THESE DE DOCTORAT DE L'ETABLISSEMENT UNIVERSITE BOURGOGNE FRANCHE-COMTE

PREPAREE A L'UNITE INSERM U1231 – Equipe GAD

Ecole doctorale n°554

Environnements – Santé

Doctorat de Sciences de la Vie et de la Santé

Par

M. DUCREUX Bastien

Exploration pangénomique des effets épigénétiques et transcriptomiques liés aux techniques d'assistance médicale à la procréation

Thèse présentée et soutenue à Dijon, le 27/02/2024

Composition du Jury :

Mme JAMMES Hélène	Directrice de Recherche, INRAE, Université Paris-Saclay	Président
Mme DURANTHON Véronique	Directrice de Recherche, INRAE, Université Paris-Saclay	Rapporteur
M. VAIMAN Daniel	Directeur de recherche, INSERM, Université Paris Cité	Rapporteur
Mme BOURC'HIS Déborah	Directrice de Recherche, INSERM, Institut Curie	Examinatrice
Mme PATRAT Catherine	Professeure des Universités-Praticien Hospitalier, AP-HP Cochin, Université Paris Cité	Examinatrice
Mme FAUQUE Patricia	Professeure des Universités-Praticien Hospitalier, CHU Dijon, Université Bourgogne Franche-Comté	Directrice de thèse

ÉCOLE DOCTORALE
Environnements - Santé
Bourgogne | Franche-Comté

Titre : Exploration pangénomique des effets épigénétiques et transcriptomiques liés aux techniques d'assistance médicale à la procréation

Mots clés : assistance médicale à la procréation, embryon, épigénétique, méthylation de l'ADN, ovocyte, transcriptome

Résumé : Des millions d'enfants sont nés à travers le monde grâce aux techniques d'assistance médicale à la procréation (AMP) dont l'innocuité n'a pas été totalement démontrée à ce jour. Ces techniques concomitantes à la reprogrammation épigénétique pourraient être en lien avec certaines des complications observées après AMP telles les pathologies liées à l'empreinte. Les expérimentions animales ont démontré que ces méthodes pouvaient avoir un impact sur la régulation épigénétique de gènes majeurs pour le développement du conceptus mais chez l'homme cela reste largement inconnu.

Nous nous proposons d'étudier les interactions entre les gamètes et l'embryon avec le milieu *in vitro* (vitrification des ovocytes, composition du milieu de culture embryonnaire) chez l'humain par une approche transcriptomique (single-oocyte et single-embryo RNA-seq). Par ailleurs, une analyse critique de la littérature sur les altérations transcriptomiques des ovocytes induites par l'AMP a permis d'identifier des mécanismes biologiques communs par lesquels différentes techniques d'AMP modifient le transcriptome ovocytaire et sa régulation épigénétique.

Ensuite, nous aborderons les conséquences à court et à long terme des techniques d'AMP sur l'ensemble du profil épigénétique chez l'humain sur trois périodes clés du développement, à savoir en phase pré-implantatoire, immédiatement à la naissance puis durant l'enfance. A cette fin nous avons réalisé une revue systématique et méta-analyse ayant comme thématique le suivi des profils de la méthylation de l'ADN chez les enfants conçus par AMP. Pour compléter ces données, nous avons mesuré les profils de méthylation chez une cohorte d'enfants de 7-8 ans conçus par FIV/ICSI à l'aide de puces EPIC (Illumina).

De façon générale, la majorité des interventions en AMP sont susceptibles d'interférer sur la reprogrammation épigénétique des gamètes et embryons. Les faibles taux de réussite en AMP et surtout leur variabilité inter-clinique pourraient être un témoin qu'aujourd'hui, les modifications épigénétiques (dans les lignées germinales ou chez l'embryon) et leurs conséquences sur l'échec d'une tentative d'AMP ne sont pas assez prises en compte dans les pratiques actuelles. Dans le prolongement de cette thèse, des protocoles d'AMP plus sûrs sont nécessaires et la recherche doit aller en ce sens.

Title : Genome-wide exploration of the epigenetic and transcriptomic effects of medically assisted reproduction techniques

Keywords : assisted reproductive technologies, embryo, epigenetics, DNA methylation, oocyte, transcriptome

Abstract : Millions of children are born worldwide thanks to medically assisted reproduction techniques (ARTs), the safety of which has not yet been fully demonstrated. These techniques, combined with epigenetic reprogramming, could be linked to some of the complications observed after ART, such as imprinting-related pathologies. Animal experiments have shown that these methods can have an impact on the epigenetic regulation of major genes for conceptus development, but in humans, this remains largely unknown.

We propose to study the interactions between gametes and embryos with the in vitro environment (oocyte vitrification, composition of embryonic culture medium) in humans using a transcriptomic approach (single-oocyte and single-embryo RNA-seq). In addition, a critical review of the literature on ART-induced oocyte transcriptomic alterations identified common biological mechanisms by which different ARTs modify the oocyte transcriptome and its epigenetic regulation.

Next, we will look at the short- and long-term consequences of ARTs on the overall epigenetic profile in humans over three key developmental periods, namely pre-implantation, immediately after birth and during childhood. To this end, we carried out a systematic review and meta-analysis focusing on the monitoring of DNA methylation profiles in children conceived by ART. To complement these data, we measured methylation profiles in a cohort of 7–8-year-old children conceived by IVF/ICSI, using EPIC arrays (Illumina).

In general, most ARTs interventions are likely to interfere with the epigenetic reprogramming of gametes and embryos. The low success rates in ART and, above all, their inter-clinical variability could be a sign that epigenetic modifications (in germ lines or embryos) and their consequences on the failure of an ART attempt are not sufficiently taken into account in current practices. As an extension of this thesis, safer ARTs protocols are needed, and research must move in this direction.

Université Bourgogne Franche-Comté
32, avenue de l'Observatoire
25000 Besançon

Remerciements

En premier lieu, je souhaite remercier les membres du jury qui ont accepté d'examiner mes travaux de thèse. J'exprime ma gratitude à Madame le Docteur Véronique Duranthon et Monsieur le Docteur Daniel Vaiman d'avoir accepté d'être les rapporteurs de cette thèse. Merci à Madame le Docteur Hélène Jammes d'avoir suivi le déroulé de cette thèse, et d'avoir toujours pris le temps de me conseiller après chacune de mes présentations. Merci à Madame le Docteur Déborah Bourc'his et Madame la Professeure Catherine Patrat pour leurs relectures constructives sur mes publications.

Je tiens à exprimer toute ma reconnaissance à ma directrice de thèse, Madame la Professeure Patricia Fauque. Je tenais à vous remercier pour votre bienveillance et votre écoute durant ces trois années. J'éprouve une très grande fierté à travailler à vos côtés et j'ai hâte de poursuivre vos nombreux projets avec vous.

Je remercie le Professeur Patrick Callier d'avoir accepté de suivre l'avancement de cette thèse.

Je remercie la Professeure Christel Thauvin de m'avoir accueilli au sein de son équipe Génétique des Anomalies du Développement. Un très grand merci à Yannis Duffourd pour son assistance en bioinformatique. Merci à tous les autres membres de l'équipe GAD que j'ai pu côtoyer durant ces trois années, et notamment Aymeric mon camarade de thèse !

Je tiens spécifiquement à remercier Julie Barberet et les très beaux articles que nous avons pu produire ensemble, et de m'avoir guidé lors de mes premiers pas dans la thèse. Je te souhaite tout le meilleur pour ta carrière. Merci également à Céline Bruno pour son accueil et ses conseils lors de mon arrivée au sein du laboratoire.

Toutes mes analyses n'auraient pas été possibles sans tous les professionnels qui ont opéré au sein du Laboratoire de Biologie de la Reproduction du CHU Dijon et m'ont permis d'obtenir les données nécessaires à l'élaboration de cette thèse : Magali, Bruno, Cindy, Déborah, Nicolas, Raymond, Clarisse, Flavie, Aurélie et Jean.

Je remercie Aurélie Teissandier pour sa grande aide sur les analyses RNA-seq de cette thèse. Un très grand merci également à Jacquetta Trasler, Raquel Pérez-Palacios et Lucile Ferreux pour leurs relectures des manuscrits. Merci à Suzanne Rankin pour son assistance en grammaire anglaise.

Si j'ai trouvé ma voie dans la recherche aujourd'hui, c'est grâce à ma rencontre avec Sarah Voisin il y a (déjà!) 6 ans en Australie. Sarah, tu as su faire naître ma vocation pour l'analyse de données épigénomiques et tu seras toujours mon mentor et mon exemple de réussite dans ce domaine. Merci pour ton aide et d'avoir toujours pris le soin de prendre de mes nouvelles pendant ces années.

Je terminerai ces remerciements pour mes proches qui me soutiennent depuis le début. Maman et Papa, vous m'avez toujours donné les moyens de faire les études que je souhaitais. A ma Clara pour son soutien indéfectible, et notre vie bientôt réunis.

Table des matières

Préambule 1

Chapitre 1 : État de l'art et analyses à partir des données de la littérature 3

I) L'assistance médicale à la procréation : principes et techniques 3
1) Stimulation ovarienne 4
2) Technique de fécondation : FIV et ICSI 5
3) Culture embryonnaire 6
4) Cryoconservation des ovocytes et embryons 10
5) Maturation ovocytaire *in vitro* 11

II) Régulation épigénétique et transcriptomique dans les premières étapes du développement et techniques de mesure 15
1) L'épigénétique 15
1.1) Les marques épigénétiques 15
1.2) La méthylation de l'ADN 18
1.3) Dynamique des profils de méthylation depuis le développement embryonnaire jusqu'à l'âge adulte 21
1.4) Techniques de mesure de méthylation à l'échelle du génome-entier 30
1.5) Analyses bioinformatiques des données de méthylation issues de puces 38
1.5.1) Contrôle qualité 39
1.5.2) Normalisation 41
1.5.3) Filtrage 46
1.5.4) Analyse différentielle 46
1.5.5) Annotation et interprétation 48
1.5.6) Les méta-analyses d'études d'association à l'échelle de l'épigénome 51
2) Le transcriptome 52
2.1) Le transcriptome ovocytaire, sentinelle du développement embryonnaire 54
2.1.1) Objectifs 54
2.1.2) Matériels et méthodes 55
2.1.3) Résultats 56
2.1.4) Article 1 - Overview of Gene Expression Dynamics during Human Oogenesis/Folliculogenesis 58
2.2) L'activation du génome embryonnaire 80
2.3) Techniques de mesure du transcriptome à l'échelle du génome-entier 80
2.4) Analyses bioinformatiques des données issues de RNA-seq 83

III) Effets épigénétiques et transcriptomiques en lien avec l'AMP depuis l'ovocyte jusque chez l'adulte : quelle évidence à ce jour ? 85
1) Effets épigénétiques des techniques AMP: une nécessité d'évaluer les modifications du profil de méthylation de l'ADN depuis l'ovocyte jusque chez l'adulte 86
1.1) Données issues du modèle animal 86
1.2) Données chez l'humain 88
1.2.1) AMP et profils de méthylation dans l'ovocyte 88
1.2.2) AMP et profils de méthylation chez l'embryon 89
1.2.3) AMP et profils de méthylation depuis la vie fœtale jusqu'à l'âge adulte 91
1.2.3.1) Objectifs 91
1.2.3.2) Matériels et méthodes 92
1.2.3.3) Résultats 96
1.2.3.4) Article 2 - DNA methylation profiles after ART during human lifespan: a systematic review and meta-analysis 103
2) Mécanismes biochimiques de modification de l'épigénome : la reprogrammation épigénétique comme période de susceptibilité 140
3) La vulnérabilité de l'ovocyte et de l'embryon humain face aux techniques d'AMP se traduit sur leur transcriptome 142
3.1) Effets sur l'ovocyte chez l'Homme 143
3.1.1) Objectifs 143

3.1.2) Matériels et méthodes 144
3.1.3) Résultats 144
3.1.4) Article 3 - Transcriptomic integrity of human oocytes used in assisted reproductive technologies: technical and intrinsic factor effects 148
3.2) Effets sur l'embryon chez l'Homme 182

Chapitre 2 : Analyses biologiques sur expérimentations réalisées au laboratoire 183

I) Le transcriptome ovocytaire et embryonnaire est-il influencé par différentes techniques d'AMP ? 184

1) Comparaison de la vitrification d'ovocytes à l'aide d'un système fermé semi-automatique ou manuel sur le transcriptome d'ovocytes humains appariés 185
1.1) Objectifs 185
1.2) Matériels et méthodes 185
1.3) Résultats 186
1.4) Article 4 - Comparison of oocyte vitrification using a semi-automated or a manual closed system in human siblings: survival and transcriptomic analyses 187
2) Évaluation de l'influence de milieux de culture embryonnaire distincts sur le transcriptome préimplantatoire humain 204
2.1) Objectifs 204
2.2) Matériels et méthodes 205
2.3) Résultats 206
2.4) Article 5 - Assessing the influence of distinct IVF culture media on human pre-implantation development using single-embryo transcriptomics 207

II) Profil de méthylation chez des enfants conçus par AMP 233

1) Objectifs 233
2) Matériels et méthodes 233
3) Résultats 234
4) Article 6 - Genome-wide analysis of DNA methylation in buccal cells of children conceived through IVF and ICSI 235

Chapitre 3 : Discussion générale 255

Conclusion 268

Bibliographie 270

Liste des illustrations

Figure 1. Organigramme des lignes directrices sur la stimulation ovarienne pour la FIV/ICSI recommandées par la Société Européenne de Reproduction Humaine et d'Embryologie (ESHRE). 5
Figure 2. Schéma du processus de FIV et d'ICSI. 6
Figure 3. Modifications du profil métabolique de l'embryon précoce à partir du stade morula. 8
Figure 4. Maturation *in vitro* des ovocytes et ses variantes utilisées actuellement. 13
Figure 5. AMP et caractéristiques parentales : une multitude de facteurs pouvant potentiellement affecter le développement de l'embryon. 14
Figure 6. Les modifications post-traductionnelles des histones régulent l'état de la chromatine. 16
Figure 7. Différents types de modifications épigénétiques à différentes échelles génomiques. 18
Figure 8. Répartition et organisation schématique des CpGs dans le génome. 20
Figure 9. Mécanisme de méthylation puis d'hydroxylation des cytosines via les enzymes ADN méthyltransférases et Ten-eleven translocator (Wu & Zhang, 2014). 21
Figure 10. Acquisition des profils de méthylation de l'ADN depuis les cellules germinales primordiales jusqu'au développement embryonnaire. 24
Figure 11. Deux exemples de régulation en *cis* et en *trans* de l'expression de gène soumis à empreinte. 26
Figure 12. Principales techniques de mesure de méthylation. 30
Figure 13. Fonctionnement des différents types de sondes retrouvées sur les puces de type Beadchip de chez Illumina. 37
Figure 14. Pipeline générique d'analyse de données issues de puces à méthylation de l'ADN. 39
Figure 15. Une représentation de la courbe de densité de distribution classique des beta-valeurs sur une puce 450k (échantillons-tests du package R minfiData). 40
Figure 16. Distributions des intensités des signaux de méthylation des types de sondes Infinium I et II pour toutes les sondes d'une puce 450k (premier échantillon-test du package R minfiData). 41
Figure 17. Distributions des intensités des signaux de méthylation des types de sondes Infinium I et II pour les sondes contenant 1,2 ou 3 CpGs sur une puce 450k (premier échantillon-test du package R minfiData). 43
Figure 18. Distributions des intensités des beta-valeurs des types de sondes Infinium I et II comparées avant et après normalisation BMIQ et SWAN. 44
Figure 19. Exemple de visualisations possibles après analyse différentielle. Issu de l'analyse du jeu de données test du package minfiData. 49
Figure 20. Dynamique du développement ovocytaire et de son transcriptome. 55
Figure 21. Organigramme de la méthode scRNA-seq pour ovocyte et embryon unique. 82
Figure 22. Le diagramme UpSet, une alternative aux diagrammes de Venn. 95
Figure 23. Résumé des résultats des études comparant les profils de méthylation de l'ADN de fœtus, nouveau-nés, enfants, adolescents et adultes conçus par AMP en comparaison de conceptions spontanées. 97
Figure 24. Résumé de l'évidence concernant les modifications épigénétiques en lien avec l'AMP depuis la grossesse jusqu'à l'âge adulte dans les articles notés avec une qualité de l'évidence très haute. 102
Figure 25. Le cycle de la méthylation simplifié. 141
Figure 26. Résumé des études évaluant les modifications du transcriptome après hyperstimulation ovarienne et ses modalités, maturation *in vitro* et cryopréservation. 147
Figure 27. Contrôle qualité des données. 234

Liste des tables

Table 1. Synthèse des troubles de la santé liés à l'empreinte parentale. 28
Table 2. Gènes soumis à empreinte très exprimés dans le placenta humain connus pour entraîner des phénotypes avec anomalies placentaires de croissance, voire létaux, lorsque leur expression est altérée chez le modèle murin. 29
Table 3. Différentes méthodes de normalisation couramment utilisées pour l'analyse de puces à méthylation et leurs caractéristiques. 45
Table 4. Recommandation de nomenclatures des régions soumises à empreinte dans le génome humain. 94

Liste des abréviations

5hmC : 5-hydroxyméthylcytosine
5mC : 5-méthylcytosine
AMP : assistance médicale à la procréation
ARNm : ARN messager
ARNnc : ARN non codant
ATP : adénosine triphosphate
BMIQ : Beta-Mixture Quantile Normalisation
bp : paire de base
CC : cellules du cumulus
CECOS : centres d'étude et de conservation des œufs et du sperme
CGM : cellules de la granulosa murale
CGPs : cellules germinales primordiales
CpG : cytosine-phosphate-guanine
DEG : differentially expressed gene (gène différentiellement exprimé)
DMP : differentially methylated position (position différentiellement méthylée)
DMR : differentially methylated region (région différentiellement méthylée)
DNMT : ADN méthyltransférases
DOHaD : developmental origins of health and disease (l'origine développementale de la santé et des maladies)
DROs : dérivés réactifs de l'oxygène
EDTA : éthylènediaminetétraacétique
EGA : activation du génome embryonnaire
ESHRE : Société Européenne de Reproduction Humaine et d'Embryologie
EWAS : epigenome-wide association study (étude d'association à l'échelle de l'épigénome)
FDR : false discovery rate
FIV : fécondation *in vitro*
FSH : follicle-stimulating hormone (hormone stimulant le follicule ovarien)
GnRH : hormone de libération de la gonadotrophine
GnRH-a : agoniste de l'hormone de libération de la gonadotrophine
GnRH-anta : antagoniste de l'hormone de libération de la gonadotrophine
GO : gene ontology
GSE : gène soumis à empreinte
GV : vésicule germinale
GVBD : germinal vesicle breakdown (rupture de la vésicule germinale)
hCG : hormone gonadotrophine chorionique humaine
hMG : gonadotrophine ménopausique humaine
ICR : imprinting control regions (régions de contrôle de l'empreinte parentale)
ICSI : injection intracytoplasmique de spermatozoïde
LH : luteinizing hormone (hormone lutéinisante)
MBD : methyl-binding domain (domaine de liaison sur l'ADN méthylé)

MCI : masse cellulaire interne
MeDIP : Methylated DNA ImmunoPrecipitation
MI : métaphase I
miRNA : microARN
MII : métaphase II
MIV : maturation *in vitro*
mQTL : traits quantitatifs de méthylation
MRE : methylation sensitive restriction enzyme
mtDNA : ADN mitochondrial
noob : normal-exponential out-of-band
PCR : polymerase chain reaction
PHATE : Potential of Heat-diffusion for Affinity-based Trajectory Embedding
rFSH : recombinant follicle-stimulating hormone (hormone recombinante stimulant le follicule ovarien)
RRBS : Reduced Representation Bisulfite Sequencing
SAH : S-adénosylhomocystéine
SAM : S-adénosylméthionine
SHSO : syndrome d'hyperstimulation ovarienne
SNP : single nucleotide polyphormism
SOPK : syndrome des ovaires polykystiques
SWAN : Subset-quantile Within Array Normalization
TET : enzymes ten-eleven translocation
TIN : transcript integrity number
TSS : transcription start site (site d'initiation de la transcription)
UTR : untranslated transcribed region (régions régulatrices non traduites)
WGBS : Whole Genome Bisulfite Sequencing

Préambule

Cela fait maintenant plus de 40 ans que les techniques d'Assistance Médicale à la Procréation (AMP) sont utilisées à travers le monde. Le recours à l'AMP est grandissant et a permis à ce jour la naissance de millions d'enfants représentant plus de 4% des naissances annuelles en Europe (De Geyter *et al.*, 2018).

Pourtant l'innocuité de ces techniques n'est aujourd'hui pas encore admise. En effet, de sérieuses préoccupations concernant la santé des enfants nés sous AMP ont été émises au début des années 2000 (Hansen *et al.*, 2002; Schieve *et al.*, 2004). Une plus forte prévalence d'anomalies congénitales a été observée chez ces enfants par rapport à la population générale, notamment de maladies cardio-vasculaires ou métaboliques (Chen & Heilbronn, 2017; Guo *et al.,* 2017b; Berntsen *et al.,* 2019). La survenue de syndromes dits de Beckwith-Wiedemann, Silver-Russell ou encore Angelman est aussi anormalement plus élevée chez les enfants conçus par AMP (Vermeiden & Bernardus, 2013). Ces pathologies rares sont liées à des dysfonctionnements bien connus de certaines régions chromosomiques dites « soumises à empreinte parentale » et à l'origine d'anomalies du développement (Argyraki *et al.*, 2019).

En outre, l'ensemble des techniques liées aux différentes étapes d'AMP, peuvent constituer un terrain stressant pour des gamètes et embryons alors soumis à un environnement *in vitro*. Elles interviennent à un moment où les gamètes et l'embryon entrent dans une phase de reprogrammation épigénétique intense. Aussi, il est probable que des éléments péri-conceptionnels en lien avec l'AMP soient responsables d'anomalies de méthylation dans les régions soumises à empreinte, et des syndromes congénitaux qui en découlent (Ramos-Ibeas *et al.*, 2019). L'hyperstimulation ovarienne et la cryoconservation pour l'ovocyte, les conditions de culture *in vitro* pour l'embryon (composition du milieu, tension en oxygène, …) sont autant d'expositions les rendant vulnérables et qui ont la capacité d'altérer leur architecture épigénétique et leur qualité transcriptomique. Des expérimentations utilisant des espèces

modèles ont mis en évidence l'importance de ces phénomènes sur la régulation épigénétique au niveau des régions de contrôle de l'empreinte parentale (Imprinting Control Regions ; ICRs) mais aussi à l'échelle du génome entier ; les connaissances restent pourtant éparses chez l'Homme (Fauque *et al.*, 2007a; Duranthon & Chavatte-Palmer, 2018).

Les objectifs de cette thèse se résument en deux grandes parties. Dans un premier temps, nous évaluerons les interactions entre les gamètes et l'embryon avec le milieu *in vitro* (vitrification des ovocytes, composition du milieu de culture embryonnaire) chez l'humain par une approche transcriptomique. Dans un second temps, nous aborderons les conséquences à court et à long terme des techniques d'AMP sur l'ensemble du profil épigénétique chez l'humain sur trois périodes clés du développement, à savoir en phase pré-implantatoire, immédiatement à la naissance puis durant l'enfance. A travers l'analyse de données de séquençage à haut débit de collections rares et uniques d'échantillons biologiques obtenus selon différentes modalités de conception et contextes d'infertilité, nous apporterons une meilleure compréhension des effets épigénétiques et transcriptomiques en lien avec les techniques d'assistance médicale à la procréation.

Chapitre 1 : État de l'art et analyses à partir des données de la littérature

I) L'assistance médicale à la procréation : principes et techniques

Le recours à l'assistance médicale à la procréation est de plus en plus élevé à travers le monde (Kushnir *et al.*, 2017; de Geyter *et al.*, 2020). Symboliquement, la barre du million de cycles d'AMP amorcés sur une année parmi les 39 pays d'Europe avec des données de registre disponibles a été atteinte pour la première fois en 2018 (Wyns *et al.*, 2022). Les techniques d'AMP doivent faire face à une infertilité croissante et deviennent un enjeu de santé publique majeur (Sun *et al.*, 2019). Depuis la naissance du premier enfant conçu par AMP en 1978, les techniques ont considérablement évolué avec notamment l'optimisation des conditions de culture, le développement de l'injection intracytoplasmique des spermatozoïdes et l'apparition de la congélation ultra-rapide. De plus, le recours à l'AMP tend à s'adresser à un public de plus en plus varié pour des raisons éthiques, cliniques et d'évolution de la société (parentalité plus tardive, gonadotoxicité de certains traitements, baisse de la fertilité due à l'obésité).

Aujourd'hui il existe une grande disparité des techniques utilisées à travers les pays, et même à une échelle nationale, qui conduisent à des taux de réussite variables (Munné *et al.*, 2017; Chambers *et al.*, 2021; Agence de la biomédecine, 2023). Lors d'un protocole d'AMP peuvent se succéder différentes interventions externes adaptées à la pluralité des facteurs d'infertilité. Il est nécessaire que ces étapes soient strictement contrôlées et n'impactent pas la qualité embryonnaire, qui est un déterminant majeur des chances de grossesse et de naissance (Fauque *et al.*, 2007b).

1) Stimulation ovarienne

La stimulation ovarienne en fécondation *in vitro*, a pour but d'obtenir une croissance multifolliculaire et ainsi plusieurs ovocytes matures afin d'augmenter les chances de succès. Les patientes reçoivent un traitement hormonal à base d'agonistes ou d'antagoniste du GnRH (hormone de libération des gonadotrophines hypophysaires) et de FSH (hormone stimulant le follicule ovarien, follicle-stimulating hormone) pendant environ 2 semaines avec des doses adaptées au profil hormonal de la patiente. Le rôle du traitement par agoniste ou antagoniste du GnRH est de mettre l'hypophyse au repos afin de bloquer l'ovulation spontanée qui pourrait surgir lors du cycle menstruel à la suite du pic de LH endogène (hormone lutéinisante, luteinizing hormone). La FSH et ses différentes isoformes (d'origine urinaire ou recombinante) permettent quant à elles de stimuler la croissance du follicule. Ainsi le traitement permet de contrôler les niveaux d'hormones et déclencher l'ovulation au moment opportun. Ce déclenchement survient généralement dès lors que les follicules ont atteint 15-16mm de diamètre. Après plusieurs heures, l'ovocyte est alors normalement mature, c'est-à-dire que les différentes stimulations l'ont conduit à passer du stade vésicule germinale (prophase I) au stade métaphase II. L'ovocyte a subi une maturation double, cytoplasmique et nucléaire, permettant la reprise de sa méiose si un pic de LH a lieu, mais également la préparation pour la fécondation. L'induction de l'ovulation est en majorité provoquée par une injection de hCG (hormone gonadotrophine chorionique humaine) et les ovocytes sont généralement collectés dans les 36-38 heures suivantes, par ponction ovarienne sous contrôle échographique et par voie vaginale. Il existe différents types de protocoles de stimulation multifolliculaire, courts ou longs en fonction d'un bilan médical préalablement réalisé. Chez certaines patientes, il peut exister un risque élevé de syndrome d'hyperstimulation ovarienne qui peut être limité en adaptant les doses prescrites ou en substituant l'administration de hCG (Fiedler & Ezcurra, 2012). Un résumé des étapes de la stimulation ovarienne et de son adaptation à différents types de patients (prévision de la réponse ovarienne faible, normale ou forte suivant les marqueurs de réserve ovarienne) est indiqué en Figure 1.

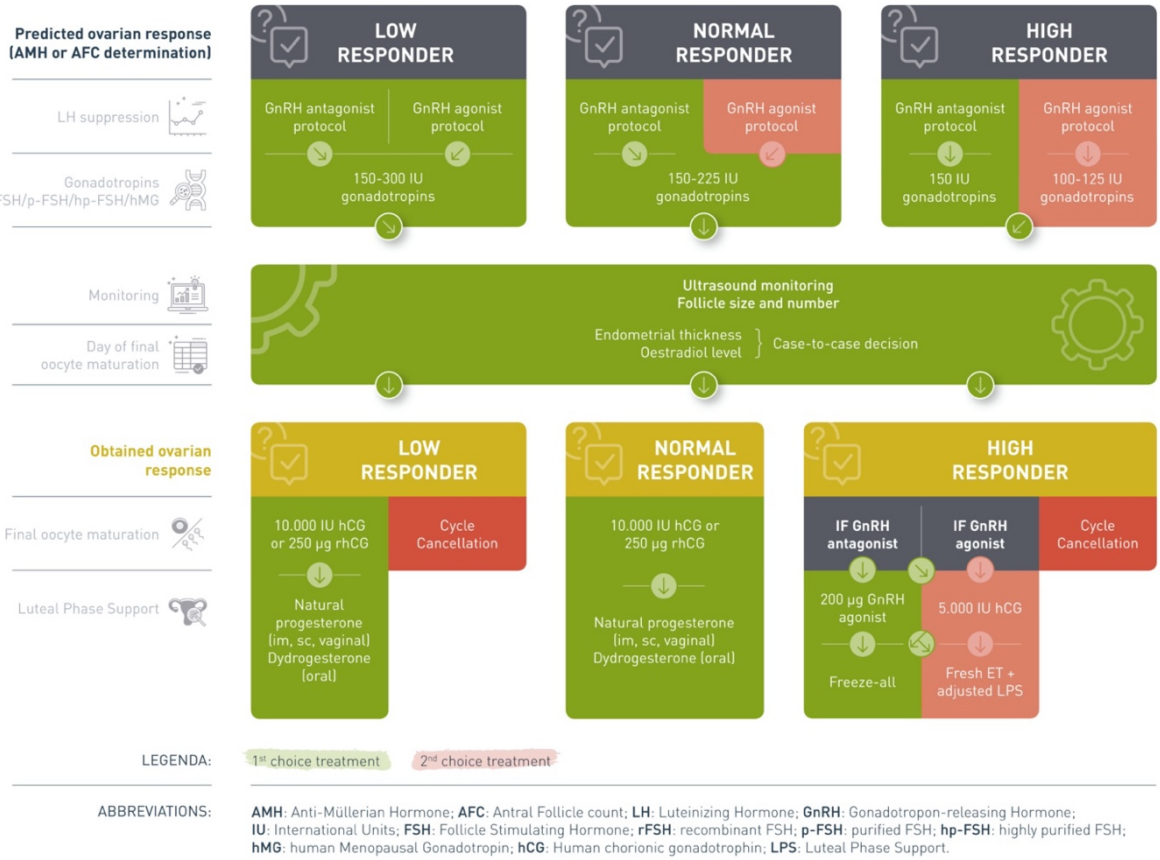

Figure 1. Organigramme des lignes directrices sur la stimulation ovarienne pour la FIV/ICSI recommandées par la Société Européenne de Reproduction Humaine et d'Embryologie (ESHRE).

2) Technique de fécondation : FIV et ICSI

Après une étape de stimulation ovarienne, les complexes cumulus-ovocytes (ovocyte plus cellules folliculaires entourant l'ovocyte) sont ponctionnés par voie transvaginale environ 36 heures après le déclenchement de l'ovulation. Les spermatozoïdes subissent également une étape de préparation après leur recueil afin de sélectionner ceux de meilleure qualité. L'étape suivante de mise en fécondation est couramment réalisée selon deux techniques : la fécondation *in vitro* (FIV) et l'injection intracytoplasmique du spermatozoïde (ICSI) (Barberet *et al.*, 2018).

Lors de la FIV, les spermatozoïdes sont sélectionnés et déposés au contact des complexes cumulus-ovocytes dans une boîte de culture (Figure 2). Depuis quelques années, l'ICSI est de plus en plus pratiquée en raison d'une hausse de l'infertilité masculine potentiellement reliée

à des facteurs environnementaux (pollution, nutrition, activité physique, perturbateurs endocriniens) (Kumar & Singh, 2015). Le biologiste établit une sélection du spermatozoïde en fonction de sa morphologie et de sa motilité. L'ovocyte est décoronisé des cellules qui l'entourent (cellules de la granulosa, cellules du cumulus) par une hyaluronidase et puis l'unique spermatozoïde est injecté avec une micropipette de verre. Les gestes supplémentaires et la sélection du spermatozoïde en ICSI fait l'objet d'une surveillance accrue de la santé des enfants conçus via cette technique.

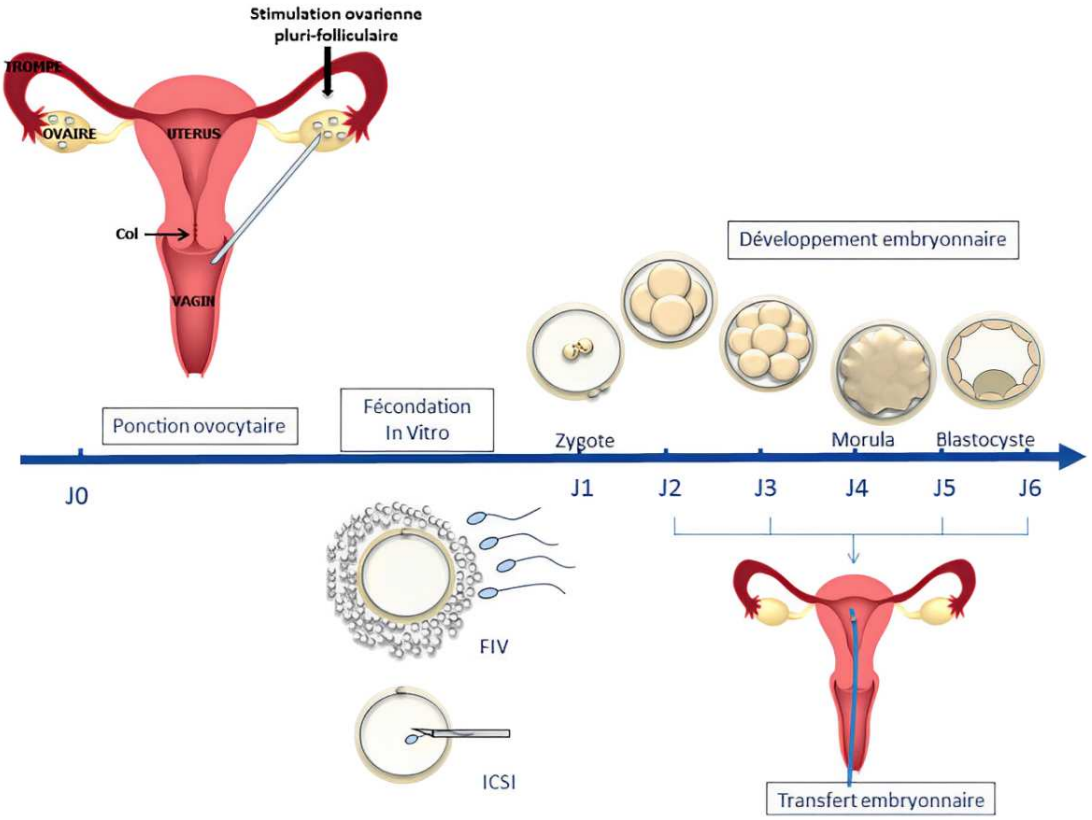

Figure 2. Schéma du processus de FIV et d'ICSI.
Issu de Barberet *et al.* (2018) (Barberet *et al.*, 2018).

3) Culture embryonnaire

La mise en culture des embryons est une étape essentielle des protocoles AMP. Elle permet d'identifier les embryons de bonne morphologie après quelques jours de culture en vue d'un transfert vers la voie utérine (au stade clivé : jour 2 ou 3, au stade de blastocyste :

jour 5/6). La composition du milieu de culture utilisé est importante et doit répondre aux besoins physiologiques de l'embryon précoce (Sunde *et al.*, 2016):

- Substrats énergétiques : le cycle de Krebs représente la principale source d'énergie pour l'embryon pré-implantatoire. La consommation d'oxygène augmente progressivement durant le développement mais la source de carbone est différente avant ou post-compaction. L'oxydation du pyruvate est la principale source d'énergie de l'embryon au stade clivé. Après compaction, ce métabolisme change radicalement, la consommation d'oxygène augmente, et l'embryon utilise la glycolyse aérobie pour compenser sa forte demande biosynthétique et ses besoins en glucose sont donc croissants.
- Acides aminés : certains sont des précurseurs du lactate, une des sources d'énergie de l'embryon au stade clivé. D'autres jouent le rôle de tampon de pH intracellulaire, de chélateurs de métaux lourds, stimulent le taux de clivage ou participent à la biosynthèse de protéines et d'antioxydants (Leese *et al.*, 2021). La méthionine, par sa conversion en S-adénosylméthionine, joue le rôle de donneur de méthyle et participe donc à la méthylation de l'ADN qui prend place lors de la reprogrammation épigénétique intense subie par le génome embryonnaire au cours de la période pré-implantatoire (Menezo *et al.*, 2022a).
- Ions : la majorité des milieux contiennent des ions sodium, potassium, chlore, calcium, magnésium, sulfate qui régulent l'osmolalité des cellules.
- EDTA (éthylènediaminetétraacétique) : la présence de glucose dans certains milieux est conditionnée à la présence d'EDTA, afin de bloquer la glycolyse. Lorsque l'embryon passe sous un régime de glycolyse aérobie, il sécrète davantage d'enzymes de la glycolyse, qui ne pourront plus être saturées par l'EDTA à partir d'une certaine concentration. Le glucose devient alors métabolisable après compaction et répond aux besoins métaboliques de l'embryon.

- Protéines : la principale protéine supplémentée dans le milieu est l'albumine. Elle régule la disponibilité de lipides, de certaines hormones et de minéraux.
- Facteurs de croissance et cytokines : Les facteurs de croissance peuvent soutenir le développement. Les cytokines soutiennent le développement embryonnaire en protégeant contre le stress cellulaire et l'apoptose.

Deux types de milieux de culture sont actuellement utilisés en AMP : les milieux uniques (dits « single step ») et les milieux séquentiels (Chronopoulou & Harper, 2015). Les premiers peuvent être utilisés pendant toute la durée de culture, depuis la fécondation jusqu'au stade blastocyste car ils contiennent tous les nutriments nécessaires au développement de l'embryon. Les milieux séquentiels doivent eux être changés après deux jours de culture car leur composition est spécifique aux besoins physiologiques de l'embryon avant et après compaction (Figure 3).

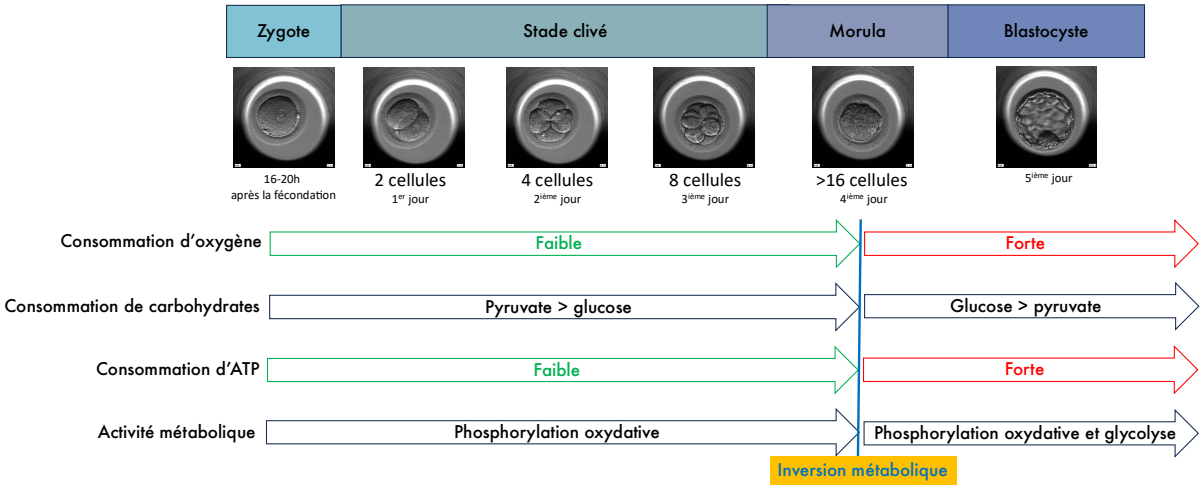

Figure 3. Modifications du profil métabolique de l'embryon précoce à partir du stade morula.
Le métabolisme de l'embryon clivé se caractérise par une activité faible reposant exclusivement sur l'oxydation du pyruvate. Après l'activation du génome embryonnaire, le blastocyste absorbe des niveaux élevés de glucose et consomme beaucoup d'ATP (adénosine triphosphate) et d'oxygène pour la glycolyse aérobie, du fait d'une forte demande biosynthétique. Inspiré de Ferrick *et al.* (2019) (Ferrick *et al.*, 2019).

Les milieux séquentiels sont très utilisés car considérés comme adaptés à la physiologie de l'embryon mais cela impose en contrepartie des manipulations additionnelles qui peuvent être source de stress cellulaire. Chaque milieu de culture possède une composition qui lui est

propre et qui est souvent incomplètement rendue transparente par les industriels, ce qui fait l'objet de nombreux débats (Sunde *et al.*, 2016). L'objectif de la culture embryonnaire n'est pas d'être un parfait miroir des conditions utérines mais d'assurer que l'environnement physiologique de l'embryon lui permette de se développer de façon optimale (Gardner, 1998). Toutefois, il y a encore des désaccords sur de nombreux paramètres physico-chimiques qui garantissent cette optimalité, la composition en acides aminés essentiels ou la supplémentation en antioxydants, vitamines, facteurs de croissance, nucléotides ou encore stéroïdes (Chronopoulou & Harper, 2015; Xu & Sinclair, 2015). D'autres paramètres restent peu étudiés mais semblent déterminants pour le développement de l'embryon, comme l'intensité lumineuse (Khodavirdilou *et al.*, 2021), la température et ses variations (Baak *et al.*, 2019), et la contamination chimique du milieu (soit déjà présente dans le milieu conditionné industriellement (Tarahomi *et al.*, 2019) soit par phénomène de lixiviation des contenants plastiques (Gatimel *et al.*, 2016)).

Les études comparant l'efficacité des milieux de culture actuellement utilisés en AMP se sont principalement concentrées sur des aspects cliniques du développement embryonnaire, à savoir les taux de blastulation, d'implantation et de naissance (Mantikou *et al.*, 2013). Les nombreuses études et méta-analyses ne mettent à ce jour pas en évidence de différences de taux de grossesse, qui est le critère principal de jugement d'efficacité de chaque technique, selon les milieux uniques et séquentiels (Biggers & Summers, 2008; Sepúlveda *et al.*, 2009; Dieamant *et al.*, 2017), alors qu'au contraire l'impact de la tension en oxygène semble avéré (Van Montfoort *et al.*, 2020; Herbemont *et al.*, 2021). Concernant les issues cliniques à court et long terme, peu d'études ont été réalisées, et la principale différence retrouvée selon les milieux de culture est au niveau du poids de naissance (Zandstra *et al.*, 2015).

4) Cryoconservation des ovocytes et embryons

La cryoconservation des ovocytes et embryons est une technique apparue en premier lieu avec la méthode dite de la « congélation lente » et permettant de préserver la fertilité des patients masculins et féminins. Rapidement, la vitrification l'a remplacée et a permis une amélioration des taux de grossesses cliniques (Rezazadeh Valojerdi *et al.*, 2009; Edgar & Gook, 2012). La vitrification consiste en la congélation ultrarapide à -196°C à l'aide d'agents cryoprotectants en forte concentration qui permettent d'éviter la formation de cristaux intra-cellulaires et de conserver la morphologie des gamètes et embryons intacte (Wolkers & Oldenhof, 2015). Cette technique est particulièrement utile pour un grand nombre de patientes. Elle permet notamment aux femmes de conserver leurs ovocytes avant l'introduction d'un traitement potentiellement gonadotoxique (chimiothérapie et/ou radiothérapie). Depuis 2021 en France, les femmes souhaitant retarder leur grossesse peuvent congeler leurs ovocytes pour conserver des ovocytes « jeunes » et donc de meilleure qualité, car la qualité ovocytaire diminue avec l'âge (Cimadomo *et al.*, 2018). La vitrification ovocytaire est également utile dans le cadre du don d'ovocytes (Cobo *et al.*, 2011). En France, les ovocytes sont conservés dans des centres autorisés comme les centres d'étude et de conservation des œufs et du sperme (CECOS). Par ailleurs, les embryons peuvent également être cryoconservés, en vue de transferts d'embryons, soit au stade clivé (au 2^{ième} ou 3^{ième} jour post-fécondation) soit au stade blastocyste (au 5^{ième} ou 6^{ième} jour post-fécondation).

Les ovocytes vitrifiés affichent un très bon taux de survie après réchauffement, de l'ordre de 90% (De Munck *et al.*, 2013; Argyle *et al.*, 2016). Les taux de fécondation, de clivage et de grossesse clinique des ovocytes vitrifiés semblent comparables à ceux des ovocytes « frais » (Cobo & Diaz, 2011; Haute Autorité de Santé, 2017). Ces résultats sont rassurants, même si plus de données obstétricales nécessitent d'être réunies. Les ovocytes collectés après la ponction ovarienne doivent être dénudés (décoronisés : élimination des cellules qui entourent l'ovocyte). Plus tard, ces ovocytes seront mis contact avec des milieux avec de fortes

concentrations en cryoprotecteurs avant leur congélation ultra-rapide au sein de dispositifs spécifiques (permettant une congélation dans un très faible volume, de l'ordre de quelques microlitres). La décongélation des ovocytes est réalisée par un réchauffement rapide à 37°C, et les ovocytes doivent ensuite être inséminés dans un délai de 2h maximum. Pour les embryons, les protocoles de vitrification et réchauffement sont sensiblement identiques à ceux des ovocytes. Toutefois les blastomères étant de taille plus petite, la congélation ultra-rapide offre des taux de survie plus élevés.

5) Maturation ovocytaire *in vitro*

Le développement ovocytaire commence dès la vie fœtale par la mise en place des cellules germinales primordiales (CGPs), les ovogonies. Elles se multiplient successivement par division mitotique pour constituer un stock d'ovogonies conséquent (7 millions vers le 7ème mois de grossesse mais le stock diminuera à terme à environ 500 000 ovocytes par atrésie folliculaire jusqu'à la puberté) (Baker, 1963; Crawford & Steiner, 2015). A la suite d'une première division méiotique, toutes les ovogonies rentrent en diapause et restent bloquées au stade diplotène de la prophase de la méiose I, avant la naissance. A la puberté, la FSH déclenche périodiquement la croissance d'un petit groupe de follicules (à chaque cycle menstruel) qui entrent en croissance et se développent parallèlement au développement ovocytaire. Cette période est cruciale pour l'ovocyte qui synthétise et stocke une grande quantité d'ARN messagers et de protéines nécessaires au développement embryonnaire précoce (Krisher, 2004). Généralement, un seul ovocyte arrive à maturité et termine la méiose I pour initier la deuxième méiose interrompue en métaphase II (MII). Après la rupture de son follicule (ovulation), l'ovocyte restera en métaphase II jusqu'à l'entrée du spermatozoïde (fécondation).

Certaines femmes sont à risque ou ont des antécédents d'hyperstimulation ovarienne, comme les patientes ayant un syndrome des ovaires polykystiques (SOPK). Une option pour ces patientes est de réaliser une maturation *in vitro* (MIV) des ovocytes qui correspond à la

maturation de plusieurs follicules antraux *in vitro* à l'aide d'un milieu de culture approprié (Figure 4). Les issues obstétricales et périnatales après maturation ovocytaire *in vitro* restent peu connues en raison du faible nombre d'enfants encore conçus avec cette technique mais les premières données sur leur santé sont rassurantes (Söderström-Anttila *et al.*, 2006; Hatırnaz *et al.*, 2018; Grynberg *et al.*, 2022). Toutefois, les taux d'implantation, de grossesse et de naissance vivante restent faibles par rapport à une FIV conventionnelle (Gremeau *et al.*, 2012). Les raisons de ces faibles performances sont encore difficiles à identifier mais pourraient être liées à un stress oxydatif accru ou à la mise sous silence de la communication bidirectionnelle entre l'ovocyte et les cellules cumulus l'entourant, qui sont nécessaires pour le transfert de métabolites énergétiques et de petites molécules de signalisation régulant la maturation et le développement de l'ovocyte (Combelles *et al.*, 2009; Russell *et al.*, 2016).

Par ailleurs, dans 10 à 30% des cas, les ovocytes collectés à la suite d'une stimulation multifolliculaire contrôlée ne sont pas matures, restant au stade vésicule germinale (GV) ou métaphase I (MI) (Mandelbaum *et al.*, 2021). Il est possible de réaliser une maturation *in vitro* « de secours » lorsque seuls (ou en forte proportion) des ovocytes immatures sont recueillis. Ces ovocytes immatures le jour de la ponction ovarienne et plus précisément après dénudation en vue d'ICSI sont alors mis en culture *in vitro* jusqu'au stade métaphase II, pendant maximum 24h, afin de maximiser les chances d'obtenir un embryon transférable.

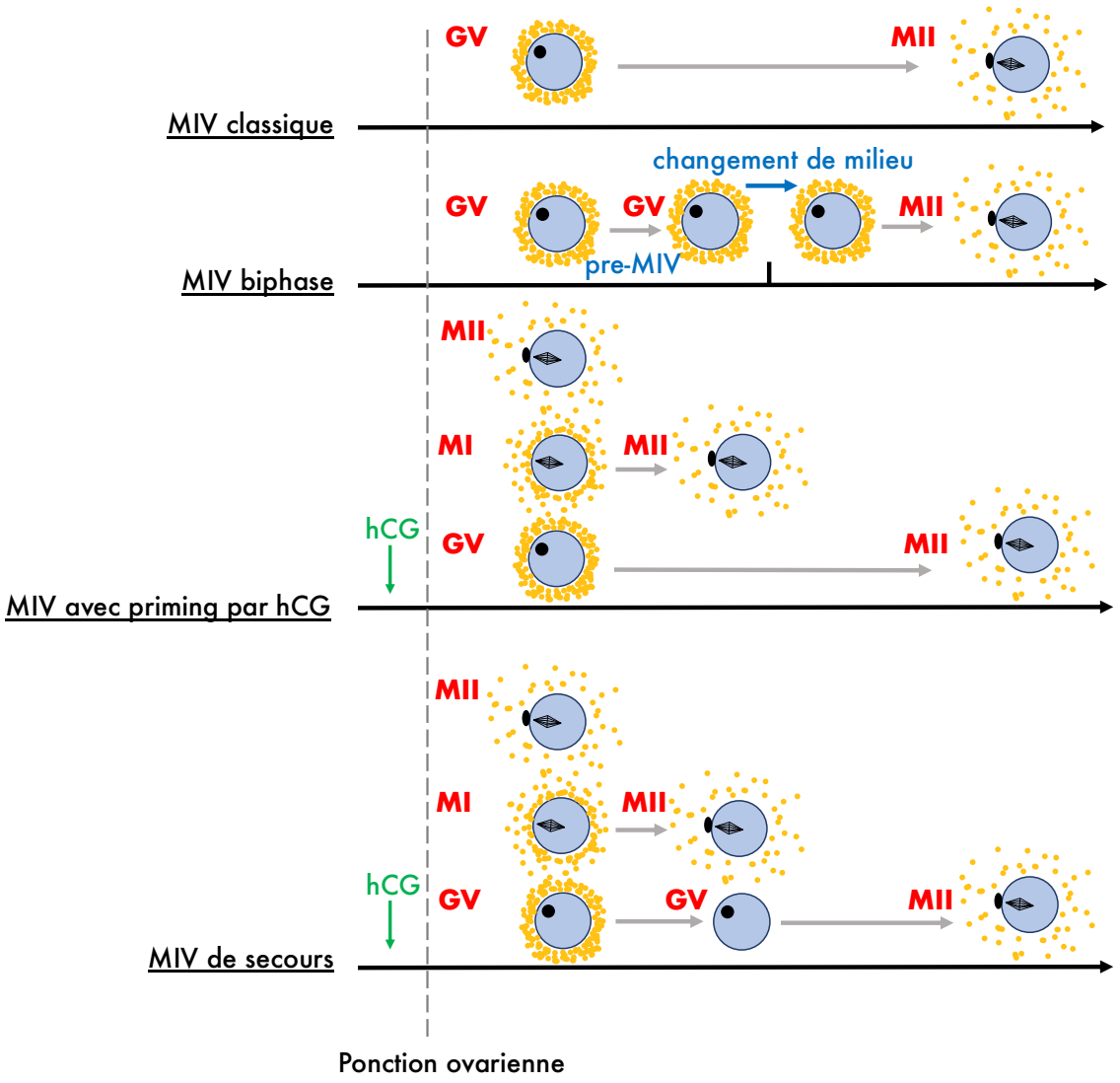

Figure 4. Maturation *in vitro* des ovocytes et ses variantes utilisées actuellement.
Dans la MIV classique, les COCs au stade GV sont maturés dans un milieu de culture *in vitro* jusqu'à atteindre le stade MII. Dans la MIV biphase, technique assez récente, les COCs sont cultivés d'abord dans un milieu inhibant la reprise de la méiose et promouvant la synchronisation entre la maturation cytoplasmique et nucléaire, avant de repasser dans un milieu classique pour terminer sa méiose et atteindre le stade MII. Dans la MIV avec « priming » par hCG (amorçage), une proportion d'ovocytes (ou tous) sont collectés à des stades immatures (GV, MI) après stimulation hormonale ou non des patients, qui seront maturés *in vitro* jusqu'au stade MII. La MIV de secours s'adresse aux patientes qui ont suivi un parcours d'ICSI avec stimulation ovarienne multifolliculaire et dont tout ou quasi-totalité des ovocytes collectés sont immatures. Les ovocytes au stade GV sont préalablement dénudés des cellules l'entourant. Inspiré de De Vos *et al*. (De Vos *et al.*, 2021).

Toutes les techniques présentées ici, si elles s'avèrent suboptimales, seraient susceptibles de fragiliser les gamètes et embryons et diminuer les chances de grossesse (Figure 5). Une augmentation des taux de réussite en AMP apparaît alors envisageable avec l'optique d'optimiser les conditions de culture et les protocoles techniques mis en place. En outre, nous

ne sommes pas totalement rassurés sur l'innocuité de toutes ces techniques. Avec prudence, on peut affirmer que les enfants conçus par AMP sont plus prédisposés à différents troubles, sans prédominance d'un en particulier, mais que cette incidence reste très modérée par rapport aux conceptions naturelles (Jouannet *et al.*, 2023). Dans les prochaines années, ces techniques sont amenées à évoluer, en lien avec la recherche sur le génome et l'épigénome des enfants ainsi conçus. Grâce à cette meilleure compréhension biologique des effets individuels de chaque technique, de meilleurs taux de succès sont envisageables.

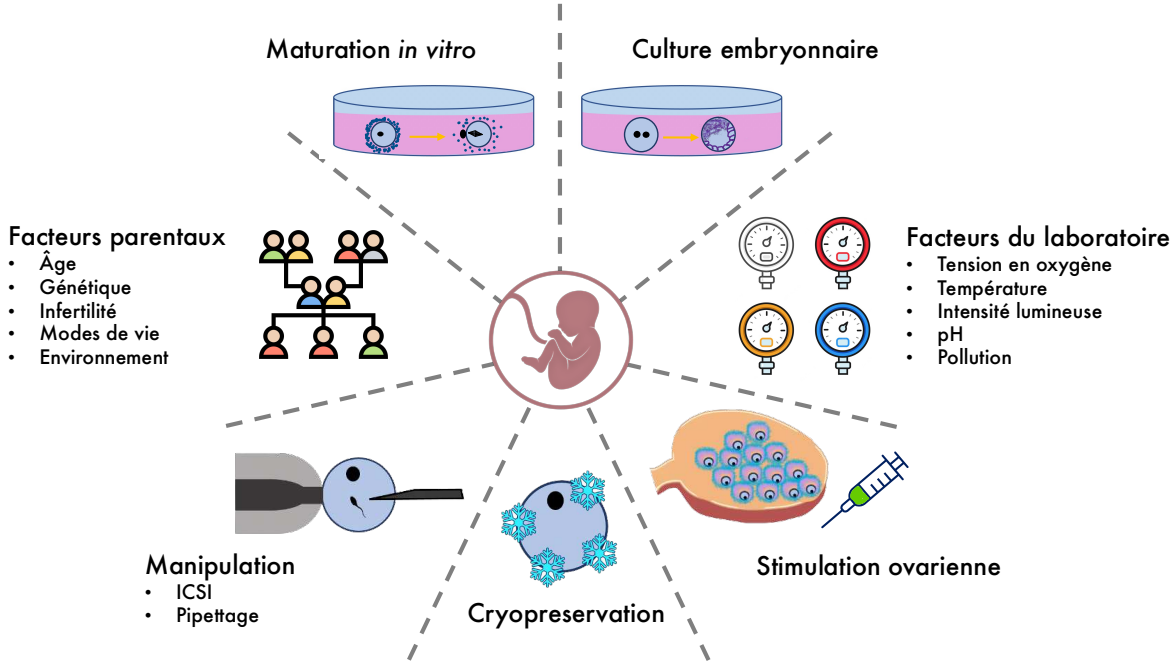

Figure 5. AMP et caractéristiques parentales : une multitude de facteurs pouvant potentiellement affecter le développement de l'embryon.

II) Régulation épigénétique et transcriptomique dans les premières étapes du développement et techniques de mesure

1) L'épigénétique

L'épigénétique est la branche de la biologie qui s'intéresse aux interactions causales entre les gènes et leurs produits aboutissant à l'avènement du phénotype comme défini pour la première fois par Conrad Waddington dans les années 1940. Le terme épigénétique qu'il accorde à cette désignation est une contraction de « épigenèse » et « génétique ». Avec le temps, la définition de l'épigénétique tend à être précisée. Pour Adrian Bird, elle correspond à « l'adaptation structurelle des régions chromosomiques de manière à enregistrer, signaler ou perpétuer des états d'activité modifiés ». Biologiquement parlant, l'épigénétique renvoie à l'étude des mécanismes modifiant l'activité des gènes, de manière réversible, n'impliquant pas de modification de la séquence ADN et qui sont transmissibles au cours des divisions cellulaires. Sommairement, les modifications épigénétiques sont provoquées par des signaux issus de l'environnement d'une cellule ou reçus de ses voisines. La conversion de ces signaux se traduit par un état de changement dans l'expression des gènes, qui peut être transitoire ou durable même en l'absence du signal.

1.1) Les marques épigénétiques

Le maintien de l'identité de chaque type cellulaire est le fruit de marques épigénétiques apposées directement sur l'ADN (Barrero *et al.*, 2010). Il existe différents mécanismes de régulation épigénétique, qui prennent place exclusivement au niveau de la chromatine en impliquant notamment des modifications biochimiques (Delcuve *et al.*, 2009). Notre ADN est enroulé autour de structures protéiques appelées histones (H2A, H2B, H3 et H4), formant les

nucléosomes (octamère d'histones, deux copies de chaque sous-unité), qui contrôlent l'état ouvert ou fermé de la chromatine, et donc l'expression des gènes. Ces histones possèdent des extrémités N-terminales qui dépassent de l'ADN et sont sujettes à des modifications post-traductionnelles de type méthylation, acétylation, phosphorylation, citrullination, ubiquitinylation, sumoylation, ribosylation, biotinylation et crotonylation qui régulent l'accessibilité de la chromatine (Millán-Zambrano *et al.*, 2022). Ces marques sont apposées par des protéines dites « writers » qui modifient chimiquement les histones, sont reconnues par des protéines « readers » qui instruisent un nouvel état chromatinien (plus ouvert ou fermé) et possiblement effacées par des protéines « erasers » qui rendent l'entièreté du processus réversible (Falkenberg & Johnstone, 2014) (Figure 6).

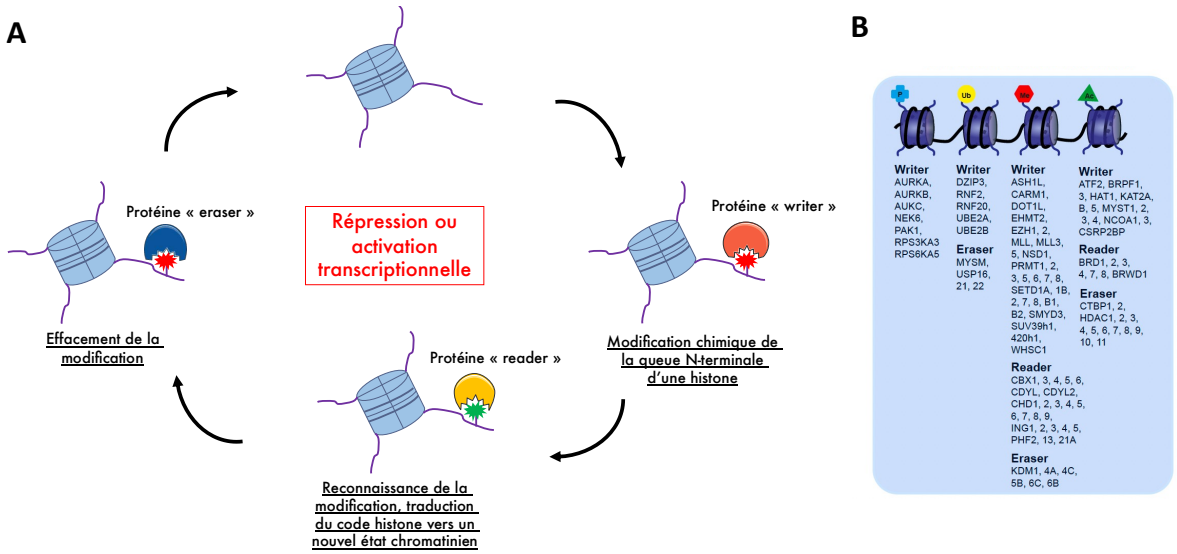

Figure 6. Les modifications post-traductionnelles des histones régulent l'état de la chromatine.
A. Dynamique de la régulation épigénétique par modification d'histones.
B. Exemples de protéines writers, readers et erasers connues en fonction de 4 grands types de modification d'histones (phosphorylation, ubiquitinylation, méthylation, acétylation).
Inspiré de Falkenberg et Johnstone (2014) (Falkenberg & Johnstone, 2014).

Une marque épigénétique bien caractérisée est l'acétylation des histones qui consiste en l'ajout d'un groupement acétyle (-COCH3) sur les lysines situées dans la queue N-terminale (Turner, 2000). Cette acétylation des lysines neutralise la charge positive de la queue N-terminale de sorte que l'interaction avec l'ADN chargé négativement est rompue. L'acétylation des lysines rend la structure de la chromatine plus lâche et donc ouverte, favorisant la fixation

des facteurs de transcription régulant la région alors ouverte. A l'inverse, la désacétylation rend la structure plus compacte et tend à réduire la transcription de la région environnante. De plus, il a été montré que les enzymes catalysant les réactions d'acétylation ou de déacétylation des histones (les acétyltransférases et déacétylases) sont recrutées spécifiquement par des facteurs de transcription de gènes cibles mais aussi par des répresseurs. Ces modifications d'histones sont un exemple parmi tant d'autres, qui représentent ensemble le code histone (Jenuwein & Allis, 2001). Le code histone associe à chaque combinaison de modifications biochimiques des histones un état chromatinien, et donc l'activation, la répression ou le silence de la transcription, mais possède également des effets biologiques sur la mitose ou la réparation de l'ADN, en fonction du contexte génomique. Une référence des modifications connues chez toutes les espèces confondues est accessible à l'adresse : https://www.cellsignal.com/learn-and-support/reference-tables/histone-modification-table.

Il existe d'autres systèmes de régulation épigénétique des gènes, impliquant les ARNs non codant (ARNnc). Les ARNnc sont issus de la transcription mais ne sont pas traduits en protéines. On en distingue deux classes suivant leur longueur : les petits ARNnc et les longs ARNnc (de composition respectivement inférieure ou supérieure à 200 nucléotides) (Wei *et al.*, 2017). Les microARNs (miARN) (18-24 nucléotides) jouent un rôle clé dans la régulation de la transcription en se liant directement à des ARNm cibles, entraînant leur dégradation ou leur inhibition (Yao *et al.*, 2019). Il y aurait environ 2300 miARN chez l'humain (Alles *et al.*, 2019). Les longs ARNnc ont eux un mécanisme d'action indirect sur l'ARNm et ciblent les activateurs et répresseurs transcriptionnels des gènes. Ce sont plus de 100 000 ARNnc longs qui sont recensés actuellement (Volders *et al.*, 2019). Il existe d'autres systèmes de régulation épigénétique des gènes, comme la méthylation de l'ADN, qui pour sa part joue un rôle fondamental dans le développement embryonnaire et fait l'objet de cette thèse (Figure 7).

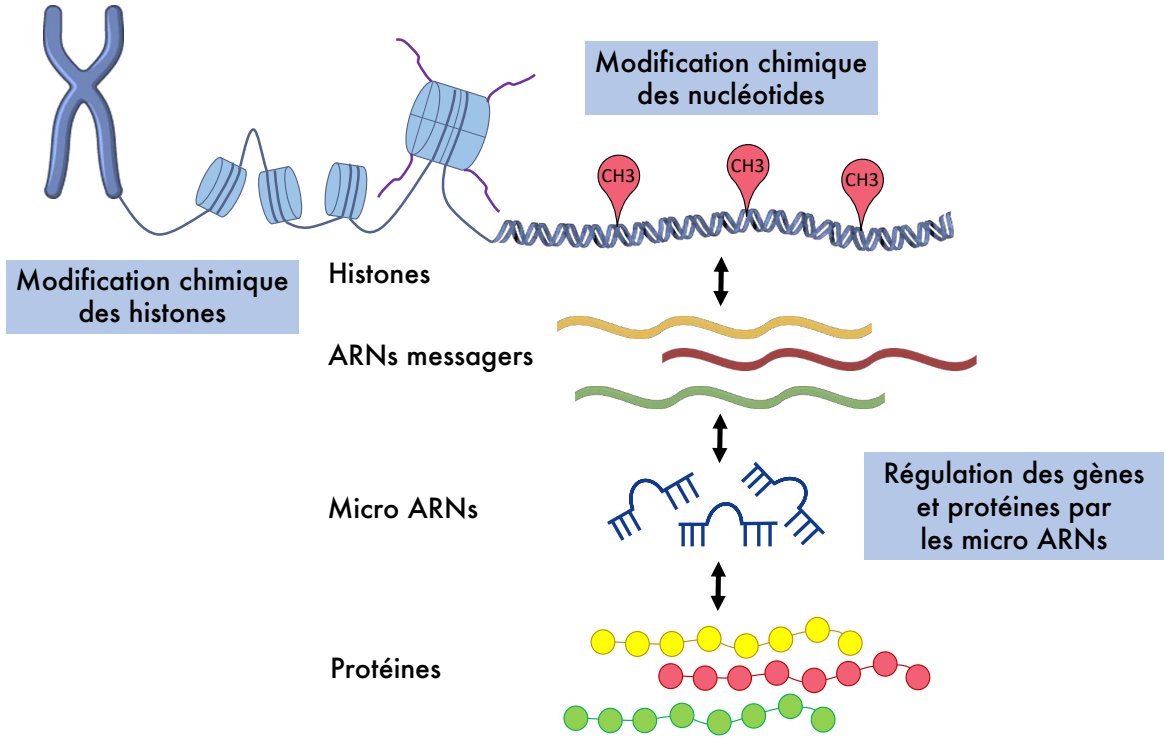

Figure 7. Différents types de modifications épigénétiques à différentes échelles génomiques. Inspiré de Barrès et Zierath (2016) (Barrès & Zierath, 2016).

1.2) La méthylation de l'ADN

La méthylation de l'ADN est une modification biochimique qui se caractérise par la présence de groupements méthyles (-CH_3) au niveau du carbone 5 des cytosines de l'ADN, principalement dans le contexte cytosine-guanine (CpG) (Greenberg & Bourc'his, 2019). Lorsque positionnée sur les régions régulatrices des gènes, de type promoteur, amplificateur ou inactiveur, la méthylation est associée à une chromatine silencieuse et une absence de transcription, jouant donc un rôle majeur dans la régulation de l'expression des gènes (Schultz *et al.*, 2015). En outre, la méthylation de l'ADN s'inscrit aussi comme un motif de recrutement de certaines protéines telles que les protéines à domaine de liaison sur l'ADN méthylé (MBD), à domaine « SET and RING associated » et Kaiso mais également d'autres facteurs de transcription (Zhu *et al.*, 2016).

Deux types d'enzymes catalysent la méthylation de l'ADN à travers le génome, les ADN méthyltransférases de maintenance (DNMT1) et les ADN méthyltransférases *de novo* (DNMT3A, DNMT3B). La première participe à la maintenance des marques de méthylation de l'ADN dans les cellules au cours de la vie d'un individu, qui subissent d'une dizaine jusqu'à une centaine de divisions cellulaires suivant le type cellulaire (à l'exception des cellules souches qui peuvent probablement se diviser davantage). Les secondes sont impliquées dans la mise en place des profils de méthylation de l'ADN lors du développement embryonnaire, qui sont globalement par la suite stables au fur et à mesure des divisions cellulaires. Par ailleurs, DNMT3L n'a pas d'activité catalytique mais elle stimule l'activité des autres methyltransférases *de novo* (Suetake *et al.*, 2004).

On recense plus de 30 millions de positions de méthylation à travers le génome humain mais leur distribution n'est pas uniforme. Les CpGs très méthylés sont principalement retrouvés dans des séquences répétées comme les éléments transposables et le corps des gènes où ils participent à la stabilité du génome (Suzuki & Bird, 2008). Les CpGs les moins méthylés sont retrouvés par cluster dans des courts motifs appelés îlots CpGs, des régions très concentrées en CpGs (Bird, 1986) (Figure 8). Il existe des exceptions à cette hypométhylation des îlots CpGs comme dans les régions soumises à empreinte qui conservent une asymétrie parentale de méthylation (partie qui sera développée plus spécifiquement dans un paragraphe suivant). On retrouve également des îlots CpGs très méthylés dans le chromosome X inactif chez la femme (mécanisme épigénétique de compensation de dose dû à la présence de deux copies du chromosome X) qui répriment l'expression de ses gènes (Hellman & Chess, 2007).

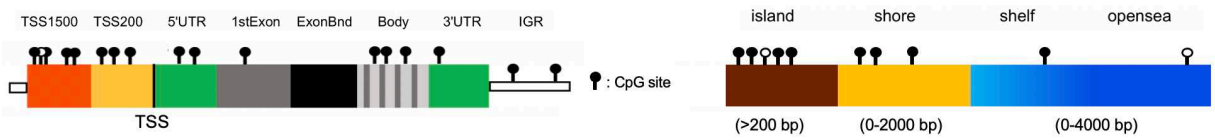

Figure 8. Répartition et organisation schématique des CpGs dans le génome.
A. Un gène peut se cartographier par plusieurs régions. Sa région promotrice se trouve en amont du site d'initiation de la transcription (TSS = transcription start site) et les nucléotides situés 1500 paires de bases (bp = base pair/paire de base) et 200 bp avant ce TSS (TSS1500 et TSS200) jouent un rôle majeur dans la régulation des gènes. Les CpGs très méthylés dans ces régions ont tendance à réprimer l'expression d'un gène, tandis que l'absence de méthylation corrèle avec leur activation. Les CpGs situés dans d'autres régions génomiques tels que les régions 5'UTR et 3'UTR (régions régulatrices non traduites), le corps du gène (région codante incluant les exons, introns et leurs frontières) et les régions intergéniques sont susceptibles d'avoir moins d'influence sur la régulation des gènes, même si cela n'est pas exclus.
B. A l'échelle du génome, les CpGs se retrouvent dans quatre grandes catégories. L'îlot CpGs (CpG island) est une courte séquence (200-3000 bp) de forte concentration en CpGs. Dans son entourage, on retrouve les rivages de l'îlot CpGs (shore) puis un peu plus loin les bords de l'îlot CpGs (shelf). Plus on s'éloigne de l'îlot CpGs, moins la concentration en CpGs est forte. Ponctuellement, on retrouve des CpGs disséminés ailleurs dans le génome dans ce qu'on appelle la pleine mer (opensea).
Issu de Ducreux *et al.* (2021) (Ducreux *et al.*, 2021).

Il existe un mécanisme biologique par lequel la méthylation est réversible, qui fonctionne via l'oxydation des cytosines méthylées (hydroxyméthylation) par les méthylcytosine dioxygénases de la famille Ten-eleven translocation (TET), ensuite reconnues par des enzymes de réparation qui les remplacent par des cytosines dépourvues de méthylation (Wu & Zhang, 2017) (Figure 9). D'autres mécanismes de déméthylation active sont connus, impliquant la désaminase induite par l'activation (AID) ou l'enzyme d'édition de l'ARNm de l'apolipoprotéine B, polypeptide catalytique 1 (APOBEC1), qui désaminent les cytosines méthylées, engendrant l'apparition d'un mésappariement thymine-guanine ensuite réparé par excision de base en intégrant une cytosine non méthylée (Hajkova *et al.*, 2010). Il est à noter qu'une déméthylation de l'ADN passive peut survenir au cours des divisions cellulaires et de la réplication de l'ADN, et surtout dans le génome maternel post-fécondation (développé dans le paragraphe suivant), via la dégradation des mécanismes de maintien de la méthylation de l'ADN (Chen & Riggs, 2011).

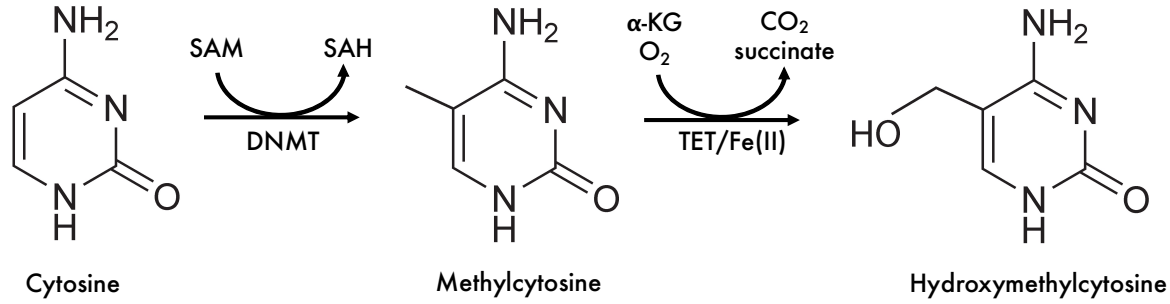

Figure 9. Mécanisme de méthylation puis d'hydroxylation des cytosines via les enzymes ADN méthyltransférases et Ten-eleven translocator (Wu & Zhang, 2014).
Alpha-KG : acide alpha-cétoglutarique. DNMT : ADN méthyltransférases. Fe : fer. SAH : S-adénosylhomocystéine. SAM : S-adénosylméthionine. TET : enzymes Ten-eleven translocation.

1.3) Dynamique des profils de méthylation depuis le développement embryonnaire jusqu'à l'âge adulte

Le développement embryonnaire précoce puis la gamétogenèse sont des fenêtres temporelles au cours desquelles une reprogrammation épigénétique intense s'établit. Chez l'Homme, la première phase prend place lors de la migration des CGPs depuis l'épiblaste embryonnaire vers les crêtes génitales avant la différenciation sexuelle qui démarre aux alentours des 3-5 premières semaines de grossesse (Fujimoto *et al.*, 1977; Molyneaux & Wylie, 2004; Richardson & Lehmann, 2010). Dès lors, ces cellules subissent une déméthylation drastique (environ 80% de méthylation à cette période) qui atteint son paroxysme à 10-11 semaines de grossesse où le niveau de méthylation globale atteint autour de 6-8% avec des différences selon le sexe (Guo *et al.*, 2015) (Figure 10). Ce seuil est le plus bas connu pour n'importe quelle cellule humaine (Guo *et al.*, 2015). Ce mécanisme de déméthylation est biphasique. D'abord, une déméthylation passive se met en place via la répression de DNMT3A et DNMT3B (Yabuta *et al.*, 2006; Kurimoto *et al.*, 2008) et du cofacteur essentiel de DNMT1, NP95 (ou UHRF1) (Kurimoto *et al.*, 2008; Seisenberger *et al.*, 2012), qui implique une maintenance altérée de la méthylation de l'ADN dans les CGPs. Certaines régions sont protégées de cette déméthylation passive, incluant les régions de contrôle de l'empreinte (ICRs : imprinting control regions), les îlots CpGs du chromosome X inactif,

certains retrovirus endogènes (Intracisternal A particles) et les promoteurs de certains gènes impliqués dans la génération des gamètes ou de la méiose (Guibert *et al.*, 2012; Seisenberger *et al.*, 2012; Hackett *et al.*, 2013; Kawasaki *et al.*, 2014; Messerschmidt *et al.*, 2014). DNMT1, malgré l'absence de son cofacteur NP95, permettrait le maintien de la méthylation dans ces régions durant cette période d'effacement global de la méthylation (Hargan-Calvopina *et al.*, 2016). Toutefois les enzymes TET1, TET2 et possiblement AID et APOBEC1 procéderont à la déméthylation active complète de ces régions environ trois jours après la phase de déméthylation passive (Popp *et al.*, 2010; Ohno *et al.*, 2013; Yamaguchi *et al.*, 2013; Kawasaki *et al.*, 2014).

Après la détermination du sexe de l'embryon, les CGPs acquièrent *de novo* la méthylation de l'ADN mais avec des différences de chronologie selon le sexe. Rapidement, le génome spermatique est reméthylé à hauteur de 75% (Hanna *et al.*, 2018). En revanche, le génome ovocytaire n'est reméthylé qu'à 54% et seulement après la puberté, durant la croissance folliculaire d'un pool de follicules engagés dans la croissance basale lors d'un cycle ovarien (Hanna *et al.*, 2018). Les mécanismes impliqués dans cette phase de re-méthylation impliquent les enzymes DNMT3A et DNMT3L, catalyseur de la méthylation *de novo* mais pas DNMT3B (Bourc'his *et al.*, 2001; Kaneda *et al.*, 2004; Shirane *et al.*, 2013).

Une deuxième phase de la reprogrammation épigénétique s'opère post-fécondation accompagnant l'activation du génome embryonnaire, passant d'un contrôle maternel à un contrôle embryonnaire (Surani, 2001). L'ADN haploïde maternel et paternel subissent ici encore des évènements de méthylation différents en raison de leur état chromatinien divergent (l'ADN paternel et maternel forment deux pronoyaux distincts) (Wang *et al.*, 2014). Le génome paternel est notamment déméthylé de manière active très rapidement grâce à l'action de l'enzyme TET3 qui va former des intermédiaires de déméthylation de l'ADN comme la 5-hydroxyméthylcytosine mais aussi la 5-formylcytosine et la 5-carboxylcytosine (Howell *et al.*, 2001; Gu *et al.*, 2011; Inoue & Zhang, 2011; Iqbal *et al.*, 2011; Guo *et al.*, 2014; Tsukada *et al.*, 2015). Ainsi, la méthylation du génome paternel passe de 75% à 50% environ, dans les

premières heures suivant la fécondation (Zhu *et al.*, 2018). Dans cette même fenêtre temporelle, le pronucleus femelle subit une faible déméthylation active par TET3, atteignant les 50% de méthylation globale également. Il s'en suit une période de déméthylation passive progressive du génome maternel qui accompagne le développement de l'embryon depuis le stade zygote (une cellule) jusqu'au stade blastocyste (environ 20% de méthylation globale) (Zhu *et al.*, 2018). Cette déméthylation passive serait liée à une déficience des mécanismes de maintien de la méthylation puisque DNMT1 apparaît comme exclusivement localisée dans le cytoplasme, laissant le génome maternel subir une dilution passive de sa méthylation au cours du clivage de l'embryon (Rougier *et al.*, 1998; Guo *et al.*, 2014). La méthylation résiduelle observée à ce stade correspond aux éléments transposables et régions soumises à empreinte, que nous détaillerons par la suite (Okae *et al.*, 2014). Ce maintien de méthylation implique la présence de mécanismes de protection contre la déméthylation, comme STELLA (autres alias connus PGC7 et DPPA3) qui inhibe l'action de TET3 ou encore le complexe ZFP57/TRIM28 qui permet de recruter DNMT1 qui ne serait pas totalement exclue du noyau (Hirasawa *et al.*, 2008; Quenneville *et al.*, 2011; Li *et al.*, 2018). A ce stade, le blastocyste est dans un état de pluripotence naïve, c'est-à-dire que les cellules ont la capacité de se différencier en n'importe quel type cellulaire.

Une fois l'embryon implanté dans la paroi utérine, une re-méthylation *de novo* s'installe à hauteur de 70-80% (Smith *et al.*, 2012; Guo *et al.*, 2014). L'embryon commence à se différencier, via les premières lignées cellulaires embryonnaires, le trophectoderme et la masse cellulaire interne, impliquant des différences d'acquisition de la méthylation suivant ces tissus. Cette apposition des marques de méthylation est médiée par les méthyltransférases DNMT3A et DNMT3B et ce profil sera globalement stable au cours de la vie dans les cellules somatiques de l'individu nouvellement formé (Okano *et al.*, 1999; Chen *et al.*, 2003).

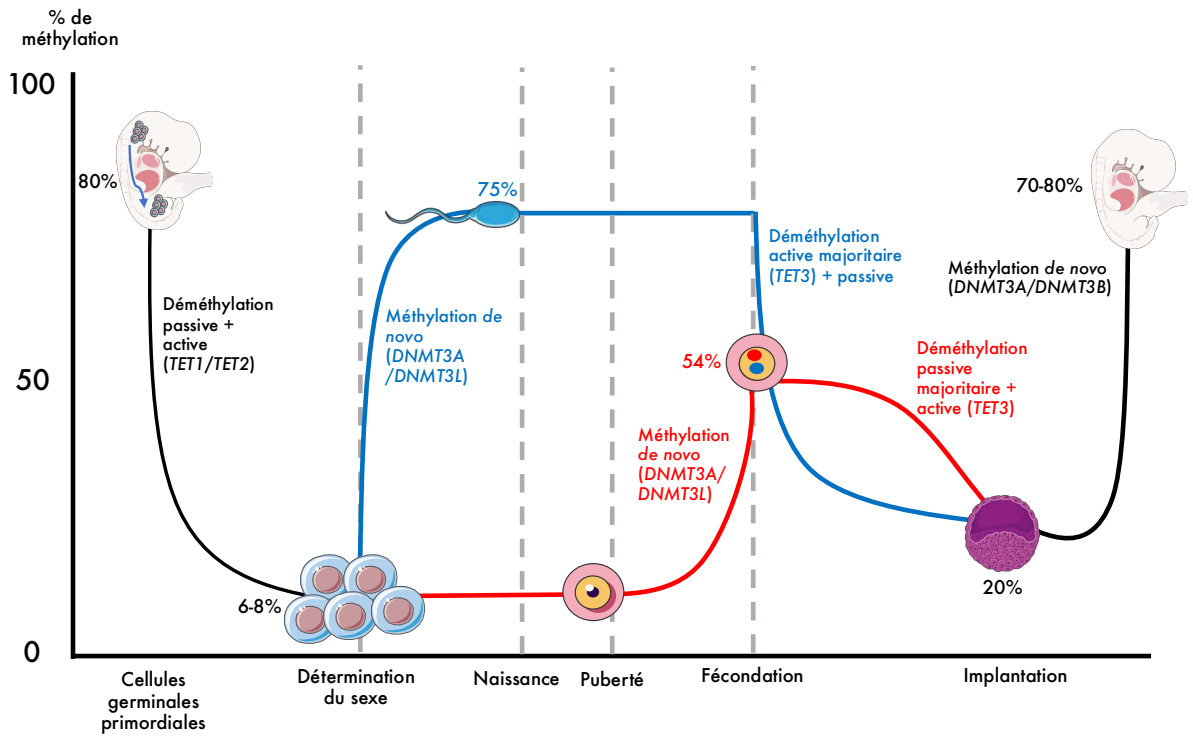

Figure 10. Acquisition des profils de méthylation de l'ADN depuis les cellules germinales primordiales jusqu'au développement embryonnaire.
Deux phases de reprogrammation épigénétique de déméthylation suivie de reméthylation ont lieu dans les cellules germinales primordiales puis après la fécondation des gamètes.

La compréhension du mécanisme de reprogrammation épigénétique a mis en évidence que certains gènes du génome sont « protégés » de la reprogrammation épigénétique (déméthylation et reméthylation) ; ils sont dits soumis à empreinte parentale. Ces gènes sont souvent retrouvés par clusters régulés par des régions régulatrices de contrôle de l'empreinte riches en CpGs, les DMRs primaires et secondaires (DMR : differentially methylated region). Les DMRs primaires qui correspondent à certaines ICRs, qui comme détaillé en amont, sont d'abord déméthylées activement dans les CGPs, reméthylées dans l'ovocyte et le spermatozoïde puis résistent à la déméthylation après fécondation. Les DMRs secondaires sont établies dans les cellules somatiques lors de la reméthylation qui survient post-fécondation sous le contrôle des DMRs primaires via des mécanismes encore peu connus (Sato *et al.*, 2011; Adalsteinsson & Ferguson-Smith, 2014). Ainsi, ces régions conservent une asymétrie de méthylation entre le chromosome paternel et maternel, issue de l'effacement puis l'apposition différentielle des marques épigénétiques lors de la gamétogenèse selon le

sexe (Reik & Walter, 2001). Cela conduit à une expression parentale différentielle des gènes contrôlés par ces régions.

Dans le cas présent, on observe que la majorité des gènes soumis à empreinte (GSE) sont exprimés soit totalement par le chromosome paternel soit totalement par le chromosome maternel, c'est-à-dire qu'un gène est contrôlé par une région totalement méthylée pour l'un des chromosomes, et totalement déméthylée pour l'autre (voir exemple Figure 11). Il existe différents types de régulation par les régions de contrôle de l'empreinte, selon qu'elles se trouvent dans une région promotrice d'un gène, ou dans des séquences inter- ou intragéniques en impliquant l'intervention d'amplificateur ou de répresseur par exemple (Figure 11) (Zwart *et al.*, 2001; Lopes *et al.*, 2003; Schoenherr *et al.*, 2003; Delaval & Feil, 2004). On dénombre 129 GSE connus chez l'humain à la date d'écriture de cette thèse d'après la base de données Geneimprint (https://www.geneimprint.com/site/genes-by-species).

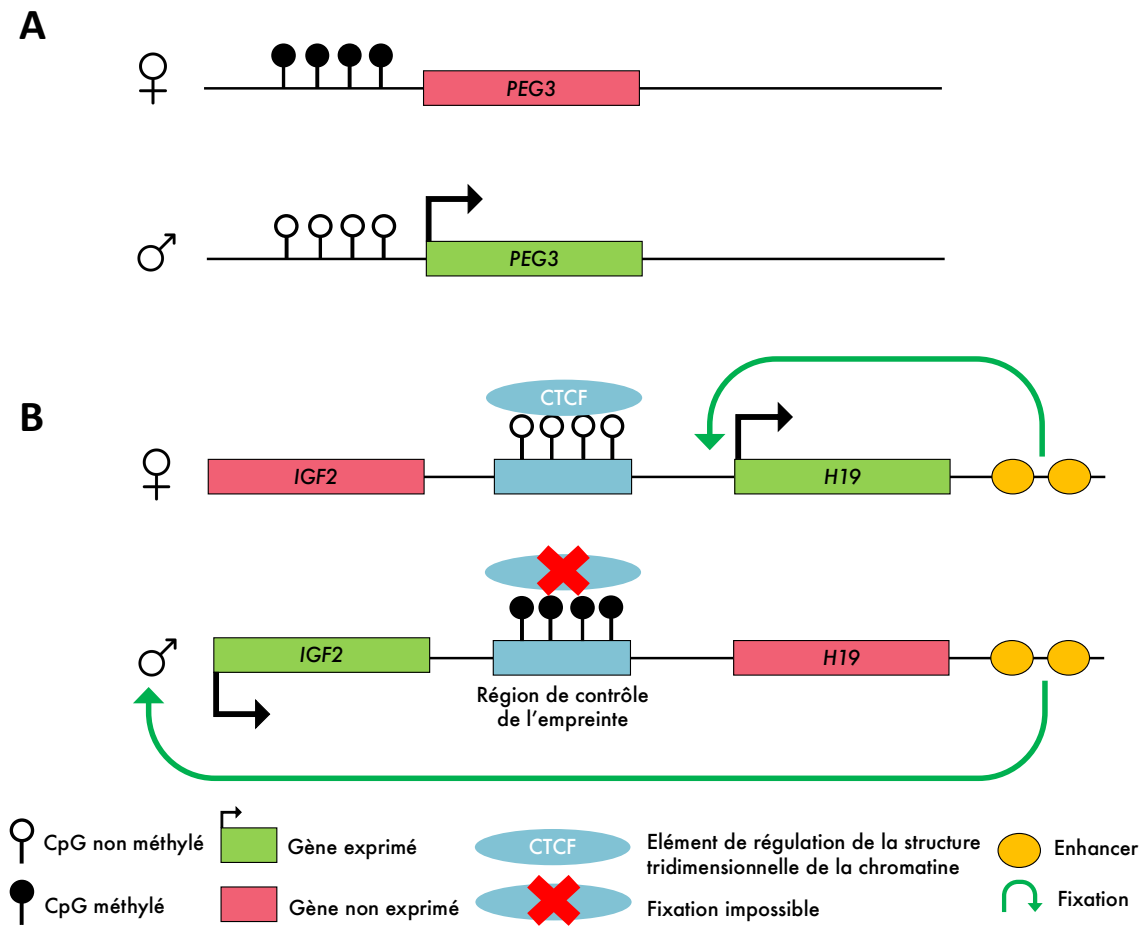

Figure 11. Deux exemples de régulation en *cis* et en *trans* de l'expression de gène soumis à empreinte.
A. La région promotrice de *PEG3* est totalement déméthylée sur l'allèle paternel, facilitant l'expression de ce gène. Sur l'allèle maternel, la région promotrice est totalement méthylée, rendant l'expression de ce gène nulle.
B. Une région de contrôle de l'empreinte se situe entre le gène *IGF2* et le gène *H19*. Sur l'allèle maternel, cette région est totalement déméthylée, rendant la fixation du facteur de transcription CTCF (régulateur de la structure tridimensionnelle de la chromatine) possible sur le motif CCCTC de la région. Les enhancers sont alors capables de se fixer sur la région promotrice de *H19* uniquement, impliquant l'expression de *H19* et la répression de *IGF2*. A l'inverse sur l'allèle paternel, le CTCF n'est pas capable de se fixer sur la région de contrôle de l'empreinte qui est totalement méthylée. La conformation de la chromatine dans cette région fait que les enhancers situés après *H19* sont uniquement capables de se fixer dans la région promotrice de *IGF2* et ainsi activer son expression. Toutefois, *IGF2* ne semble pas soumis à empreinte dans le cerveau.

Les gènes soumis à empreinte occupent une place de choix dans l'étude des effets épigénétiques et transcriptomiques en lien avec les techniques d'AMP. Leurs caractéristiques de régulation impliquant l'apposition des marques de méthylation lors de la gamétogenèse et leur protection vis-à-vis de la reprogrammation épigénétique de l'embryon sont susceptibles d'être perturbées par les nombreuses manipulations réalisées lors d'un protocole d'AMP qui surviennent dans la même fenêtre temporelle. De plus, l'haploïdie des GSE est fondamentale

au bon développement de l'embryon car de nombreux cas de perte d'expression (aucun allèle exprimé) ou d'expression bi-allélique sont associés à des syndromes chez l'humain et semblent favoriser l'émergence de certains troubles de la santé (Table 1). Par ailleurs, l'expression monoallélique de certains GSE est requise sans quoi des malformations fœtales et placentaires léthales pourraient survenir comme rapportés dans le modèle souris (Moore *et al.*, 2015) (Table 2). Toutefois, dans certains types cellulaires, on retrouve une expression biallélique de certains GSE, comme pour *IGF2* dans le cerveau (Pham *et al.*, 1998) et d'autres gènes ont une empreinte spécifique à certains types cellulaires comme *GNAS*, *KCNQ1* et *UBE3A* (Varrault *et al.*, 2020).

Troubles	Locus (gènes/régions supposément impliqués)
Syndromes	
Syndrome de Beckwith-Wiedemann	11p.15.5 (*IGF2*, *H19*, *KCNQ1OT1*, *CDKN1C*)
Syndrome de Silver-Russell	7q32 (*PEG1*/*MEST*), 7p12 (*GRB10*), 11p15.5 (*IGF2*, *H19*)
Syndrome de Prader-Willi	15q11.2-q13 (*SNRPN*, *MAGEL2*, *NDN*, *MKRN3*)
Syndrome d'Angelman	15q11.2-q13 (*UBE3A*, *ATP10C*)
Pseudohypoparathyroïdisme	20q13 (*GNAS*)
Diabète néonatal transitoire	6q24 (*PLAGL1*, *HYMAI*)
Syndrome de Temple	14q32 (*MEG3*)
Syndrome de Kagami-Ogata	14q32 (IG-DMR, *MEG3*)
Autres troubles	
Neuroblastome	14q32.2 (*DLK1-MEG3*)
Leucémie myéloblastique aiguë	20q11.2 (*NNAT*)
Léiomyome utérin	7q32 (*PEG1*/*MEST*)
Cancer de la prostate	Dérégulation d'un réseau de gènes soumis à empreinte
Carcinome colorectal	11p15.5 (*H19*, *IGF2* DMR0)
Cancer du sein	7q32 (*PEG1*/*MEST*)
Cancer de l'ovaire	11p15.5 (*H19*/*IGF2*), 19q13.4 (*PEG3*)
Diabète	14q32.2 (*DLK1-MEG3*)
Développement neurocomportemental	Dérégulation d'un réseau de gènes soumis à empreinte
Obésité	11p15.5 (*H19*/*IGF2*)
Échec et complications de la grossesse	11p15.5 (*IGF2*, *CDKN1C*, *PHLDA2*), 7q21 (*PEG10*)

Table 1. Synthèse des troubles de la santé liés à l'empreinte parentale.
Issu de Argyraki *et al.* (2019) et Wallace et Bean (2017) (Wallace & Bean, 2017; Argyraki *et al.*, 2019).

Locus	Gène	Origine	Description/rôle	Phénotypes après knockout chez la souris
6q24	*PLAGL1*	Paternel	Protéine à doigt de zinc	Retard de croissance fœtale, malformation osseuse, létalité néonatale élevée
6q25	*IGF2R*	Maternel	Clairance d'IGF2	Surcroissance fœtale et placentaire, anomalies des organes et squelettique
7p12	*GRB10*	Maternel/Paternel	Protéine liée au récepteur GF	Surcroissance fœtale et placentaire
7q21.3	*PEG10*	Paternel	Dérivé d'un rétrotransposon	Létalité embryonnaire due à une malformation placentaire
7q32.2	*MEST*	Paternel	α/β hydrolase	Retard de croissance fœtale et placentaire, létalité postnatale élevée, comportement maternel anormal
11p15	*H19*	Maternel	ARN non-codant long	Surcroissance fœtale et placentaire
11p16	*IGF2*	Paternel	Facteur de croissance	Retard de croissance fœtale et placentaire
11p17	*CDKN1C*	Maternel	Suppresseur de tumeur	Surcroissance fœtale et placentaire gestationnelle
11p19	*PHLDA2*	Maternel	Domaine d'homologie de la pleckstrine	Surcroissance placentaire
14q32	*DLK1*	Paternel	Glycoprotéine transmembranaire	Retard de croissance pré- et postnatal, létalité périnatale élevée, obésité postnatale
14q33	*MEG3*	Maternel	ARN non-codant	Létalité postnatale, retard de croissance pré- et postnatale
19q13.4	*PEG3*	Paternel	Protéine à doigt de zinc	Retard de croissance placentaire et fœtale, comportement maternel anormal

Table 2. Gènes soumis à empreinte très exprimés dans le placenta humain connus pour entraîner des phénotypes avec anomalies placentaires de croissance, voire létaux, lorsque leur expression est altérée chez le modèle murin.
Travaux synthétisés dans l'article de Moore *et al.* (2015) (Moore *et al.*, 2015).

1.4) Techniques de mesure de méthylation à l'échelle du génome-entier

Il existe de nos jours beaucoup de méthodes permettant de mesurer la méthylation, à l'échelle d'un CpG unique, d'une région (quelques CpGs consécutifs), d'un gène, d'éléments génomiques et également à l'échelle du génome entier (Figure 12). Le choix de la méthode à appliquer dépend de la résolution et de la couverture de l'étude (changements globaux ou régionaux de méthylation de l'ADN), du coût, de la quantité d'ADN disponible, de la sensitivité et la spécificité requise pour l'étude ou encore de la disponibilité d'infrastructures pour l'analyse bioinformatique. Nous détaillons ici quelques méthodes couramment utilisées pour l'évaluation de la méthylation sur l'ensemble du génome.

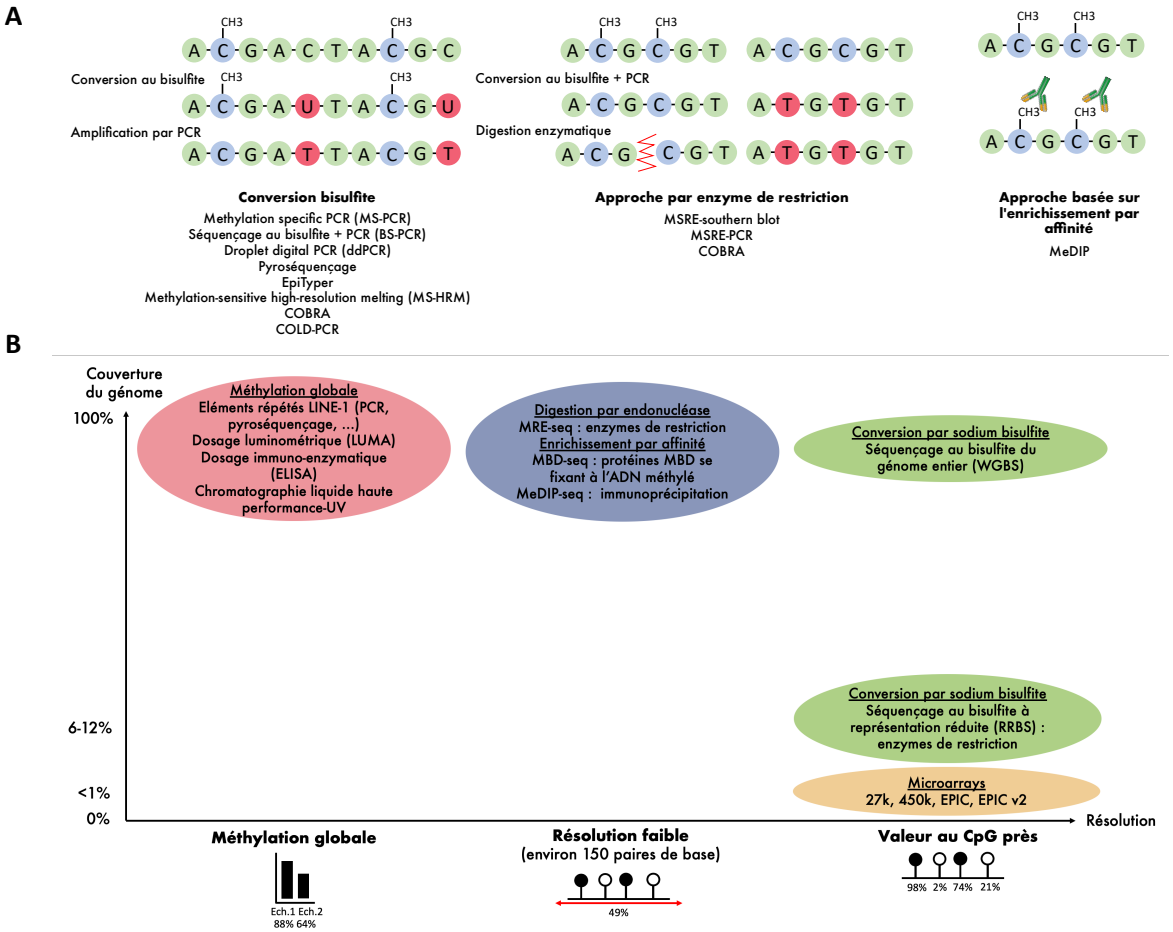

Figure 12. Principales techniques de mesure de méthylation.
A. Techniques utilisées pour mesurer la méthylation de gènes/régions cibles.
B. Techniques utilisées pour mesurer la méthylation à l'échelle du génome entier.

Méthylation globale

Les retrotransposons LINE1 sont des séquences répétées qui représentent environ 17% du génome (Cordaux & Batzer, 2009). Ainsi, mesurer leur méthylation constitue un bon indicateur pour inférer la méthylation globale d'un génome (Yang *et al.*, 2004). Cette mesure s'effectue préférentiellement selon la technique du pyroséquençage. Ses avantages se résument à son faible coût par échantillon, et sa fiabilité à indiquer les niveaux globaux de méthylation. On notera également sa facilité de mise en œuvre et sa rapidité.

Un dosage enzymatique reposant sur la technique ELISA (anticorps ciblant les 5-méthylcytosines (5mC) couplé à une détection colorimétrique) est également utilisé pour mesurer la méthylation globale d'un génome (Kurdyukov & Bullock, 2016). Ses avantages incluent sa facilité et rapidité de mise en œuvre et l'existence de nombreux kits nécessitant peu d'ADN pour mesurer la méthylation.

Le luminometric methylation assay (LUMA) repose sur la comparaison de l'efficacité de coupure de l'ADN par les enzymes de restriction MspI et HpaII qui clivent le site de restriction C^CGG (Karimi *et al.*, 2006). En effet, MspI clive le site indépendamment de l'état de méthylation du CpG alors que HpaII le clive si le CpG n'est pas méthylé, permettant d'évaluer par pyroséquençage la méthylation globale d'un échantillon par le ratio de l'intensité des signaux générés par l'ADN digéré par les deux enzymes. Ses avantages incluent sa rapidité de mise en œuvre, sa faible quantité d'ADN nécessaire et la présence d'un contrôle interne tenant compte de la quantité d'ADN présente dans les deux digestions parallèles. Ses inconvénients correspondent au fait que l'ADN doit être d'excellente qualité pour que la digestion soit optimale, et qu'elle ne cible que les sites CCGG qui est une valeur biaisée de la méthylation globale d'un génome. Elle possède également moins de spécificité et sensitivité que des techniques équivalentes (Kurdyukov & Bullock, 2016).

La chromatographie liquide haute performance (HPLC) repose sur le principe de l'hydrolysation de l'ADN en ses bases nucléotidiques 5mC et désoxycytidine, puis séparation

de ces produits par chromatographie (Kuo *et al.*, 1980). Le rapport entre les quantifications de 5mC et désoxycytidine indique alors le niveau de méthylation globale de l'échantillon. La HPLC est un « gold standard » de mesure globale de la méthylation en raison de sa précision. L'intérêt pour cette méthode reste toutefois très limité en raison de l'équipement nécessaire et de la quantité d'ADN très élevée requise.

Toutes ces techniques mesurant la méthylation globale peuvent être finalisées avec des tests statistiques simples (t-test, ANOVA, …) pour comparer plusieurs échantillons et ne sont donc pas coûteuses en analyse bioinformatique. Leurs applications préférentielles incluent la corrélation entre niveau de méthylation et le mode de vie, le vieillissement, le régime alimentaire, et la détection de méthylation aberrante dans différents types de tumeurs qui est un marqueur d'initiation et de progression d'un cancer. L'inconvénient majeur de ces techniques réside toutefois dans le fait qu'elles n'indiquent qu'une mesure globale de méthylation par échantillon, ne permettant pas de trouver des liens fonctionnels pouvant expliquer une différence de méthylation.

Digestion par endonucléase

La technique de MRE-seq (Methylation sensitive Restriction Enzyme sequencing, également connue sous le nom de Methyl-seq) repose sur des enzymes de restriction sensibles à la méthylation qui ne sont pas capables de couper les résidus de cytosine méthylés, laissant ainsi l'ADN méthylé non clivé (Maunakea *et al.*, 2010). Le MRE-seq consiste ainsi à séquencer des fragments de 100-300 pb issus de digestions parallèles de l'ADN par différentes enzymes sensibles à la méthylation dans des contextes CpG différents, comme HapII, Hin6I et AciI. L'identification des sites de coupure par séquençage fournit des informations sur l'état de méthylation des CpGs. L'avantage du MRE-seq est qu'elle mesure la méthylation de l'ADN à la résolution d'un CpG unique, avec une bonne répartition dans tout le génome, pour un coût compétitif. Son inconvénient est qu'elle dépend des propriétés des enzymes de restriction, et offre une couverture assez limitée de tous les CpGs du génome (Saini *et al.*, 2023). De plus,

une digestion incomplète par les enzymes augmente significativement les faux positifs (Li & Tollefsbol, 2021).

Enrichissement par affinité

La technique de MBD-seq repose sur la capture de l'ADN, préalablement fragmenté par sonication, par des protéines à domaine de liaison méthyl-CpG (MBD : methyl-binding domain) couplée à des billes pour capturer l'ADN méthylé (Lan *et al.*, 2011). L'ADN est ensuite lavé et élué avec des concentrations croissantes de sel, les fractions à faible teneur en sel contenant des fragments à faible densité de CpG, tandis que les fractions à teneur élevée en sel contiennent une forte densité d'ADN méthylé. Les fragments récupérés sont ensuite séquencés sur une plateforme à haut débit et nécessitent des infrastructures bioinformatiques pour analyser les données de séquençage. Ses avantages incluent sa couverture assez complète du génome. Il y a cependant quelques inconvénients notables, comme sa résolution faible (mesure de méthylation par région de 150pb et non au CpG unique), sa faible couverture des régions peu méthylées comme les îlots CpGs (la sélection basée sur l'affinité est généralement biaisée en faveur des régions hyperméthylées), et son incapacité à distinguer la méthylation 5mC de l'hydroxyméthylation 5hmC (Li & Tollefsbol, 2021). Ces limites sont cependant compensées par son coût intéressant.

Le MeDIP-seq (Methylated DNA ImmunoPrecipitation sequencing) est souvent comparé au MBD-seq étant donné leurs similarités en termes de principe technique, d'avantages et d'inconvénients. Cette technique consiste à isoler des fragments d'ADN méthylés (150-200bp) à l'aide d'un anticorps dirigé contre la 5mC (immunoprécipitation) puis de leur séquençage à haut débit (Weber *et al.*, 2005). Les inconvénients liés au MeDIP-seq sont sa résolution faible, et son biais en faveur des régions hyperméthylées, même si elle couvre mieux les régions avec une faible densité de CpGs que le MRE-seq. Son coût reste avantageux et elle peut donc être favorisée pour des études souhaitant réaliser une cartographie globale d'un méthylome et non destinées à la recherche de biomarqueurs précis tels que des CpGs uniques. De plus

son application ne se limite pas à la méthylation des CpGs mais la méthylation des cytosines dans tous les contextes nucléotidiques de l'ADN (Li & Tollefsbol, 2021).

Séquençage après conversion par sodium bisulfite

Le Reduced Representation Bisulfite Sequencing (RRBS) est une technique de séquençage réduite ciblant des régions génomiques sélectionnées via des enzymes de restriction (Meissner *et al.*, 2005). L'ADN est d'abord digéré à l'aide d'enzymes de restriction insensibles à la méthylation (comme MspI) générant des fragments contenant des CpGs à leurs extrémités. Les fragments sont sélectionnés en fonction de leur taille (40-220pb) pour conserver des régions riches en CpGs suffisamment petites pour être séquencées. Les fragments sont ensuite convertis par sodium bisulfite, transformant sélectivement les cytosines non méthylées en uraciles par désamination, tout en laissant les cytosines méthylées inchangées (5mC et 5hmC). Les fragments sont amplifiés par PCR puis séquencés sur une technologie à haut débit. Ses avantages incluent le fait de ne pas réaliser un séquençage complet (très coûteux à l'heure actuelle, environ 1-3% du génome) avec une profondeur de séquençage excellente tout en ciblant des régions génomiques d'intérêt (Beck *et al.*, 2022). Cette technique offre de plus des résultats hautement reproductibles, même à partir de faibles quantités d'ADN ou dégradé (fort intérêt pour des tissus précieux). La démocratisation de la bioinformatique rend cette technique de plus en plus accessible, avec des pipelines d'analyse de moins en moins coûteux en temps. Les régions pauvres en CpGs sont toutefois difficilement couvertes, ce qui peut refreiner son utilisation pour certaines recherches (régions soumises à empreinte parentale notamment).

Enfin il est possible d'établir l'entièreté du profil de méthylation d'une cellule ou d'un tissu. Via la technique de Whole Genome Bisulfite Sequencing (WGBS), chaque CpG du génome peut être évalué, ce qui constitue la meilleure cartographie possible de la méthylation d'un ADN (Frommer *et al.*, 1992). L'ADN est simplement converti par sodium bisulfite, amplifié puis séquencé sur une plateforme à haut débit. Il existe des recommandations des paramètres de

séquençage, comme de réaliser un séquençage paired-end (fragment d'ADN séquencé à partir de ses deux extrémités) pour augmenter le taux d'alignement, avec une profondeur d'au moins 30X (nombre de lectures uniques qui incluent un nucléotide donné) (Rivera & Ren, 2013). Cependant, le WGBS reste peu utilisé en raison de son coût, même s'il est incontournable si l'on veut étudier de façon précise des régions à faible densité en CpGs, non couvertes via le RRBS.

Microarrays (puces à ADN)

Les techniques fréquemment utilisées afin d'avoir une couverture satisfaisante du génome avec des coûts qui restent raisonnables par échantillon sont les puces à méthylation de l'ADN. Cette technologie est notamment développée par Illumina qui en a développé 4 modèles. Le premier couvrait 1536 CpGs répartis dans 371 gènes essentiellement connus pour être impliqués dans différents cancers (GoldenGate Assay, Illumina). Par la suite, les puces se sont étendues à toutes les régions du génome, couvrant respectivement plus de 27,000 (27k, Illumina), 450,000 (450k, Illumina) et 850,000 (EPIC, Illumina) positions de méthylation au fur et à mesure des générations. La puce EPIC a d'ailleurs récemment été élargie à plus de 935,000 positions sur sa version 2.

Prenons l'exemple du fonctionnement de la puce EPIC que j'ai eu l'occasion de traiter lors de mes travaux de thèse. Après une extraction d'ADN des échantillons à étudier, celui-ci est traité au bisulfite de sodium, puis par amplification par PCR, les cytosines méthylées converties en uracile sont transformées en thymines. Cet ADN amplifié est disposé sur la puce EPIC, où se trouvent des millions de sondes d'hybridation de 50 nucléotides correspondant aux milliers de loci ciblés. Il existe deux types de sondes avec chacune leurs propriétés. Les sondes de type I fonctionnent par paire : l'une mesure l'état méthylé et l'autre l'état non méthylé (Figure 13). Si le locus est méthylé, la cytosine a été conservée dans le fragment d'ADN et s'hybride avec la sonde mesurant l'état méthylé. Lors de l'élongation des sondes, un nucléotide possédant un fluorochrome peut donc être ajouté, libérant un signal lumineux. Pour ce même locus

méthylé, il n'y a pas d'hybridation avec la sonde mesurant l'état non méthylé et donc pas de fluorescence dégagée.

Similairement, si le locus n'est pas méthylé, la cytosine du motif CpG a été convertie en thymine via traitement au bisulfite de sodium. Ainsi ce locus ne s'hybride pas sur la sonde mesurant l'état méthylé et ne dégage pas de fluorescence. En revanche, sur la sonde mesurant l'état non méthylé, le fragment d'ADN amplifié s'hybride et par élongation, un nucléotide sera ajouté, émanant un fluorochrome de la même lumière que celui dégagé pour le locus méthylé. Ainsi, le niveau de méthylation d'un locus peut s'établir par le rapport fluorescence de la sonde méthylée divisé par la somme des fluorescences de toutes les sondes. Ce type de sondes a été utilisé pour la conception de la puce 27k mais est retrouvé sur l'ensemble des autres puces des générations suivantes, permettant donc la comparaison et la reproductibilité d'études ayant utilisé cette technologie.

Les sondes de type II possèdent un fonctionnement plus direct. La sonde s'hybride avec la guanine du motif CpG du fragment d'ADN. Lors de l'élongation, deux cas de figure peuvent se produire. Si le locus est méthylé, alors le nucléotide suivant est une cytosine, et par élongation et complémentarité des bases, une adénine sera ajoutée à la sonde, libérant un fluorochrome rouge. Si le locus est déméthylé, c'est une thymine qui se trouve sur le brin d'ADN, et donc par élongation et complémentarité des bases, une guanine est ajoutée à la sonde, libérant un fluorochrome vert. La mesure de la méthylation d'un locus se fait donc simplement par le rapport entre l'intensité lumineuse verte et la somme des intensités lumineuses. Ce type de sonde permet un gain de place, divisant par deux le nombre de sondes par rapport aux sondes de type I.

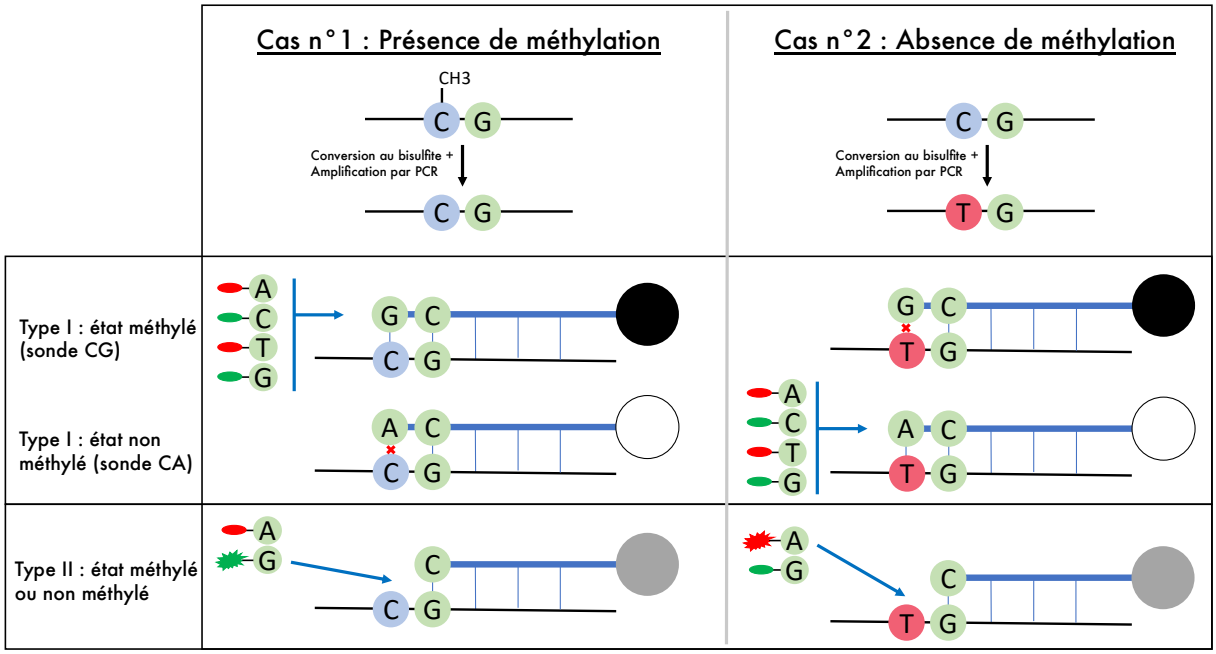

Figure 13. Fonctionnement des différents types de sondes retrouvées sur les puces de type Beadchip de chez Illumina.
Les sondes de type I fonctionnent par paire de sondes mesurent l'état méthylé et l'état non méthylé. En présence de méthylation (Cas n°1), la sonde mesurant l'état méthylé s'hybride complètement avec le fragment d'ADN au niveau du locus CpG, permettant l'élongation de la sonde et la libération d'un fluorochrome. La sonde mesurant l'état non méthylé ne s'hybride pas avec le fragment d'ADN au niveau du locus CpG, ne libérant pas de signal lumineux. L'inverse se produit lors de l'absence de méthylation (Cas n°2).
Les sondes de type II s'hybrident directement au niveau de la guanine du motif CpG. Si le fragment d'ADN était initialement méthylé (Cas n°1), un fluorochrome vert associé à la guanine est ajouté lors de l'élongation de la sonde par complémentarité avec la cytosine. Si le fragment d'ADN n'était initialement pas méthylé (Cas n°2), un fluorochrome rouge associé à l'adénosine est ajouté lors de l'élongation de la sonde par complémentarité avec la thymine.

Les avantages des puces incluent leur coût par échantillon, leur comparabilité entre différents jeux de données (mêmes CpGs couverts), leur praticité à mettre en œuvre, et leur couverture du génome (au moins une sonde dans 99% de tous les gènes connus). En revanche, la dernière des puces (EPIC) ne représente que 0,4% de tous les loci de méthylation du génome ce qui offre une couverture limitée de certaines régions. Il existe également plusieurs biais statistiques qui doivent être corrigés lors de l'analyse (détaillé dans le paragraphe suivant).

Le choix de la technique de mesure de la méthylation de l'ADN que l'on veut appliquer dépend donc du budget (€ WGBS > € RRBS/microarray > € MeDIP/MBD/MRE-seq > € mesure de la méthylation globale), de la résolution (CpG unique, région ou global), de la couverture souhaitée (génome entier, régions denses en CpGs, régions spécifiques, global) et des

compétences et infrastructures disponibles pour l'analyse bioinformatique et statistique (cluster de calcul pour traitement des données de séquençage, tests statistiques simples pour la méthylation globale).

1.5) Analyses bioinformatiques des données de méthylation issues de puces

La méthylation de l'ADN mesurée sur puces faisant l'objet de cette thèse, intéressons-nous plus précisément à la méthodologie du traitement des données et permettant d'évaluer *in fine* l'état méthylé ou non d'un CpG suivant différents échantillons. Après une étape de lavage, les puces sont soumises à un scanner qui va mesurer l'intensité des signaux de méthylation, c'est-à-dire la fluorescence émise par les nucléotides marqués par fluorochromes et hybridés à chaque sonde complémentaire identifiée. L'intensité de ce signal dépend de la quantité d'hybridation à chaque locus pour chaque échantillon. Il existe des sondes contrôles (c'est-à-dire sans signal attendu) permettant d'estimer le signal de fond, afin d'éviter la création de bruit de fond dans les données finales. En sortie, la lecture des plaques permet d'obtenir des fichiers au format .idat, qui possèdent l'information de la fluorescence pour chaque échantillon déposé sur la plaque et pour chaque couleur (un fichier vert et un fichier rouge correspondant à des longueurs d'onde de scanner différentes).

Un traitement bioinformatique permet de convertir ce fichier d'intensité lumineuse à une valeur de méthylation pour chaque locus étudié et de réaliser une analyse différentielle de la méthylation entre échantillons, dont un résumé est fourni en Figure 14.

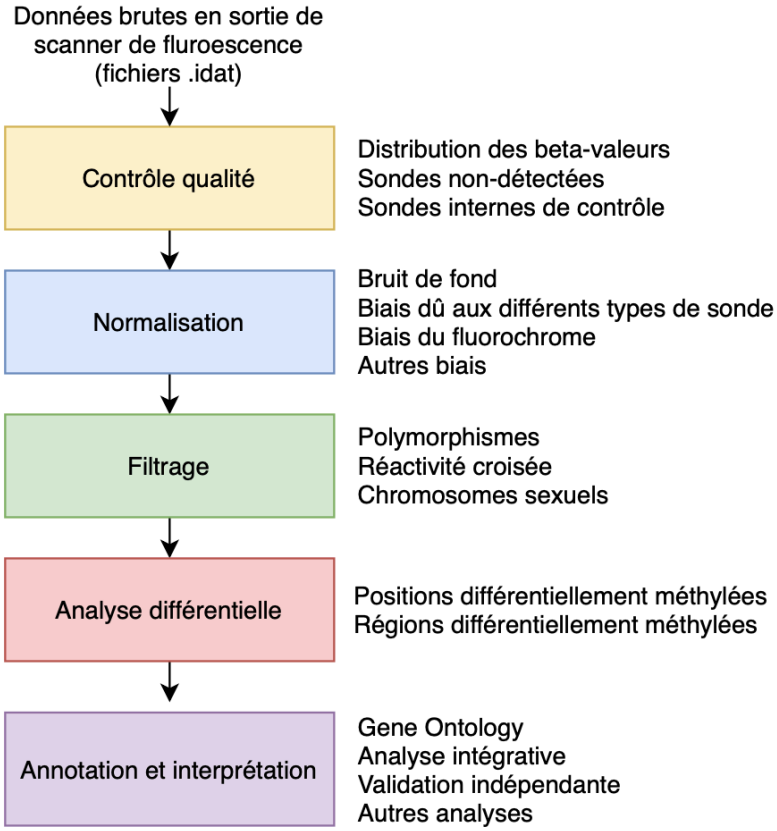

Figure 14. Pipeline générique d'analyse de données issues de puces à méthylation de l'ADN.

1.5.1) Contrôle qualité

Une fois le signal lumineux converti, on obtient pour chaque CpG une beta-valeur qui correspond au pourcentage de méthylation du CpG, comprise entre 0 et 100%. Ces valeurs ont un fort pouvoir d'interprétation du fait de leur simplicité de compréhension, mais statistiquement, elles ont une puissance faible à cause de leur hétéroscédasticité pour les très fortes et très faibles valeurs de méthylation (Du *et al.*, 2010). Cela signifie que dans le contexte de régression linéaire, notamment utilisée par la suite pour réaliser les analyses différentielles, la variance des erreurs du modèle de régression n'est pas la même pour toutes les observations (variance non homogène), ce qui représente un biais statistique. Les M-valeurs pallient ce problème, en se définissant par le logarithme base 2 du rapport entre intensité méthylée et non-méthylée. Une M-valeur positive indique que l'intensité lumineuse du signal méthylé est plus forte, et si elle est négative, à l'inverse, l'intensité lumineuse est plus faible. Il

est donc recommandé d'utiliser les M-valeurs lors de tout calcul statistique (valeur entre -Inf et +Inf) et d'utiliser les beta-valeurs pour toute interprétation et visualisation des données (valeur entre 0 et 100%) (Du *et al.*, 2010).

Avant tout calcul statistique, il est nécessaire de contrôler la qualité des données ainsi obtenues. Les puces à méthylation de l'ADN possèdent de nombreuses sondes permettant de l'évaluer. Principalement, il convient d'éliminer toutes les sondes dont le signal n'est pas différenciable du bruit de fond, à l'aide des sondes de contrôle négatif qui sont conçues de telle sorte qu'elles ne peuvent pas s'hybrider à l'ADN et ne dégagent pas de fluorescence. Chaque sonde de la puce se voit attribuer une p-valeur de détection indiquant si l'intensité mesurée est probablement un véritable signal et non un bruit de fond, et les sondes ne pouvant pas être discernées doivent être exclues. On peut également s'interroger sur la pertinence d'un échantillon comportant un trop grand nombre de sondes non détectées. Une deuxième information utile est la densité de distribution des beta-valeurs, qui doit afficher deux pics (distribution bimodale), un pour les valeurs très méthylées et un pour les très faiblement méthylées (Figure 15).

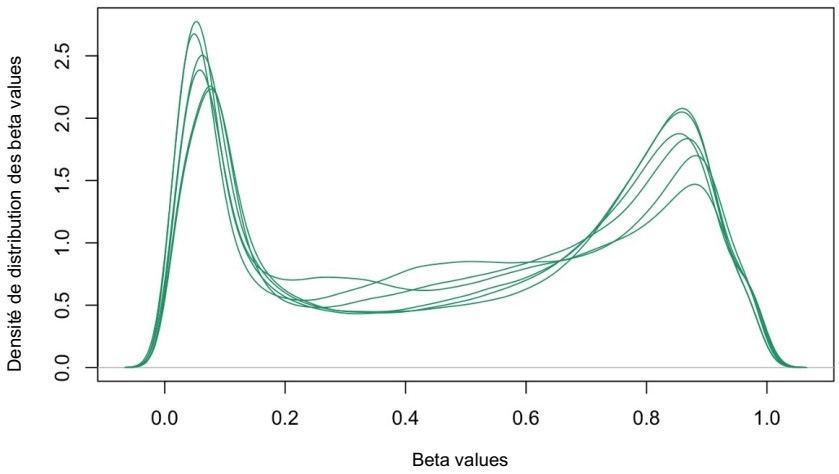

Figure 15. Une représentation de la courbe de densité de distribution classique des beta-valeurs sur une puce 450k (échantillons-tests du package R minfiData).

Ces deux paramètres sont principalement utilisés et permettent d'identifier les échantillons à potentiellement exclure avant de futures analyses. Des sondes internes de contrôle permettent

par ailleurs la vérification de la bonne conversion au bisulfite, des performances d'hybridation, du nettoyage des fragments non hybridés ou encore de l'extension.

1.5.2) Normalisation

Le rôle de la normalisation est d'éliminer les sources de variation technique sur une même puce, tout en maintenant les différences biologiques importantes pour l'interprétation des données. Une des particularités des techniques de mesure de méthylation via puces est la présence des deux types de sondes I et II qui sont techniquement très différentes. Spécifiquement, sur la puce 450k il est estimé que 57% des sondes de type I mesurent des CpGs se trouvant dans des régions d'îlots CpGs (comportant généralement un faible niveau de méthylation), contre 21% seulement pour les sondes de type II (Maksimovic *et al.*, 2012). Ainsi les sondes de type I et II affichent des distributions d'intensité de méthylation très différentes du fait de leur couverture, avec un signal non-méthylé plus fort pour les sondes de type I en raison de leur couverture préférentielle de CpGs situés dans des îlots CpGs (Figure 16).

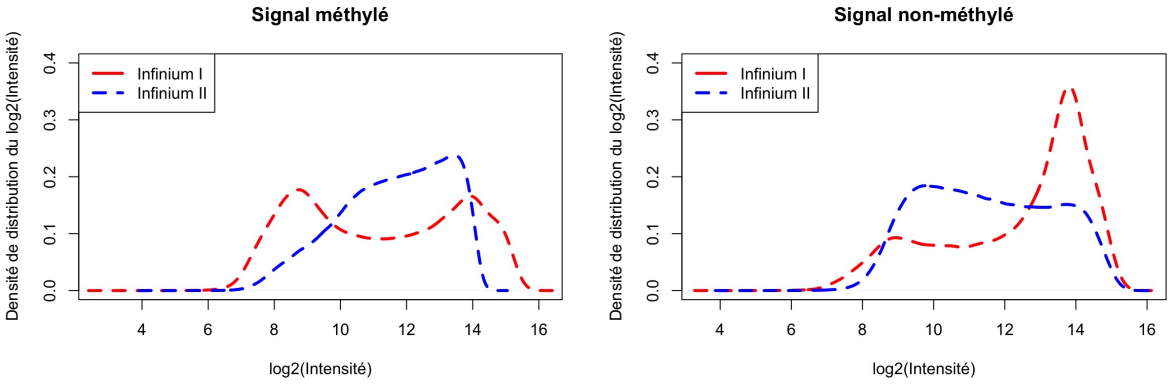

Figure 16. Distributions des intensités des signaux de méthylation des types de sondes Infinium I et II pour toutes les sondes d'une puce 450k (premier échantillon-test du package R minfiData).
Les différences qualitatives de distributions d'intensité sont probablement dues aux différences biologiques entre les régions que les deux types de sondes couvrent.

Pour minimiser les variations indésirables au sein d'un même échantillon et entre les échantillons, plusieurs méthodes de normalisation des données peuvent être appliquées. En fonction du type de tissu, du plan expérimental, et des hypothèses de recherche, chaque

méthode présente des avantages et des inconvénients (Hicks & Irizarry, 2015). Deux normalisations sont principalement utilisées car elles ont été développées spécifiquement pour l'analyse de données de puce à méthylation et les contraintes liées à la présence des différents types de sondes (I et II) sur une même puce.

La méthode SWAN ("Subset-quantile Within Array Normalization") consiste à appliquer à une sélection aléatoire de sondes de type I et II la normalisation classique par quantiles, et d'interpoler linéairement la normalisation au reste de la puce. Plus spécifiquement, la sélection se fait sur des sondes similaires (1, 2 ou 3 CpGs sur leur contenu en CpG), car une sonde nucléotidique peut contenir plusieurs CpGs sur sa séquence même si un seul est interrogé. Il y a proportionnellement plus de sondes de type I contenant deux voire trois CpGs du fait qu'elles couvrent biologiquement plus d'îlots CpGs. Sur ces sondes à plusieurs CpGs, la méthylation des CpGs adjacents est considérée comme très similaire d'un CpG à l'autre pour les sondes de type I et sont conçues de sorte que les CpGs en amont de la sonde aient le même statut de méthylation que le CpG ciblé (CG si méthylé, CA sinon). A l'opposé, les sondes de type II sont plus souples et permettent de mesurer la méthylation d'un CpG ciblé de façon indépendante de la présence d'autres CpGs méthylés ou non en amont de la sonde grâce au polymorphisme de la sonde (combinaison de CA et CG). On remarque que la distribution des intensités de méthylation pour les sondes contenant respectivement 1, 2 ou 3 CpGs est proche avant normalisation entre les sondes de type I ou II (Figure 17). La normalisation SWAN repose sur le principe d'égalité de distribution des signaux de méthylation suivant les sondes de type I et II lorsqu'elles sont égales en nombre de CpG contenus.

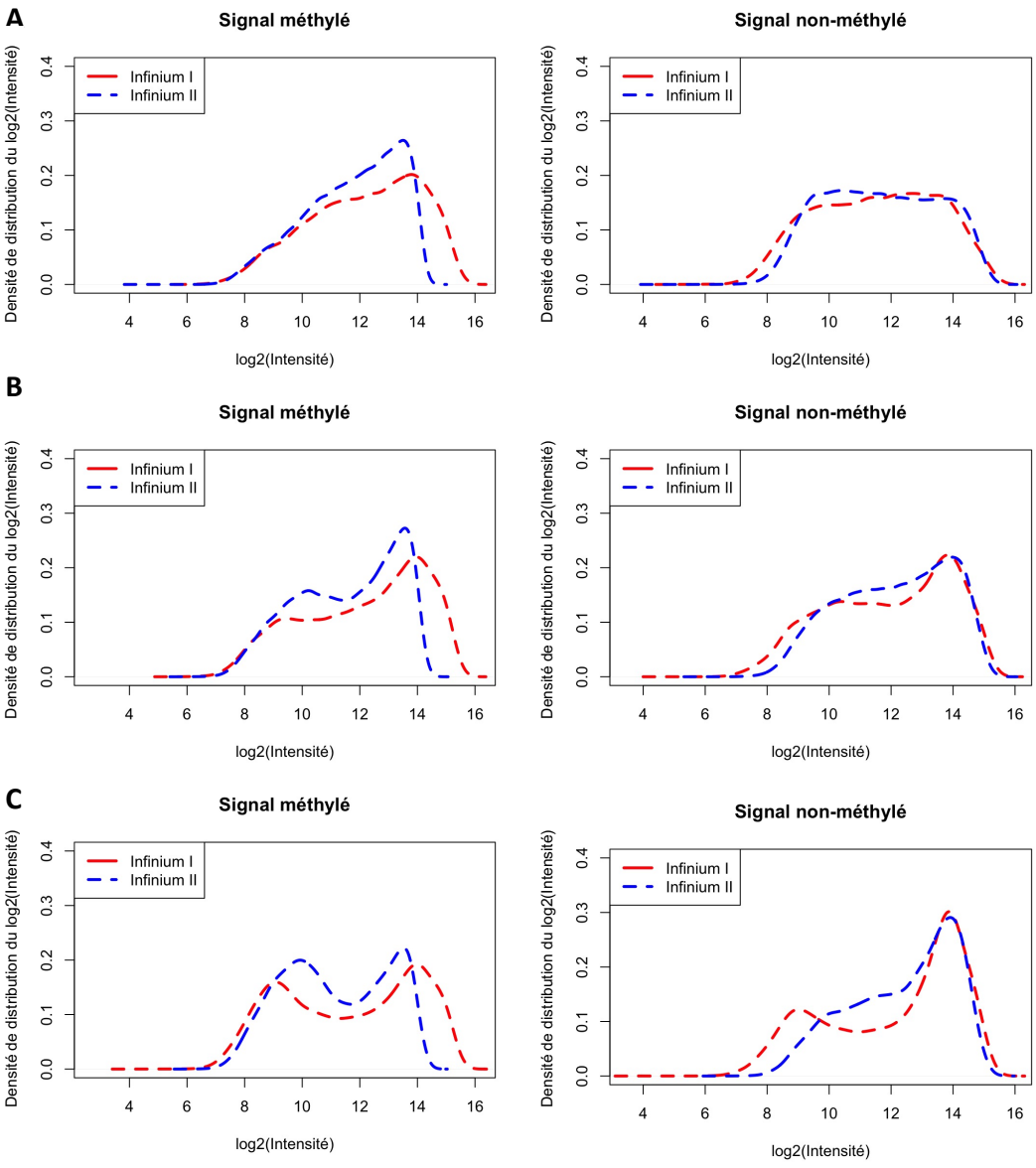

Figure 17. Distributions des intensités des signaux de méthylation des types de sondes Infinium I et II pour les sondes contenant 1,2 ou 3 CpGs sur une puce 450k (premier échantillon-test du package R minfiData).
A. Un seul CpG dans le corps de la sonde.
B. Deux CpGs dans le corps de la sonde.
C. Trois CpGs dans le corps de la sonde.

La deuxième méthode couramment utilisée est la normalisation BMIQ (« Beta-MIxture Quantile normalisation ») (Figure 18). Elle repose sur la décomposition des signaux de méthylation en trois distributions détaillant l'état non-méthylé (0%), hémi-méthylé (50%) ou totalement méthylé (100%), la transformation de ces probabilités en quantile avant une étape de transformation de dilatation. Le détail statistique complexe de cette démarche est décrit dans Teschendorff *et al.* (2013) (Teschendorff *et al.*, 2013). En résumé, cette méthode ajuste les valeurs obtenues via les sondes de type II sur celles obtenues via les sondes de type I, car il a été observé que les valeurs de méthylation issues de sondes de type II tombaient dans une fenêtre plus réduite (moins de sensibilité aux valeurs extrêmes de méthylation) que celles de type I et qu'elles étaient moins reproductibles (Dedeurwaerder *et al.*, 2011).

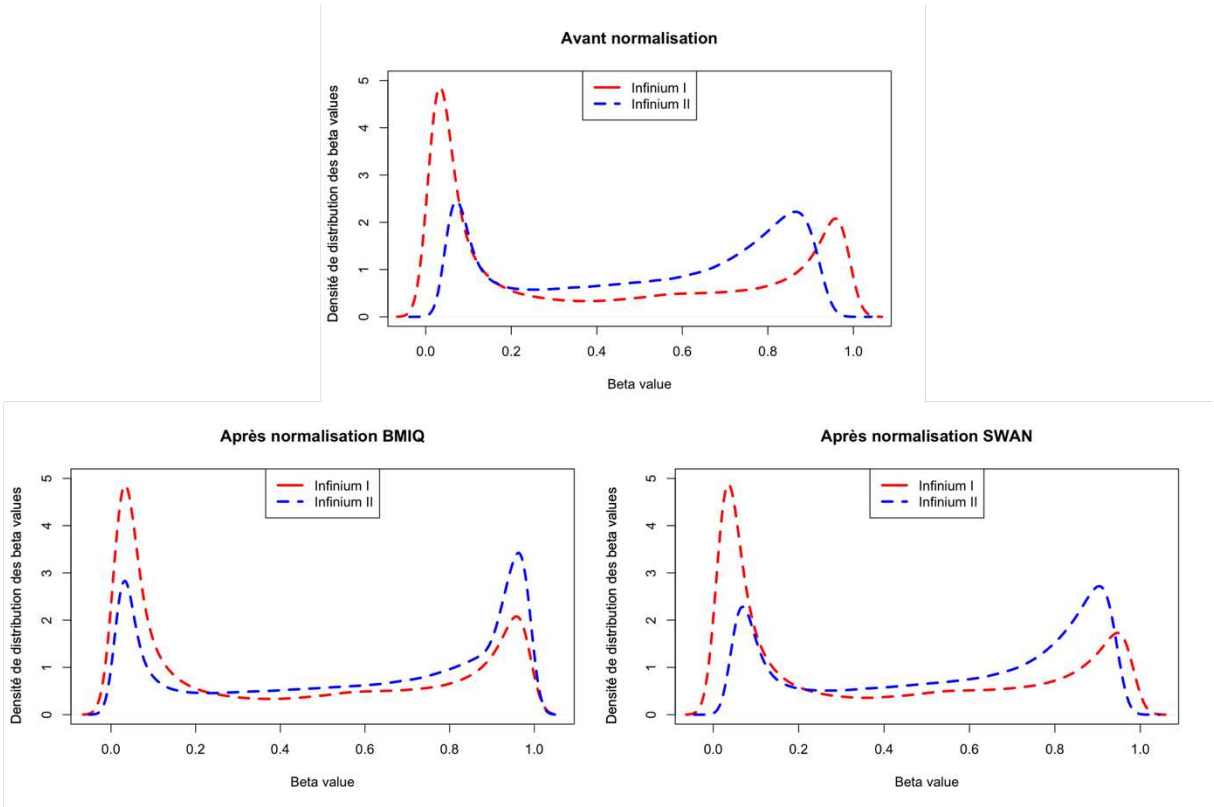

Figure 18. Distributions des intensités des beta-valeurs des types de sondes Infinium I et II comparées avant et après normalisation BMIQ et SWAN.

D'autres méthodes de normalisation peuvent être appliquées pour ces technologies et utilisent la correction du bruit de fond ou le biais du fluorochrome, comme la correction noob (« normal-exponential out-of-band »). Un résumé des différentes méthodes de normalisation couramment utilisées et leur fondement statistique est fourni en Table 3.

	SWAN	**BMIQ**	**noob**	**FunNorm**	**dasen**	**pQuantile**	**RCP**
Correction du bruit de fond	Non	Oui	Oui	Non	Oui	Non	Oui
Biais corrigé	Biais dû aux sondes de type I/II	Biais dû aux sondes de type I/II	Biais du flurorochrome	Biais dû au batch	Biais dû aux sondes de type I/II	Biais dû aux sondes de type I/II, biais de sexe	Biais dû aux sondes de type I/II
Régions génomiques ajustées	Non	Non	Non	Non	Non	Oui (même contexte CpG)	Oui (paires de sondes proches de 25 paires de base + même contexte CpG)
Méthode statistique	Normalisation des sous-ensembles par les quantiles	Normalisation par les quantiles basée sur un modèle de mélanges de 3 distributions beta	Normalisation normale-exponentielle par les quantiles	Normalisation fonctionnelle	Normalisation par les quantiles basée sur un modèle de mélanges de distributions beta	Normalisation stratifiée par les quantiles	Normalisation par les quantiles
Type de normalisation	Dans une même puce	Dans une même puce	Dans une même puce	Entre puces	Entre puces	Entre puces	Dans une même puce

Table 3. Différentes méthodes de normalisation couramment utilisées pour l'analyse de puces à méthylation et leurs caractéristiques.
Comme elles ne corrigent pas les mêmes biais, il peut être intéressant de combiner plusieurs approches, comme la méthode noob+BMIQ pour corriger le biais dû au type de sondes ainsi que le biais du fluorochrome. L'intérêt statistique de ces différentes méthodes et leur puissance est discutée dans Liu et Siegmund (2016) (Liu & Siegmund, 2016). Table adaptée depuis Sala *et al.* (2020) (Sala *et al.*, 2020).

1.5.3) Filtrage

En dehors des sondes de mauvaises qualité exclues en raison de leur faible signal, d'autres sondes ciblant des régions du génome peuvent afficher des M-valeurs et beta-valeurs biaisées. En effet, la présence de polymorphismes nucléotidiques (single nucleotide polyphormism, SNPs) dans le corps d'une sonde ou au niveau de son extension peut modifier l'affinité de la sonde avec les fragments d'ADN (Daca-Roszak *et al.*, 2015; Pidsley *et al.*, 2016). Il existe également des sondes qui ne sont pas spécifiques à une seule région de génome, dites à réactivité croisée car elles capturent des fragments d'ADN correspondant à des positions du génome multiples (Chen *et al.*, 2013). L'exclusion de ces sondes est nécessaire pour la fiabilité de l'analyse. Dans certains cas, on peut exclure les sondes situées sur les chromosomes sexuels car leur méthylation est naturellement asymétrique suivant le sexe, mais ce n'est pas obligatoire du moment que le sexe est pris en compte dans la suite des analyses. Certains packages R proposent des fonctions qui permettent d'éliminer ces sondes comme le package *minfi* (Aryee *et al.*, 2014).

1.5.4) Analyse différentielle

Après avoir adéquatement préparé les données vient le moment de chercher à répondre aux questions biologiques posées, par exemple savoir s'il existe des niveaux de méthylation spécifiques d'une condition dans certaines parties du génome. On peut distinguer deux grands types d'analyse : la recherche de CpGs individuels différentiellement méthylés (DMPs, differentially methylated positions) ou plus largement de régions (plusieurs CpGs) différentiellement méthylées (DMRs, differentially methylated regions).

La recherche de DMPs est intéressante dans le sens où les puces à méthylation de l'ADN couvrent l'ensemble du génome mais dans des proportions restreintes. Elle peut donc donner une idée des gènes, des types de régions génomiques (promoteur, exon, région régulatrice, …) susceptibles d'être épigénétiquement dérégulés suivant les conditions évaluées.

Pour identifier des DMPs, on utilise principalement la régression linéaire qui permet d'évaluer pour une variable quantitative ou qualitative la différence de méthylation entre individus comparés. Dans ce cas, la variable expliquée est le niveau de méthylation d'un CpG (M-valeur) et les variables explicatives sont la condition à évaluer plus les facteurs de confusion. Ces facteurs de confusion peuvent être d'ordres techniques et biologiques. Au sens technique, l'effet « batch » peut survenir lorsque pour une même expérience, des échantillons ont été préparés à des moments différents, quand bien même le protocole était le même. Il peut aussi y avoir des différences techniques entre puces préparées au même moment, et même entre échantillons d'une même puce suivant leur positionnement. Au sens biologique, on connaît une multitude de facteurs influençant les profils de méthylation. Les plus importants sont l'âge (Boks *et al.*, 2009; Christensen *et al.*, 2009; Rakyan *et al.*, 2010; Seale *et al.*, 2022), la composition cellulaire du tissue étudié (Houseman *et al.*, 2012, 2015) et le sexe mais suivant le tissu et la population étudiée, il est judicieux d'ajuster pour d'autres facteurs connus (exemple : phase du cycle menstruel pour l'endomètre (Saare *et al.*, 2016; Tsai *et al.*, 2018), tabagisme, traitement médical, co-morbidité, polymorphisme génétique). Lorsque la composition cellulaire est inconnue, des algorithmes de déconvolution permettent de l'estimer à partir des niveaux de méthylation provenant d'échantillons référence de chaque sous-type cellulaire purifié (Teschendorff *et al.*, 2017). En effet, certains CpGs sont caractéristiques de certains types cellulaires et ont un très fort pouvoir discriminant (très méthylé dans un type cellulaire alors que très déméthylé dans tous les autres types cellulaires). Ils établissent ainsi un profil de référence de chaque type cellulaire. La déconvolution consiste à interpréter le profil de méthylation d'un échantillon comme la somme linéaire pondérée des profils de référence de méthylation de chaque type cellulaire.

Les moyennes et les erreurs standard de méthylation estimées pour chaque groupe comparé sont ensuite utilisées pour calculer une statistique de test-t modéré et une p-valeur indiquant le niveau de méthylation différentielle entre les groupes. Comme un nombre très conséquent de CpGs est testé (>800 000 pour la puce EPIC), on augmente proportionnellement la

probabilité que chaque CpG testé soit déclaré à tort significativement différentiellement méthylé (on parle d'erreur de type I, on encore de taux de faux positifs). Il convient corriger les p-valeurs pour que le risque d'erreur de type I soit contrôlé via une technique de correction des tests multiples comme le « false discovery rate » (FDR) ou la correction de Bonferroni. La sélection finale des DMPs significatives doit se faire sur la base du seuil de significativité de la correction des tests multiples (généralement FDR<0.05) et également sur la différence de méthylation entre groupes comparés (taille de l'effet ou deltabeta) qui doit être réglée pour que >80% des CpGs testés aient >80% de puissance statistique à détecter cette différence (Mansell *et al.*, 2019). Cette dernière valeur est dépendante de la taille d'échantillon et du nombre de CpGs testés.

La recherche de régions différentiellement méthylées (DMRs) est possible à partir du moment où plusieurs DMPs ont été identifiées. Les DMRs permettent de se défaire de la redondance spatiale des DMPs car il est prouvé que des CpGs adjacents ont souvent des valeurs de méthylation très corrélées (Guo *et al.*, 2017a; Affinito *et al.*, 2020). De plus, elles apportent une information robuste et possèdent une implication fonctionnelle plus importante qu'une DMP individuelle. Le package R *dmrcate* repose sur le principe de lissage des p-valeurs des DMPs dans une fenêtre de 1000 paires de base ajustable, à l'aide d'un noyau gaussien (Peters *et al.*, 2015). Les paramètres de définition d'une région sont adaptables par chaque utilisateur. Dans nos études par exemple, nous utilisons les critères qu'une région doit contenir au moins 2 CpGs et qu'une région ne peut contenir de CpGs distants de plus de 1000 paires de base. Ce sont les paramètres recommandés par le package *dmrcate* pour optimiser la recherche de DMRs.

1.5.5) Annotation et interprétation

La compréhension globale d'un jeu de données de méthylation de l'ADN grâce à de nombreux outils statistiques et de visualisation est importante. Par exemple, l'application de techniques de réduction de dimension comme l'analyse en composantes principales et la classification

ascendante hiérarchique sont des outils utiles pour inspecter les similarités globales entre échantillons biologiques. Après analyse différentielle, les diagrammes en volcan (« volcanoplot ») et les diagrammes de Manhattan permettent d'inspecter la distribution de tous les CpGs respectivement en terme d'hypo-/hyper-méthylation et de localisation dans le génome (Figure 19).

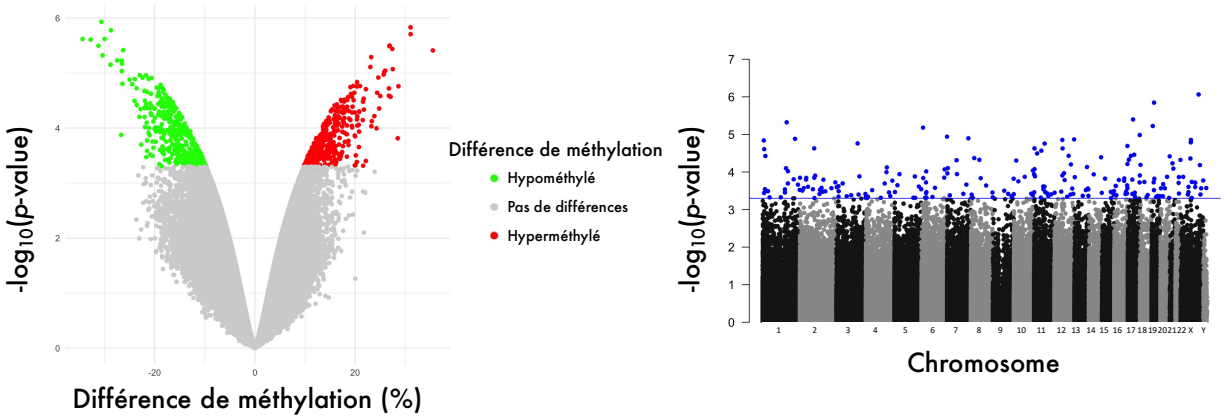

Figure 19. Exemple de visualisations possibles après analyse différentielle. Issu de l'analyse du jeu de données test du package minfiData.
A. Le volcanoplot montre les différences de méthylation entre deux groupes testés, et leur significativité.
B. Le Manhattan plot montre la répartition des CpGs différentiellement méthylés le long du génome.

L'annotation de chaque CpG et région différentiellement méthylés est cruciale pour leur interprétation. Il existe des bases d'annotation préconçues fournies par le constructeur de puces ou développées dans des packages R qui donnent une indication du gène où se localisent les CpGs mais aussi dans quels éléments génomiques, comme les régions régulatrices (promoteur, exon, intron, …). Chacun est libre d'annoter sa propre base, à l'aide de bases d'annotation fournies par le NCBI, l'UCSC ou Ensembl.

A l'issue de l'obtention d'une liste de DMPs et de DMRs il est possible de réaliser une analyse d'enrichissement en Gene Ontology (GO) sur les gènes où elles sont localisées (en séparant les DMPs/DMRs suivant leur hypo- ou hyper-méthylation). Cette méthode repose sur un test hypergéométrique qui évalue la sur- ou sous-représentation d'un ensemble de gènes d'une même ontologie (groupe de gènes qui ont les mêmes fonctions moléculaires, ou impliqués dans les mêmes processus biologiques, ou localisés dans les mêmes compartiments

cellulaires) en comparaison de l'ensemble des gènes exprimés pour le tissu et la condition étudiés. Cette approche est possible avec les puces à méthylation de l'ADN mais doit prendre en compte que la couverture en CpGs par les puces n'est pas identique pour chaque gène, ce qui constitue un biais si l'on veut utiliser l'approche GO classique car certains gènes ont plus de probabilité d'être identifiés comme différentiellement méthylés. La fonction *gometh* du package R *missMethyl* corrige ce biais et permet d'appliquer de façon juste le principe de la GO (Maksimovic *et al.*, 2021).

Les analyses dites « intégratives » de données multi-omiques offrent la possibilité de mieux comprendre des processus biologiques complexes en combinant des données biologiques à différentes échelles, de la séquence ADN en elle-même, au protéome et au métabolome, en passant par l'épigénome et le transcriptome. La corrélation entre les niveaux de méthylation dans le corps d'un gène, son promoteur et d'autres régions régulatrices avec des données d'expression des gènes permet de mesurer les conséquences biologiques de certaines modifications de méthylation de l'ADN (Roadmap Epigenomics Consortium *et al.*, 2015). L'association entre des variations génétiques types SNPs et des niveaux de méthylation permet d'établir des traits quantitatifs de méthylation (mQTL). En outre on peut identifier pour certaines maladies avec des variations génétiques connues si ces variations influent sur la méthylation des CpGs environnants, à l'aide d'outils comme *ANNOVAR* (Wang *et al.*, 2010; McRae *et al.*, 2018).

Dans l'idéal, le recours à des cohortes indépendantes de validation des résultats doit être systématisé pour attester de la robustesse d'un résultat. Pour les DMRs les plus fortes ou les gènes avec une forte prévalence de DMPs, il peut être intéressant d'utiliser une méthode expérimentale alternative d'évaluation de la méthylation, comme le pyroséquençage afin de vérifier la reproductibilité et la précision des résultats.

Pour aller encore plus loin, l'application d'algorithmes de machine learning a pris son essor depuis quelques années. Depuis 2013, l'établissement d'une horloge épigénétique via la

méthode de régression « Elastic net » permet de déterminer l'âge biologique de n'importe quel être humain (Horvath, 2013). En effet, en réduisant l'âge chronologique de 8000 échantillons de tous types cellulaires sur un ensemble de plus de 20 000 CpGs, cet algorithme a sélectionné 353 CpGs prédictifs de l'âge, permettant de calculer un « âge épigénétique ». Il s'avère qu'une différence positive entre l'âge épigénétique et l'âge chronologique (qualifiée d'accélération épigénétique) témoigne d'une accélération du vieillissement cellulaire et augmente la susceptibilité à de nombreuses maladies (Horvath & Raj, 2018; Seale *et al.*, 2022).

La recherche de biomarqueurs de méthylation est un axe prometteur pour le diagnostic clinique de nombreuses maladies. De façon plus spécifique, on peut également inférer la composition cellulaire d'un individu à partir de niveaux de méthylation comme évoqué précédemment (package R *EpiDISH*) (Teschendorff *et al.*, 2017), mais également prédire la méthylation aux loci situés dans les éléments transposables à partir d'un nombre réduit de CpGs (package R *REMP*) (Zheng *et al.*, 2017).

1.5.6) Les méta-analyses d'études d'association à l'échelle de l'épigénome

Les études d'association à l'échelle de l'épigénome (EWAS) reposant sur des échantillons de petite taille ne permettent pas de détecter de faibles différences de méthylation et sont susceptibles de contenir un taux de faux positifs élevé. Il est notamment évalué que pour détecter une différence de méthylation de 2% entre deux groupes avec une puissance statistique supérieure à 80% via la puce EPIC, il faudrait plus de 500 échantillons par groupe, et au moins 100 par groupe pour une différence de 5% (Mansell *et al.*, 2019). La plupart des EWAS sont très éloignées de ces valeurs. Au vu de l'importance d'explorer les effets épigénétiques en lien ou causés par certaines conditions, il apparaît nécessaire que les résultats individuels des petites et larges études soient valorisés par le biais d'une méta-analyse. Cette synthèse statistique permet une réexploitation beaucoup plus fine des données

de chaque étude individuelle par l'agrégation des différentes cohortes étudiées. Cette méthode robuste a donc vocation d'identifier des biomarqueurs de méthylation de l'ADN associés à une condition (DMPs et DMRs).

Pour la méta-analyse, l'outil METAL adapté pour les méta-analyses des études d'association à l'échelle du génome est couramment utilisé pour les données de méthylation de l'ADN (Willer *et al.*, 2010). METAL calcule une taille d'effet groupé pour chaque position génomique étudiée en pondérant chaque effet d'études individuelles par l'inverse de l'écart-type. Un modèle à effet aléatoire ou fixe peut être choisi suivant l'hétérogénéité des populations étudiées, qui est généralement calculée avec un test Q de Cochran (Cochran, 1954). Les positions génomiques de méthylation franchissant le seuil d'une p-valeur ajustée inférieure à 0.05 sont généralement considérées comme DMPs. Il est possible de rajouter des critères de sélection des DMPs suivant la différence de méthylation moyenne entre les groupes ou le nombre d'études où l'association entre phénotype et méthylation était positive ou négative.

Pour des études ciblées de la méthylation (PCR, pyroséquençage, …), les méta-analyses sont également applicables avec des outils statistiques standards (modèle à effet aléatoire ou fixe) mais il faut s'assurer auparavant que les régions étudiées dans chaque étude indépendante soient identiques.

2) Le transcriptome

Le transcriptome comprend l'ensemble des ARNm issus du génome. Il représente ainsi l'expression des gènes d'une cellule ou d'un tissu à un moment donné (National Human Genome Research Institute, 2020).

Les ARNm sont issus de la transcription, qui est le mécanisme biologique se déroulant dans le noyau correspondant à la copie d'un segment d'ADN en ARN. Elle se déroule en 3 phases, l'initiation, l'élongation et la terminaison. Lors de l'initiation, une ARN polymérase se fixe dans la région promotrice d'un gène, ce qui entraîne le déroulement de la double hélice d'ADN.

Cette fixation est permise par un ensemble de protéines qu'on appelle facteurs de transcription et qui reconnait certains motifs nucléotidiques spécifiques des régions promotrices, comme les boites TATA (séquences riches en motif TA). L'ARN polymérase progresse ensuite le long du brin matrice d'ADN en synthétisant un transcrit d'ARN dans le sens 5' -> 3' (élongation), en appariant les nouveaux nucléotides de l'ARN au brin matrice d'ADN. La molécule d'ARN se détache progressivement du brin d'ADN transcrit au fur et à mesure de l'avancée de la polymérase. L'ARN est finalement clivé (terminaison) après transcription d'une séquence de polyadénylation. On obtient alors un ARN pré-messager qui doit être maturé post-transcription avant d'être traduit en protéine. Cette maturation implique différentes modifications enzymatiques comme l'ajout d'une coiffe méthylguanosine en 5' permettant la reconnaissance de l'ARNm par les ribosomes pour la traduction, l'ajout d'une queue poly-A de 50 à 250 adénines en 3' par une poly-A polymérase permettant la stabilité de l'ARNm (facilite le transport, protège de la dégradation, aide à la fixation sur les ribosomes). Enfin, l'ARN pré-messager est excisé de certaines séquences, puis suturé. On parle du processus d'épissage de l'ARN, qui élimine les introns (séquences non codantes d'un gène) et conserve les exons (séquences destinées à être exprimées). Il est réalisé à l'aide d'un complexe de particules ribonucléoprotéiques appelé splicéosome. On obtient alors un ARNm mature, qui pourra être transféré en dehors du noyau, vers les ribosomes afin d'initier la traduction en protéines.

En lien avec la reproduction, il est primordial de connaître l'effet de différentes techniques d'AMP sur le transcriptome de l'ovocyte et de l'embryon précoce, des étapes du développement où le transcriptome apparaît très vulnérable.

2.1) Le transcriptome ovocytaire, sentinelle du développement embryonnaire

2.1.1) Objectifs

La folliculogenèse et la maturation ovocytaire se manifestent par des changements transcriptionnels et physiologiques/morphologiques qui devraient fournir des conditions optimales pour la fécondation et le transport de transcrits maternels essentiels qui contrôleront les premières divisions embryonnaires (Eppig, 1996; Watson, 2007; Conti & Franciosi, 2018) (Figure 20).

Dans les follicules pré-antraux, la chromatine est décondensée, ce qui rend l'activité transcriptionnelle élevée et répond aux besoins de croissance du follicule à cette période (Luciano *et al.*, 2012; Gu *et al.*, 2019). A partir du follicule tertiaire, la chromatine des ovocytes se condense progressivement et l'activité transcriptionnelle est finalement interrompue lorsque les ovocytes atteignent la rupture de la vésicule germinale (GVBD), ce qui entraîne une dégradation drastique de l'ARNm, comme constaté dans le modèle murin (Wu & Dean, 2020; Jiang *et al.*, 2023). Une dégradation maternelle (M-decay), nécessaire pour ouvrir la voie à l'activation du génome embryonnaire, a lieu pendant la maturation finale de l'ovocyte tandis que la dégradation zygotique (Z-decay) a lieu après la fécondation (Sha *et al.*, 2020; Cornet-Bartolomé *et al.*, 2021; Tora & Vincent, 2021; Jiang *et al.*, 2023).

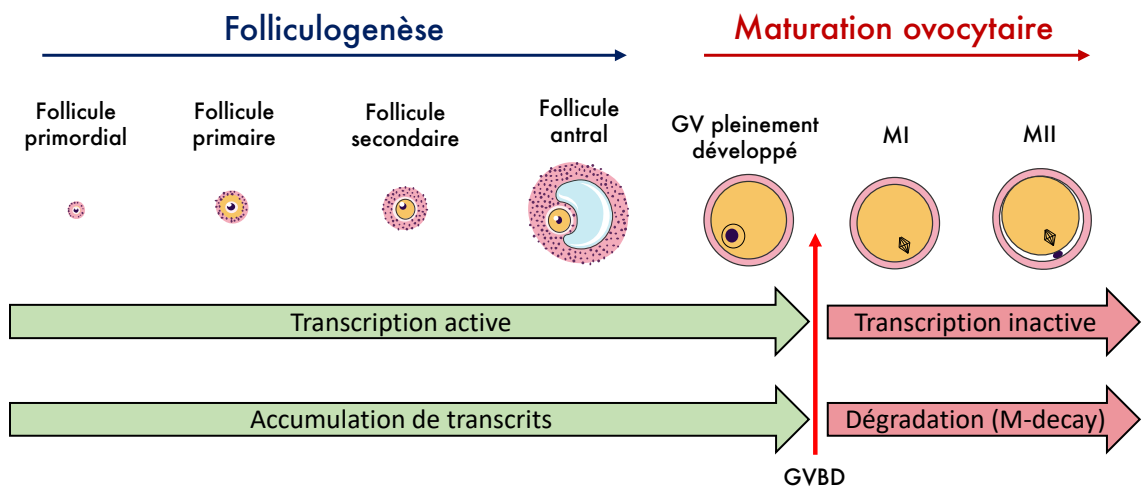

Figure 20. Dynamique du développement ovocytaire et de son transcriptome.
GVBD. Germinal Vesicle Breakdown.

Au cours des dernières années, la technique de RNA-seq a été utilisée pour établir le profil du transcriptome des ovocytes en croissance et en maturation chez l'Homme, mais aucune étude n'a agrégé de manière exhaustive les données qui en émanent. Évaluer l'ensemble de ces données afin de mieux identifier les processus clés impliqués dans la croissance et la maturation des ovocytes devrait permettre d'identifier les exigences transcriptomiques fondamentales de l'ovocyte à tout moment de sa croissance et la régulation des ARNm qui en résulte.

2.1.2) Matériels et méthodes

Une réanalyse bioinformatique de 7 jeux de données précédemment publiés quantifiant le transcriptome ovocytaire humain depuis le follicule primordial jusqu'au stade MII a été réalisée, en standardisant la quantification de l'expression des gènes pour chacun d'entre eux pour assurer leur comparabilité.

Dans un premier temps, un jeu de données single-cell RNA-seq a permis de retracer la cinétique du transcriptome depuis le stade follicule primordial jusqu'au follicule antral. La folliculogenèse étant probablement un processus dynamique, une analyse « pseudotime » a été mise en œuvre en utilisant la méthode de réduction de dimension PHATE (Potential of Heat-diffusion for Affinity-based Trajectory Embedding) pour trouver les gènes

différentiellement exprimés (DEGs) tout au long de la folliculogenèse. Le « pseudotime » est une métrique qui peut être interprétée comme une distance temporelle entre 1 cellule et son précurseur. Cette méthode permet d'identifier les gènes dont l'expression change dynamiquement au cours de la croissance de l'ovocyte, de manière continue et indépendamment du stade du follicule dans lequel se trouve l'ovocyte. Nous avons choisi PHATE en raison de sa capacité à capturer l'hétérogénéité et à réduire le bruit mieux que les autres méthodes de réduction de la dimensionnalité (Moon *et al.*, 2019).

Concernant la maturation ovocytaire depuis le stade vésicule germinale (GV) jusqu'au stade métaphase II (MII, ovocyte mature), les résultats d'analyse différentielle individuelle (MII-GV) (taille de l'effet (logFC) et p-valeur) pour chaque gène de 6 jeux de données ont été méta-analysés en utilisant un modèle à effets aléatoires.

2.1.3) Résultats

Nous avons décodé les événements régulateurs des ARNm maternels qui conduisent l'ovocyte à croître puis à subir de multiples types de maturation (cytoplasmique, nucléaire, épigénétique, structurale). L'atlas des modifications transcriptomiques décrit dans cette étude permettra à l'avenir d'identifier plus précisément les transcrits impliqués dans la croissance folliculaire et les échecs de maturation ovocytaire.

Notre analyse comparative a révélé des voies biologiques signatures activées et réprimées dans les ovocytes à différents stades folliculaires. Le stade primordial peut refléter une forte communication entre l'ovocyte et ses cellules environnantes, qui se manifeste par une régulation à la hausse des gènes liés à l'adhésion cellulaire, à la prolifération des cellules épithéliales et à l'organisation des fibrilles de collagène, qui tendent à être réduites par la suite. De plus, une régulation à la baisse de la traduction cytoplasmique a été observée dans les follicules antraux alors que l'activité la plus élevée a été observée dans les follicules primordiaux, ce qui corrobore les résultats selon lesquels les ARNm maternels ne sont progressivement plus traduits mais stockés jusqu'à ce qu'ils soient dégradés ou traduits après

la reprise de la méiose à la suite de la GVBD. Les ovocytes des follicules primordiaux présentent également une régulation à la baisse des voies du cycle cellulaire, ce qui correspond à leur arrêt au stade diplotène de la méiose I jusqu'à leur activation. Dans le follicule antral, les gènes de transition du cycle cellulaire sont régulés à la hausse, ce qui pourrait correspondre à l'acquisition de la compétence méiotique pour soutenir la maturation prochaine des ovocytes.

Les ovocytes au stade du follicule primaire ne présentent pas un profil transcriptomique très spécifique par rapport au follicule primordial. La transition entre les deux stades est probablement liée à une accumulation non-spécifique d'ARNm, ce qui signifie que les ovocytes du follicule primaire accumulent l'ARNm de manière drastique mais non sélective.

Ensuite, la transition d'un ovocyte de follicule primaire à un ovocyte de follicule secondaire est marquée par un changement dans les voies métaboliques mobilisées pour consommer de l'énergie (activation de la synthèse d'ATP mitochondriale, respiration aérobie et phosphorylation oxydative).

Enfin, les ovocytes des follicules antraux semblent arrêter cette activité énergétique, peut-être passivement (régulation à la baisse de la respiration aérobie et des voies de phosphorylation oxydative) en raison de la difficulté d'accès à l'oxygène dans un micro-environnement clos (Redding *et al.*, 2008; Thompson *et al.*, 2015; Lim *et al.*, 2021). Nous avons également observé que les ovocytes des follicules antraux présentent une capacité accrue à réparer les altérations de l'ADN par rapport aux autres stades (régulation à la hausse de la voie de recombinaison homologue), ce qui est confirmé par des observations antérieures (Winship *et al.*, 2018).

Par ailleurs, nous avons mieux caractérisé la dégradation subie par les ARNm maternels pendant la fin de l'ovogenèse. Nous avons constaté une baisse moyenne de 30 % de l'ARNm total entre le stade GV et le stade MII dans l'ensemble des études. Nous montrons par ailleurs la régulation négative sélective de certains transcrits; ceux associés à la production d'énergie et aux fonctions mitochondriales ont été largement régulés à la baisse, tandis que ceux

associés à la traduction cytoplasmique, à la modification des histones, aux processus méiotiques et aux processus de l'ARN ont été conservés.

2.1.4) Article 1 - Overview of Gene Expression Dynamics during Human Oogenesis/Folliculogenesis

International Journal of
Molecular Sciences

MDPI

Article

Overview of Gene Expression Dynamics during Human Oogenesis/Folliculogenesis

Bastien Ducreux [1], Lucile Ferreux [2,3], Catherine Patrat [2,3] and Patricia Fauque [1,4,*]

[1] Université Bourgogne Franche-Comté-Equipe Génétique des Anomalies du Développement (GAD) INSERM UMR1231, 2 Rue Angélique Ducoudray, F-21000 Dijon, France; bastien.ducreux@outlook.fr
[2] Faculty of Medicine, Inserm 1016, Université de Paris Cité, F-75014 Paris, France; lucile.ferreux@aphp.fr (L.F.); catherine.patrat@aphp.fr (C.P.)
[3] Department of Reproductive Biology-CECOS, Aphp.Centre-Université Paris Cité, Cochin, F-75014 Paris, France
[4] Laboratoire de Biologie de la Reproduction-CECOS, CHU Dijon Bourgogne, 14 Rue Gaffarel, F-21000 Dijon, France
* Correspondence: patricia.fauque@chu-dijon.fr

Abstract: The oocyte transcriptome follows a tightly controlled dynamic that leads the oocyte to grow and mature. This succession of distinct transcriptional states determines embryonic development prior to embryonic genome activation. However, these oocyte maternal mRNA regulatory events have yet to be decoded in humans. We reanalyzed human single-oocyte RNA-seq datasets previously published in the literature to decrypt the transcriptomic reshuffles ensuring that the oocyte is fully competent. We applied trajectory analysis (pseudotime) and a meta-analysis and uncovered the fundamental transcriptomic requirements of the oocyte at any moment of oogenesis until reaching the metaphase II stage (MII). We identified a bunch of genes showing significant variation in expression from primordial-to-antral follicle oocyte development and characterized their temporal regulation and their biological relevance. We also revealed the selective regulation of specific transcripts during the germinal vesicle-to-MII transition. Transcripts associated with energy production and mitochondrial functions were extensively downregulated, while those associated with cytoplasmic translation, histone modification, meiotic processes, and RNA processes were conserved. From the genes identified in this study, some appeared as sensitive to environmental factors such as maternal age, polycystic ovary syndrome, cryoconservation, and in vitro maturation. In the future, the atlas of transcriptomic changes described in this study will enable more precise identification of the transcripts responsible for follicular growth and oocyte maturation failures.

Keywords: folliculogenesis; maturation; oocyte; RNA-seq; transcriptome

Citation: Ducreux, B.; Ferreux, L.; Patrat, C.; Fauque, P. Overview of Gene Expression Dynamics during Human Oogenesis/Folliculogenesis. *Int. J. Mol. Sci.* **2024**, *25*, 33. https://doi.org/10.3390/ijms25010033

Academic Editor: Christine Wyns

Received: 20 November 2023
Revised: 7 December 2023
Accepted: 12 December 2023
Published: 19 December 2023

1. Introduction

Obtaining a mature oocyte is a lengthy and complex process. It results from two processes, folliculogenesis and oogenesis, which set the stage for early embryonic development. Interestingly, these multistep procedures are characterized by specific transcriptional states and are associated with notable transcriptomic transitions. To date, there is still much we do not know about the tight regulation of oogenesis.

The long journey of an oocyte is initiated in the primordial germ cells during fetal life when oogonia enter meiosis (approximately at week 9 in humans) and is subsequently arrested at the diplotene stage of prophase I (germinal vesicle stage, GV) [1,2]. The nuclear maturation is stopped for several years and resumes after puberty at each menstrual cycle, when a surge of luteinizing hormone triggers the final maturation of a dominant follicle recruited to develop until the oocyte reaches the metaphase of meiosis II (MII) stage. The oocyte has then completed both cytoplasmic and nuclear maturation. This maturation is manifested by transcriptional and physiological/morphological changes that

should provide optimal conditions for fertilization and the transport of essential maternal transcripts that will control the first embryonic divisions [3–5]. Concomitantly, oocyte nuclear maturation is also conditioned by two other biological modifications: organelle maturation, which situates mitochondria/ribosomes/endoplasmic reticulum/cortical granules and the Golgi apparatus, and epigenetic maturation, because important epigenetic reprogramming takes place at the same time (de novo methylation, histone modifications and exchanges) [6]. Thus, oocyte growth and maturation are the main factors determining early embryonic competence.

In the pre-antral follicles, the chromatin is decondensed, making the transcriptional activity high and fitting the needs required by the follicle to grow [7,8]. As the tertiary follicle develops, gradual condensation of chromatin occurs, and the transcriptional activity is finally stopped when oocytes reach the GV breakdown (GVBD) and could initiate drastic mRNA degradation, as found in the mouse model [9,10]. The degradation of maternal transcripts is needed to pave the way for the embryonic transcriptome and occurs in two big waves. Maternal decay (M-decay) takes place during final oocyte maturation and is thought to eliminate 30–50% of maternal factors, while zygotic decay (Z-decay) occurs after fertilization and clears the remaining material in such a way that approximately 80% of polyadenylated (poly(A)) mRNAs stored at the GV stage are not present in the eight-cell mouse embryo [10–14]. This degradation is notably governed by RNA-binding proteins, microRNAs, nonsense-mediated decay factors, or siRNA [15–18]. Reaching the MII stage does not guarantee that the embryo will fully develop, and oocyte competence should be decoded from their transcriptome [5,19,20]. The key process in oocyte maturation that will determine embryo quality may lie (i) in the selective degradation and conservation of maternal transcripts from the fully grown GV to MII stage and (ii) in the appropriate and timely regulation of a set of specific transcripts at each stage of oocyte development.

Advances in the knowledge of oocyte maturation and folliculogenesis may also be beneficial for the success of fertility preservation. It may lead to the optimization of in vitro maturation and culture processes in fertility clinics by identifying key factors conditioning the favorable outcome of oocyte maturation. In addition, it may lead to a better understanding of what causes deficient maturation, because excessive transcript accumulation and defects in the degradation machinery were shown to be associated with embryonic genome activation failure [11,15,21,22]. Moreover, the development of RNA-seq techniques has expanded our knowledge of the transcriptome-wide landscape of tissues and even single cells (scRNA-seq). Capturing polyadenylated RNA in a sample provides a snapshot of the existing mRNA population and reflects its gene expression identity. Over the last few years, RNA-seq has been used to profile the transcriptome of growing and maturing oocytes, but no studies have comprehensively aggregated the resulting data.

In the current review, we comprehensively evaluated these data to better identify key processes involved in human oocyte growth and maturation. We first applied a Gene Ontology and a pseudotime analysis to identify the fundamental transcriptomic requirements of the oocyte at any stage of folliculogenesis and the resultant mRNA regulation. Secondly, we performed a meta-analysis of studies comparing fully grown GV and MII oocytes to decode the accumulation/degradation of maternal transcripts occurring during this final maturation. In closing, we evaluated whether the transcripts supposedly having a role in the oocyte growth and maturation processes are sensitive to environmental factors, which could help us better understand the origin of oocyte maturation defects.

2. Results

2.1. Folliculogenesis

Global observation via principal component analysis (PCA) of transcriptomes from oocytes originating from primordial to antral follicles indicated overall differences between the different groups, but there was little difference between primordial and primary follicles, suggesting high transcriptional profile proximity for those cells (Figure 1A). The accumulation of maternal transcripts in the oocyte throughout folliculogenesis was con-

firmed, but there was no significant variation from the primary to the secondary follicle stage (Figure 1B).

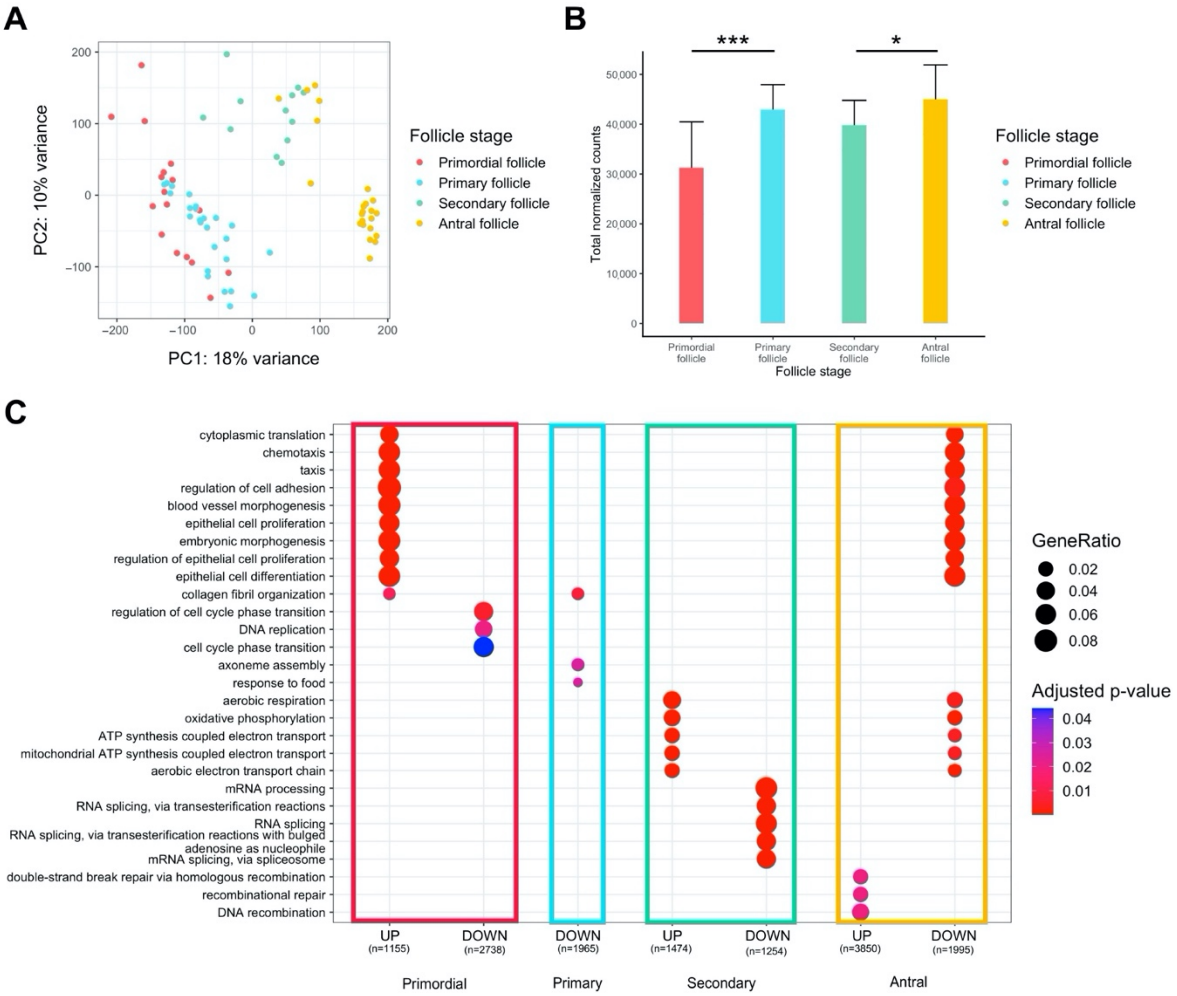

Figure 1. Differential expression analysis of transcriptomic signature changes along the different stages of folliculogenesis (dataset from Zhang et al. (2018) [23]). (**A**) Principal component analysis of the whole expression dataset removing the 10% genes with the lowest variance. (**B**) Comparison of the normalized read counts total between the different follicle stages (significance assessed with a *t*-test, * $p < 0.05$, *** $p < 0.005$). (**C**) Comparative Gene Ontology enrichment analysis according to the up- or downregulation of transcripts between all four follicle stages. GeneRatio corresponds to the fraction of differentially expressed genes (DEGs) found in each Gene Ontology set.

We carried out a gene ontology over-representation analysis on genes differentially expressed between one stage and all others to reveal the biological signatures of oocytes from each follicle type (Figure 1C, Supplementary Table S1).

Oocytes of primordial follicles are characterized by the upregulation of genes involved in cytoplasmic translation, chemotaxis, regulation of cell adhesion, and regulation of epithelial cells, while the cell cycle phase transition is downregulated. Primary follicle oocytes do not display strong transcript identity compared to oocytes from other stages of follicle development, since few pathways are significantly downregulated and there is low biological function linked to oocyte development. Oocytes of secondary follicles manifest a

rise in aerobic respiration, mitochondrial ATP synthesis, and oxidative phosphorylation, while RNA processes (mRNA processing, RNA splicing) tend to be slowed down. Finally, oocytes of antral follicles reveal a pattern that is opposite to primordial follicles (downregulation of cytoplasmic translation, chemotaxis, epithelial cell regulation, upregulation of cell cycle transition regulation) and secondary follicles (downregulation in aerobic respiration, mitochondrial ATP synthesis, and oxidative phosphorylation). Oocytes of antral follicles are also characterized by higher expression of genes involved in recombinational repair.

Folliculogenesis is likely a dynamic process since oocytes in follicles undergo continuous transcriptomic modifications and are not arrested at definite stages. As such, we performed a pseudotime analysis to temporally assess which genes show variation of expression in the window of folliculogenesis and to characterize the activation or repression behavior of these transcripts throughout follicular development. We first applied PHATE dimension reduction to normalized counts and discerned a transcriptomic trajectory (Figure 2A). We observed that primordial and primary follicles were almost indistinguishable in the first two dimensions (Figure 2A). A heatmap comparing differentially expressed genes all in one stage versus all other stages confirmed this observation considering that hierarchical clustering hardly separates primordial from primary follicles, revealing their transcriptomic proximity (Supplementary Figure S1A). We also observed that in the same follicle stage group, the transcriptome could be temporally different. Specifically, some antral follicles were close to secondary follicles, while the remaining antral follicles formed a clearly separated cluster later in the follicle developmental trajectory (Figure 2A), which turned out to be related to a patient effect (Patients E and G in Supplementary Figure S1B). The patients included in this study were notably healthy or suffering from reproductive pathologies of varying degrees of severity.

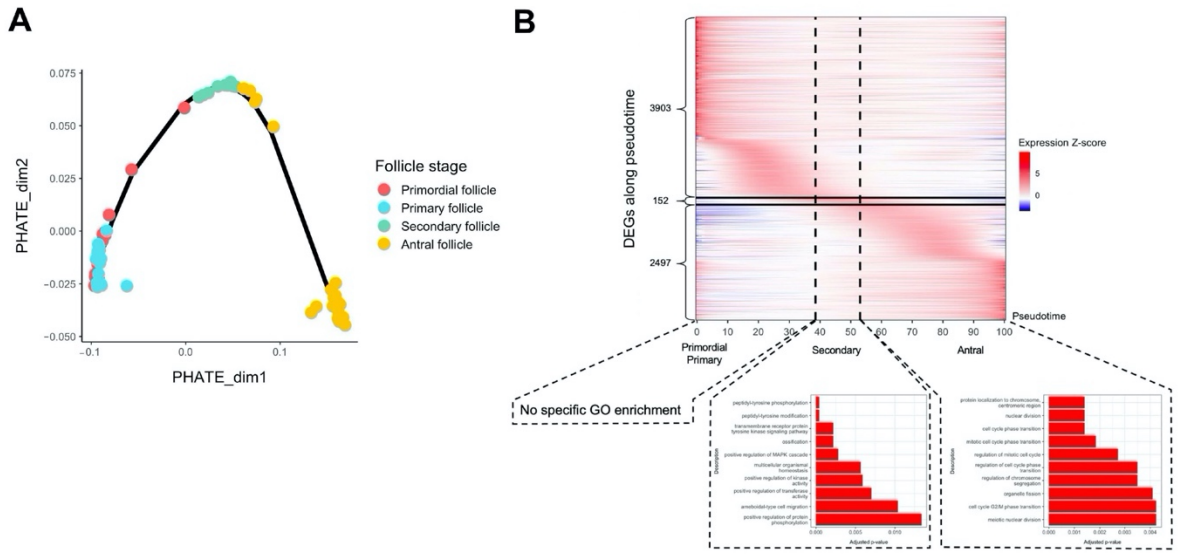

Figure 2. *Cont.*

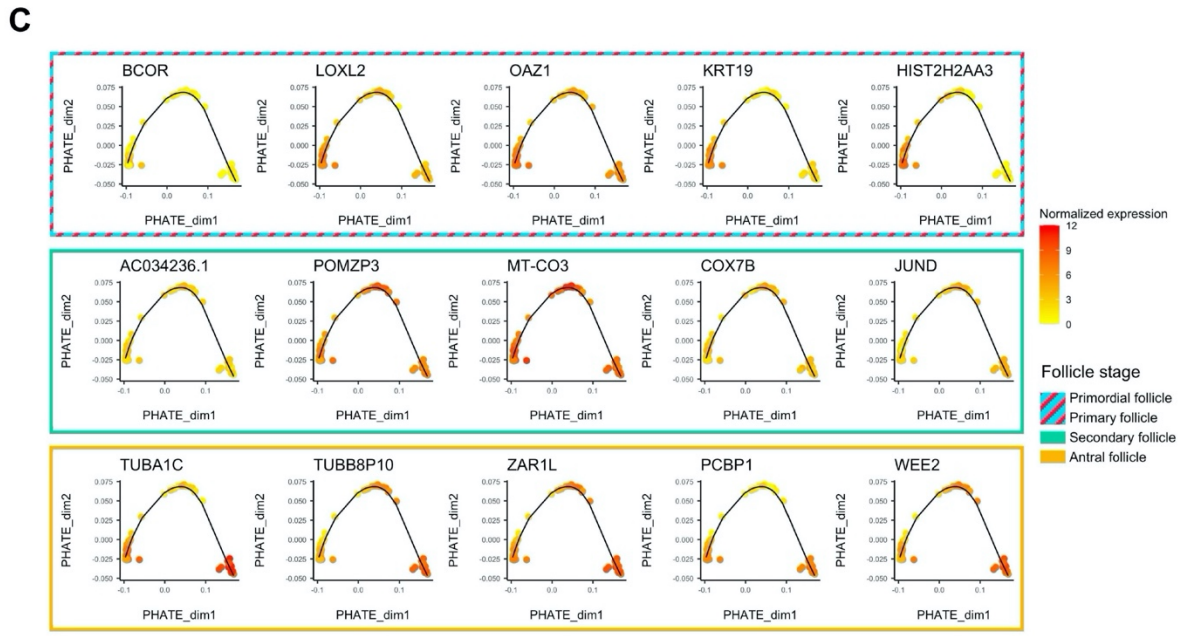

Figure 2. Trajectory analysis of transcriptomic changes along folliculogenesis. (**A**) PHATE dimensionality reduction analysis of the whole expression dataset. (**B**) Heatmap of inferred expression of the most variable significant genes along folliculogenesis (6552 genes showing average expression changed by at least logFC > 1 within the oocyte developmental trajectory). Pseudotime is a metric that could be interpreted as a timing distance between one cell and its precursor cell and helps identify the ordering of cells along a lineage based on their gene expression profile. In this analysis, pseudotime 0 represents oocytes in the beginning of the window of the oocyte developmental trajectory (early follicles), while pseudotime 100 represents oocytes in the end of the window (antral follicles). Vertical lines delimit oocytes from the primordial/primary, secondary, and antral follicle groups. Horizontal lines delimit significantly differentially expressed genes along folliculogenesis reaching their peak expression during the primordial/primary (3903), secondary (152), and antral follicle groups (2497). (**C**) Variation of expression, for each follicle stage group, of the top 5 genes differentially expressed along folliculogenesis reaching their peak expression at this stage.

Then, we generated a list of 6552 transcripts whose expression varied temporally during folliculogenesis according to our pseudotime analysis (FDR < 0.05, logFC > 1) (Supplementary Table S2). The heatmap in Figure 2B highlights the sequential waves of transcriptional activity modifications from the primordial to the antral stage (Figure 2B). Successive activation and repression of these genes may drive folliculogenesis and regulate the transition from early to late stages, which is particularly the case for transcription factors (Supplementary Figure S2). Most of the 6552 transcripts are highly expressed inside the primordial and primary follicles and show lower expression in the following stages (3903 transcripts) (Figure 2B) but they are not enriched for a specific gene ontology. The transition to a secondary follicle oocyte is marked by the activation of a small set of genes (152) related to peptidyl-tyrosine modification and kinase activity, while final follicle oocyte growth is associated with the upregulation of 2497 transcripts enriched in cell cycle pathway genes (Figure 2B). The top five genes for each follicle stage group (primordial/primary, secondary, and antral) are displayed in Figure 2C, and their function is described in Table 1.

Table 1. Description, for each follicle stage group, of the top 5 genes differentially expressed along folliculogenesis reaching their peak expression at this stage. Their function was retrieved and simplified from Uniprot database.

Gene	Timing of Peak Expression	Full Name	Function (Uniprot Description)
BCOR	Primordial Primary	BCL6 Interacting Corepressor	Transcriptional corepressor May specifically inhibit gene expression when recruited to promoter regions by sequence-specific DNA-binding proteins such as BCL6 and MLLT3
LOXL2	Primordial Primary	Lysyl oxidase homolog 2	Mediates the post-translational oxidative deamination of lysine residues on target proteins leading to the formation of deaminated lysine Acts as a transcription corepressor and specifically mediates deamination of H3K4me3, a specific tag for epigenetic transcriptional activation
OAZ1	Primordial Primary	Ornithine decarboxylase antizyme 1	Ornithine decarboxylase (ODC) antizyme protein that negatively regulates ODC activity and intracellular polyamine biosynthesis and uptake in response to increased intracellular polyamine levels
KRT19	Primordial Primary	Keratin, type I cytoskeletal 19	Involved in the organization of myofibers
HIST2H2AA3	Primordial Primary	Histone H2A type 2-A	Core component of nucleosome
AC034236.1	Secondary		Unknown
POMZP3	Secondary	POM121 and ZP3 fusion protein	Unknown
MT-CO3	Secondary	Cytochrome c oxidase subunit 3	Component of the cytochrome c oxidase, the last enzyme in the mitochondrial electron transport chain which drives oxidative phosphorylation
COX7B	Secondary	Cytochrome c oxidase subunit 7B, mitochondrial	Component of the cytochrome c oxidase, the last enzyme in the mitochondrial electron transport chain which drives oxidative phosphorylation
JUND	Secondary	Transcription factor JunD	Transcription factor binding AP-1 sites
TUBA1C	Antral	Tubulin alpha-1C chain	Tubulin is the major constituent of microtubules, a cylinder consisting of laterally associated linear protofilaments composed of alpha- and beta-tubulin heterodimers
TUBB8P10	Antral	Tubulin Beta 8 Class VIII Pseudogene 10	Pseudogene
ZAR1L	Antral	Protein ZAR1-like	mRNA-binding protein required for maternal mRNA storage, translation, and degradation during oocyte maturation Probably promotes formation of some phase-separated membraneless compartment that stores maternal mRNAs in oocytes: acts by undergoing liquid–liquid phase separation upon binding to maternal mRNAs
PCBP1	Antral	Poly(rC)-binding protein 1	Single-stranded nucleic acid binding protein that binds preferentially to oligo dC
WEE2	Antral	Wee1-like protein kinase 2	Oocyte-specific protein tyrosine kinase that phosphorylates and inhibits CDK1/CDC2 and acts as a key regulator of meiosis during both prophase I and metaphase II Required to maintain meiotic arrest in oocytes during the germinal vesicle (GV) stage Also required for metaphase II exit during egg activation

2.2. Oocyte Maturation

- Re-analysis of individual studies

Standard re-analysis of six studies comparing the transcriptome of fully grown GV and MII oocytes obtained after controlled ovarian stimulation confirmed the existence of intense modulation of maternal transcript abundance [24–29]. First, a clear separation between fully grown GV and MII oocytes was observed in all datasets using dimension reduction (PCA method) (Supplementary Figure S3). Secondly, the number of differentially expressed genes between GV and MII oocytes was high in all datasets, with an average of

33% (9–51%) of transcripts undergoing modification between the two stages (Figure 3A). According to several independent studies, the main pathways modified were related to mitochondrial processes (downregulated in MII compared to fully grown GV), cytoplasmic translation, and chromatin organization (upregulated in MII compared to fully grown GV) (Supplementary Figure S4A,B). Correlations in all transcript expressions were high between datasets, but there were some differences, likely due to technical variation, justifying the need for a meta-analysis (Figure 3B). The six RNA-seq datasets showed high correlation in all expressed gene counts (Pearson's correlation coefficient > 0.75, Figure 3B), but as seen on PCA on merged datasets, the various techniques have an influence on transcript abundance even after batch correction (Supplementary Figure S5).

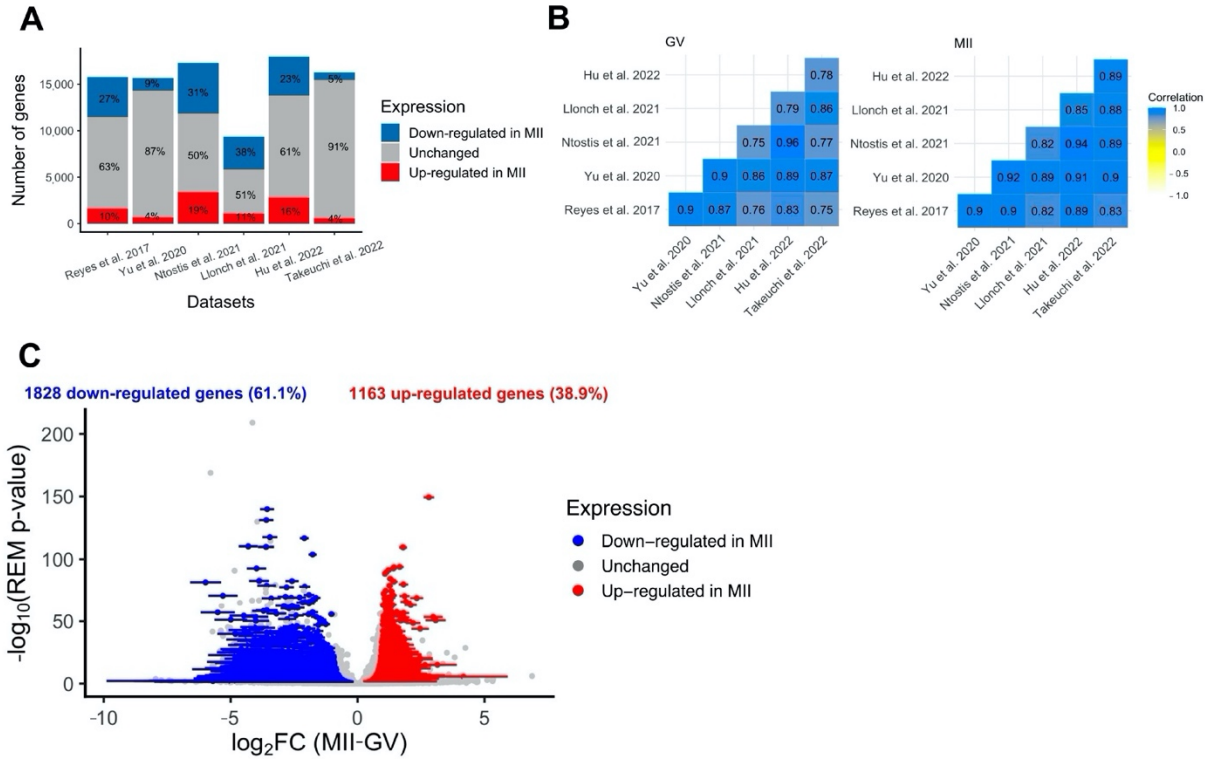

Figure 3. Differential expression analysis of genes during the GV-to-MII oocyte transition. (**A**) Results of individual differential expression analysis for the six datasets evaluated in this study. Numbers represent the percentage of genes upregulated, downregulated, or stable in MII versus GV oocytes. (**B**) Correlation of the normalized expression of all expressed genes for the six datasets evaluated in this study, respectively, for GV and MII oocytes. (**C**) Volcanoplot of the meta-analysis result for the six datasets evaluated in this study. A random effects model based on effect size (log2FC, difference of expression between MII and GV oocytes) and *p*-values from each dataset was applied. One gene is represented by one dot. A total of 2991 significant DEGs were identified (summary adjusted *p*-value from the random effect model < 0.05 and sign of log2FC consistent in all 6 studies). Blue dots represent significant DEGs downregulated in MII oocytes compared to GV. Similarly, red dots represent significant DEGs upregulated in MII oocytes compared to GV oocytes. The interval confidence of the summary log2FC is represented by the bars associated with the dots for each DEG [24–29].

- Meta-analysis

To eliminate parameters likely to influence biological effects (such as age or health condition) and increase statistical power, we conducted a meta-analysis of differentially

expressed genes (DEGs) between fully grown GV and MII oocytes. In total, the six datasets included 87 fully grown GV and 70 MII oocytes, collected from patients ranging from young to advanced maternal ages (18–44 yo). The random effects model meta-analysis identified 2991 DEGs with consistent modifications across all six datasets (Figure 3C, Supplementary Table S3). While most were downregulated in MII oocytes (61%) (Figure 3C), some displayed a higher level of transcripts in MII oocytes. Upregulated pathways were related to histone modification, nuclear maturation, and RNA processes, while downregulated pathways were related to mitochondrial processes (Figure 4). Transcript annotation revealed that DEGs were mainly protein-coding genes and, in small proportions, transposable elements or long non-coding RNAs (lncRNA) (Supplementary Figure S6A). Long terminal repeats (LTR) were mostly upregulated in MII, while long interspersed nuclear elements (LINE) elements were downregulated (Supplementary Figure S6B).

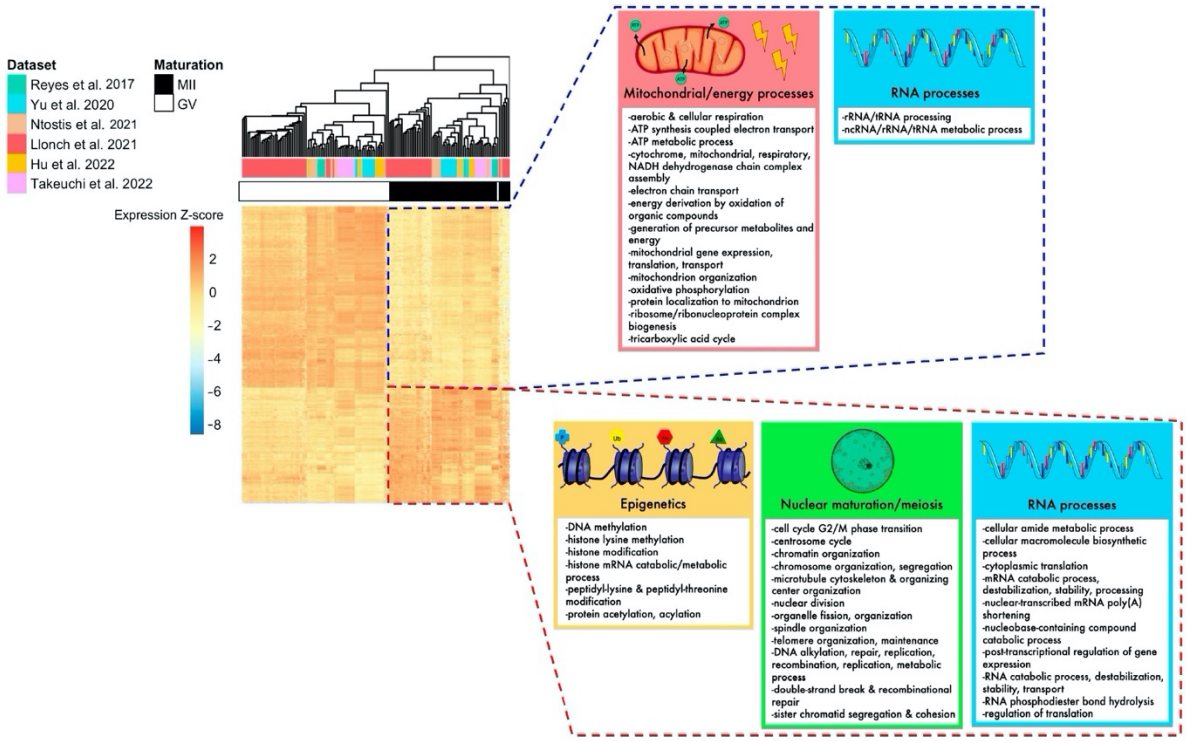

Figure 4. Summary of biological pathways enriched for DEGs identified in the meta-analysis, according to their up- or downregulation. The heatmap of DEGs identified with the meta-analysis shows that MII and GV oocytes are correctly segregated according to their expression for these genes. Mitochondrial processes, energy processes, and some RNA processes were downregulated in MII oocytes (framed in blue), while nuclear maturation/meiosis, epigenetics, and some other RNA processes were upregulated in MII oocytes (framed in red) [24–29].

We evaluated the extent of mRNA degradation during the transition from fully grown GV to MII oocyte stage according to the meta-analysis results. A substantial proportion of the transcripts was highly degraded (>70% loss) (Figure 5A). The mean degradation per transcript was 53% for downregulated transcripts (Figure 5B). Between fully grown GV and MII stages, there was a significant drop in total maternal mRNA quantity, which could be evaluated at 31% (Figure 5C). The degradation concerned transcripts from all chromosomes, whereas mtDNA gene expression was increased in MII oocytes (Figure 5D).

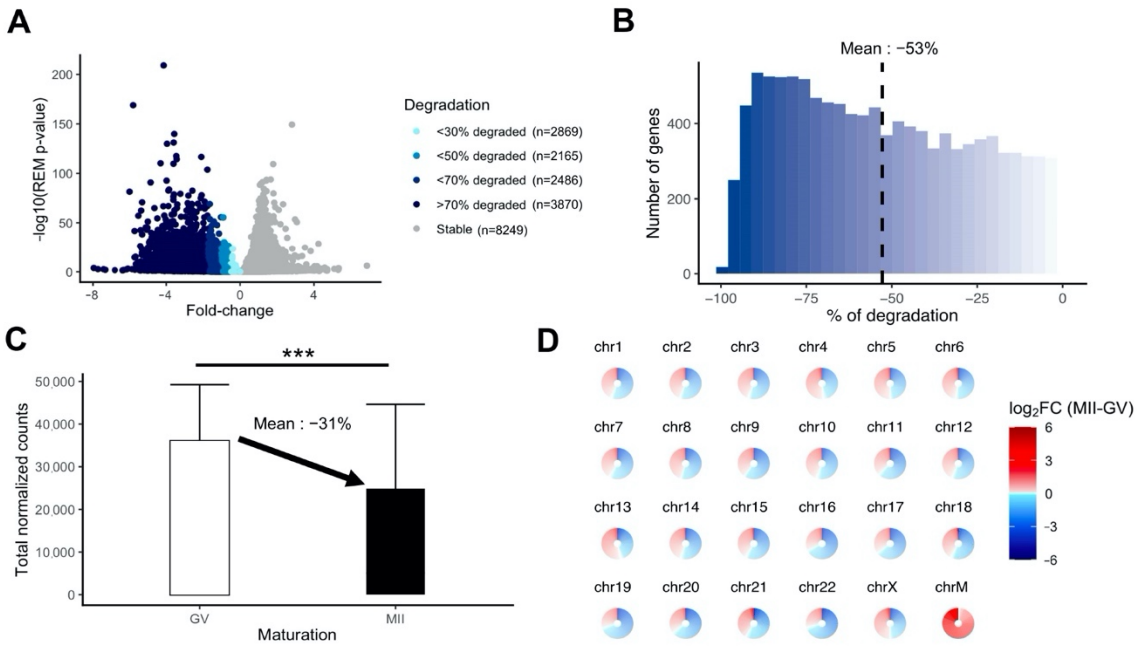

Figure 5. Measurement of the degradation of the maternal mRNA content in MII oocytes. (**A**) Volcanoplot of the meta-analysis result (MII versus GV) colored by the intensity of degradation between GV and MII stages (stable, <30% of degradation, <50% of degradation, <70% of degradation, or >70% of degradation). (**B**) Histogram focusing on the extent of degradation in downregulated transcripts in MII versus GV oocytes. (**C**) Comparison of total normalized counts between the GV and MII oocytes (significance assessed with a *t*-test, *** $p < 0.005$). (**D**) Assessment of degradation by chromosome. Each circle is divided into sections according to the number of genes on the chromosome and each section, representing one gene, is colored by the summary log2FC resulting from the meta-analysis result (MII versus GV) corresponding to the gene. ChrM: mitochondrial chromosome.

2.3. Influence of the Environment on Human Oogenesis/Folliculogenesis

We identified transcripts differentially expressed during folliculogenesis or the GV-to-MII transition; these transcripts are also putative transcripts susceptible to environmental stressors occurring in the window of oocyte development (maternal age, polycystic ovary syndrome (PCOS), in vitro maturation (IVM), cryopreservation). A list of these genes is available in Table 2 and a summary of studies on the factors evaluated can be found in Supplementary Table S4.

Table 2. Comparison of folliculogenesis and oogenesis-specific genes identified in this review with previous putative genes sensitive to the environment (PCOS, maternal age, IVM, cryoconservation). Only DEGs retrieved in >2 studies for each factor were considered to increase robustness of the analysis.

Factor	Folliculogenesis Cross-Checking	GV-to-MII Cross-Checking
PCOS	*ARHGAP18 ATRX CNOT6 EEA1 KLHL32 LAMP3 LRRTM4 POMP RASA1 SCAMP2 SERPINB5 UBE2V2 ZDHHC6*	*AMOT ARHGAP18 ATRX C3orf14 CASP8 CNOT6 CTNND1 EEA1 FKBP4 NFRKB NIF3L1 PRPS2 SERPINB5 TNRC6A*
Maternal age	*ABHD5 ATRX C12orf75 C1orf146 C5orf58 CNIH4 COX7B DEAF1 GCA GPX1 HAL LGALS12 LSM8 MRFAP1 MRPL22 NDUFA1 NDUFB6 PIN1 PIR PLEKHF2 POMZP3 PTBP2 RAD23B SAA1 SCGB3A2 SLC10A3 SNAP23 STYK1 TICAM1 TMEM65 TSPAN13 TSPYL5 TUBA3E TXNDC12 UCHL3 ZAR1L*	*ABHD5 ARPC1A ARPC3 ATRX BDH2 C5orf58 CFL2 CNIH4 CYB5A DYNLL1 EIF6 ELP1 LGALS12 LSM6 MRPL22 MYL12A NDUFA1 NDUFAF6 NDUFS6 PDCD5 PIN1 PPA1 PPRC1 PSMB1 PTS RECQL4 RMI2 SCCPDH SNRPA1 SRRM1 TMEM65 UCHL3*
IVM	*ATP5MG DCTN6 LYPLAL1 NFE2L2 PAOX PCF11 TAF1A*	*DAZL DDX59 DEPDC7 EXOSC8 MKKS MRPL20 PSMB1*
Oocyte cryoconservation	*FOXO3B PRKCSH RSPH4A SF3A2 TRPC3 TYMS UBXN4 USP4 ZWINT*	*DYSF UBXN4 ZNF530*

DEGs: differentially expressed genes; IVM: in vitro maturation; PCOS: polycystic ovary syndrome.

3. Discussion

The oocyte is the largest human cell and one of the richest in mRNA quantity [30]. It determines early embryonic competence and its transcriptome contains many secrets waiting to be revealed [31]. In this study, we comprehensively gathered scRNA-seq datasets from human oocytes at multiple stages during the long process of oocyte growth and maturation and decrypted the transcriptomic reorganization required to ensure that the oocyte becomes fully competent. We believe it is important to focus on human oocyte regulation exclusively, as previous studies comparing human oocyte maturation with other mammalian species revealed very few overlaps in the individual transcripts modified, even if major biological processes activation/repression were similar [18].

Folliculogenesis and oocyte maturation imply specific regulation during oocyte development. First, variation in chromatin accessibility determines the activity of transcription, which is high within early follicles but absent after GV breakdown [7,32]. Secondly, transcription factor activity shapes the oocyte transcriptome during folliculogenesis by upregulating or downregulating specific transcripts to allow the transition from a primary to a pre-ovulatory follicle oocyte [33]. Thirdly, selective degradation or translation of maternal transcripts is a prerequisite for cytoplasmic maturation, leading to a fertilizable MII oocyte that can ensure the first embryonic divisions [14].

Our chronological gene ontology comparison analysis revealed signature pathways activated and repressed in oocytes from the different follicle stages. The primordial stage may reflect strong communication between the oocyte and its surrounding cells, manifested by an upregulation of genes related to cell adhesion, epithelial cell proliferation, and collagen fibril organization pathways, which tend to be reduced afterwards. Communication with the surrounding cells, such as granulosa, plays a pivotal role in oocyte growth via the action of paracrine factors [34]. Oocytes mobilize specific transcripts such as *GDF9*, *TGFB1*, and *ACTN1*, to act on granulosa cell proliferation and maintain gap junctions [35,36]. Moreover, downregulation of cytoplasmic translation was seen in antral follicles while the highest activity was observed in primordial follicles, which corroborates the findings that progressively maternal mRNAs are not translated but stored until they are degraded or translated after meiosis resumption following GVBD. Oocytes from primordial follicles also show downregulation of cell cycle pathways which agrees with their arrest at the diplotene stage of meiosis I until their activation [37]. In the antral follicle, cell cycle phase transition pathways are upregulated, possibly correlating with the acquisition of meiotic competence to sustain proximate oocyte maturation [38]. One of our conclusions would be that the oocytes at the primary follicle stage do not display a highly specific transcriptomic profile compared to the primordial follicle. The transition between both stages is likely to be mRNA quantity-specific rather than pathway-specific, meaning that primary follicle oocytes accumulate mRNA drastically but not selectively. This primary-to-primordial transition may be driven by a specific regulatory network involving transcription factors and long non-coding RNAs according to previous evidence [23,39]. Then, the transition from an early follicle oocyte to a secondary follicle oocyte is marked by a switch in energy consumption. Activation of mitochondrial ATP synthesis, aerobic respiration, and oxidative phosphorylation sustain major structural and biochemical evolution, which are energy-intensive processes [40]. Furthermore, mRNA processing and notably splicing are slowed down in secondary follicle oocytes compared to other stages. Finally, oocytes in antral follicles turn off energy activity possibly passively (downregulation of aerobic respiration and oxidative phosphorylation pathways) because of the difficulty of accessing O_2 in a restricted micro-environment, according to mathematical modelling in humans [41–43]. We also observed that oocytes in antral follicles show an increased ability to repair DNA alterations compared to other stages (upregulation of recombinational repair pathway), which is confirmed by previous observations [44].

Taking advantage of the single-cell nature of the Zhang et al. dataset [23], we then applied trajectory analysis along folliculogenesis to characterize continuous transcriptomic changes. We identified a bunch of genes showing significant variation in expression from

primordial-to-antral follicle oocyte development and characterized their temporal regulation. This revealed that a large majority of them were highly upregulated during the early follicle stages, seemingly biologically unspecific as no Gene Ontology showed enrichment for them. This confirms our hypothesis of an unspecific accumulation of transcripts during the primary follicle stage. Surprisingly, only about a hundred folliculogenesis variable genes show a peak of expression in the window of the secondary follicle stage, which appeared to be related to peptidyl-tyrosine modification and regulation of kinase (notably the MAPK cascade) and transferase activity. Following transcriptional waves of upregulation may involve the preparation for meiosis resumption in the antral follicle oocyte.

Furthermore, we observed that depending on the patients, the transcriptome dynamic displayed different kinetics of progression. Differences between patients in the previously published dataset used herein could stem from the inclusion of patients with particular pathological conditions (cervical cancer, endometrial cancer, lymphoma), which may affect reproductive functions. This could lead to unwanted bias in the interpretation of the results as a small number of patients for each follicle stage were included.

Next, we better characterized the downfall undergone by maternal mRNAs during late oogenesis. We found an average decline of 30% in total mRNA from fully grown GV to the MII stage across studies. Previous studies indicated that 60% of maternal transcripts are degraded from the fully grown GV to MII stage, using mass measures [45,46]. The difference observed may be a direct consequence of the fact that mRNAs with short polyA tails are not captured by the employed sequencing technologies. Therefore, our analysis mirrors the biological pathways that are recruited in a timely manner (mRNAs with long polyA tails on the verge of being degraded or translated) rather than how degraded all maternal transcripts are. However, this approach displays the selective downregulation of specific transcripts. Indeed, transcripts associated with energy production and mitochondrial functions were extensively downregulated, while those associated with cytoplasmic translation, histone modification, meiotic processes, and RNA processes were conserved. The downregulation of mitochondrial processes is highly conserved across mammals and may be a protective system with respect to oxidative stress via ROS production and the inability of the early embryo to protect against these stressors as reported in rhesus monkey, mouse, and cow models [18,47]. Concomitantly, MII oocytes should have already synthesized sufficient mtDNA to support key developmental events such as epigenetic programming [48]. The new meta-analysis we proposed found that genes involved in mobilization of cytoplasmic translation, histone modification, meiotic processes, and RNA processes are upregulated in MII oocytes, which are metabolic pathways crucial for the multiplicity of maturations (cytoplasmic-nuclear-epigenetic) required by the oocyte.

Interestingly, the transition from fully grown GV to MII oocytes displayed upregulation of a substantial number of transcripts, whereas oocytes are thought to be transcriptionally quiescent. This could be explained by several hypotheses. First, as explained, the scRNA-sequencing methods used in the meta-analyzed studies captured mRNA with long polyA tails, thus reflecting the amount of mRNA that can be recruited for translation and not silenced or set to degrade mRNAs with short polyA tails. Some transcripts are still enrolled for translation during the GV-MII transition via polyA lengthening, showing them to be upregulated in MII oocytes. A second hypothesis that still needs investigation is that transcriptional quiescence after the GVBD stage is not total [49,50]. This theory is contrasted by a third hypothesis, only proven in *C. elegans*, assuming that oocytes after GVBD cannot synthetize mRNA but can accumulate transcripts from surrounding somatic cells, supposedly via extracellular vesicles [51].

Furthermore, we intended to re-analyze studies comparing failed-to-mature oocytes versus mature oocytes. In Pietroforte et al., the authors did not identify any DEG between both groups, while the low number of samples in Li et al. (three oocytes per group) would be too low to detect expression differences with satisfactory power [52,53]. Then, it remains crucial to assess the biological reasons behind oocyte maturation failure and whether transcriptomic abnormalities would be responsible for it. In some cases, defects in the

maternal mRNA degradation machinery would be involved, notably an alteration in the expression of *Btg4* or *Msy2* in mice [22,54,55]. This would lead to the unwanted maintenance of certain categories of transcripts detrimental to oocyte fertility or embryonic development.

In addition, throughout growth and maturation, oocytes are exposed to multiple environmental stressors, which can alter the sequential gene expression changes governing oocyte development [56]. Our identification of transcripts expressed along oocyte development that are highly susceptible to those factors is of major importance, as they may be the key to understanding the apparition of oocyte defects and deficiencies and overcoming these outcomes [27–29,57–67]. For oocyte in vitro maturation and cryoconservation, regaining expected levels of expression of those transcripts by adapting assisted reproductive protocols may become a path of research to increase mature oocyte rates in the future. For age and PCOS, identification of those transcripts is also important to understand the precise underlying mechanisms. In future studies, it would be highly interesting to observe transcriptomic modifications in the same patient from the primordial follicle stage and compare the dynamic of transcriptional changes between several donors, particularly under pathological conditions (pathology versus control).

To conclude, the oocyte transcriptome follows a dynamic that is tightly controlled. Overall, we have decoded the regulatory events of maternal mRNAs that lead the oocyte to grow and undergo multiple types of maturation, which we synthetized in Figure 6. The atlas of transcriptomic modifications described here will facilitate the precise identification of the transcripts involved in the failure of oocyte growth and maturation in future research.

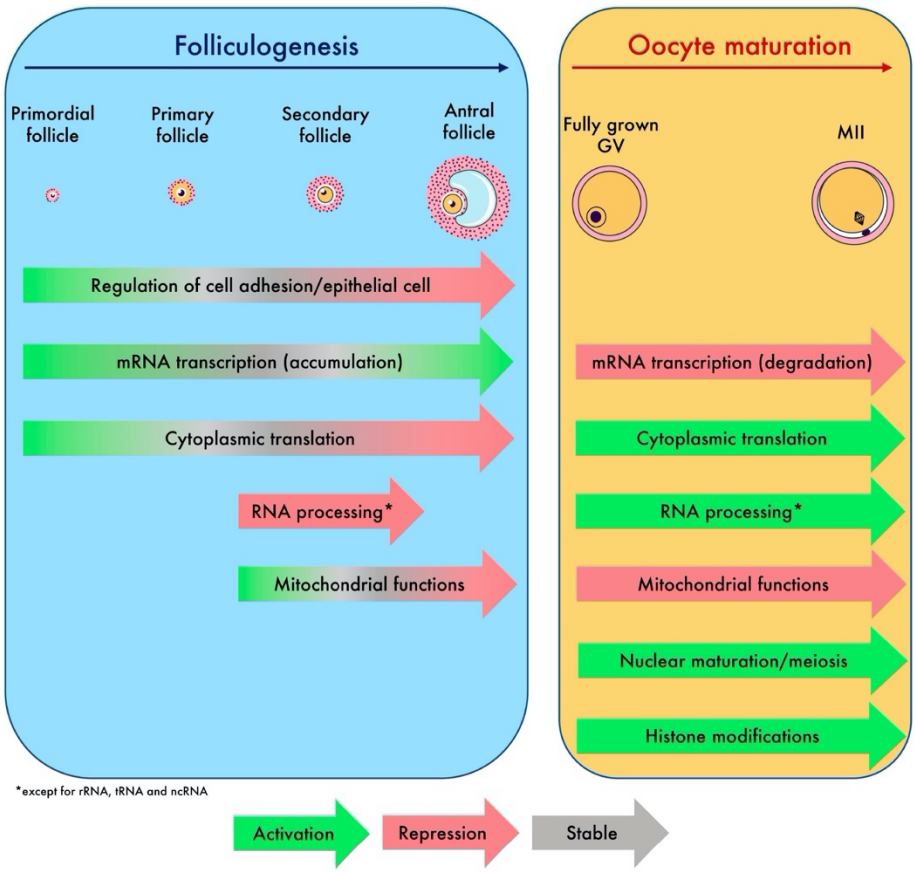

Figure 6. Summary of biological processes and global transcriptomic events driving oocyte growth and maturation identified in this study.

4. Materials and Methods

4.1. Population

To examine the transcriptomic modifications experienced by the oocyte along human folliculogenesis, we included datasets comprising human primary oocytes from primordial to antral follicles (at least two different stages). To examine the transcriptomic modifications experienced by the oocyte throughout human oogenesis, we included datasets comprising human immature fully grown GV (prophase I arrested), MI (metaphase of meiosis I), and MII oocytes collected from controlled ovarian hyperstimulation protocols. Inclusion was also conditional on the sequencing method, which had to be single-oocyte RNA-seq. Only single-denuded oocytes were considered, meaning that oocytes surrounding cells were excluded from this review. Oocytes recovered in all clinical contexts were included, whether they were collected from donors or patients seeking infertility treatment, from in vitro or in vivo maturation, and at all maternal ages. No restrictions were placed on the publication date of datasets. A summary of the included studies with information on population characteristics, study design, and sequencing protocol is presented in Table 3.

4.2. Dataset Collection

All the datasets used in this study are available in public repositories. Raw data (.fastq) were downloaded from European Nucleotide Archive accessions: PRJNA666614, PRJNA508772, PRJNA377237, PRJNA811110, PRJNA701233, PRJNA690226 and PRJNA421274.

4.3. Dataset Processing

For each dataset, adapters and low-quality sequences were trimmed using TrimGalore! V0.6.6. Next, paired-end alignment was performed onto human reference genome (hg38) with STAR v2.7.9a, reporting randomly one position and allowing 6% of mismatches. Transposable element (TE) annotation was downloaded from RepeatMasker and joined with Gencode v19 gene annotation [68] to measure their expression level as TEs are crucial in the regulation of gametes and embryos gene expression. Finally, gene expression was quantified with featureCounts v2.0.1.

All datasets were processed following a standard procedure. Genes with low counts were removed with the filterByExpr function from the edgeR R package. Counts were normalized using the limma-voom method. When clinical information was available, we used duplicateCorrelation to account for samples from the same patients (considered as technical replicates).

For comparison of folliculogenesis stages (oocytes from primordial, primary, secondary, and antral follicles), differential analysis was performed between oocytes from one stage versus all stages using limma (differentially expressed if FDR < 0.05 and FC > 2 or FC < 0.5). This analysis was designed to identify a specific signature for each follicular stage. Because folliculogenesis is likely a dynamic process, a pseudotime analysis was implemented using tradeSeq using PHATE reduction to find differentially expressed genes throughout folliculogenesis rather than separating oocytes into distinct clusters [69,70]. This will identify precisely in time which genes are activated and repressed in oocytes during the development of follicles, from the primordial to the antral stage. The advantage of PHATE reduction is that it relies on diffusion dynamics and is thus particularly suitable to assess developmental trajectories such as oocyte growth.

For the comparison between GV, MI, and MII oocytes, differential analysis was performed between stage groups for each independent dataset using limma. Maternal age was incorporated as a covariate when available. Genes were considered differentially expressed when FDR < 0.05 and FC > 2 or FC < 0.5.

All PCAs in this article were performed using PCAtools on normalized expression (log2(cpm + 1)) removing the 10% genes with the lowest variance. Pathway analyses were run with clusterProfiler using the enrichGO function. For the purpose of visualization, independent datasets were corrected for batch effects using ComBat. All heatmaps were created with the pheatmap R package.

Table 3. Characteristics of studies re-analyzed in this review.

Study	Year	Population	nGV	nMI	nMII	Ovarian Stimulation	Oocytes/Follicles Collection and Processing	RNA-Seq
Reyes et al. [29].	2017	*n* = 5 (1 GV and 1 IVM-MII for each patient) Age: *n* = 5 < 30 yo (26.8, 20–29/*n* = 5 >= 40 yo (41.6, 40–43) Varying causes of infertility	10		10	FSH + hCG for final follicular maturation	GV processed immediately MII obtained after 24 h IVM	Isolation: PicoPure RNA Isolation kitRT: anchored oligo(dT) Library: Thruplex DNA-seq kit Sequencing: Illumina paired-end 100 bp (HiSeq2500)
Yu et al. [26]	2020	*n* = 17 Age: GV 35.3 yo (28–41), MI 36.1 yo (32–41), MII 32.6 yo (27–39)	7	7	7	Unknown	MII from oocyte donors who had excess oocytes that removed them from donor list	RT: SMART-Seq v4 ultra low input RNA kit Library: Illumina TruSeq
Ntostis et al. [28]	2021	*n* = 12 Age: *n* = 6 21.6 yo (21–26 yo)/*n* = 6 42.0 yo (41–44 yo) Young maternal age group = oocyte donor Advanced maternal age = unexplained infertility, male infertility or age	10		11	Short GnRH agonist protocol + rFSH + hCG trigger	In vivo matured	RT: SMART-Seq v4 ultra low input RNA kit Library: Illumina's Nextera XT Sequencing: Illumina sequencing 150 bp (HiSeq3000)
Llonch et al. [27]	2021	*n* = 37 (25 donors, 12 patients) Age: 28.8 yo (18–43) AFC: 22.1 (4–46) Patient: advanced maternal age or male factor infertility	44		31	GnRH antagonist + FSH or HP-hMG + hCG or triptorelin	GV processed immediately MII obtained after 30 h IVM	Smart-seq2 protocol RT: SuperScript II with oligo-dT Library: Illumina's Nextera XT Sequencing: Illumina paired-end 75 bp (HiSeq4000)
Hu et al. [25]	2022	Age: <35 yo	9		5	GnRH antagonist or long agonist protocol, hCG trigger	2 replicates of 10 pooled oocytes from different donors (for GV and MII) or single oocytes Oocytes were vitrified/thawed	T&T-seq Isolation: TRIzol + isopropanol RT: Single Cell Full-Length mRNA-Amplification Kit Library: TruePrep® DNA Library Prep Kit V2 Sequencing: (Novaseq 6000)

Table 3. *Cont.*

Study	Year	Population	nGV	nMI	nMII	Ovarian Stimulation	Oocytes/Follicles Collection and Processing	RNA-Seq
Takeuchi et al. [24]	2022	*n* = 11 Age: 30–39 yo	7	6	6		Surplus oocytes other than the MII stage were subjected to IVM: GV, MI, and MII collected after IVM Oocytes that remained immature at the time sampling were left in the maturation medium overnight and examined on the next day of the oocyte retrieval 4 GV, 3 MI, 3 MII after 7.5–9 h IVM 3 GV, 3 MI, 3 MII after 15–16.5 h IVM	RT: SMART-seq v4 Ultra Low Input RNA Kit Library: Nextera XT DNA Library Preparation Kit Sequencing: paired-end 50 bp + 25 bp (NextSeq)
			87	13	70			
Zhang et al. [23]	2018	*n* = 8 Age: 27.7 yo (24–32) Sex reassignment surgery, cervical cancer, endometrial cancer, benign ovarian mass, or lymphoma but without histopathological abnormality	*n* = 17 primordial follicles *n* = 25 primary follicles *n* = 12 secondary follicles *n* = 23 antral follicles			NA		Library: Kappa Hyper Prep Kit

AFC: antral follicle count; FSH: follicle-stimulating hormone; GnRH-a: gonadotrophin-releasing hormone; GV: germinal vesicle; hCG: human chorionic gonadotrophin; HP-hMG: highly purified human menopausal gonadotrophin; IVM: in vitro maturation; MI: metaphase I; MII: metaphase II; RT: retrotranscription.

4.4. Meta-Analysis

A meta-analysis between all datasets comparing fully grown GV, MI, and MII oocytes was performed with MetaVolcanoR, which relies on the metafor package [71,72]. We summarized the expression fold change for each gene across the six independent datasets, implementing a random effects model using effect size (log2FC) and raw *p*-values from each dataset as input. The resulting estimation of a summary *p*-value for each gene indicates the probability of the summary expression fold-change being equal to zero. The advantage of the random effects model is the consideration of heterogeneity between studies (between-study effect variance) in addition to the within-study effect variance. For each gene, we considered significant expression change with an adjusted summary *p*-value < 0.05 and consistency (same sign of log2FC) in all studies.

Degradation or accumulation of mRNA quantity for each transcript through final oocyte maturation was calculated by converting the summary log(fold-change) to the percentage difference of normalized expression between baseline and the compared group. Transcripts with higher level of transcripts in MII than in fully grown GV were considered stable due to the assumed transcriptional quiescence of oocytes during the GV-to-MII transition (difference in polyadenylation and not quantity).

Because of the low number of studies that included MI oocytes (n = 2) and their reduced sample size (respectively, 6 and 7 MI), results including the comparison of MI with fully grown GV and MII oocytes are not discussed further (high risk of bias).

4.5. Influence of the Environment on Human Oogenesis/Folliculogenesis

In a previous review on the transcriptomic integrity of human oocytes used in assisted reproductive techniques (ARTs), we discussed the biological mechanisms likely to be altered in the context of ART interventions, maternal aging, a suboptimal lifestyle, or reproductive health issues [56]. We believe it would be highly interesting to identify oocyte growth and maturation-specific transcripts dysregulated by those factors. Thereby, available lists of DEGs from each study discussed in our previous review were retrieved and cross-checked for each environmental factor considered (endometriosis, PCOS, maternal age, smoking, body mass index (BMI), ovarian stimulation, IVM, and cryopreservation) to find common transcripts dysregulated between at least two studies. Those lists were in turn cross-checked with lists of DEGs identified in our folliculogenesis and oocyte maturation differential expression analyses. Previous studies on granulosa and cumulus cells were not considered here.

Supplementary Materials: The following supporting information can be downloaded at: https://www.mdpi.com/article/10.3390/ijms25010033/s1.

Author Contributions: Conceptualization, B.D. and P.F.; Methodology, B.D.; Software, B.D.; Formal Analysis, B.D.; Investigation, B.D. and P.F.; Data Curation, B.D.; Writing—Original Draft Preparation, B.D. and P.F.; Writing—Review and Editing, B.D. and P.F.; Visualization, B.D.; Supervision, P.F.; Critical Revision and Editing, L.F. and C.P. All authors have read and agreed to the published version of the manuscript.

Funding: This work was supported by funding from the Agence Nationale pour la Recherche ('CARE'-ANR JCJC 2017).

Informed Consent Statement: Not applicable.

Data Availability Statement: Data are contained within the article and supplementary materials.

Acknowledgments: We thank Suzanne Rankin for her help in proofreading the manuscript.

Conflicts of Interest: The authors declare no conflict of interest.

References

1. Bendsen, E.; Byskov, A.G.; Andersen, C.Y.; Westergaard, L.G. Number of Germ Cells and Somatic Cells in Human Fetal Ovaries during the First Weeks after Sex Differentiation. *Hum. Reprod.* **2006**, *21*, 30–35. [CrossRef] [PubMed]

2. Tripathi, A.; Prem Kumar, K.V.; Chaube, S.K. Meiotic Cell Cycle Arrest in Mammalian Oocytes. *J. Cell Physiol.* **2010**, *223*, 592–600. [CrossRef] [PubMed]
3. Eppig, J.J. Coordination of Nuclear and Cytoplasmic Oocyte Maturation in Eutherian Mammals. *Reprod. Fertil. Dev.* **1996**, *8*, 485–489. [CrossRef] [PubMed]
4. Watson, A.J. Oocyte Cytoplasmic Maturation: A Key Mediator of Oocyte and Embryo Developmental Competence. *J. Anim. Sci.* **2007**, *85*, E1–E3. [CrossRef] [PubMed]
5. Conti, M.; Franciosi, F. Acquisition of Oocyte Competence to Develop as an Embryo: Integrated Nuclear and Cytoplasmic Events. *Hum. Reprod. Update* **2018**, *24*, 245–266. [CrossRef]
6. Fan, H.-Y.; Sun, Q.-Y. Oocyte Meiotic Maturation. In *The Ovary*; Elsevier: Amsterdam, The Netherlands, 2019; pp. 181–203.
7. Gu, C.; Liu, S.; Wu, Q.; Zhang, L.; Guo, F. Integrative Single-Cell Analysis of Transcriptome, DNA Methylome and Chromatin Accessibility in Mouse Oocytes. *Cell Res.* **2019**, *29*, 110–123. [CrossRef]
8. Luciano, A.M.; Lodde, V.; Franciosi, F.; Tessaro, I.; Corbani, D.; Modina, S.C. Large-Scale Chromatin Morpho-Functional Changes during Mammalian Oocyte Growth and Differentiation. *Eur. J. Histochem.* **2012**, *56*, 231–235. [CrossRef]
9. Wu, D.; Dean, J. EXOSC10 Sculpts the Transcriptome during the Growth-to-Maturation Transition in Mouse Oocytes. *Nucleic Acids Res.* **2020**, *48*, 5349–5365. [CrossRef]
10. Jiang, Y.; Adhikari, D.; Li, C.; Zhou, X. Spatiotemporal Regulation of Maternal MRNAs during Vertebrate Oocyte Meiotic Maturation. *Biol. Rev.* **2023**, *98*, 900–930. [CrossRef]
11. Sha, Q.Q.; Zheng, W.; Wu, Y.W.; Li, S.; Guo, L.; Zhang, S.; Lin, G.; Ou, X.H.; Fan, H.Y. Dynamics and Clinical Relevance of Maternal MRNA Clearance during the Oocyte-to-Embryo Transition in Humans. *Nat. Commun.* **2020**, *11*, 4917. [CrossRef]
12. Cornet-Bartolomé, D.; Barragán, M.; Zambelli, F.; Ferrer-Vaquer, A.; Tiscornia, G.; Balcells, S.; Rodriguez, A.; Grinberg, D.; Vassena, R. Human Oocyte Meiotic Maturation Is Associated with a Specific Profile of Alternatively Spliced Transcript Isoforms. *Mol. Reprod. Dev.* **2021**, *88*, 605–617. [CrossRef]
13. Tora, L.; Vincent, S.D. What Defines the Maternal Transcriptome? *Biochem. Soc. Trans.* **2021**, *49*, 2051–2062. [CrossRef] [PubMed]
14. Su, Y.Q.; Sugiura, K.; Woo, Y.; Wigglesworth, K.; Kamdar, S.; Affourtit, J.; Eppig, J.J. Selective Degradation of Transcripts during Meiotic Maturation of Mouse Oocytes. *Dev. Biol.* **2007**, *302*, 104–117. [CrossRef] [PubMed]
15. Jiang, Z.Y.; Fan, H.Y. Five Questions toward MRNA Degradation in Oocytes and Preimplantation Embryos: When, Who, to Whom, How, and Why? *Biol. Reprod.* **2022**, *107*, 62–75. [CrossRef] [PubMed]
16. Christou-Kent, M.; Dhellemmes, M.; Lambert, E.; Ray, P.F.; Arnoult, C. Diversity of RNA-Binding Proteins Modulating Post-Transcriptional Regulation of Protein Expression in the Maturing Mammalian Oocyte. *Cells* **2020**, *9*, 662. [CrossRef] [PubMed]
17. Svoboda, P.; Franke, V.; Schultz, R.M. Sculpting the Transcriptome During the Oocyte-to-Embryo Transition in Mouse. In *Current Topics in Developmental Biology*; Academic Press Inc.: Cambridge, MA, USA, 2015; Volume 113, pp. 305–349, ISBN 9780124095236.
18. Schall, P.Z.; Latham, K.E. Essential Shared and Species-Specific Features of Mammalian Oocyte Maturation-Associated Transcriptome Changes Impacting Oocyte Physiology. *Am. J. Physiol. Cell Physiol.* **2021**, *321*, C3–C16. [CrossRef] [PubMed]
19. Labrecque, R.; Sirard, M.A. The Study Ofmammalian Oocyte Competence by Transcriptome Analysis: Progress and Challenges. *Mol. Hum. Reprod.* **2014**, *20*, 103–116. [CrossRef] [PubMed]
20. Suo, L.; Zhou, Y.X.; Jia, L.L.; Wu, H.B.; Zheng, J.; Lyu, Q.F.; Sun, L.H.; Sun, H.; Kuang, Y.P. Transcriptome Profiling of Human Oocytes Experiencing Recurrent Total Fertilization Failure. *Sci. Rep.* **2018**, *8*, 17890. [CrossRef]
21. Rong, Y.; Ji, S.Y.; Zhu, Y.Z.; Wu, Y.W.; Shen, L.; Fan, H.Y. ZAR1 and ZAR2 Are Required for Oocyte Meiotic Maturation by Regulating the Maternal Transcriptome and MRNA Translational Activation. *Nucleic Acids Res.* **2019**, *47*, 11387–11402. [CrossRef]
22. Medvedev, S.; Pan, H.; Schultz, R.M. Absence of MSY2 in Mouse Oocytes Perturbs Oocyte Growth and Maturation, RNA Stability, and the Transcriptome. *Biol. Reprod.* **2011**, *85*, 575–583. [CrossRef]
23. Zhang, Y.; Yan, Z.; Qin, Q.; Nisenblat, V.; Chang, H.M.; Yu, Y.; Wang, T.; Lu, C.; Yang, M.; Yang, S.; et al. Transcriptome Landscape of Human Folliculogenesis Reveals Oocyte and Granulosa Cell Interactions. *Mol. Cell* **2018**, *72*, 1021–1034.e4. [CrossRef] [PubMed]
24. Takeuchi, H.; Yamamoto, M.; Fukui, M.; Inoue, A.; Maezawa, T.; Nishioka, M.; Kondo, E.; Ikeda, T.; Matsumoto, K.; Miyamoto, K. Single-Cell Profiling of Transcriptomic Changes during in Vitro Maturation of Human Oocytes. *Reprod. Med. Biol.* **2022**, *21*, e12464. [CrossRef] [PubMed]
25. Hu, W.; Zeng, H.; Shi, Y.; Zhou, C.; Huang, J.; Jia, L.; Xu, S.; Feng, X.; Zeng, Y.; Xiong, T.; et al. Single-Cell Transcriptome and Translatome Dual-Omics Reveals Potential Mechanisms of Human Oocyte Maturation. *Nat. Commun.* **2022**, *13*, 5114. [CrossRef] [PubMed]
26. Yu, B.; Jayavelu, N.D.; Battle, S.L.; Mar, J.C.; Schimmel, T.; Cohen, J.; Hawkins, R.D. Single-Cell Analysis of Transcriptome and DNA Methylome in Human Oocyte Maturation. *PLoS ONE* **2020**, *15*, e0241698. [CrossRef] [PubMed]
27. Llonch, S.; Barragán, M.; Nieto, P.; Mallol, A.; Elosua-Bayes, M.; Lorden, P.; Ruiz, S.; Zambelli, F.; Heyn, H.; Vassena, R.; et al. Single Human Oocyte Transcriptome Analysis Reveals Distinct Maturation Stage-Dependent Pathways Impacted by Age. *Aging Cell* **2021**, *20*, e13360. [CrossRef] [PubMed]
28. Ntostis, P.; Iles, D.; Kokkali, G.; Vaxevanoglou, T.; Kanavakis, E.; Pantou, A.; Huntriss, J.; Pantos, K.; Picton, H.M. The Impact of Maternal Age on Gene Expression during the GV to MII Transition in Euploid Human Oocytes. *Hum. Reprod.* **2021**, *37*, 80–92. [CrossRef] [PubMed]
29. Reyes, J.M.; Silva, E.; Chitwood, J.L.; Schoolcraft, W.B.; Krisher, R.L.; Ross, P.J. Differing Molecular Response of Young and Advanced Maternal Age Human Oocytes to IVM. *Hum. Reprod.* **2017**, *32*, 2199–2208. [CrossRef]

30. Kataruka, S.; Modrak, M.; Kinterova, V.; Malik, R.; Zeitler, D.M.; Horvat, F.; Kanka, J.; Meister, G.; Svoboda, P. MicroRNA Dilution during Oocyte Growth Disables the MicroRNA Pathway in Mammalian Oocytes. *Nucleic Acids Res.* **2020**, *48*, 8050–8062. [CrossRef]
31. Kocabas, A.M.; Crosby, J.; Ross, P.J.; Otu, H.H.; Beyhan, Z.; Can, H.; Tam, W.L.; Rosa, G.J.M.; Halgren, R.G.; Lim, B.; et al. The Transcriptome of Human Oocytes. *Proc. Natl. Acad. Sci. USA* **2006**, *103*, 14027–14032. [CrossRef]
32. De La Fuente, R.; Eppig, J.J. Transcriptional Activity of the Mouse Oocyte Genome: Companion Granulosa Cells Modulate Transcription and Chromatin Remodeling. *Dev. Biol.* **2001**, *229*, 224–236. [CrossRef]
33. Hamazaki, N.; Kyogoku, H.; Araki, H.; Miura, F.; Horikawa, C.; Hamada, N.; Shimamoto, S.; Hikabe, O.; Nakashima, K.; Kitajima, T.S.; et al. Reconstitution of the Oocyte Transcriptional Network with Transcription Factors. *Nature* **2021**, *589*, 264–269. [CrossRef] [PubMed]
34. Emori, C.; Sugiura, K. Role of Oocyte-Derived Paracrine Factors in Follicular Development. *Anim. Sci. J.* **2014**, *85*, 627–633. [CrossRef] [PubMed]
35. Mcginnis, L.K.; Kinsey, W.H. Role of Focal Adhesion Kinase in Oocyte-Follicle Communication. *Mol. Reprod. Dev.* **2015**, *82*, 90–102. [CrossRef] [PubMed]
36. Gilchrist, R.B.; Ritter, L.J.; Myllymaa, S.; Kaivo-Oja, N.; Dragovic, R.A.; Hickey, T.E.; Ritvos, O.; Mottershead, D.G. Molecular Basis of Oocyte-Paracrine Signalling That Promotes Granulosa Cell Proliferation. *J. Cell Sci.* **2006**, *119*, 3811–3821. [CrossRef] [PubMed]
37. Adhikari, D.; Liu, K. Molecular Mechanisms Underlying the Activation of Mammalian Primordial Follicles. *Endocr. Rev.* **2009**, *30*, 438–464. [CrossRef] [PubMed]
38. Mehlmann, L.M. Stops and Starts in Mammalian Oocytes: Recent Advances in Understanding the Regulation of Meiotic Arrest and Oocyte Maturation. *Reproduction* **2005**, *130*, 791–799. [CrossRef] [PubMed]
39. Ernst, E.H.; Nielsen, J.; Ipsen, M.B.; Villesen, P.; Lykke-Hartmann, K. Transcriptome Analysis of Long Non-Coding RNAs and Genes Encoding Paraspeckle Proteins during Human Ovarian Follicle Development. *Front. Cell Dev. Biol.* **2018**, *6*, 78. [CrossRef]
40. Kirillova, A.; Smitz, J.E.J.; Sukhikh, G.T.; Mazunin, I. The Role of Mitochondria in Oocyte Maturation. *Cells* **2021**, *10*, 2484. [CrossRef]
41. Thompson, J.G.; Brown, H.M.; Kind, K.L.; Russell, D.L. The Ovarian Antral Follicle: Living on the Edge of Hypoxia or Not? *Biol. Reprod.* **2015**, *92*, 153. [CrossRef]
42. Lim, M.; Thompson, J.G.; Dunning, K.R. Hypoxia and Ovarian Function: Follicle Development, Ovulation, Oocyte Maturation. *Reproduction* **2021**, *161*, F33–F40. [CrossRef]
43. Redding, G.P.; Bronlund, J.E.; Hart, A.L. Theoretical Investigation into the Dissolved Oxygen Levels in Follicular Fluid of the Developing Human Follicle Using Mathematical Modelling. *Reprod. Fertil. Dev.* **2008**, *20*, 408–417. [CrossRef] [PubMed]
44. Winship, A.L.; Stringer, J.M.; Liew, S.H.; Hutt, K.J. The Importance of DNA Repair for Maintaining Oocyte Quality in Response to Anti-Cancer Treatments, Environmental Toxins and Maternal Ageing. *Hum. Reprod. Update* **2018**, *24*, 119–134. [CrossRef] [PubMed]
45. Bachvarova, R. Gene Expression During Oogenesis and Oocyte Development. In *Developmental Biology*; Springer: Boston, MA, USA, 1985; Volume 1, pp. 453–524.
46. Paynton, B.V.; Rempel, R.; Bachvarova, R. Changes in State of Adenylation and Time Course of Degradation of Maternal MRNAs during Oocyte Maturation and Early Embryonic Development in the Mouse. *Dev. Biol.* **1988**, *129*, 304–314. [CrossRef] [PubMed]
47. Ruebel, M.L.; Zambelli, F.; Schall, P.Z.; Barragan, M.; Vandevoort, C.A.; Vassena, R.; Latham, K.E. Shared Aspects of Mrna Expression Associated with Oocyte Maturation Failure in Humans and Rhesus Monkeys Indicating Compromised Oocyte Quality. *Physiol. Genom.* **2021**, *53*, 137–149. [CrossRef] [PubMed]
48. St John, J.C.; Okada, T.; Andreas, E.; Penn, A. The Role of MtDNA in Oocyte Quality and Embryo Development. *Mol. Reprod. Dev.* **2023**, *90*, 621–633. [CrossRef] [PubMed]
49. Reyes, J.M.; Chitwood, J.L.; Ross, P.J. RNA-Seq Profiling of Single Bovine Oocyte Transcript Abundance and Its Modulation by Cytoplasmic Polyadenylation. *Mol. Reprod. Dev.* **2015**, *82*, 103–114. [CrossRef] [PubMed]
50. Mamo, S.; Carter, F.; Lonergan, P.; Leal, C.L.V.; Al Naib, A.; McGettigan, P.; Mehta, J.P.; Evans, A.C.O.; Fair, T. Sequential Analysis of Global Gene Expression Profiles in Immature and in Vitro Matured Bovine Oocytes: Potential Molecular Markers of Oocyte Maturation. *BMC Genom.* **2011**, *12*, 151. [CrossRef]
51. Trimmer, K.A.; Zhao, P.; Seemann, J.; Chen, S.Y.; Mondal, S.; Ben-Yakar, A.; Arur, S. Spatial Single-Cell Sequencing of Meiosis I Arrested Oocytes Indicates Acquisition of Maternal Transcripts from the Soma. *Cell Rep.* **2023**, *42*, 112544. [CrossRef]
52. Pietroforte, S.; Barragan Monasterio, M.; Ferrer-Vaquer, A.; Irimia, M.; Ibáñez, E.; Popovic, M.; Vassena, R.; Zambelli, F. Specific Processing of Meiosis-Related Transcript Is Linked to Final Maturation in Human Oocytes. *Mol. Hum. Reprod.* **2023**, *29*, gaad021. [CrossRef]
53. Li, J.; Lu, M.; Zhang, P.; Hou, E.; Li, T.; Liu, X.; Xu, X.; Wang, Z.; Fan, Y.; Zhen, X.; et al. Aberrant Spliceosome Expression and Altered Alternative Splicing Events Correlate with Maturation Deficiency in Human Oocytes. *Cell Cycle* **2020**, *19*, 2182–2194. [CrossRef]
54. Yu, C.; Ji, S.Y.; Sha, Q.Q.; Dang, Y.; Zhou, J.J.; Zhang, Y.L.; Liu, Y.; Wang, Z.W.; Hu, B.; Sun, Q.Y.; et al. BTG4 Is a Meiotic Cell Cycle-Coupled Maternal-Zygotic-Transition Licensing Factor in Oocytes. *Nat. Struct. Mol. Biol.* **2016**, *23*, 387–394. [CrossRef] [PubMed]

55. Pasternak, M.; Pfender, S.; Santhanam, B.; Schuh, M. The BTG4 and CAF1 Complex Prevents the Spontaneous Activation of Eggs by Deadenylating Maternal MRNAs. *Open Biol.* **2016**, *6*, 160184. [CrossRef] [PubMed]
56. Ducreux, B.; Patrat, C.; Trasler, J.; Fauque, P. Transcriptomic Integrity of Human Oocytes Used in ARTs: Technical and Intrinsic Factor Effects. *Hum. Reprod. Update* **2023**. [CrossRef]
57. Li, J.; Chen, H.; Gou, M.; Tian, C.; Wang, H.; Song, X.; Keefe, D.L.; Bai, X.; Liu, L. Molecular Features of Polycystic Ovary Syndrome Revealed by Transcriptome Analysis of Oocytes and Cumulus Cells. *Front. Cell Dev. Biol.* **2021**, *9*, 735684. [CrossRef] [PubMed]
58. Wood, J.R.; Dumesic, D.A.; Abbott, D.H.; Strauss, J.F. Molecular Abnormalities in Oocytes from Women with Polycystic Ovary Syndrome Revealed by Microarray Analysis. *J. Clin. Endocrinol. Metab.* **2007**, *92*, 705–713. [CrossRef]
59. Grøndahl, M.L.; Yding Andersen, C.; Bogstad, J.; Nielsen, F.C.; Meinertz, H.; Borup, R. Gene Expression Profiles of Single Human Mature Oocytes in Relation to Age. *Hum. Reprod.* **2010**, *25*, 957–968. [CrossRef]
60. Jones, G.M.; Cram, D.S.; Song, B.; Magli, M.C.; Gianaroli, L.; Lacham-Kaplan, O.; Findlay, J.K.; Jenkin, G.; Trounson, A.O. Gene expression profiling of human oocytes following in vivo or in vitro maturation. *Hum. Reprod.* **2008**, *23*, 1138–1144. [CrossRef]
61. Lee, A.W.T.; Ng, J.K.W.; Liao, J.; Luk, A.C.; Suen, A.H.C.; Chan, T.T.H.; Cheung, M.Y.; Chu, H.T.; Tang, N.L.S.; Zhao, M.P.; et al. Single-Cell RNA Sequencing Identifies Molecular Targets Associated with Poor in Vitro Maturation Performance of Oocytes Collected from Ovarian Stimulation. *Hum. Reprod.* **2021**, *36*, 1907–1921. [CrossRef]
62. Virant-Klun, I.; Bauer, C.; Ståhlberg, A.; Kubista, M.; Skutella, T. Human Oocyte Maturation in Vitro Is Improved by Co-Culture with Cumulus Cells from Mature Oocytes. *Reprod. Biomed. Online* **2018**, *36*, 508–523. [CrossRef]
63. Barberet, J.; Ducreux, B.; Bruno, C.; Guilleman, M.; Simonot, R.; Lieury, N.; Guilloteau, A.; Bourc'his, D.; Fauque, P. Comparison of Oocyte Vitrification Using a Semi-Automated or a Manual Closed System in Human Siblings: Survival and Transcriptomic Analyses. *J. Ovarian Res.* **2022**, *15*, 128. [CrossRef]
64. Chamayou, S.; Bonaventura, G.; Alecci, C.; Tibullo, D.; di Raimondo, F.; Guglielmino, A.; Barcellona, M.L. Consequences of Metaphase II Oocyte Cryopreservation on MRNA Content. *Cryobiology* **2011**, *62*, 130–134. [CrossRef] [PubMed]
65. Huo, Y.; Yuan, P.; Qin, Q.; Yan, Z.; Yan, L.; Liu, P.; Li, R.; Yan, J.; Qiao, J. Effects of Vitrification and Cryostorage Duration on Single-Cell RNA-Seq Profiling of Vitrified-Thawed Human Metaphase II Oocytes. *Front. Med.* **2021**, *15*, 144–154. [CrossRef] [PubMed]
66. Monzo, C.; Haouzi, D.; Roman, K.; Assou, S.; Dechaud, H.; Hamamah, S. Slow Freezing and Vitrification Differentially Modify the Gene Expression Profile of Human Metaphase II Oocytes. *Hum. Reprod.* **2012**, *27*, 2160–2168. [CrossRef] [PubMed]
67. Stigliani, S.; Moretti, S.; Anserini, P.; Casciano, I.; Venturini, P.L.; Scaruffi, P. Storage Time Does Not Modify the Gene Expression Profile of Cryopreserved Human Metaphase II Oocytes. *Hum. Reprod.* **2015**, *30*, 2519–2526. [CrossRef] [PubMed]
68. Teissandier, A.; Servant, N.; Barillot, E.; Bourc'His, D. Tools and Best Practices for Retrotransposon Analysis Using High-Throughput Sequencing Data. *Mob. DNA* **2019**, *10*, 52. [CrossRef] [PubMed]
69. Moon, K.R.; van Dijk, D.; Wang, Z.; Gigante, S.; Burkhardt, D.B.; Chen, W.S.; Yim, K.; van den Elzen, A.; Hirn, M.J.; Coifman, R.R.; et al. Visualizing Structure and Transitions in High-Dimensional Biological Data. *Nat. Biotechnol.* **2019**, *37*, 1482–1492. [CrossRef]
70. van den Berge, K.; Roux de Bézieux, H.; Street, K.; Saelens, W.; Cannoodt, R.; Saeys, Y.; Dudoit, S.; Clement, L. Trajectory-Based Differential Expression Analysis for Single-Cell Sequencing Data. *Nat. Commun.* **2020**, *11*, 1201. [CrossRef]
71. Prada, C.; Lima, D.; Nakaya, H. MetaVolcanoR: Gene Expression Meta-Analysis Visualization Tool. *R Package Version* **2020**, *1*, 2020.
72. Viechtbauer, W. Conducting Meta-Analyses in R with the Metafor Package. *J. Stat. Softw.* **2010**, *36*, 1–48. [CrossRef]

Supplementary Figure S1. Transcriptomic analysis of variable genes along folliculogenesis. A. Heatmap of all DEGs in all comparisons between the follicle stages. **B.** PHATE dimensionality reduction of the whole expression dataset colored by follicle stage with patient origin for each oocyte notified by a letter.

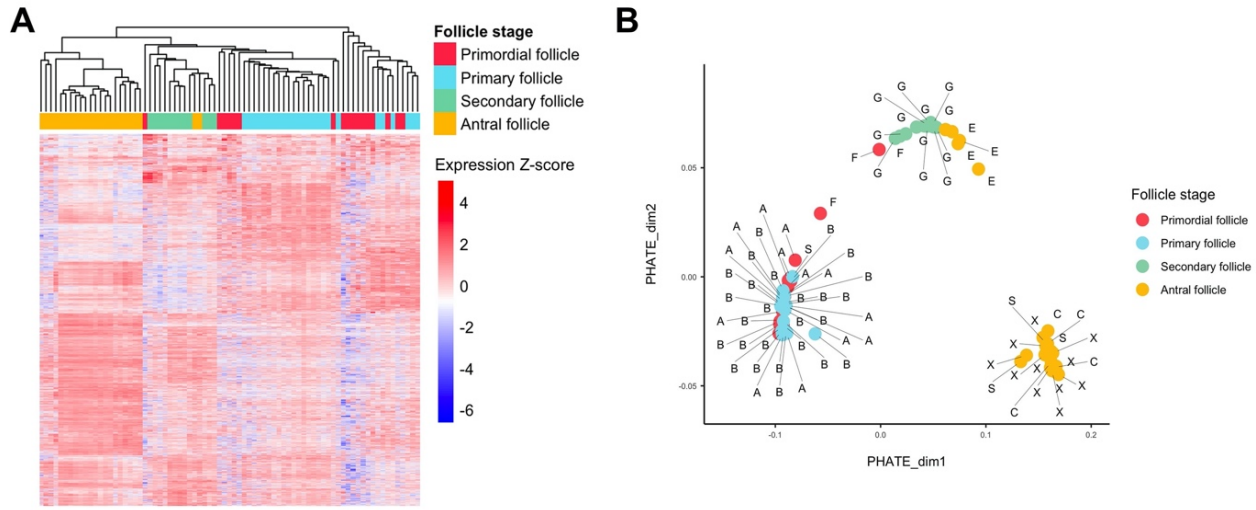

Supplementary Figure S2. Expression variation of transcription factors with significant variation along folliculogenesis according to the trajectory analysis (logFC>3).

Supplementary Figure S3. Individual PCA plots of the six datasets analyzed in this study comparing GV, MI, and MII transcriptomes.

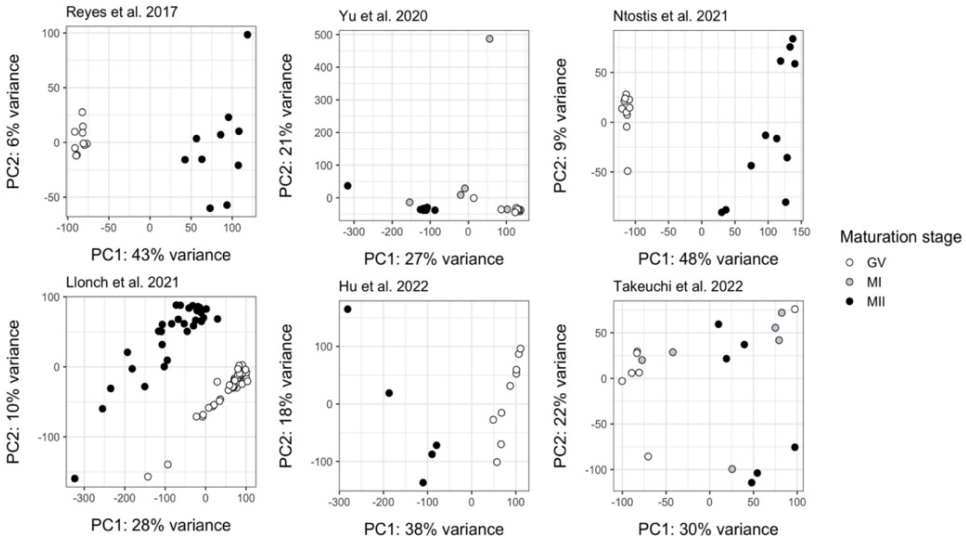

Supplementary Figure S4. Individual results of GO enrichment analysis of the six datasets analyzed in this study comparing GV and MII transcriptomes. The top 10 GOs are displayed for each study. GOs in grey did not reach significance. **A.** For up-regulated genes identified in MII *versus* GV oocytes. The highlighted terms are significant among at least two studies. **B.** For down-regulated genes identified in MII *versus* GV oocytes. The highlighted terms are significant among at least two studies.

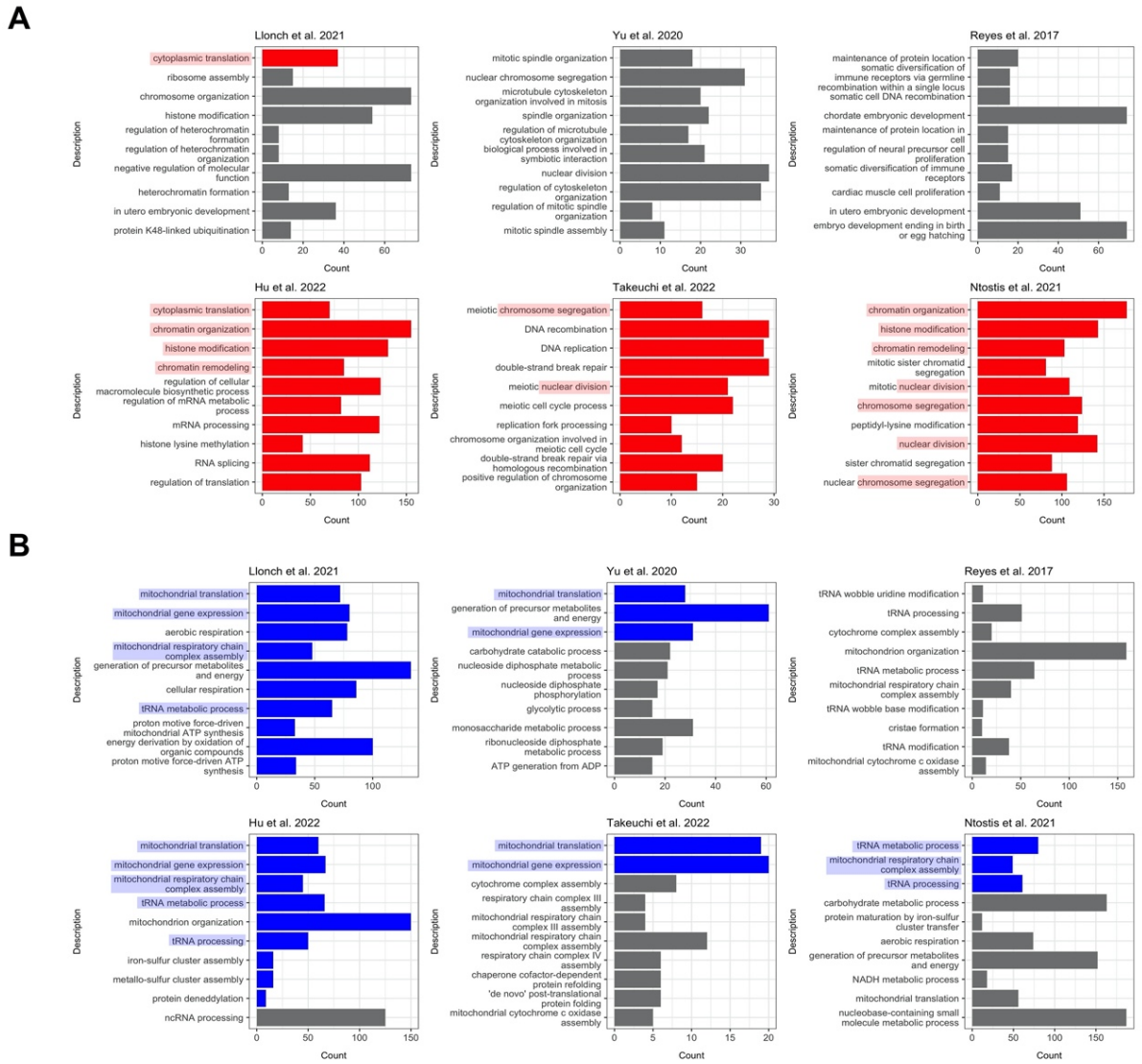

Supplementary Figure S5. PCA plots of merged expression of all samples from the six datasets analyzed in this study comparing GV and MII transcriptomes. A. Using raw expression. **B.** After batch correction with ComBat.

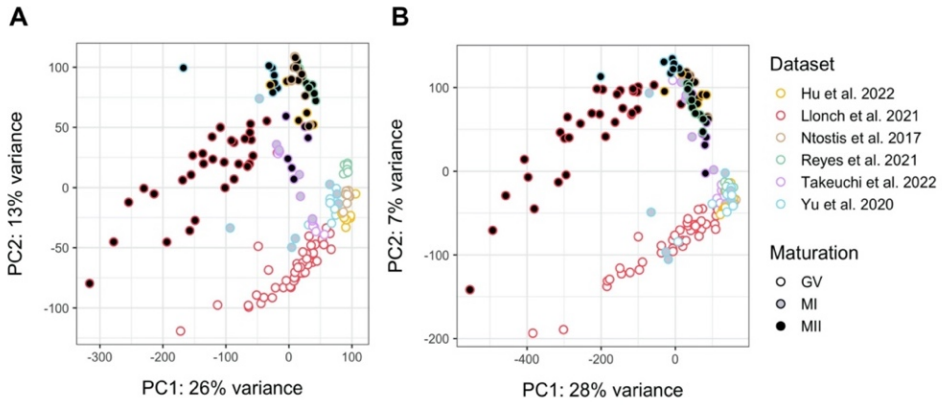

Supplementary Figure S6. Genomic class annotation analysis of DEGs identified in the meta-analysis of MII *versus* GV oocytes. LINE : long interspersed nuclear elements, lncRNA : long non-coding RNA, LTR : long terminal repeats, SINE : short interspersed nuclear elements, TE : transposable elements. **A.** General genomic class annotation of DEGs identified in the meta-analysis of MII *versus* GV oocytes (right circle), compared to the representation in expressed genes (left circle). **B.** Heatmap of transposable elements in the DEGs identified in the meta-analysis of MII *versus* GV oocytes and information on their family.

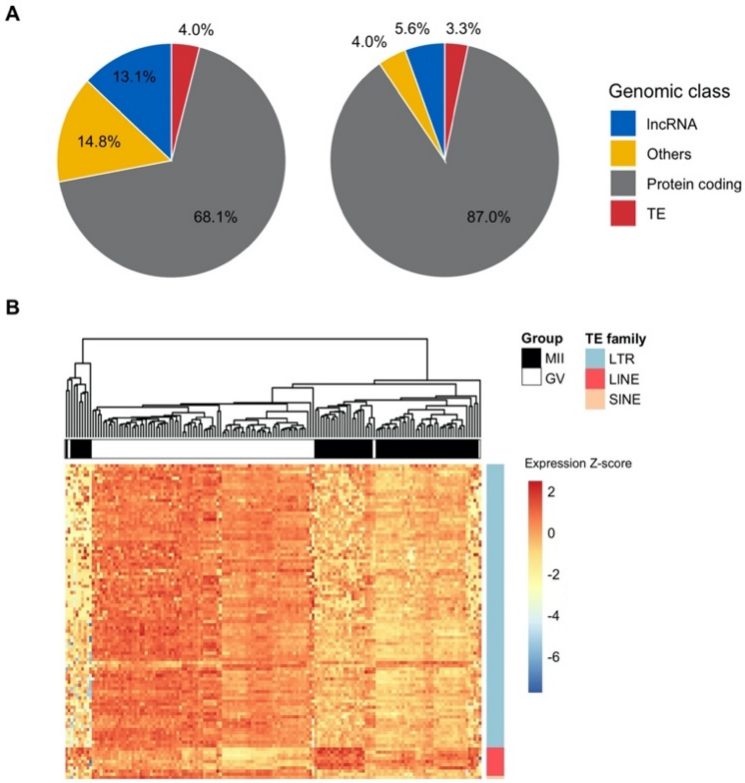

Supplementary Table S1. Results of the differential expression analysis for one follicle stage *versus* all others.

Supplementary Table S2. Results of the differential expression analysis along pseudotime during oocyte growth.

Supplementary Table S3. Results of the differential expression meta-analysis between GV and MII oocytes, and associated gene ontology enrichment for significant differentially expressed genes (separated for up- and down-regulated).

Supplementary Table S4. Summary of studies assessing the influence of PCOS, age, IVM and cryoconservation on oocyte transcriptome.

Available at https://www.mdpi.com/article/10.3390/ijms25010033/s1

2.2) L'activation du génome embryonnaire

Chez l'homme comme chez tous les mammifères, un remodelage des génomes transcriptionnellement inactifs haploïdes maternel et paternel après fécondation doit impérativement avoir lieu pour constituer un génome embryonnaire diploïde fonctionnel. Les études de la dynamique du transcriptome depuis la fécondation jusqu'au stade 8-cellule chez l'homme montrent qu'aucune activité transcriptionnelle, ou très peu, ne se produit, c'est-à-dire qu'il n'y a pas d'ARNm synthétisé par l'embryon durant cette période (Tadros & Lipshitz, 2009; Vassena *et al.*, 2011; Schulz & Harrison, 2019; Perry *et al.*, 2022). Les transcrits maternels stockés dans l'ovocyte dictent ainsi la physiologie de l'embryon jusqu'à l'activation du génome embryonnaire, qui s'établit progressivement via différentes vagues de transcription depuis le stade 1-cellule chez l'homme (Asami *et al.*, 2022). En parallèle de la mise en route de l'activité transcriptionnelle propre à l'embryon, les ARNm maternels sont dégradés. On parle alors de transition materno-zygotique pour qualifier le passage d'un contrôle du développement embryonnaire maternel à un contrôle zygotique (Schultz, 2002; Schier, 2007; Zhao *et al.*, 2019b).

2.3) Techniques de mesure du transcriptome à l'échelle du génome-entier

Il existe deux catégories principales de techniques de mesure du transcriptome à grande échelle, basées sur les puces à ADN et le séquençage à haut débit (Lowe *et al.*, 2017).

Puces (microarrays)

Pour réaliser une analyse sur puce, les ARNm collectés doivent être rétrotranscrits en ADN complémentaire (ADNc) puis amplifiés. Il existe deux types de puces suivant la méthodologie expérimentale suivie. Si l'on veut comparer directement des échantillons expérimentaux avec une référence, on peut utiliser l'approche à « double marquage » (plus connu en anglais sous

le nom de « dual-channel »). Les ADNc sont marqués par un fluorochrome, différents pour chaque condition étudiée. Typiquement, on utilise les fluorochromes verts (cyanine3) et rouges (cyanine5). Les ADNc marqués sont ensuite mis en contact ensemble avec la puce où se trouvent des milliers de sondes d'hybridation correspondant à des séquences de gènes connus. Une étape de lavage permet d'éliminer les fragments non hybridés. Enfin, la puce est analysée grâce à un scanner de fluorescence qui va mesurer l'intensité de la fluorescence de chaque fluorochrome. On peut ainsi déterminer le ratio d'intensité des signaux pour chaque gène étudié et quantifier si l'échantillon expérimental est plus ou moins exprimé par rapport à l'échantillon de référence. La deuxième technologie de puce permet de mesurer l'expression individuelle d'un seul échantillon, sans comparaison directe (technologie « simple marquage » ou « one-channel »). Cette technique est utile pour comparer des échantillons provenant de différentes origines ou de différents batchs. Elle repose sur la même méthodologie, si ce n'est qu'un seul fluorochrome est utilisé.

RNA-seq

Le RNA-seq (RNA-sequencing) est quant à lui une technique de séquençage de seconde génération. Il requiert une étape de préparation des librairies d'ADNc à séquencer, rétrotranscrits depuis les ARNm polyadénylés collectés puis préamplifiés. Pour le séquençage Illumina, l'ADNc est fragmenté en petits morceaux généralement d'une longueur entre 100 et 300 paires de base et qui varie selon le séquenceur à disposition. Des séquences adaptatrices spécifiques à chaque technologie sont ajoutées à chaque fragment, ce qui va permettre leur fixation sur la lame de verre (« flowcell »), leur amplification par des cycles de PCR successifs et donc le séquençage. Chaque fragment séquencé est appelé lecture ou « read ». En sortie du séquenceur, on obtient un fichier au format .fastq qui répertorie toutes les lectures et des informations sur la qualité du séquençage de chaque base nucléotidique.

En 2009, la méthode RNA-seq est optimisée pour analyser une cellule unique jusqu'alors impossible en raison de la trop faible quantité de matériel génétique (Tang *et al.*, 2009) ; on

parle de single-cell RNA-seq. La méthode utilisée dans cette thèse est une adaptation de la méthode originelle de Tang *et al.* (2009) spécifiquement appliquée pour l'étude des premiers stades du développement embryonnaire, soit en séquençage sur cellule unique soit en embryon unique. La Figure 21 détaille dans les grandes lignes le protocole mis en œuvre pour réaliser ici le séquençage d'ovocytes et d'embryons uniques (adapté de Perez-Palacios *et al.* (2021) (Pérez-Palacios *et al.*, 2021)).

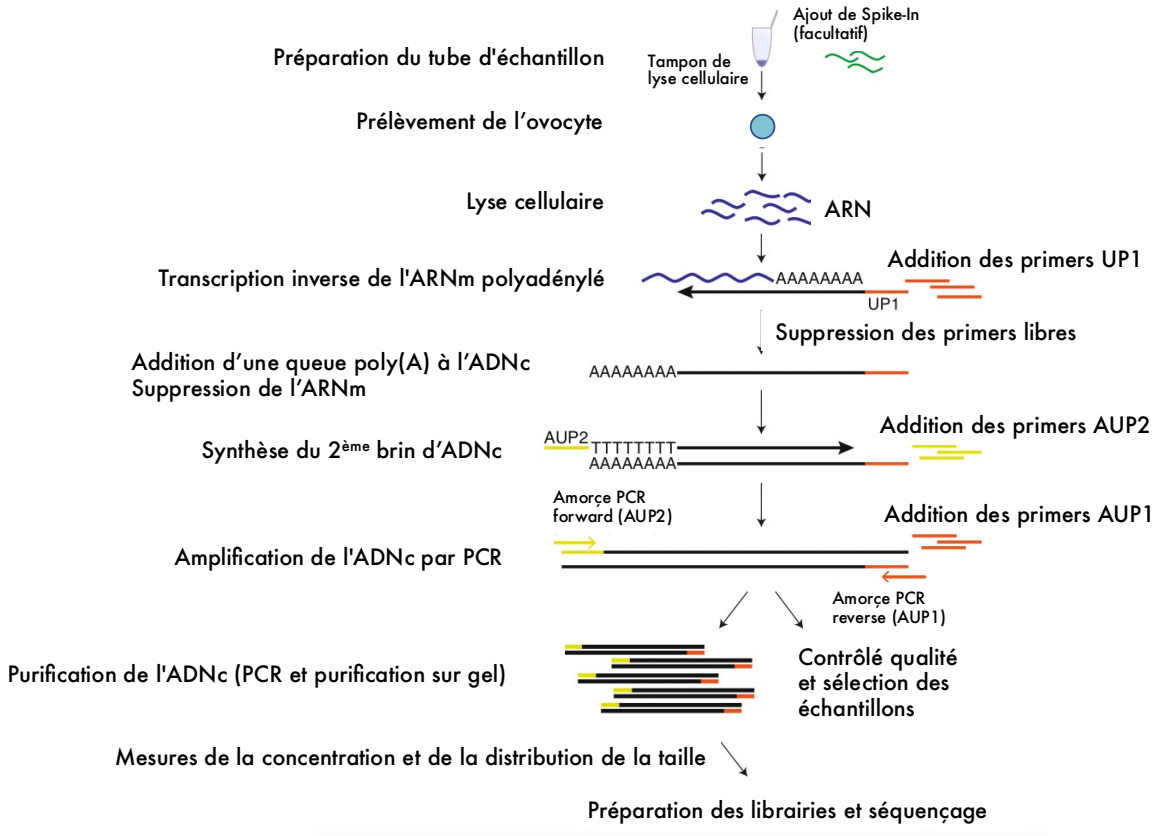

Figure 21. Organigramme de la méthode scRNA-seq pour ovocyte et embryon unique.
Avant la collecte des ovocytes et embryons, des tubes d'échantillonnage contenant du tampon de lyse cellulaire sont préparés avec l'ajout facultatif de molécules Spike-In au mélange réactionnel. Les échantillons sont ensuite lysés et les ARNm polyadénylés sont rétrotranscrits. Après l'ajout d'une queue Poly(A) à l'ADNc de premier brin, l'ADNc du second brin est synthétisé et les ADNc sont amplifiés par PCR à l'aide d'amorces oligo-dT. Enfin, les ADNc sont purifiés et sélectionnés sur gel d'agarose avant la préparation des librairies d'ADN et le séquençage à haut débit. Traduit et adapté depuis Perez-Palacios *et al.* (2021) (Pérez-Palacios *et al.*, 2021).

RNA-seq et puces reposent donc sur deux technologies différentes, séquençage ou hybridation. Les avantages des puces sont la simplicité de leurs protocoles et leur coût très modique par échantillon comparé au RNA-seq. En revanche, elles ont une très faible

sensibilité pour les gènes très peu exprimés et ne peuvent pas détecter de nouveaux transcrits du fait qu'elles reposent sur l'hybridation de séquences prédéfinies. Le RNA-seq reste aujourd'hui le « gold standard » pour l'analyse du transcriptome. Son très bon rapport qualité/prix et les progrès technologiques de la bioinformatique rendent cette technique privilégiée par les équipes de recherches, ce qui se traduit par une quantité de données générées exponentielle sur les dernières années et la multiplication des outils d'analyse. Ses avantages sont multiples : détection de nouveaux transcrits, des SNPs et ARNs non codant, forte sensibilité pour les gènes même faiblement exprimés et faible quantité d'ARN nécessaire. Ses inconvénients en comparaison des puces restent leur coût plus élevé et la complexité de l'analyse bioinformatique des données générées.

Dans le paragraphe suivant, nous nous intéresserons à détailler spécifiquement les étapes d'analyse de données RNA-seq après obtention des données issues du séquenceur.

2.4) Analyses bioinformatiques des données issues de RNA-seq

Conventionnellement il y a trois grandes étapes de traitement bioinformatique pour transformer les données brutes en une matrice d'expression exploitable pour des analyses biologiques. Dans un premier temps il est nécessaire de s'assurer de la qualité des données du séquençage, et de supprimer les échantillons dont elle n'est pas satisfaisante ou de raccourcir les lectures en éliminant les bases de mauvaise qualité (« trimming »). Chez l'humain, nous possédons un génome de référence qui correspond à la séquence complète d'ADN à partir de laquelle les ARN séquencés ont été obtenus. Toutes les lectures obtenues sont alignées sur le génome de référence. Le dernier assemblage de référence du génome humain, initialement publié par le Genome Reference Consortium, est le GRCh38 (hg38) en 2013. Ce génome de référence est amené à évoluer dans le temps car certaines régions sont encore non résolues (estimé à 8%), et l'utilisation du génome Telomere-to-Telomere (T2T) paru en 2022 devrait se généraliser à moyen terme (Nurk *et al.*, 2022).

Enfin, lorsque la position de chaque lecture sur le génome est connue, on peut compter pour chaque gène le nombre de lectures alignées. On obtient une matrice de comptage qui illustre l'abondance des lectures par gène et qu'il faut traiter statistiquement pour quantifier l'expression de chaque gène. En RNA-seq, comme évoqué précédemment pour la méthylation de l'ADN, il est principalement d'intérêt de réaliser une analyse différentielle entre plusieurs échantillons. Avant de séquencer des échantillons, il faut planifier les expériences qui seront réalisées, la taille des échantillons et la profondeur de séquençage (le nombre de lecture total pour chaque échantillon). Ces paramètres sont cruciaux pour que l'analyse différentielle soit statistiquement puissante et constitue donc un résultat biologiquement valide.

Pour rendre des comptages comparables entre échantillons, il faut normaliser les données. En effet, la profondeur de séquençage est différente entre échantillons ce qui constitue un biais. Il existe une multitude de méthodes de normalisation dont les détails statistiques ne seront pas détaillés ici (médiane, moyenne géométrique, …). Les méthodes implémentées dans *DESeq2* et *edgeR* apparaissent comme les plus performantes parmi celles existantes et seront utilisées dans cette thèse (Dillies *et al.*, 2013).

Pour chaque gène, l'analyse différentielle teste l'hypothèse d'une différence de la moyenne d'expression entre les conditions testées (test de Wald, t-test modéré, etc … suivant les packages (c'est-à-dire un ensemble de logiciels) utilisés). Les p-valeurs brutes résultants de ces tests individuels doivent être corrigées pour contrôler le taux de faux positifs dus aux tests multiples, comme évoqué précédemment sur la partie méthylation de l'ADN.

III) Effets épigénétiques et transcriptomiques en lien avec l'AMP depuis l'ovocyte jusque chez l'adulte : quelle évidence à ce jour ?

Comme les techniques d'AMP coïncident avec les périodes de reprogrammation épigénétique, de quiescence transcriptionnelle de l'ovocyte et de l'embryon puis d'activation du génome embryonnaire, elles apparaissent particulièrement à risque pour l'intégrité du transcriptome et de l'épigénome ovocytaire et embryonnaire. Toute altération épigénétique, qu'elle soit directe en modifiant les profils de méthylation de l'ADN ou indirecte en perturbant la machinerie de régulation de la reprogrammation épigénétique, est susceptible d'avoir des conséquences à court terme pour le développement. De plus, de nombreuses publications ont suggéré un lien entre la fréquence accrue de syndromes liés à l'empreinte parentale et l'utilisation des techniques d'AMP (Amor & Halliday, 2008; Manipalviratn *et al.*, 2009; Hattori *et al.*, 2019). Cette association reste difficile à étudier du fait de la rareté de l'occurrence de ces troubles et des effets sous-jacents de l'infertilité des patients ayant recours à l'AMP. Quant au transcriptome, des vagues transcriptionnelles successives agissent comme la partition garantissant la capacité de l'embryon à se développer. Si les ARNm ne sont pas transcrits/dégradés au moment juste, c'est comme si des musiciens manquaient dans un orchestre, ou ne jouaient pas dans la bonne cadence, la mélodie deviendrait dissonante.

1) Effets épigénétiques des techniques AMP: une nécessité d'évaluer les modifications du profil de méthylation de l'ADN depuis l'ovocyte jusque chez l'adulte

1.1) Données issues du modèle animal

Le modèle animal occupe une place de choix dans l'étude des effets épigénétiques en lien avec les techniques d'AMP. En effet, celles-ci sont exclusivement appliquées dans un contexte d'infertilité chez l'humain, ce qui peut constituer un très grand facteur confondant car des anomalies de l'épigénome paternel et maternel sous-jacentes sont susceptibles d'être transmises à la descendance. De plus chez l'animal, il est possible de mettre en œuvre des protocoles simples permettant d'évaluer l'impact individuel de chaque technique, et donc d'identifier à quelles étapes les altérations épigénétiques peuvent survenir. En raison de lois restrictives encadrant l'utilisation d'embryons pour la recherche et des questions éthiques qu'elles soulèvent, peu d'études chez l'Homme ont été et peuvent être réalisées à des stades précoces.

Les effets épigénétiques des techniques d'AMP chez l'animal, principalement chez la souris, ont fait l'objet de nombreuses revues, avec un focus particulier sur l'hyperstimulation ovarienne et les conditions de culture embryonnaire et leurs effets sur les gènes soumis à empreinte (Van Montfoort *et al.*, 2012; Fauque, 2013; Ramos-Ibeas *et al.*, 2019). En synthèse, la superovulation semble contribuer à une incidence accrue d'épimutations au niveau des embryons pré-implantatoires dans les nombreux gènes soumis à empreinte étudiés (*PEG1*, KvDMR1, *ZAC*, *H19*, *SNRPN*, *PEG3*), avec un effet dose marqué (Market-Velker *et al.*, 2009; De waal *et al.*, 2012; Fauque, 2013). De façon intrigante, alors que seul l'ovocyte est impacté par cette technique, des gènes paternels sont aussi affectés dans le blastocyste, comme *H19* qui subit une perte de méthylation en lien avec la superovulation (Market-Velker *et al.*, 2009). Dans l'ovocyte issu de superovulation, il n'y avait cependant pas de modifications de

méthylation dans les régions précédemment retrouvées comme altérées dans le blastocyste (*SNRPN*, *PEG3*, KvDMR1), suggérant un défaut des mécanismes de maintien de la méthylation au cours du développement précoce de l'embryon plutôt qu'un défaut d'acquisition pendant l'ovogenèse à l'origine des altérations embryonnaires (Denomme *et al.*, 2011; Duranthon & Chavatte-Palmer, 2018). Les conditions de culture *in vitro* influencent également largement le profil de méthylation de plusieurs gènes soumis à empreinte chez l'ovocyte, l'embryon pré- et post-implantatoire de souris (*IGF2R*, *MEST/PEG1*, *H19*) (Doherty *et al.*, 2000; Khosla *et al.*, 2001; Kerjean *et al.*, 2003; Fernández-Gonzalez *et al.*, 2004; Mann *et al.*, 2004; Fauque *et al.*, 2007a; Anckaert *et al.*, 2010). Notamment, les milieux de culture supplémentés en acides aminés présentaient des marques épigénétiques similaires aux conditions *in vivo* (Doherty *et al.*, 2000; Fauque *et al.*, 2007a). La fragilité des GSE aux techniques d'AMP est d'autant plus marquante que la simple manipulation d'embryons pour transfert altère leur expression, comme pour *IGF2* (Rivera *et al.*, 2008). Plus de recul sur l'ensemble du méthylome est toutefois manquant, avec très peu d'études chez l'animal sur des gènes autres que soumis à empreinte mais qui alertent sur la répercussion des techniques d'AMP sur la méthylation d'autres gènes impliqués dans le développement (Li *et al.*, 2011b; Saenz-De-Juano *et al.*, 2019; Lira-Albarrán *et al.*, 2022). Dans d'autres modèles animaux moins utilisés que la souris, les profils épigénétiques d'embryons conçus *in vitro* apparaissent également modifiés (cochon, (Tyler *et al.*, 2017)) et à l'origine de certains syndromes (veau, « large offspring syndrome », (Young *et al.*, 2001)).

Néanmoins, on ne peut pas être certain que le modèle animal reflète totalement la situation de l'AMP chez l'humain (espèces polyovulatoires, timing différent de l'activation du génome embryonnaire (EGA), reprogrammation épigénétique à des niveaux de méthylation différents, DNMT3L non exprimée dans l'ovocyte humain) (Ménézo & Hérubel, 2002; Hanna *et al.*, 2018). Les paragraphes suivants ont vocation à synthétiser l'état de l'art concernant l'influence des techniques d'AMP sur le méthylome humain, à différents stades de développement depuis l'ovocyte jusqu'à l'âge adulte.

1.2) Données chez l'humain

Comme admis chez l'animal, les techniques d'assistance médicale à la procréation sont susceptibles d'engendrer des modifications du profil de méthylation dès l'ovocyte chez l'humain. En comparaison de l'épigénome paternel, les marques épigénétiques maternelles sont apposées tardivement (juste avant l'ovulation), de façon concomitante aux techniques spécifiques telles que la stimulation ovarienne multifolliculaire, la MIV ou la congélation. Toutefois, les études chez l'humain restent peu nombreuses.

1.2.1) AMP et profils de méthylation dans l'ovocyte

Stimulation ovarienne

L'hyperstimulation ovarienne semble accroître les erreurs de méthylation aux loci soumis à empreinte dans les gènes *PEG1*, *H19* et la région KvDMR1 (Sato *et al.*, 2007; Khoureiry *et al.*, 2008).

Maturation ovocytaire *in vitro*

L'incidence des défauts d'empreinte parentale pourrait également être plus élevée chez les ovocytes maturés *in vitro* en comparaison de conditions *in vivo* (Borghol *et al.*, 2006) même si une récente étude utilisant des technologies de séquençage dernière génération n'a retrouvé aucune différence sur le méthylome global (Ye *et al.*, 2020).

Vitrification

Concernant la vitrification, il ne semble pas y avoir de modifications du méthylome ovocytaire induites par cette technique chez l'homme (Barberet *et al.*, 2020).

Toutefois, il y a beaucoup d'incertitudes sur ces résultats liées aux caractéristiques intrinsèques des patients mais aussi la contamination par l'ADN des cellules entourant l'ovocyte comme les cellules cumulus qui ont un profil épigénétique de cellules somatiques.

L'impact de la maturation *in vitro* a toutefois été analysé dans le sang de cordon et les villosités choriales de nouveau-nés issus d'ovocytes maturés *in vitro* ou *in vivo* sur quelques gènes cibles (soumis à empreinte, suppresseurs de tumeur, impliqués dans le métabolisme ou la pluripotence, éléments répétés) sans montrer de différences entre les deux groupes (Pliushch *et al.*, 2015). Ne pas retrouver de grandes différences de méthylation au stade ovocytaire entre ovocytes conditionnés en vue de FIV/ICSI et conditions *in vivo* ne garantit toutefois pas que les mécanismes de maintien de méthylation soient inaltérés et n'aient pas un impact ultérieur.

1.2.2) AMP et profils de méthylation chez l'embryon

Après la fécondation de l'ovocyte, le zygote subit des divisions cellulaires successives et se développe pour atteindre le stade blastocyste au 5ème jour chez l'humain. Avant l'activation du génome embryonnaire qui prend place préférentiellement autour du stade 8-cellules (Braude *et al.*, 1988; Vassena *et al.*, 2011), l'embryon est particulièrement vulnérable aux facteurs extérieurs en raison d'une quiescence transcriptionnelle et donc l'absence de mobilisation possible de mécanismes de défense aux stress. Il est ainsi important de distinguer l'embryon pré-compaction de l'embryon post-compaction qui semblent montrer des degrés de fragilité différents vis-à-vis de l'environnement *in vitro* (Zander *et al.*, 2006). De plus, comme décrit plus en amont, le profil épigénétique de l'embryon évolue de manière dynamique, avec l'effacement de la méthylation puis la méthylation *de novo* ou la maintenance de la méthylation dans les régions soumises à empreinte. Cette reprogrammation épigénétique, est donc sensible aux interventions et manipulations artificielles, qui sont, comme pour l'ovocyte, nombreuses dans le cadre d'un protocole d'AMP. Dans les régions soumises à empreinte, plusieurs études ont mis en cause l'influence néfaste des techniques d'AMP sur le profil de méthylation, notamment dans les régions *H19*, *PEG1* et KvDMR1 (Chen *et al.*, 2010; Ibala-Romdhane *et al.*, 2011; Shi *et al.*, 2014) mais sans comparatif avec des embryons conçus naturellement.

<u>FIV ou ICSI</u>

De façon intéressante, la technique d'ICSI suspectée d'engendrer plus de perturbations en raison des manipulations additionnelles réalisées en comparaison de la FIV classique (injection du spermatozoïde directement dans l'ovocyte à l'aide d'une pipette) ne montre pas d'augmentation de l'incidence d'erreurs de méthylation (Santos *et al.*, 2010).

Vitrification

La vitrification embryonnaire au jour 3 n'induit également pas de modification du niveau de méthylation de *H19/IGF2* DMR au stade blastocyste (Derakhshan-Horeh *et al.*, 2016).

Autres techniques

Récemment, des études ont réalisé des analyses comparatives de techniques d'AMP qui n'ont jusqu'alors pas été incriminées comme potentielles sources de perturbation du méthylome. Cela démontre une prise de conscience collective que chaque intervention et paramètre en AMP est un facteur susceptible de perturber la physiologie des gamètes et de l'embryon. En effet, comme le Groupe de consensus sur les conditions de culture en FIV du Caire 2018 l'a fait remarquer, « il y a une seule chose qui est importante dans le laboratoire d'AMP, tout » (Consensus Group, 2020). Par exemple, Zhu *et al.* (2023) a comparé le méthylome d'embryons au stade 8-cellules cultivés de façon interrompue (déplacés à plusieurs reprises pour évaluation morphologique) ou ininterrompue (incubateurs avec imagerie temporelle) (Zhu *et al.*, 2023). En effet, ces déplacements peuvent être source de variation de conditions physico-chimiques (température, lumière, humidité, oxygène, pH, …) qui peuvent être détrimentaires pour l'embryon. Toutefois dans cette étude, il n'y avait pas de différences majeures de méthylation entre les deux groupes même si quelques DMRs ont été identifiées et nécessitent davantage d'investigation concernant l'effet des variations de paramètres physico-chimiques pour l'embryon et l'utilisation de matériel pouvant les limiter.

1.2.3) AMP et profils de méthylation depuis la vie fœtale jusqu'à l'âge adulte

1.2.3.1) Objectifs

Lors de la réalisation de cette thèse, il est apparu qu'une analyse critique de la littérature des modifications des profils de méthylation induites par les techniques liées à l'AMP manquait afin d'avoir un regard plus clairvoyant. Une revue systématique publiée en 2014 a tenté d'adresser cette problématique ; néanmoins elle apparaît aujourd'hui caduc au vu du nombre d'études publiées sur la dernière décennie et des progrès méthodologiques concernant en particulier le séquençage (Lazaraviciute *et al.*, 2014). Nous avons donc réalisé une revue systématique de la littérature et établi une méta-analyse ayant comme thématique le suivi des profils de la méthylation de l'ADN chez les enfants conçus par AMP (Barberet *et al.*, 2022b). Cela a permis de mieux évaluer l'existence de modifications propres à l'AMP de façon critique et de cibler les manques actuels dans la littérature.

1.2.3.2) Matériels et méthodes

Une revue systématique est une méthode de synthèse bibliographique rigoureuse et reproductible. Elle demande un travail de collecte exhaustif et une évaluation critique des connaissances récoltées. Toute revue systématique doit être enregistrée auprès d'un registre prospectif, tel que PROSPERO, qui enregistre son protocole et garantit toute transparence dans sa réalisation. Le protocole dressé avec mon équipe pour la réalisation d'une revue systématique et méta-analyse sur les effets épigénétique en AMP est décrit ci-dessous et enregistré dans PROSPERO sous le numéro d'enregistrement CRD42021267425.

En collaboration avec Julie Barberet, nous avons conduit une recherche bibliographique extensive dans les bases de données PubMed et Embase le 15 juillet 2021. Celle-ci a été réalisée au moyen d'une équation de recherche large mais précise permettant de couvrir l'ensemble de la littérature du domaine ciblé (méthylation et AMP). Pour être analysées de manière comparable, les études ont été divisées en groupes suivant la période de vie à laquelle ont été collectés les échantillons (grossesse, naissance, enfance, adolescence, adulte), le type cellulaire et la résolution à laquelle la méthylation est mesurée (gène/région ou ensemble du génome). Pour les études ciblées, les paires de primers utilisées pour le séquençage des régions d'intérêt ont été récupérées et soumises à une PCR bisulfite *in silico* pour retrouver précisément les coordonnées chromosomiques de la région séquencée dans chaque étude (Tusnády *et al.*, 2005). Ainsi, chaque région soumise à empreinte de chaque étude a été attribuée à une région soumise à empreinte clairement identifiée en fonction des coordonnées génomiques étudiées (Monk *et al.*, 2018) (Table 4).

Nomenclature	Chromosome	Début	Fin	Nombre de CpGs	Origine maternelle ou paternelle
PPIEL:Ex1-DMR	1	40,024,626	40,025,540	39	M
DIRAS3:TSS-DMR	1	68,515,433	68,517,545	88	M
DIRAS3:Ex2-DMR	1	68,512,505	68,513,486	39	M
GPR1-AS:TSS-DMR	2	207,066,967	207,069,445	86	M
ZDBF2/*GPR1*:IG-DMR	2	207,114,583	207,136,544	439	P
NAP1L5:TSS-DMR	4	89,618,184	89,619,237	57	M
VTRNA2–1:DMR	5	135,414,802	135,416,645	76	M
FAM50B:TSS-DMR	6	3,849,082	3,850,359	90	M
PLAGL1:alt-TSS-DMR	6	144,328,078	144,329,888	143	M
IGF2R:Int2-DMR	6	160,426,558	160,427,561	74	M
WDR27:Int13-DMR	6	170,054,504	170,055,618	58	M
GRB10:alt-TSS-DMR	7	50,848,726	50,851,312	171	M
PEG10:TSS-DMR	7	94,285,537	94,287,960	119	M
MEST:alt-TSS-DMR	7	130,130,122	130,134,388	226	M
SVOPL:alt-TSS-DMR	7	138,348,118	138,349,069	31	M
HTR5A:TSS-DMR	7	154,862,719	154,863,382	55	M
ERLIN2:Int6-DMR	8	37,604,992	37,606,088	37	M
PEG13:TSS-DMR	8	141,108,147	141,111,081	193	M
FANCC:Int1-DMR	9	98,075,400	98,075,744	26	M
INPP5F:Int2-DMR	10	121,578,046	121,578,727	52	M
H19/*IGF2*:IG-DMR	11	2,018,812	2,024,740	250	P
IGF2:Ex9-DMR	11	2,153,991	2,155,112	63	P
IGF2:alt-TSS-DMR	11	2,168,333	2,169,768	33	P
KCNQ1OT1:TSS-DMR	11	2,719,948	2,722,259	192	M
RB1:Int2-DMR	13	48,892,341	48,895,763	195	M
MEG3/*DLK1*:IG-DMR	14	101,275,427	101,278,058	64	P
MEG3:TSS-DMR	14	101,290,524	101,293,978	188	P
MEG8:Int2-DMR	14	101,370,741	101,371,419	43	M
MKRN3:TSS-DMR	15	23,807,086	23,812,495	109	M
MAGEL2:TSS-DMR	15	23,892,425	23,894,029	51	M
NDN:TSS-DMR	15	23,931,451	23,932,759	108	M
SNRPN:alt-TSS-DMR	15	25,068,564	25,069,481	19	M
SNRPN:Int1-DMR1	15	25,093,008	25,193,829	44	M
SNRPN:Int1-DMR2	15	25,123,027	25,123,905	45	M
SNURF:TSS-DMR	15	25,200,004	25,201,976	113	M
IGF1R:Int2-DMR	15	99,408,496	99,409,650	55	M
ZNF597:3' DMR	16	3,481,801	3,482,388	29	M
ZNF597:TSS-DMR	16	3,492,828	3,494,463	76	P
ZNF331:alt-TSSDMR1	19	54,040,510	54,042,212	125	M

ZNF331:alt-TSSDMR2	19	54,057,086	54,058,425	102	M
PEG3:TSS-DMR	19	57,348,493	57,353,271	221	M
MCTS2P:TSS-DMR	20	30,134,663	30,135,933	47	M
NNAT:TSS-DMR	20	36,148,604	36,150,528	135	M
L3MBTL1:alt-TSSDMR	20	42,142,365	42,144,040	84	M
GNAS-NESP:TSS-DMR	20	57,414,039	57,418,612	257	P
GNAS-AS1:TSS-DMR	20	57,425,649	57,428,033	128	M
GNAS-XL:Ex1-DMR	20	57,428,905	57,431,463	200	M
GNAS A/B:TSS-DMR	20	57,463,265	57,465,201	198	M
WRB:alt-TSS-DMR	21	40,757,510	40,758,276	43	M
SNU13:alt-TSS-DMR	22	42,077,774	42,078,873	63	M

Table 4. Recommandation de nomenclatures des régions soumises à empreinte dans le génome humain.
Les coordonnées génomiques sont fournies pour la version GRCh37/hg19. Issu de Monk *et al.* (Monk *et al.*, 2018).

Pour chaque gène, dans chaque type cellulaire et à chaque période d'échantillonnage, une méta-analyse a été appliquée dès lors qu'au moins deux études fournissaient la moyenne de méthylation et les écarts-types associés de l'analyse différentielle entre groupe AMP et contrôle.

Pour les études à l'échelle du génome, seule une analyse comparative qualitative s'est avérée possible en l'absence de données quantitatives disponibles pour une forte proportion d'études. L'analyse a consisté en un recoupement des gènes où ont été retrouvées des DMPs ou DMRs d'une étude à l'autre. Les intersections de gènes contenant des DMPs ou DMRs ont ensuite été visualisées à l'aide de diagrammes de type « UpSet plot » séparément pour les DMPs et DMRs (Figure 22).

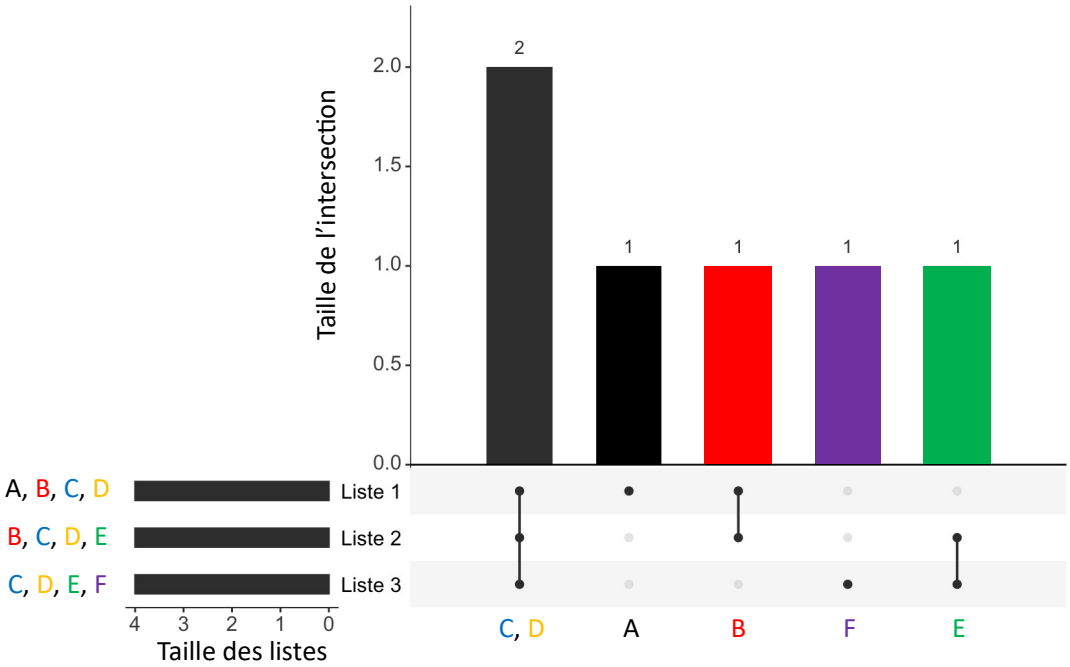

Figure 22. Le diagramme UpSet, une alternative aux diagrammes de Venn.
Il permet de visualiser plus facilement des intersections avec un très grand nombre de listes. Dans cet exemple, C et D est commun aux trois listes, B est commun aux Listes 1 et 2, E est commun aux Listes 2 et 3. A n'est retrouvé que dans la Liste 1, de même que F n'est retrouvé que dans la Liste 3.

1.2.3.3) Résultats

Grossesse

Dans les villosités choriales, une étude a retrouvé une hypométhylation chez les enfants conçus par AMP dans la région KvDMR1, même si ce résultat n'a pas été retrouvé précédemment dans une autre cohorte (Kobayashi *et al.*, 2009; Zechner *et al.*, 2010) (Figure 23). Deux études à large échelle de la même équipe (>450,000 et >730,000 CpGs testés) ont respectivement montré une absence puis la présence de 195 DMPs pour des conceptions via FIV, dont une seule dans un gène soumis à empreinte jusqu'alors non suspecté d'être altéré (*RASGEF1A*) (Xu *et al.*, 2017; Gonzalez *et al.*, 2023) (Figure 23). Cela va dans le sens des études sur des gènes soumis à empreinte cibles qui n'ont également pas mis en évidence de différence (Zheng *et al.*, 2011; Liu *et al.*, 2018). L'effet des techniques d'AMP sur la méthylation de l'ADN a également été évalué sur des tissus fœtaux, mais les conclusions ne semblent pas généralisables à l'AMP en elle-même en raison du recours à la réduction embryonnaire pour l'obtention des échantillons (Lou *et al.*, 2014, 2019; Liu *et al.*, 2021).

A

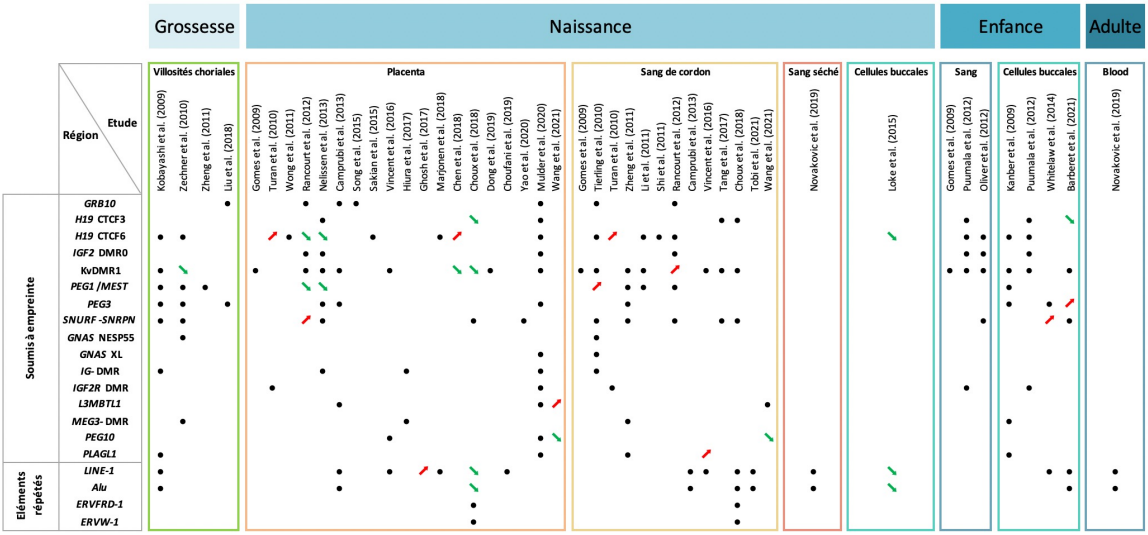

B

		Etude	Nombre de contrôle	Nombre de sujets	Nombre de CpGs testés	Nombre de DMP	Nombre de DMR
Grossesse	Villosités choriales	Xu et al. (2017)	5	5	485 148	0	-
		Gonzalez et al. (2023)	56	44	730 325	195	-
Naissance	Placenta	Katari et al. (2009)	13	10	1 536	246	-
		Camprubi et al. (2013)	121	73	384	-	3
		Litzky et al. (2017)	158	18	1730	-	-
		Choufani et al. (2019)	44	44	414 320	0	-
		Mani et al. (2022)	45	147	793 205	1004	-
	Sang de cordon	Katari et al. (2009)	13	10	1 536	358	-
		Camprubi et al. (2013)	121	73	384	-	0
		Melamed et al. (2015)	8	10	26 486	733	-
		Castillo-Fernandez et al. (2017)	60	46	Génome entier	-	1
		El Hajj et al. (2017)	46	48	428 227	4 730	-
		Gentilini et al. (2018)	41	23	>450 000	0	-
		Chen et al. (2020) (IVF)	34	30	Génome entier	-	4 361
		Chen et al. (2020) (ICSI)	34	26	Génome entier	-	4 831
		Tobi et al. (2021)	70	87	441 836	19	-
		Caramaschi et al. (2021)	2439	205	485 512	5	-
		Håberg et al. (2022)	983	962	770 586	607	-
		Romanowska et al. (2023)	963	982	16 841 (chromosome X)	5 (3 pour ♀ et 2 pour ♂)	15 (12 pour ♀ et 3 pour ♂)
	Sang séché	Estill et al. (2016)	43	94	394 454	-	>1000
		Novakovic et al. (2019)	58	149	722 301	2340	18
		Yeung et al. (2021)	520	158	836 001	12	9
Enfance	Cellules buccales	Barberet et al. (2021)	12	36	4 193	401	33
	Sang	Yeung et al. (2021)	95	23	833 355	1	1
Adolescence	Sang	Penova-Veselinovic et al. (2021)	1188	231	792 104	0	0
Adulte	Sang	Novakovic et al. (2019)	75	158	722 301	0	4

Figure 23. Résumé des résultats des études comparant les profils de méthylation de l'ADN de fœtus, nouveau-nés, enfants, adolescents et adultes conçus par AMP en comparaison de conceptions spontanées.
A. Résumé des études ciblées sur quelques gènes. Une flèche verte indique une hypométhylation avec AMP. Une flèche rouge indique une hyperméthylation avec AMP. Un point noir indique l'absence de différence entre groupe contrôle et AMP.
B. Résumé des études analysant le méthylome global. DMP : position différentiellement méthylée. DMR : région différentiellement méthylée.

Naissance

Chez les nouveau-nés, les différents tissus comparés entre les enfants conçus par FIV/ICSI ou spontanément indiquent des résultats variables. Il y a donc nécessité d'analyser les études par type cellulaire (Figure 23).

Dans le placenta, plusieurs études ciblées indiquent une méthylation altérée de plusieurs régions soumises à empreinte, notamment *H19* (dans les régions régulatrices CTCF3 et CTCF6), KvDMR1, *SNRPN*, *L3MBTL1* et *PEG10* (Turan *et al.*, 2010; Rancourt *et al.*, 2012; Nelissen *et al.*, 2013; Vincent *et al.*, 2016; Chen *et al.*, 2018; Choux *et al.*, 2020; Wang *et al.*, 2021). Ces résultats restent toutefois à confirmer ou infirmer car de nombreuses études n'ont pas retrouvé ces différences et la méta-analyse n'a pas révélé de différences statistiques entre groupe AMP et contrôle (Gomes *et al.*, 2009; Chan Wong *et al.*, 2011; Camprubí *et al.*, 2013; Sakian *et al.*, 2015; Song *et al.*, 2015; Hiura *et al.*, 2017; Marjonen *et al.*, 2018; Dong *et al.*, 2019; Mulder *et al.*, 2020; Yao *et al.*, 2020). Seule la région *PEG1*/*MEST* indique une hypométhylation avérée par le biais de notre méta-analyse (–3.83[–6.83,–0.83], p=0.012) mais seulement deux études ont été incluses en raison de l'absence de données supplémentaires. En outre, certaines régions transposables montrent des niveaux de méthylation modifiés avec AMP, comme dans les éléments mobiles LINE1 ou Alu (Ghosh *et al.*, 2017; Choux *et al.*, 2018) même si cela reste un résultat conflictuel (Camprubí *et al.*, 2013; Vincent *et al.*, 2016; Choufani *et al.*, 2019). De façon plus globale, les premières études à l'échelle de l'épigénome ont rapporté soit une absence, soit peu de modifications ponctuelles de la méthylation de l'ADN dans le placenta (Katari *et al.*, 2009; Camprubí *et al.*, 2013; Litzky *et al.*, 2017; Choufani *et al.*, 2019). La couverture génomique de ces études en termes de CpGs analysés reste toutefois faible et la plus large étude à ce jour a révélé un nombre élevé de DMPs entre groupes AMP (transferts frais ou congelé confondus) et contrôle (Mani *et al.*, 2022).

Dans le sang de cordon, des hyperméthylations en lien avec l'AMP ont été rapportées dans les régions soumises à empreinte *H19* CTCF6, KvDMR1, *PLAGL1* tout en étant non

confirmées par d'autres études et par notre méta-analyse (Gomes *et al.*, 2009; Tierling *et al.*, 2010; Turan *et al.*, 2010; Li *et al.*, 2011a; Shi *et al.*, 2011; Rancourt *et al.*, 2012; Camprubí *et al.*, 2013; Zheng *et al.*, 2013; Vincent *et al.*, 2016; Tang *et al.*, 2017; Choux *et al.*, 2020; Tobi *et al.*, 2021). Notre méta-analyse confirme statistiquement une hyperméthylation dans la région *PEG1*/*MEST* (0.88 [0.17–1.60], p=0.015), mais seulement deux études ont à nouveau pu être incluses. Les études à l'échelle de l'épigénome demeurent également conflictuelles, rapportant à tour de rôle un large panel de CpG/régions différentiellement méthylés ou tout autrement une totale ou faible absence de différences (Katari *et al.*, 2009; Camprubí *et al.*, 2013; El Hajj & Haaf, 2013; Gentilini *et al.*, 2015; Melamed *et al.*, 2015; Castillo-Fernandez *et al.*, 2017; Chen *et al.*, 2020; Caramaschi *et al.*, 2021; Tobi *et al.*, 2021; Håberg *et al.*, 2022; Romanowska *et al.*, 2023).

A partir de sang périphérique prélevé au talon à la naissance, quelques DMPs et DMRs ont été rapportées par Estill *et al.* (2016), Novakovic *et al.* (2019) et Yeung *et al.* (2021) suggérant une possible association entre conception par FIV/ICSI et profil de méthylation altéré dans certaines régions (Estill *et al.*, 2016; Novakovic *et al.*, 2019; Yeung *et al.*, 2021).

Une étude individuelle a par ailleurs rapporté dans les cellules buccales une hypométhylation dans la région *H19* CTCF6 mais aussi dans les éléments LINE1 et Alu parmi le groupe conçu par AMP (Loke *et al.*, 2015).

En conclusion, à la naissance et quel que soit le type cellulaire étudié, les résultats sont conflictuels et restent difficiles à interpréter (Figure 23). Cela est potentiellement dû à la variabilité des techniques et méthodologies statistiques employées, ce qui implique des différences de qualité de l'évidence des résultats présentés. Pris dans son ensemble, la littérature semble toutefois nous indiquer une récurrence de modifications dans les gènes/régions soumis/es à empreinte parentale chez les nouveau-nés. Une question qui demeure en suspens est le degré de responsabilité de chaque type d'AMP dans le profil de méthylation. Certaines pratiques actuelles sont-elles plus à risque d'altérer le méthylome que

d'autres? Dans le placenta et le sang de cordon, des études ont cherché à distinguer les effets spécifiques de certaines techniques utilisées. Le transfert d'embryons congelés semble modifier de façon globale les niveaux de méthylation par hyperméthylation dans le placenta en comparaison de transferts frais (Ghosh *et al.*, 2017; Barberet *et al.*, 2021b; Mani *et al.*, 2022). La tension en oxygène à 20% en comparaison de 5% pourrait être délétère d'après les niveaux de méthylation dans les éléments répétés LINE1 (Ghosh *et al.*, 2017). Aucune différence selon le milieu de culture (G5 vs HTF) n'est retrouvée dans le méthylome du sang de cordon ou dans des régions soumises à empreinte du placenta (Mulder *et al.*, 2020; Koeck *et al.*, 2022a).

Enfance

Durant l'enfance, un faible nombre d'études ont assuré un suivi des enfants nés sous AMP (Figure 23). Dans les cellules buccales, ces études semblent toutefois indiquer la présence de profils de méthylation différents en comparaison de grossesses naturelles, notamment dans les régions soumises à empreinte *SNRPN*, *PEG3* ou *H19* CTCF3 même si certaines études ne les retrouvent pas (Kanber *et al.*, 2009; Puumala *et al.*, 2012; Whitelaw *et al.*, 2014; Barberet *et al.*, 2021a). Notre méta-analyse ne retrouve d'ailleurs aucune différence dans les régions *H19* CTCF3 et *H19* CTCF6, KvDMR1 et *PEG3* entre les groupes conçus naturellement et par AMP. Les régions génomiques autres que soumises à empreinte n'ont pas été investiguées avant la réalisation de cette thèse dans les cellules buccales. En revanche, dans le sang périphérique, Yeung *et al.* ont identifié une unique DMR dans le gène soumis à empreinte *GNAS*, qui de façon intrigante était déjà présente dans une cohorte de nouveau-nés FIV de la même étude (Yeung *et al.*, 2021). D'autres études sur des gènes ciblés dans le sang ne rapportent pas de différences pour les régions testées *H19* CTCF6, *IGF2* DMR0 et KvDMR1, ce qui est confirmé par la méta-analyse (Gomes *et al.*, 2009; Oliver *et al.*, 2012; Puumala *et al.*, 2012). De plus, Barberet *et al.* et Koeck *et al.* ont successivement montré l'absence de différences de méthylation dans les cellules buccales d'enfants entre 7 et 9 ans suivant la culture embryonnaire dans différents milieux (respectivement Global/LifeGlobal vs

SSM/Irvine Scientific et G3/Vitrolife vs K-SICM/Cook) (Barberet *et al.*, 2021a; Koeck *et al.*, 2022b).

Adolescence et vie adulte

A l'adolescence, une étude à l'échelle de l'épigénome utilisant la technologie de pointe de puces EPIC n'a retrouvé aucune différence en comparant le sang de 231 enfants conçus par AMP contre 1188 conçus naturellement (Penova-Veselinovic *et al.*, 2021) (Figure 23). Chez l'adulte, quatre DMRs sont retrouvées dans le sang (Novakovic *et al.*, 2019) (Figure 23). Ces études sont rassurantes quant à la sécurité des techniques d'AMP pour la santé à long terme.

Conclusion

En conclusion, les résultats semblent souvent conflictuels et peu répliqués d'une étude à l'autre concernant les profils de méthylation des enfants conçus sous AMP. Si l'on considère seulement les études avec une très forte qualité de l'évidence, on remarque une prévalence plus forte d'évènements affectant la méthylation des gènes soumis à empreinte (Figure 24). Notre méta-analyse met notamment en évidence de façon robuste des altérations de la région *PEG1*/*MEST* à la naissance (hypométhylation dans le placenta, hyperméthylation dans le sang de cordon).

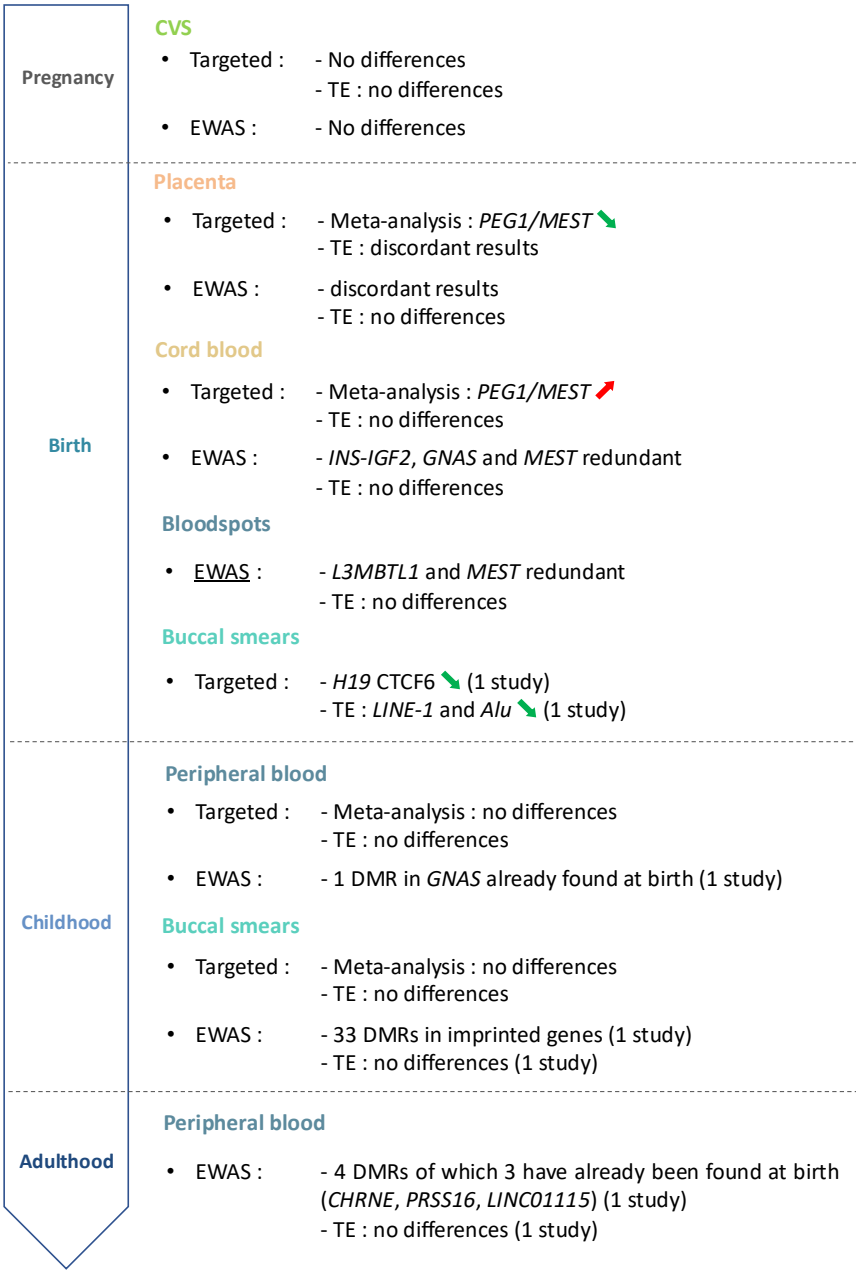

Figure 24. Résumé de l'évidence concernant les modifications épigénétiques en lien avec l'AMP depuis la grossesse jusqu'à l'âge adulte dans les articles notés avec une qualité de l'évidence très haute.

Par ailleurs, même si l'intérêt des études sur les gènes soumis à empreinte est crucial au vu de leurs fonctions biologiques au cours du développement embryonnaire et du cycle cellulaire plus tard dans la vie, il ne faut pas omettre que des altérations de méthylation dans tous les autres gènes peuvent être fréquentes, avec des conséquences inconnues à ce jour. Une des hypothèses en réponse à la variabilité des résultats obtenus réside dans le fait que l'AMP ne

provoque pas de modifications communes d'un individu à l'autre mais plutôt, elle pourrait augmenter le nombre de modifications stochastiques anormales de méthylation en comparaison de conceptions spontanées. Même si de façon évidente la très grande majorité des enfants issus d'AMP sont aujourd'hui en bonne santé, on ne peut exclure que ces légères modifications épigénétiques accroissent la susceptibilité à des maladies aux étiologies complexes de façon aléatoire dans la population d'individus conçus par FIV/ICSI. Des études longitudinales sur la santé de ces populations devront être menées pour écarter ou non ce risque. De plus, il est de fort enjeu de réduire la variabilité épigénétique retrouvée chez l'embryon conçu *in vitro* car elle pourrait expliquer les échecs d'implantation ou les arrêts de développement embryonnaire post-implantation.

1.2.3.4) Article 2 - DNA methylation profiles after ART during human lifespan: a systematic review and meta-analysis

Human Reproduction Update, pp. 1–27, 2022
https://doi.org/10.1093/humupd/dmac010

human reproduction update

DNA methylation profiles after ART during human lifespan: a systematic review and meta-analysis

Julie Barberet [1,2,†], Bastien Ducreux [1,†], Magali Guilleman [1], Emmanuel Simon [1,3], Céline Bruno [1,2], and Patricia Fauque [1,2,*]

[1]Université Bourgogne Franche-Comté – Equipe Génétique des Anomalies du Développement (GAD) INSERM UMR1231, Dijon, France [2]Laboratoire de Biologie de la Reproduction—CECOS, CHU Dijon Bourgogne, Dijon, France [3]Gynécologie—Obstétrique et Biologie de la Reproduction, CHU Dijon Bourgogne, Dijon, France

*Correspondence address. Laboratoire de Biologie de la Reproduction—CECOS, CHU Dijon Bourgogne, 14 rue Gaffarel, Dijon F-21000, France. E-mail: patricia.fauque@chu-dijon.fr https://orcid.org/0000-0002-9708-1710

Submitted on October 22, 2021; resubmitted on February 4, 2022; editorial decision on February 11, 2022

TABLE OF CONTENTS

- Introduction
  - Methylation dynamics during primordial germ cell development
  - Methylation dynamics in the embryo
- Methods
  - Search strategy
  - Eligibility criteria and study selection
  - Data collection
  - Quality assessment
  - Statistical analysis
- Results
  - Study selection
  - Study characteristics
  - Risk of bias and quality assessment
  - Results of individual studies
- Discussion
  - Overall summary of findings
  - Current challenges and recommendations for future research
  - Strengths and limitations of the systematic review
- Conclusion

BACKGROUND: The many manipulations and processes used in ART coincide with the timing of epigenetic reprogramming and imprinting during female gametogenesis and pre-implantation embryo development, leading to concerns that the actual ART could negatively affect epigenetic reprogramming and imprinting in gametes and early embryos. A growing body of literature suggests that ART may affect epigenetic marks, such as DNA methylation, in the fetus and placenta. Potentially, this may be responsible later in life for the increased risk of adverse outcomes associated with ART. Unfortunately, the conclusions are inconsistent and, despite the increasing usage of ART, its safety at the epigenetic level is still not established.

[†]These authors equally contributed to this work.

OBJECTIVE AND RATIONALE: To examine whether ART is associated with DNA methylation modifications and if these modifications persist throughout life, we provide an update on the current understanding of epigenetic reprogramming in human gametes and embryos, and then focus on the assessment of fetal and postnatal DNA methylation modifications that may remain until adulthood following the use of ART in humans.

SEARCH METHODS: We reviewed studies using targeted or epigenome-wide techniques to assess the DNA methylation patterns of the conceptus after ART compared with natural conceptions. A search for relevant studies was performed in the PubMed and EMBASE databases on 15 July 2021 with an extensive search equation. Studies on animals, gametes and embryos were subsequently excluded. After an in-depth review of full-text articles, studies on specific populations with imprinting disorders were removed and not further discussed. Before comprehensive analysis, the risk of bias of each included study was assessed with the Newcastle–Ottawa scale and quality of evidence was graded using the Grading of Recommendations, Assessment, Development and Evaluations criteria.

OUTCOMES: In total, 928 records were initially identified, and 51 were finally included in the systematic review. Given the variability in the genomic scale at which DNA methylation was measured in the different studies, they were separated into two categories: targeted DNA methylation or genome-wide DNA methylation study. The present systematic review has made it possible to assess a substantial number of children since more than 4000 DNA methylation profiles of ART concepti were compared to more than 7000 controls. There is evidence that ART conception is associated with aberrant DNA methylation in imprinted loci and other genes in various tissues. One isolated modification notably occur in the paternally expressed gene 1/mesoderm-specific transcript homologue (*PEG1/MEST*) region, and we cannot rule out other studied sequences owing to the heterogeneity of the evidence base.

WIDER IMPLICATIONS: Differences in DNA methylation after ART conceptions are modest, and the functional relevance in adult tissues is unknown. Functional effects in terms of gene expression as well as the roles of other epigenetic marks need to be further explored. Moreover, there is little overlap of findings obtained in targeted and genome-scale analyses owing to the lack of comparability of CpGs analyzed between both techniques. This issue also stems from small sample sizes and marked differences in methodology and cohort characteristics. Standardization of methodologies and large collaborative efforts are required to reduce the inconsistency of results and increase the robustness of findings. Finally, further studies are required to determine the contribution of parental infertility per se from the ART treatment.

Key words: systematic review / meta-analysis / ART / DNA methylation / imprinted gene / IVF / ICSI

Introduction

The number of offspring conceived through ART has extensively increased over the years, and more than 5 million children have been born with the aid of ART so far. ART includes various processes, from mild interventions, such as hormone treatment, to the more invasive procedures of IVF or ICSI. Even if ART techniques are largely thought to be harmless, the safety of the procedures has gained significant attention. While the great majority of ART infants are healthy, the use of ART is associated with an increased risk of several adverse health outcomes, including obstetric complications and worse perinatal outcomes, e.g. low birth rate and preterm birth (Qin *et al.*, 2017; Berntsen *et al.*, 2019), as well as suboptimal cardiovascular and metabolic function (Hart and Norman, 2013; Guo *et al.*, 2017b). Furthermore, ART-conceived offsprings are reported to have an increased risk of rare imprinting disorders, such as Beckwith–Wiedemann syndrome (BWS), Silver–Russell syndrome (SRS), Angelman syndrome (AS) and Prader–Willi syndrome (PWS), when compared with naturally-conceived (NC) children (Vermeiden and Bernardus, 2013; Lazaraviciute *et al.*, 2014; Cortessis *et al.*, 2018), raising concerns about potential epigenetic dysregulations in the context of ART (Kopca and Tulay, 2021). Notably, a recent meta-analysis reported a positive association between ART conceptions and BWS with a summary odds ratio of 5.8 (95% CI: 3.1–11.1) (Cortessis *et al.*, 2018). The phenotype of BWS, characterized by an overgrowth condition, recalls the previously described large offspring syndrome (LOS) observed in bovine and ovine offspring generated by IVF, suggesting that these conditions have a common mechanism of origin (Young *et al.*, 1998). LOS in animals has been found to be associated with epigenome dysregulations, especially in imprinted genes (IGs) (Young *et al.*, 2001; Farin *et al.*, 2010; Chen *et al.*, 2015). In addition, in humans, parental subfertility may also play a role in the increased incidence of these imprinting disorders, as underlined in a Dutch study performed in families with a child with BWS (Doornbos *et al.*, 2007). Thus, these associations probably originate through epigenetic mechanisms in the gametes and/or early embryonic stage since major epigenetic events during gametogenesis and embryo development overlap with ART interventions (Fleming *et al.*, 2018). During these periods of epigenetic programming, the genome is particularly vulnerable to environmental factors. More particularly, epigenetics refers to the processes leading to heritable variations in gene expression during mitotic or meiotic cell divisions that do not result from changes in the primary DNA sequence. In mammals, epigenetic mechanisms include DNA methylation, post-translational modification of histones (known as the 'histone code'), long non-coding RNAs and microRNAs. These distinct but interrelated marks contribute to the establishment and maintenance of specific gene expression patterns that determine cell identity and can regulate the stable inheritance of cellular memory during mitotic division. DNA methylation and post-translational biochemical modifications in histones change chromatin accessibility and packaging, allowing gene activation or repression. Among the various epigenetic marks in humans, DNA methylation, in which a methyl group (–CH3) is added to unmethylated cytosine in cytosine–guanine (CpG) dinucleotides, is a major covalent modification of DNA and the most widely investigated epigenetic mark. Consequently, we have made DNA methylation the focus of this review.

DNA methylation mostly takes places in palindromic CpG dinucleotides, while non-CpG methylation can be found in cells with high *de*

novo methylation activity, such as neuronal cells and oocytes (Okae *et al.*, 2014; Yu *et al.*, 2017). Regions with high-density CpG dinucleotides, called CpG islands, are predominantly unmethylated and commonly located at promoters of developmental genes (Deaton and Bird, 2011). On the contrary, the rest of the genome, including repetitive elements and intergenic and intronic regions, is considered to be CpG poor and usually methylated. In most human somatic cells, 60–80% of the ~28 million CpGs are methylated (Smith and Meissner, 2013).

The association between DNA methylation and gene silencing has long been recognized. Silencing occurs through the recruitment of methylated DNA-binding proteins or changes in accessibility of the DNA sites, but the mechanisms are still poorly understood. The correlation between DNA methylation and gene silencing increases with the density of CpG dinucleotides at promoters (i.e. low CpG density promoters, generally hypermethylated, remain transcriptionally active regardless of their methylation state) (Weber *et al.*, 2007). However, DNA methylation-based gene regulation is more complex and multifaceted than previously thought. Recent insights suggest that DNA methylation is associated with functional interaction and recruitment of sequence-specific transcription factors (Hu *et al.*, 2013; Yin *et al.*, 2017), chromatin remodelers and modifiers (Greenberg and Bourc'his, 2019) and even gene activation through binding with transcription activators (Yu *et al.*, 2013).

On the other hand, lifelong DNA methylation-based silencing is particularly important in three major classes of genes in somatic tissues: genes in inactivated X-chromosomes, IGs and transposable elements (TEs). Among them, X-inactivation and imprinting are both forms of non-Mendelian inheritance in which only one allele is expressed. IGs are thus a subset of autosomal genes preferentially expressed from only one of the two parental chromosomes. This targeted parent-of-origin-dependent expression results from DNA methylation monoallelic apposition via *de novo* methyltransferase activity (DNMT3A/B) during gametogenesis in male and female germlines. DNA methylation can be inherited by the daughter cells during subsequent cell divisions by maintaining methylation status with the help of the maintenance DNA methyltransferase DNMT1, characterizing parental imprinting. Genomic imprinting plays a key role in maintaining normal embryogenesis, prenatal and postnatal growth (Barlow and Bartolomei, 2014). In humans, more than 100 IGs have been identified, and they are generally clustered in differentially methylated regions (DMRs), allowing *cis*-regulation of monoallelic expression (Monk *et al.*, 2019). Imprinted DMRs (iDMRs) are classified into two groups: primary and secondary DMRs (Ferguson-Smith, 2011). Over 20 primary DMRs, also called germline DMRs, acquire their methylation status during gametogenesis and remain stable throughout life. These DMRs are the crucial imprinted control regions (ICRs) that are needed to achieve monoallelic parent-of-origin-specific expression. A single ICR can control the expression of the nearest single IG or the entire gene cluster, and serve as either a methylation-sensitive insulator or promoter for long non-coding RNAs (Barlow and Bartolomei, 2014). Secondary DMRs, also referred to as somatic DMRs, acquire their methylation modifications after fertilization and are regulated by germline DMRs (Okae *et al.*, 2014).

Beyond being essential for parental imprinting, the acquisition and maintenance of gametic identity, and pluripotency embryonic lineage decisions, DNA methylation is one of the epigenetic mechanisms that silences the expression and mobility of TEs (Fauque and Bourc'his, 2014). Approximately 45% of the human genome is composed of TEs, representing millions of copies (Kazazian and Moran, 2017), and the ectopic recombination of TEs may lead to insertional mutations and detrimental structural rearrangements. By restricting the mechanisms of TEs expression, DNA methylation is a major means of limiting retrotransposition (Kazazian and Moran, 2017).

DNA methylation profiles are stably inherited in mitotically dividing cells. However, the mammalian genome undergoes two widespread waves of CpG methylation profile reprogramming during early embryonic and germline development. These two periods have been shown to be crucial for proper development in mammals (Hackett and Surani, 2013). Thanks to genome-wide methods assessing DNA methylation with single nucleotide resolution from a few cells, much progress has been recently made in understanding the genetic requirements for these epigenome reprogramming processes (Greenberg and Bourc'his, 2019; Monk *et al.*, 2019; Wen and Tang, 2019). Mechanisms of DNA methylation reprogramming in early embryogenesis and in germline development differ mainly in the number of sequences that resist DNA methylation loss. The germline wave of demethylation is more extensive than the pre-implantation development wave (Fig. 1). The following evidence relates to human data.

Methylation dynamics during primordial germ cell development

In human embryos, the first wave of genome-wide DNA demethylation in primordial germ cells (PGCs) takes place before 4–7 weeks: the entire genome of PGCs undergo significant demethylation. At ~10–11 weeks of gestation, the overall DNA methylation levels reach the lowest point, with <10% residual methylation (Guo *et al.*, 2014; Gkountela *et al.*, 2015). Probably both passive dilution and active demethylation mediated by DNA demethylases TET1 and TET2 contribute to this extensive erasure of the parental DNA methylation memory (Guo *et al.*, 2014; Gkountela *et al.*, 2015).

ICRs undergo demethylation in developing PGCs, which is a necessity for later acquisition of sex-specific DNA methylation patterns during male and female germline differentiation. Conversely, some genomic loci, referred to as 'escapees' and mostly associated with retrotransposable elements, remain methylated in the PGCs. In particular, evolutionarily younger families of repetitive elements in humans, such as LINE-1 from the long interspersed nuclear elements (LINE) family and Alu from the short interspersed nuclear elements family, still retain abundant residual DNA methylation (Okae *et al.*, 2014; Gkountela *et al.*, 2015; Guo *et al.*, 2015; Tang *et al.*, 2015). The KAP1-Krüppel-associated box zinc-finger protein (KRAB-ZFP) co-repressor complex may be involved in recruiting DNMT1 to maintain DNA methylation in retrotransposons (Tang *et al.*, 2015). This state of residual DNA methylation and less accessible chromatin in the probably more active and deleterious transposable elements suggest a mechanism to repress transcription and transposition, and raises the possibility of the existence of epigenetic inheritance (Guo *et al.*, 2014, 2017a; Tang *et al.*, 2015).

Following the period of DNA demethylation in PGCs, sex-specific patterns of DNA methylation are established in the male and female germlines, asynchronously between the sexes. In the male germline, *de novo* methylation occurs before birth and is maintained through many

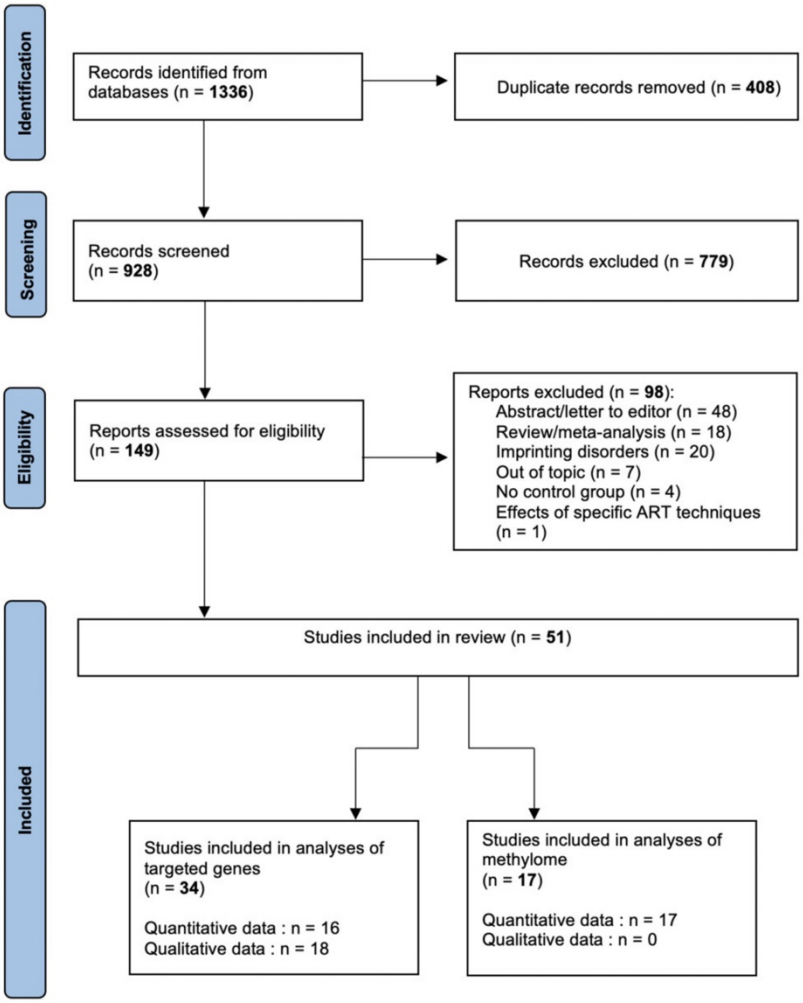

Figure 1. Flow chart of selection of records for the systematic review, assembled according to PRISMA guidelines. PRISMA, Preferred Reporting Items for Systematic Reviews and Meta-Analysis.

cycles of mitotic division before entry into meiosis, while female germ cells remain hypomethylated throughout the fetal period. Methylation levels remain low in female and male PGCs until at least 19 weeks of development, implying that global re-methylation occurs later (Guo *et al.*, 2015). Male germ cells initiate *de novo* methylation between 59 and 137 days of development (Gkountela *et al.*, 2015). At the end of gametogenesis, the sperm genome exhibits ~80% CpG methylation (Zhu *et al.*, 2018). In contrast, oocytes remain hypomethylated until maturation in the post-pubertal period (Smallwood and Kelsey, 2012). During each menstrual cycle, DNA methylation is gradually re-established throughout oocyte growth. At the end of gametogenesis, the Metaphase II oocyte genome exhibits ~50–55% CpG methylation (Yu *et al.*, 2017; Zhu *et al.*, 2018). The fact that processes of *de novo* DNA methylation of oocytes are progressive and not established until the final stages of the oocyte draws attention to the risk of potential deregulations induced by reproductive techniques. Particularly, controlled ovarian hyperstimulation, *in vitro* oocyte maturation, and oocyte manipulations required in the oocyte freezing protocols are at high risk of causing methylation dysregulations (Barberet *et al.*, 2020).

Methylation dynamics in the embryo

Following fertilization and before the blastocyst stage, a genome-wide loss of DNA methylation is required to establish pluripotency and

develop embryonic lineages. Initial rapid demethylation primarily affects the paternal genome of human zygotes, 10–12 h after fertilization to the early male pronucleus (Zhu *et al.*, 2018). Through a combination of passive dilution of 5 mC and TET3-mediated demethylation, the demethylation rate of the male genome is faster and deeper than that of the maternal genome at the zygote stage. Indeed, demethylation of the maternal genome is more limited, and some oocyte-specific methylated regions maintain maternal allele-specific methylation during pre-implantation development (Okae *et al.*, 2014). Additionally, members of the subcortical maternal complex, such as NLRP5 and its associated proteins, are involved in oocyte-specific imprint establishment and maintenance (Monk *et al.*, 2019). Despite genome-wide DNA demethylation after fertilization, imprinting centers escape the DNA methylation reprogramming, thanks to a KRAB-KZFP protection mechanism. The recognition of the specific TGCCGC sequence in oocyte ICRs by ZFP57 and ZFP445 recruits DNA methyltransferases, KAP1 (KRAB-associated protein 1), and other silencing factors (Strogantsev *et al.*, 2015; Takahashi *et al.*, 2019). In humans, mutations of the *ZFP57* gene are associated with the phenotype of transient neonatal diabetes mellitus with multilocus imprinting disturbances (Touati *et al.*, 2019), whose incidence was reported to be higher after ART (Fauque *et al.*, 2020). As a result, the parent-specific DNA methylation of ICRs acquired in the germline is maintained during pre-implantation development.

Interestingly, two waves of *de novo* methylation occur from the early to mid-pronuclear stage and from the four-cell to the eight-cell stage, along with embryonic genome activation. These are strongly enriched for evolutionarily young subfamilies, such as the Alu and LINE-1 transposable elements. This underscores that the DNA methylation dynamic during pre-implantation development is a balance between strong genome-wide demethylation and focused remethylation (Zhu *et al.*, 2018). Furthermore, from the two-cell stage onward, residual methylation is consistently higher on the maternal than the paternal genome, and the trend continues in post-implantation embryos and extra-embryonic lineages (Zhu *et al.*, 2018).

After reaching a minimal methylation level at the blastocyst stage, the embryo undergoes genome-wide remethylation that establishes the methylation landscape in somatic cells. Based on human implantation embryos from *in vitro* culture system, the three major lineages [pluripotent epiblast (EPI), trophectoderm (TrE) and primitive endoderm (PrE), giving rise to the embryo proper, placenta and yolk sac, respectively] have different gene-expression signatures but also show distinct and asynchronous DNA re-methylation patterns (Zhou *et al.*, 2019). The increase in TrE methylation is weaker than that of EPIs. Although both the PrE and EPI are generated from the inner cell mass, PrE has a slower DNA remethylation pattern than both EPI and TrE. Moreover, the promoters of many lineage-specific genes are methylated in reciprocal cell lineages in which they are silenced, suggesting that DNA methylation has an important role in regulating the expression of lineage-specific genes (Zhou *et al.*, 2019). In addition, the greater part of remaining DNA methylation at the blastocyst stage is related to evolutionarily young and potentially active transposable elements, in particular the LINE-1 and Alu elements, probably to maintain stronger repression of their transcription and activity (Guo *et al.*, 2014).

After implantation, most genomic features (e.g. gene bodies, TEs and CpG-poor promoters) become remethylated, while CGIs mostly remain unmethylated. Compared with somatic tissues, the cells of the placenta have a unique epigenetic profile and they are mostly hypomethylated (Schroeder *et al.*, 2013; Robinson and Price, 2015). In the placenta, a large number of oocyte-derived methylation differences persist in a unique manner as transiently methylated DMRs (Sanchez-Delgado *et al.*, 2016). In somatic tissues, IGs show intermediate methylation levels in ICR DMRs, concordant with monoallelic gene expression and silencing of a reciprocal parental allele through DNA methylation (Pervjakova *et al.*, 2016).

Finally, all ART procedures occur in the time frame during which drastic global epigenetic reprogramming occurs (i.e. during female gametogenesis and pre-implantation embryo development), and when the embryonic epigenome may be more vulnerable to external changes. Ovarian stimulation, IVM, fertilization, embryo culture, embryo biopsy, transfer and cryopreservation all have the potential to disrupt epigenetic reprogramming and imprinting in gametes and early embryos. Owing to the potential impact of ART on gamete and embryo epigenetic competence, subsequent embryo development and placentation, ART techniques might consequently affect pregnancy or neonatal and long-term DNA methylation in children conceived through ART compared to natural conception. Little is known about the human ART offspring methylome even if the last two decades have seen an increase in the number of studies investigating the epigenetic signatures of human conceptions after ART. While the evidence was reviewed most recently in 2014 (Lazaraviciute *et al.*, 2014), it is now out of date as microarray-based technologies are now available.

To examine whether ART is associated with DNA methylation modifications and if these modifications persist during the human lifespan, we systematically reviewed trials using epigenome-wide or targeted techniques to assess the DNA methylation patterns of the conceptus after ART compared with NC pregnancies and children. Our main objective was to perform a meta-analysis of quantitative targeted studies and to summarize the findings from genome-wide cohorts. The included studies were organized according to the timing of sampling (during pregnancy, at birth, during childhood, adolescence and adulthood) and also according to the source tissue (chorionic villus samples, placenta, cord blood, peripheral blood and buccal samples). Finally studies were sorted by the resolution at which DNA methylation was assessed (at specific loci or across the methylome). Finally, we propose concrete recommendations for future research in the field.

Methods

A protocol for this systematic review was registered on the international prospective register for systematic reviews, PROSPERO (ID number CRD42021267425). The Preferred Reporting Items for Systematic Reviews and Meta-Analysis (PRISMA) guidelines for systematic reviews were followed in the development of this review and meta-analysis (Page *et al.*, 2021).

Search strategy

We conducted a systematic search of the literature published in Medline/PubMed and Embase on 15 July 2021. An elaborate search strategy can be found in Supplementary Table SI. Records obtained

from each database were merged and duplicates were removed with reference management software (Mendeley). A flow diagram of the selection process, including the number of articles filtered at each step of the process, is shown in Fig. 1.

Eligibility criteria and study selection

This review focuses on the assessment of fetal and postnatal DNA methylation modifications that may occur following the use of ART in humans. Eligibility criteria were chosen according to the Patients, Interventions, Comparison and Outcomes framework. Eligible studies examined epigenome-wide or targeted associations among DNA methylation of source tissues accessible/representative of the conceptus after ART, at any point from the onset of pregnancy to adulthood (fetuses, neonates, children, adolescents, adults). The different types of ART included were conventional IVF and ICSI with fresh and frozen embryo transfers (FETs), and IUI. Comparisons were made with a population of NC counterparts. The outcome of interest was any type of analysis method of DNA methylation at specific loci or across the methylome.

We excluded studies in which the tissue was not a result of ART (e.g. gametes) and non-human studies. Second, articles were excluded by screening if they were not original research articles (reviews, conference abstracts, case reports and commentaries), if they did not include a control population, or if the population included only patients with imprinting disorders (such as BWS cohorts). Two reviewers (J.B. and B.D.) independently performed the literature search and screening according to the eligibility criteria. Any discrepancies were resolved through discussion and, if needed, a third author (P.F.) was consulted to reach consensus. All these steps were processed with the Covidence© software.

Data collection

Information extracted from every identified study was recorded according to a data extraction form (Supplementary Table SII) by the first primary author and independently verified by the second primary author. Any disagreements were resolved through discussion with a third author. We divided the included studies according to the stage at which samples were collected (during pregnancy, at birth, during childhood, adolescence and adulthood). We then arranged them according to the source tissue (chorionic villus samples, placenta, cord blood, peripheral blood or buccal samples) and to the resolution at which DNA methylation was assessed (single gene or genome-wide approach).

The means and SDs of DNA methylation at each region were obtained or calculated from original articles. When necessary, authors were contacted to seek additional data in a format suitable for meta-analyses. Methylation values for ICSI and IVF groups were pooled with the *dmetar* package (Harrer *et al.*, 2019) to avoid 'double-counting' of the control group, when applicable. As a substantial number of studies are uncontrolled and retrospective studies or matched studies without quantitative measures; we performed meta-analyses wherever appropriate and also added narrative data descriptions.

Quality assessment

The quality assessment of studies was independently performed by two separate reviewers (J.B. and B.D.) and any disagreement was resolved by discussion between the two parties or by including a third reviewer (P.F.). First, each study was given a maximum of nine stars according to three categories following the Newcastle–Ottawa scale for cohort studies: selection, comparability and outcome (Wells *et al.*, 2013). Risk of bias was rated as high (0–5), moderate (6–7) or low (8-9), depending on whether or not they met the evaluation criteria. Questions adapted to the topic of interest can be found in Supplementary Table SIII. Furthermore, we applied the Grading of Recommendations Assessment, Development and Evaluation (GRADE) approach to score the quality of evidence on two key concepts: magnitude of effect and quality of evidence (considering the risk of bias, study design, consistency, directness and precision of findings) (Ryan and Hill, 2016). The evaluation was performed with a custom GRADE form inspired by a previous systematic review on DNA methylation in human sperm (Supplementary Table SIV) (Åsenius *et al.*, 2020). Specifically, targeted studies were penalized for imprecision when their sample size was not sufficient to detect a 2.5% methylation difference with 80% power between ART and control groups, which required a sample size of at least 63 individuals per group with a 1:1 ratio. Genome-wide studies were penalized when they did not reach a total arbitrary sample size >100 or when one group contained <30 samples. Targeted studies analyzing less than three genes were penalized because they are suspected of publication bias. Publications with GRADE ratings of ≥ 0 were assigned a quality score of 'high', -1 were assigned 'moderate', -2 were assigned 'low' and ≤ -3 were assigned 'very low'.

Statistical analysis

We conducted two separate data pre-processing and analyses according to the resolution at which DNA methylation was assessed (single gene or genome-wide). Targeted DNA methylation studies were defined as those scanning CpGs across reduced regions (selected genomic families or genes) including bisulfite sequencing, pyrosequencing, methylation-specific polymerase chain reaction (PCR), bisulfite PCR, combined bisulfite restriction analysis, single-nucleotide primer extension (SNuPE), sequence-based quantitative methylation analysis, methylation-specific quantitative PCR, single nucleotide primer extension reaction ion pair reverse-phase high performance liquid chromatography (SIRPH), methylation-sensitive restriction endonuclease assay, MassARRAY EpiTYPER and luminometric methylation assay. Genome-wide DNA methylation studies were defined as those scanning CpGs across the complete set of DNA at high resolution using arrays, reduced representation bisulfite sequencing (RRBS) or methylated DNA immunoprecipitation sequencing (MeDIP-seq).

Targeted DNA methylation studies

If precise genomic coordinates of the studied sequences were not directly available, pairs of primers collected from data extraction used in the study protocol were subjected to *in silico* bisulfite PCR with BiSearch (Tusnády *et al.*, 2005). All coordinates were converted to GRch37/hg19 and were attributed to a clearly identified iDMR (i.e. a set of CpGs located in ICRs) if they were overlapping coordinates of a consensus list of iDMRs (Monk *et al.*, 2018). For the *H19/IGF2* DMR, we retrieved CTCF-binding sites coordinates from NCBI Genome Data Viewer (Rangwala *et al.*, 2021).

Regions where mean DNA methylation ± SD was available at least twice for one tissue were subjected to a meta-analysis according to the timing of sampling and the source tissue. A random effects model with a DerSimonian–Laird estimate for between-study variance was chosen and the weighted mean difference (95% CI) was calculated with the R *meta* package (Balduzzi *et al.*, 2019). Heterogeneity was assessed using the Higgins and Thompson I2 statistic (Higgins and Thompson, 2002). When exceeding 50%, it indicates considerable heterogeneity between studies. According to the recommendations in Higgins *et al.* (2019), we performed a meta-analysis for both random effects and fixed effects, and we chose to present results obtained from the random effects model because the results were similar in the case when heterogeneity was low (Higgins *et al.*, 2019). A *P*-value < 0.05 was used to set statistical significance. Forest plots were generated and in order to improve visualization of missing numerical data, the direction of significant DNA methylation modifications was indicated (left arrow for hypomethylation with ART, right arrow for hypermethylation with ART, dot for no difference between conception groups). Regions studied at least two times in different articles but where quantitative assessment of methylation was not available were grouped for a comparative analysis without meta-analysis (referred to as 'supplementary' studied IGs). Finally, regions studied only once were not further discussed.

Genome-scale DNA methylation studies

We were able to extract differentially methylated probes (DMPs) and DMRs data according to a variety of definitions and statistical thresholds set in each individual study (Supplementary Tables SV and SVI). In those studies, DMP refers to a single differentially methylated CpG, whereas a DMR is a block of adjacent CpGs that display differential methylation. Two studies solely displayed DMPs located in genes containing at least two DMPs (Katari *et al.*, 2009; Melamed *et al.*, 2015). To ensure comparability between studies, we selected and defined DMPs as those located in genes with two or more DMPs for downstream analysis for the 10 studies left (Supplementary Table SV). Then, CpG identifications were checked for any overlap between studies that were performed with Illumina 27k/450k/EPIC BeadChip arrays. Every CpG was rematched to the nearest gene using matchGenes function from the *bumphunter* R package (Jaffe *et al.*, 2012) so as to have the same gene annotation between studies and to avoid alias ambiguity. IGs containing DMPs were identified by crossmatching within a list of 76 genes known to be imprinted (Pervjakova *et al.*, 2016).

Raw or preprocessed datasets used in a majority of epigenome-wide association studies were provided in only 9 out of 17 (Supplementary Table SV). However, various tissues were analyzed in these studies, explaining why only a qualitative comparative analysis was feasible.

Analysis of DMRs required all coordinates to be converted to GRCh37/hg19 with *liftOver* (Hinrichs *et al.*, 2006). As previously carried out for DMPs, we cross-checked the genomic coordinates between DMRs found in each study to identify similar DMRs across studies. We re-annotated DMR coordinates to the closest gene. For one study that had more DMRs than its contemporaries, since DMRs were given for two subgroups (IVF and ICSI), we chose to select common DMRs with the same methylation direction as DMRs representative of an ART group inside their cohort. Intersections of sets of genes containing DMPs or DMRs are visualized, thanks to an UpSet plot, which is an alternative for Venn diagrams when there is a large number of datasets. Finally, reporting biases were graphically examined through the inspection of funnel plots displaying sample size against standard error for each study.

Results

Study selection

The literature search returned 1336 records. After duplicate removal, 928 studies were identified in total. After exclusion and eligibility criteria were applied, 51 studies were included in the systematic review. Compared with the most recently published meta-analysis, which included 18 targeted studies (Lazaraviciute *et al.*, 2014), we included an additional 23 studies in targeted DNA methylation analysis and 17 methylome studies. The PRISMA flowchart in Fig. 1 presents the selection process. For 18 studies, quantitative data regarding methylation were not available for meta-analysis.

Study characteristics

The 51 included studies are presented according to the timing of sampling (during pregnancy, at birth, during childhood, adolescence and adulthood) and source tissue (chorionic villus samples, placenta, cord blood, peripheral blood and buccal samples) in Fig. 2. Characteristics of the included studies are detailed in Supplementary Table SVII. The majority of studies were conducted in neonates using placenta or cord blood. In pregnancy, six studies were conducted by chorionic villus sampling (CVS). Seven studies focused on children younger than 10 years using buccal smears or blood samples. Among adolescents and adults, only two studies were performed using blood samples, but both had large cohorts.

Risk of bias and quality assessment

Details on how each study was graded are available in Supplementary Table SVII. Twenty out of 51 studies were considered as having a high risk of bias. This was mainly the case for pioneering studies that did not adjust methylation assessment for confounders. Targeted studies were largely considered as low or very low quality of evidence because of their weak statistical power for detecting small methylation differences, the small number of genes studied (publication bias) and the high risk of bias. Genome-wide studies were better classified thanks to their larger sample sizes, the inclusion of a validation cohort or because they adjusted for important confounders. For the remaining studies, the main risks of bias remained the oversight of cell-type composition adjustment, the inclusion of cases with unknown types of ART and too little information on the selection of controls.

Results of individual studies

The characteristics of the main findings of the studies and methylation measures are available in Supplementary Tables SVI and SVII.

Methylation differences during pregnancy

CVS provides the earliest time point that can be used to study the influence of the mode of conception on DNA methylation levels. Mostly

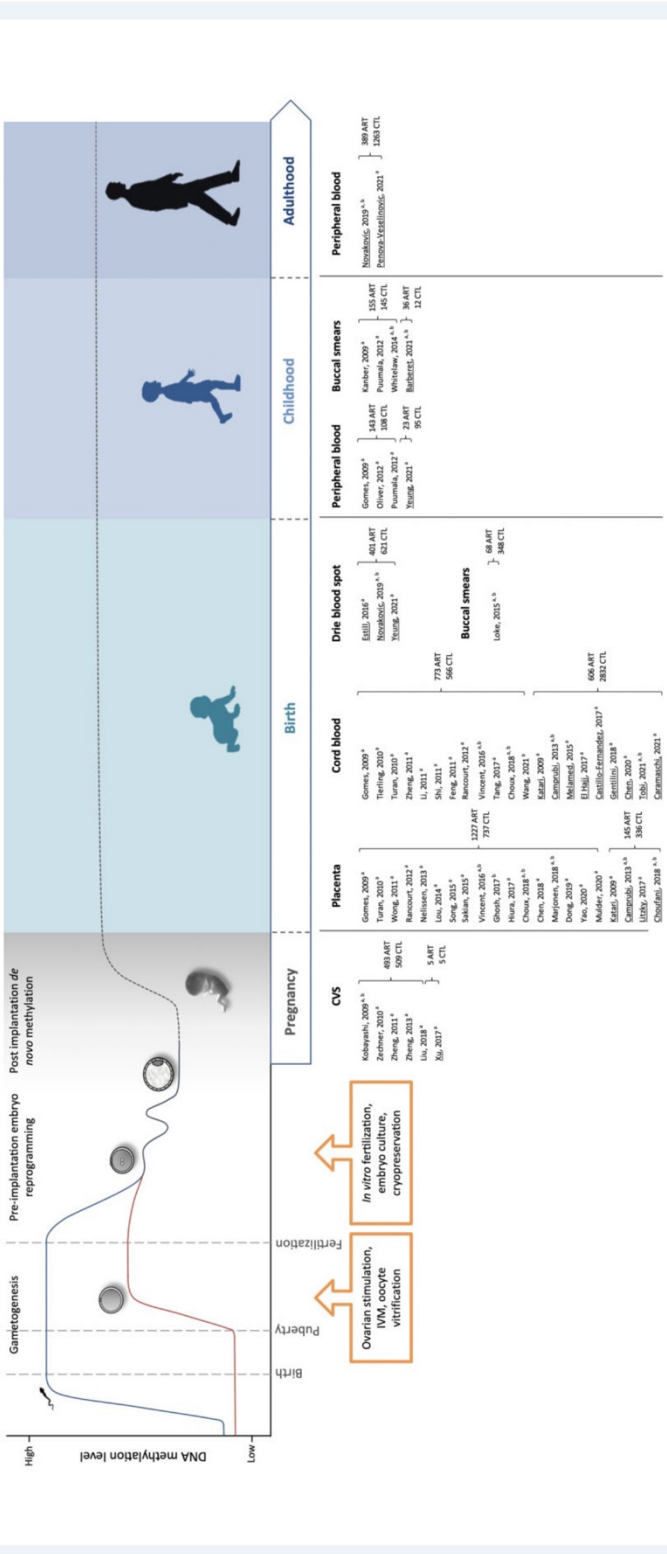

Figure 2. DNA methylation reprogramming during human development and overview of included studies. Studies assessing the effect of ART conception on DNA methylation in Human are classified according to the timing of sampling (during pregnancy, at birth, during childhood, adolescence and adulthood) and source tissue (chorionic villus samples, placenta, cord blood, peripheral blood and buccal sample). Blue line represents DNA methylation in the male germline (or after fertilization, the male genome). Red signifies the female germline/genome. Genome-wide approaches are underlined. [a]DNA methylation of imprinted genes. [b]DNA methylation of transposable elements. Numbers represent the total number of children born after ART or after natural conception. CTL, controls; CVS, chorionic villus sampling.

based on CVS from abortions (spontaneous or induced) or stillbirth, five studies reported targeted DNA methylation analyses, comparing a total of 493 ART fetuses and 509 spontaneously conceived abortions or reductions (Fig. 2). One study was excluded from the qualitative and quantitative assessment of DNA methylation after ART because the results for CVS and muscle samples were indivisible (Zheng *et al.*, 2013). Owing to the lack of available data in this tissue, a meta-analysis was not feasible on targeted IGs. Among the entire studied sample, significant differences of DNA methylation levels between ART and NC children were reported for only 42 ART and 29 NC.

In the KvDMR1 region, while Zechner et al. (2010) uncovered significant hypomethylation associated with ART, Kobayashi *et al.* (2009) found no difference between conception groups. Across the four targeted CVS studies, our qualitative analysis revealed no DNA methylation differences between conception groups for KvDMR1, and there was no additional discordance between studies for nine other imprinted regions (*GRB10, H19 CTCF6, PEG1/MEST, PEG3, SNRPN, GNAS NESP55, IG-DMR, MEG3-DMR, PLAGL1*) (Zheng *et al.*, 2011b; Liu *et al.*, 2018) (Fig. 3). Kobayashi *et al.* found no further differences in LINE-1 and Alu transposable elements (Kobayashi *et al.*, 2009).

Only one study undertook genome-wide DNA methylation assessment of *in vitro* conception in first-trimester CVS samples from gestations delivered after 20 weeks (Xu *et al.*, 2017). This study did not demonstrate a difference between ART and NC groups among more than 400 000 probes tested on a very small sample size (n = 5 IVF and 5 NC).

In conclusion, there is limited evidence that DNA methylation levels of IGs are comparable in IVF and ICSI versus NC, based on CVS.

Methylation differences at birth

Many of the values needed for meta-analyses (e.g. means and standard error) were missing for a significant number of studies (only 10 studies out of 24 had available numerical data).

Placenta. With 18 studies targeting IG and repetitive element DNA methylation, placenta was the most studied tissue in neonates. A total of 1372 DNA methylation profiles of ART children (1227 in targeted studies and 145 in methylome studies) were compared to those from 1073 NC children (737 in targeted and 336 in methylome cohorts) (Fig. 2). Among the ART children, the vast majority was conceived by IVF or ICSI, but 161 were conceived after FETs and 27 after the use of ovulation induction (OI) medication. Results varied among the studies since significant differences in DNA methylation levels between ART and NC children were reported for 514 ART and 530 NC out of the total, i.e. on less than a half of the entire studied sample.

Among candidate gene studies of DNA methylation, there was a consensus toward *PEG1/MEST* as two studies showed significant hypomethylation after ART in this region (Rancourt *et al.*, 2012; Nelissen *et al.*, 2013) (Fig. 3A). Meta-analysis of data from these two sets of samples demonstrated significant hypomethylation after ART: –3.83 (–6.83 to –0.83), $P = 0.012$ (Fig. 4).

The KvDMR1 region has been extensively studied (Fig. 3A). Two studies out of nine reported significant hypomethylation of KvDMR1 after ART (Chen *et al.*, 2018; Choux *et al.*, 2018) but the meta-analysis was not significant (–1.15 (–2.69 to 0.39), $P = 0.144$, n = 4 studies) (Gomes *et al.*, 2009; Rancourt *et al.*, 2012; Camprubí *et al.*, 2013; Nelissen *et al.*, 2013; Vincent *et al.*, 2016; Chen *et al.*, 2018; Choux *et al.*, 2018; Dong *et al.*, 2019; Mulder *et al.*, 2020) (Fig. 4).

For the *H19* gene, the results are conflicting (Fig. 3A). In the CTCF3 region, one study brought to light hypomethylation after ART (Choux *et al.*, 2018), while two others found no difference (Mulder *et al.*, 2020; Nelissen *et al.*, 2013). In the CTCF6 region, two studies showed evidence of hypomethylation (Rancourt *et al.*, 2012; Nelissen *et al.*, 2013) while two reported hypermethylation after ART (Turan *et al.*, 2010; Chen *et al.*, 2018) and four others found no differences (Wong *et al.*, 2011; Sakian *et al.*, 2015; Marjonen *et al.*, 2018; Mulder *et al.*, 2020) (Fig. 3A). Overall, the pooled mean methylation difference for *H19* in meta-analysis suggests that there is not a statistically significant difference (CTCF3: –1.80 (–4.09 to 0.48), $P = 0.122$, n = 3 studies; CTCF6: –0.45 (–1.81 to 0.91), $P = 0.516$, n = 6 studies) (Fig. 4).

In *SNRPN*, it is also unclear how placenta methylation reacts to ART. Whilst significant hypermethylation after ART was reported by Rancourt *et al.* (2012), three other studies found no differences (Nelissen *et al.*, 2013; Choux *et al.*, 2018; Yao *et al.*, 2020). Meta-analysis was not significant (–0.41 (–2.76 to 1.93), $P = 0.730$, n = 3 studies) (Fig. 4).

Among 'supplementary' studied IGs, four studies analyzed the effects of ART conception on *L3MBTL1* and *PEG10* DNA methylation (Fig. 3B). While two of them found no difference on *L3MBTL1* (Camprubí *et al.*, 2013; Mulder *et al.*, 2020) or *PEG10* (Vincent *et al.*, 2016; Mulder *et al.*, 2020), a recent study concluded that there was, respectively, hyper- and hypomethylation of *L3MBTL1* and *PEG10* after ART (Wang *et al.*, 2021). Nevertheless, this study relied on MS-PCR, which is used for qualitative assessment of methylation and cannot be deemed as a strong level of evidence. No difference was reported for the other 'supplementary' sequences (Turan *et al.*, 2010; Nelissen *et al.*, 2013; Lou *et al.*, 2014; Hiura *et al.*, 2017).

In *GRB10*, *IGF2*, *IGF2R* and *PEG3*, DNA methylation levels in placenta do not appear to be modified by ART procedures (Rancourt *et al.*, 2012; Camprubí *et al.*, 2013; Nelissen *et al.*, 2013; Song *et al.*, 2015; Mulder *et al.*, 2020) ($P > 0.05$, Figs 3A and B and 4).

Among transposable elements, LINE-1 was reported as differentially methylated in two out of six studies (Ghosh *et al.*, 2017; Choux *et al.*, 2018), but in inverse directions. Concerning Alu sequences, Choux *et al.* reported hypomethylation in ART children, which was not corroborated by a previously published study (Camprubí *et al.*, 2013) (Fig. 3C).

Among studies using a genome-wide approach to assess DNA methylation in placenta, Katari *et al.* (2009) identified 38 differently methylated genes, some of which were imprinted (*GRB10*, *MEST*, *PEG3*, *SLC22A2*) (Fig. 5A). Another study, using a custom Illumina Veracode GoldenGate assay inspecting 25 iDMRs, reported that *PEG3* and KvDMR1 were hypermethylated with ART (Camprubí *et al.*, 2013) (Fig. 5B). Katari *et al.* (2009) and Camprubí *et al.* (2013) found no difference in DNA methylation among ART and NC conception groups (Litzky *et al.*, 2017; Choufani *et al.*, 2019). Nevertheless, Choufani *et al.* (2019) highlighted that a group of ART outliers displayed specific methylation patterns with a substantial number of DMPs compared with the NC group (n = 252).

Overall, there is limited and conflicting evidence regarding the associations between ART interventions and altered DNA methylation in placenta. Based on the meta-analysis from two sample sets, a decrease

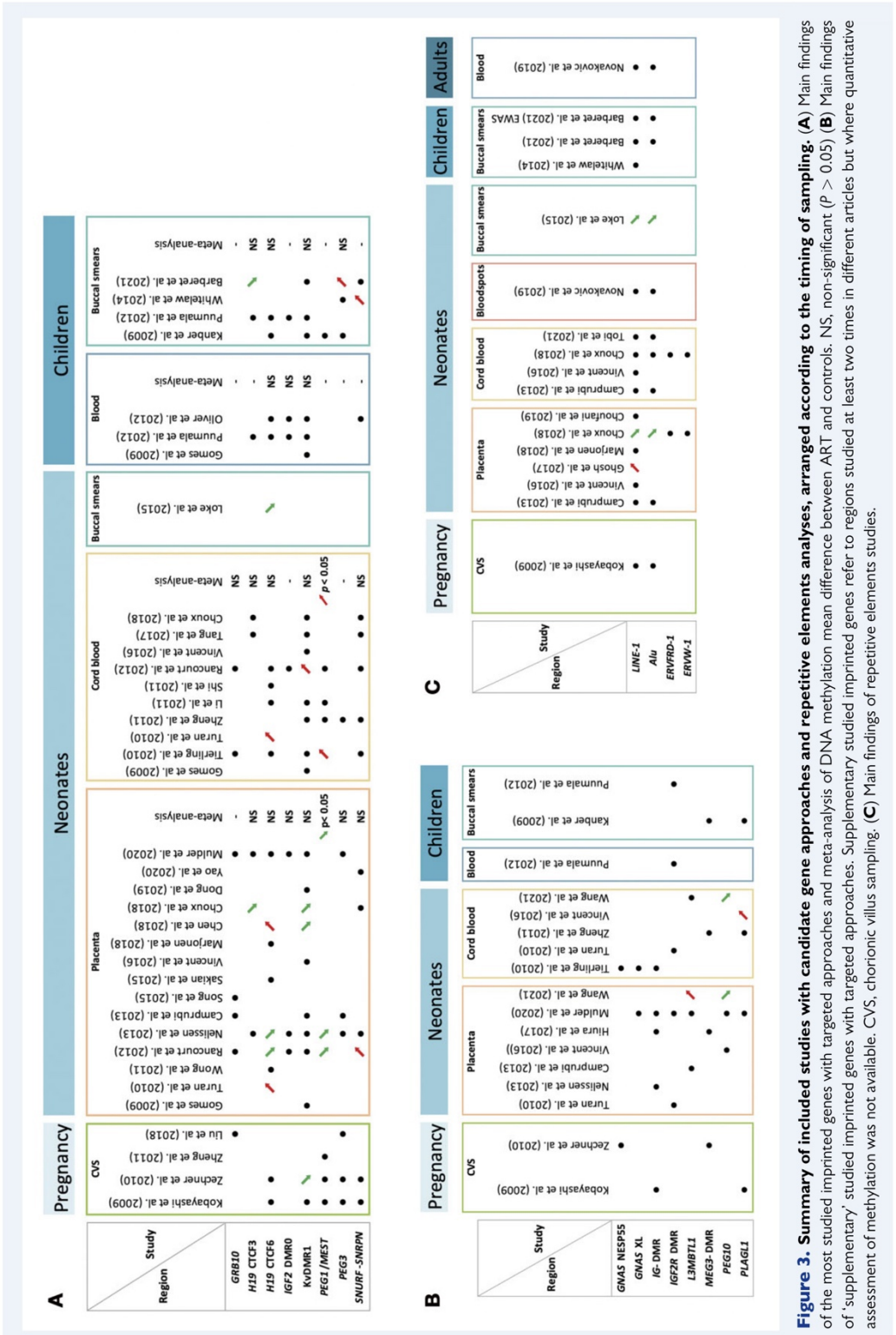

Figure 3. Summary of included studies with candidate gene approaches and repetitive elements analyses, arranged according to the timing of sampling. (**A**) Main findings of the most studied imprinted genes with targeted approaches and meta-analysis of DNA methylation mean difference between ART and controls. NS, non-significant ($P > 0.05$) (**B**) Main findings of 'supplementary' studied imprinted genes with targeted approaches. Supplementary studied imprinted genes refer to regions studied at least two times in different articles but where quantitative assessment of methylation was not available. CVS, chorionic villus sampling. (**C**) Main findings of repetitive elements studies.

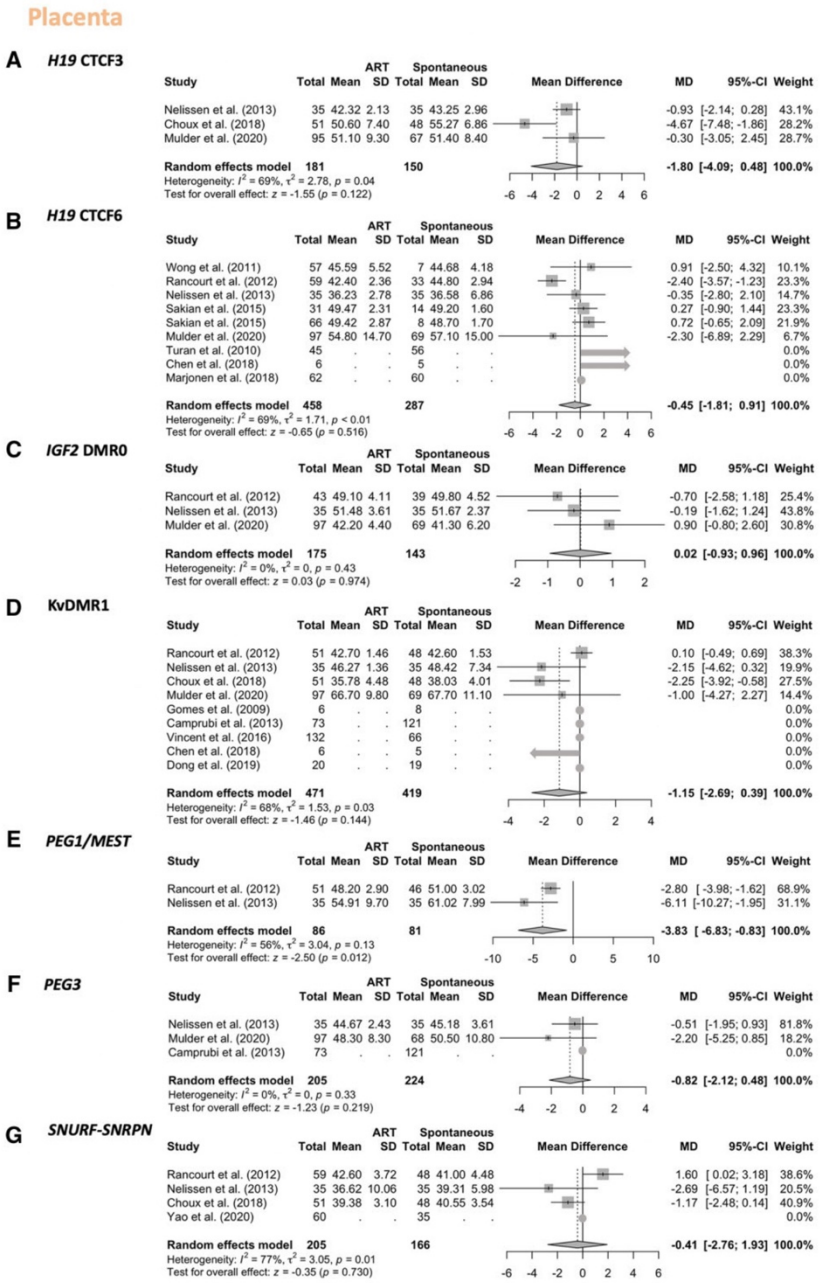

Figure 4. Forest plot analyses of overall weighted mean difference in targeted DNA methylation in ART children compared to naturally conceived children, from placenta. For studies where numerical data were not accessible, visualization is made with arrows depending on the direction of DNA methylation changes between conception groups: left arrow for hypomethylation after ART, right arrow for hypermethylation after ART, dot for no difference between conception groups. MD, mean difference.

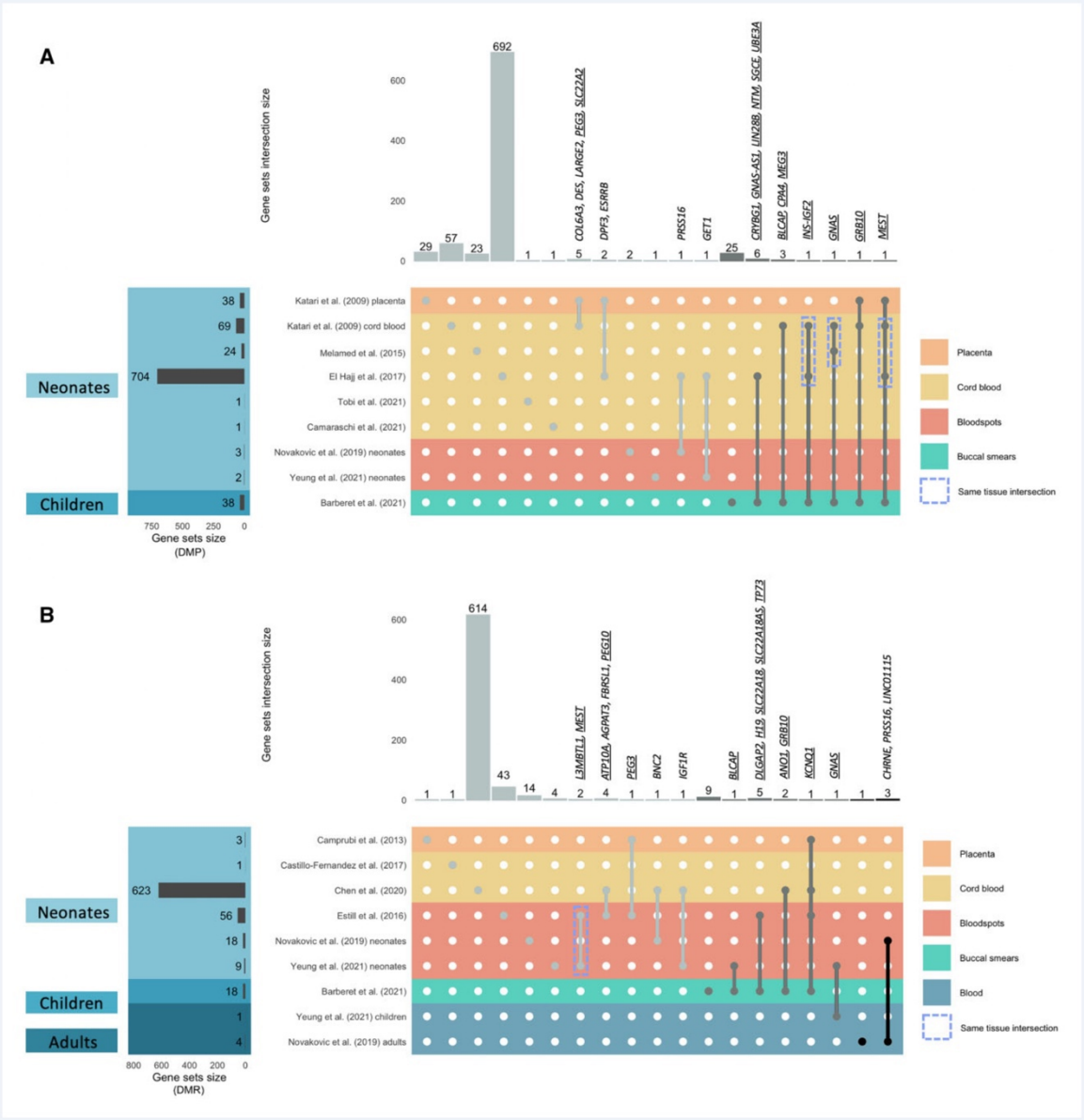

Figure 5. Comparative analysis of methylome studies main findings. (**A**) Upset plot representing intersections of genes containing differentially methylated probes (DMPs) across studies. (**B**) Upset plot representing intersections of genes containing differentially methylated regions (DMRs) across studies. Imprinted genes are underlined. Studies are grouped according to the timing of sampling (from light to dark blue: birth, childhood, adulthood) and to the source tissue. Light gray plots and lines: intersections between neonatal samples, dark gray: intersections between childhood and other timings of sampling, black: intersections between adulthood and others. Imprinted genes are underlined. Redundant gene sets in the same tissue are circled by blue dotted line. Illustration for intersection between Katari *et al.* (2009) genes containing DMPs in placenta and other studies: with 38 DMPs reported, 29 are not redundant with any other study. Their findings are intersecting with five of their same cohort in cord blood (*COL6A3, DES, LARG2E2, PEG3 and SLC22A2*), two with El Hajj *et al.* (2017) in cord blood (*DPF3, ESRRB*), one (*GRB10*) with cord blood of Katari *et al.* (2009) and buccal smears of Barberet *et al.* (2021), and one (*MEST*) with cord blood of Katari *et al.* (2009) and El Hajj *et al.* (2017) and buccal smears of Barberet *et al.* (2021).

in DNA methylation of the *PEG1/MEST* region is found after ART conception. Moreover, the DNA methylation of imprinted regions KvDMR1, *H19* CTCF3, *H19* CTCF6 and *SNRPN* might be perturbed by ART techniques as reported by individual results, although the results of meta-analysis did not reach statistical significance. Discordant results were reported for DNA methylation differences in *L3MBTL1*, *PEG10* and repeated elements LINE-1 and Alu. Despite a considerable aggregated sample size, the meta-analysis for placenta remains inconclusive and significant modifications found in individual studies have not been replicated to date.

Cord blood. A total of 1379 DNA methylation profiles of ART children (773 in candidate genes and 606 in methylome studies) were compared to those from 3398 NC children (566 in targeted studies and 2832 in methylome cohorts). Among them, significant differences between ART and NC children were reported for 939 ART and 2978 NC cases, i.e. on the vast majority of the entire sample. Data from Tierling *et al.* (2010) were incorporated into meta-analysis even though they reported a mean methylation index because it corresponds to the mean methylation of a tested region measured with a specific technique (SNuPE). One study was excluded from the analysis (Feng *et al.*, 2011) because the ART group contained a case of child with loss of imprinting and no statistical tests were performed to compare the groups.

Including two sample sets of targeted methylation data in cord blood, the meta-analysis revealed significant hypermethylation of the *PEG1/MEST* region associated with ART conception (0.88 (0.17–1.60), $P = 0.015$, n = 2 studies) (Figs 3A and 6). In the *H19* CTCF6 region, one study (Turan *et al.*, 2010) out of five reported hypermethylation of this region after ART (Tierling *et al.*, 2010; Turan *et al.*, 2010; Li *et al.*, 2011; Shi *et al.*, 2011; Rancourt *et al.*, 2012), but the meta-analysis was not statistically significant (0.46 (–0.08 to 1.01), $P = 0.097$, n = 3 studies) (Figs 3A and 6). The KvDMR1 region was found to be significantly hypermethylated in ART children in only one (Rancourt *et al.*, 2012) of eight studies (Gomes *et al.*, 2009; Tierling *et al.*, 2010; Li *et al.*, 2011; Zheng *et al.*, 2011a; Rancourt *et al.*, 2012; Vincent *et al.*, 2016; Tang *et al.*, 2017; Choux *et al.*, 2018) (Figs 3A and 6). Overall, the meta-analysis of data from four eligible studies showed no significant difference in DNA methylation of the KvDMR1 region (0.35 (–0.64 to 1.34), $P = 0.493$, n = 4 studies) (Fig. 6). Additionally, the only study analyzing *PEG10* found significant hypomethylation in ART children (Wang *et al.*, 2021), and *PLAGL1* was reported to be hypermethylated after ART in one (Vincent *et al.*, 2016) of two studies (Fig. 3B). There was no evidence of differential methylation in other major IGs *GRB10*, *H19* CTCF3 and *SNRPN* as no studies reported differences associated with ART, which was corroborated by the results of the meta-analysis (Figs 3A and 6). Moreover, there was a consensus that there was no differential methylation in repetitive elements (Fig. 3C).

Concerning epigenome-wide cord blood studies (n = 9), it is worth noting that there are conflicting results regarding the number of DNA methylation discrepancies between NC and ART conceptuses. Indeed, El Hajj *et al.* (2017) identified more than 700 genes containing DMPs and correlated with ART, whereas five other studies found no (Gentilini *et al.*, 2018) or a limited number of DMPs (Katari *et al.*, 2009; Melamed *et al.*, 2015; Caramaschi *et al.*, 2021; Tobi *et al.*, 2021). On the whole, 15 of 796 genes containing DMPs were imprinted. Redundant genes containing DMPs, defined as those reported differentially methylated among different studies, were found between cord blood studies, and noticeably all were located inside IGs: *INS-IGF2*, *GNAS and MEST* (Fig. 5A).

At a regional scale, no DMR was reported by Camprubí *et al.* (2013), while no common DMR was found between the two cord blood studies screening for DMRs with two different techniques of methylome assessment (Castillo-Fernandez *et al.*, 2017; Chen *et al.*, 2020) (Fig. 5B). With a genome-wide coverage at a 500 bp region resolution using MeDIP-seq, Castillo-Fernandez *et al.* (2017) found only one DMR that reached statistical significance between NC and ART conceptuses. Using a more restricted genome coverage but providing a measure of single CpG methylation, Chen *et al.* (2020) found more than 4000 DMRs associated with IVF or ICSI status with RRBS.

Overall, there is evidence that an increase in DNA methylation of the *PEG1/MEST* region is associated with ART conception. As suggested by the meta-analysis and despite extensive studies, there is no noticeable change in DNA methylation levels after ART for other regions. Individual modifications reported in *H19* CTCF6 and KvDMR1 by two studies were not replicated to date. Additionally, even if a small proportion of reported genes containing DMPs was imprinted in epigenome-wide studies (1.9%), the only three redundant genes in cord blood studies were all imprinted (*INS-IGF2, GNAS, MEST*).

Dried bloodspots. DNA methylation was compared between conception groups with a genome-wide approach in dried bloodspots in 401 ART children (of which 38 were conceived by FET) and 621 NC (n = 3 studies, Fig. 2). Among them, significant differences between ART and NC children were reported for the entire studied sample.

Very few DMPs (n = 10 in five genes) were found in dried bloodspots from newborns, and none was found in the same gene in the two reports (Novakovic *et al.*, 2019; Yeung *et al.*, 2021) (Fig. 5A). Three studies investigated DNA methylation differences, defining DMRs with different criteria (Supplementary Table SV) (Estill *et al.*, 2016; Novakovic *et al.*, 2019; Yeung *et al.*, 2021). The only similarities were between Estill *et al.* (2016) and Yeung *et al.* (2021): both studies found DMRs inside the IGs *L3MBTL1* and *MEST* (Fig. 5B). Finally, Novakovic *et al.* (2019) also analyzed methylation at repetitive elements inside a large cohort and reported no differences for LINE-1 and Alu (Fig. 3C).

Although three studies suggest a possible association between ART conception and modified DNA methylation in dried bloodspots at birth, there is insufficient evidence to draw conclusions in this tissue.

Buccal smears. Only one team studied targeted DNA methylation on buccal samples of twin pairs younger than 2 weeks (Loke *et al.*, 2015). They highlighted significant hypomethylation after ART of the *H19* CTCF6 region as well as LINE-1 and Alu elements (Fig. 3A and C).

In conclusion, at birth there is evidence of DNA methylation perturbations in placenta and cord blood, mainly in IGs. In particular, the meta-analysis highlights significant differences in DNA methylation levels of the imprinted *PEG1/MEST* gene after ART. However, the magnitude of the aggregated differences remains limited in both tissues, and the heterogeneity of the evidence base does not allow us to rule out other studied sequences. There was less evidence in other tissues such as bloodspots.

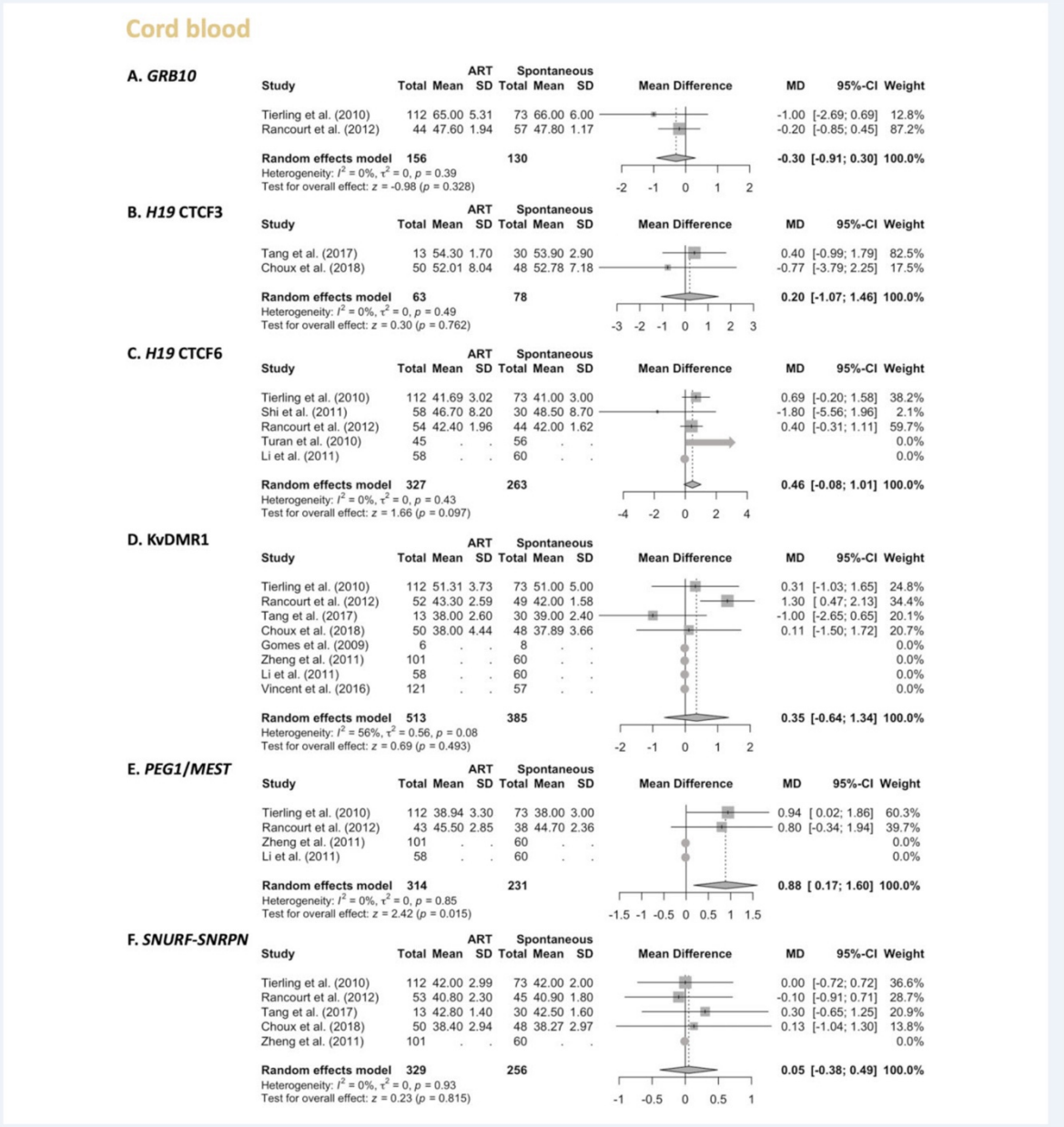

Figure 6. Forest plot analyses of overall weighted mean difference in targeted DNA methylation in ART children compared to naturally conceived children, from cord blood. For studies where numerical data were not accessible, visualization is made with arrows depending on the direction of DNA methylation changes between conception groups: left arrow for hypomethylation after ART, right arrow for hypermethylation after ART, dot for no difference between conception groups. MD, mean difference.

Methylation differences during childhood

Peripheral blood. Among candidate gene approaches, three studies focused on the methylation of IGs in peripheral blood during childhood at various ages (average age from 2 to 6 years) (Gomes *et al.*, 2009; Oliver *et al.*, 2012; Puumala *et al.*, 2012), for a total of 143 ART and 108 NC children. None of the studies reported evidence of DNA

methylation differences between NC and ART in the most studied IGs (Fig. 3A) and the meta-analysis remains non-significant for *H19* CTCF6, *IGF2* DMR0 and KvDMR1 (Fig. 7).

Only one high-quality methylome study looked at peripheral blood in children aged 8–10 years (Yeung *et al.*, 2021) (Fig. 5B). They reported a single significant DMR that was intriguingly identical to the one they found in dried bloodspots of their neonate cohort. The DMR was located in IG *GNAS* and had the same methylation direction (decreased DNA methylation levels in ART children as compared with NC).

Buccal smears. In four sets of samples from candidate gene approaches (Kanber *et al.*, 2009; Puumala *et al.*, 2012; Whitelaw *et al.*, 2014) and one from both candidate and genome-wide analysis focusing on imprinted and repetitive elements with a relatively small sample size (Barberet *et al.*, 2021), 155 ART children aged 2–8 years old were compared to 145 NC children. In these studies, significant differences between ART and NC children were reported for 69 ART and 86 NC out of the entire studied sample.

A significant hypermethylation of *SNRPN* in ART children (2.8 ± 1.9 years old—birth to 7 years old) was described in Whitelaw *et al.* (2014) but was not confirmed by Barberet *et al.* (2021) in a cohort of 8-year-old children (Fig. 3A). On the contrary, while Whitelaw *et al.* (2014) and Kanber *et al.* (2009) (in 4–7 year olds) found no differences in *PEG3* among conception groups, Barberet *et al.* (2021) found this region to be hypermethylated after ART. The results of the meta-analysis for this region did not reach statistical significance (1.83 (–0.26 to 3.92), $P = 0.086$, n = 2 studies) (Fig. 8). Furthermore, Barberet *et al* (2021) also reported hypomethylation in *H19* CTCF3 after ART, whereas no difference was observed for younger children in Puumala *et al.* (2012) (2.5 ± 0.9 years old). Once again, the pooled difference was not significant in the meta-analysis (–2.67 (–7.71 to 2.38), $P = 0.300$, n = 2 studies). Meta-analysis of the 'supplementary' studied IGs in buccal smears revealed no significant DNA modifications associated with ART status (Fig. 8). Additionally, there was no evidence of differences between NC and ART groups in other IGs or repetitive elements (Fig. 3B and C).

However, differences in IGs were uncovered in the buccal smears of ART children using genome resolution (Barberet *et al.*, 2021). Thirty-three iDMRs were highlighted between ART and NC children, but without associations between ART conception and global DNA methylation levels or DNA methylation of repeated elements (Fig. 5).

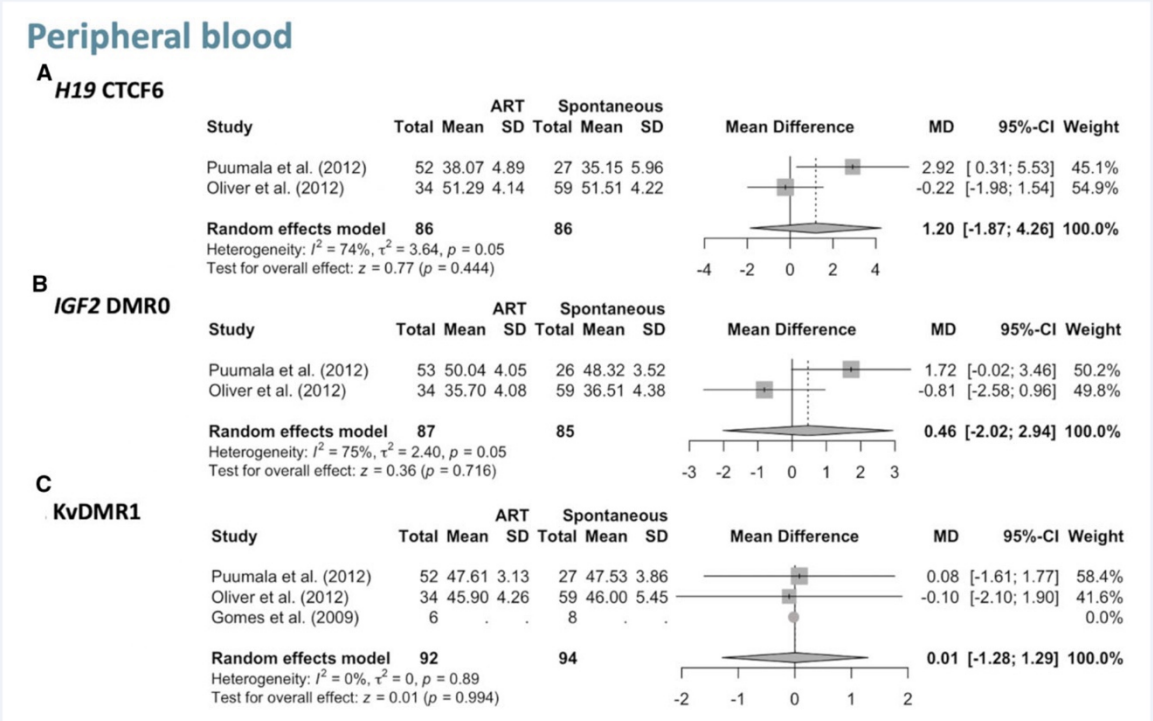

Figure 7. Forest plot analyses of overall weighted mean difference in targeted DNA methylation in ART children compared to naturally conceived children, from peripheral blood. For studies where numerical data were not accessible, visualization is made with arrows depending on the direction of DNA methylation changes between conception groups: left arrow for hypomethylation after ART, right arrow for hypermethylation after ART, dot for no difference between conception groups. MD, mean difference.

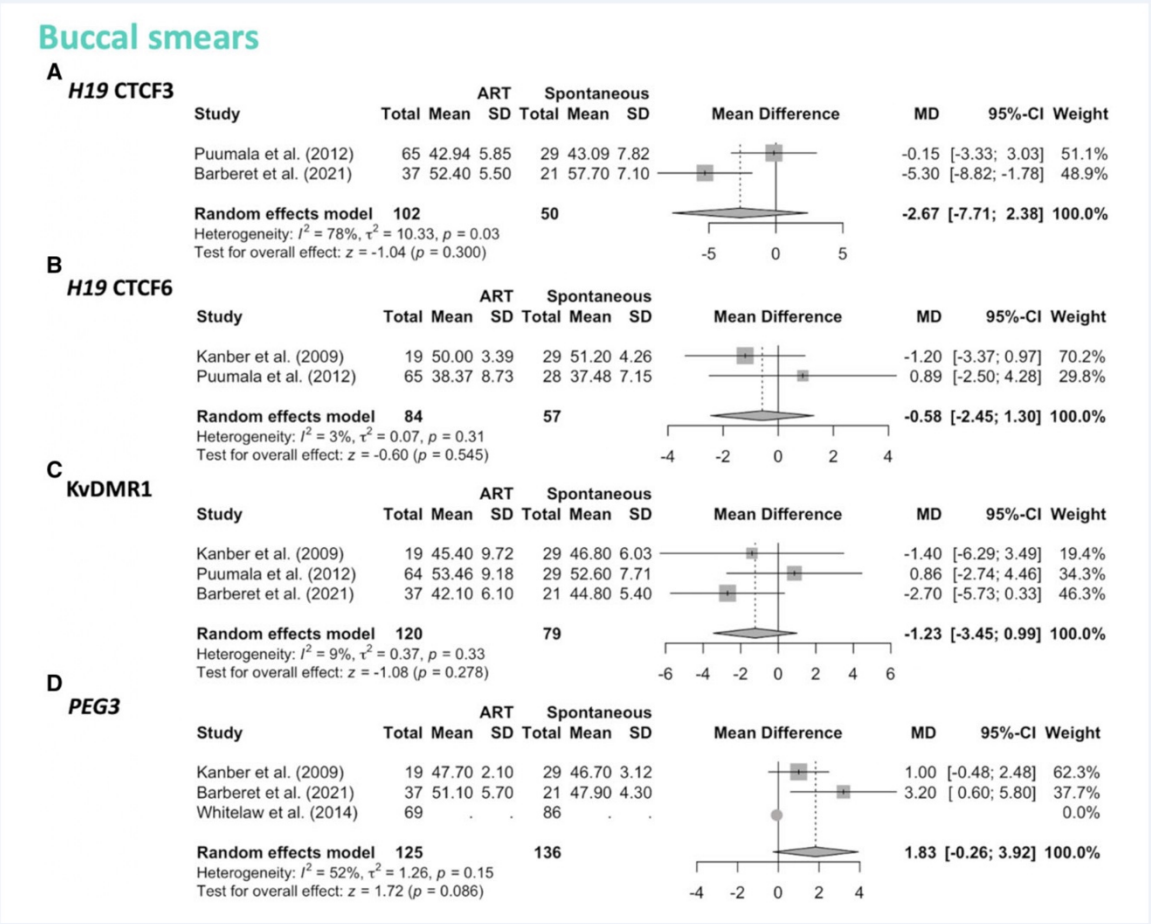

Figure 8. Forest plot analyses of overall weighted mean difference in targeted DNA methylation in ART children compared to naturally conceived children, from buccal cells. For studies where numerical data were not accessible, visualization is made with arrows depending on the direction of DNA methylation changes between conception groups: left arrow for hypomethylation after ART, right arrow for hypermethylation after ART, dot for no difference between conception groups. MD, mean difference.

Overall, quantitative analysis of candidate gene studies suggests that DNA methylation in imprinted regions remained unmodified during childhood after ART. Epigenome-wide qualitative assessment of genes disturbed by ART might show that IGs are sensitive to these techniques. Nevertheless, given that only IGs were studied in buccal smears and the sample size was small, these last results must be interpreted with caution. The limited number of studies and the small number of children studied highlight the need for larger scale, longitudinal analyses of ART conceptions during childhood.

Methylation differences during adolescence

Blood. Only one high-quality study investigated the effects of ART conception on DNA methylation during adolescence (15.9 ± 1.6 years old). On the basis of two large prospective cohorts with a subset of 231 ART adolescents and 1188 NC profiles, Penova-Veselinovic *et al.* (2021) did not identify any DMP or DMR inside the adolescent blood methylome but they applied a conservative *P*-value threshold. Epigenetic aging was also tested, but none of the different measures of DNA methylation age displayed accelerated epigenetic aging with ART.

Methylation differences during adulthood

Blood. The longest longitudinal analysis of blood collected soon after birth and in adulthood (22–35 years old) identified four DMRs in the adult blood methylome (Novakovic *et al.*, 2019). Three of them were the same as those discovered in neonatal bloodspots (*CHRNE*, *PRSS16*, *LINC01115*). There was no evidence of LINE-1 or Alu

repetitive elements or mean methylation changes in association with ART (Fig. 3C).

Common methylation differences across tissues in epigenome studies during lifespan

The cross-over between methylome studies in different tissues and at various ages yields some interesting results (Fig. 5).

At birth, we found few similarities in DNA methylation modifications between neonatal tissues (DNA from placenta, cord blood and dried blood spots) according to ART status. First, some common findings were highlighted in DMPs. Redundant DMPs after ART were spotted in cord blood and placenta in genes *COL6A3*, *DES*, *GRB10*, *LARGE2*, *MEST*, *PEG3*, *SLC22A2* (Katari *et al.*, 2009; El Hajj *et al.*, 2017) (Fig. 5A). Nevertheless, it is worth noting that there were sometimes opposing differences found in placenta and cord blood (hypomethylation in placenta (Katari *et al.*, 2009) and hypermethylation in cord blood for *PEG1/MEST* (Katari *et al.*, 2009; El Hajj *et al.*, 2017)). Among them, the IGs *GRB10* and *MEST* were also reported in buccal smears collected during childhood (Barberet *et al.*, 2021). Interestingly, only 7 out of 100 common differentially methylated genes were shared between placenta and cord blood samples in the same cohort of newborns (Katari *et al.*, 2009).

Two genes in cord blood and neonatal bloodspots were redundant between studies (*PRSS16* and *GET1*, respectively, hyper- and hypomethylated for the same CpGs) (El Hajj *et al.*, 2017; Novakovic *et al.*, 2019; Yeung *et al.*, 2021), while 13 other redundant IGs were common between cord blood and later in life in buccal cell studies (*BLCAP, CPA4, CRYBG1, GNAS, GNAS-AS1, GRB10, INS-IGF2, LIN28B, MEST, NTM, SGCE, UBE3A or MEG3*) (Katari *et al.*, 2009; Melamed *et al.*, 2015; El Hajj *et al.*, 2017; Barberet *et al.*, 2021) (Fig. 5A).

Then, in DMRs, seven redundant genes were observed between cord blood and bloodspot studies (*ATP10A, AGPAT3, BNC2, FBRSL1, IGF1R, KCNQ1, PEG10*), among which three were IGs (Estill *et al.*, 2016; Novakovic *et al.*, 2019; Chen *et al.*, 2020; Yeung *et al.*, 2021) (Fig. 5B). Two IGs containing DMRs, *PEG3* and *KCNQ1*, were also differentially methylated in cord blood and placenta studies after ART compared with natural conceptions. Despite being redundant between the placenta cohort in Camprubí *et al.* (2013) and newborn bloodspots in Estill *et al.* (2016), *PEG3* displayed DNA methylation profiles going in opposite directions (hypermethylated in Camprubí *et al.*, 2013; hypomethylated in Estill *et al.*, 2016). *KCNQ1* was reported as containing DMR to a larger extent: it was redundant in placentas (Camprubí *et al.*, 2013, hypermethylated), cord blood (Chen *et al.*, 2020, hypermethylated), dried bloodspots (Estill *et al.*, 2016, hypomethylated) and, later in life, in buccal samples of 8-year-old ART children (Barberet *et al.*, 2021, hypo- and hypermethylated).

Given the paucity of ART DNA methylation studies later in life, few redundancies between studies were reported after childhood.

Evidence of few persistent differences in DMRs between ART and NC across various ages is provided by Novakovic *et al.* (2019) since only 3 out of the 18 DMRs found at birth were found in adulthood. This was also the case in Yeung *et al.* (2021) where only one of nine DMRs persisted between birth and childhood.

Discussion

To date, this systematic review is the largest critical evaluation of studies of DNA methylation in human conception following the use of ART.

Overall summary of findings

In the existing literature, there is some evidence that ART conception is associated with aberrant DNA methylation in imprinted loci and other genes in various tissues (Fig. 9). Although the results are often conflicting and poorly replicated in the high quality of evidence genome-wide analyses, alterations in imprinted regions were detected after ART in 11 out of 17 epigenome studies. Few genes were redundant between studies, except for the *PEG1/MEST* region, which was differentially methylated in both candidate and array-based DNA methylation analyses at birth and later in life. *PEG1/MEST* (paternally expressed gene 1/mesoderm-specific transcript homologue) encodes an α/β-hydrolase fold family enzyme that is expressed during the entire embryonic period. Its precise function is still unknown in humans, but disruption of the homologous *Peg1/Mest* gene in a mouse model led to embryonic growth retardation and abnormal maternal behavior (Lefebvre *et al.*, 1998). Initially reported to be predominantly expressed in the mesoderm and its derivatives, the *MEST* gene is in fact widely expressed in all major fetal organs, tissues and placenta, suggesting a crucial effect on placental and fetal growth (Salpekar *et al.*, 2001; Huntriss *et al.*, 2013). In humans, Sato *et al.* (2007) proposed that DNA methylation of *PEG1/MEST* is sensitive to ART manipulation as aberrant demethylation of superovulated oocytes was observed in this region (Sato *et al.*, 2007). DNA methylation of *MEST* is directly inherited from oocytes (Lucifero *et al.*, 2002), thus hypothetically linked to a contribution of maternal factors. Even if epimutation at the *PEG1/MEST* locus in 7q31 is not a major determinant in SRS (Schöherr *et al.*, 2008), a case of loss of imprinting was reported in this locus in a Silver–Russell patient conceived *in vitro* (Kagami *et al.*, 2007). In addition, a putative loss of imprinting of *PEG1/MEST* in humans has been described in different cancer types (lung cancer cell lines, colorectal and breast cancer) (Pedersen *et al.*, 1999; Kohda *et al.*, 2001; Nakanishi *et al.*, 2004). These observations indicate a need to monitor over the long term the potential consequences of differences in *PEG1/MEST* DNA methylation observed between children conceived *in vitro* and *in vivo*.

The existence of differentially methylated genes after ART in several tissues and at various ages also emerged for several IGs across targeted and methylome studies (*ANO1, ATP10A, BLCAP, CPA4, CRYBG1, DLGAP2, GNAS, GRB10, H19, INS-IGF2, KCNQ1, L3MBTL1, LIN28B, MEG3, MEST, NTM, PEG3, PEG10, SGCE, SLC22A1, SLC22A2, UBE3A*).

Nevertheless, these results should be interpreted with caution since possibly the most striking conclusion from this systematic review is the limited replication of findings found in each individual study. The detected DNA methylation changes were mild and widespread, and opposing methylation trends were sometimes observed (*H19, IGF2, KCNQ1, SNRPN*). In addition, the conclusions supported by our systematic review and meta-analysis rely partially on studies classified as having a low quality of evidence for the reasons previously mentioned. We provide in Supplementary Table SVIII a review of IGs and regions

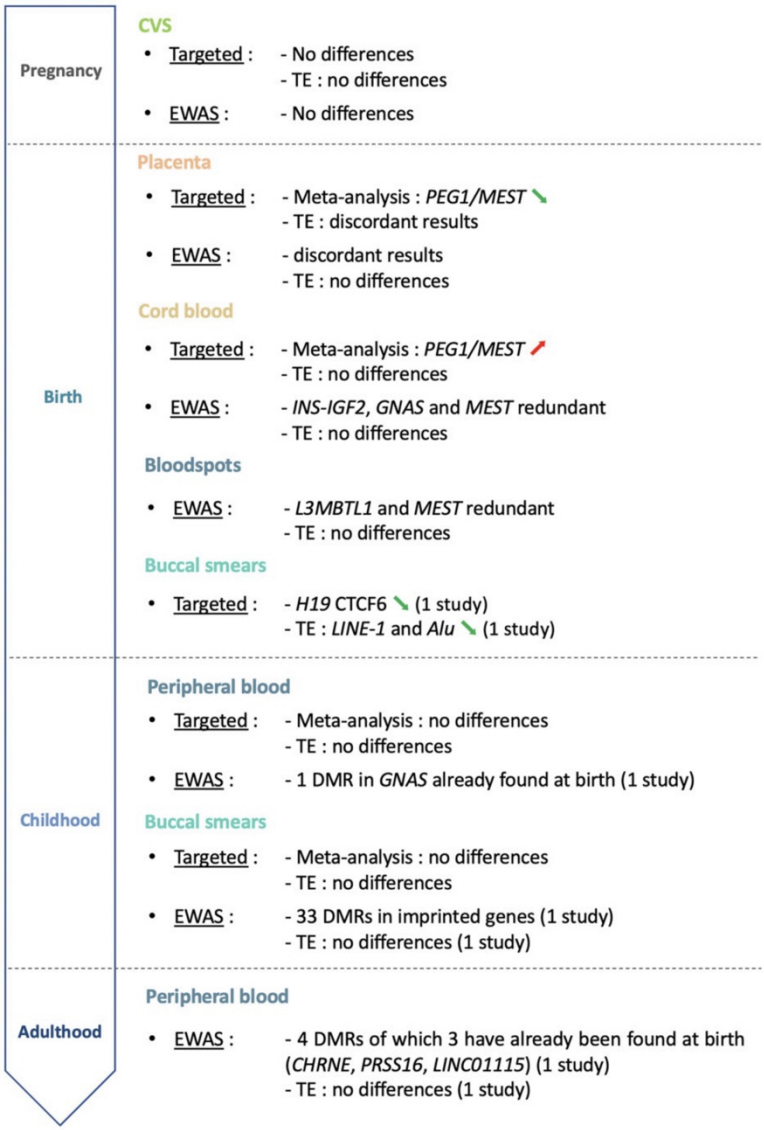

Figure 9. Overview of the conclusions. CVS, chorionic villus sampling; DMR, differentially methylated region; EWAS, epigenome-wide association studies; TE, transposable element.

worthy of further investigation according to the results of studies with a good quality of evidence.

It is also true that the limited overlap of findings between targeted and genome-scale analyses likely stems not only from marked differences in CpGs localization, but also the high variability in methodology and sample characteristics (see below), as well as insufficient statistical power to detect small differences in methylation. From a methodological perspective, it is clear that there are vast disparities between studies. However, the meta-analysis aggregates mean differences instead of DNA methylation levels, overcoming the potential differences between different techniques.

First, targeted and genome-wide methods of investigating DNA methylation yielded different results for technical causes, making them challenging to compare. There may indeed be an association between DNA methylation and ART in candidate genes, but it is not strong enough to withstand genome-wide thresholds of significance.

Furthermore, methylation arrays only partially covered imprinted regions and may have captured the differences in those regions to a limited extent. The most prominent examples are the *IGF2* DMR0 and *IG*-DMR regions, which only contain two CpGs on the EPIC probes, thus not reflecting the status of methylation established in these regions (Hernandez Mora *et al.*, 2018). Moreover, commonly available array technologies only cover 2–4% of CpG sites across the genome. Whole genome bisulfite sequencing could be used to overcome this problem, but its cost remains dissuasive. Two studies screened CpGs at a higher coverage than arrays: Chen et al. (2020) used RRBS and Castillo-Fernandez *et al.* (2017) used MeDIP-seq, which covers the entire genome. Both are interesting pangenomic approaches, but further studies are needed to compare their findings since their coverage of imprinted regions remains uncertain.

Second, the comparison of methylome studies is particularly tricky. Studies on arrays used a wide range of DMR detection algorithms, which can vary widely in terms of sensitivity and false-positive rates (Mallik *et al.*, 2019). DMP and DMR detection settings and filters are also important factors that can limit comparisons between studies. For example, three studies eliminated DMPs for which the difference in DNA methylation between the natural conception and ART groups was <5% (Melamed *et al.*, 2015; Novakovic *et al.*, 2019; Barberet *et al.*, 2021) even though there may have been CpGs of interest. The criteria for determining DMRs were also highly variable from one study to another, notably according to the maximal distance allowed between consecutive CpGs, multiple testing correction methods (Bonferroni, false discovery rate, sliding linear model) and thresholds for minimal differences between groups (deltabeta < or > to 5%).

While ART is associated with differences in DNA methylation *in utero* and after birth, the clinical significance of these observations is not well understood. ART probably causes some epigenetic changes in the offspring, which might be the molecular basis of complex traits and diseases. However, it is still unclear whether the small differences observed in several studies represent a real difference between ART-conceived and NC children, and whether these differences could lead to the adverse perinatal outcomes reported after ART.

Another issue is that it is unclear whether epigenetic changes are attributable to patient characteristics related to infertility, or the ART techniques, or a combination of both. ART children have mostly been compared with NC children in the general population, while only rare studies included a subfertile population (Litzky *et al.*, 2017; Choufani *et al.*, 2019). Subfertility itself, with or without assisted conception, may be found to be significantly associated with a higher rate of epigenetic dysregulations. There is some evidence that epigenetic defects in the sperm used in ART techniques could also play a crucial role. In fact, alterations in the normal epigenetic state of gametes have been highlighted in infertile male patients (Jenkins *et al.*, 2017) as well as association of aberrant sperm DNA methylation patterns on IGs or TEs with compromised semen parameters (Santi *et al.*, 2017). Additionally, a causative relation has been suggested between advanced paternal age and impaired epigenetic marks in the male germline (Jenkins *et al.*, 2014). Case reports have found the same epigenetic defects on specific imprinted loci in infertile men and their offspring (Kagami *et al.*, 2007; Kobayashi *et al.*, 2009), reinforcing the idea that male infertility may increase the risk of epigenetic defects in offspring. The contribution of female infertility to epigenetic defects is more complex, multifactorial and less explored considering the diversity of conditions including ovulation problems, endometriosis and age-related factors. However, extensive evidence underlines the potential contribution of the maternal and gestational environment to the regulation of epigenetic patterns, including IGs, primarily in the placenta (Argyraki *et al.*, 2019). For example, acquisition of methylation in *Peg1* has been shown to be delayed or altered in connexin37-deletion mice, as a model of female infertility, leading to defective transport of methyl donors or other metabolites from granulosa cells to the oocyte (Denomme *et al.*, 2012). Additionally, a large cohort follow-up study determined that underlying maternal infertility, particularly endometriosis, contributed to an increased risk of imprinting-related disorders associated with ART (Fauque *et al.*, 2020). Further studies are required to clarify the contribution of parental infertility per se versus the ART treatments.

In the current study, we chose not to include populations with imprinting-related disorders since they may display dissimilar epigenetic patterns on IGs compared with healthy populations. The conclusions of this review may consequently not be transposable to the population with imprinting-related disorders. To our knowledge, only two studies compared the methylome from a cohort of patients with imprinting-related disorders (SRS, BWS, AS and PWS) conceived after ART with those who were conceived naturally. Tenorio *et al.* (2016) did not find imprinted methylation differences in BWS patients born after ART compared with BWS patients conceived naturally (Tenorio *et al.*, 2016). In contrast, higher DNA methylation variability was found in SRS following ART compared with NC patients with SRS (Hattori *et al.*, 2019). It has been reported that patients with BWS conceived by ART with a KvDMR1 hypomethylation present multi-locus methylation alterations in at least three imprinting loci, and remarkably with a greater tendency in maternal DMRs (Mangiavacchi *et al.*, 2021). It could be useful to further study cohorts of patients with imprinting-related disorders to decipher the mechanistic processes associated specifically with ART.

Finally, the included cohorts were recurrently heterogeneous in terms of ART techniques, with IVF/ICSI/IUI/OI medication, and fresh and FETs, making it impossible to assess the specific effect of each technique.

Overall, marked differences in methodology and sample characteristics currently limit the comparability of findings and our ability to fully answer these questions.

Current challenges and recommendations for future research

Epigenetics and ART is an emerging field which requires rigorous interpretation and methodology. In this section, we present some ways in which future research can meet the challenges of studying the epigenetic field in ART conception.

Sample size

To date, genome-scale DNA methylation studies of ART conceptus have had relatively low statistical power, despite larger recent cohorts, and hence a substantial false-negative rate. The field would benefit from large collaborative efforts for cohorts to increase statistical power, optimize the use of resources and strengthen the evidence for reported associations. Indeed, detecting mean differences of 5% at genome-wide significance with >80% power would require 100

participants in each group with the EPIC array (Mansell et al., 2019). Whether they are targeted or genome-wide, studies should take into consideration power calculations before running analyses.

Moreover, to obtain important new insights into the development of the epigenome, prospective cohorts, whereby children are followed throughout their development (ideally from pregnancy), would be valuable. This type of study design makes it possible to study changes in DNA methylation over time while adjusting for prenatal environmental factors, and to discern whether there are specific windows for DNA methylation modifications. A number of large prospective birth cohorts already exist (MoBa, ALSPAC, CHART, GUHS, Upstate KIDS) (Caramaschi et al., 2021; Penova-Veselinovic et al., 2021; Yeung et al., 2021), and this type of cohort should be encouraged. The inclusion of validation cohorts from independent populations would also be beneficial, as would multicenter collaborations.

Uniformity of included groups—tissue specificity

To complicate matters, DNA methylation varies by age, sex, tissue type and cell type. This makes it challenging to characterize how an exposure, such as ART, impacts epigenetic patterns at a given point in time, in a given type of tissue. Differences in DNA methylation may consequently stem from the different sources of genomic DNA, as placenta is derived from the TE and the vast majority of other accessible tissues from the EPI. This also means that DNA methylation profiles in easily accessible peripheral tissues, such as cord blood, peripheral blood or saliva, may partially reflect what is happening in other tissues if adequately isolated. That is why studies should ideally aim to collect DNA from multiple tissue sources, in order to establish the extent and correlation of the DNA methylation modifications between tissues.

Furthermore, what remains to be determined, in broader studies with homogeneous groups of techniques, is whether specific ART techniques, including fresh versus frozen embryo transfer, fertilization method, culture media composition and other ART-specific techniques may play a role. To fully answer this question, future research should consider including homogeneous groups of ART technique (e.g. all fresh or all FET, exclusion of OI medication).

Methodology

Several early studies described associations between DNA methylation and assisted conceptions with a limited number of assessed CpG sites. The emergence of Illumina Infinium Human Methylation Arrays, which are capable of interrogating around 27 000 CpGs for the 27K array, 450 000 CpGs for the 450K array and more than 800 000 for the recent EPIC array, has allowed scientists to investigate more sites than candidate approaches in single assays. Future studies should consider confirming the microarray findings with targeted techniques at the same CpGs to ensure their robustness.

In addition, the methylome studies differed widely in the number of associations reported (and the specific DNA methylation sites identified). A number of these differences stem from the heterogeneous methodology, for example correction of key factors known to influence DNA methylation levels (see below), criteria for DMP and DMR selection (considering probes or not, or regions where effect size was <2.5 or 5%), and threshold of significance. A critical evaluation of the EPIC array statistical analysis method recently suggested a significance threshold of $P < 9 \times 10^{-8}$ to control for false-positive rates on these arrays (Mansell et al., 2019). These methods must be standardized to reduce the inconsistency of results related to the use of independent statistical methods and to allow cross-study comparisons, increasing the robustness of findings.

Moreover, epigenetic outliers may be a cause for inconsistent results when studying methylation differences between ART and natural conceptions (Gentilini et al., 2018; Mani and Mainigi, 2018). The emerging hypothesis that ART could induce stochastic epigenetic variability rather than global effects would be interesting to explore in future studies.

Accounting for confounding factors

Considering that observational studies in general are subject to confounding, there are several drawbacks to studying DNA methylation patterns.

First, the ART population is inherently different from the general population. DNA methylation is a dynamic process that may change under the influence of genetic and environmental factors, so it is necessary to control for possible confounding factors. Gestational age and sex can affect DNA methylation even in natural conceptions, in non-imprinted as well as imprinted regions (Yousefi et al., 2015; Merid et al., 2020; Bozack et al., 2021). Considering that mothers who conceive by ART are older than those who conceive without ART, maternal age is important to take into account. Furthermore, for methylome studies, even if imprinted regions are highly stable across tissues (Murphy et al., 2012), the cell composition must be considered for the analysis of a wide range of CpGs, even outside of these regions. Authors should aim to report findings with adjustments that are standard in the field, including sex, age and gestation length, cell-type composition and technical covariates (batch effect and positional effects). Furthermore, adjustment for additional features, such as maternal smoking, obesity and history of high blood pressure or diabetes, could be performed because the maternal environment may modify epigenetic regulation during pregnancy (Fauque et al., 2020). Most essential in the design of the study is the measurement of potential confounding factors. These facilitate statistical adjustment and ensure the comparability between NC and ART children.

Second, another major driver of DNA methylation variation is genetic variation (Czamara et al., 2019). In ART, it is currently unclear to what extent DNA methylation associations vary depending on genetic background. One way of accounting for genetic influences is to directly measure DNA sequence variation, or to use genetic data on methylation quantitative trait loci (Gaunt et al., 2016) or publicly accessible online resources. The use of a twin study design is also possible, even if prematurity and obstetric complications can also influence DNA methylation. Consequently, the variance explained by genetic background should be controlled in upcoming studies to exclude the possibility that part of the difference in DNA methylation is explained by genetic variation. Furthermore, DNA methylation patterns are known to vary between tissues, and even in different cell types within tissues (Rahmani et al., 2019). In ART cohort studies, cord blood, placenta and peripheral blood are typically the main sources of DNA. This presents challenges regarding the generalization of the findings. One way to address this limitation and to evaluate the estimated effect is to have recourse to methods imputing the major cell types in the different sources of genomic DNA.

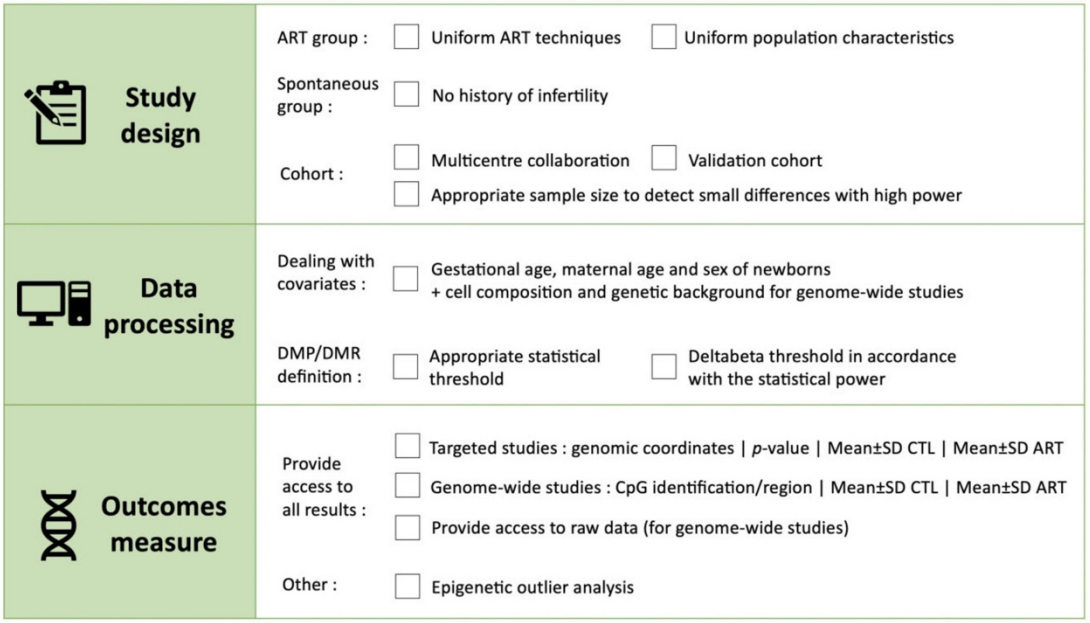

Figure 10. Overview of the recommendations for future research in the field of DNA methylation after ART. CpG, cytosine–guanine dinucleotides; CTL, controls; DMP, differentially methylated probe; DMR, differentially methylated region.

Access to raw data/transparent reports

Another issue concerns reporting practices, since key statistics needed for pooling estimates in meta-analyses, such as mean and standard errors, are often not provided. For example, regarding the KvDMR1 region, four studies with available data found a trend for hypomethylation after ART. Four additional studies indicated that there was a tendency toward hypomethylation inside this region but did not provide access to their data. Consequently, the mean weighted difference in that region remained non-significant despite various results suggesting hypomethylation after ART. Furthermore, in the case of array-based studies, only associations that meet a certain threshold of significance are usually presented among the hundreds of thousands of tested sites, whereas the full results are seldom provided. As only 9 out of 17 studies provided their materials on a public repository (e.g. GEO), we encourage forthcoming studies to provide complete access to their data in a suitable format. Authors should provide all the statistics needed for meta-analyses and fully available results (e.g. genome-wide data) in the supplementary material or uploaded to a public repository to facilitate future reviews and meta-analyses.

A summary of the recommendations for future studies on DNA methylation and ART is provided in Fig. 10.

Strengths and limitations of the systematic review

This systematic review is an exhaustive literature search that includes a large number of publications studying DNA methylation variations in conceptuses conceived through assisted reproduction, including different source tissues, and at any point from the onset of pregnancy to adulthood. A meta-analysis was attempted across targeted studies to allow the reader to navigate a vast and often contradictory field, updating the previous meta-analysis from 2014 (Lazaraviciute *et al.*, 2014) with numerous recent studies. This is a valuable tool for assessing overall effects across heterogeneous cohorts and study designs. A further strength of this review remains the approach used to compare DNA methylation results among various designs of studies, particularly on IGs. Indeed, we ensured that the imprinted region coordinates in each region of analysis for each of the included studies were similar. This was particularly important when focusing on *H19/IGF2* ICR (ICR1) since *H19* CTCF3 and CTCF6 have been described several times as differentially methylated after ART.

Additionally, we provide a systematic review according to the type of tissue studied as well as the age at which samples were analyzed. Indeed, as imprints differ between cell types, we were able to distinguish the tissue-specific effects of ART. The drawbacks of this design, which split up the various studies, is that the size of each group decreased, reducing the power of the meta-analysis and highlighting the lack of 'replication' studies.

Finally, the results of this meta-analysis must be interpreted in light of the limitations of the contributing studies since a potential bias is introduced when reporting on studies with a low quality of evidence. Many of the included studies had small sample sizes with inadequate power to assess differences in rates of DNA methylation, and some

did not stratify for singletons and multiples. Most of the outcome data came from retrospective observational studies with considerable heterogeneity and differences in ART techniques and control groups. Additionally, a substantial number of studies did not account for many of the confounding factors known to cause epigenetic dysregulations. Finally, we had only limited access to key statistics in targeted analysis or raw data for epigenome-wide studies, which are essential for conducting meta-analyses.

As a final point, it should be noted that longitudinal and long-term follow-up studies are difficult to carry out in ART children. Far too few studies are regrettably performed during childhood, which contributes to the limited evidence we were able to report. Although it has been over 20 years since the first concerns were voiced about the safety of ART at an epigenetic level, studies conducted later in life are still inconclusive. It also remains unknown if ART could induce detrimental DNA methylation modifications at later ages and, if so, whether they lead to harmful outcomes in the offspring. The first babies conceived via ART are now entering their 40s. This could be an appropriate moment to follow-up on these individuals and to perform testing at the epigenetic level using epigenomic arrays.

While the identification of DNA methylation changes induced by ART was complex and most studies presented small sample sizes, the present systematic review has made it possible to assess a substantial number of children. Overall, more than 4000 DNA methylation profiles of ART conceptuses were compared to over 7000 controls.

Conclusion

Even though around half of the studies did not report any differences, our review does suggest the existence of DNA methylation differences after ART compared to natural conception. Our analyses indicate that IGs may be particularly sensitive to ART. Nevertheless, we are not able to rule out other studied sequences owing to the heterogeneity of the evidence base. Most evidence regarding DNA methylation and assisted conception stems from neonatal studies. Less is known about DNA methylation in childhood/adulthood, and there was no strong evidence of persistent modifications into later life. Further longitudinal follow-up studies will thus be needed to elucidate the persistence of these differences throughout life. The observed differences were modest, and the functional relevance in adult tissue is unknown. To understand the importance of these small differences, we need to shed more light on the functional effects in terms of gene expression as well as the roles of other epigenetic marks. Moreover, while some differences in DNA methylation profiles may be related to the ART procedures, they may also result from the parental contribution in a context of infertility.

Aggregating data from different cohorts will help to identify the global effects that are difficult to observe in individual studies, and it may be helpful to pool results to resolve these discrepancies in future work. Although great strides have already been taken in the field of epigenetics in ART, there is still much to discover.

Supplementary data

Supplementary data are available at *Human Reproduction Update* online.

Data availability

All data are incorporated into the article and its online supplementary material.

Acknowledgements

We thank Callista Mulder, Thomas Haaf and Marcus Dittrich for their reactivity in sharing their raw data. We appreciate the feedback from Aafke van Montfoort and Déborah Bourc'his during the discussion of this study. We also thank Suzanne Rankin for her help in writing the manuscript.

Authors' roles

J.B. and B.D. screened articles, selected articles and performed data extraction. B.D. performed statistical analysis. J.B., B.D. and P.F. contributed to the design of the study, interpretation of the data and writing of the manuscript. M.G., E.S. and C.B. contributed to the discussion. All authors approved the final version for submission.

Funding

This work was supported by funding from the Agence Nationale pour la Recherche ('CARE'-ANR JCJC 2017).

Conflict of interest

The authors declare no conflict of interest.

References

Argyraki M, Damdimopoulou P, Chatzimeletiou K, Grimbizis GF, Tarlatzis BC, Syrrou M, Lambropoulos A. In-utero stress and mode of conception: impact on regulation of imprinted genes, fetal development and future health. *Hum Reprod Update* 2019;**25**:777–801.

Åsenius F, Danson AF, Marzi SJ. DNA methylation in human sperm: a systematic review. *Hum Reprod Update* 2020;**26**:841–873.

Balduzzi S, Rücker G, Schwarzer G. How to perform a meta-analysis with R: a practical tutorial. *Evid Based Ment Health* 2019;**22**:153–160.

Barberet J, Barry F, Choux C, Guilleman M, Karoui S, Simonot R, Bruno C, Fauque P. What impact does oocyte vitrification have on epigenetics and gene expression? *Clin Epigenetics* 2020;**12**:121.

Barberet J, Binquet C, Guilleman M, Doukani A, Choux C, Bruno C, Bourredjem A, Chapusot C, Bourc'his D, Duffourd Y *et al.* Do assisted reproductive technologies and in vitro embryo culture influence the epigenetic control of imprinted genes and transposable elements in children? *Hum Reprod* 2021;**36**:479–492.

Barlow DP, Bartolomei MS. Genomic imprinting in mammals. *Cold Spring Harb Perspect Biol* 2014;**6**:a018382.

Berntsen S, Söderström-Anttila V, Wennerholm U-B, Laivuori H, Loft A, Oldereid NB, Romundstad LB, Bergh C, Pinborg A. The health of children conceived by ART: 'the chicken or the egg?'. *Hum Reprod Update* 2019;**25**:137–158.

Bozack AK, Colicino E, Just AC, Wright RO, Baccarelli AA, Wright RJ, Lee AG. Associations between infant sex and DNA methylation across umbilical cord blood, artery, and placenta samples. *Epigenetics* 2021;1–18.

Camprubí C, Iglesias-Platas I, Martin-Trujillo A, Salvador-Alarcon C, Rodriguez MA, Barredo DR, Court F, Monk D. Stability of genomic imprinting and gestational-age dynamic methylation in complicated pregnancies conceived following assisted reproductive technologies. *Biol Reprod* 2013;**89**:50.

Caramaschi D, Jungius J, Page CM, Novakovic B, Saffery R, Halliday J, Lewis S, Magnus MC, London SJ, Håberg SE *et al.* Association of medically assisted reproduction with offspring cord blood DNA methylation across cohorts. *Hum Reprod* 2021;**36**:2403–2413.

Castillo-Fernandez JE, Loke YJ, Bass-Stringer S, Gao F, Xia Y, Wu H, Lu H, Liu Y, Wang J, Spector TD *et al.* DNA methylation changes at infertility genes in newborn twins conceived by in vitro fertilisation. *Genome Med* 2017;**9**:28.

Chen W, Peng Y, Ma X, Kong S, Tan S, Wei Y, Zhao Y, Zhang W, Wang Y, Yan L *et al.* Integrated multi-omics reveal epigenomic disturbance of assisted reproductive technologies in human offspring. *EBioMedicine* 2020;**61**:103076.

Chen X-J, Chen F, Lv P-P, Zhang D, Ding G-L, Hu X-L, Feng C, Sheng J-Z, Huang H-F. Maternal high estradiol exposure alters CDKN1C and IGF2 expression in human placenta. *Placenta* 2018;**61**:72–79.

Chen Z, Hagen DE, Elsik CG, Ji T, Morris CJ, Moon LE, Rivera RM. Characterization of global loss of imprinting in fetal overgrowth syndrome induced by assisted reproduction. *Proc Natl Acad Sci U S A* 2015;**112**:4618–4623.

Choufani S, Turinsky AL, Melamed N, Greenblatt E, Brudno M, Bérard A, Fraser WD, Weksberg R, Trasler J, Monnier P; 3D Cohort Study Group. Impact of assisted reproduction, infertility, sex and paternal factors on the placental DNA methylome. *Hum Mol Genet* 2019;**28**:372–385.

Choux C, Binquet C, Carmignac V, Bruno C, Chapusot C, Barberet J, Lamotte M, Sagot P, Bourc'his D, Fauque P. The epigenetic control of transposable elements and imprinted genes in newborns is affected by the mode of conception: ART versus spontaneous conception without underlying infertility. *Hum Reprod* 2018;**33**:331–340.

Cortessis VK, Azadian M, Buxbaum J, Sanogo F, Song AY, Sriprasert I, Wei PC, Yu J, Chung K, Siegmund KD. Comprehensive meta-analysis reveals association between multiple imprinting disorders and conception by assisted reproductive technology. *J Assist Reprod Genet* 2018;**35**:943–952.

Czamara D, Eraslan G, Page CM, Lahti J, Lahti-Pulkkinen M, Hämäläinen E, Kajantie E, Laivuori H, Villa PM, Reynolds RM *et al.*; Major Depressive Disorder Working Group of the Psychiatric Genomics Consortium. Integrated analysis of environmental and genetic influences on cord blood DNA methylation in new-borns. *Nat Commun* 2019;**10**:2548.

Deaton AM, Bird A. CpG islands and the regulation of transcription. *Genes Dev* 2011;**25**:1010–1022.

Denomme M, White C, Gillio-Meina C, MacDonald W, Deroo B, Kidder G, Mann M. Compromised fertility disrupts Peg1 but not Snrpn and Peg3 imprinted methylation acquisition in mouse oocytes. *Front Genet* 2012;**3**:129.

Dong J, Wen L, Guo X, Xiao X, Jiang F, Li B, Jin N, Wang J, Wang X, Chen S *et al.* The increased expression of glucose transporters in human full-term placentas from assisted reproductive technology without changes of mTOR signaling. *Placenta* 2019;**86**:4–10.

Doornbos ME, Maas SM, McDonnell J, Vermeiden JPW, Hennekam RCM. Infertility, assisted reproduction technologies and imprinting disturbances: a Dutch study. *Hum Reprod* 2007;**22**:2476–2480.

El Hajj N, Haertle L, Dittrich M, Denk S, Lehnen H, Hahn T, Schorsch M, Haaf T. DNA methylation signatures in cord blood of ICSI children. *Hum Reprod* 2017;**32**:1761–1769.

Estill MS, Bolnick JM, Waterland RA, Bolnick AD, Diamond MP, Krawetz SA. Assisted reproductive technology alters deoxyribonucleic acid methylation profiles in bloodspots of newborn infants. *Fertil Steril* 2016;**106**:629–639.

Farin CE, Farmer WT, Farin PW, Farin CE, Farmer WT, Farin PW. Pregnancy recognition and abnormal offspring syndrome in cattle. *Reprod Fertil Dev* 2010;**22**:75–87.

Fauque P, Bourc'his D. Genes are not the whole story. In: Sermon K and Viville S (eds). *Textbook of Human Reproductive Genetics*. Cambridge University Press. 2014.

Fauque P, De Mouzon J, Devaux A, Epelboin S, Gervoise-Boyer M-J, Levy R, Valentin M, Viot G, Bergère A, De Vienne C *et al.* Reproductive technologies, female infertility, and the risk of imprinting-related disorders. *Clin Epigenet* 2020;**12**:9.

Feng C, Tian S, Zhang Y, He J, Zhu X-M, Zhang D, Sheng J-Z, Huang H-F. General imprinting status is stable in assisted reproduction-conceived offspring. *Fertil Steril* 2011;**96**:1417–1423.

Ferguson-Smith AC. Genomic imprinting: the emergence of an epigenetic paradigm. *Nat Rev Genet* 2011;**12**:565–575.

Fleming TP, Watkins AJ, Velazquez MA, Mathers JC, Prentice AM, Stephenson J, Barker M, Saffery R, Yajnik CS, Eckert JJ *et al.* Origins of lifetime health around the time of conception: causes and consequences. *Lancet* 2018;**391**:1842–1852.

Gaunt TR, Shihab HA, Hemani G, Min JL, Woodward G, Lyttleton O, Zheng J, Duggirala A, McArdle WL, Ho K *et al.* Systematic identification of genetic influences on methylation across the human life course. *Genome Biol* 2016;**17**:61.

Gentilini D, Somigliana E, Pagliardini L, Rabellotti E, Garagnani P, Bernardinelli L, Papaleo E, Candiani M, Di Blasio AM, Viganò P. Multifactorial analysis of the stochastic epigenetic variability in cord blood confirmed an impact of common behavioral and environmental factors but not of in vitro conception. *Clin Epigenet* 2018;**10**:13.

Ghosh J, Coutifaris C, Sapienza C, Mainigi M. Global DNA methylation levels are altered by modifiable clinical manipulations in assisted reproductive technologies. *Clin Epigenetics* 2017;**9**:14.

Gkountela S, Zhang KX, Shafiq TA, Liao W-W, Hargan-Calvopiña J, Chen P-Y, Clark AT. DNA demethylation dynamics in the human prenatal germline. *Cell* 2015;**161**:1425–1436.

Gomes MV, Huber J, Ferriani RA, Amaral Neto AM, Ramos ES. Abnormal methylation at the KvDMR1 imprinting control region in clinically normal children conceived by assisted reproductive technologies. *Mol Hum Reprod* 2009;**15**:471–477.

Greenberg MVC, Bourc'his D. The diverse roles of DNA methylation in mammalian development and disease. *Nat Rev Mol Cell Biol* 2019;**20**:590–607.

Guo F, Yan L, Guo H, Li L, Hu B, Zhao Y, Yong J, Hu Y, Wang X, Wei Y *et al.* The transcriptome and DNA methylome landscapes of human primordial germ cells. *Cell* 2015;**161**:1437–1452.

Guo H, Hu B, Yan L, Yong J, Wu Y, Gao Y, Guo F, Hou Y, Fan X, Dong J *et al.* DNA methylation and chromatin accessibility profiling of mouse and human fetal germ cells. *Cell Res* 2017a;**27**:165–183.

Guo H, Zhu P, Yan L, Li R, Hu B, Lian Y, Yan J, Ren X, Lin S, Li J *et al.* The DNA methylation landscape of human early embryos. *Nature* 2014;**511**:606–610.

Guo X-Y, Liu X-M, Jin L, Wang T-T, Ullah K, Sheng J-Z, Huang H-F. Cardiovascular and metabolic profiles of offspring conceived by assisted reproductive technologies: a systematic review and meta-analysis. *Fertil Steril* 2017b;**107**:622–631.

Hackett JA, Surani MA. DNA methylation dynamics during the mammalian life cycle. *Philos Trans R Soc Lond B Biol Sci* 2013;**368**: 20110328.

Harrer M, Cuijpers P, Furukawa T, Ebert DD. *Dmetar: Companion R Package for the Guide 'Doing Meta-Analysis in R'*. R package version 0.0.9000, 2019. http://dmetar.protectlab.org

Hart R, Norman RJ. The longer-term health outcomes for children born as a result of IVF treatment. Part II-Mental health and development outcomes. *Hum Reprod Update* 2013;**19**:244–250.

Hattori H, Hiura H, Kitamura A, Miyauchi N, Kobayashi N, Takahashi S, Okae H, Kyono K, Kagami M, Ogata T *et al.* Association of four imprinting disorders and ART. *Clin Epigenetics* 2019;**11**:21.

Hernandez Mora JR, Tayama C, Sánchez-Delgado M, Monteagudo-Sánchez A, Hata K, Ogata T, Medrano J, Poo-Llanillo ME, Simón C, Moran S *et al.* Characterization of parent-of-origin methylation using the Illumina Infinium MethylationEPIC array platform. *Epigenomics* 2018;**10**:941–954.

Higgins JPT, Thomas J, Chandler J, Cumpston M, Li T, Page M, Welch V. *Cochrane Handbook for Systematic Reviews of Interventions Version 6.0 (Updated July 2019)*. 2019. www.training.cochrane.org/handbook.

Higgins JP, Thompson SG. Quantifying heterogeneity in a meta-analysis. *Stat Med* 2002;**21**:1539–1558.

Hinrichs AS, Karolchik D, Baertsch R, Barber GP, Bejerano G, Clawson H, Diekhans M, Furey TS, Harte RA, Hsu F *et al.* The UCSC genome browser database: update 2006. *Nucleic Acids Res* 2006;**34**:D590–D598.

Hiura H, Hattori H, Kobayashi N, Okae H, Chiba H, Miyauchi N, Kitamura A, Kikuchi H, Yoshida H, Arima T. Genome-wide microRNA expression profiling in placentae from frozen-thawed blastocyst transfer. *Clin Epigenetics* 2017;**9**:79.

Hu S, Wan J, Su Y, Song Q, Zeng Y, Nguyen HN, Shin J, Cox E, Rho HS, Woodard C *et al.* DNA methylation presents distinct binding sites for human transcription factors. *eLife* 2013;**2**:e00726.

Huntriss JD, Hemmings KE, Hinkins M, Rutherford AJ, Sturmey RG, Elder K, Picton HM. Variable imprinting of the MEST gene in human preimplantation embryos. *Eur J Hum Genet* 2013;**21**:40–47.

Jaffe AE, Murakami P, Lee H, Leek JT, Fallin MD, Feinberg AP, Irizarry RA. Bump hunting to identify differentially methylated regions in epigenetic epidemiology studies. *Int J Epidemiol* 2012;**41**:200–209.

Jenkins TG, Aston KI, James ER, Carrell DT. Sperm epigenetics in the study of male fertility, offspring health, and potential clinical applications. *Syst Biol Reprod Med* 2017;**63**:69–76.

Jenkins TG, Aston KI, Pflueger C, Cairns BR, Carrell DT. Age-associated sperm DNA methylation alterations: possible implications in offspring disease susceptibility. *PLoS Genet* 2014;**10**:e1004458.

Kagami M, Nagai T, Fukami M, Yamazawa K, Ogata T. Silver–Russell syndrome in a girl born after in vitro fertilization: partial hypermethylation at the differentially methylated region of PEG1/MEST. *J Assist Reprod Genet* 2007;**24**:131–136.

Kanber D, Buiting K, Zeschnigk M, Ludwig M, Horsthemke B. Low frequency of imprinting defects in ICSI children born small for gestational age. *Eur J Hum Genet* 2009;**17**:22–29.

Katari S, Turan N, Bibikova M, Erinle O, Chalian R, Foster M, Gaughan JP, Coutifaris C, Sapienza C. DNA methylation and gene expression differences in children conceived in vitro or in vivo. *Hum Mol Genet* 2009;**18**:3769–3778.

Kazazian HH, Moran JV. Mobile DNA in health and disease. *N Engl J Med* 2017;**377**:361–370.

Kobayashi H, Hiura H, John RM, Sato A, Otsu E, Kobayashi N, Suzuki R, Suzuki F, Hayashi C, Utsunomiya T *et al.* DNA methylation errors at imprinted loci after assisted conception originate in the parental sperm. *Eur J Hum Genet* 2009;**17**:1582–1591.

Kohda M, Hoshiya H, Katoh M, Tanaka I, Masuda R, Takemura T, Fujiwara M, Oshimura M. Frequent loss of imprinting of IGF2 and MEST in lung adenocarcinoma. *Mol Carcinog* 2001;**31**:184–191.

Kopca T, Tulay P. Association of assisted reproductive technology treatments with imprinting disorders. *Glob Med Genet* 2021;**8**:1–6.

Lazaraviciute G, Kauser M, Bhattacharya S, Haggarty P, Bhattacharya S. A systematic review and meta-analysis of DNA methylation levels and imprinting disorders in children conceived by IVF/ICSI compared with children conceived spontaneously. *Hum Reprod Update* 2014;**20**:840–852.

Lefebvre L, Viville S, Barton SC, Ishino F, Keverne EB, Surani MA. Abnormal maternal behaviour and growth retardation associated with loss of the imprinted gene Mest. *Nat Genet* 1998;**20**:163–169.

Li L, Wang L, Le F, Liu X, Yu P, Sheng J, Huang H, Jin F. Evaluation of DNA methylation status at differentially methylated regions in IVF-conceived newborn twins. *Fertil Steril* 2011;**95**:1975–1979.

Litzky JF, Deyssenroth MA, Everson TM, Armstrong DA, Lambertini L, Chen J, Marsit CJ. Placental imprinting variation associated with assisted reproductive technologies and subfertility. *Epigenetics* 2017;**12**:653–661.

Liu Y, Tang Y, Ye D, Ma W, Feng S, Li X, Zhou X, Chen X, Chen S. Impact of abnormal DNA methylation of imprinted loci on human spontaneous abortion. *Reprod Sci* 2018;**25**:131–139.

Loke YJ, Galati JC, Saffery R, Craig JM. Association of in vitro fertilization with global and IGF2/H19 methylation variation in newborn twins. *J Dev Orig Health Dis* 2015;**6**:115–124.

Lou H, Le F, Zheng Y, Li L, Wang L, Wang N, Zhu Y, Huang H, Jin F. Assisted reproductive technologies impair the expression and methylation of insulin-induced gene 1 and sterol regulatory element-binding factor 1 in the fetus and placenta. *Fertil Steril* 2014; **101**:974.e2–980.e2.

Lucifero D, Mertineit C, Clarke HJ, Bestor TH, Trasler JM. Methylation dynamics of imprinted genes in mouse germ cells. *Genomics* 2002;**79**:530–538.

Mallik S, Odom GJ, Gao Z, Gomez L, Chen X, Wang L. An evaluation of supervised methods for identifying differentially methylated regions in Illumina methylation arrays. *Brief Bioinform* 2019;**20**: 2224–2235.

Mangiavacchi PM, Caldas-Bussiere MC, Mendonça M da S, Dias AJB, Rios ÁFL. Multi-locus imprinting disturbances of Beckwith–Wiedemann and large offspring syndrome/abnormal offspring syndrome: a brief review. *Theriogenology* 2021;**173**:193–201.

Mani S, Mainigi M. Embryo Culture Conditions and the Epigenome. Semin Reprod Med 2018;**36**:211–220.

Mansell G, Gorrie-Stone TJ, Bao Y, Kumari M, Schalkwyk LS, Mill J, Hannon E. Guidance for DNA methylation studies: statistical insights from the Illumina EPIC array. *BMC Genomics* 2019;**20**:366.

Marjonen H, Auvinen P, Kahila H, Tšuiko O, Kõks S, Tiirats A, Viltrop T, Tuuri T, Söderström-Anttila V, Suikkari A-M *et al.* rs10732516 polymorphism at the IGF2/H19 locus associates with genotype-specific effects on placental DNA methylation and birth weight of newborns conceived by assisted reproductive technology. *Clin Epigenetics* 2018;**10**:80.

Melamed N, Choufani S, Wilkins-Haug LE, Koren G, Weksberg R. Comparison of genome-wide and gene-specific DNA methylation between ART and naturally conceived pregnancies. *Epigenetics* 2015;**10**:474–483.

Merid SK, Novoloaca A, Sharp GC, Küpers LK, Kho AT, Roy R, Gao L, Annesi-Maesano I, Jain P, Plusquin M *et al.* Epigenome-wide meta-analysis of blood DNA methylation in newborns and children identifies numerous loci related to gestational age. *Genome Med* 2020;**12**:25.

Monk D, Mackay DJG, Eggermann T, Maher ER, Riccio A. Genomic imprinting disorders: lessons on how genome, epigenome and environment interact. *Nat Rev Genet* 2019;**20**:235–248.

Monk D, Morales J, den Dunnen JT, Russo S, Court F, Prawitt D, Eggermann T, Beygo J, Buiting K, Tümer Z; Nomenclature group of the European Network for Human Congenital Imprinting Disorders. Recommendations for a nomenclature system for reporting methylation aberrations in imprinted domains. *Epigenetics* 2018;**13**:117–121.

Mulder CL, Wattimury TM, Jongejan A, De Winter-Korver CM, Van Daalen SKM, Struijk RB, Borgman SCM, Wurth Y, Consten D, Van Echten-Arends J *et al.* Comparison of DNA methylation patterns of parentally imprinted genes in placenta derived from IVF conceptions in two different culture media. *Hum Reprod* 2020;**35**: 516–528.

Murphy SK, Huang Z, Hoyo C. Differentially methylated regions of imprinted genes in prenatal, perinatal and postnatal human tissues. *PLoS One* 2012;**7**:e40924.

Nakanishi H, Suda T, Katoh M, Watanabe A, Igishi T, Kodani M, Matsumoto S, Nakamoto M, Shigeoka Y, Okabe T *et al.* Loss of imprinting of PEG1/MEST in lung cancer cell lines. *Oncol Rep* 2004; **12**:1273–1278.

Nelissen ECM, Dumoulin JCM, Daunay A, Evers JLH, Tost J, van Montfoort APA. Placentas from pregnancies conceived by IVF/ICSI have a reduced DNA methylation level at the H19 and MEST differentially methylated regions. *Hum Reprod* 2013;**28**:1117–1126.

Novakovic B, Lewis S, Halliday J, Kennedy J, Burgner DP, Czajko A, Kim B, Sexton-Oates A, Juonala M, Hammarberg K *et al.* Assisted reproductive technologies are associated with limited epigenetic variation at birth that largely resolves by adulthood. *Nat Commun* 2019;**10**:3922.

Okae H, Chiba H, Hiura H, Hamada H, Sato A, Utsunomiya T, Kikuchi H, Yoshida H, Tanaka A, Suyama M *et al.* Genome-wide analysis of DNA methylation dynamics during early human development. *PLoS Genet* 2014;**10**:e1004868.

Oliver VF, Miles HL, Cutfield WS, Hofman PL, Ludgate JL, Morison IM. Defects in imprinting and genome-wide DNA methylation are not common in the in vitro fertilization population. *Fertil Steril* 2012;**97**:147–153.

Page MJ, Moher D, Bossuyt PM, Boutron I, Hoffmann TC, Mulrow CD, Shamseer L, Tetzlaff JM, Akl EA, Brennan SE et al. PRISMA 2020 explanation and elaboration: updated guidance and exemplars for reporting systematic reviews. *BMJ* 2021;**372**:n160. https://www.bmj.com/content/372/bmj.n160. (15 July 2021, date last accessed).

Pedersen IS, Dervan PA, Broderick D, Harrison M, Miller N, Delany E, O'Shea D, Costello P, McGoldrick A, Keating G *et al.* Frequent loss of imprinting of PEG1/MEST in invasive breast cancer. *Cancer Res* 1999;**59**:5449–5451.

Penova-Veselinovic B, Melton PE, Huang RC, Yovich JL, Burton P, Wijs LA, Hart RJ. DNA methylation patterns within whole blood of adolescents born from assisted reproductive technology are not different from adolescents born from natural conception. *Hum Reprod* 2021;**36**:2035–2049.

Pervjakova N, Kasela S, Morris AP, Kals M, Metspalu A, Lindgren CM, Salumets A, Mägi R. Imprinted genes and imprinting control regions show predominant intermediate methylation in adult somatic tissues. *Epigenomics* 2016;**8**:789–799.

Puumala SE, Nelson HH, Ross JA, Nguyen RH, Damario MA, Spector LG. Similar DNA methylation levels in specific imprinting control regions in children conceived with and without assisted reproductive technology: a cross-sectional study. *BMC Pediatr* 2012;**12**:33.

Qin J-B, Sheng X-Q, Wu D, Gao S-Y, You Y-P, Yang T-B, Wang H. Worldwide prevalence of adverse pregnancy outcomes among singleton pregnancies after in vitro fertilization/intracytoplasmic sperm injection: a systematic review and meta-analysis. *Arch Gynecol Obstet* 2017;**295**:285–301.

Rahmani E, Schweiger R, Rhead B, Criswell LA, Barcellos LF, Eskin E, Rosset S, Sankararaman S, Halperin E. Cell-type-specific resolution epigenetics without the need for cell sorting or single-cell biology. *Nat Commun* 2019;**10**:3417.

Rancourt RC, Harris HR, Michels KB. Methylation levels at imprinting control regions are not altered with ovulation induction or in vitro fertilization in a birth cohort. *Hum Reprod* 2012;**27**:2208–2216.

Rangwala SH, Kuznetsov A, Ananiev V, Asztalos A, Borodin E, Evgeniev V, Joukov V, Lotov V, Pannu R, Rudnev D *et al.* Accessing NCBI data using the NCBI Sequence Viewer and Genome Data Viewer (GDV). *Genome Res* 2021;**31**:159–169.

Robinson WP, Price EM. The human placental methylome. *Cold Spring Harb Perspect Med* 2015;**5**:a023044.

Ryan R, Hill S. *How to GRADE the Quality of the Evidence*. 2016. http://cccrg.cochrane.org/author-resources (2016, date last accessed).

Sakian S, Louie K, Wong EC, Havelock J, Kashyap S, Rowe T, Taylor B, Ma S. Altered gene expression of H19 and IGF2 in placentas from ART pregnancies. *Placenta* 2015;**36**:1100–1105.

Salpekar A, Huntriss J, Bolton V, Monk M. The use of amplified cDNA to investigate the expression of seven imprinted genes in human oocytes and preimplantation embryos. *Mol Hum Reprod* 2001;**7**:839–844.

Sanchez-Delgado M, Court F, Vidal E, Medrano J, Monteagudo-Sánchez A, Martin-Trujillo A, Tayama C, Iglesias-Platas I, Kondova I, Bontrop R *et al.* Human oocyte-derived methylation differences persist in the placenta revealing widespread transient imprinting. *PLoS Genet* 2016;**12**:e1006427.

Santi D, De Vincentis S, Magnani E, Spaggiari G. Impairment of sperm DNA methylation in male infertility: a meta-analytic study. *Andrology* 2017;**5**:695–703.

Sato A, Otsu E, Negishi H, Utsunomiya T, Arima T. Aberrant DNA methylation of imprinted loci in superovulated oocytes. *Hum Reprod* 2007;**22**:26–35.

Schöherr N, Jäger S, Ranke MB, Wollmann HA, Binder G, Eggermann T. No evidence for isolated imprinting mutations in the PEG1/MEST locus in Silver–Russell patients. *Eur J Med Genet* 2008; **51**:322–324.

Schroeder DI, Blair JD, Lott P, Yu HOK, Hong D, Crary F, Ashwood P, Walker C, Korf I, Robinson WP *et al.* The human placenta methylome. *Proc Natl Acad Sci U S A* 2013;**110**:6037–6042.

Shi X, Ni Y, Zheng H, Chen S, Zhong M, Wu F, Xia R, Luo Y. Abnormal methylation patterns at the IGF2/H19 imprinting control region in phenotypically normal babies conceived by assisted reproductive technologies. *Eur J Obstet Gynecol Reprod Biol* 2011; **158**:52–55.

Smallwood SA, Kelsey G. De novo DNA methylation: a germ cell perspective. *Trends Genet* 2012;**28**:33–42.

Smith ZD, Meissner A. DNA methylation: roles in mammalian development. *Nat Rev Genet* 2013;**14**:204–220.

Song S, Ghosh J, Mainigi M, Turan N, Weinerman R, Truongcao M, Coutifaris C, Sapienza C. DNA methylation differences between in vitro- and in vivo-conceived children are associated with ART procedures rather than infertility. *Clin Epigenetics* 2015;**7**:41.

Strogantsev R, Krueger F, Yamazawa K, Shi H, Gould P, Goldman-Roberts M, McEwen K, Sun B, Pedersen R, Ferguson-Smith AC. Allele-specific binding of ZFP57 in the epigenetic regulation of imprinted and non-imprinted monoallelic expression. *Genome Biol* 2015;**16**:112.

Takahashi N, Coluccio A, Thorball CW, Planet E, Shi H, Offner S, Turelli P, Imbeault M, Ferguson-Smith AC, Trono D. ZNF445 is a primary regulator of genomic imprinting. *Genes Dev* 2019;**33**: 49–54.

Tang L, Liu Z, Zhang R, Su C, Yang W, Yao Y, Zhao S. Imprinting alterations in sperm may not significantly influence ART outcomes and imprinting patterns in the cord blood of offspring. *PloS One* 2017;**12**:e0187869.

Tang WWC, Dietmann S, Irie N, Leitch HG, Floros VI, Bradshaw CR, Hackett JA, Chinnery PF, Surani MA. A unique gene regulatory network resets the human germline epigenome for development. *Cell* 2015;**161**:1453–1467.

Tenorio J, Romanelli V, Martin-Trujillo A, Fernández G-M, Segovia M, Perandones C, Pérez Jurado LA, Esteller M, Fraga M, Arias P *et al.*; SOGRI Consortium. Clinical and molecular analyses of Beckwith–Wiedemann syndrome: comparison between spontaneous conception and assisted reproduction techniques. *Am J Med Genet A* 2016;**170**:2740–2749.

Tierling S, Souren NY, Gries J, LoPorto C, Groth M, Lutsik P, Neitzel H, Utz-Billing I, Gillessen-Kaesbach G, Kentenich H *et al.* Assisted reproductive technologies do not enhance the variability of DNA methylation imprints in human. *J Med Genet* 2010;**47**: 371–376.

Tobi EW, Almqvist C, Hedman A, Andolf E, Holte J, Olofsson JI, Wramsby H, Wramsby M, Pershagen G, Heijmans BT *et al.* DNA methylation differences at birth after conception through ART. *Hum Reprod* 2021;**36**:248–259.

Touati A, Errea-Dorronsoro J, Nouri S, Halleb Y, Pereda A, Mahdhaoui N, Ghith A, Saad A, de Nanclares GP, Brahim DHB. Transient neonatal diabetes mellitus and hypomethylation at additional imprinted loci: novel ZFP57 mutation and review on the literature. *Acta Diabetol* 2019;**56**:301–307.

Turan N, Katari S, Gerson LF, Chalian R, Foster MW, Gaughan JP, Coutifaris C, Sapienza C. Inter- and intra-individual variation in allele-specific DNA methylation and gene expression in children conceived using assisted reproductive technology. *PLoS Genet* 2010;**6**:e1001033.

Tusnády GE, Simon I, Váradi A, Arányi T. BiSearch: primer-design and search tool for PCR on bisulfite-treated genomes. *Nucleic Acids Res* 2005;**33**:e9

Vermeiden JPW, Bernardus RE. Are imprinting disorders more prevalent after human in vitro fertilization or intracytoplasmic sperm injection? *Fertil Steril* 2013;**99**:642–651.

Vincent RN, Gooding LD, Louie K, Chan Wong E, Ma S. Altered DNA methylation and expression of PLAGL1 in cord blood from assisted reproductive technology pregnancies compared with natural conceptions. *Fertil Steril* 2016;**106**:739–748.

Wang Y-X, Yue L-F, Zhang J-W, Xiong Y-W, Hu J-J, Wang L-L, Li Z, Liu Y, Yang L, Sun L-J. Expression and DNA methylation status of the imprinted genes PEG10 and L3MBTL1 in the umbilical cord blood and placenta of the offspring of assisted reproductive technology. *Reprod Sci* 2021;**28**:1133–1141.

Weber M, Hellmann I, Stadler MB, Ramos L, Pääbo S, Rebhan M, Schübeler D. Distribution, silencing potential and evolutionary impact of promoter DNA methylation in the human genome. *Nat Genet* 2007;**39**:457–466.

Wells G, Shea B, Peterson J, Welch V, Losos M, Tugwell P. *The Newcastle-Ottawa Scale (NOS) for Assessing the Quality of Nonrandomised Studies in Meta-Analyses*. 2013. http://www.ohri.ca/programs/clinical_epidemiology/oxford.asp (2 September 2021, date last accessed).

Wen L, Tang F. Human germline cell development: from the perspective of single-cell sequencing. *Mol Cell* 2019;**76**:320–328.

Whitelaw N, Bhattacharya S, Hoad G, Horgan GW, Hamilton M, Haggarty P. Epigenetic status in the offspring of spontaneous and assisted conception. *Hum Reprod* 2014;**29**:1452–1458.

Wong EC, Hatakeyama C, Robinson WP, Ma S. DNA methylation at H19/IGF2 ICR1 in the placenta of pregnancies conceived by in vitro fertilization and intracytoplasmic sperm injection. *Fertil Steril* 2011;**95**:2524–2526.

Wu X, Zhang Y. TET-mediated active DNA demethylation: mechanism, function and beyond. *Nat Rev Genet* 2017;**18**:517–534.

Xu N, Barlow GM, Cui J, Wang ET, Lee B, Akhlaghpour M, Kroener L, Williams J 3rd, Rotter JI, Chen YI *et al.* Comparison of genome-wide and gene-specific DNA methylation profiling in first-trimester chorionic villi from pregnancies conceived with infertility treatments. *Reprod Sci* 2017;**24**:996–1004.

Yao J-F, Huang Y-F, Huang R-F, Lin S-X, Guo C-Q, Hua C-Z, Wu P-Y, Hu J-F, Li Y-Z. Effects of vitrification on the imprinted gene Snrpn in neonatal placental tissue. *Reprod Dev Med* 2020;**4**:25–31.

Yeung EH, Mendola P, Sundaram R, Zeng X, Guan W, Tsai MY, Robinson SL, Stern JE, Ghassabian A, Lawrence D *et al.* Conception by fertility treatment and offspring deoxyribonucleic acid methylation. *Fertil Steril* 2021;**116**:493–504.

Yin Y, Morgunova E, Jolma A, Kaasinen E, Sahu B, Khund-Sayeed S, Das PK, Kivioja T, Dave K, Zhong F *et al.* Impact of cytosine methylation on DNA binding specificities of human transcription factors. *Science* 2017;**356**:eaaj2239.

Young LE, Fernandes K, McEvoy TG, Butterwith SC, Gutierrez CG, Carolan C, Broadbent PJ, Robinson JJ, Wilmut I, Sinclair KD. Epigenetic change in IGF2R is associated with fetal overgrowth after sheep embryo culture. *Nat Genet* 2001;**27**:153–154.

Young LE, Sinclair KD, Wilmut I. Large offspring syndrome in cattle and sheep. *Rev Reprod* 1998;**3**:155–163.

Yousefi P, Huen K, Davé V, Barcellos L, Eskenazi B, Holland N. Sex differences in DNA methylation assessed by 450 K BeadChip in newborns. *BMC Genomics* 2015;**16**:911.

Yu B, Dong X, Gravina S, Kartal Ö, Schimmel T, Cohen J, Tortoriello D, Zody R, Hawkins RD, Vijg J. Genome-wide, single-cell DNA methylomics reveals increased non-CpG methylation during human oocyte maturation. *Stem Cell Reports* 2017;**9**:397–407.

Yu D-H, Ware C, Waterland RA, Zhang J, Chen M-H, Gadkari M, Kunde-Ramamoorthy G, Nosavanh LM, Shen L. Developmentally programmed 3' CpG island methylation confers tissue- and cell-type-specific transcriptional activation. *Mol Cell Biol* 2013;**33**:1845–1858.

Zechner U, Pliushch G, Schneider E, El Hajj N, Tresch A, Shufaro Y, Seidmann L, Coerdt W, Müller AM, Haaf T. Quantitative methylation analysis of developmentally important genes in human pregnancy losses after ART and spontaneous conception. *Mol Hum Reprod* 2010;**16**:704–713.

Zheng H-Y, Shi X-Y, Wang L-L, Wu Y-Q, Chen S-L, Zhang L. Study of DNA methylation patterns of imprinted genes in children born after assisted reproductive technologies reveals no imprinting errors: a pilot study. *Exp Ther Med* 2011a;**2**:751–755.

Zheng H-Y, Shi X-Y, Wu F-R, Wu Y-Q, Wang L-L, Chen S-L. Assisted reproductive technologies do not increase risk of abnormal methylation of PEG1/MEST in human early pregnancy loss. *Fertil Steril* 2011b;**96**:84–89.

Zheng H-Y, Tang Y, Niu J, Li P, Ye D-S, Chen X, Shi X-Y, Li L, Chen S-L. Aberrant DNA methylation of imprinted loci in human spontaneous abortions after assisted reproduction techniques and natural conception. *Hum Reprod* 2013;**28**:265–273.

Zhou F, Wang R, Yuan P, Ren Y, Mao Y, Li R, Lian Y, Li J, Wen L, Yan L *et al.* Reconstituting the transcriptome and DNA methylome landscapes of human implantation. *Nature* 2019;**572**:660–664.

Zhu P, Guo H, Ren Y, Hou Y, Dong J, Li R, Lian Y, Fan X, Hu B, Gao Y *et al.* Single-cell DNA methylome sequencing of human preimplantation embryos. *Nat Genet* 2018;**50**:12–19.

Supplementary Table SI: Search strategy

PubMed search
("assisted reproduct*
OR "in vitro conception"
OR ICSI
OR "intracytoplasmic sperm injection"
OR "in vitro fertili*"
OR IVF
OR insemination)
AND (DNA methylation)
NOT review[Publication Type]

Number of results : 647
Date of search : 15th July 2021

EMBASE search
('assisted reprod*':ti,ab,kw
OR 'in vitro conception':ti,ab,kw
OR icsi:ti,ab,kw
OR 'intracytoplasmic sperm injection':ti,ab,kw
OR ivf:ti,ab,kw
OR 'in vitro fertili*':ti,ab,kw
OR insemination:ti,ab,kw)
AND 'dna methylation':ti,ab,kw
NOT review:it

Number of results : 689
Date of search : 15th July 2021

Supplementary Table SII: Data extraction form and PRISMA checklist

Title			
Authors			
Date of publication			
Journal			
Study period			
Recruitment method			
Single or multi-center			
Study design			
Information on population			
	ART	**CTL**	
Age			
Gestational age at birth			
Maternal age			
…			
Sample size			n ART= n CTL=
Validation cohort			
Tissue			
Regions analyzed			chr:coordinates (genome assembly)
DNA methylation technique			
Data/results			CpG ID (DMP) or DMR or targeted region Deltabeta *p*val Mc Sc Me Se

Section and Topic	Item #	Checklist item	Location where item is reported
TITLE			
Title	1	Identify the report as a systematic review.	1
ABSTRACT			
Abstract	2	See the PRISMA 2020 for Abstracts checklist.	3
INTRODUCTION			
Rationale	3	Describe the rationale for the review in the context of existing knowledge.	11-12
Objectives	4	Provide an explicit statement of the objective(s) or question(s) the review addresses.	12
METHODS			
Eligibility criteria	5	Specify the inclusion and exclusion criteria for the review and how studies were grouped for the syntheses.	12-13
Information sources	6	Specify all databases, registers, websites, organisations, reference lists and other sources searched or consulted to identify studies. Specify the date when each source was last searched or consulted.	12-13
Search strategy	7	Present the full search strategies for all databases, registers and websites, including any filters and limits used.	Supp Table 1
Selection process	8	Specify the methods used to decide whether a study met the inclusion criteria of the review, including how many reviewers screened each record and each report retrieved, whether they worked independently, and if applicable, details of automation tools used in the process.	13
Data collection process	9	Specify the methods used to collect data from reports, including how many reviewers collected data from each report, whether they worked independently, any processes for obtaining or confirming data from study investigators, and if applicable, details of automation tools used in the process.	13
Data items	10a	List and define all outcomes for which data were sought. Specify whether all results that were compatible with each outcome domain in each study were sought (e.g. for all measures, time points, analyses), and if not, the methods used to decide which results to collect.	13-16
	10b	List and define all other variables for which data were sought (e.g. participant and intervention characteristics, funding sources). Describe any assumptions made about any missing or unclear information.	13-16
Study risk of bias assessment	11	Specify the methods used to assess risk of bias in the included studies, including details of the tool(s) used, how many reviewers assessed each study and whether they worked independently, and if applicable, details of automation tools used in the process.	14
Effect measures	12	Specify for each outcome the effect measure(s) (e.g. risk ratio, mean difference) used in the synthesis or presentation of results.	14
Synthesis methods	13a	Describe the processes used to decide which studies were eligible for each synthesis (e.g. tabulating the study intervention characteristics and comparing against the planned groups for each synthesis (item #5)).	14-15
	13b	Describe any methods required to prepare the data for presentation or synthesis, such as handling of missing summary statistics, or data conversions.	15-16
	13c	Describe any methods used to tabulate or visually display results of individual studies and syntheses.	15-16

Section and Topic	Item #	Checklist item	Location where item is reported
	13d	Describe any methods used to synthesize results and provide a rationale for the choice(s). If meta-analysis was performed, describe the model(s), method(s) to identify the presence and extent of statistical heterogeneity, and software package(s) used.	15-16
	13e	Describe any methods used to explore possible causes of heterogeneity among study results (e.g. subgroup analysis, meta-regression).	NA
	13f	Describe any sensitivity analyses conducted to assess robustness of the synthesized results.	NA
Reporting bias assessment	14	Describe any methods used to assess risk of bias due to missing results in a synthesis (arising from reporting biases).	14
Certainty assessment	15	Describe any methods used to assess certainty (or confidence) in the body of evidence for an outcome.	14
RESULTS			
Study selection	16a	Describe the results of the search and selection process, from the number of records identified in the search to the number of studies included in the review, ideally using a flow diagram.	17
	16b	Cite studies that might appear to meet the inclusion criteria, but which were excluded, and explain why they were excluded.	18&21
Study characteristics	17	Cite each included study and present its characteristics.	Supp table 7
Risk of bias in studies	18	Present assessments of risk of bias for each included study.	Supp table 3 & 7
Results of individual studies	19	For all outcomes, present, for each study: (a) summary statistics for each group (where appropriate) and (b) an effect estimate and its precision (e.g. confidence/credible interval), ideally using structured tables or plots.	Figure 4
Results of syntheses	20a	For each synthesis, briefly summarise the characteristics and risk of bias among contributing studies.	17
	20b	Present results of all statistical syntheses conducted. If meta-analysis was done, present for each the summary estimate and its precision (e.g. confidence/credible interval) and measures of statistical heterogeneity. If comparing groups, describe the direction of the effect.	18-28
	20c	Present results of all investigations of possible causes of heterogeneity among study results.	NA
	20d	Present results of all sensitivity analyses conducted to assess the robustness of the synthesized results.	NA
Reporting biases	21	Present assessments of risk of bias due to missing results (arising from reporting biases) for each synthesis assessed.	17
Certainty of evidence	22	Present assessments of certainty (or confidence) in the body of evidence for each outcome assessed.	Supp table 4 & 7
DISCUSSION			
Discussion	23a	Provide a general interpretation of the results in the context of other evidence.	28-37
	23b	Discuss any limitations of the evidence included in the review.	35-37
	23c	Discuss any limitations of the review processes used.	29-32
	23d	Discuss implications of the results for practice, policy, and future research.	36-37

Section and Topic	Item #	Checklist item	Location where item is reported
OTHER INFORMATION			
Registration and protocol	24a	Provide registration information for the review, including register name and registration number, or state that the review was not registered.	12
	24b	Indicate where the review protocol can be accessed, or state that a protocol was not prepared.	12
	24c	Describe and explain any amendments to information provided at registration or in the protocol.	12
Support	25	Describe sources of financial or non-financial support for the review, and the role of the funders or sponsors in the review.	39
Competing interests	26	Declare any competing interests of review authors.	39
Availability of data, code and other materials	27	Report which of the following are publicly available and where they can be found: template data collection forms; data extracted from included studies; data used for all analyses; analytic code; any other materials used in the review.	Supp table 6

From: Page MJ, McKenzie JE, Bossuyt PM, Boutron I, Hoffmann TC, Mulrow CD, *et al*. The PRISMA 2020 statement: an updated guideline for reporting systematic reviews. BMJ 2021;372:n71. doi: 10.1136/bmj.n71

Supplementary Table SIII: Quality assessment of cohort studies by the Newcastle-Ottawa scale

Criteria	
Selection	1) Representativeness of the Exposed Cohort? (scored 1 star) 2) Selection of the Non-Exposed Cohort (same community scored 1 star) 3) Ascertainment of Exposure (scored 1 star) 4) Demonstration That Outcome of Interest Was Not Present at Start of Study (no history of infertility scored 1 star)
Comparability	5) Comparability of Cohorts on the Basis of the Design or Analysis (control or population matched for important factor scored 1 star; control for additional factor scored 1 star among maternal age, gestational age, sex, age)
Outcome	6) Assessment of Outcome (Targeted gene studies : several CpGs and quantitative measure, Genome-wide : control for gender/cell-type composition scored 1 star) 7) Same method of ascertainment of outcome for exposed and non-exposed (scored 1 star) 8) Was Follow-Up Long Enough for Outcomes to Occur (scored 1 star) Total stars (maximum: 9)

Supplementary Table SIV: GRADE of evidence criteria

GRADE criteria	Rating	Footnotes	Quality of the evidence
Risk of Bias	No serious (-1) very serious (-2)	As assessed with Newcastle-Ottawa scale : High - Moderate - Low	
Inconsistency	No serious (-1) very serious (-2)	Contradicting studies Overlapping effect estimates	⊕ ⊕ ⊕ ⊕ High
Indirectness	No serious (-1) very serious (-2)	Generalizability Particular population/intervention (FH-FZ, autologous and donor oocytes) Indirect comparison, Validation of gene expression changes Lack of appropriate controls Lack of descriptive statistics of participants	⊕ ⊕ ⊕ Moderate ⊕ ⊕ Low ⊕ Very Low
Imprecision	No serious (-1) very serious (-2)	Targeted : n<63 per group with 1:1 ratio (or 47 ART/94 NC with 1:2 ratio, or 42 ART/126 NC with 1:3 ratio) EWAS : n<100 in total or one group n<30 Non-quantitative assessment	
Publication Bias	Undetected Strongly suspected (-1)	Less than 3 genes studied	
Other (upgrading factors)	Large effect (+1 or +2) Dose response (+1 or +2) No Plausible confounding (+1 or +2)	Inconsistency: +1 if validation cohort Imprecision: +1 +2 if large sample size	

From GRADE (Grading of Recommendations Assessment, Development and Evaluation

Supplementary Table SV: Definition of DMPs and DMRs and statistical thresholds set in each study.

							DMPs					DMRs		
Study	**Age**	**Tissue**	**DMP**	**DMR**	**Raw data accessibility**	**Location of raw data**	**Number of DMP found**	**Criteria**	**Number of DMP with available data**	**Criteria**	**DMP in genes with 2 DMP**	**Number of DMR**	**Algorithm**	**Criteria**
Katari *et al.*, (2009)	neonates	cord blood	yes	no	no		358	P<0.05 (2-way ANOVA)	163	*p*<0.08 in gene with 2 or more CpGs	163	-	-	-
	neonates	placenta	yes	no	no		246	P<0.05 (2-way ANOVA)	86	*p*<0.08 in gene with 2 or more CpGs	86	-	-	-
Camprubi *et al.,* (2013)	neonates	placenta	no	yes	no but processed data available	Supplementary Table S3 and S4 in Camprubi *et al.* (2013)	-	-	-	-	-	3	t-test	25 iDMRs AND *p*<0.05 (Bonferroni)
	neonates	cord blood	no	yes	no but processed data available		-	-	-	-	-	0	t-test	26 iDMRs AND *p*<0.05 (Bonferroni)
Melamed *et al.,* (2014)	neonates	cord blood	yes	no	no		733	FDR<0.05	61	FDR<0.05 in gene with 2 or more CpGs OR with deltabeta>10% OR in imprinted gene	48	-	-	-
Estill *et al.,* (2016)	neonates	bloodspots	no	yes	yes	GEO : GSE79257	-	-	-	-	-	unknown	A-clustering	FDR<0.05 AND average Δβ ≥2.5% AND (in enhancer or IG)
Castillo-Fernandez *et al.,* (2017)	neonates	cord blood	no	yes	yes	EGA : EGAS00001002248	-	-	-	-	-	1	linear mixed-effects model	FDR<0.05
Xu *et al.,* (2017)	pregnancy	CVS	yes	no	no		0	FDR<0.05	0	FDR<0.05	0	-	-	-
El Hajj *et al.,* (2017)	neonates	cord blood	yes	no	no		4730	FDR<0.05	4730	FDR<0.05	1596	-	-	-
Litzky *et al.,* (2017)	neonates	placenta	no	no	yes	GEO : GSE75248	-	-	-	-	-	-	-	-

Gentilini *et al.,* (2018)	neonates	cord blood	yes	no	yes	GEO : GSE152380	0	$P<10^{-7}$	0	$p<10^{-7}$	0	-	-	-
Choufani *et al.,* (2019)	neonates	placenta	yes	no	yes	GEO : GSE120250	0	FDR<0.05	0	FDR<0.05	0	-	-	-
Novakovic *et al.,* (2019)	neonates	bloodspots	yes	yes	yes	GEO : GSE131433	2340	FDR<0.05	136	FDR<0.05, Δβ ≥5%	8	18	DMRcate	>=3DMP with 1DMP Δβ ≥5% AND FDR<0.05
	adults	blood	yes	yes	yes		0	FDR<0.05	0	FDR<0.05, Δβ ≥5%	0	4	DMRcate	>=3DMP with 1DMP Δβ ≥5% AND FDR<0.05
Chen *et al.,* (2020)	neonates	cord blood	no	yes	yes	GEO : GSE136849	-	-	-	-	-	4361	calculateDiffMeth() from MethylKit (logistic regression)	adjusted *p*<0.05 (SLIM method) AND Δβ ≥5% AND (in 4 out of 6 group comparison)
	neonates	cord blood	no	yes	yes		-	-	-	-	-	4831	calculateDiffMeth() from MethylKit (logistic regression)	adjusted *p*<0.05 (SLIM method) AND Δβ ≥5% AND (in 4 out of 6 group comparison)
Barberet *et al.,* (2021)	children	buccal cells	yes	yes	yes	GEO : GSE150901	401	FDR<0.05, Δβ ≥5%	401	FDR<0.05, Δβ ≥5%	391	33	DMRcate	>=3DMP AND (maximum 1000bp between DMP)
Tobi *et al.,* (2021)	neonates	cord blood	yes	no	no		19	FDR<0.05	19	FDR<0.05	3	-	-	-
Yeung *et al.,* (2021)	neonates	bloodspots	yes	yes	no		12	FDR<0.05	12	FDR<0.05	4	9	DMRff	888 probes in imprinting regions AND *p*<0.05 (Bonferroni)
	children	blood	yes	yes	no		1	FDR<0.05	1	FDR<0.05	0	1	DMRff	889 probes in imprinting regions AND *p*<0.05 (Bonferroni)
Penova-Veselinovic *et al.,* (2021)	adolescent	blood	yes	yes	no		0	$P<6.31x10^{-8}$	0	$p<6.31x10^{-8}$	0	0	DMRff	*p*<0.05 (Bonferroni) AND (maximum 500 bp between DMP)
Camaraschi *et al.,* (2021)	neonates	cord blood	yes	no	no		5	FDR<0.05	5	FDR<0.05	2	-	-	-

Supplementary Table SVI: Extracted data of DNA methylation in each included publication

Available online at https://academic.oup.com/humupd/article/28/5/629/6544694#369820865

Supplementary Table SVII: Studies characteristics

Available online at https://academic.oup.com/humupd/article/28/5/629/6544694#369820865

Supplementary Table SVIII: Imprinted region high quality studies

		Birth	Childhood	Adulthood
Targeted studies	Placenta	*H19* CTCF3[1], KvDMR1[1]	-	-
	Cord blood	*PEG1/MEST*[2], *PLAGL1*[3]	-	-
	Dried bloodspots	No studies	-	-
	Buccal smears	*H19* CTCF63[4]	*SNRPN*[5]	No studies
	Peripheral blood	No studies	No differences	No studies
Genome-wide studies	Placenta	No studies reaching quality criteria	-	-
	Cord blood	*NTM*[6], *RTL1*[6], *UBE3A*[6], *LIN28B*[6], *MESTIT1*[6], *MEST*[6], *SGCE*[6]	-	-
	Dried bloodspots	*GNAS*[7], *L3MBTL1*[7], *BLCAP*[7], *HYMAI*[7], *MEST*[7]	-	-
	Buccal smears	No studies	No studies reaching quality criteria	No studies
	Peripheral blood	No studies	*GNAS*[7]	No differences

[1]Choux *et al.* (2018), [2]Tierling *et al.* (2010), [3]Vincent *et al.* (2016), [4]Loke *et al.* (2015), [5]Whitelaw *et al.* (2014), [6]El Hajj *et al.* (2017), [7]Yeung *et al.* (2021)

2) Mécanismes biochimiques de modification de l'épigénome : la reprogrammation épigénétique comme période de susceptibilité

Les modifications subies par le méthylome ovocytaire et embryonnaire pourraient être engendrées par deux mécanismes principaux. Le premier impliquerait la perturbation biochimique de la reprogrammation épigénétique via les cycles de la méthionine et des folates, et le second l'action du stress oxydant.

Dans des conditions normales, la méthionine réagit avec l'ATP pour former la S-adénosylméthionine (SAM) qui sous l'action des DNMTs libère le groupe méthyle et donne la S-adénosylhomocystéine (SAH) (Figure 25). Une hydrolase spécifique de la SAH la transforme en homocystéine et adénosine, et l'homocystéine est à nouveau retransformée en méthionine. Cela constitue le cycle de la méthionine. Un des principaux points de blocage du cycle se situe au niveau de l'hydrolysation de la SAH qui est une réaction hautement réversible et favorise davantage la synthèse de la SAH plutôt que son hydrolysation. La SAH possède plus d'affinité avec les méthyltransférases que la SAM, inhibant ainsi l'activité des méthyltransférases. L'accumulation de SAH via une concentration plus élevée d'homocystéine a donc tendance à bloquer le cycle de la méthylation, en limitant la disponibilité de groupement méthyle (Barroso *et al.*, 2017). Par exemple, la stimulation ovarienne augmenterait la concentration en homocystéine dans le liquide folliculaire, et a donc la capacité de perturber la reprogrammation épigénétique de l'embryon (Boxmeer *et al.*, 2008).

Toute concentration inadaptée de méthionine dans le milieu de culture embryonnaire (concentrations supra- ou infra-physiologiques) est susceptible d'altérer la mise en place des profils de méthylation de l'embryon précoce issus de sa reprogrammation épigénétique, même si cela reste à démontrer chez l'humain (Ikeda *et al.*, 2011).

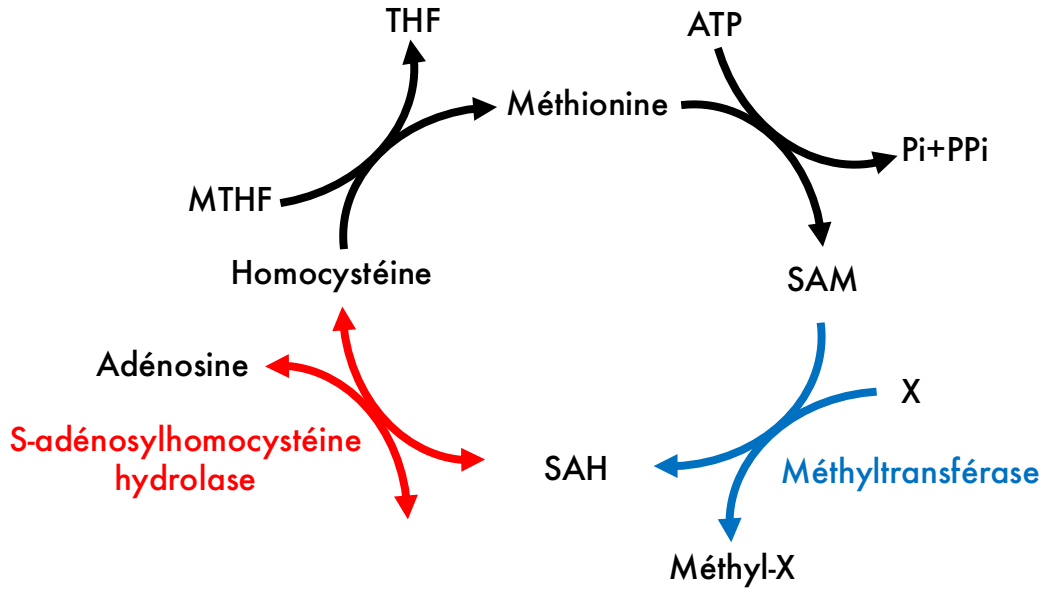

Figure 25. Le cycle de la méthylation simplifié.
En rouge, l'hydrolysation de la SAH est réversible et favorise davantage la synthèse de SAH à partir d'homocystéine et d'adénosine. En bleu, le mécanisme de méthylation de l'ADN : les méthyltransférases ont plus d'affinité avec la SAH que la SAM. ATP : adénosine triphosphate. MTHF : méthyltétrahydrofolate. Pi : phosphate inorganique. PPi : pyrophosphate inorganique. SAH : S-adénosylhomocystéine. SAM : S-adénosylméthionine. THF : tétrahydrofolate. X : molécule pouvant être méthylée.

En outre, le cycle des folates est intimement lié à celui de la méthionine. Il est démontré que des supplémentations en acide folique chez les femmes enceintes modulent la méthylation des nouveau-nés dans les régions soumises à empreinte *IGF2* ou *PEG3*, et dans des gènes impliqués dans le neurodéveloppement, et même à long-terme (Steegers-Theunissen *et al.*, 2009; Haggarty *et al.*, 2013; Richmond *et al.*, 2018; Ondičová *et al.*, 2022). Les milieux de culture embryonnaire ne possèdent pas de folates dans leur composition à la différence du fluide tubaire, et la privation en folates pourrait perturber la disponibilité de groupements méthyles (Morbeck *et al.*, 2014; Menezo *et al.*, 2019, 2022b).

Il existe donc un risque accru en AMP de créer un déséquilibre des cycles des folates et de la méthionine qui coïncide avec la reprogrammation épigénétique, et qui peuvent induire des altérations du méthylome gamétique et embryonnaire, potentiellement durables. L'embryon et les gamètes possèdent des capacités d'homéostasie pour corriger ces déséquilibres, mais

l'accumulation des interventions en AMP pourraient induire *in fine* des modifications épigénétiques tangibles.

Par ailleurs, les multiples manipulations effectuées en AMP sont génératrices de stress oxydant qui a pour origine un déséquilibre entre la production de dérivés réactifs de l'oxygène (DROs) et les mécanismes de protection face aux dégradations qu'ils induisent (Agarwal *et al.*, 2022). Ces DROs peuvent oxyder les cytosines méthylées, qui se retrouvent dans un état hydroxyméthylé qui caractérise un signal de reconnaissance de déméthylation active pour les enzymes thymine-DNA glycosylases (TDG), TETs et potentiellement AID et APOBECs (Shen *et al.*, 2014). Les embryons précoces ne sont pas capables de se défendre dans un environnement *in vitro* dépourvus d'antioxydants. La synthèse de cystéine à partir d'homocystéine n'est pas active aux stades où interviennent les manipulations en AMP, alors qu'elle est le précurseur du glutathion censé maintenir le potentiel redox du cytoplasme cellulaire (Menezo *et al.*, 2022a). L'accumulation d'expositions à des conditions suboptimales en AMP est donc à risque pour le profil épigénétique entre l'absence de mécanisme de défense au stress oxydant et la perturbation des cycles des folates et de la méthionine. Il n'est pas exclu que d'autres mécanismes encore inconnus influencent les profils de méthylation.

3) La vulnérabilité de l'ovocyte et de l'embryon humain face aux techniques d'AMP se traduit sur leur transcriptome

L'exposition des gamètes et embryons à un environnement stressant les oblige à s'adapter, et l'acquisition du matériel transcriptionnel nécessaire au développement de l'embryon peut être compromise. Similairement à l'épigénome, le transcriptome serait sensible aux interventions réalisées en AMP, qui surviennent alors que les gamètes et l'embryon sont transcriptionnellement silencieux, partiellement ou complètement (Mermillod *et al.*, 2008; Krisher, 2013). Les effets de la stimulation ovarienne, de la vitrification, de la maturation *in*

vitro et des conditions de culture ont été évalués afin de mesurer l'impact de ces interventions sur le stockage des ARN maternels.

3.1) Effets sur l'ovocyte chez l'Homme

3.1.1) Objectifs

L'ovocyte est à la fois la cellule la plus grosse du corps humain mais aussi une des plus vulnérables à son environnement. Pendant des années, les investigations sur les effets des techniques d'AMP se sont focalisées sur l'embryon, tandis que c'est avant tout, la qualité ovocytaire qui détermine la compétence développementale du futur embryon et son issue clinique. L'exposition de l'ovocyte à des environnements stressants le force à s'adapter et modifie les modalités d'acquisition des transcrits nécessaires pour supporter les premières étapes du développement embryonnaire (O'Neill *et al.*, 2012; Bertoldo *et al.*, 2015). L'objectif de cette étude est d'identifier dans la littérature existante les facteurs intrinsèques à l'AMP susceptibles de perturber le transcriptome ovocytaire chez l'humain (stimulation ovarienne, cryopréservation, maturation and conditions *in vitro*) mais aussi ceux liés au contexte maternel (pathologies utérines, environnement et mode de vie des mères) qui ont la capacité de modifier l'expression de ses gènes. Trois points fondamentaux ont été discutés :

i) les concordances dans les résultats obtenus entre différentes études pour un même facteur étudié
ii) les dérégulations transcriptionnelles communes ou de certaines voies biologiques entre différents facteurs étudiés
iii) l'existence de régions ou de groupes de gènes particulièrement sensibles à l'ensemble des facteurs étudiés

3.1.2) Matériels et méthodes

Une recherche bibliographique approfondie d'articles originaux mesurant l'expression de certains gènes (approches gène candidat) ou le transcriptome (approche pangénomique) en lien avec les facteurs techniques et intrinsèques à l'AMP et en lien avec le contexte maternel a été réalisée dans PubMed (endométriose, syndrome des ovaires polykystiques, réserve ovarienne diminuée, âge maternel, tabagisme, obésité, pollution, stimulation ovarienne, maturation *in vitro*, cryopréservation). Pour chacune des études, le design (facteurs étudiés, populations comparées, …), le nombre et l'identité des gènes différentiellement exprimés selon la condition analysée et les voies biologiques altérées ont été notés. En l'absence d'études directement sur l'ovocyte lui-même pour certains facteurs, les études sur les cellules entourant l'ovocyte (cellules du cumulus ou de la granulosa murale) ont également été considérées. Ainsi, un total de 50 études est évalué de façon critique dans cette revue.

3.1.3) Résultats

L'absence d'études directement sur l'ovocyte humain et seulement sur les cellules qui l'entourent (cellules cumulus (CC) et cellules de la granulosa (CGM)) conduit à des conclusions limitées quant à l'effet de la stimulation ovarienne sur le transcriptome ovocytaire (Figure 26). Le recours à un protocole hormonal réalisée avec des agonistes ou antagonistes de l'hormone de libération de la gonadotrophine pour inhiber une augmentation prématurée de l'hormone lutéinisante ne semble pas influencer l'expression des gènes dans les CC (Devjak *et al.*, 2012). Toutefois, le type de protocole de stimulation par gonadotrophines (hormone de stimulation folliculaire recombinante ou non ou urinaire (FSH, rFSH), gonadotrophine ménopausique humaine (hMG), supplémentation en hormone lutéinisante (LH)) module l'expression des CC et CGM, avec un effet dose prononcé (Grøndahl *et al.*, 2009; Adriaenssens *et al.*, 2010; Brannian *et al.*, 2010; Barberi *et al.*, 2012; Assou *et al.*, 2013; Gatta *et al.*, 2013; Gurgan *et al.*, 2014; Cruz *et al.*, 2017; Liu *et al.*, 2022). Les principales voies biologiques différentiellement exprimées dans les CC et CGM semblent être au niveau de la

stéroïdogenèse, de l'angiogenèse, des interactions cellulaires et du métabolisme lipidique. L'induction de l'ovulation via différentes hormones (choriogonadotrophine humaine (hCG) ou agoniste de la gonadolibérine ou une combinaison des deux) dans les CC résulte en une expression différentielle de nombreux gènes impliqués dans la maturation ovocytaire (*AREG*, *EREG*) et des gènes à effets anti-angiogéniques (*PEDF*, *VEGF*), prévenant le risque de développement d'un syndrome d'hyperstimulation ovarienne (SHSO) (Borgbo *et al.*, 2013; Haas *et al.*, 2014, 2016; Vuong *et al.*, 2017; Fuchs Weizman *et al.*, 2019). Collectivement, il semble que l'hyperstimulation ovarienne impacte négativement l'achèvement de la maturation cytoplasmique de l'ovocyte (De Los Santos *et al.*, 2012; Papler *et al.*, 2014; Lu *et al.*, 2019; Taher *et al.*, 2021) et que différentes stimulations façonnent le contenu transcriptomique des cellules entourant l'ovocyte notamment celui impliqué dans le métabolisme lipidique.

Les récentes études utilisant les techniques de dernière génération de séquençage montrent que la maturation *in vitro* augmente l'expression de gènes impliqués dans la phosphorylation oxydative ou l'apoptose, et dérégule des fonctions mitochondriales et métaboliques dans l'ovocyte (Zhao *et al.*, 2019a; Ye *et al.*, 2020; Lee *et al.*, 2021; Yang *et al.*, 2022). Ces résultats suggèrent une maturation cytoplasmique incomplète due à une déficience des processus énergétiques mobilisables par l'ovocyte. Les paramètres physico-chimiques de l'environnement *in vitro* doivent être strictement contrôlés d'après le modèle souris, sous peine de favoriser l'apoptose et la réponse au stress sous hyperoxie (Naillat *et al.*, 2021; Takashima *et al.*, 2021) ou la dérégulation de la signalisation hormonale et du cycle cellulaire par exposition au bisphénol A (Ferris *et al.*, 2016). Toutes les sources de variation de ces paramètres nécessitent davantage de surveillance (température, phtalates, tension en oxygène, lumière, composition du milieu de culture, temps d'incubation, …).

Par ailleurs, la vitrification ovocytaire chez l'Homme pourrait dégrader la qualité et le nombre d'ARNm maternels en comparaison d'ovocytes frais, indépendamment de la durée de conservation (Huo *et al.*, 2021). L'étude du transcriptome ovocytaire confirme par ailleurs l'effet délétère de la congélation lente vis-à-vis de la vitrification (Monzo *et al.*, 2012).

Si toutes ces études sont nécessaires, elles n'indiquent pas si les modifications transcriptomiques en lien avec les différentes techniques d'AMP évaluées ont un effet à court et long terme. Compte tenu des processus biologiques impactés (métabolisme, activité mitochondriale, cycle cellulaire) qui sont connus pour gouverner le développement embryonnaire jusqu'à la transition materno-zygotique, davantage d'études sont nécessaires pour mieux évaluer leurs répercussions. De plus il faut également prendre en compte que les ovocytes collectés en AMP proviennent souvent de patientes avec des problèmes d'infertilité variés (endométriose, âge avancé, faible réserve ovarienne, tabagisme, obésité, …) qui eux-mêmes pourraient avoir un impact négatif sur le transcriptome ovocytaire.

		Tissu	Comparaison	Etude	Nombre d'échantillons par groupe	Nombre de transcrits testés	Nombre de DEGs
Hyperstimulation ovarienne contrôlée	Stimulation ovarienne	CC	Agoniste vs antagoniste de la GnRH	Devjak et al. (2012)	15 vs 10	28 869	-
		CC	HP-hMG vs rFSH	Adriaenssens et al. (2010)	35 vs 28	10	2
		CC	HP-hMG vs rFSH	Assou et al. (2013)	53 vs 93	>47 000	94
		CC	HP-hMG vs rFSH	Cruz et al. (2017)	6 vs 5	>41 000	75
		CC	HP-hMG vs rFSH urinaire	Cruz et al. (2017)	6 vs 5	>41 000	155
		CC	rFSH vs FSH urinaire	Cruz et al. (2017)	5 vs 5	>41 000	43
		CC	HP-hMG vs rFSH	Gatta et al. (2013)	4 vs 8	30 968	3369
		CC	rLH+rFSH vs rFSH	Gatta et al. (2013)	4 vs 8	30 968	499
		CGM	HP-hMG vs rFSH	Brannian et al. (2010)	4 vs 4	19 426	1736
		CGM	HP-hMG vs rFSH	Grondahl et al. (2009)	15 vs 15	>47 000	85
		CC	FSH+rFSH (séquentiel) vs FSH ou rFSH seules	Gurgan et al. (2014)	15 vs 15	>47 000	579
		CC	rFSH seule vs supplémentation en r-LH	Barberi et al. (2012)	11 vs 7	3	2
		CGM	Modérée vs conventionnelle	Liu et al. (2022)	27 vs 21	Ensemble du génome	425
	Induction de l'ovulation	CC	hCG vs agoniste de la GnRH	Borgbo et al. (2013)	10 vs 9	28 869	391
		CGM	hCG vs agoniste de la GnRH	Borgbo et al. (2013)	10 vs 6	28 869	252
		CGM	hCG vs agoniste de la GnRH	Haas et al. (2014)	12 vs 12	11	8
		CGM	hCG vs hCG+agoniste de la GnRH	Haas et al. (2016)	15 vs 15	8	4
		CGM	Différentes doses d'agoniste de la GnRH	Vuong et al. (2017)	10	3	-
		CC	hCG ou agoniste de la GnRH vs hCG+agoniste de la GnRH	Weizman et al. (2019)	4 vs 5	Ensemble du génome	3106
	Stimulation vs cycle naturel	CC	Stimulation vs cycle naturel	de los Santos et al. (2012)	4 vs 4	>41 000	18
		CGM	Stimulation vs cycle naturel	Lu et al. (2019)	3 vs 4	Ensemble du génome	1002
		CC	Stimulation vs cycle naturel modifié	Papler et al. (2013)	3 vs 5	28 869	66
Maturation *in vitro*	MIV	Ovocyte	MIV vs *in vivo*	Yang et al. (2022)	12 vs 8	Ensemble du génome	2281
		Ovocyte	MIV vs *in vivo*	Ye et al. (2020)	7 vs 8	Ensemble du génome	507
	MIV de secours	Ovocyte	MIV de secours vs *in vivo*	Jones et al. (2008)	3 vs 11	19 426	2766
		Ovocyte	MIV de secours vs *in vivo*	Lee et al. (2021)	11 vs 10	Ensemble du génome	1559
		Ovocyte	MIV de secours vs *in vivo*	Virant-Klun et al. (2018)	30 vs 30	50 599	?
		Ovocyte	MIV de secours vs *in vivo*	Wells et Patricio (2007)	10 vs 15	29 098	?
		Ovocyte	MIV de secours vs *in vivo*	Zhao et al. (2019)	3 vs 3	Ensemble du génome	2230
		Ovocyte	MIV de secours vs MIV de secours avec hormone de croissance	Li et al. (2019)	3 vs 3	Ensemble du génome	507
		CC	MIV de secours vs *in vivo* (SOPK)	Ouandaogo et al. (2012)	9 vs 9	>47 000	5219
Cryopreservation	MIV	Ovocyte	Frais vs vitrifié	Barberet et al. (2022)	6 vs 14	Ensemble du génome	108
		Ovocyte	Vitrification semi -automatique vs manuelle	Barberet et al. (2022)	7 vs 6	Ensemble du génome	5
		Ovocyte	Frais vs cryopréservé (congélation lente + vitrification)	Chamayou et al. (2011)	15 vs 30	19	17
		Ovocyte	Vitrification vs congélation lente	Chamayou et al. (2011)	15 vs 15	19	-
		Ovocyte	Frais vs vitrifié	D'Aurora et al. (2019)	16 vs 16	5	-
		Ovocyte	Frais vs vitrifié	Di Pietro et al. (2010)	10 vs 15	7	-
		Ovocyte	Frais vs vitrifié	Huo et al. (2020)	3 vs 13	Ensemble du génome	1987
		Ovocyte	Frais vs vitrifié	Monzo et al. (2012)	54 vs 86	>47 000	608
		Ovocyte	Frais vs congélation lente	Monzo et al. (2012)	54 vs 59	>47 000	388
		Ovocyte	Frais vs congélation lente	Stigliani et al. (2015)	31 vs 68	>41 000	102

Figure 26. Résumé des études évaluant les modifications du transcriptome après hyperstimulation ovarienne et ses modalités, maturation *in vitro* et cryopréservation.
CC : cellules du cumulus. CGM : cellules de la granulosa murale. hCG : choriogonadotrophine humaine. HP-hMG : gonadotrophine ménopausique humaine hautement purifiée. GnRH : hormone de libération de la gonadotrophine. LH : hormone lutéinisante. MIV : maturation *in vitro*. rFSH : hormone de stimulation folliculaire recombinante. SOPK : syndrome des ovaires polykystiques.

3.1.4) Article 3 - Transcriptomic integrity of human oocytes used in assisted reproductive technologies: technical and intrinsic factor effects

OXFORD

human reproduction update

Human Reproduction Update, 2023, **00(0)**, 1–22
https://doi.org/10.1093/humupd/dmad025

Transcriptomic integrity of human oocytes used in ARTs: technical and intrinsic factor effects

Bastien Ducreux[1], Catherine Patrat [2,3], Jacquetta Trasler[4,5,6], and Patricia Fauque [1,7,*]

[1]Université Bourgogne Franche-Comtés—Equipe Génétique des Anomalies du Développement (GAD) INSERM UMR1231, Dijon, France
[2]Université de Paris Cité, Faculty of Medicine, Inserm 1016, Paris, France
[3]Department of Reproductive Biology-CECOS, aphp.centre-Université Paris Cité, Paris, France
[4]Department of Pediatrics, McGill University and Research Institute of the McGill University Health Centre, Montreal, QC, Canada
[5]Department of Human Genetics, McGill University and Research Institute of the McGill University Health Centre, Montreal, QC, Canada
[6]Department of Pharmacology & Therapeutics, McGill University and Research Institute of the McGill University Health Centre, Montreal, QC, Canada
[7]CHU Dijon Bourgogne, Laboratoire de Biologie de la Reproduction—CECOS, Dijon, France

*Correspondence address. CHU Dijon Bourgogne, Laboratoire de Biologie de la Reproduction—CECOS, Dijon, France. E-mail: patricia.fauque@chu-dijon.fr https://orcid.org/0000-0002-9708-1710

TABLE OF CONTENTS

- Introduction
- Methods
- Patients' characteristics
  - Infertility
  - Lifestyle and environmental exposure
- Ovarian stimulation
  - Ovarian stimulation protocols
  - Ovulation triggering protocol
  - Ovarian stimulation effects compared with natural cycles
- *In vitro* conditions
  - IVM of oocytes
  - Oxygen tension
  - Temperature
  - Pollutants
- Cryopreservation and storage time
- ART factors not studied to date
- Implications of different ART and external factors for common transcriptional regulation mechanisms
- Conclusion and perspective

Received: April 28, 2023. **Revised:** July 4, 2023. **Editorial decision:** August 23, 2023.

GRAPHICAL ABSTRACT

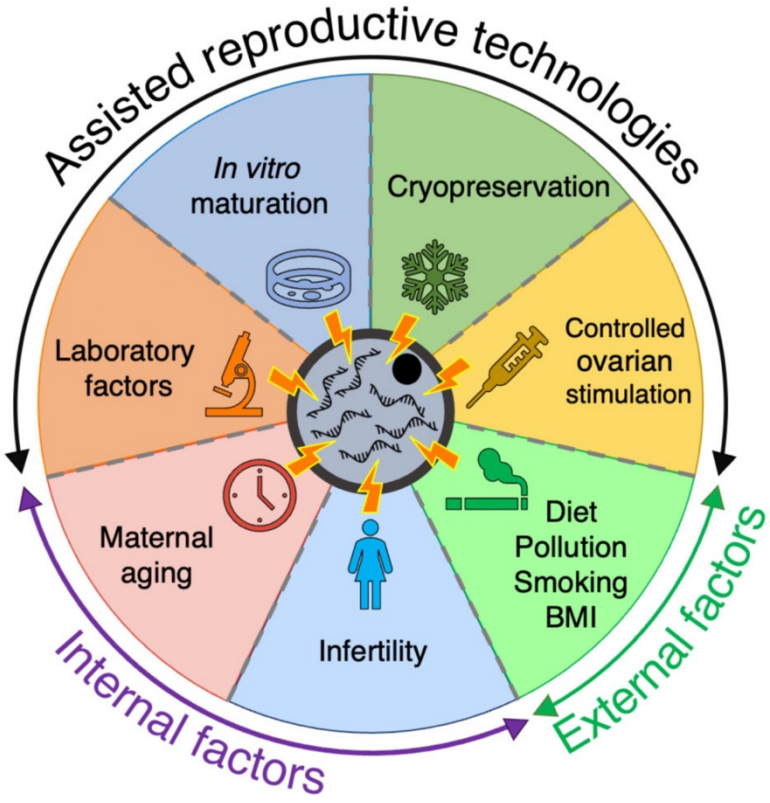

The multiplicity of assisted reproductive interventions has the potential to modify the oocyte or follicle transcriptome, which has possibly been previously modulated by patient characteristics and their environmental exposures.

ABSTRACT

BACKGROUND: Millions of children have been born throughout the world thanks to ARTs, the harmlessness of which has not yet been fully demonstrated. For years, efforts to evaluate the specific effects of ART have focused on the embryo; however, it is the oocyte quality that mainly dictates first and foremost the developmental potential of the future embryo. Ovarian stimulation, cryopreservation, and IVM are sometimes necessary steps to obtain a mature oocyte, but they could alter the appropriate expression of the oocyte genome. Additionally, it is likely that female infertility, environmental factors, and lifestyle have a significant influence on oocyte transcriptomic quality, which may interfere with the outcome of an ART attempt.

OBJECTIVE AND RATIONALE: The objective of this review is to identify transcriptomic changes in the human oocyte caused by interventions specific to ART but also intrinsic factors such as age, reproductive health issues, and lifestyle. We also provide recommendations for future good practices to be conducted when attempting ART.

SEARCH METHODS: An in-depth literature search was performed on PubMed to identify studies assessing the human oocyte transcriptome following ART interventions, or in the context of maternal aging, suboptimal lifestyle, or reproductive health issues.

OUTCOMES: ART success is susceptible to external factors, maternal aging, lifestyle factors (smoking, BMI), and infertility due to endometriosis or polycystic ovary syndrome. Indeed, all of these are likely to increase oxidative stress and alter mitochondrial processes in the foreground. Concerning ART techniques themselves, there is evidence that different ovarian stimulation regimens shape the oocyte transcriptome. The perturbation of processes related to the mitochondrion, oxidative phosphorylation, and metabolism is observed with IVM. Cryopreservation might dysregulate genes belonging to transcriptional regulation, ubiquitination, cell cycle, and oocyte growth pathways. For other ART laboratory factors such as temperature, oxygen tension, air pollution, and light, the evidence remains scarce. Focusing on genes involved in chromatin-based processes such as DNA methylation, heterochromatin modulation, histone modification, and chromatin remodeling complexes, but also genomic imprinting, we observed systematic dysregulation of such genes either after ART intervention or lifestyle exposure, as well as due to internal factors such as maternal aging and reproductive diseases. Alteration in the expression of such epigenetic regulators may be a common mechanism linked to adverse oocyte environments, explaining global transcriptomic modifications.

WIDER IMPLICATIONS: Many IVF factors and additional external factors have the potential to impair oocyte transcriptomic integrity, which might not be innocuous for the developing embryo. Fortunately, it is likely that such dysregulations can be minimized by adapting ART protocols or reducing adverse exposure.

Keywords: assisted reproduductive technologies / human oocyte / IVF / RNA-seq / transcriptome

Introduction

ARTs have allowed the birth of millions of children worldwide and the proportion of couples undergoing infertility treatments is in continuing expansion (de Geyter *et al.*, 2020; Wyns *et al.*, 2020, 2021). ARTs have been recognized as safe, but >40 years after the first baby born via IVF (Steptoe and Edwards, 1978) numerous studies have reported a higher incidence of birth defects and congenital disorders including imprinting disorders in the population conceived '*in vitro*' (Davies *et al.*, 2012; Vermeiden and Bernardus, 2013). Over recent years, efforts have been made to improve the safety of such techniques after identification of several factors that may be detrimental for gametes and embryos.

There is no doubt that during an IVF cycle, oocytes are particularly vulnerable to exogenous exposure, notably at the MII (metaphase II) stage when there is transcriptional quiescence. Transcriptional activity of the oocyte dictates the developmental potential of the future embryo, and small perturbations of the oocyte microenvironment have the capacity to impair oocyte quality and developmental competence, with potential long-lasting effects (Mermillod *et al.*, 2008; Krisher, 2013). Assessing the integrity of the oocyte transcriptome has been proposed as a tool to evaluate oocyte quality following several ART exogenous exposures including ovarian stimulation, IVM and culture conditions, cryopreservation, oocyte denudation, pipetting, and other *in vitro* external factors such as thermal stress and plastic pollution. Additionally, it is likely that environmental factors and lifestyle have a significant influence on oocyte transcriptomic quality that may interfere with the success of an IVF/ICSI protocol (Krisher, 2013; Carré *et al.*, 2017).

For years, efforts have focused mainly on the optimization of *in vitro* culture conditions of the embryos, known to be crucial for the outcomes (Wale and Gardner, 2016). However, the impact of environment for oocyte quality should not be underestimated; the quality of the oocyte quality at fertilization is the fundamental checkpoint to ensure correct early embryo development. Exposing the oocyte to stressful environment forces the oocyte to adaptations, and the acquisition of necessary transcriptional material to support embryo development may be compromised. Intrinsically, the embryo expresses pro-death pathways, which are tightly repressed by autocrine trophic signals (such as growth factors) which activate cAMP response element-binding protein (CREB) and AKT signaling, playing a pro-survival role (O'Neill *et al.*, 2012). An inherited defective maternal-effect machinery, as hypothesized by Bertoldo *et al.* (2015) based on evidence from early mouse embryos, would deprive the embryo of those trophic signals, and switch the embryonic transcriptome from pro-survival to pro-apoptotic settings via accumulation of TRP53 protein (Bertoldo *et al.*, 2015). The purpose of this review is to identify and interpret changes in the transcriptome or expression of targeted genes in the human oocyte caused by interventions specific to ART but also external factors such as maternal age, reproductive diseases and lifestyle. The three main objectives of our study were: (i) to determine whether there is concordance between the findings of the studies carried out in humans according to each disruptive factor; (ii) to identify whether common transcriptional dysregulations of molecular pathways exist between the different disruptive factors; and (iii) to identify whether some regions/genes are particularly sensitive to the different disruptive factors.

Methods

The focus of this review is human oocyte gene expression in the context of ART technical and intrinsic factors; thus, an in-depth literature search was performed on PubMed to identify studies relevant to this subject, without publication date limit. The factors considered included: endometriosis, polycystic ovary syndrome (PCOS), diminished ovarian reserve (DOR), maternal age, smoking, BMI, pollutants, ovarian stimulation, IVM, and cryopreservation. Studies evaluating both the full (via microarrays, RNA-seq or scRNA-seq) or partial transcriptome (using RT-qPCR) or only a small number of genes were considered in this review. Due to the narrative nature of this review, no formal quality of evidence assessment of studies was conducted. For all studies, we recorded information on study design, the number, and the list of differentially expressed genes (DEGs), and information of biological pathways altered in the context considered. In the absence of studies directly on human oocytes for some factors, studies on somatic cells surrounding the oocytes (i.e. mural granulosa cells (MGCs) or cumulus cells (CCs)) were also considered. In total, 50 studies were recorded evaluating specific ART interventions or intrinsic factor effects on the human oocyte transcriptome or that of its surrounding cells. In some cases, studies on animal oocytes were also discussed in the absence of studies directly on human oocytes.

To facilitate and justify the comparison of studies, we gathered lists of DEGs retrieved in each individual study. No custom significance threshold was applied for the selection of DEGs; all DEGs have been selected based on the criteria applied in each study. Then, we separated DEGs into up- and down-regulated genes according to the two groups compared (reference versus other condition tested) and subjected them to gene symbol update with the *UpdateSymbolList* function from Seurat package for harmonization (Hao *et al.*, 2021). This function finds current gene symbol of old or alias gene symbols from the HGNC database. All lists of DEGs were intersected with each other to find overlaps in affected genes between studies, and Venn diagrams were used for visualization. We also sought to cross-reference these genes with a list of genes involved in chromatin-based processes such as DNA methylation, heterochromatin modulators, histone modifiers, and remodeling complexes.

Patients' characteristics

The interaction between patients' characteristics and ART remains a grey area, but if clarified, this could lead to improve patient management in the future. The fact that oocytes have lower competence with specific patients' conditions might be seen at the transcriptomic level and that could help scientists to develop new personalized ART protocols.

Infertility

Endometriosis

Endometriosis is a common disorder in the general population (~1 in 10 women) (Eisenberg *et al.*, 2018) and it is estimated that 35–50% of infertile women are affected by this disease (Meuleman *et al.*, 2009; Bulletti *et al.*, 2010). Several studies have shown that endometriosis does not reduce endometrial receptivity and have suggested that decreased oocyte quality could be the reason why patients have reduced implantation rates (Sung *et al.*, 1997; Garcia-Velasco *et al.*, 2015; Miravet-Valenciano *et al.*, 2017; Tan *et al.*, 2021). The transcriptomic profile of MII oocytes from patients with endometriosis has recently been compared with healthy controls to understand the molecular mechanisms altering oocyte quality (Ferrero *et al.*, 2019) (Supplementary Table S1). Using scRNA-seq on 16 MII oocytes from 5 healthy oocyte donors and 16 MII oocytes from 7 patients with ovarian

endometrioma, the authors identified 520 DEGs (the majority up-regulated due to endometriosis), which were enriched for processes such as steroid metabolism, response to oxidative stress, cell growth regulation, mitochondrial function, methylation, and angiogenesis functions. Interestingly, robust sub-group analysis when oocytes came from an affected or unaffected ovary from the same patient showed no difference between the groups, suggesting that endometriosis decreases globally oocyte quality independently of the presence of an endometrioma. A study on RNA-seq in pools of cumulus cells from patients with endometrioma reached the same conclusions (da Luz *et al.*, 2021), while another study with a similar protocol found different pathways and defective functions such as MAPK and Wnt signaling, apoptosis, and cell junctions (Shi *et al.*, 2022). The small number of samples (9 and 5, respectively) could explain the heterogeneity of the results. It remains to be determined to what extent these transcriptomic modifications could compromise oocyte fertility and have a negative influence on ART outcomes for patients with endometriosis (Senapati *et al.*, 2016). Elevated levels of reactive oxygen species (ROS) in follicular and peritoneal fluids may explain a substantial number of these transcriptomic alterations, and cumulus-oophorus rinsing rapidly after follicular puncture may prevent them. Additionally, half of the causes of endometriosis can be attributed to genetic factors (Saha *et al.*, 2015), and polymorphisms may impact the expression of some oocyte transcripts, but this is unclear to date.

Polycystic ovary syndrome

A second reproductive disorder that has been comprehensively studied at the molecular level is PCOS. The frequency of PCOS is also high in the infertile population with great variability depending on ethnicity and world regions (5–20%) (Lizneva *et al.*, 2016; Wolf *et al.*, 2018). It is an endocrine and metabolic disorder characterized by hyperandrogenism, ovulatory dysfunction, and polycystic ovaries. Of concern, an altered endocrine microenvironment could alter the quality of the oocyte and compromise its ability to develop.

Single-cell RNA-seq and microarray studies in small cohorts of germinal vesicle (GV) and MII oocytes (n = 6, 11, and 3 PCOS versus n = 6, 9, and 6 controls) demonstrated that oocytes from patients with PCOS show transcriptomic abnormalities in genes related to meiosis (such as genes encoding microtubules) (Wood *et al.*, 2007; Liu *et al.*, 2016; Li *et al.*, 2021). In addition, a recurrent observation in PCOS oocyte studies is the perturbation of mitochondrial processes, which would cause impaired energy metabolism and oxidative phosphorylation (Qi *et al.*, 2020; Li *et al.*, 2021). The suggested mechanism in PCOS is that mitochondrial functions are prematurely activated at the GV stage instead of the MII stage, leading to the production of ROS with detrimental effects for oocyte competence (Qi *et al.*, 2020). Abnormal expression of 826 transposable elements was also reported in oocytes from women with PCOS (Li *et al.*, 2021). As the authors noticed, some of these elements may be involved in complex transcriptional regulation processes, negatively affecting the oocyte transcriptome, or could be biomarkers of aberrant expression of important genes for oocyte developmental competence, such as tubulin genes (Li *et al.*, 2021).

An adaptation of stimulation and maturation protocols (using mild controlled ovarian stimulation or medical IVM) may assist PCOS patients in obtaining oocytes with higher competence while also decreasing the risk of OHSS.

Women's age

Over the last few decades, maternal age at birth has significantly increased worldwide (Attali and Yogev, 2021) and now it is common for women to rely on ART after the age of 35. Advanced maternal age is associated with a higher proportion of poor-competence oocytes and difficulty in achieving a successful IVF outcome (Cimadomo *et al.*, 2018). Studies agree that the main biological processes involved in reproductive aging are cell cycle, mitosis and meiosis, oxidative stress, mitochondrial functions, and RNA metabolism (Steuerwald *et al.*, 2007; Grøndahl *et al.*, 2010; Reyes *et al.*, 2017; Zhang *et al.*, 2020b; Llonch *et al.*, 2021; Ntostis *et al.*, 2021; Yuan *et al.*, 2021) (Supplementary Table S1). Specifically, aging is associated with an increased production of ROS, a decrease in the expression of oxidation-protective genes, and a gradual alteration of mitochondrial activity (Llonch *et al.*, 2021). The completion of oocyte maturation is energy intensive, thus relying on a minimum level of mitochondrial activity to ensure basal energy production. Reduced ATP production and subsequent reduced protein metabolism could negatively affect oocyte maturation if the basal activity is not ensured (Schatten *et al.*, 2014).

Interestingly, GV and MII oocytes do not seem to be equally affected by maternal age revealing that maturation differentially mediates the transcriptomic effects of maternal aging. Llonch *et al.* (studying continuous changes from 18 to 43 years old), Ntostis *et al.* and Reyes *et al.* (studying <30 versus >40 years old) showed with scRNA-seq that MII oocytes display more age-related transcriptional abnormalities than oocytes at the GV stage (Reyes *et al.*, 2017; Llonch *et al.*, 2021; Ntostis *et al.*, 2021). There was not even a partial overlap between age-related DEGs at both stages, signifying that age-related modifications at the GV stage were not carried over to MII oocytes despite transcription being less active during the transition between stages. The deviation in gene expression occurring during maturation may be caused by elevated cellular stress as maternal age increases, and the lack of compensatory mechanisms in response to stress, with the transcriptional quiescence occurring at MII. A limitation to those conclusions is that the IVM used in the Llonch *et al.* and Reyes *et al.* studies, which could have engendered a confusion between IVM and age-related effects between GV and MII oocytes. Nevertheless, aging effects may preferentially occur within the time frame of oocyte maturation and protecting oocytes from oxidative stress during this period is crucial in women with advanced maternal age. Adapting ART protocols toward the use of antioxidant molecules during IVM might be beneficial for women aged over 35 (Liang *et al.*, 2017; Liu *et al.*, 2018; Cao *et al.*, 2020), and oxidative stress could also be limited by minimizing the exposure to *in vitro* environments, with short and soft processes. Counteracting the degradation of mitochondrial activity with age is also one of the reasons given for using mitochondrial transfer. While there may be research opportunities to improve IVM for these women and increase pregnancy rates, at present, oocyte vitrification might be a safer alternative for women who plan to delay childbearing.

Diminished ovarian reserve

DOR naturally occurs with maternal aging but is also found in a small proportion of women under 40 years old in cases of premature ovarian insufficiency and other infertility factors (Kaur and Arora, 2013; Chon *et al.*, 2021). A microarray study determined whether the quantity of antral follicles in the ovary could directly be related to the transcriptomic quality of oocytes (Barragán *et al.*, 2017) (Supplementary Table S1). For that purpose, four

groups of healthy fertile women were recruited, including women of young and advanced maternal age, with low (5–10) or high (20–35) antral follicle count, and their MII oocytes were collected from natural cycles. The authors determined that ovarian reserve levels are associated with particular non-coding RNA profiles (mainly long ncRNAs), which have key roles in transcription and regulation of development (Bouckenheimer *et al.*, 2016, 2018). In addition, the few mRNAs found dysregulated in relation to DOR were not related to any pathways. It is interesting that long ncRNAs are supposed to be involved in the pathological mechanisms leading to DOR because they directly regulate follicle development via the activation of different signaling cascades (Tu *et al.*, 2020; Dong *et al.*, 2022; Lv *et al.*, 2023). Unfortunately, the absence of annotation for a very large proportion of those ncRNAs restrict the analysis to a superficial interpretation and the functional importance of those specific ncRNA for the oocyte quality remains unknown.

However, there was limitation to this study lying in the absence of a description of the potential causes of DOR, notably for the young group. Definitively, more studies are needed to explore the oocyte transcriptome from DOR patients and to determine whether DOR due to maternal aging impacts the same biological pathways as DOR caused by other infertility factors.

Lifestyle and environmental exposure

Oocytes that have been exposed to multiple detrimental exposures over the lifecourse are even more susceptible to stress exposure induced *in vitro*. A current threat to oocyte quality is pollution and exposure to environmental contaminants such as drug residues in food and water, toxicants or chlorinated organic compounds (Foster *et al.*, 2008; Carré *et al.*, 2017). Unfortunately, the literature is sparse for human oocytes due to the difficulty in establishing comparative groups. Mouse exposed to particulate matter <2.5 µm during 12 weeks (8 h per day, 6 days per week) yielded a lower number of oocytes and with increased ROS compared with their counterparts exposed to filtered air (Guo *et al.*, 2021). This correlated with data at the transcriptomic level as the DEGs were mainly related to mitochondrial protein complexes. Differences were even assessed until the blastocyst stage, in which metabolism and metabolic regulation genes were dysregulated by particulate exposure, suggesting that increased oxidative stress may have potential long-term health consequences (Guo *et al.*, 2021). Other harmful substances such as persistent endocrine disruptors, nonylphenols, showed alterations in mitochondrial and apoptosis genes expression that may also be mediated by accumulation of ROS in mice (Xu *et al.*, 2020). Phthalates are also suspected to disrupt oocyte gene expression, according to a study in bovines (Kalo and Roth, 2017).

Along the same lines, some lifestyle habits are generators of oxidative stress. One study on mouse oocytes hypothesized that cytotoxic smoke constituents may be metabolized by the cytochrome P450 2E1, which in turn increases ROS production (Sobinoff *et al.*, 2013). This may consecutively trigger complex ovotoxicity mechanisms negatively influencing pathways involved in cancer, cellular development, cell death, inflammatory responses, and detoxification pathways (Sobinoff *et al.*, 2013; Mai *et al.*, 2014). In human, up-regulation of oxidative stress genes in GC and CC has been reported with smoking, confirming the oxidant–antioxidant imbalance generated by smoking observed in animals (Budani *et al.*, 2017; Konstantinidou *et al.*, 2021). Research should go further and evaluate daily cigarette consumption how many cycles after stopping smoking are required for significant improvements in oocyte competencies.

Additionally, increased BMI (>25 kg/m^2) as compared with normal BMI (18.5–24.9 kg/m^2) in GV, MI, and MII human oocytes is associated with an up-regulation of metabolic, inflammation and oxidative stress-related genes (Ruebel *et al.*, 2017). Modifications in the follicular fluid composition (insulin, leptin, triglyceride, C-reactive protein, cytokine, polyunsaturated fatty acids concentrations) might create a pro-inflammatory, oxidant, and altered metabolic environment which has repercussions on the follicle. However, the cohort in this study comprised patients undergoing IVF treatment for a multitude of infertility factors including endometriosis and ovulatory disorders, which may weaken some results (Ruebel *et al.*, 2017).

It is likely that many other lifestyle factors and environmental exposures have detrimental effects (Varghese *et al.*, 2011). Alcohol consumption is associated with reduced quantities of oocytes collected in IVF cycles, reduced fertilization rates, reduced live birth rates, and increased pregnancy loss (Firns *et al.*, 2015), and also with oocyte dimorphisms (dark cytoplasm, fragmented polar body, zona pellucida hardening) (Setti *et al.*, 2022). Those dimorphisms may also be negatively influenced by refined sugar consumption but ameliorated by consumption of vegetables, highlighting nutritional habits as an important parameter in oocyte quality (Setti *et al.*, 2022).

Remaining to be studied are the effects at the transcriptomic level, and the constitution of human cohorts to study the effects of disruptive environmental factors, such as particulate matter, is important. Moreover, the studies have often been performed on young individuals, and age is a cumulative risk factor for all these lifestyle factors and exposures, potentially augmenting their individual effects. It is thus important to adopt a healthy lifestyle in the context of an IVF attempt.

As the proceeding sections outlined, before attempting an IVF cycle, the oocyte may have been exposed to multiple exposures which are potentially harmful to its transcriptomic integrity. Furthermore, specific ART interventions involving gene expression modifications can exacerbate or superimpose on these pre-existing alterations. The following sections discuss the interactions between the transcriptome of the oocyte or its surrounding cells with current ART practices.

Ovarian stimulation

Ovarian stimulation is a conventional step in IVF protocols, with the aim of artificially triggering maturation and ovulation to obtain a high number of oocytes and increase the chances of a successful live birth per attempt. This process may be damaging to oocyte quality because of the forced growth and maturation of some antral follicles.

Due to obvious ethical considerations, the transcriptomic effects of ovarian stimulation directly on mature human oocytes have never been investigated. Nevertheless, studies on cumulus cells and MGCs provide a non-invasive indication of the influence of ovarian stimulation on oocyte transcriptomic patterns. Both cell types originate from undifferentiated granulosa cells that divides into two cell lineages. CC constitute the layers of cells in contact with the oocyte while MGC delineate the follicle (Uyar *et al.*, 2013). Bidirectional communication is established between an oocyte and its surrounding cells and this has led investigators to consider MGC and CC as indirect markers of oocyte quality (Uyar *et al.*, 2013; Dumesic *et al.*, 2015).

Ovarian stimulation protocols

Effects of hormonal protocols used to inhibit a premature rise in luteinizing hormone

Ovarian stimulation is practiced with gonadotropins in combination with gonadotropin releasing hormone agonists (GnRH-a) or antagonists (GnRH-anta). Their role is to put the pituitary gland at rest and thus block the risk of spontaneous ovulation by preventing the risk of an LH surge. From a gene expression perspective, Devjak *et al.* (2012) demonstrated with microarrays that the use of GnRH-a or GnRH-anta does not result in transcriptomic divergence in CC of MI (metaphase I) and MII oocytes. This supports the observation that both treatments are clinically and molecularly equally effective (Al-Inany *et al.*, 2016).

Effects of gonadotropin stimulation protocols

Each fertility clinic relies on their own gonadotropin stimulation protocols, which are adapted to ensure for heterogeneous groups of patients the best chance of retrieving a relatively good number of mature oocytes, as expected for their age and ovarian reserve. Studies on CC and MGC suggest that different hormone treatments used for stimulation do not result in similar gene expression profiles in patients with similar characteristics (ART prescribed for male factor or tubal disease or unexplained infertility, <35 years old, normal BMI) (Supplementary Table S2). We identified nine studies assessing gene expression profiles at both candidate genes (with RT-PCR) and with the whole transcriptome level (using different versions of microarrays). Six of the studies were interested in comparing recombinant FSH (rFSH) stimulation versus highly purified hMG (HP-hMG, human menopausal gonadotropin) and all reported differentially expressed genes in both MGC and CC (Grøndahl *et al.*, 2009; Adriaenssens *et al.*, 2010; Brannian *et al.*, 2010; Assou *et al.*, 2013; Gatta *et al.*, 2013; Cruz *et al.*, 2017).

rFSH versus HP-hMGH

Concerning CC analyses, investigations showed little consensus in either the number of differentially expressed genes between rFSH and HP-hMG regimens and the biological significance of the pathways retrieved disturbed in four different studies (Adriaenssens *et al.*, 2010; Assou *et al.*, 2013; Gatta *et al.*, 2013; Cruz *et al.*, 2017) (Supplementary Table S2). This might stem from heterogeneities in methodology and the populations analyzed including either oocyte donors or patients with unexplained infertility (Supplementary Table S2). However, Assou *et al.* (2013) and Gatta *et al.* (2013) found DEGs in identical molecular pathways, related to cell-to-cell interactions, lipid metabolism and cellular assembly and organization, while Gatta *et al.* (2013) and Cruz *et al.* (2017) found DEGs related to system development. Lipid metabolism represents the principal energy source for resuming oocyte maturation (Khan *et al.*, 2021) and defective cell-cell interactions of an oocyte and its surrounding CC might break a cascade of essential hormonal and metabolic signals (Russell and Robker, 2007; Li and Albertini, 2013). Our cross-over of DEGs between studies revealed common genes up- or down-regulated following HP-hMG stimulation compared with rFSH when studies were compared one by one (Fig. 1A and B): *COL1A1*, *DKFZp451A211*, *ENDOD1*, *GAL*, *HS3ST1*, *MT3*, *NFIB*, *NPY1R*, *OSBPL6*, *WNT3A*. Notably, up-regulation of *NPY1R* in CC was associated with good embryo quality at day-3; NPY receptors are implicated in the modulation of steroid production (Assou *et al.*, 2013). In the same study, *OSBPL6* up-regulation in CC was associated with higher blastocyst grading and is a modulator of cholesterol synthesis (Assou *et al.*, 2013). The nuclear factor I B (*NFIB*) expression in CC was also associated with the oocyte capacity to generate embryos capable of implanting and may play a role in embryogenesis and organ development (Steele-Perkins *et al.*, 2005; Assou *et al.*, 2008). In bovine CC, *COL1A1*, a sub-unit of type I collagen and component of the extracellular matrix may regulate several important biological pathways such as ovarian cell cycle, proliferation or apoptosis (Fu *et al.*, 2019). Taking the comparisons together, there is evidence that rFSH and HP-hMG stimulations do not mobilize similar CC metabolic pathways.

The main difference between rFSH and HP-hMG stimulation was the absence of exogenous LH activity when rFSH was administered alone and surprisingly, there were no differences in the expression of LH/hCG receptor in the three microarray studies in CC. This suggests that despite activating different molecular mechanisms that mobilize distinct intracellular pathways, both treatments have nonetheless a similar potency to induce hormonal receptors. However, the results still must be interpreted with caution owing to the limited sample size in the two studies (Supplementary Table S2) (Gatta *et al.*, 2013; Cruz *et al.*, 2017).

In parallel, in MGC, although Grøndahl *et al.* (2009) found only 85 DEGs and Brannian *et al.* (2010) 20 times more but with a small sample size (n = 4 per group), the main observations pointed to the perturbation of metabolic processes (lipid metabolism, protein phosphorylation, cholesterol and steroid synthesis). Genes found to be down-regulated with HP-hMG common to both studies included *ATP2C1*, *EPHA4*, *FGG*, *HMGCS1*, *RNGTT*, and *TFRC* (Fig. 1C and D). *HMGCS1* is notably required for cholesterol biosynthesis but contrary to the results of CC studies, the gene *LHCGR* encoding the LH/hCG receptor was down-regulated with HP-hMG in Grøndahl *et al.* (2009), which could explain the shutdown of the cholesterol de novo synthesis pathway.

Recombinant LH supplementation

In a small study on three markers of developmental competence (*HAS2*, *GREM1*, and *PTGS2*), recombinant LH (rLH) supplementation during the rFSH stimulation protocol suggested a positive effect on oocyte maturation manifested by the up-regulation of *HAS2* and *PTGS2* with rLH in CC, as assessed via RT-PCR (Barberi *et al.*, 2012). In a larger study using microarrays, rLH supplementation was associated with a differential expression of 496 genes (Gatta *et al.*, 2013), but the results were not discussed and the expression of *HAS2* and *PTGS2* was similar between the rLH + rFSH and rFSH groups.

Origin of FSH

Two studies have investigated different origins of FSH stimulation, but the results have not yet been replicated to date (Gurgan *et al.*, 2014; Cruz *et al.*, 2017). In CC, stimulation with either rFSH or human-derived FSH alone versus rFSH + FSH together showed variable responses on gene expression, notably on genes related to cholesterol metabolism, cell growth and proliferation, cell morphology and death, cell adhesion and differentiation, as well as protein synthesis (Gurgan *et al.*, 2014). A limitation in this study is the absence of the description of the population analyzed and underlying infertility causes that is important regarding the response to treatment (Supplementary Table S2). Urinary FSH was also compared with rFSH and HP-hMG in CC from healthy oocyte donors (Cruz *et al.*, 2017). Unsurprisingly, urinary FSH and rFSH stimulation had similar effects on the transcriptome with only 44 DEGs and without enrichment in any biological process. Three times more DEGs were found between urinary FSH and

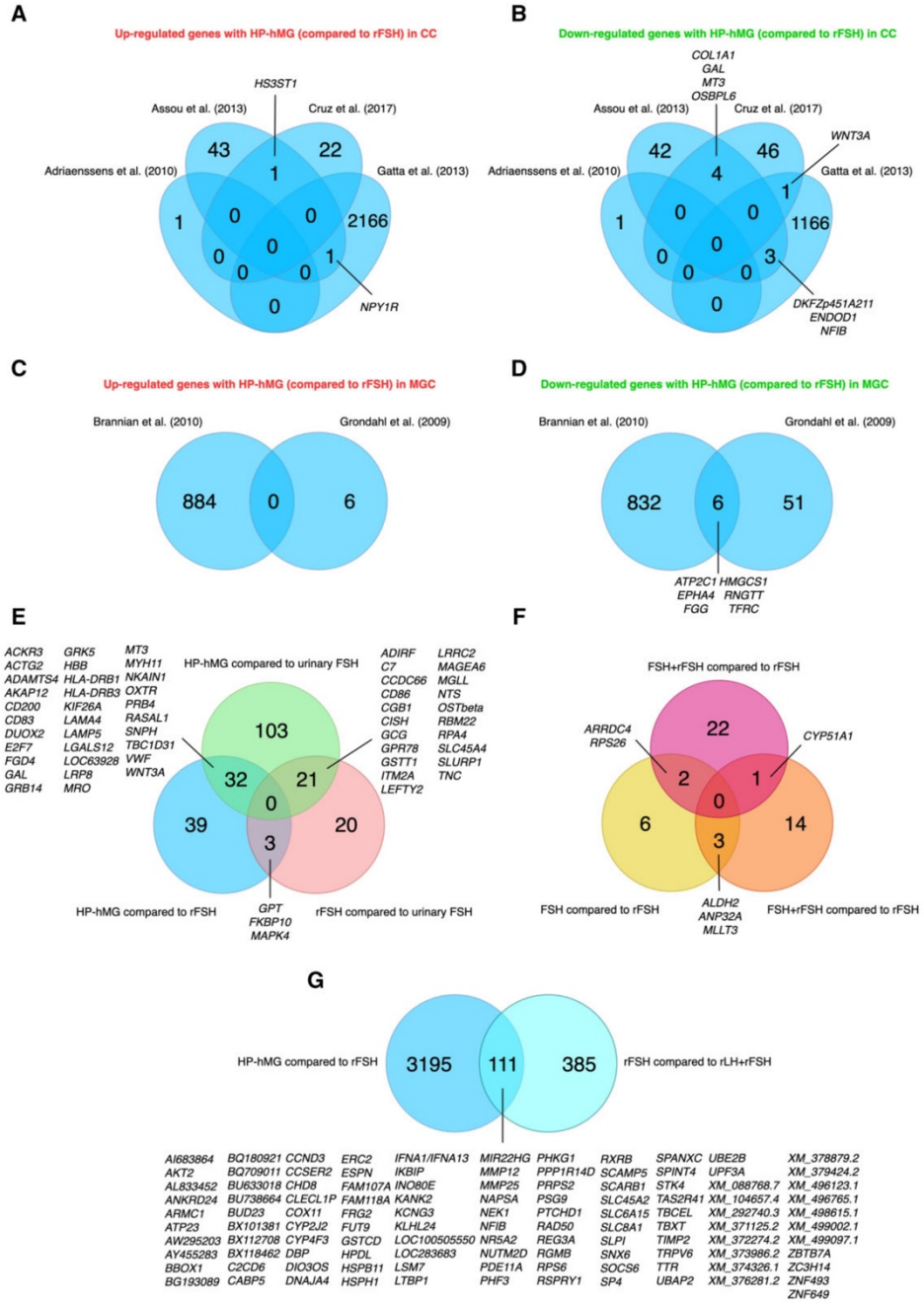

Figure 1. Differentially expressed genes between studies comparing different types of gonadotropin stimulation protocols. (**A**) Genes up-regulated with HP-hMG in CC as compared to rFSH. (**B**) Genes down-regulated with HP-hMG in CC as compared to rFSH. (**C**) Genes up-regulated with HP-hMG in MGC as compared to rFSH. (**D**) Genes down-regulated with HP-hMG in MGC as compared to rFSH. (**E**) Overlap of genes differentially expressed between stimulation protocols in Cruz *et al.* HP-hMG, urinary FSH and rFSH compared. (**F**) Overlap of genes differentially expressed between stimulation protocols in Gatta *et al.* (FSH, rFSH, and FSH + rFSH compared). (**G**) Overlap of genes differentially expressed between stimulation protocols in Gurgan *et al.* (HP-hMG, rFSH, and rLH + rFSH compared). CC: cumulus cells; HP-hMG: highly purified human menopausal gonadotrophin; MGC: mural granulosa cells; rFSH: recombinant follicle stimulating hormone.

HP-hMG, related to metabolic processes, which corroborates previous observations on the various effects of HP-hMG and FSH isoforms on metabolic activity.

Differences in induced regulation from the different FSH isoforms may stem from their different glycosylation profiles, which play an essential role in FSH pharmacokinetics, metabolic

stability, and receptor signaling (Ulloa-Aguirre *et al.*, 1999; Gurgan *et al.*, 2014). For example, human urinary FSH is more sialylated than rFSH, thus more acidic (Andersen *et al.*, 2004). It has been shown that less acidic isoforms have a higher half-life and potency in estrogen stimulation, which may result in different oocyte biological activity (Timossi *et al.*, 2000). Recently, a new FSH analog with an increased half-life (corifollitropin alfa) has entered the clinic (Anderson *et al.*, 2018). Now, transcriptomic comparisons have to be performed with other FSH isoforms.

In the end, studies comparing more than three different regimens support the observation that proximal treatments of different origins have variable effects on the transcriptome, which is manifested by the low number of overlaps between DEGs (Gatta *et al.*, 2013; Gurgan *et al.*, 2014; Cruz *et al.*, 2017) (Fig. 1E–G).

Dose effects

A recent study investigated the benefits of a mild ovarian stimulation protocol compared with the conventional ovarian stimulation in CC from poor ovarian responders with advanced maternal age (Liu *et al.*, 2022). The main difference between the two protocols was the daily gonadotropin dose administered to patients, which was closer to the physiological environment in mild treatments. The RNA-seq analysis revealed 425 DEGs (192 up-regulated and 233 down-regulated with mild stimulation) which were mainly involved in cytokine activities, regulation activities, immune responses, oocyte development, cytokine–cytokine receptor interactions, the TGF-β signaling pathway, the cGMP-PKG signaling pathway, and metabolic pathways. The authors concluded that the mild protocol is beneficial for poor responders because they further demonstrated, via western blot and hormone assays, the importance of the up-regulation of the TGF-β signaling pathway in this group for the cross-talk between MGC and oocyte and embryo quality.

Ovulation triggering protocol

Following ovarian stimulation, ovulation induction is artificially triggered. This ovulatory surge is the crucial step in oocyte meiosis and maturation, as well as in maturation of its supporting cells. Various effective triggering methods are commonly used, including hCG (classically recombinant) or GnRH-a administration or the combination of both. As assessed with microarrays, genes related to steroidogenesis were up-regulated with GnRH-a compared with hCG in CC and notably the expression of the *LHCGR* gene was up-regulated, which may promote progesterone production and facilitate implantation (Borgbo *et al.*, 2013). In contrast, Haas *et al.* (2014), still studying CC but by using RT-qPCR, reported lower expression of genes related to steroidogenesis (*CYP19A1*, *CYP11A1*, *HSD3B1*) with a GnRH-a trigger and no difference in *LHR* expression (Fig. 2A and B, Supplementary Table S2). Again, discrepancies in the results might stem from variability in the populations analyzed, notably the inclusion or exclusion of endometriosis patients who may have a particular local intrafollicular environment (presence of ROS, high estrogen, and progesterone levels) (Sanchez *et al.*, 2017). In MGC, the principal findings suggest that GnRH-a might reduce the risk of developing OHSS by down-regulating the angiogenesis pathway (Borgbo *et al.*, 2013). Interestingly, these observations were partially confirmed by a study in MGC from OHSS patients with RT-qPCR on *VEGF* (a central vasoactive factor) whose expression was lowered with the use of GnRH-a compared with hCG (Haas *et al.*, 2014). In addition, high or low doses of GnRH showed similar effects on three regulator genes of oocyte maturation, *HSD3B1*, *LHCGR*, and *IHNBA* expression in both CC and MGC of healthy oocyte donors (Vuong *et al.*, 2017).

By using RNA-seq to compare hCG single versus double (hCG + GnRH-a) regimens in CC from poor and normal responders to stimulation, dual triggering showed up-regulation of pathways such as oocyte maturation, cell cycle, and apoptosis (Fuchs Weizman *et al.*, 2019). However, the few similarities in the genes disturbed by the triggering method in both responder groups (Fig. 2C and D, Supplementary Table S2) revealed that patients' characteristics, such as advanced maternal age (>40 years old) or low levels of anti-Müllerian hormone resulting in poor ovarian response to stimulation, are associated with variable effects of the triggering method compared with a cohort of normal responders. In MGC, comparison of the hCG single trigger versus the double trigger showed *AREG*, *EREG*, and *SERPINF1* up-regulation and *GJA1* down-regulation with the double trigger, which was not observed in the Fuchs Weizman *et al.* study on CC (Haas *et al.*, 2016; Fuchs Weizman *et al.*, 2019) (Fig. 2C and D). Higher levels of amphiregulin (AREG) and epiregulin (ERG) may be associated with improved oocyte maturation, while higher levels of PEDF (SERPINF1), which has anti-angiogenic actions, may reduce the risk of OHSS.

Collectively, despite the inter-patient and inter-cell type heterogeneity of pathway responses to the triggers, these results still highlight the benefit of using a dual trigger to promote oocyte developmental competence while preserving patients from the detrimental effects of a single hCG trigger (Haas *et al.*, 2016). Nonetheless, GnRH-a still has apoptotic effects, notably on GC, which could induce premature demise of the corpus luteum (Gonen *et al.*, 2021).

Ovarian stimulation effects compared with natural cycles

Different ovarian stimulation regimens shape the oocyte transcriptome but with differences that may remain limited when one is compared with another. However, recourse to ovarian stimulation itself may substantially affect oocyte gene expression compared with natural cycles and could give hints as to why oocytes have lower developmental competence after ovarian stimulation (Blondin *et al.*, 1996; Lee *et al.*, 2017). A study on CC from oocyte donors showed a mild effect of ovarian stimulation on the transcriptome using microarray (18 DEGs related to immune processes, meiosis and ovulation) but even in the natural cycles, recombinant hCG was administered to trigger ovulation which could have hidden ovulation induction effects (de los Santos *et al.*, 2012). In contrast, Papler *et al.* (2014) reported that in CC from natural cycles and ovarian stimulation, 66 DEGs were revealed by microarray, mainly related to RNA degradation and transport, ribosomes, metabolism and oxidation-reduction processes. Finally, Lu *et al.* (2019), this time analyzing MGC by using RNA-seq, identified 1002 DEGs, enriched for genes related to immune processes for those up-regulated, and genes related to cell cycle, meiosis, steroidogenesis, and oocyte maturation for those down-regulated with ovarian stimulation. Cross-over between up- and down-regulated genes in those three studies showed limited overlap, as only *GSTA1*, *GSTA2*, and *CTSV* were found to have similar effects associated with ovarian stimulation in at least two studies (Fig. 3A and B). *GSTA1* and *GSTA2* down-regulation might be a manifestation of lower steroidogenesis with ovarian stimulation, as demonstrated in bovine MGC (Rabahi *et al.*, 1999). The low sample size in all these studies and the lack of replication remain a serious limit in assessing the transcriptomic effects of ovarian stimulation and results should be taken with caution (Supplementary Table S2).

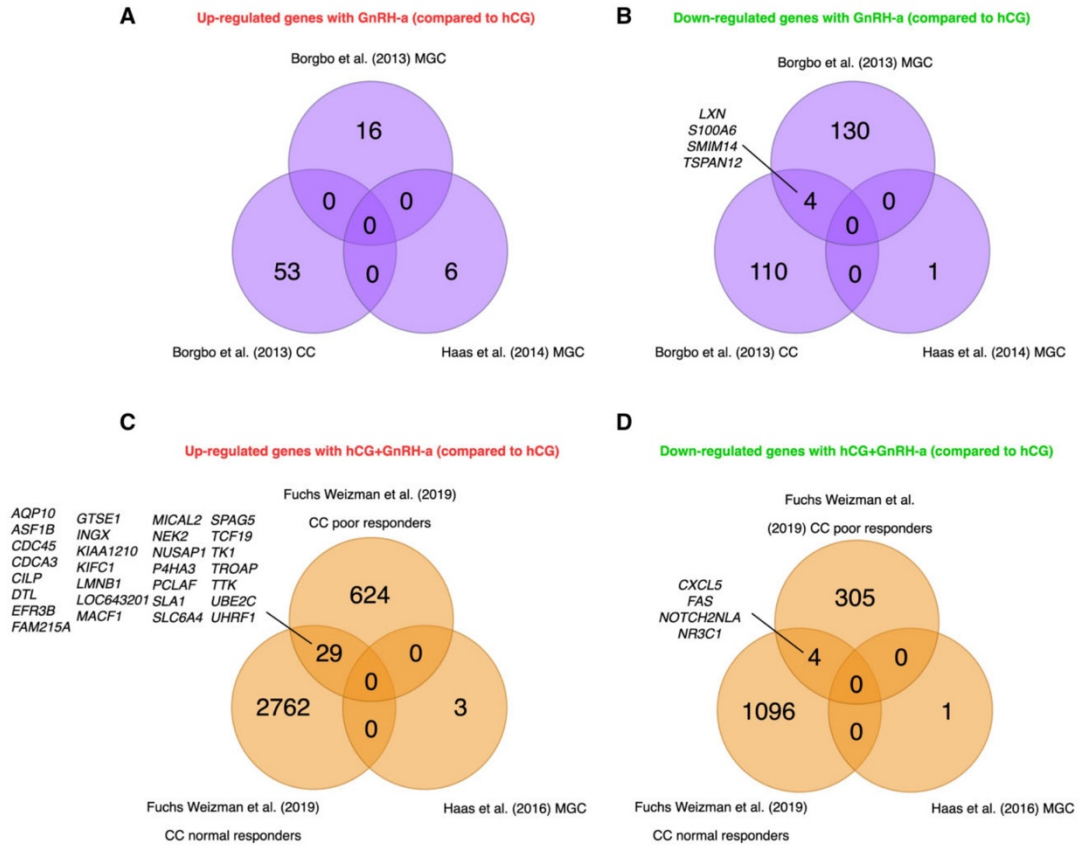

Figure 2. Differentially expressed genes between studies comparing different types of ovulation triggering protocols (GnRH-agonist trigger, hCG, and dual trigger). (A) Genes up-regulated with GnRH-a as compared to hCG. (**B**) Genes down-regulated with GnRH-a as compared to hCG. (**C**) Genes up-regulated with hCG + GnRH-a as compared to hCG. (**D**) Genes down-regulated with hCG + GnRH-a as compared to hCG. GNRH-a: gonadotrophin releasing hormone agonist; hCG: human chorionic gonadotrophin.

Overall, it remains unknown whether modifications in CC and MGC may reflect oocyte integrity, even if there is a close interaction between these cell types. Evidence of alterations in gene expression in ovarian stimulation protocols in the oocyte is only available from mouse and farm animals. The expression of some maternal effect genes, which could be considered molecular markers of oocyte quality, has been investigated in mouse oocytes following superovulation by RT-qPCR (Jahanbakhsh-Asl *et al.*, 2018). The expression of *BMP15*, *HDGF*, *DNMT1*, *DPPA3*, and *ZFP53* was significantly reduced in superovulated oocytes compared with naturally ovulated oocytes. The three latter genes are involved in epigenetic reprogramming, which could explain the presence of methylation errors in superovulated oocytes (Market-Velker *et al.*, 2010). *BMP15*, along with two others preferentially expressed growth factors in oocytes (*GDF9*, *FGF8*), showed no difference in FSH stimulated mouse oocytes compared with those produced *in vivo* (Sánchez *et al.*, 2010). However, the increase in FSH dose resulted in significant up-regulation of *BMP15*, *GDF9*, and *FGF8*. A recent study compared, at the same time, the transcriptome and proteome of superovulated mouse oocytes with their counterparts *in vivo* (Taher *et al.*, 2021). The transcriptomes were very similar in contrast to the proteomes, and the results indicated that superovulation does not cause direct harmful effects on oocytes but rather it produces oocytes that have not reached complete cytoplasmic maturity.

In conclusion, the lack of studies directly on oocytes in humans is a notable barrier in our understanding of how ovarian stimulation could affect oocyte quality at the molecular level. A striking aspect of the studies is the almost complete absence of genes commonly dysregulated under the same conditions. This may stem from the various technologies used (different arrays versus RNA-seq), the low sample size which may over-estimate the magnitude of an association between gene expression and a specific condition, the heterogeneity between the clinical characteristics of patients, and the CC and MGC heterogeneity in response to treatment in the same patient, which is unknown. Evidence from CC and MGC and studies in small and large animal models suggest there are no drastic transcriptomic damages, but oocytes produced via ovarian stimulation appear not to have achieved complete cytoplasmic maturation compared with their naturally produced counterparts. A fundamental step forward in the field would be to assess if there is a heterogeneous response of sibling CC/MGC and sibling oocytes (i.e. from the same follicle and patient) following an identical ovarian stimulation treatment. Some ovarian stimulation protocols might be a risk for patients by increasing the risk of developing OHSS and therefore

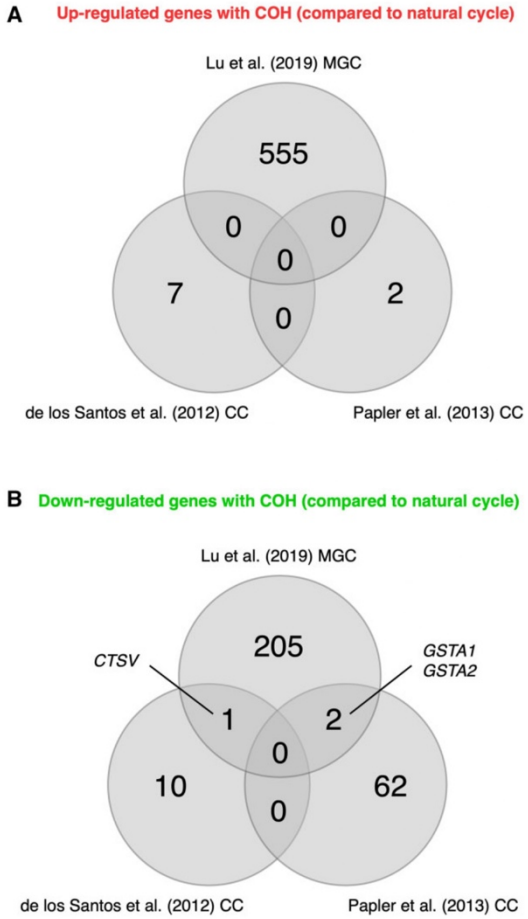

Figure 3. Differentially expressed genes between studies comparing ovarian stimulation and natural cycles. Natural cycles were set as the reference group. (**A**) Genes up-regulated with COH as compared to natural cycles. (**B**) Genes down-regulated with COH as compared to natural cycles. COH: (controlled) ovarian stimulation.

moving toward mild ovarian stimulation and dual trigger is beneficial. For most patients (male factor or tubal disease infertility, <35 years old, normal BMI), the standard protocols used for decades are well adapted, but approaches to reduce unpleasant treatment experiences with the use of dual trigger and doses closer to physiological environment could become more widely used. A main limit to the scientific evidence regarding transcriptomic effects of ovarian stimulation is the low number of studies on specific populations, including those with PCOS, poor ovarian responders, or aged patients, who display a hormonal profile suboptimal for the effectiveness of standard protocols. In the era of personalized medicine, individualized ovarian stimulation will soon be preferred above standard protocols (la Marca and Sunkara, 2014).

In vitro conditions

IVM of oocytes

Medical IVM is defined as the maturation of oocytes (most often as cumulus–oocyte complexes) collected from small and intermediate antral follicles (generally diameter <13 mm) to MII *in vitro* using an appropriate IVM medium (Dahan *et al.*, 2016). It must be differentiated from rescue IVM (rIVM), which is performed on GV-stage oocytes denuded of their CC and collected from ovarian stimulation cycles and thus not a common procedure (de Vos *et al.*, 2016). Medical IVM is an effective method for women with resistant ovary syndrome and for reducing the risk of developing OHSS; it can also be used for oncological patients to preserve fertility over time before a cryopreservation step (Shalom-Paz *et al.*, 2012; Virant-Klun *et al.* 2022).

Problematically, there is a high heterogeneity among fertility clinics in the techniques used to perform IVM/rIVM (e.g. standard or biphasic IVM, follicular priming methods, choice of the culture medium and supplementations, time of culture (Yang *et al.*, 2021)) that may contribute to their high variability in clinical outcomes (Dahan *et al.*, 2016). Additionally, IVM/rIVM is affected by reports depicting poor oocyte developmental competence and multiple other clinical outcomes despite decades of research (Hatırnaz *et al.*, 2018; Krisher, 2022). Oocyte transcriptomic analysis appears to be crucial to unravel the molecular cause behind the altered oocyte competencies.

The first study on the transcriptomic effects of rIVM compared with *in vivo* maturation on pools of human oocytes revealed, on the one hand, up-regulation of genes related to signal

transduction and metabolism (nucleic acids, tRNA, lipids, steroids) and, on the other hand, down-regulation of genes involved in protein biosynthesis, translational regulation, cell cycle, and homeostasis (Wells and Patrizio, 2008). Although the differences remained mild and MII oocytes produced via rIVM had an expression pattern highly similar to the *in vivo* matured oocytes, this study suggested that their expression pattern displayed vestiges of the GV stage, which could explain the greater difficulties in producing successful pregnancies following rIVM. Additionally, other studies on pooled oocytes have established that rIVM alters the regulation of transcription, cell cycle, transport, cellular metabolism, respiratory process, epigenetics, and embryogenesis (Jones *et al.*, 2008; Virant-Klun *et al.*, 2013) (Supplementary Table S3). The high number of DEGs identified in those studies could be indicative of failure in the correct post-transcriptional regulatory events during nuclear maturation, such as poly- or de-adenylation, and thus explains the low developmental competence of rIVM oocytes that still resemble GV oocytes (Jones *et al.*, 2008).

More recently, next-generation sequencing has brought a finer resolution of transcriptomic changes related to IVM and rIVM in oocytes. The high number of DEGs retrieved in four studies between *in vitro* and *in vivo* maturation confirmed previous observations (Zhao *et al.*, 2019; Ye *et al.*, 2020; Lee *et al.*, 2021; Yang *et al.*, 2022) (Supplementary Table S3). In rIVM oocytes, Zhao *et al.* (2019) identified key genes related to metabolism that turned out to be kinases and enzymes related to CoA production. All are key regulators of oocyte maturation as kinases are necessary for completing the meiosis cycle and CoA is critical in the regulation of substrate production in the Krebs cycle, and down-regulation of CoA-related enzymes observed with IVM would cause a decline in energy metabolism leading to deficient maturation (Palmer *et al.*, 1998; Downs *et al.*, 2009). DEGs associated with rIVM in the Lee *et al.* study (Lee *et al.*, 2021) were over-represented for genes participating in metabolic processes, biosynthesis and oxidative phosphorylation. The *GATA-1/CREB1/WNT* signaling pathway was particularly down-regulated with rIVM, promoting apoptosis and decreasing the chance of correct cytoplasmic maturation. Corroborating the observations from rIVM, DEGs identified by scRNA-seq in Ye *et al.* (2020) with IVM in a population of healthy volunteers undergoing caesarean delivery were related to cell cycle, mRNA metabolism, mitochondrial respiration biogenesis and ATP metabolism notably. In Yang *et al.*, using oocytes collected from pregnant women undergoing caesarean delivery (Yang *et al.*, 2022), among the 2281 DEGs identified from IVM oocytes, 160 were mitochondria related genes and were involved in oxidative phosphorylation, amino acid and carbon metabolism, and fatty acid degradation. DEGs were also enriched in mitochondrial respiration processes, cellular structure, metabolic process, NADH dehydrogenase activity and ribosomal activity. This might highlight compensatory mitochondrial mechanisms activated by the oocyte to adjust for the energy needed to complete cytoplasmic maturation. These results could not be extrapolated to patients needing medical IVM (e.g. PCOS patients).

Transcriptomic effects of rIVM have also been assessed in patients with PCOS, who are most likely to benefit from this treatment, but only in CC. Corroborating previous observations, >5000 DEGs have been identified in CC from patients with PCOS and involve the down-regulation of oocyte maturation and cumulus expansion-related genes with rescue IVM (Ouandaogo *et al.*, 2012).

Overall, due to the inability to access complete data for most studies on *in vitro* oocyte maturation, analysis of DEGs common to multiple studies was not pertinent. From a methodological standpoint, most studies did not provide sufficient clinical information on the patients included, and the quality of the evidence for the results presented could be questioned, particularly for medical IVM (Supplementary Table S3). To gain insight on how IVM/rIVM has different effects regarding the population studied, information on maternal age and causes of infertility must be clearly presented. However, a clear message emanating from all studies is the perturbation of processes related to the mitochondrion, oxidative phosphorylation and metabolism. Incomplete cytoplasmic maturation might be explained by these deficient energy processes. Improvement of energy availability for the oocyte could be a lever of development for the future of IVM culture conditions (Katz-Jaffe *et al.*, 2009; Gao *et al.*, 2017; Zhang *et al.*, 2021). Refinement of the culture medium composition is also a promising field of research. Notably, co-culture of immature oocytes with CC of mature oocytes from the same patient led to a transcriptomic profile with reduced divergence compared with the differences observed between classic IVM and *in vivo* matured oocytes (Virant-Klun *et al.*, 2018). Addition of growth hormone in the IVM media was associated with the up-regulation of *AURKA*, *CENPE*, *PDIA6*, *LINGO2*, and *CENPJ*, which probably contribute to accelerating meiotic progression, balancing redox homeostasis, and thus promoting oocyte maturation (Li *et al.*, 2019). Protection of oocytes against oxidative stress during IVM with antioxidant supplementation offers a new perspective in improving IVM efficiency (Cao *et al.*, 2020; Sallem *et al.*, 2022).

Oxygen tension

A key component in *in vitro* steps that is largely overlooked in human is oxygen tension. Depending on the species in mammals, it is estimated that the physiological intrauterine and intratubal oxygen tension *in vivo* varies between 2% and 8%, with levels that decrease as a follicle develops. Current practices in IVF laboratories are either performed at 5% O_2 or 20% O_2 but, transiently, follicles and oocytes extracted from the genital tract could be exposed to variable oxygen concentrations (Christianson *et al.*, 2014). Clinical outcomes comparing low (5%) and high (20%) oxygen tension effects indicated no positive effects in a high O_2 environment (Eppig and Wigglesworth, 1995; Kasterstein *et al.*, 2013; Lim *et al.*, 2021). It is known that O_2 increases the production of ROS and could have cytotoxic effects and activate stress pathways. Oocytes would adapt in response to different oxygen environments, notably through genes regulated by the hypoxia-inducible factor (HIF) (Lim *et al.*, 2021).

Whether the transcriptional content of oocytes is altered depending on physiological or ambient oxygen tension is currently unknown in human. In mice, using RNA-seq on pools of primary oocytes cultured to the GV phase for 9 days under 5% O_2 or 14 days under 20% O_2, ontologies corresponding to female gamete genes and chromatin organization tended to be up-regulated with 20% O_2, whereas stress response genes were up-regulated with 5% O_2 (Naillat *et al.*, 2021). In another mouse study, this time using scRNA-seq, oocytes from secondary follicles cultured to GV for 12 days under 20% O_2 versus 7% O_2 were compared (Takashima *et al.*, 2021). Oocytes grown in 20% O_2 showed up-regulation of genes related to apoptosis and the sphingolipid signaling pathway, including ceramide metabolism. The authors concluded that mitochondrial dysfunction and impaired developmental abilities were associated with ambient oxygen tension as compared to *in vivo* conditions, whereas the *in vivo* and 7% O_2 environments resulted in oocytes highly similar in their transcriptomic profiles. Studies in a large animal model,

yak oocytes matured under 5% or 20% O_2 revealed, for the hypoxia group, up-regulation of genes involved in the cell cycle (ERK1 and ERK2 cascade, PI3K-Akt signaling) and maturation with a decrease in the expression of genes involved in oxidative phosphorylation; the authors concluded that there was an improved quality of oocytes grown under hypoxic conditions (Li et al., 2020).

In conclusion, three studies with different animal models showed contradictory results on whether hypoxia or normoxia is beneficial at the transcriptomic scale. The studies suggest the need to further assess to what extent non-physiological gas conditions disturb key oocyte biological processes in humans.

Temperature

IVM is rigorously performed at 37°C but the temperature could transiently vary during oocyte transfer from collection to the IVF laboratory and then during the further oocyte manipulations (e.g. during oocyte denudation and fertilization). After oocyte collection, it is important to minimize the time for CC removal and manipulations because dishes are also prone to temperature decreases, with the risk of slightly modifying pH conditions of the buffered media and generating ROS (Agarwal et al., 2022). IVM performed under large temperature differences (38.5°C versus 41°C) does not alter the expression of major heat shock proteins and oocyte quality markers in bovine (*BMP15*, *GDF9*) but the overall effect of temperature on the whole transcriptome remains to be evaluated (Payton et al., 2011; Roth, 2018).

Pollutants

While maternal exposure to pollutants can affect the oocyte, additional pollution specific to the laboratory environment is directly in close contact with the oocyte. It involves plastic consumables such as tips for oocyte holding and denudation, tubes or plastic dishes for collection, maturation, fertilization and cryopreservation, as the worrying presence of bisphenol A, S, and AF was measured in those consumables from different brands, even if they do not leach into ART media (Togola et al., 2021). Contrary to *in vivo* conditions, there is no glucuronidation in IVM and bisphenols cannot be turned into their inactive form (Togola et al., 2021). Gene expression changes with exposure to bisphenol A in double-strand break signaling and repair related genes has been observed with RT-qPCR in human fetal oocytes (Brieño-Enríquez et al., 2012). In mouse oocytes, IVM under supraphysiological concentrations of bisphenol A showed alterations in gene expression of major genes involved in cell cycle, hormone signaling, and translational regulation (Ferris et al., 2016). In addition, there could be a synergetic or additive effect of different pollutants on oocyte transcriptome, and the careful assessment of all sources of pollution and their uncontrolled effects on the transcriptome of gametes is necessary.

Cryopreservation and storage time

Cryopreservation was first introduced in the 1980s with the slow freezing method but has been gradually replaced by vitrification among IVF clinics, an ultrarapid freezing and cost-effective technique. For ethical and clinical reasons, there is a growing use of cryopreservation with respect to delayed childbearing, maternal aging, donation programs, and cryopreservation before gonadotoxic therapy (Cobo et al., 2021).

A recurrent observation is the overall decrease in total mRNA content following slow freezing (Chamayou et al., 2011; Monzo et al., 2011; Stigliani et al., 2015) and vitrification (Huo et al., 2021) as compared with fresh human oocytes. Maternal mRNAs drive early embryo development until the maternal-to-zygotic transition and sufficient maternal mRNAs should be stored in the oocyte beforehand (Flach et al., 1982; Dworkin and Dworkin-Rastl, 1990; Sirard et al., 2006). Additionally, it is likely that major pathways including DNA structural organization, chromosomal structure maintenance and organization, cell cycle processes, response to DNA damage stimuli, and cellular response to stress and DNA repair are altered by the slow freezing method according to two microarray and one RT-PCR studies on pools of oocytes (Chamayou et al., 2011; Monzo et al., 2011; Stigliani et al., 2015) (Supplementary Table S4). Vitrification and slow freezing do not have the same influence compared with fresh oocyte, and genes modified by both techniques are partially different. The study by Monzo et al., using microarrays (Monzo et al., 2011), showed that only 88 DEGs were common to both techniques, among respectively 389 and 608 DEGs identified for slow-frozen and vitrified MII unfertilized oocytes. Slowly frozen oocytes showed down-regulation of genes associated with DNA repair, transcriptional regulation in response to DNA damage, cell cycle regulation and maintenance of chromosome stability, which were absent when comparing vitrified to fresh oocytes (Monzo et al., 2011). Differences between vitrified and fresh oocytes appear less deleterious than those after slow freezing, as confirmed by the mRNA content of a panel of genes involved in important oocyte functions (cell cycle, chromosome structure, mitochondrial pathways) which are more conserved in supernumerary vitrified MII oocytes than with slow freezing (Chamayou et al., 2011). Vitrification also showed no differential expression in genes related to cytokinesis (*PLK1*, *DCTN1*,2,3 and 6), known to be involved in zygotic arrest, and no difference for genes involved in basic oocyte functions such as *GAPDH*, *BMP15*, *GDF9*, and *OCT4* in supernumerary MII oocytes (Di Pietro et al., 2010; D'Aurora et al., 2019). Although it has less of an impact than slow freezing, pathways altered by vitrification are related to transcriptional regulation, ubiquitination, cell cycle and oocyte growth (Monzo et al., 2011; Huo et al., 2021), which is not insignificant regarding oocyte and embryo developmental competence. Recent work by Barberet et al., using both scRNA-seq and a strong study design consisting of sibling oocytes from the same patients, was reassuring regarding the use of vitrification. The number of DEGs remained low (108 versus 1987 DEGs in Huo et al.) and the difference between the fresh and vitrified groups was largely limited (fold change <1) (Huo et al., 2021; Barberet et al., 2022). In addition, the use of either manual of semi-automated vitrification is also without consequence for the oocyte (Barberet et al., 2022). By comparing the DEGs of the studies, we did not find any overlapping genes from one study to another, either for vitrification or slow freezing, but complete data were not available for one study (Monzo et al., 2011). Evidence from animal studies globally corroborates the observations in human oocytes, notably, alterations in cell cycle, ubiquitination, and transcriptional regulation linked to cryopreservation (Wang et al., 2017; Huang et al., 2018; Barberet et al., 2020; Ma et al., 2022).

Finally, it does not seem that storage time exacerbates differences after cryopreservation for a few months compared with >5 years periods (Stigliani et al., 2015; Huo et al., 2021).

The nature and the concentration of cryoprotective agents might be a source of variation for the oocyte transcriptome and oocyte quality due to vitrification, as indicated by studies in bovines (Zhang et al., 2020a). Indeed, decreased concentrations of CPAs reduced the number of aberrant transcriptional modifications in immature oocytes vitrified in liquid helium, but not

Table 1. List of chromatin modifier genes, imprinted genes, and transposable elements shown to be differentially expressed in studies investigating ART, maternal aging, lifestyle, and endometrial diseases' effects.

Comparison	Cell type	Study	Direction of regulation	Chromatin modifiers *	Imprinted genes *	Transposable elements
Ovarian stimulation						
HP-hMG vs rFSH	CC	Gatta et al. (2013)	UP	*BRD3 CHD7 DZIP3 HDAC2 ING5 PAK1 PBRM1 PRMT3 PRMT6 SMYD3 UBE2B UTY*	*DLX5 KCNK9*	
			DOWN	*CBX3 CHD8 MBD4 MECP2 PHF10*	*NNAT ZFAT*	
		Assou et al. (2013)	DOWN		*H19*	
	MGC	Brannian et al. (2010)	UP	*BRD3 BRD4 HDAC7 KAT2A PCGF2 MTA1 NSD2 SMARCA4 SMARCD3*	*CDKN1C DLK1 PHLDA2*	
			DOWN	*BMI1 EED NCOA3 RPS6KA5 RNF2*	*CMKLR2*	
		Grondahl et al. (2009)	DOWN	*PHF10*		
rFSH vs rLH+rFSH	CC	Gatta et al. (2013)	UP	*CHD8*	*SNURF*	
			DOWN	*DNMT3B UBE2B*		
HP-hMG vs urinary FSH	CC	Cruz et al. (2017)	DOWN		*DIRAS3*	
FSH+rFSH vs rFSH	CC	Gurgan et al. (2014)	UP	*SUZ12*	*NAP1L5*	
GnRH-a vs hCG	CC	Borgbo et al. (2013)	UP	*SETDB2*		
			DOWN		*TFPI2*	
	MGC	Borgbo et al. (2013)	DOWN		*DIRAS3 DLK1 SGCE ZC3H12C*	
hCG+GnRH-a vs hCG	CC	Fuchs Weizman et al. (2019) normal responders	UP	*AURKB ESCO2 HDAC9 INGX UTY*	*CPA4 DDC DLGAP2 KCNQ1OT1*	
			DOWN	*MBD2 MBD4*	*IGF2 TFPI2*	
		Fuchs Weizman et al. (2019) poor responders	UP	*CBX1 CHD1 DNMT3B ING1 INGX KDM6B KMT2C PHF13*	*DLX5 GLIS3 H19 MAGEL2 MEG3 TFPI2 ZDBF2 ZNF597*	
			DOWN	*EZH2*	*ATP10A CPA4 CMKLR2 DIRAS3 GRB10 KCNQ1OT1 PHLDA2*	
Ovarian stimulation vs natural cycle	MGC	Lu et al. (2019)	UP		*ATP10A CRYBG1 PHLDA2*	
			DOWN	*AURKA AURKB*	*IGF2 ZIM2*	
	CC	Papler et al. (2013)	UP		*IGF2*	
IVM						
Rescue IVM vs in vivo	Oocyte	Jones et al. (2008)	UP	*ATF2 BRD7 MBD4*		
	Oocyte	Lee et al. (2021)	UP	*HDAC11 SMYD3*	*GNAS KCNQ1OT1 NLRP2*	
			DOWN	*ACTL6A PRMT1 SMARCD1 RNF20*	*BLCAP ZNF597*	
	Oocyte	Virant-Klun et al. (2018)	UP		*DLGAP2*	
	CC (from PCOS patients)	Ouandaogo et al. (2012)	UP	*ASH1L ATF2 BAZ2B BMI1 BRWD1 CHD6 CKDM5B DOT1L EZH1 HDAC4 ING1 ING4 ING5 NCOA3 KAT6A KDM4C KDM5B KMT5B PHF10 PRMT2 RING1 RPS6KA3 RPS6KA5 SETDB1 SETDB2 SMARCA2 UBE2B*	*BLCAP DLK1 CRYBG1 GRB10 NAP1L5 PEG3 SLC22A18 SGCE SGK3 TFPI2 UBE3A ZDBF2*	
			DOWN	*ACTL6A AURKA AURKB BPTF BRD2 BRD4 BRD7 CARM1 CBX5 CDYL CHD1 CHD4 CHD8 CHD9 CTBP2 DNMT1 EHMT2 EZH2 HDAC2 HDAC8 KAT6B KMT2E*	*MEG3 GNAS PEG10 UBE3A IGF2R MEST DNMT1*	

(continued)

Table 1. Continued

				KMT5A *PBRM1* *PRMT3* PRMT5 *PRMT6* *MBD3* *MTA1* NEK6 *NSD2* SETD2 *SMARCD3* *SMARCA4* SPEN *SUZ12* UBE2A		
Cryopreservation						
Vitrification vs fresh	Oocyte	Huo et al. (2021)	UP	*DOT1L* *EHMT2*	*RB1*	
			DOWN	BRPF1 CBX4 *CBX8* *EZH2* INO80 *KAT8* *KDM4C* KMT2A SETD1A *SMARCA4*	*ANO1* *GLIS3* LIN28B *SLC22A2*	
		Barberet et al. (2022)	UP	*PBRM1*	*KCNK9* *ZIM2*	
			DOWN	*AURKC*		LTR13A LTR16C MLT1A1 PABL_A-in
Slow freezing vs fresh	Oocyte	Stigliani et al. (2015)	UP		*BLCAP* *ZFAT*	
			DOWN	*BRD1*		
Endometriosis						
Endometriosis vs healthy	Oocyte	Ferrero et al. (2019)	UP	*SPEN*	*SNRPN*	
			DOWN	*CHD2* *DNMT1* *RNF20*	*DNMT1*	
PCOS						
PCOS vs healthy	Oocyte	Li et al. (2021)	UP	*BPTF* *BRD3* *BRD4* *CHD1* *CHD2* *CHD6* *CHD7* *CHD8* *DNMT1* *KAT6A* *KAT6B* KDM4A *KMT2C* *KMT2E* NSD1 PHF21A *PRMT1* *PRMT2* *SPEN*	*DNMT1* *ZDBF2* *CMKLR2*	ERV1
			DOWN	HAT1 *PHF10* *RPS6KA3* *SMARCA2* *SMYD3* *UBE2B*	*GNAS*	
		Wood et al. (2007)	UP	*CBX1*		
			DOWN	*KAT6A*		
Maternal age						
Young vs advanced maternal age	Oocyte	Grondahl et al. (2010)	UP	*ARID1A*		
			DOWN		*CDKN1C* *GRB10*	
		Llonch et al. (2021)	UP	*ASH1L* *BAZ1A* *BAZ1B* *BAZ2B* *CHD8* *DNMT1* DZIP3 ESCO1 *ESCO2* ING3 *KMT2E* *PBRM1* *PHF10* *RNF20* USP16	*DNMT1* *SGK3* *UBE3A*	
			DOWN	*KAT8* KDM1A *KDM5B* *RING1* *RNF2* *SMARCA4* *SUZ12*		
		Ntostis et al. (2021)	UP	*ING4* *MBD3* *SMARCD3*	*SL22A2*	
			DOWN		*ANO1*	
BMI						
Obese vs normal BMI	Oocyte	Ruebel et al. (2017)	DOWN	*CBX8* *PRTM7*	*ZFAT*	

CC: cumulus cells; GnRH-a: gonadotrophin releasing hormone agonist; hCG: human chorionic gonadotrophin; HP-hMG: highly purified human menopausal gonadotrophin; MGC: mural granulosa cells; PCOS: polycystic ovary syndrome; rFSH: recombinant follicle-stimulating hormone; rLH: recombinant luteinizing hormone.

* Genes in red, blue, and green are found in, respectively, two, three, and four different studies.

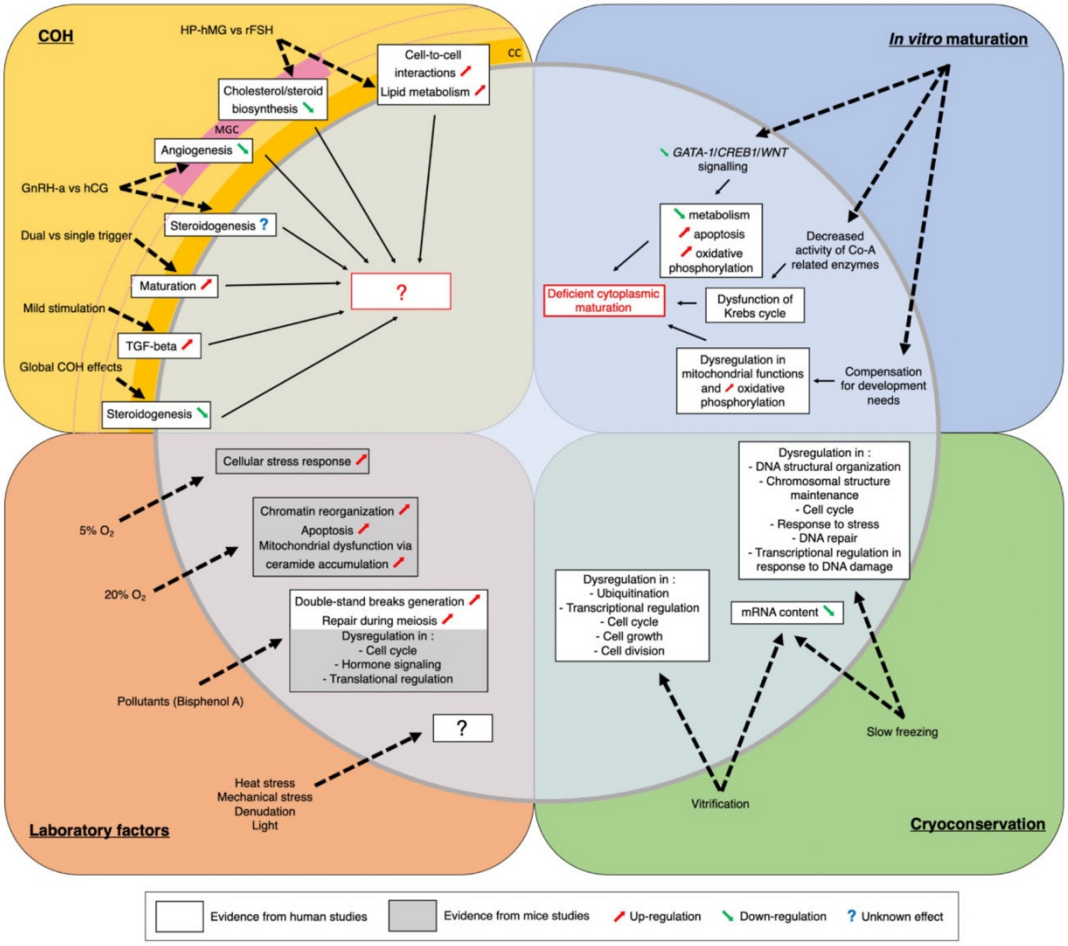

Figure 4. Summary of the current evidence regarding factors affecting the transcriptomic integrity of human oocyte during ART protocols. CC: cumulus cells; COH: (controlled) ovarian stimulation; MGC: mural granulosa cells.

liquid nitrogen (Zhang *et al.*, 2020a). Optimization of the vitrification technique is still possible to reduce the few molecular side effects reported to date in human oocytes and to ameliorate clinical outcomes.

ART factors not studied to date

The Cairo consensus recently noticed that 'there is only one thing that is truly important in an IVF laboratory: everything'. It would be interesting to investigate to what extent overlooked factors such as light exposure could affect gene expression since early mouse embryos at different stages showed light-induced changes in genes related to regulation of transcription, apoptosis, cell cycle and cellular responses to stimulus (Lv *et al.*, 2019). Variations in oocyte handling media formulation also exist among fertility clinics, but there are no studies comparing their transcriptomic effects to date. Whether micromanipulation or vigorous pipetting could trigger severe mechanical stress is unknown as well. The exposure time to hyaluronidase treatment for oocyte denudation might also influence the oocyte transcriptome. We still do not know whether the incubation time of oocytes before insemination or sperm microinjection, which can delay the fertilization step, could induce *in vitro* aging and directly impact fertilization and developmental abilities. While all these factors may have a limited impact on oocyte competence independently, the combination of all these factors cannot be neglected.

Implications of different ART and external factors for common transcriptional regulation mechanisms

Examining common genes dysregulated due to different exposures is challenging owing to the different methodologies and significance thresholds employed in each study. However, we grouped all the DEGs found per ART interventions (ovarian stimulation versus natural cycle, cryopreservation versus fresh, IVM versus *in vivo* maturation) independently of the study and we observed that 8 DEGs were common to the different exposures evaluated in this review: *CDC45*, *CENPA*, *GINS1*, *IQGAP3*, *MED17*, *TNFRSF1B*, *TNNI3*, and *UHRF1*. For most of them, their precise role in oocytes is unknown, but they may be linked to centromere position (*CENPA*), initiation of DNA replication (*CDC45*, *GINS1*), mediation of RNA polymerase II transcription (*MED17*), and apoptosis (*TNFRSF1B*). Interestingly, UHRF1 plays a major role in

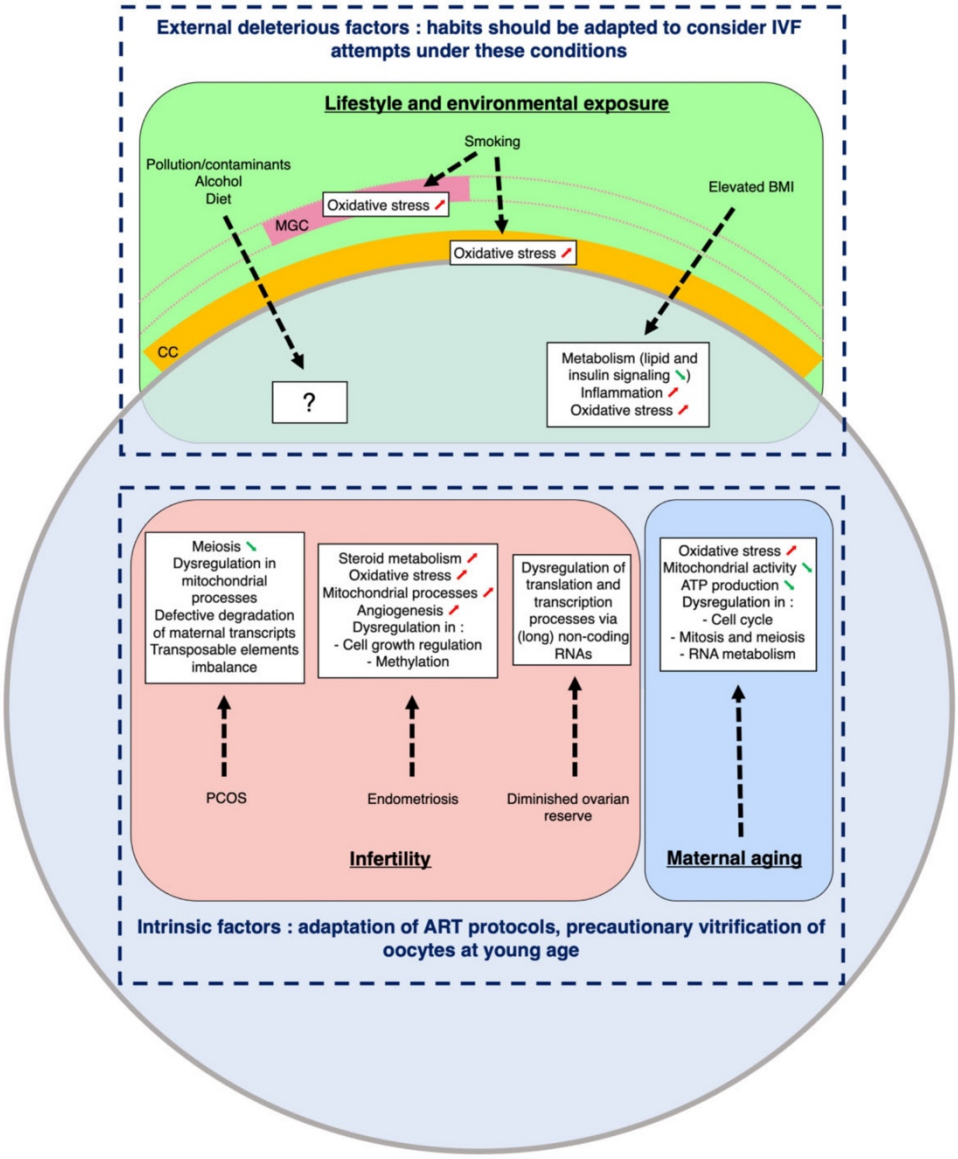

Figure 5. Summary of the current evidence regarding environmental factors, infertility and aging effects on the transcriptomic integrity of human oocyte. CC: cumulus cells; MGC: mural granulosa cells.

DNA methylation by recruiting DNMT1 (Maenohara *et al.*, 2017). Mouse *Uhrf1*-null oocytes notably showed increased aneuploidy rates, DNA double-strand breaks, and spindle aberrations (Cao *et al.*, 2019). However, these results need to be interpreted with caution because it remains a qualitative assessment of genes deregulated in different studies (i.e. common genes of three ART processes yet not reported by all studies).

We can still hypothesize that dysregulation in genes involved in chromatin-based processes such as DNA methylation, heterochromatin modulation, histone modification, and complex remodeling, but also otherwise genomic imprinting, may be a common mechanism linked to an adverse oocyte environment and explaining global transcriptomic modifications. Indeed, when we focused on chromatin modifier genes, we systematically found dysregulations of such genes either after ART intervention or lifestyle exposure, as well as due to internal factors such as maternal aging and reproductive diseases (Table 1). Among the most frequently found dysregulated genes with such functions were *CHD8*, *DNMT1*, *PBRM1*, *PHF10*, and *SMARCA4* (Table 1). The role of *DNMT1* is particularly crucial for global DNA methylation patterns and genomic imprints, as DNMT1 is primarily required for maintaining methylation patterns established in gametogenesis. DNMT1 can also participate in the de novo methylation of a small but essential part of the genome (Edwards *et al.*, 2017). Careful assessment of genes involved in chromatin-based regulation appears warranted in future research regarding

ART and external factors influencing the oocyte transcriptome because these genomic regions seem to be particularly at risk for oocyte quality.

Transposable elements have barely been studied to date but would also deserve more attention as they are key regulators of genomic stability.

Conclusion and perspective

We have seen that many IVF factors and additional external factors have the potential to impair oocyte transcriptomic integrity, which might not be innocuous for the developing embryo. In line with our research questions, our findings include three aspects. (i) We found similarities in dysregulated biological pathways, but not genes, between studies for each factor considered (summarized in Figs 4 and 5). (ii) We provide an overview of oocyte transcriptomic effects integrating all the types of intervention and we identified common oocyte alterations in cell cycle and division, energy (metabolism, mitochondria activity), and transcriptional and translational regulation pathways, which are essential for governing the development of the embryo until the maternal-to-zygotic transition. Additionally, each factor may mobilize other distinct biological pathways. (iii) For the first time, we also revealed a repetitive hypersensitivity of genes related to epigenetic mechanisms, which deserves more attention regarding the influence of ARTs, as they are considered risk factors for epigenetic defects, notably, at the DNA methylation level.

However, it is unclear whether all these alterations are detrimental for the future embryo and prone to be pathogenic later in life. Maternal transcripts are recruited in a temporally complex manner to fit in with the biological needs of the early embryo. Some of them, designated as maternal effect genes, have already proven associations with structural birth defects in the absence of expression in mouse models (Mitchell, 2022). Further identification of all the maternal transcripts crucial before the embryo takes control of its own genome will help in our understanding of how the oocyte environment determines the success or failure of the first mitotic divisions. One limit to the scientific evidence of all of the studies assessed in this review lies in the heterogeneity of ART factors transcriptomic effects that is rarely studied in populations of sibling oocytes. Indeed, the studies considered here mainly pooled oocytes or did not report data per patient. The fact that ART effects might not be similar from one oocyte to another in the same patient under the same conditions is an important parameter for the success of an ART attempt. It also remains undetermined whether the oocyte transcriptomic modifications associated with ART have a short- or long-term effect in humans, although two mice studies have considered this question for cryoinjuries and ovarian stimulation (Eroglu *et al.*, 2020; Taher *et al.*, 2021). Overall, it is completely unknown for human oocytes whether the transcriptomic and individual gene alterations described in this review correlate with proteomic modifications. Simultaneous assessment of the human oocyte proteome and transcriptome could give better insights on the consequences of transcriptomic alterations found with ART and intrinsic factors, but there are still technical challenges to overcome.

Although we lack considerable evidence for some aspects of ART, the majority of children born through those techniques remain healthy (Hart and Norman, 2013). Even so, this review could identify the weakest points in ART to ameliorate in the near future in order to improve ART outcomes. From this perspective, we have elaborated on some recommendations for ART practices which include adaptations in hormonal treatment and culture conditions, and a reduction in exposure factors in the *in vitro* environment. These adaptations must be set against the small number of studies, the absence of human oocyte evidence and their sometimes conflicting results for certain factors (Supplementary Fig. S1).

ART should not force the oocyte to adapt to a modified environment but should put the oocyte in the best possible conditions so as not to have a detrimental impact on embryonic development. While it is not possible to act on certain parameters such as maternal age, it is necessary to avoid any cumulative stress during gamete manipulation and embryo development, and efforts to provide safer ART protocols are still required in this direction.

Supplementary data

Supplementary data are available at *Human Reproduction Update* online.

Data availability

No new data were generated or analyzed in support of this research.

Authors' roles

B.D. performed the literature search and data extraction. B.D. and P.F. drafted the manuscript. C.P. and J.T. provided critical revision and edited the article. All the authors approved the final version of the article.

Funding

This work was supported by funding from the Agence Nationale pour la Recherche ('CARE'-ANR JCJC 2017).

Conflict of interest

The authors declare no conflict of interest.

References

Adriaenssens T, Wathlet S, Segers I, Verheyen G, de Vos A, van der Elst J, Coucke W, Devroey P, Smitz J. Cumulus cell gene expression is associated with oocyte developmental quality and influenced by patient and treatment characteristics. *Hum Reprod* 2010; **25**:1259–1270.

Agarwal A, Rosas IM, Anagnostopoulou C, Cannarella R, Boitrelle F, Munoz LV, Finelli R, Durairajanayagam D, Henkel R, Saleh R. Oxidative stress and assisted reproduction: a comprehensive review of its pathophysiological role and strategies for optimizing embryo culture environment. *Antioxidants* 2022;**11**:477.

Al-Inany HG, Youssef MA, Ayeleke RO, Brown J, Lam WS, Broekmans FJ ; Cochrane Gynaecology and Fertility Group. Gonadotrophin-releasing hormone antagonists for assisted reproductive technology. *Cochrane Database Syst Rev* 2016;**2016**:1–139.

Andersen CY, Westergaard LG, van Wely, M. FSH isoform composition of commercial gonadotrophin preparations: a neglected aspect? *Reprod Biomed Online* 2004;**9**:231–236. Reproductive Healthcare Ltd.

Anderson RC, Newton CL, Anderson RA, Millar RP. Gonadotropins and their analogs: current and potential clinical applications. *Endocr Rev* 2018;**39**:911–937.

Assou S, Haouzi D, Dechaud H, Gala A, Ferrières A, Hamamah S. Comparative gene expression profiling in human cumulus cells according to ovarian gonadotropin treatments. *Biomed Res Int* 2013;**2013**:354582.

Assou S, Haouzi D, Mahmoud K, Aouacheria A, Guillemin Y, Pantesco V, Rème T, Dechaud H, Vos J, de Hamamah S *et al.* A non-invasive test for assessing embryo potential by gene expression profiles of human cumulus cells: a proof of concept study. *Mol Hum Reprod* 2008;**14**:711–719.

Attali E, Yogev Y. The impact of advanced maternal age on pregnancy outcome. *Best Pract Res Clin Obstet Gynaecol* 2021;**70**:2–9.

Barberet J, Barry F, Choux C, Guilleman M, Karoui S, Simonot R, Bruno C, Fauque P. What impact does oocyte vitrification have on epigenetics and gene expression? *Clin Epigenetics* 2020;**12**:121.

Barberet J, Ducreux B, Bruno C, Guilleman M, Simonot R, Lieury N, Guilloteau A, Bourc'his D, Fauque P. Comparison of oocyte vitrification using a semi-automated or a manual closed system in human siblings: survival and transcriptomic analyses. *J Ovarian Res* 2022;**15**:128.

Barberi M, Ermini B, Morelli MB, Ermini M, Cecconi S, Canipari R. Follicular fluid hormonal profile and cumulus cell gene expression in controlled ovarian hyperstimulation with recombinant FSH: Effects of recombinant LH administration. *J Assist Reprod Genet* 2012;**29**:1381–1391.

Barragán M, Pons J, Ferrer-Vaquer A, Cornet-Bartolomé D, Schweitzer A, Hubbard J, Auer H, Rodolosse A, Vassena R. The transcriptome of human oocytes is related to age and ovarian reserve. *Mol Hum Reprod* 2017;**23**:535–548.

Bertoldo MJ, Locatelli Y, O'Neill C, Mermillod P. Impacts of and interactions between environmental stress and epigenetic programming during early embryo development. *Reprod Fertil Dev* 2015;**27**:1125–1136.

Blondin P, Coenen K, Guilbault LA, Sirard M-A. Superovulation can reduce the developmental competence of bovine embryos. *Theriogenology* 1996;**46**:1191–1203.

Borgbo T, Povlsen BB, Andersen CY, Borup R, Humaidan P, Grøndahl ML. Comparison of gene expression profiles in granulosa and cumulus cells after ovulation induction with either human chorionic gonadotropin or a gonadotropin-releasing hormone agonist trigger. *Fertil Steril* 2013;**100**:994–1001.

Bouckenheimer J, Assou S, Riquier S, Hou C, Philippe N, Sansac C, Lavabre-Bertrand T, Commes T, Lemaître J-M, Boureux A *et al.* Long non-coding RNAs in human early embryonic development and their potential in ART. *Hum Reprod Update* 2016;**23**:19–40.

Bouckenheimer J, Fauque P, Lecellier CH, Bruno C, Commes T, Lemaître JM, Vos De J, Assou S. Differential long non-coding RNA expression profiles in human oocytes and cumulus cells. *Sci Rep* 2018;**8**:2202.

Brannian J, Eyster K, Mueller BA, Bietz MG, Hansen K. Differential gene expression in human granulosacells from recombinant FSH versus humanmenopausal gonadotropin ovarian stimulation-protocols. *Reprod Biol Endocrinol* 2010;**8**:25.

Brieño-Enríquez MA, Reig-Viader R, Cabero L, Toran N, Martínez F, Roig I, Garcia Caldés M. Gene expression is altered after bisphenol A exposure in human fetal oocytes in vitro. *Mol Hum Reprod* 2012;**18**:171–183.

Budani MC, Carletti E, Tiboni GM. Cigarette smoke is associated with altered expression of antioxidant enzymes in granulosa cells from women undergoing in vitro fertilization. *Zygote* 2017;**25**:296–303.

Bulletti C, Coccia ME, Battistoni S, Borini A. Endometriosis and infertility. *J Assist Reprod Genet* 2010;**27**:441–447.

Cao Y, Li M, Liu F, Ni X, Wang S, Zhang H, Sui X, Huo R. Deletion of maternal UHRF1 severely reduces mouse oocyte quality and causes developmental defects in preimplantation embryos. *FASEB J* 2019;**33**:8294–8305.

Cao Y, Zhao H, Wang Z, Zhang C, Bian Y, Liu X, Zhang C, Zhang X, Zhao Y. Quercetin promotes in vitro maturation of oocytes from humans and aged mice. *Cell Death Dis* 2020;**11**:965.

Carré J, Gatimel N, Moreau J, Parinaud J, Léandri R. Does air pollution play a role in infertility?: A systematic review. *Environ Health* 2017;**16**:82.

Chamayou S, Bonaventura G, Alecci C, Tibullo D, Raimondo F, di Guglielmino A, Barcellona ML. Consequences of metaphase II oocyte cryopreservation on mRNA content. *Cryobiology* 2011;**62**:130–134.

Chon SJ, Umair Z, Yoon MS. Premature ovarian insufficiency: past, present, and future. *Front Cell Dev Biol* 2021;**9**:672890.

Christianson MS, Zhao Y, Shoham G, Granot I, Safran A, Khafagy A, Leong M, Shoham Z. Embryo catheter loading and embryo culture techniques: results of a worldwide web-based survey. *J Assist Reprod Genet* 2014;**31**:1029–1036.

Cimadomo D, Fabozzi G, Vaiarelli A, Ubaldi N, Ubaldi FM, Rienzi L. Impact of maternal age on oocyte and embryo competence. *Front Endocrinol (Lausanne)* 2018;**9**:327.

Cobo A, García-Velasco JA, Remohí J, Pellicer A. Oocyte vitrification for fertility preservation for both medical and nonmedical reasons. *Fertil Steril* 2021;**115**:1091–1101.

Cruz M, Requena A, Agudo D, García-Velasco JA. Type of gonadotropin used during controlled ovarian stimulation induces differential gene expression in human cumulus cells: a randomized study. *Eur J Obstet Gynecol Reprod Biol* 2017;**215**:124–133.

da Luz CM, da Broi MG, Plaça JR, Silva Jr, WA, Meola J, Navarro PA. Altered transcriptome in cumulus cells of infertile women with advanced endometriosis with and without endometrioma. *Reprod Biolmed Online* 2021;**42**.

Dahan MH, Tan SL, Chung J, Son WY. Clinical definition paper on in vitro maturation of human oocytes. *Hum Reprod* 2016;**31**:1383–1386.

D'Aurora M, Budani MC, Franchi S, Sarra A, Stuppia L, Tiboni GM, Gatta V. Dynactin pathway-related gene expression is altered by aging, but not by vitrification. *Reprod Toxicol* 2019;**88**:48–55.

Davies MJ, Moore VM, Willson KJ, Essen P, van Priest K, Scott H, Haan EA, Chan A. Reproductive technologies and the risk of birth defects. *Obstet Gynecol Surv* 2012;**67**:527–528.

de los Santos MJ, García-Láez V, Beltrán-Torregrosa D, Horcajadas JA, Martínez-Conejero JA, Esteban FJ, Pellicer A, Labarta E. Hormonal and molecular characterization of follicular fluid, cumulus cells and oocytes from pre-ovulatory follicles in stimulated and unstimulated cycles. *Hum Reprod* 2012;**27**:1596–1605.

Devjak R, Fon Tacer K, Juvan P, Virant Klun I, Rozman D, Vrtačnik Bokal E. Cumulus cells gene expression profiling in terms of oocyte maturity in controlled ovarian hyperstimulation using GnRH agonist or GnRH antagonist. *PLoS One* 2012;**7**:e47106.

Di Pietro C, Vento M, Guglielmino MR, Borzì P, Santonocito M, Ragusa M, Barbagallo D, Duro LR, Majorana A, De Palma A *et al.* Molecular profiling of human oocytes after vitrification strongly suggests that they are biologically comparable with freshly isolated gametes. *Fertil Steril* 2010;**94**:2804–2807.

Dong L, Xin X, Chang HM, Leung PCK, Yu C, Lian F, Wu H. Expression of long noncoding RNAs in the ovarian granulosa cells of women with diminished ovarian reserve using high-throughput sequencing. *J Ovarian Res* 2022;**15**:119.

Downs SM, Mosey JL, Klinger J. Fatty acid oxidation and meiotic resumption in mouse oocytes. *Mol Reprod Dev* 2009;**76**:844–853.

Dumesic DA, Meldrum DR, Katz-Jaffe MG, Krisher RL, Schoolcraft WB. Oocyte environment: Follicular fluid and cumulus cells are critical for oocyte health. *Fertil Steril* 2015;**103**:303–316.

Dworkin MB, Dworkin-Rastl E. Functions of maternal mRNA in early development. *Mol Reprod Dev* 1990;**26**:261–297.

Edwards JR, Yarychkivska O, Boulard M, Bestor TH. DNA methylation and DNA methyltransferases. *Epigenetics Chromatin* 2017;**10**:23.

Eisenberg VH, Weil C, Chodick G, Shalev V. Epidemiology of endometriosis: a large population-based database study from a healthcare provider with 2 million members. *BJOG* 2018;**125**:55–62.

Eppig JJ, Wigglesworth K. Factors affecting the developmental competence of mouse oocytes grown in vitro: oxygen concentration. *Mol Reprod Dev* 1995;**42**:447–456.

Eroglu B, Szurek EA, Schall P, Latham KE, Eroglu A. Probing lasting cryoinjuries to oocyte-embryo transcriptome. *PLoS One* 2020;**15**: e0231108.

Ferrero H, Corachán A, Aguilar A, Quiñonero A, Carbajo-García MC, Alamá P, Tejera A, Taboas E, Muñoz E, Pellicer A *et al.* Single-cell RNA sequencing of oocytes from ovarian endometriosis patients reveals a differential transcriptomic profile associated with lower quality. *Hum Reprod* 2019;**34**:1302–1312.

Ferris J, Mahboubi K, MacLusky N, King WA, Favetta LA. BPA exposure during in vitro oocyte maturation results in dose-dependent alterations to embryo development rates, apoptosis rate, sex ratio and gene expression. *Reprod Toxicol* 2016;**59**:128–138.

Firns S, Cruzat VF, Keane KN, Joesbury KA, Lee AH, Newsholme P, Yovich JL. The effect of cigarette smoking, alcohol consumption and fruit and vegetable consumption on IVF outcomes: a review and presentation of original data. *Reprod Biol Endocrinol* 2015;**13**: 134.

Flach G, Johnson MH, Braude PR, Taylor RA, Bolton VN. The transition from maternal to embryonic control in the 2-cell mouse embryo. *EMBO J* 1982;**1**:681–686.

Foster WG, Neal MS, Han MS, Dominguez MM. Environmental contaminants and human infertility: Hypothesis or cause for concern? *J Toxicol Environ Health B Crit Rev* 2008;**11**:162–176.

Fu XH, Chen CZ, Wang Y, Peng YX, Wang WH, Yuan B, Gao Y, Jiang H, Zhang JB. COL1A1 affects apoptosis by regulating oxidative stress and autophagy in bovine cumulus cells. *Theriogenology* 2019;**139**:81–89.

Fuchs Weizman N, Wyse BA, Gat I, Balakier H, Sangaralingam M, Caballero J, Kenigsberg S, Librach CL. Triggering method in assisted reproduction alters the cumulus cell transcriptome. *Reprod Biomed Online* 2019;**39**:211–224.

Gao L, Jia G, Li A, Ma H, Huang Z, Zhu S, Hou Y, Fu X. RNA-Seq transcriptome profiling of mouse oocytes after in vitro maturation and/or vitrification. *Sci Rep* 2017;**7**:13245.

Garcia-Velasco JA, Fassbender A, Ruiz-Alonso M, Blesa D, D'Hooghe T, Simon C. Is endometrial receptivity transcriptomics affected in women with endometriosis? A pilot study. *Reprod Biomed Online* 2015;**31**:647–654.

Gatta V, Tatone C, Ciriminna R, Vento M, Franchi S, d'Aurora M, Sperduti S, Cela V, Borzì P, Palermo R *et al.* Gene expression profiles of cumulus cells obtained from women treated with recombinant human luteinizing hormone + recombinant human follicle-stimulating hormone or highly purified human menopausal gonadotropin versus recombinant human follicle-stimulating hormone alone. *Fertil Steril* 2013;**99**:2000–2008.e1.

Geyter C, de Calhaz-Jorge C, Kupka MS, Wyns C, Mocanu E, Motrenko T, Scaravelli G, Smeenk J, Vidakovic S, Goossens V *et al.* ART in Europe, 2015: results generated from European registries by ESHRE. *Hum Reprod Open* 2020;**2020**:1–17.

Gonen N, Casper RF, Jurisicova A, Yung Y, Friedman-Gohas M, Orvieto R, Haas J. Does gonadotropin-releasing hormone agonist cause luteolysis by inducing apoptosis of the human granulosa-luteal cells? *J Assist Reprod Genet* 2021;**38**:2301–2305.

Grøndahl ML, Borup R, Lee YB, Myrhøj V, Meinertz H, Sørensen S. Differences in gene expression of granulosa cells from women undergoing controlled ovarian hyperstimulation with either recombinant follicle-stimulating hormone or highly purified human menopausal gonadotropin. *Fertil Steril* 2009;**91**: 1820–1830.

Grøndahl ML, Yding Andersen C, Bogstad J, Nielsen FC, Meinertz H, Borup R. Gene expression profiles of single human mature oocytes in relation to age. *Hum Reprod* 2010;**25**:957–968.

Guo Y, Cao Z, Jiao X, Bai D, Zhang Y, Hua J, Liu W, Teng X. Pre-pregnancy exposure to fine particulate matter (PM2.5) increases reactive oxygen species production in oocytes and decrease litter size and weight in mice. *Environmental Pollution* 2021;**268**: 115858.

Gurgan T, Montjean D, Demirol A, Menezo YJR. Sequential (hFSH + recFSH) vs homogenous (hFSH or recFSH alone) stimulation: Clinical and biochemical (cumulus cell gene expression) aspects. *J Assist Reprod Genet* 2014;**31**:657–665.

Haas J, Ophir L, Barzilay E, Machtinger R, Yung Y, Orvieto R, Hourvitz A. Standard human chorionic gonadotropin versus double trigger for final oocyte maturation results in different granulosa cells gene expressions: a pilot study. *Fertil Steril* 2016;**106**:653–659.e1.

Haas J, Ophir L, Barzilay E, Yerushalmi GM, Yung Y, Kedem A, Maman E, Hourvitz A. GnRH agonist vs. hCG for triggering of ovulation—Differential effects on gene expression in human granulosa cells. *PLoS One* 2014;**9**:e90359.

Hao Y, Hao S, Andersen-Nissen E, Mauck WM, Zheng S, Butler A, Lee MJ, Wilk AJ, Darby C, Zager M *et al.* Integrated analysis of multimodal single-cell data. *Cell* 2021;**184**:3573–3587.e29.

Hart R, Norman RJ. The longer-term health outcomes for children born as a result of ivf treatment: Part i-general health outcomes. *Hum Reprod Update* 2013;**19**:232–243.

Hatırnaz Ş, Ata B, Hatırnaz ES, Dahan MH, Tannus S, Tan J, Tan SL. Oocyte in vitro maturation: a sytematic review. *Turk J Obstet Gynecol* 2018;**15**:112–125.

Huang J, Ma Y, Wei S, Pan B, Qi Y, Hou Y, Meng Q, Zhou G, Han H. Dynamic changes in the global transcriptome of bovine germinal vesicle oocytes after vitrification followed by in vitro maturation. *Reprod Fertil Dev* 2018;**30**:1298–1313.

Huo Y, Yuan P, Qin Q, Yan Z, Yan L, Liu P, Li R, Yan J, Qiao J. Effects of vitrification and cryostorage duration on single-cell RNA-Seq profiling of vitrified-thawed human metaphase II oocytes. *Front Med* 2021;**15**:144–154.

Jahanbakhsh-Asl E, Salehi M, Ghaffari-Novin M, Kato Y. Superovulation affects the gene expression patterns of mice oocytes and preimplantation embryos produced by different assisted reproductive technologies. *Int J Women's Health Reprod Sci* 2018;**6**:444–451.

Jones GM, Cram DS, Song B, Magli MC, Gianaroli L, Lacham-Kaplan O, Findlay JK, Jenkin G, Trounson AO. Gene expression profiling of human oocytes following in vivo or in vitro maturation. *Hum Reprod* 2008;**23**:1138–1144.

Kalo D, Roth Z. Low level of mono(2-ethylhexyl) phthalate reduces oocyte developmental competence in association with impaired gene expression. *Toxicology* 2017;**377**:38–48.

Kasterstein E, Strassburger D, Komarovsky D, Bern O, Komsky A, Raziel A, Friedler S, Ron-El R. The effect of two distinct levels of oxygen concentration on embryo development in a sibling oocyte study. *J Assist Reprod Genet* 2013;**30**:1073–1079.

Katz-Jaffe MG, McCallie BR, Preis KA, Filipovits J, Gardner DK. Transcriptome analysis of in vivo and in vitro matured bovine MII oocytes. *Theriogenology* 2009;**71**:939–946.

Kaur M, Arora M. Diminished ovarian reserve, causes, assessment and management. *Int J Infertil Fetal Med* 2013;**4**:45–55.

Khan R, Jiang X, Hameed U, Shi Q. Role of lipid metabolism and signaling in mammalian oocyte maturation, quality, and acquisition of competence. *Front Cell Dev Biol* 2021;**9**:639704.

Konstantinidou F, Budani MC, Sarra A, Stuppia L, Tiboni GM, Gatta V. Impact of cigarette smoking on the expression of oxidative stress-related genes in cumulus cells retrieved from healthy women undergoing IVF. *Int J Mol Sci* 2021;**22**:13147.

Krisher RL. In vivo and in vitro environmental effects on mammalian oocyte quality. *Annu Rev Anim Biosci* 2013;**1**:393–417.

Krisher RL. Present state and future outlook for the application of in vitro oocyte maturation in human infertility treatment. *Biol Reprod* 2022;**106**:235–242.

Lee AWT, Ng JKW, Liao J, Luk AC, Suen AHC, Chan TTH, Cheung MY, Chu HT, Tang NLS, Zhao MP *et al.* Single-cell RNA sequencing identifies molecular targets associated with poor in vitro maturation performance of oocytes collected from ovarian stimulation. *Hum Reprod* 2021;**36**:1907–1921.

Lee M, Ahn J, Il Lee AR, Ko DW, Yang WS, Lee G, Ahn JY, Lim JM. Adverse effect of superovulation treatment on maturation, function and ultrastructural integrity of murine oocytes. *Mol Cells* 2017;**40**:558–566.

Li J, Chen H, Gou M, Tian C, Wang H, Song X, Keefe DL, Bai X, Liu L. Molecular features of polycystic ovary syndrome revealed by transcriptome analysis of oocytes and cumulus cells. *Front Cell Dev Biol* 2021;**9**:735684.

Li R, Albertini DF. The road to maturation: somatic cell interaction and self-organization of the mammalian oocyte. *Nat Rev Mol Cell Biol* 2013;**14**:141–152.

Li R, Luo Y, Xu J, Sun Y, Ma Z, Chen S. Effects of oxygen concentrations on developmental competence and transcriptomic profile of yak oocytes. *Zygote* 2020;**28**:459–469.

Li Y, Liu H, Yu Q, Liu H, Huang T, Zhao S, Ma J, Zhao H. Growth hormone promotes in vitro maturation of human oocytes. *Front Endocrinol (Lausanne)* 2019;**10**:485.

Liang LF, Qi ST, Xian YX, Huang L, Sun XF, Wang WH. Protective effect of antioxidants on the pre-maturation aging of mouse oocytes. *Sci Rep* 2017;**7**:1434.

Lim M, Thompson JG, Dunning KR. Hypoxia and ovarian function: follicle development, ovulation, oocyte maturation. *Reproduction* 2021;**161**:F33–F40.

Liu MJ, Sun AG, Zhao SG, Liu H, Ma SY, Li M, Huai YX, Zhao H, Liu HB. Resveratrol improves in vitro maturation of oocytes in aged mice and humans. *Fertil Steril* 2018;**109**:900–907.

Liu Q, Li Y, Feng Y, Liu C, Ma J, Li Y, Xiang H, Ji Y, Cao Y, Tong X *et al.* Single-cell analysis of differences in transcriptomic profiles of oocytes and cumulus cells at GV, MI, MII stages from PCOS patients. *Sci Rep* 2016;**6**:39638.

Liu X, Mai H, Chen P, Zhang Z, Wu T, Chen J, Sun P, Zhou C, Liang X, Huang R. Comparative analyses in transcriptome of human granulosa cells and follicular fluid micro-environment between poor ovarian responders with conventional controlled ovarian or mild ovarian stimulations. *Reprod Biol Endocrinol* 2022;**20**:54.

Lizneva D, Suturina L, Walker W, Brakta S, Gavrilova-Jordan L, Azziz R. Criteria, prevalence, and phenotypes of polycystic ovary syndrome. *Fertil Steril* 2016;**106**:6–15.

Llonch S, Barragán M, Nieto P, Mallol A, Elosua-Bayes M, Lorden P, Ruiz S, Zambelli F, Heyn H, Vassena R *et al.* Single human oocyte transcriptome analysis reveals distinct maturation stage-dependent pathways impacted by age. *Aging Cell* 2021;**20**:e13360.

Lu CL, Yan ZQ, Song XL, Xu YY, Zheng XY, Li R, Liu P, Feng HL, Qiao J. Effect of exogenous gonadotropin on the transcriptome of human granulosa cells and follicular fluid hormone profiles. *Reprod Biol Endocrinol* 2019;**17**.

Lv B, Liu C, Chen Y, Qi L, Wang L, Ji Y, Xue Z. Light-induced injury in mouse embryos revealed by single-cell RNA sequencing. *Biol Res* 2019;**52**:48.

Lv Z, Lv Z, Song L, Zhang Q, Zhu S. Role of lncRNAs in the pathogenic mechanism of human decreased ovarian reserve. *Front Genet* 2023;**14**:1056061.

Ma Y, Long C, Liu G, Bai H, Ma L, Bai T, Zuo Y, Li S. WGBS combined with RNA-seq analysis revealed that Dnmt1 affects the methylation modification and gene expression changes during mouse oocyte vitrification. *Theriogenology* 2022;**177**:11–21.

Maenohara S, Unoki M, Toh H, Ohishi H, Sharif J, Koseki H, Sasaki H. Role of UHRF1 in de novo DNA methylation in oocytes and maintenance methylation in preimplantation embryos. *PLoS Genet* 2017;**13**:e1007042.

Mai Z, Lei M, Yu B, Du H, Liu J. The effects of cigarette smoke extract on ovulation, oocyte morphology and ovarian gene expression in mice. *PLoS One* 2014;**9**:e95945.

Marca la A, Sunkara SK. Individualization of controlled ovarian stimulation in IVF using ovarian reserve markers: From theory to practice. *Hum Reprod Update* 2014;**20**:124–140.

Market-Velker BA, Fernandes AD, Mann MRW. Side-by-side comparison of five commercial media systems in a mouse model: Suboptimal in vitro culture interferes with imprint maintenance. *Biol Reprod* 2010;**83**:938–950.

Mermillod P, Dalbiès-Tran R, Uzbekova S, Thélie A, Traverso JM, Perreau C, Papillier P, Monget P. Factors affecting oocyte quality: who is driving the follicle? *Reprod Domest Anim* 2008;**43**:393–400.

Meuleman C, Vandenabeele B, Fieuws S, Spiessens C, Timmerman D, D'Hooghe T. High prevalence of endometriosis in infertile women with normal ovulation and normospermic partners. *Fertil Steril* 2009;**92**:68–74.

Miravet-Valenciano J, Ruiz-Alonso M, Gómez E, Garcia-Velasco JA. Endometrial receptivity in eutopic endometrium in patients with endometriosis: it is not affected, and let me show you why. *Fertil Steril* 2017;**108**:28–31.

Mishina T, Tabata N, Hayashi T, Yoshimura M, Umeda M, Mori M, Ikawa Y, Hamada H, Nikaido I, Kitajima TS. Single-oocyte transcriptome analysis reveals aging-associated effects influenced by life stage and calorie restriction. *Aging Cell* 2021;**20**:e13428.

Monzo C, Haouzi D, Assou S, Dechaud H, Hamamah S. Slow-freezing-thawing significantly alters gene expression profile of human metaphase II oocytes than that vitrification procedure: genomic results in lights of transcriptomic. *Fertil Steril* 2011;**96**:S209.

Naillat F, Saadeh H, Nowacka-Woszuk J, Gahurova L, Santos F, Tomizawa SI, Kelsey G. Oxygen concentration affects de novo DNA methylation and transcription in in vitro cultured oocytes. *Clin Epigenetics* 2021;**13**:132.

Ntostis P, Iles D, Kokkali G, Vaxevanoglou T, Kanavakis E, Pantou A, Huntriss J, Pantos K, Picton HM. The impact of maternal age on gene expression during the GV to MII transition in euploid human oocytes. *Hum Reprod* 2021;**37**:80–92. NLM (Medline).

O'Neill C, Li Y, Jin XL. Survival signaling in the preimplantation embryo. *Theriogenology* 2012;**77**:773–784.

Ouandaogo ZG, Frydman N, Hesters L, Assou S, Haouzi D, Dechaud H, Frydman R, Hamamah S. Differences in transcriptomic profiles of human cumulus cells isolated from oocytes at GV, MI and

MII stages after in vivo and in vitro oocyte maturation. *Hum Reprod* 2012;**27**:2438–2447.

Palmer A, Gavin A-C, Nebreda AR. A link between MAP kinase and p34 cdc2/cyclin B during oocyte maturation: p90 rsk phosphorylates and inactivates the p34 cdc2 inhibitory kinase Myt1. *EMBO J* 1998;**17**:5037–5047.

Papler TB, Bokal EV, Tacer KF, Juvan P, Klun IV, Devjak R. Differences in cumulus cells gene expression between modified natural and stimulated in vitro fertilization cycles. *J Assist Reprod Genet* 2014; **31**:79–88.

Payton RR, Rispoli LA, Saxton AM, Lannett Edwards J. Impact of heat stress exposure during meiotic maturation on oocyte, surrounding cumulus cell, and embryo RNA populations. *J Reprod Dev* 2011;**57**:481–491.

Qi L, Liu B, Chen X, Liu Q, Li W, Lv B, Xu X, Wang L, Zeng Q, Xue J *et al.* Single-cell transcriptomic analysis reveals mitochondrial dynamics in oocytes of patients with polycystic ovary syndrome. *Front Genet* 2020;**11**:396.

Reyes JM, Silva E, Chitwood JL, Schoolcraft WB, Krisher RL, Ross PJ. Differing molecular response of young and advanced maternal age human oocytes to IVM. *Hum Reprod* 2017;**32**:2199–2208.

Rabahi F, Brûlé S, Sirois J, Beckers JF, Silversides DW, Lussier JG. High expression of bovine glutathione S-transferase (GSTA1, GSTA2) subunits is mainly associated with steroidogenically active cells and regulated by gonadotropins in bovine ovarian follicles. *Endocrinology* 1999;**140**:3507–3517.

Roth Z. Stress-induced alterations in oocyte transcripts are further expressed in the developing blastocyst. *Mol Reprod Dev* 2018;**85**: 821–835.

Ruebel ML, Cotter M, Sims CR, Moutos DM, Badger TM, Cleves MA, Shankar K, Andres A. Obesity modulates inflammation and lipid-metabolism oocyte gene expression: a single-cell transcriptome perspective. *J Clin Endocrinol Metab* 2017;**102**:2029–2038.

Russell DL, Robker RL. Molecular mechanisms of ovulation: coordination through the cumulus complex. *Hum Reprod Update* 2007;**13**:289–312.

Saha R, Pettersson H, Svedberg P, Olovsson M, Bergqvist A, Marions L, Tornvall P, Kuja-Halkola R. Heritability of endometriosis. *Fertil Steril* 2015;**104**:947–-952.

Sallem A, Denizot A-L, Ziyyat A, L'Hostis A, Favier S, Burlet P, Lapierre J-M, Dimby SF, Patrat C, Sifer C *et al.* A fertilin-derived peptide improves in vitro maturation and ploidy of human oocytes. *F S Sci* 2022;**3**:21–28.

Sanchez AM, Vanni VS, Bartiromo L, Papaleo E, Zilberberg E, Candiani M, Orvieto R, Viganò P. Is the oocyte quality affected by endometriosis? A review of the literature. *J Ovarian Res* 2017;**10**: 43.

Sánchez F, Adriaenssens T, Romero S, Smitz J. Different follicle-stimulating hormone exposure regimens during antral follicle growth alter gene expression in the cumulus-oocyte complex in mice. *Biol Reprod* 2010;**83**:514–524.

Schatten H, Sun QY, Prather R. The impact of mitochondrial function/dysfunction on IVF and new treatment possibilities for infertility. *Reprod Biol Endocrinol* 2014;**12**:111.

Senapati S, Sammel MD, Morse C, Barnhart KT. Impact of endometriosis on in vitro fertilization outcomes: an evaluation of the Society for Assisted Reproductive Technologies Database. *Fertil Steril* 2016;**106**:164–171.e1.

Setti AS, Halpern G, de Braga DA, Iaconelli A, Borges E. Maternal lifestyle and nutritional habits are associated with oocyte quality and ICSI clinical outcomes. *Reprod Biomed Online* 2022;**44**:370–379.

Shalom-Paz E, Holzer H, Young Son W, Levin I, Tan SL, Almog B. PCOS patients can benefit from in vitro maturation (IVM) of oocytes. *Eur J Obstet Gynecol Reprod Biol* 2012;**165**:53–56. Elsevier Ireland Ltd.

Shi L, Wei X, Wu B, Yuan C, Li C, Dai Y, Chen J, Zhou F, Lin X, Zhang S. Molecular signatures correlated with poor IVF outcomes: insights from the mRNA and lncRNA expression of endometriotic granulosa cells. *Front Endocrinol (Lausanne)* 2022;**13**:825934.

Sirard MA, Richard F, Blondin P, Robert C. Contribution of the oocyte to embryo quality. *Theriogenology* 2006;**65**:126–136.

Sobinoff AP, Beckett EL, Jarnicki AG, Sutherland JM, McCluskey A, Hansbro PM, McLaughlin EA. Scrambled and fried: cigarette smoke exposure causes antral follicle destruction and oocyte dysfunction through oxidative stress. *Toxicol Appl Pharmacol* 2013; **271**:156–167.

Steele-Perkins G, Plachez C, Butz KG, Yang G, Bachurski CJ, Kinsman SL, Litwack ED, Richards LJ, Gronostajski RM. The transcription factor gene Nfib is essential for both lung maturation and brain development. *Mol Cell Biol* 2005;**25**:685–698.

Steptoe PC, Edwards RG. Birth after the reimplantation of a human embryo. *Lancet* 1978;**2**:366.

Steuerwald NM, Bermúdez MG, Wells D, Munné S, Cohen J. Maternal age-related differential global expression profiles observed in human oocytes. *Reprod Biomed Online* 2007;**14**:700–708.

Stigliani S, Moretti S, Anserini P, Casciano I, Venturini PL, Scaruffi P. Storage time does not modify the gene expression profile of cryopreserved human metaphase II oocytes. *Hum Reprod* 2015;**30**: 2519–2526.

Stigliani S, Moretti S, Casciano I, Canepa P, Remorgida V, Anserini P, Scaruffi P. Presence of aggregates of smooth endoplasmic reticulum in MII oocytes affects oocyte competence: Molecularbased evidence. *Mol Hum Reprod* 2018;**24**:310–317.

Sung L, Mukherjee T, Takeshige T, Bustillo M, Copperman AB. Endometriosis is not detrimental to embryo implantation in oocyte recipients. *J Assist Reprod Genet* 1997;**14**:152–156.

Taher L, Israel S, Drexler HCA, Makalowski W, Suzuki Y, Fuellen G, Boiani M. The proteome, not the transcriptome, predicts that oocyte superovulation affects embryonic phenotypes in mice. *Sci Rep* 2021;**11**:23731.

Takashima T, Fujimaru T, Obata Y. Effect of in vitro growth on mouse oocyte competency, mitochondria and transcriptome. *Reproduction* 2021;**162**:307–318.

Tan J, Cerrillo M, Cruz M, Cecchino GN, Garcia-Velasco JA. Early pregnancy outcomes in fresh versus deferred embryo transfer cycles for endometriosis-associated infertility: a retrospective cohort study. *J Clin Med* 2021;**10**:1–9.

Timossi CM, Barrios-De-Tomasi J, González-Suárez R, Arranz MC, Padmanabhan V, Conn PM, Ulloa-Aguirre A. Differential effects of the charge variants of human follicle-stimulating hormone. *J Endocrinol* 2000;**165**:193–205.

Togola A, Desmarchais A, Téteau O, Vignault C, Maillard V, Buron C, Bristeau S, Guérif F, Binet A, Elis S. Bisphenol S is present in culture media used for ART and cell culture. *Hum Reprod* 2021;**36**: 1032–1042.

Tu J, Tu J, Chen Y, Li Z, Yang H, Chen H, Yu Z. Long non-coding RNAs in ovarian granulosa cells. *J Ovarian Res* 2020;**13**:63.

Ulloa-Aguirre A, Timossi C, Damián-Matsumura P, Dias JA. Role of glycosylation in function of follicle-stimulating hormone. *Endocrine* 1999;**11**:205–215.

Uyar A, Torrealday S, Seli E. Cumulus and granulosa cell markers of oocyte and embryo quality. *Fertil Steril* 2013;**99**:979–997.

Varghese AC, Ly KD, Corbin C, Mendiola J, Agarwal A. Oocyte developmental competence and embryo development: Impact of lifestyle and environmental risk factors. *Reprod Biomed Online* 2011; **22**:410–420.

Vermeiden JPW, Bernardus RE. Are imprinting disorders more prevalent after human in vitro fertilization or intracytoplasmic sperm injection? *Fertil Steril* 2013;**99**:642–651.

Virant-Klun I, Bauer C, Ståhlberg A, Kubista M, Skutella T. Human oocyte maturation in vitro is improved by co-culture with cumulus cells from mature oocytes. *Reprod Biomed Online* 2018;**36**:508–523.

Virant-Klun I, Bedenk J, Jancar N. In vitro maturation of immature oocytes for fertility preservation in cancer patients compared to control patients with fertility problems in an in vitro fertilization program. *Radiol Oncol* 2021;**56**:119–128.

Virant-Klun I, Knez K, Tomazevic T, Skutella T. Gene expression profiling of human oocytes developed and matured in vivo or in vitro. *Biomed Res Int* 2013;**2013**:879489–871144.

Vos M, De Smitz J, Thompson JG, Gilchrist RB. The definition of IVM is clear—variations need defining. *Hum Reprod* 2016;**31**:2411–2415.

Vuong TNL, Ho MT, Ha TQ, Jensen MB, Andersen CY, Humaidan P. Effect of GnRHa ovulation trigger dose on follicular fluid characteristics and granulosa cell gene expression profiles. *J Assist Reprod Genet* 2017;**34**:471–478.

Wale PL, Gardner DK. The effects of chemical and physical factors on mammalian embryo culture and their importance for the practice of assisted human reproduction. *Hum Reprod Update* 2016;**22**:2–22.

Wang N, Li C-Y, Zhu H-B, Hao H-S, Wang H-Y, Yan C-L, Zhao S-J, Du W-H, Wang D, Liu Y *et al.* Effect of vitrification on the mRNA transcriptome of bovine oocytes. *Reprod Domest Anim* 2017;**52**:531–541.

Wells D, Patrizio P. Gene expression profiling of human oocytes at different maturational stages and after in vitro maturation. *Am J Obstet Gynecol* 2008;**198**:455.e1.

Wolf WM, Wattick RA, Kinkade ON, Olfert MD. Geographical prevalence of polycystic ovary syndrome as determined by region and race/ethnicity. *Int J Environ Res Public Health* 2018;**15**:2589.

Wood JR, Dumesic DA, Abbott DH, Strauss JF. Molecular abnormalities in oocytes from women with polycystic ovary syndrome revealed by microarray analysis. *J Clin Endocrinol Metab* 2007;**92**:705–713.

Wyns C, Bergh C, Calhaz-Jorge C, Geyter C, de Kupka MS, Motrenko T, Rugescu I, Smeenk J, Tandler-Schneider A, Vidakovic S *et al.* ART in Europe, 2016: results generated from European registries by ESHRE. *Hum Reprod Open* 2020;**2020**:1–17.

Wyns C, de Geyter C, Calhaz-Jorge C, Kupka MS, Motrenko T, Smeenk J, Bergh C, Tandler-Schneider A, Rugescu IA, Vidakovic S *et al.* ART in Europe, 2017: results generated from European registries by ESHRE. *Hum Reprod Open* 2021;**2021**:1–17.

Xu Y, Sun MH, Xu Y, Ju JQ, Pan MH, Pan ZN, Li XH, Sun SC. Nonylphenol exposure affects mouse oocyte quality by inducing spindle defects and mitochondria dysfunction. *Environ Pollut* 2020;**266**:114967.

Yang H, Kolben T, Meister S, Paul C, Dorp J, van Eren S, Kuhn C, Rahmeh M, Mahner S, Jeschke U *et al.* Factors influencing the in vitro maturation (IVM) of human oocyte. *Biomedicines* 2021;**9**:1904.

Yang ZY, Ye M, Xing YX, Xie QG, Zhou JH, Qi XR, Kee K, Chian RC. Changes in the mitochondria-related nuclear gene expression profile during human oocyte maturation by the IVM technique. *Cells* 2022;**11**:297.

Ye M, Yang ZY, Zhang Y, Xing YX, Xie QG, Zhou JH, Wang L, Xie W, Kee KK, Chian RC. Single-cell multiomic analysis of in vivo and in vitro matured human oocytes. *Hum Reprod* 2020;**35**:886–900.

Yuan L, Yin P, Yan H, Zhong X, Ren C, Li K, Chin Heng B, Zhang W, Tong G. Single-cell transcriptome analysis of human oocyte ageing. *J Cell Mol Med* 2021;**25**:6289–6303.

Zhang F, Zhang ZY, Cai MD, Li XX, Li YH, Lei Y, Yu XL. Effect of vitrification temperature and cryoprotectant concentrations on the mRNA transcriptome of bovine mature oocytes after vitrifying at immature stage. *Theriogenology* 2020a;**148**:225–235.

Zhang HL, Xu Y, Ju JQ, Pan ZN, Liu JC, Sun SC. Increased environment-related metabolism and genetic expression in the in vitro matured mouse oocytes by transcriptome analysis. *Front Cell Dev Biol* 2021;**9**:642010.

Zhang J, Liu X, Chen L, Zhang S, Zhang X, Hao C, Miao Y. Advanced maternal age alters expression of maternal effect genes that are essential for human oocyte quality. *Aging (Albany NY)* 2020b;**12**:3950–3961.

Zhao H, Li T, Zhao Y, Tan T, Liu C, Liu Y, Chang L, Huang N, Li C, Fan Y *et al.* Single-cell transcriptomics of human oocytes: environment-driven metabolic competition and compensatory mechanisms during oocyte maturation. *Antioxid Redox Signal* 2019;**30**:542–559.

Supplementary Table S1. Summary of studies investigating transcriptomic effects of lifestyle and environmental factors. FC : absolute fold change.

Authors	Year	Tissue	Groups compared	Sample size	Population	Technique	Significance threshold	Main results
Endometriosis								
Ferrero *et al.*	2019	Oocyte (MII)	Endometriosis vs healthy	Endometriosis : n=16 Control : n=16	Age : 18-31 yo for control, 24-34 yo for endometriosis BMI : 18.6-31.2 kg/m2 Endometriosis : ovarian endometrioma (bilateral or unilateral) Control : healthy egg donors, no infertility problems	scRNA-seq	FDR<0.05 (t-test)	520 DEGs involved in steroid metabolism, response to oxidative stress, cell growth regulation, mitochondrion, methylation, angiogenesis Affected or unaffected ovaries show similar pattern
PCOS								
Li *et al.*	2021	Oocyte (GV stage)	PCOS vs healthy	PCOS : n=3 Control : n=3	Age : 35.60±2.23 for control, 32.40±1.29 for PCOS BMI : 17.7-28.1 kg/m2 Control : regular menstrual cycle, normal appearance of ovaries, no clinical signs of PCOS	RNA-seq	FDR<0.05, log2FC>1.5 (DESeq2)	2755 DEGs involved in chromatin, microtubule, cytoskeleton, actin, MAPK signaling, mTOR signaling, FOXO signaling, spliceosome, gap junction, meiosis, oxidative phosphorylation 826 transposable elements dysregulated
Liu *et al.*	2016	Oocyte (GV, MI, MII stage)	PCOS vs healthy	PCOS : n=11 (3 GV, 4 MI, 4 MII) Control : n=9 (3 GV, 3 MI, 3 MII)	Age : 28.5±3.7 for control, 27.4 ±3.0 for PCOS BMI : 22.7±3.1 and 22.7±3.9 kg/m2 Control : regular menstrual cycle, normal luteum serum progesterone levels, normal ovarian morphology	scRNA-seq	FDR<0.05 (?)	GV : 606 DEGs MI : 437 DEGs MII : 839 DEGs (notably hormone receptors) Meiosis and maturation down-regulated at GV but normal at MI and MII Cell-cell communication down-regulated between oocytes and its CCs at all stages
Qi *et al.*	2020	Oocyte (GV, MI, MII stage)	PCOS vs healthy	PCOS : n=20 (7 GV, 4 MI, 9 MII) Control : n=14 (6 GV, 5 MI, 3 MII)	Age : 29.7±0.6 for control, 27.4 ±1.1 for PCOS BMI : 18.6±0.4 and 19.7±0.6 kg/m2 Control : regular menstrual cycle, normal luteum serum progesterone levels, normal ovarian morphology	scRNA-seq	p-value<0.05, FC>=2 (DESeq2)	GV : 2426 DEGs related to mitochondria-related processes and oocyte development MI : 1298 DEGs MII : 1181 DEGs No mitochondrial function alteration at MI and MII
Wood *et al.*	2007	Oocyte (MII)	PCOS vs healthy	PCOS : n=6 Control : n=6	Age : 31.3±0.8 for control, 30.6±1.4 for PCOS	HG-U133 Plus 2.0 (Affymetrix)	p-value<0.05 (one-way ANOVA)	374 DEGs related to signal transduction, cellular metabolism,

					BMI : 23.6±1.3 and 31.0±3.8 kg/m2 Control : regular menstrual cycle, normal luteum serum progesterone levels, male or tubal factor infertility			DNA transcription, RNA processing, cellular architecture + maternal effect genes and meiosis/mitotic cell cycle
Age								
Grondahl *et al.*	2010	Oocyte (MII)	Young vs advanced maternal age	Young group : n=10 Advanced group : n=5	Age : <36 yo for young, 37-39 for advanced No ovarian cysts and endometrial thickness	HG-U133 Plus 2.0 (Affymetrix)	p-value<0.05, FC>=1.5, difference of means>50 (univariate two-sample t-test)	342 DEGs involved in cell cycle regulation, chromosome aligment, sister chromatid separation, oxidative stress, ubiquitination
Llonch *et al.*	2021	Oocyte (GV and MII)	Changes with aging	GV : n=40 MII : n=32	Age : 18-43 yo BMI : 18.8-30 kg/m2 except two (17 and 32) Infertility : advanced maternal age and male factor (exclusion of endometriosis, history of cancer, chronic infection)	scRNA-seq	p-value<0.01, FC>2 (seurat)	GV : 596 DEGs related to no GO term MII : 1219 DEGs related to chromosome segregation, mitochondrial function, RNA metabolism Only 29 genes overlapping in both comparisons
Ntostis *et al.*	2021	Oocyte (GV and MII)	Young vs advanced maternal age	Young : n=5 GV and n=5 MII Advanced : n=5 GV and n=6 MII	Age : 21-26 yo for young, 41-44 yo for advanced Infertility : male factor or unexplained Young group with no infertility (donor)	scRNA-seq	FDR<0.05, FC>2 (GLM)	GV : 10 DEGs MII : 1191 DEGs (111↗ and 1080↘ with age) -> mitochondria related biological process, translation
Reyes *et al.*	2017	Oocyte (GV and MII)	Young vs advanced maternal age	Young : n=5 GV and n=5 MII Advanced : n=5 GV and n=5 MII	Age : 20-29 yo for young, 40-43 yo for advanced Oocyte donors Infertility : varying causes	scRNA-seq	FDR<0.05, FC>2 (DESeq2)	GV : 1 DEG with age MII : 255 DEGs related to oocyte maturation, mitochondria, cell cycle and cytoskeleton
Steuerwald *et al.*	2007	Oocyte (MII)	Young vs advanced maternal age	Young : 2 pools of 10 oocytes intermediate : 1 pool of 10 oocytes Advanced : 2 pools of 10 oocytes	Age : <32 yo for young, >40 yo for advanced, >32 & <40 for intermediate Infertility : tubal disorder, advanced maternal age, male factor	Affymetrix GeneChip® Human Genome Focus Arrays	FC>1.5	608 DEGs related to cell cycle regulation and control,cell signaling, cytoskeletal structure, energy pathways and mitochondrial function, DNA damage response and repair, protein transport and trafficking, transcription, protein phosphorylation
Yuan *et al.*	2021	Oocyte (MII)	Young vs advanced maternal age	Young : n=3 Advanced : n=6	Age : <30 yo for young, >40 yo for advanced BMI : 21.5±1.6 and 22.4±2.1 kg/m2 Infertility : unknown	scRNA-seq	q-value<0.05, FC>2 (DESeq2)	481 DEGs related to transcription, ubiquitination, epigenetic regulation, cellular processes, cell cycle, protein-protein interactions
Zhang *et al.*	2020	Oocyte (MII)	Young vs advanced maternal age	Young : n=3 Advanced : n=3	Age : <30 yo for young, >40 yo for advanced Infertility : non-ovarian reasons, tubal blockage, uterine disease, male factor	scRNA-seq	No information	357 DEGs involved in transcriptional activation, oxidative stress, immune function and catalytic activity

Diminished ovarian reserve								
Barragan *et al.*	2017	Oocyte (MII)	Low vs high antral follicle count (AFC)	Low AFC : n=18 (young + advanced maternal age) High AFC : n=17 (young + advanced maternal age)	Age : 21±1 /24±2 yo for young, 32±2/34±1 yo for advanced BMI <30 kg/m2 Healthy oocyte donors : no evidence of systemic or reproductive conditions, negative for HIV, no sexually transmitted diseases, no hepatitis C and B Low AFC : 8±2/7±1 follicles High : 24±3/29±7 follicles	GeneChip Human Transcriptome Array 2.0 (Affymetrix) RT-qPCR validation	FDR<0.05, FC>2 (linear regression)	77 DEGs : 22 mRNAs and 55 ncRNAs
Smoking								
Budani *et al.*	2017	MGC	Smokers vs non-smokers	Smokers : n=20 Control : n=20	Age : 32.8±4.1 and 33.7±3.8 yo BMI : 21.5±3.5 and 22.5±3.6 kg/m2 Infertility : male factor, unexplained, tubal or unknown Patients taking micronutrient supplements excluded Smoking habits were assessed by a questionnaire	RT-qPCR	p-value<0.05 (t-test)	Higher expression of SOD2 with smoking
Konstantinidou *et al.*	2021	CC	Smokers vs non-smokers	Smokers : n=5 Control : n=5	Age : <39 yo BMI : 19–25 kg/m2 Infertility : tubal or male factors (exclusion of endometriosis, history of poor response in previous ART cycles or history of severe OHSS, AFC<7, >3 ART attempts without clinical pregnancy) Patients taking micronutrient supplements excluded Smoking habits were assessed by a questionnaire	RT-qPCR	p-value<0.05 (one-way ANOVA)	26 DEGs related to cell death and survival, cell cycle, cell signaling, cellular growth and proliferation, gene expression, free radical scavenging, cellular function and maintenance and DNA replication, recombination and repair
BMI								
Ruebel *et al.*	2017	Oocytes (GV, MI and MII)	Obese vs normal weight	Obese : n=11 Control : n=13	Age : 18-38 yo BMI : 22.3±0.6 for normal, 32.3±1.8 kg/m2 for obese Infertility : male factor, ovulatory disorder, tubal factor, endometriosis, unexplained (PCOS, diabete, cardiovascular disease excluded)	scRNA-seq	p-value<0.05, FC>2 (DESeq2)	GV : 192 DEGs (cytokine-cytokine receptor) MI : 624 DEGs (metabolic pathways/MAPk signalling) MII : 468 DEGs (metabolic pathways and mTOR signaling)

Supplementary Table S2. Summary of studies investigating transcriptomic effects of ovarian stimulation. FC : absolute fold change.

Authors	Year	Tissue	Groups compared	Sample size	Population	Technique	Significance threshold	Main results
Ovarian stimulation								
Devjak *et al.*	2012	CC	GnRH-a & GnRH-anta	GnRH-a : n=6 MI and 9 MII GnRH-anta : n=4 MI and 6 MII	Age : <35 yo BMI : 17-26 kg/m2 Infertility : tubal factor	Human Gene 1.0ST Arrays (Affymetrix)	FDR<0.05 (two-way ANOVA)	No difference
Adriaenssens *et al.*	2010	CC	HP-hMG & rFSH	HP-hMG : n=35 rFSH : n=28	Age : 33±6 and 34±5 yo BMI : 23±5 and 22±3 kg/m2 Infertility : male factor (69% of HP-hMG/82% of rFSH), female factor (7%/6%), unknown (10%/6%) or male+female (14%/6%)	RT-qPCR	p-value<0.05 (regression model)	with rFSH : ↗SPROUTY4, ↘SDC4
Assou *et al.*	2013	CC	HP-hMG & rFSH	HP-hMG : n=53 (6 abnormal, 17 immature, 30 MII) rFSH : n=93 (1 abnormal, 21 immature, 71 MII)	Age : 21–34 yo BMI : 18–25 kg/m2 Infertility : unexplained or mild male factor	HG-U133 Plus 2.0 (Affymetrix)	FDR<0.05, FC>=1.5 (Wilcoxon test)	94 DEGs : lipid metabolism, cell-cell interaction, cellular assembly and organization, tumour necrosis factor
Cruz *et al.*	2017	CC	HP-hMG & rFSH & urinary FSH	HP-hMG : n=6 rFSH : n=5 urinary FSH : n=5	Age : 18-35 yo BMI : 20.6±0.9, 22.9±0.9 and 21.5±1.3 kg/m2 Healthy oocyte donors (regular menstrual cycle, no hereditary or chromosomal diseases, negative for sexually transmitted diseases)	Whole Human Genome Microarray 4x44k (Agilent)	p-value<0.05, FC>2 (non-parametric test)	rFSH vs hMG : 75 DEG involved in regulation of developmental process and anatomical structure development urinary FSH vs hMG : 155 DEG involved in biosynthetic and metabolic process rFSH vs urinary FSH : 43 DEG
Gatta *et al.*	2013	CC	HP-hMG & rFSH & rLH+rFSH	HP-hMG : n=4 rFSH : n=8 rLH+rFSH : n=4	Age : <35 yo BMI : 18.5–24.9 kg/m2 Infertility : male factor, tubal disease, unexplained infertility	Human Whole Genome OneARRAy Microarray V5 (Phalanx)	Clustering analysis of genes with FC>1.7, measurable expression in >80% of samples	499 DEGs with rLH+rFSH compared to rFSH 3369 DEGs with HP-hMG compared to rFSH
Brannian *et al.*	2010	MGC	HP-hMG & rFSH	HP-hMG : n=4 rFSH : n=4	Age : <35 yo BMI : 22.3±0.3 & 22.2±0.9 kg/m2 Infertility : tubal or male factor	CodeLink Whole Human Genome Bioarrays	p-value<0.05, FC>2 (t-test)	1736 DEGs : signal transduction, transcription regulation, metabolism
Grondahl *et al.*	2009	MGC	HP-hMG & rFSH	HP-hMG : n=15 rFSH : n=15	Age : 21-39 yo (30.9±4.8 & 31.7±3.6) BMI : unknown Infertility : male factor, tubal disease, unexplained, mild endometriosis	HG-U133 Plus 2.0 (Affymetrix)	p-value<0.05 (Welch t-test), FC>1.5, mean difference of 40 expression units	85 DEGs : cellular lipid metabolism, lipid metabolism, phosphate metabolism, phosphorus metabolism, protein amino acid dephosphorylation

Gurgan *et al.*	2014	CC	FSH+rFSH (sequential) & FSH or rFSH alone	FSH : n=15 rFSH : n=15 FSH+rFSH : n=15	Age : 30.2±4.8 yo BMI : 24.3±4.0 kg/m2 Infertility : no PCOS	HG-U133 Plus 2.0 (Affymetrix)	p-value<0.05 (one-way ANOVA and unpaired t-test), FC>=1.5	579 DEGs : cholesterol metabolism, cell morphology, cell death, cell growth and proliferation, embryonic development, cell adhesion, differentiation, transformation, protein synthesis
Barberi *et al.*	2012	CC	rFSH alone & r-LH supplementation	rFSH : n=11 rFSH+rLH : n=7	Age : 31–42 yo (32.3±0.3 & 34.1±1.4) BMI : 18–25 kg/m2 Infertility : tubal or unexplained or partners with semen abnormalities	multiplex RT-PCR	p-value<0.05 (two-tailed t-test)	With r-LH : ↗ PTGS2 and HAS2
Liu *et al.*	2022	MGC	Mild ovarian stimulation & conventional COS	Mild COS : n=27 Conventional COS : n=21	Age : 39.2±3.2 & 38.0±3.7 yo BMI : 23.1±2.7 & 21.7±1.9 kg/m2 Poor ovarian responders (exclusion of endocrine disorders, ovarian surgery history, radio- or chemo-therapy, ovulatory dysfunction, endometriosis and PCOS)	RNA-seq	FDR<0.05 (edgeR)	425 DEGs : cytokine activity, regulation activity, immune response, oocyte development, cytokine-cytokine receptor, TGF-beta signaling pathway, cGMP-PKG signaling pathway, metabolic pathway
Triggering method								
Borgbo *et al.*	2013	CC and MGC	hCG & GnRH-a trigger	CC : n=19 (10 GnRH-a/9 hCG) MGC : n=16 (10 GnRH-a/6 hCG)	Age : 24-35 yo BMI : 18.9-30.7 kg/m2 (24.9 & 23.8) Infertility : male factor, tubal disease, unexplained, mild endometriosis	Human Gene 1.0ST Arrays (Affymetrix)	p-value<0.05, FC>1.5 (t-test)	CC : 391 DEGs involved in lipid metabolism, steroidogenesis MGC : 252 DEGs involved in cellular movement, cardiovascular development
Haas *et al.*	2014	MGC	hCG & GnRH-a trigger	hCG : n=12 GnRH-a : n=12	Age : <40 yo (31.8±3.3 & 31.7±4.8) BMI : unknown Infertility : tubal factors, male factor (PCOS and endometriosis excluded) Preimplantation genetic diagnosis	RT-qPCR	p-value<0.05 (two-tailed t-test)	↘ VEGF, inhibin beta B, CYP19A1, CYP11A1, 3betaHSD, FSHR, with GnRH-a Amphiregulin ↗ with GnRH-a
Haas *et al.*	2016	MGC	hCG & hCG+GnRH-a trigger	hCG : n=15 hCG+GnRH-a : n=15	Age 35.6±7.4 & 36.1±7.2 yo BMI : unknown Infertility : male, unexplained, mechanical Preimplantation genetic diagnosis Two subsequent cycled within 1 year	RT-qPCR	p-value<0.05 (two-tailed t-test)	Amphiregulin, epirgulin and PEDF ↗ with dual trigger conexin43 ↘ with dual trigger
Vuong *et al.*	2017	MGC	GnRH-a trigger at different doses (0.2, 0.3, 0.4 mg)	0.2mg : n=10 0.3mg : n=10 0.4mg : n=10	Age : 18–35 yo BMI : <28 kg/m2 Oocyte donors : normal ovarian reserve or antral follicle count (exclusion of	RT-qPCR	p-value<0.05 (two-tailed test)	No difference in genes tested

					PCOS/anovulation/chronic medical condition)			
Weizman *et al.*	2019	CC	Single trigger (hCG or GnRH-a) & dual trigger (hCG+GnRH-a)	High responder : n=5 single vs n=6 dual Normal responder : n=4 single vs n=5 dual Poor responder : n=4 single vs n=6 dual	Age : 27-42 yo (34.0±1.3, 33.0±2.1, 38.3±2.1, 35.8±1.2, 36.3±1.9, 36.5±2.1) BMI : 19-32 kg/m2 High responder : PCOS/OHSS/previous cycle cancellation or coasting/high levels of anti-Müllerian hormone/>13 follicle >=11mm on triggering day Poor responder : Age >40 or low ovarian reserve/previous poor response/low levels of anti-Müllerian hormone/<4 retrieved oocytes No chronic disease	RNA-seq	FDR<0.05, FC>1.5 (edgeR)	High responder : 1766 DEGs related to apoptosis, cell-cycle regulation, extracellular matrix synthesis and remodelling, angiogenic and cell adhesion Normal responder : 3106 DEGs related to apoptosis, cell-cycle regulation, immune response, oocyte growth and maturation, extracellular matrix Poor responder : 1825 DEGs related to PEDF pathway, cell-cycle regulation, apoptosis, metabolism, transcription activation, angiogenesis, cell adhesion, migration, inflammation, oocyte maturation
COS vs natural cycles								
de los Santos *et al.*	2012	CC	COS vs natural cycle	Natural : n=4 COS : n=4	Age : <35 yo BMI : 19.3–28.9 kg/m2 Oocyte donors	Whole Human Genome Oligo Microarray (Agilent)	p-value<0.05, FC>2 (non-parametric test)	18 DEGs : cellular developmental process, cell activation, cell differentiation, immune system development, regulation of biological quality
Lu *et al.*	2019	MGC	COS vs natural cycle	Natural : n=3 COS : n=4	Age : <36 yo BMI : 18.8-26.6 kg/m2 Infertility : male or tubal factors (exclusion ovulatory disorder or follicular dysplasia)	RNA-seq	FDR<0.05 (DEGSeq)	1002 DEGs : cell cycle, chromosome segregation, oocyte meiosis, steroid hormone biosynthesis, oocyte maturation, ovarian steroidogenesis, immune response or processes, cyotkine-cytokine receptor, chemokine signiling, NF-kapp B signialing
Papler *et al.*	2013	CC	COS vs modified natural cycle (MNIVF)	MNIVF : n=3 COS : n=5	Age : <35 yo BMI : 17-26 kg/m2 Infertility : tubal cause, normal partners spermiogram Natural IVF cycle and COH in subsequent cycle	Human Gene 1.0ST Arrays (Affymetrix)	FDR<0.05 (mixed model ANOVA)	66 DEGs : olfactory transduction, RNA degradation, RNA transport, neuroactive ligand receptor interaction, ribosome biogenesis and ribosome, glutathione metabolic process, xenobiotic metabolic process, oxidation-reduction, gene expression

Supplementary Table S3. Summary of studies investigating transcriptomic effects of oocyte in vitro maturation (IVM). FC : absolute fold change.

Authors	Year	Tissue	Groups compared	Sample size	Population	Technique	Significance threshold	Main results
Rescue IVM								
Jones *et al.*	2008	Oocyte	*In vivo* maturation vs rescue IVM	*In vivo* : n=11 IVM : n=3	No information	Codelink Whole Human Genome Bioarrays	FDR<0.05 (Welch t-test)	2766 DEGs : 198 GO involved transcription, cell cycle, transport, cellular protein metabolism (all ↗ with IVM)
Lee *et al.*	2021	Oocyte	*In vivo* maturation vs rescue IVM IVM low vs high quality oocytes IVM low vs high MII ratio	*In vivo* : n=10 IVM : n=11	Age : 35.1±1.9 & 35.4±4.9 yo BMI : 23.4±2.6 & 23.3±4.5 kg/m2 Infertility : no information	Single-cell RNA-seq	FDR<0.05, FC>2 (DESeq2)	1559 DEGs : metabolic process, biosynthesis, oxidative phosphorylation
Virant-Klun *et al.*	2018	Oocyte	In vivo maturation vs rescue IVM IVM with CC or not	*In vivo* : n=30 IVM : n=30	Infertility : male factor	Agilent Whole Human Genome Oligo Microarray 8x60K v2	FDR<0.05 (t-test)	Positive regulation of transcription, placenta development, fatty acid beta-oxidation, histone H3 acetylation, and cortical actin cytoskeleton organization, nucleic acid binding transcription factor activity and microtubule motor activity, and cellular component of intracellular organelle ↗ *in vivo* mRNA metabolic process, translation, mitochondrion organization, and respiratory electron transport chain, RNA binding and structural constituent of ribosome, and intracellular membranebounded organelle as a cellular component ↘ *in vivo*
Wells and Patricio	2007	Oocyte	In vivo maturation vs rescue IVM	*In vivo* : n=15 IVM : n=10	Age : 35.3±2.1 yo Infertility : male factor (no ovarian pathology)	Applied Biosystems Human Genome Survey Microarray	No information on threshold	Biological process in ↗ genes with IVM : signal transduction, nucleic acid metabolism, protein metabolism, tRNA metabolism, lipid and steroid metabolism Biological process in ↘ genes with IVM : protein biosynthesis, protein metabolism, translational regulation, cell cycle, cell surface receptor mediated signal transduction, homeostasis

Zhao *et al.*	2019	Oocyte	In vivo maturation vs rescue IVM	*In vivo* : n=3 IVM : n=3 (same patients)	Age : 28-32 yo BMI : 18.3-25.4 kg/m2 Infertility : male factor	scRNA-seq	q-value<0.05, FC>2 (DESeq)	8260, 9168, 11263 DEGs per women with 2230 in common : metabolic and signaling pathways (kinases and CoA production)
Li *et al.*	2019	Oocyte	rescue IVM vs rescue IVM with growth hormone	*In vivo* : n=3 IVM : n=3 (same patients)	Infertility : male factor	scRNA-seq	adjusted p-value<0.05 (DESeq)	507 DEGs : meiotic progression, redox homeostasis of cellular environment, oocyte developmental competence
Ouandaogo *et al.*	2012	CC	*In vivo* maturation vs rescue IVM in PCOS patients	*In vivo* : n=9 IVM : n=9	Age : 32.3+3.3 & 33.8+3.1 yo Infertility : PCOS	HG-U133 Plus 2.0 (Affymetrix)	FDR<0.05, FC>2 (SAM)	5219 DEGs : cumulus expansion, oocyte maturation, cell cycle, DNA replication, recombination and repair
IVM								
Yang *et al.*	2022	Oocyte	*In vivo* maturation vs IVM	*In vivo* : n=8 IVM : n=12	No information	scRNA-seq	p-value<0.05 (Wilcoxon test)	2281 DEGs : cell-substrate adherens junction, cytosolic ribosome, focal adhesion, mitochondrial protein complex, mitochondrial respiratory chain complex, ribosomal subunit, ribosome, nucleoside triphosphate metabolic process, protein targeting, cadherin binding, NADH dehydrogenase activity, ubiquitin-like protein ligase binding
Ye *et al.*	2020	Oocyte	*In vivo* maturation vs IVM	*In vivo* : n=8 IVM : n=7	No information	scTrioseq	roc (0.7) method (Seurat)	507 DEGs : cell cycle, mRNA metabolism, DNA metbaolism, mitochondrial respiratory chain complex I biogenesis, response to endomplasmic reticulum stress, ATP metabolism

Supplementary Table S4. Summary of studies investigating transcriptomic effects of oocyte cryopreservation. FC : absolute fold change.

Authors	Year	Tissue	Groups compared	Sample size	Population	Technique	Significance threshold	Main results
Barberet *et al.*	2022	Oocyte	Fresh vs vitrification Semi-automated vs manual vitrification	Fresh : n=7 Semi-automated : n=7 Manual : n=6	Age : 21-36 yo Sibling oocytes (3 conditions for each patient) One oocyte donor	scRNA-seq	FDR<0.05 (DESeq2)	Manual vs semi-automated : 5 DEGs Fresh vs vitrification : 108 DEGs involved in mRNA catabolic process and ribonucleoprotein complex biogenesis
Chamayou *et al.*	2011	Oocyte	Fresh vs cryopreservation Slow freezing vs vitrification	Fresh : n=15 Slow freezing : n=15 Vitrification : n=15	No information	RT-qPCR	p-value<0.001 (z-test)	NAP1L1, TOP1, H1F0H1, SMC, SCC3, RAD21, SMC1A, SMC1B, STAG3, ATP5GJ, SDHC, CLTA, MAPK6, CKS2, DPPA3, OCTA4, FOXJ2 differentially expressed with freezing Decrease in mRNA content in both freezing procedures compared with fresh oocytes
D'Aurora *et al.*	2019	Oocyte	Fresh vs vitrification	Fresh : n=16 Vitrification : n=16	Age : two groups (<35yo and >35yo) BMI : normal Infertility : male, tubal or unexplained (exclusion of endometriosis)	RT-qPCR	p-value<0.05 (Wilcoxon)	No difference
Di Pietro *et al.*	2010	Oocyte	Fresh vs vitrification	Fresh : n=10 Vitrification : n=15	Infertility : male factor (exclusion of endometriosis, ovarian insufficiency, PCOS)	RT-qPCR	p-value<0.01 (t-test)	No difference
Huo *et al.*	2020	Oocyte	Fresh vs vitrification Storage time	Fresh : n=3 Vitrification : n=13 (1 months : 3/2 months : 3/3 months : 4/12 months : 3)	Age : 30-32 yo Infertility : tubal (exclusion of ovarian pathology)	scRNA-seq	FDR<0.05, FC>2 (multiple t-tests)	Storage time : 0 DEG 1987 DEGs between fresh and vitrified oocytes : cell cycle, meiosis, oocyte growth, oocyte development, microtubule-based process, methylation, ubiquinone biosynthetic process, tricarboxylic acid cycle, MAPK cascade
Monzo *et al.*	2012	Oocyte	Fresh vs cryopreservation Slow freezing vs vitrification	Fresh : n=3 pools (54 oocytes from 11 patients) Slow freezing : n=3 pools (59 oocytes from 16 patients) Vitrification : n=4	Age : <36 yo Infertility : male factor (exclusion of gynecological disorders)	HG-U133 Plus 2.0 (Affymetrix)	FC>5 (SAM)	Fresh vs slow freezing : 388 DEGs involved in role of BRCA1 in DNA damage response, aldosterone signaling pathway, cell cycle Fresh vs vitrification : 608 DEGs involved in ubiquitination pathway, growth hormone signaling pathway, cell cycle

				pools (86 oocytes from 21 patients)				
Stigliani *et al.*	2015	Oocyte	Fresh vs slow freezing Storage time	Fresh : n=3 pools (31 oocytes from 13 patients, two pools of 10 and one pool of 11) Slow freezing : n=4 pools for the 3 years storage group (32 oocytes from 6 patients, pools of 8 oocytes), n=4 pools for the 6 years storage group (36 oocytes from 6 patients, pools of 9 oocytes)	Age : 26-38 yo Infertility : no ovarian pathology	Human GE 4x44 K v2 (Agilent)	FDR<0.1, FC>3 (t-test)	Overall decrease of mRNA content between fresh and cryopreserved No difference between storage time group in mRNA content and differential expression Fresh vs cryopreserved : 102 DEGs involved in chromosome organization, RNA splicing, cell-cycle, process, response to DNA damage stimulus, cellular response to stress, DNA repair

Supplementary Figure S1. Concordance in the main findings of the 50 studies evaluated in this review, depending on the factors studied. *Some studies have assessed multiple conditions and should not be counted twice in the total (total number of studies included is 50). A : animal, CC : cumulus cells, H : human, MGC : mural granulosa cells, OO : oocyte.

	Condition	Human (H) or animal (A) evidence	Are results consistent between studies ?
	PCOS	H (OO)	4/4
	Endometriosis	H (OO)	1/1
	Ovarian reserve	H (OO)	1/1
	Maternal aging	H (OO)	7/7
	Smoking	A (OO) and H (MGC/CC)	2/2
	Obesity/diet	H (OO)	1/1
	GnRH-a protocol	H (CC)	1/1
	FSH isoforms and HP-hMG stimulations	H (MGC/CC)	rFSH vs HP-hMG : 3/6 rLH supplementation : 0/2* FSH origin : 2/2* Dose effect : 1/1
	hCG trigger	H (MGC/CC)	hCG vs GnRH-a : 0/2 hCG vs dual trigger : 0/2 Dose : 1/1
	COH itself	A (OO) and H (MGC/CC)	0/3
	Rescue IVM	H (OO)	5/6 Growth hormone supplementation : 1/1
	Medical IVM	H (OO)	2/2
	O2	A (OO)	-
	T°C	A (OO)	-
	Pollutants	A (OO)	-
	Cryoconservation	H (OO)	7/7

3.2) Effets sur l'embryon chez l'Homme

L'embryon est transcriptionnellement silencieux chez l'Homme jusqu'au jour 3 après la fécondation et dépend exclusivement des ARNm maternels fournis par l'ovocyte (Braude *et al.*, 1988; Vassena *et al.*, 2011). Durant cette période, la capacité de l'embryon à maintenir son métabolisme et son homéostasie cellulaire peut donc être compromise si des modifications suboptimales de son micro-environnement surviennent (Edwards *et al.*, 1998; Lane & Gardner, 2001). Par exemple, chez la souris, une courte exposition de l'embryon pré-compaction compromet les capacités de développement ultérieur par rapport à la même exposition post-compaction (Zander *et al.*, 2006). Les nombreux processus impliqués dans les techniques d'AMP, notamment au niveau de la culture embryonnaire (stress osmotique, variation des substrats, volatilité de certaines substances organiques) sont susceptibles de déclencher des mécanismes de réponse au stress chez l'embryon (Puscheck *et al.*, 2015). Ainsi, de nombreux paramètres dans les pratiques d'AMP doivent être étroitement contrôlés, en particulier ceux qui entourent la culture embryonnaire.

Avant cette thèse, seules deux études ont comparé le profil transcriptomique d'embryons humains cultivés dans deux milieux de culture différents, mais au stade blastocyste (post-compaction). Utilisant la technologie du microarray, elles ont tout de même rapporté des dérégulations des gènes impliqués dans le cycle cellulaire, l'apoptose, la dégradation des protéines et le métabolisme, qui ont la capacité d'altérer le développement de l'embryon (Kleijkers *et al.*, 2015; Mantikou *et al.*, 2016).

Chapitre 2 : Analyses biologiques sur expérimentations réalisées au laboratoire

Ainsi ces analyses à partir des données de la littérature et cet état de l'art concernant le transcriptome et le méthylome façonnés par les interventions en AMP amène de nombreuses interrogations concernant la sécurité de ces techniques et définissent un certain nombre d'enjeux auxquels mes travaux de thèse ont tenté de répondre.

Ces données nous font prendre conscience que le contenu transcriptomique de l'ovocyte et de l'embryon pré-implantatoire dictent de façon cruciale l'issue du développement embryonnaire. Ces périodes représentent les moments où l'ovocyte et l'embryon sont les plus vulnérables à leur environnement alors que les techniques d'AMP les plus invasives prennent place dans cette même fenêtre temporelle. Il apparaît notamment un manque de données concernant les effets de la vitrification ovocytaire au niveau transcriptomique, que cette thèse permet d'adresser par une étude originale comparant des ovocytes frais à des ovocytes vitrifiés manuellement ou semi-automatiquement (Barberet *et al.*, 2022a). De plus, pour la première fois, cette thèse évalue l'impact du choix du milieu de culture embryonnaire sur des embryons pré-implantatoires au jour 2 et au jour 5 afin d'identifier le comportement du transcriptome embryonnaire face à des conditions de culture différentes (Ducreux *et al.*, 2023).

Par ailleurs l'analyse critique de la littérature des modifications des profils de méthylation par notre revue systématique et méta-analyse a mis en lumière un manque de données produites en post-natal. Aucune étude n'évaluait les profils de méthylation d'enfants de 7-8 ans conçus par FIV/ICSI. Nous avons donc mis en place une telle étude (Ducreux *et al.*, 2021).

I) Le transcriptome ovocytaire et embryonnaire est-il influencé par différentes techniques d'AMP ?

L'ovocyte et l'embryon pré-implantatoire subissent de nombreuses interventions en AMP alors même que paradoxalement, ces périodes du développement constituent celles où ils sont extrêmement vulnérables à l'environnement extérieur. En accord avec la DOHaD (Developmental Origins of Health and Disease), il est d'intérêt de santé publique d'avoir un regard critique sur les effets potentiels de ces interventions sur l'expression des gènes.

Comme vu plus en amont, nous avons examiné si différentes techniques (stimulation ovarienne, cryopréservation, maturation *in vitro*, etc) modulent l'expression de gènes impliqués dans des fonctions biologiques analogues. Cette thèse a pour objectif de renforcer cette littérature existante par une nouvelle étude évaluant les effets de la vitrification ovocytaire, manuelle ou semi-automatique, afin de préciser l'influence de cette technique sur le contenu transcriptomique ovocytaire alors que cette technique fait face à une demande croissante de la population pour des raisons cliniques, éthiques et sociales.

Pour terminer, cette thèse ira plus en aval du développement embryonnaire, au stade 4-cellules et blastocyste pour mieux cerner les enjeux de la culture embryonnaire. Les effets de différentes formulations de milieux de culture embryonnaire pré-compaction seront comparés, une période où l'embryon apparaît fragile du fait de l'absence de contrôle embryonnaire.

1) Comparaison de la vitrification d'ovocytes à l'aide d'un système fermé semi-automatique ou manuel sur le transcriptome d'ovocytes humains appariés

1.1) Objectifs

Jusqu'à présent, six études ont examiné l'impact de la cryoconservation des ovocytes sur leur transcriptome chez l'Homme. Parmi elles, une seule étude a utilisé le scRNA-seq et sur un échantillon assez réduit de 16 ovocytes, les autres ayant eu recours aux technologies de microarrays ou PCR. Dans cette étude scRNA-seq, l'absence de groupe contrôle provenant du même « batch » que les ovocytes vitrifiés est une limite sérieuse aux conclusions tirées (dégradation de l'intégrité de l'ARN et dérégulation de gènes du cycle cellulaire et du développement avec la vitrification) (Huo *et al.*, 2021). Nous avons tenu à proposer la plus grande étude évaluant l'effet de la vitrification sur le transcriptome ovocytaire humain à ce jour, réalisée avec une technologie de pointe (scRNA-seq) et un schéma expérimental statistiquement robuste. De plus aucune étude à ce jour n'a comparé la méthode de vitrification manuelle et semi-automatique. Cette étude permettra de comparer le transcriptome d'ovocytes humains vitrifiés selon ces deux méthodes.

1.2) Matériels et méthodes

Cette étude a été menée prospectivement au CHU de Dijon entre juin 2018 et février 2020. Elle inclut, après recueil de consentement, des patientes réalisant une tentative de FIV ou ICSI pour des raisons médicales et des patientes faisant partie d'un programme de don d'ovocytes.

Pour chaque patiente, trois ovocytes ayant atteint le stade MII au cours des 24 premières heures de culture (stade MIV-MII) ont été répartis de façon randomisée entre les groupes

ovocytes frais, vitrifiés manuellement ou vitrifiés semi-automatiquement, et les transcriptomes ont été analysés et comparés. Trois ovocytes MII *in vivo* supplémentaires ont été inclus le jour du prélèvement des ovocytes collectés chez une patiente faisant partie d'un programme de don d'ovocytes. Les ovocytes ont été vitrifiés manuellement dans un système fermé tandis que les ovocytes MII ont été vitrifiés semi-automatiquement à l'aide de GAVI®.

L'analyse bioinformatique a été réalisée comme évoqué en introduction : contrôle qualité avec *FastQC*, « trimming » avec *TrimGalore!*, alignement sur le génome de référence hg38 avec *STAR*, quantification des lectures pour chaque gène avec *featureCounts*. Le numéro d'intégrité de la transcription (TIN, « transcript integrity number ») a été estimé pour évaluer la qualité de l'ARN post-séquençage pour chaque transcrit canonique à l'aide du logiciel *RSeQC*. Cela nous donnera une indication de l'effet de la vitrification sur la qualité globale du transcriptome. La proportion d'ADN mitochondrial (%mtDNA) (i.e. le pourcentage de lectures de séquençage alignées sur des gènes mitochondriaux) est un marqueur de qualité cellulaire, qui est intéressant pour évaluer sa capacité à être fécondé (Reynier *et al.*, 2001; Santos *et al.*, 2006). Nous l'avons calculé pour chaque ovocyte séquencé en divisant le nombre total de lectures correspondant aux 38 gènes mitochondriaux annotés par la taille de la librairie pour chaque échantillon.

La normalisation et l'analyse différentielle entre les groupes d'ovocytes vitrifiés et frais, puis entre vitrifiés manuellement et semi-automatiquement, ont été réalisé avec *DESeq2*.

1.3) Résultats

Nos résultats affichent des différences largement limitées entre les ovocytes frais et vitrifiés (108 DEGs mais logFC<1) ce qui est rassurant quant à la sécurité de cette technique pour l'intégrité du transcriptome ovocytaire. Il est possible que certains gènes soient sous-exprimés en lien avec la vitrification comme l'indiquent plusieurs études dont la nôtre mais la mesure de l'intégrité des transcrits (TIN) nous indique que la vitrification ne dégrade pas le contenu transcriptomique ovocytaire dans sa globalité. De plus les deux modes de vitrification

testés affichaient des différences minimes (5 gènes différentiellement exprimés). Notre étude sur la vitrification des ovocytes apporte la preuve que cette technique est une avancée notable pour de nombreuses femmes car elle permet de conserver ses ovocytes à des moments opportuns, où les chances qu'ils soient fertilisables sont les plus hautes et sans risque majeur d'altération.

1.4) Article 4 - Comparison of oocyte vitrification using a semi-automated or a manual closed system in human siblings: survival and transcriptomic analyses

Barberet *et al. Journal of Ovarian Research* (2022) 15:128
https://doi.org/10.1186/s13048-022-01064-3

Journal of Ovarian Research

RESEARCH Open Access

Comparison of oocyte vitrification using a semi-automated or a manual closed system in human siblings: survival and transcriptomic analyses

Julie Barberet[1,2†], Bastien Ducreux[1†], Céline Bruno[1,2], Magali Guilleman[1,2], Raymond Simonot[2], Nicolas Lieury[2], Adrien Guilloteau[3], Déborah Bourc'his[4] and Patricia Fauque[1,2,5*]

Abstract

Background: Indications of oocyte vitrification increased substantially over the last decades for clinical and ethical reasons. A semi-automated vitrification system was recently developed making each act of vitrification reproducible. In this study, we evaluated the efficiency of the semi-automated technique of oocyte vitrification by survival rate, morphometric assessment and resistance to empty micro-injection gesture as compared with a manual method. Additionally, we intended to evaluate transcriptomic consequences of both techniques using single-cell RNA-seq technology.

Results: Post-warming survival rate, oocyte surfaces and resistance to empty micro-injection were comparable between semi-automated and manual vitrification groups. Both oocyte vitrification techniques showed limited differences in the resulting transcriptomic profile of sibling oocytes since only 5 differentially expressed genes were identified. Additionally, there was no difference in median transcript integrity number or percentage of mitochondrial DNA between the two groups. However, a total of 108 genes were differentially expressed between fresh and vitrified oocytes (FDR < 0.05) and showed over-represented of genes related to important cellular process.

Conclusions: Our results provide reassurance about the influence of semi-automation as compared with the manual vitrification method. Concerning oocyte vitrification itself, no tight common transcriptomic signature associated has been observed across studies.

Trial registration: NCT03570073.

Keywords: Assisted reproductive technology, Cryopreservation, Oocyte, Single-cell RNA-seq, Vitrification

Background

Following its introduction, and despite the first birth from a frozen oocyte in 1986 [10], oocyte cryopreservation remained a challenging technique for many years. The unique structure of mature oocytes, with a low surface area to volume ratio, makes them particularly sensitive to osmotic stress and high concentrations of cryoprotectant. As an alternative to slow freezing, the introduction of vitrification led to improved outcomes.

†Julie Barberet and Bastien Ducreux equally contributed to this work.

*Correspondence: patricia.fauque@chu-dijon.fr

[5] Laboratoire de Biologie de la Reproduction, CHU Dijon, BP 77908, 14, rue Gaffarel, 21079 Dijon Cedex, France
Full list of author information is available at the end of the article

Authorized in the United Kingdom since 2000 and classified as a non-experimental technique by the American Society for Reproductive Medicine (ASRM) in 2013, survival rates after vitrification have surpassed slow freezing [35], becoming the norm in terms of oocyte cryopreservation. Consequently, indications and the number of oocyte vitrifications are rising worldwide in the field of assisted reproductive technology (ART). In addition to fertility preservation in cases of infertility risk due to gonadotoxic treatments or other medical conditions, oocyte vitrification is used for egg banking in donation programs, to postpone embryo transfer to prevent ovarian hyperstimulation, to build larger cohorts for poor responders, or to delay childbearing [11].

While early randomized controlled trials reported reproductive outcomes similar to those achieved with fresh oocytes [12, 31, 36], some recent cohort studies highlighted lower reproductive outcomes with the use of vitrified oocytes [13, 14, 25]. The loss of oocytes after thawing, leading to a diminished pool of oocytes available for insemination, is likely a reason for the inferior clinical results reported in these studies [13]. Thus, variations in the efficiency of the vitrification/warming technique performed may lead to lower reproductive outcomes. The event of degeneration after warming is known to be centre- and operator-dependent [21]. Qualified as a highly skilled procedure requiring precision and speed, vitrification thus needs high-trained operators. To improve reproducibility and consistency of processes, a semi-automated system was developed and is commercially available for clinical use: Gavi® (Genea, Sydney, Australia). Important variables such as temperature, exposures times, media volume and replacement are entirely automated, suggesting that the survival rate and inter-operator variability could be improved. At the same time, making each act of vitrification is traceable. Assessment of the efficiency of the semi-automated platform as compared with the reference method (manual) was recently made at the zygote [22], cleaved embryo [20] or blastocyst stages [29]. However, there is no comparative study on the expected oocyte survival rate using the Gavi® system.

In addition to concerns about efficiency of oocyte vitrification, there are safety apprehensions in terms of the vulnerability of intracellular content and structures. To date, much of our knowledge is obtained from animal models, but there are inherent differences between oocyte maturation and fertilization in animals and humans, which limits the generalization of findings relative to molecular alterations following oocyte vitrification to human [51]. So far, six studies have investigated the impact of oocyte cryopreservation on gene expression in humans, but none of them compared the vitrification method (i.e. manual vs semi-automated) [9, 15, 16, 23, 30, 41]. Among them, only one used single-cell RNA-sequencing technology (scRNA-seq) on 16 oocytes [23]. In this study, the transcriptome of the vitrified oocytes was altered notably through degradation of RNA integrity and the down-regulation of genes involved in major cell cycle and development processes, but there was no control group from the same batch experiment [23].

It is therefore of utmost importance to comprehensively assess the efficiency and transcriptional "safety" of oocyte vitrification as well as the recent semi-automated technique of vitrification provided by the Gavi® system as compared with the manual method. The primary objective of the current study was thus to investigate survival using of both methods of vitrification with a sibling oocyte design. Secondly, we investigated the transcriptomic landscape associated with the oocyte vitrification method using scRNA-seq. Finally, we compared the scRNA-seq data obtained after vitrification with those from a cohort of fresh sibling oocytes.

Results

Oocytes were prospectively collected from 69 donors of sibling *in vitro* matured oocytes, aged 33.3 ± 4.7 years old. In total, 173 sibling oocytes were randomly allocated between three groups: 82 in the semi-automated and manual vitrification, and 9 in the "fresh" group. The Fig. 1 summarizes the inclusion flow-chart.

Survival rate, resistance to micro-injection, morphometric assessment

A total of 164 oocytes were thawed (Table I). The post-warming survival rate was comparable between the two groups, despite the difference being near the statistical threshold for significance: 82.9% (68/82) and 92.7% (76/82) in the Gavi® and Rapid-I™ groups, respectively (OR: 2.91, 95% CI: 0.98–8.63, $p = 0.053$). Among the intact oocytes included in Group 1 and subjected to an empty micro-injection gesture three hours after warming, the survival rate was comparable between the two groups: 93.2% (55/59) and 94.0% (63/67) in the Gavi® and Rapid-ITM groups, respectively (OR: 1.16, 95% CI: 0.27–5.03, $p = 0.837$).

Reflecting the post-thawing rehydration of the oocytes, oocyte surfaces were comparable between the semi-automated and the manual group (Additional file 1) and followed the same rehydration kinetics when surface before vitrification is used as a reference (Fig. 2). Immediately after thawing, the oocyte surface was reduced, whatever the mode of vitrification, compared with the same oocytes before vitrification ($p < 0.001$). However, the difference did not persist one hour after post-thawing ($p = 0.068$).

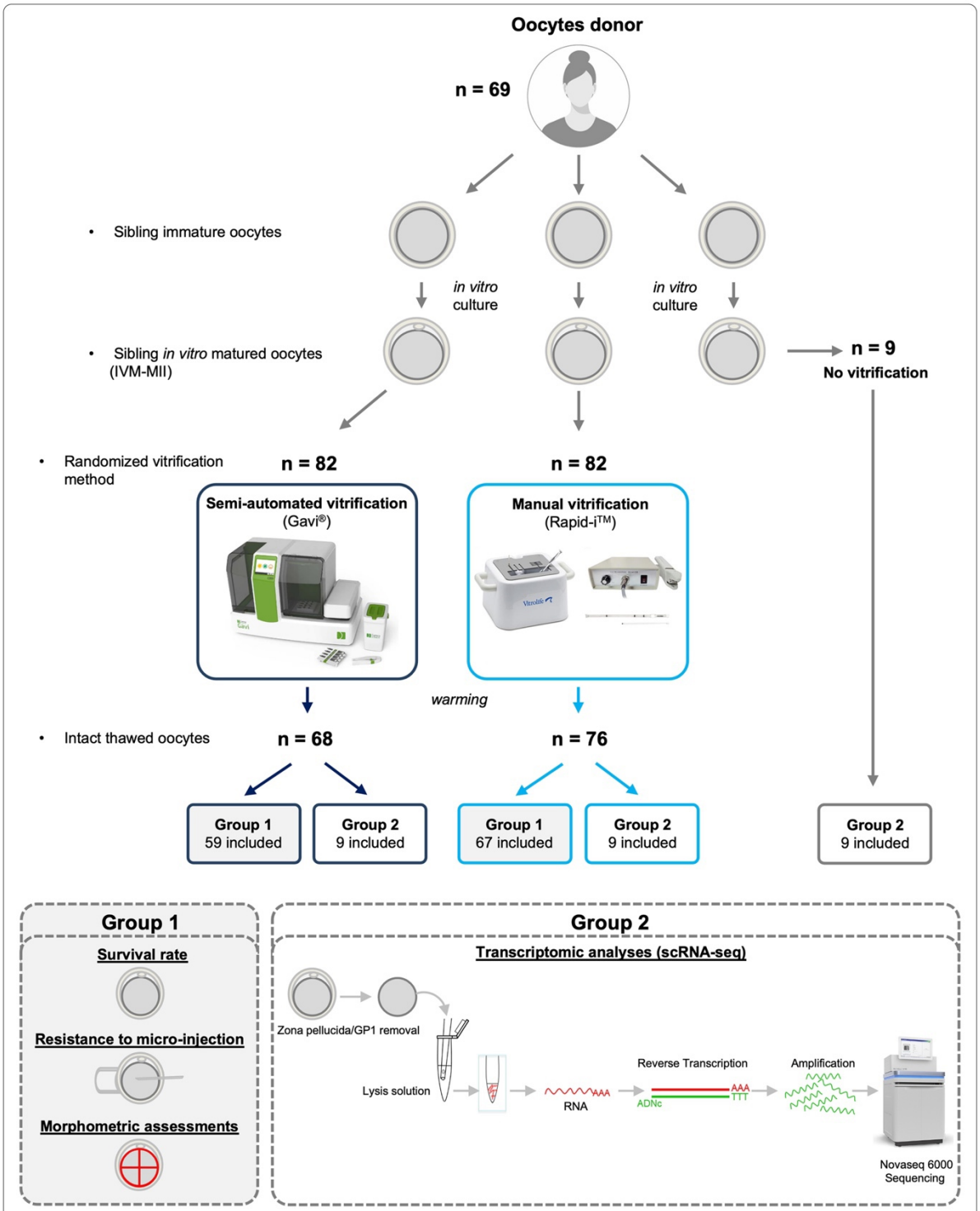

Fig. 1 Summary of the study design. After patient selection and oocyte collection, sibling oocytes were allocated to two different groups; Group 1: Manually or semi-automatically vitrified sibling oocytes for morphometric, resistance to micro-injection and survival rate assessments. Group 2: Fresh, manually or semi-automatically vitrified sibling oocytes for transcriptomic analyses by scRNA-seq

Table 1 Survival rate after thawing and resistance rate after micro-injection gesture

	Manual	GAVI	OR (95%CI)	*p-value*[a]
No. warmed oocytes	82	82		
No. survived oocytes	76	68		
Survival rate	92.7%	82.9%	2.91 (0.98–8.63)	0.053
No. injected oocytes	67	59		
No. viable oocytes post injection	63	55		
Post injection viability	94.0%	93.2%	1.16 (0.27–5.03)	0.837

For categorical variables, n (%) is presented. *OR* Odds Ratio; *95%CI* 95% Confidence Interval

[a] Logistic mixed models with random effect on donor were estimated

Single-cell RNA-seq assessment

Nine oocyte donors were included, and single-cell RNA sequencing (scRNA-seq) analysis was conducted on 20 oocytes from 7 oocytes donors for technical reasons. Among them, six patients donated *in vitro* matured oocytes (IVM-MII) and one donor was part of an oocyte donation program and donated 3 MII oocytes.

After quality checks and filters, 12,808 transcripts expressed across all samples were subjected to analysis, which is consistent with previous studies [18, 46]. The medTIN of the samples ranged between 32.3 and 46.0, and reads were uniformly distributed along the gene body, reflecting the high quality of our samples (Additional file 2). To identify potential confounders in our dataset, we performed a principal component analysis (PCA) to visually inspect the similarity between samples according to their log-transformed gene counts (Fig. 3A and B). The first two principal components (PC1 and PC2) separated samples according to patient effects such as maternal age rather than whether oocytes were vitrified or not. This was further demonstrated by unsupervised clustering of log transformed gene counts in which samples nearly clustered together according to their patient's origin (Fig. 3C).

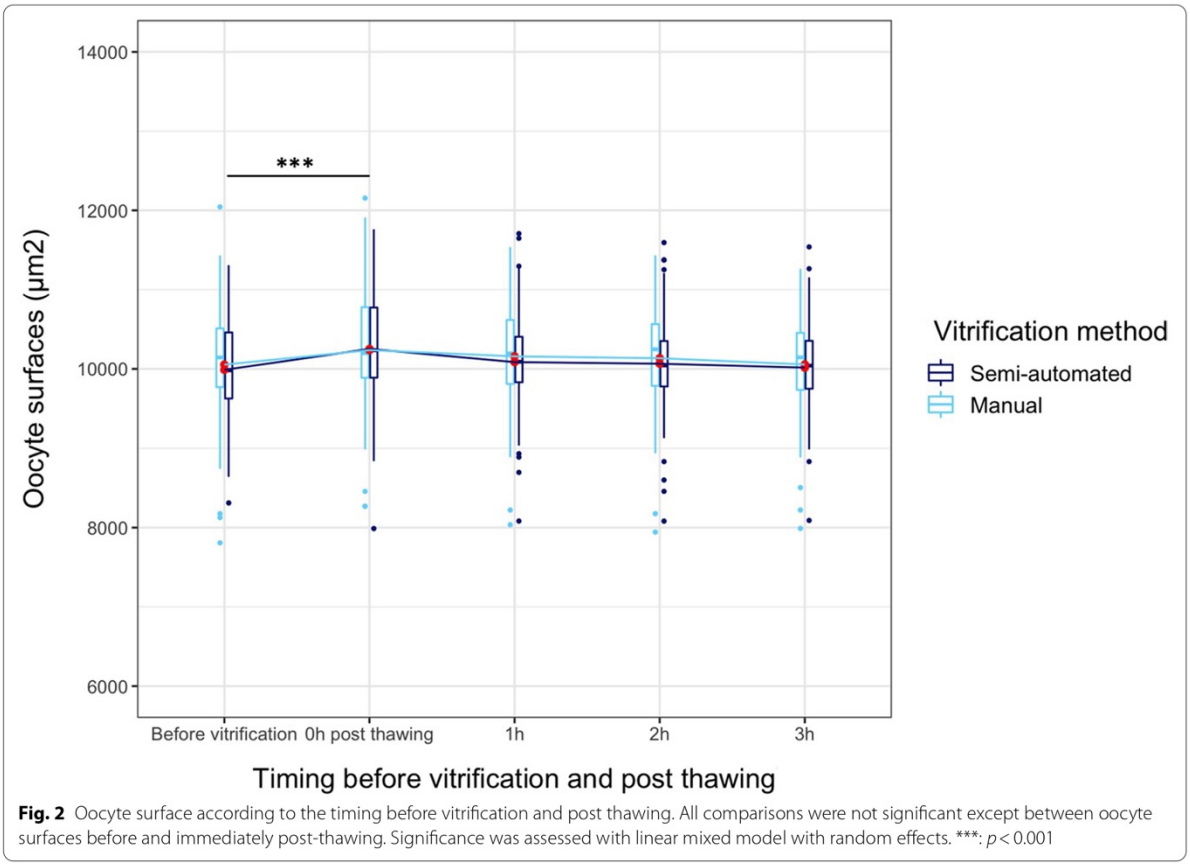

Fig. 2 Oocyte surface according to the timing before vitrification and post thawing. All comparisons were not significant except between oocyte surfaces before and immediately post-thawing. Significance was assessed with linear mixed model with random effects. ***: $p < 0.001$

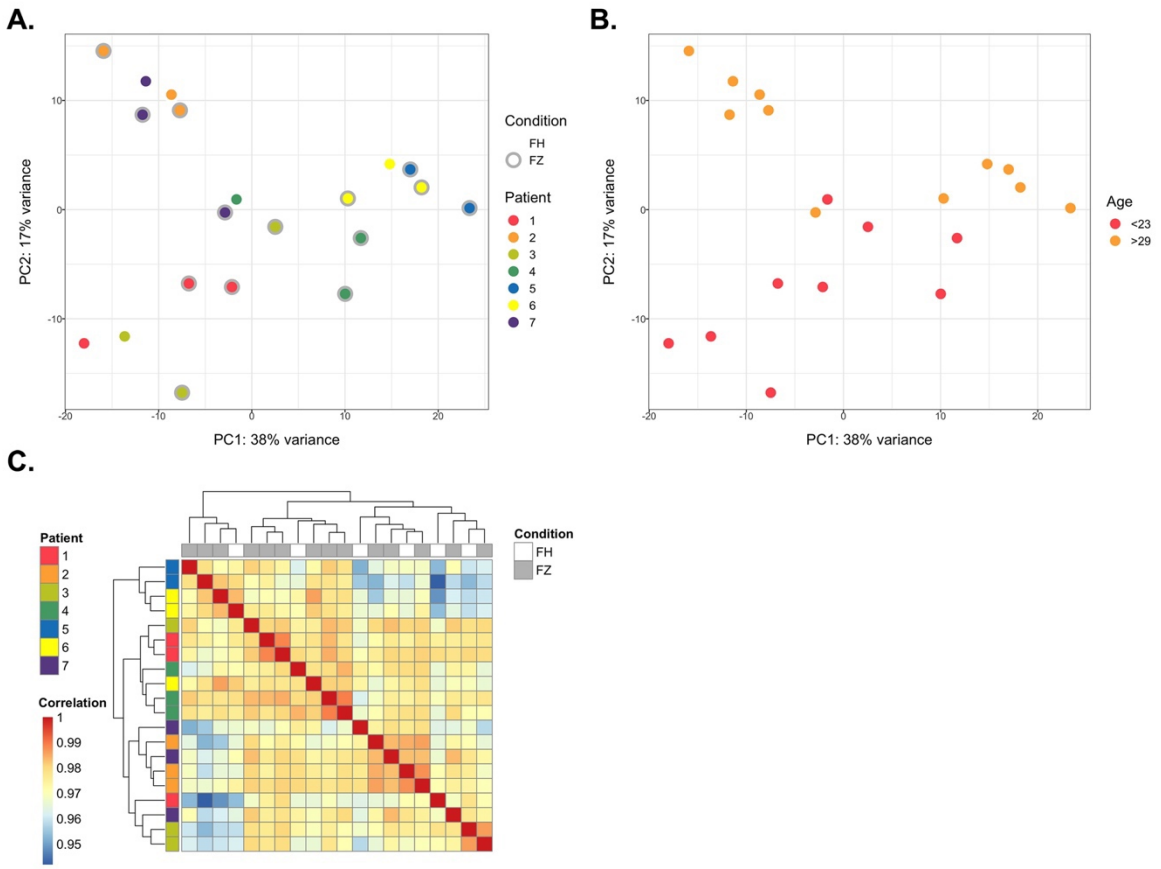

Fig. 3 Global transcriptome analysis of oocytes according to sample characteristics. **A** Principal component analysis of all samples highlighting the vitrification status and the patient origin. PC: principal component. FH: fresh oocyte. FZ: frozen oocyte. **B** Principal component analysis of all samples highlighting the patients' age. **C** Unsupervised hierarchical clustering of samples according to their global gene expression

Manual vs. semi-automated vitrification

Firstly, to elucidate whether the type of vitrification process had an impact on the oocyte transcriptome, scRNA-seq libraries were generated from seven pairs of sibling oocytes following semi-automated or manual vitrification. RNA integrity was similar between the two modes of vitrification because the medTIN was not different between the two groups (Fig. 4A, $p = 0.14$). Oocytes exhibited limited differential expression between these sample groups since only 5 DEGs were identified: *ARSD*, *CCDC124*, *CLPS*, *PLCH2*, *RHBDF1*. All were upregulated with semi-automated vitrification and 3 of them showed absolute log2(FC) > 1: *CCDC124*, *CLPS*, *PLCH2*, (Fig. 4B). These five genes have a low level of expression in oocytes (Additional file 3), and no interaction between them has been recorded in the STRING database. Comparing the expression profile of *in vivo* mature oocytes, no genes were differentially expressed depending on the mode of vitrification, revealing limited effects (Additional file 4).

Fresh vs. vitrified oocytes

Secondly, our study design allowed us to test for the potential effects of vitrification in the transcriptome of MII oocytes, whatever the mode of vitrification. We therefore performed a differential expression analysis between fresh (FH) versus vitrified (FZ) oocytes while accounting for individual baseline expression for each patient. We observed no degradation of the RNA quality in vitrified oocytes ($p = 0.02$, but indicating vitrified oocytes had higher TIN) and vitrification had no effect on mitochondrial proportion ($p = 0.41$) (Additional file 2). A total of 108 differentially expressed genes (DEGs) (54 up-regulated, 54 down-regulated) emerged, but none of them reached log2(FC) > 1, revealing small significant differences between the two

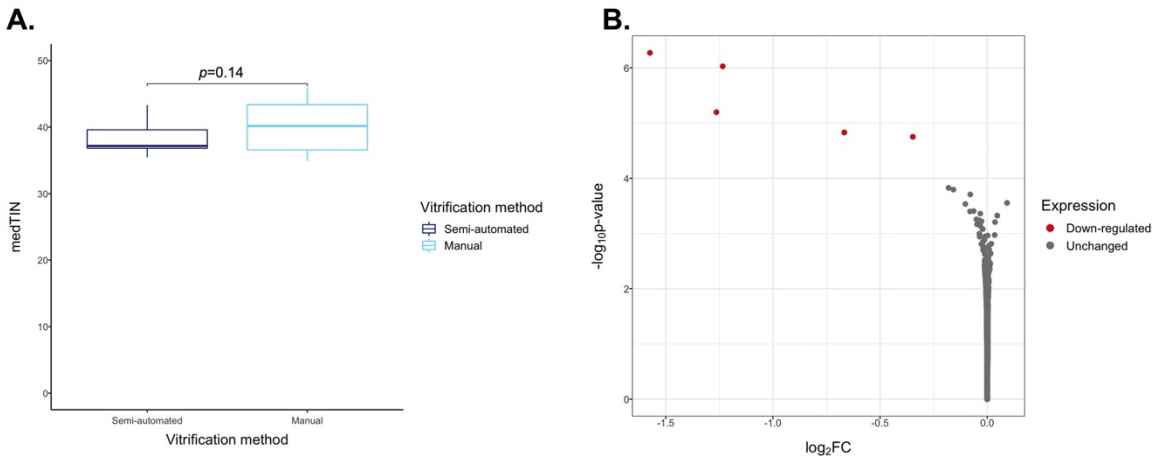

Fig. 4 Differential gene expression and RNA quality of semi-automatically and manually vitrified oocytes. **A** Comparison of mean medTIN between semi-automated and manual vitrification groups. Significance was assessed using a linear mixed model with random effects. **B** Volcano plot representation of the differential expression analysis with semi-automated vitrification compared with manual vitrification (Semi-automated minus Manual). Each point represents one of the genes expressed with log2(FC) on the x-axis and –log10 of the unadjusted *p*-value calculated with DESeq2 on the y-axis

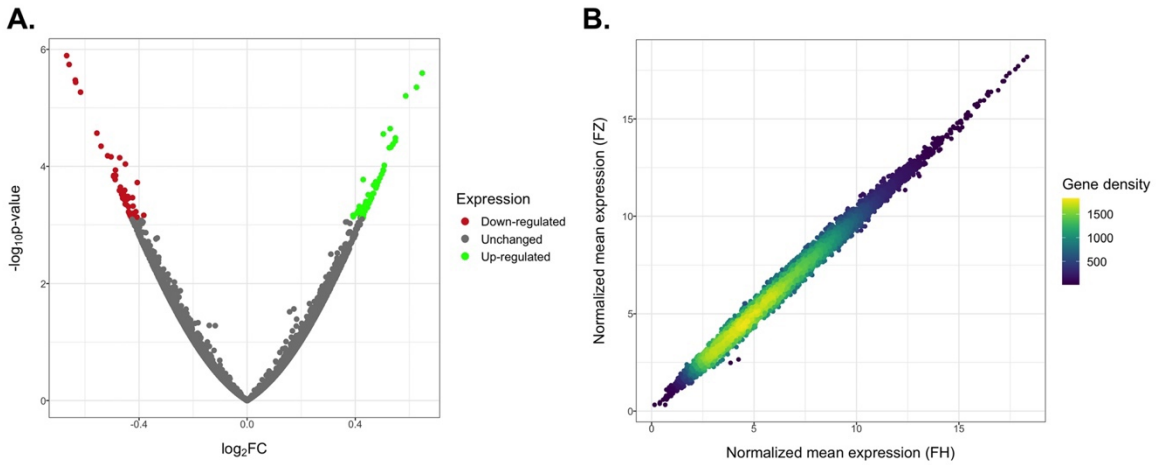

Fig. 5 Differential gene expression analysis of FH and FZ oocytes. **A** Volcano plot representation of the differential expression analysis with FZ compared with FH oocytes (FZ minus FH). **B** Correlation of the normalized mean expression (relative log expression computed with DESeq2) between FH and FZ oocytes for each gene

conditions (Fig. 5A, Additional file 5). The high comparability of the transcriptome in FH vs FZ oocytes can be detected by comparing the mean expression level of FH and FZ oocytes (Pearson's correlation, Coefficient = 0.996) (Fig. 5B). Seven of our DEGs were common with the study of Huo et al. [23], but all displayed the opposite variation of expression with vitrification (*DYSF*, *KIAA0319L*, *USP4*, *TRPC3*, *SH3RF1*, *FOXO3B*, *ZNF530*). We further explored the biological relevance of the 108 DEGs by subjecting them to Gene Ontology over-representation analysis. Two pathways reached statistical significance (FDR < 0.05) and referred to mRNA catabolic process and ribonucleoprotein complex biogenesis. An over-representation analysis on subsets of DEGs revealed no significant pathways for up-regulated DEGs but 27 significant pathways for down-regulated DEGs, mainly related to mRNA and RNA catabolic processes (Fig. 6).

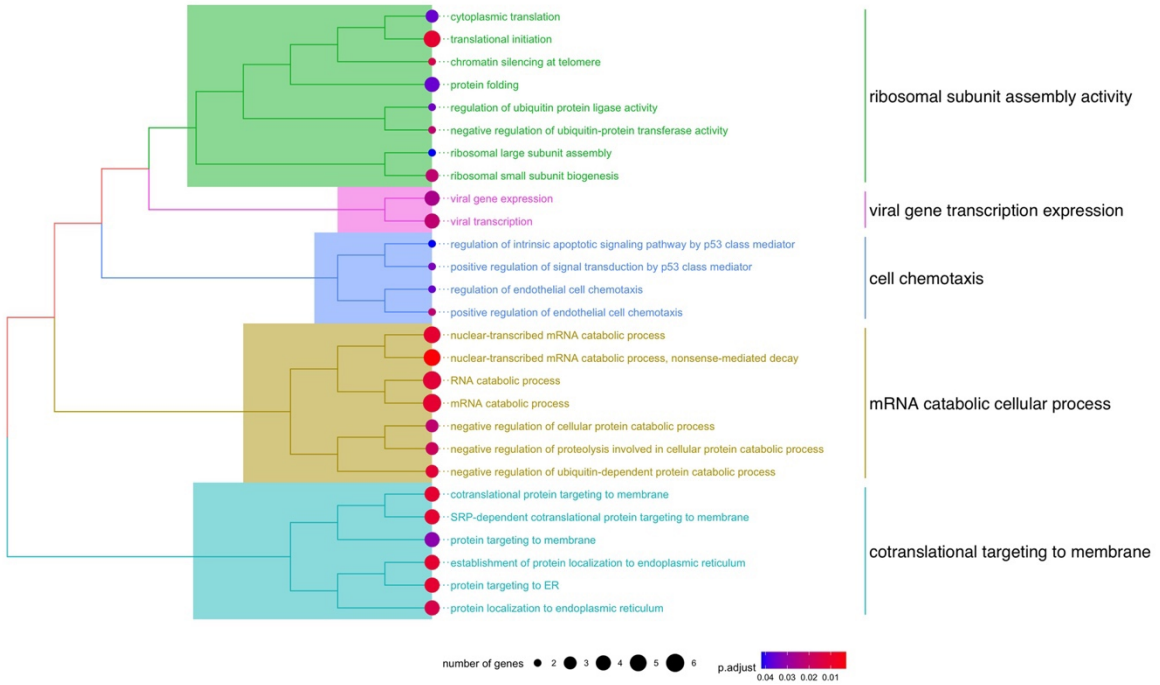

Fig. 6 Hierarchical clustering of the significant ontologies related to the down-regulated DEGs with vitrification. Each group of ontologies was assigned a denomination according the semantic similarity of the enriched biological processes

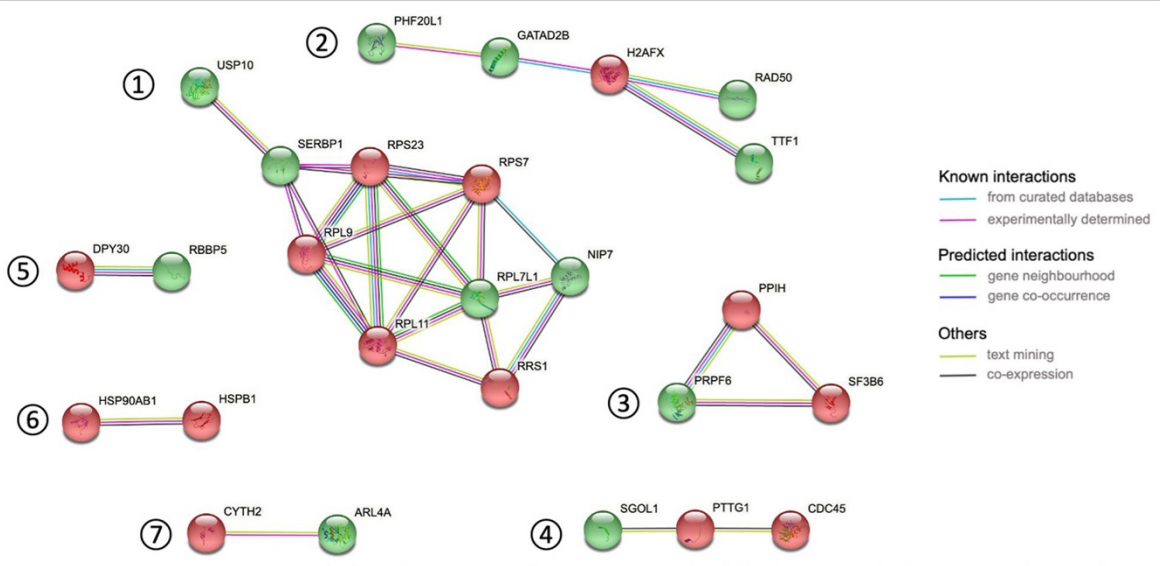

Fig. 7 Protein-protein interaction network of DEGs between FH and FZ oocytes. Genes highlighted in green and red are respectively up- and down-regulated with vitrification

The protein-protein interaction analysis of DEGs in Fig. 7 displays high-confidence networks. A single network involved more than 5 proteins and consisted in interactions of proteins related to ubitiquin hydrolysis, RNA-binding and ribosomal biogenesis (network 1). Secondary networks were related to transcriptional regulation (network 2), pre-mRNA splicing (network 3), cell division control and chromosome stability (network 4), methylation of histone 3 (network 5), heat shock proteins involved in cell cycle control (network 6) and guanine nucleotide exchange (network 7).

Using an extensive genome annotation, we quantified the expression of transposable elements (TEs). Four TEs were present in the 108 DEGs, and all of the TEs were downregulated with vitrification (LTR16C, MLT1A1, LTR13A, PABL_A-int). These elements are not among the most expressed TEs in the oocyte genome (a heatmap of the top 20 most expressed TEs and their expression profile is shown in Fig. 8). We also specifically checked for the expression of DNA methylation-related genes (*TET2*, *TET3*, *TDG*, *DNMT1*, *UHRF1*, *DNMT3A*, *DNMT3B*), but we did not observe any difference between the vitrified and fresh oocytes groups (Additional file 6).

Discussion

The introduction of Gavi®, a semi-automated vitrification device, provides an opportunity to improve the standardization of incubation duration, temperatures, and cooling rates in order to increase survival rates and lower inter-operator variability. To date, there is no available data for oocyte outcomes in terms of efficiency and safety.

The first aim of this unique study was to assess the efficiency of the semi-automated closed Gavi® oocyte vitrification method as compared with a manual closed Vitrolife method. Even if survival rates following manual vitrification tended to be higher, we reported statistically comparable survival rates between techniques, which was similar to what has been previously reported in the literature at different stages of embryonic development. Indeed, vitrification with the Gavi® system previously showed no difference in survival rate after vitrification at the zygote [22] or blastocyst stage [29] as compared with the manual open Cryotop® method. Comparable intact survival rate (with 100% intact blastomeres) and clinical pregnancy rate were recently reported after embryo vitrification at Day 2 or 3 after Gavi® vitrification than manually with Irvine®-CBS® system [20]. In the current study,

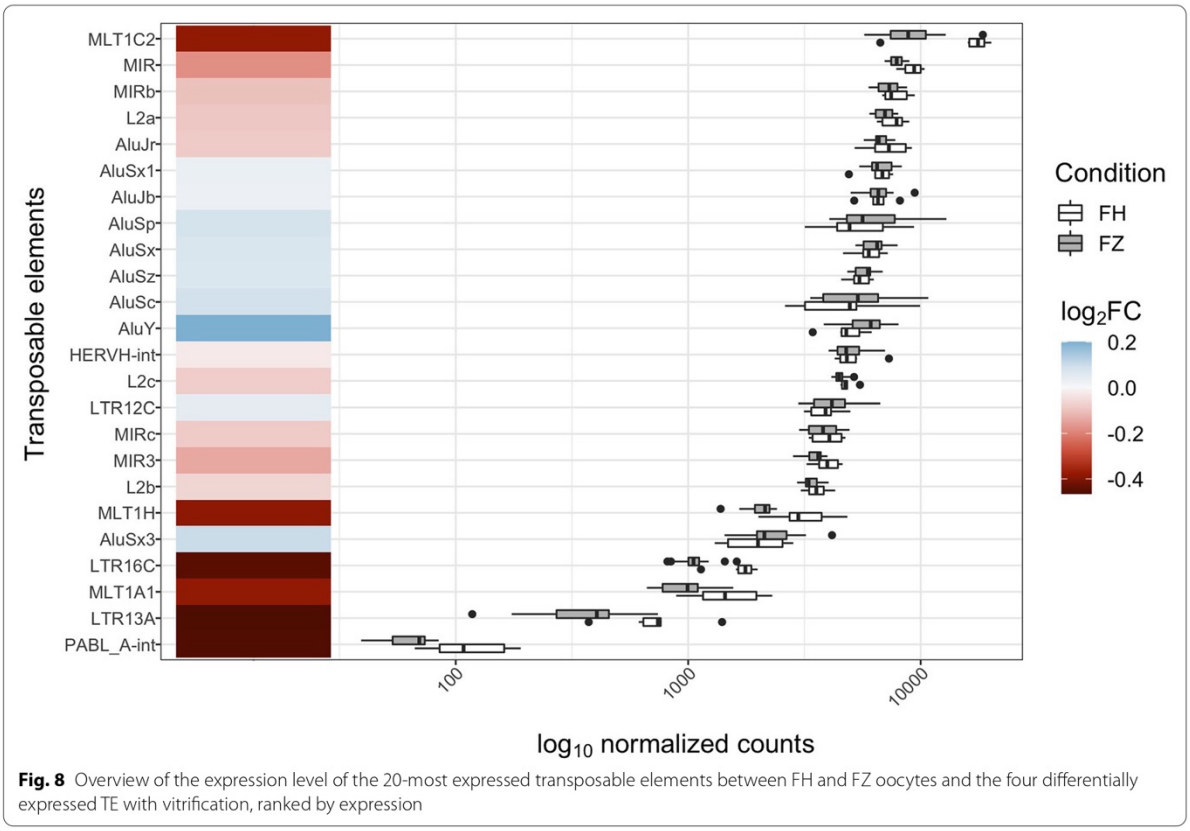

Fig. 8 Overview of the expression level of the 20-most expressed transposable elements between FH and FZ oocytes and the four differentially expressed TE with vitrification, ranked by expression

we also investigated the degree and kinetics of post-thawing rehydration through morphometric measurements, as well as thawed-oocyte resistance to a micro-injection gesture without spermatozoa. There was no difference in morphometric assessments and in the proportions of oocyte lysis after micro-injection between the vitrification methods. The results for the viability of oocytes provided by the semi-automated system compared with the closed manual method thus seem reassuring, suggesting that it could be used as an alternative vitrification procedure in ART.

The second aim of this study was to assess the impact of the semi-automated method on the transcriptome and to enrich current knowledge about the transcriptomic effects of vitrification, which has not yet been thoroughly explored in the literature. We performed single-cell RNA-sequencing with a high throughput method. The transcriptomic profiles obtained with semi-automated and manual vitrification revealed similar patterns except for three DEGs with absolute log2(FC) > 1. Among them is *CLPS*, which is a colipase involved in lipid hydrolysis whose downregulation has already been observed in relation to oocyte aging [7]. The two remaining DEGs encode for a phospholipase (*PLCH2*), and a coiled-coil domain containing protein required for proper progression of late cytokinetic stages (*CCDC124*). In addition, there was no degradation of the RNA integrity caused by any of the vitrification method in our samples according to the medTIN measure. This result is reassuring as to the preserved quality of the transcriptional material stored in the oocyte, which will be necessary for the proper development of the future embryo.

Finally, our study design made it possible to comprehensively compare the transcriptome of fresh and vitrified oocytes originating from the same patient. Among the differentially expressed genes, the overall magnitude of the differences remains largely limited between the two cohorts of sibling oocytes, reinforcing the reports of Di Pietro et al. [16] and D'Aurora et al. [15], based on a targeted approach using RTqPCR. However, the transcriptional differences between fresh and vitrified oocytes were reported more extensive by two other studies using genome-wide approach [23, 30]. Huo et al. [23], with scRNA-sequencing technology, and Monzo et al. [30], with pooled microarray, respectively found 1987 and 608 DEGs associated with vitrification, with a decrease in the mRNA content for the large majority of the DEGs. A decrease in the mean expression of 18 genes tested with a PCR approach was also reported by Chamayou et al. [9]. No tight common transcriptomic signature associated with vitrification has been observed across studies, including ours. This is potentially the result of disparate techniques and questionable study designs. Unlike PCR and microarrays, scRNA-seq has the advantage of an unbiased vision of all transcripts. Additionally, the choice of an appropriate control group should be tightly controlled and for this reason we opted for a paired design consisting in triplets of oocytes from the same patients. Indeed, one limitation of the study by Huo et al. [23] stems from the choice of the fresh oocytes comparison group, which came from a previously published experiment [46] and may have led to difficulties distinguishing between the batch and vitrification effects. However, a consensus towards the disturbance of the RNA process, cell cycle process, meiotic process, response to stress and ubiquitination may occur following vitrification. Interestingly, the down-regulation of genes involved in important cellular processes has been a recurrent observation in studies on transcriptomic effects in relation to vitrification. In our study, up-regulated genes were likely to function independently seeing as they were not related to common genetic ontologies, contrary to down-regulated genes. However, applying the same statistical threshold set in Huo's and Monzo's genome-wide studies (absolute log2(Fold Change) > 1), no significant genes (FDR < 0.05) were detected in the current study. In addition, there was no change in RNA integrity, as highlighted by the comparable medTIN between our two groups. This result was not in accordance with Huo et al. [23], who observed a drastic decrease in RNA integrity associated with vitrification [23], but the TIN is highly variable depending on sample processing.

As our team recently pointed out, the control of transposable elements is crucial for gametes and embryos [5]. In mouse oocytes, over-expression of LINE-1 elements was associated with aneuploidy and embryonic death [28]. The mechanisms regulating TEs involve epigenetic events driven by microRNAs, histone modifications and DNA methylation [8, 38, 44]. Despite being a major concern, epigenetic changes in TEs following human oocyte vitrification have not yet been assessed with high-throughput sequencing. For the first time, we tested the impact of vitrification on repetitive elements with an extensive annotation database of TE families, particularly the long terminal repeat (LTR) families, which are highly expressed in the oocytes and regulate the expression of host genes in the early embryo [32]. Four elements which are endogenous retroviruses (which belong in the LTR retrotransposons class) were significantly downregulated in the vitrified oocytes group, but they are not among the most expressed families in human oocytes and the differences were very limited. Vitrification has also been suggested to reduce the copy number of mitochondrial DNA in mice and cows [2, 4]. mtDNA is a key determinant in oocyte quality and low levels of mtDNA might indicate low developmental competence [34, 39]. Reassuringly,

we observed no difference in mitochondrial proportion between the fresh and frozen oocyte groups.

To date, this is the only study to investigate the oocyte survival rate with semi-automated vitrification process and the biggest scRNA-seq experiment on vitrified oocytes performed. However, most of our oocytes underwent an *in vitro* maturation step. Even though the *in vitro* maturation of the oocyte could be associated with some changes in the gene expression profiles assessed by scRNA-seq [48, 50], the oocyte sibling design allowed us to draw strong conclusions when we compared the two techniques. In addition, we confirmed that there was no difference between the two vitrification methods for donor oocytes that were matured *in vivo*. One of the key strengths of this study is that it was able to compare oocytes from the same patient with the use of sibling oocytes. This study design allowed us to control for potential confounders related to patient effects, so the survival rates and transcriptomic profiles were not related to the patient's characteristics.

This study is only the second to analyse the differential expression of genes by sc-RNAseq in a single oocyte rather than in a pool of oocytes. Further validation, for instance with recently developed single-cell multi-omics, would be valuable for comprehensively understand the relationship with transcriptional modifications observed after vitrification and DNA methylation dynamics, chromatin accessibility and histone modifications [47].

Conclusions

This study provides the first results on oocyte vitrification efficiency and the transcriptional impact of the automated Gavi® system compared with a closed manual vitrification method. Based on a sibling oocyte design, we showed that the oocyte survival rate, morphometric measures, and resistance to micro-injection are similar in the two methods.

In addition, for the first time, we explored the transcriptomic profiles of both techniques using single-cell RNA-sequencing. The fact that the observed transcriptional changes were infrequent and of low intensity provides reassurance about the influence of semi-automation when compared with the manual method. Our study highlights the specific adverse effects of oocyte vitrification on genomic expression. Research in this field must be continued considering that fertility preservation through oocyte vitrification is bound to develop worldwide in the coming years. Comparing clinical outcomes such as fertilization, cleavage, embryo quality, pregnancy rates, implantation, births as well as monitoring the health of children following oocyte vitrification via both techniques would also be needed in the future.

Methods

Patient selection and oocyte collection

This study was prospectively conducted at the University Hospital of Dijon between June 2018 and February 2020. Patients undergoing an attempt of *in vitro* fertilization with microinjection (ICSI, IntraCytoplasmic Sperm Injection) for medical reasons and patients who were part of an oocyte donation program were informed of this study, and their written consent was obtained before oocyte stimulation. Oocyte collection was declared (Clinical Trial NCT03570073) and approved by the ethics committee (2017-A02444–49). The controlled ovarian hyperstimulation and oocyte retrieval were performed as previously described [6].

On the day of oocyte retrieval, after removing the cumulus cells (hyaluronidase treatment plus mechanical pipetting), oocytes were classified as mature (Metaphase II) or immature (Germinal Vesicle or Metaphase I oocyte). When more than one immature oocyte was present, they were cultured in Global culture media (Global, LifeGlobal, USA) in a time-lapse incubator (EmbryoScope, Unisense FertiliTech, Denmark), at 37.0°C, 6%CO2, 5%O2 for a maximum period of 24 hours. Images and related data were stored in the EmbryoViewer (Unisense FertiliTech, Denmark) and subsequently analyzed. Oocytes that had progressed to the MII stage within the first 24 h of culture (IVM-MII stage) were selected for subsequent inclusion. Patient inclusion was based on the presence of more than two IVM-MII (siblings).

With two or an even number of IVM-MII, sibling oocytes were included in Group 1 "Survival rate, morphometric assessment, resistance to micro-injection". In that case, IVM-MII siblings were randomly and equally assigned into manual or semi-automated vitrification groups.

When there were three IVM-MII, sibling oocytes were included in Group 2: "scRNA-seq assessment". In this case, sibling oocytes were randomized between fresh, manual or semi-automated vitrified oocytes, and single-cell transcriptomes were analyzed and compared. Three *in vivo* MII oocytes were also included in Group 2 on the day of oocyte retrieval from a patient who was part of an oocyte donation program.

Oocyte conditioning

Vitrification and warming processes were performed by the two same operators.

Manual vitrification-warming procedure (Reference method)

MII were vitrified in a closed system (Rapid-I™, Vitrolife, Sweden) using the RapidVit™ Oocyte kit (Vitrolife,

Sweden) containing ethylene glycol and propanediol, which are permeable cryoprotectants, and sucrose, acting as an extracellular cryoprotectant. The vitrification procedure was performed according to the manufacturer's protocol. Each solution (Vitri 1™ Oocyte, Vitri2™ Oocyte and Vitri 3™ Oocyte) was warmed to 37 °C in a multi-well plate. The oocyte was transferred for 7 minutes in Vitri 1™ Oocyte, 4 minutes in Vitri 2™ Oocyte, and a maximum of 25 seconds in drops of Vitri 3™ Oocyte including the loading on cryodevice (Rapid-I) and immersion into liquid nitrogen. The vitrified oocytes were warmed with a RapidWarm™ Oocyte kit (Vitrolife, Sweden) at 37 °C. The Rapid-I was plunged into Warm 1™ Oocyte for 1 minute. The oocyte was then moved into Warm 2™ Oocyte for 3 minutes, Warm 3™ Oocyte for 5 minutes, and Warm 4™ Oocyte for 7 minutes. Immediately after warming, oocytes were loaded into the Embryoscope with Global media (Global, LifeGlobal, Denmark) for morphometric assessments or in a 4-well culture dish for transcriptomic assessment.

Semi-automated vitrification and warming with the GAVI® system

MII oocytes were vitrified in the semi-automated vitrification group using GAVI®, as previously described by Roy et al. [37]. Oocytes were first equilibrated in VitBase solution for 5 minutes in an un-gassed incubator at 37 °C. In the meantime, the medium cartridge containing vitrification solutions VS1 and VS2 (ethylene glycol, dimethyl sulfoxide, trehalose and supplemented human serum albumin) and tip and seal cartridges were loaded into the GAVI® system. The oocytes were then individually loaded into a device called a "Pod" and loaded into GAVI®. The oocyte vitrification protocol was selected, run and once finished, the cassette was manually removed and dunked into liquid nitrogen. Oocytes were stored in a liquid nitrogen tank before being warmed as per Genea BIOMEDX protocol using Gems Warming solutions® (Genea, Sydney, Australia). After a brief warming in a 37 °C water batch, 10 µl of WarmSol1 was dispensed in less than 20 seconds in the Pod, over a period of 1 minute. Oocytes were then transferred for 1 minute in WarmSol1, 3 minutes in WarmSol2, 5 minutes in WarmSol3, 1 minute in WarmSol3 before being transferred into Global media (Global, LifeGlobal, Denmark).

Survival rate, Morphometric assessment, Resistance to micro-injection

The primary outcome of this study was the survival rate (i.e. the number of intact oocytes after thawing divided by the total number of warmed oocytes). To evaluate post thawing oocyte rehydration for oocytes included in Group 1, the oocyte surfaces (i.e. ooplasm surface) were estimated with the Embryoscope tool immediately after thawing, and then one, two and three hours post thawing. To assess the oocyte's resistance to micro-injection in Group 1, a secondary outcome was the survival rate after "empty" micro-injection (without spermatozoa) performed 3 hours after thawing, specified as the number of intact oocytes after the micro-injection gesture.

We considered the benchmark value of 85% for oocyte survival after manual vitrification and thawing in infertile patients, as suggested by our lab results and the Alpha Scientists [1]. To test the hypothesis that the survival rate is significantly higher (95%) after semi-automated vitrification than manual vitrification (85%), we estimated necessary to include 75 oocytes (150 oocytes total) per group when taking into account the correlation between donors using a McNemar test in the least favorable situation (two-sided test, alpha = 0.05, beta = 0.2, OR = 3, proportion of discordant pairs = 0.2). Sample size estimation was done using Gpower v 3.1.9.7. Categorical variables were expressed as number of cases and percentage of occurrence, and continuous variables as means and standard deviations. To account for donor-related oocyte correlation, mixed models with random effects on donors were estimated (logistic for binary criteria, linear for quantitative criteria). No other adjustments were made in the models to assess the effect of the freezing method. Analyses were performed in R v4.0.3 and using the lme4 package. A P value of <0.05 was considered statistically significant.

RNA isolation and quantification

The sc-RNAseq method was performed as recently described by this team [33]. Briefly, the free-zona pellucida oocyte (after using acidic Tyrode's solution) was individually placed in a lysis buffer containing $MgCl_2$ (4,379,878, Applied Biosystems), DTT, Nonidet P-40 (11,332,473,001, Roche), SUPERase-In (AM2694, Ambion) and RNase-inhibitor (AM2682, Ambion). Then, we performed a reverse transcription reaction (SuperScript III reverse transcriptase - 18,080-044, Invitrogen) and a poly(A) tailing to the 3′ end of the first-strand cDNA (by using terminal deoxynucleotidyl transferase - 10,533-073, Invitrogen). After the second-strand cDNA synthesis, 20 cycles of PCR were performed to amplify the oocyte cDNA using the TaKaRa ExTaq HS (TAKRR006B, Takara) and IS PCR primer (IDT). Following purification with Zymoclean Gel DNA Recovery Kit (ZD4008, Takara), product size distribution and quantity were assessed on a Bioanalyzer using an Agilent 2100 high-sensitivity DNA assay kit (5067–4626, Agilent Technologies). The library preparation (KAPA Hyper Plus Library prep kit) and the sequencing of the scRNA-seq was performed by the ICGex - NGS platform (Curie Institute) on

NovaSeq 6000 Illumina sequencer (Illumina, San Diego, USA) for 100-bp paired-end sequencing.

Bioinformatic analysis

We carried out sequencing quality checks with FastQC [3], and the trimming of adapters and low-quality sequences was done using TrimGalore! [24]. Paired-end reads were aligned onto Human reference genome (hg38) with STAR (v2.5.2) [17] reporting randomly one position, allowing 6% of mismatches. Repeat annotation was downloaded from RepeatMasker and merged with gene annotation from Gencode v29 [19]. The combined file was used as input for quantification with *featureCounts* [26], as recommended in Teissandier et al. [43] [43]. The Transcript Integrity Number (TIN) was estimated to assess post-sequencing RNA quality for each canonical transcript with the RSeQC package [45]. For each sample, we calculated the median non-zero TIN (medTIN) and compared mean medTIN between oocyte groups via mixed linear models with a random effect on donor. The proportion of mitochondrial DNA (%mtDNA) was calculated by dividing the total number of read counts that mapped to the 38 annotated mitochondrial genes with the library size for each sample. Next, only genes with a minimum of 10 reads in at least 3 samples were retained for further analysis. Differential expression analysis was performed after relative log expression normalization of read counts using DESeq2 following the recommendations for paired samples [27]. Log2 fold changes were shrunk with the *lfcShrink* function using the *ashr* method [40] in order to remove the noise associated with fold changes from genes with low expression. Genes were declared as differentially expressed if FDR < 5%. We used *rlog* read counts transformation from DESeq2 as input to perform hierarchical clustering of samples and principal component analysis (PCA). Gene Ontology over-representation analysis was conducted using the *enrichGO* function from the clusterProfiler R package [49]. Protein-protein interaction of differentially expressed genes (DEGs) was mapped using STRING database online tool (version 11.5) [42], selecting a high-confidence minimum required interaction score (≥0.7).

Supplementary Information

The online version contains supplementary material available at https://doi.org/10.1186/s13048-022-01064-3.

Additional file 1. Oocyte surfaces before and after vitrification process.

Additional file 2. A. Comparison of mean medTIN between FH and FZ oocytes. Significance was assessed using a linear mixed model with random effects. B. Gene body scRNA-seq read coverage across all samples. C. Comparison of the proportion of mitochondrial DNA (%mtDNA) between FH and FZ oocytes. Significance was assessed using a linear mixed model with random effects.

Additional file 3 Semi-automated *vs.* manual vitrification differential expression analysis results for all genes.

Additional file 4 Semi-automated *vs.* manual vitrification differential expression analysis results for all genes only for *in vivo* mature oocytes.

Additional file 5 FH *vs.* FZ oocytes differential expression analysis results for all genes.

Additional file 6. Expression of DNA methylation-related genes across fresh, manual and semi-automated vitrification groups. None of these genes were significantly differentially expressed in the comparisons between semi-automated vs manual and FH vs FZ.

Acknowledgements

For bioinformatics, we thank Aurélie Teissandier of the Institut Curie. We thank Maud Carpentier of the "Direction de la Recherche Clinique et de l'Innovation" of Dijon University Hospital for the financial management of the study. We also thank Suzanne Rankin for her help in writing the manuscript.

Authors' contributions

P.F., J.B. and B.D. take primary responsibility for conceptualization and investigation. P.F. and J.B. were responsible for the methodology. M.G., N.L., R.S., J.B., C.B. and P.F. were involved in resources, experiments and visualization. B.D. and A.G. did the data curation and formal analysis. J.B., B. D and P.F. were involved in original draft preparation. D.B. participated to review and editing. The author(s) read and approved the final manuscript.

Funding

This work was supported by funding from the "University Hospital of Dijon", "Conseil Régional de Bourgogne", "Agence Nationale de Biomédecine" and "Agence Nationale pour la Recherche ("CARE"-ANR JCJC 2017)".

Availability of data and materials

The datasets generated during the current study are available in the NCBI Gene Expression Omnibus repository (GEO; https://www.ncbi.nlm.nih.gov/geo/) under accession number GSE205417.

Declarations

Ethics approval and consent to participate

The patients provided their written informed consent to participate in this study. Oocyte collection was declared and approved by the ethics committee (2017-A02444–49).

Consent for publication

Not applicable.

Competing interests

The authors declare that they have no competing interests.

Author details

[1]Université Bourgogne Franche-Comté - Equipe Génétique des Anomalies du Développement (GAD) INSERM UMR1231, 2 Rue Angélique Ducoudray, F-21000 Dijon, France. [2]CHU Dijon Bourgogne, Laboratoire de Biologie de la Reproduction – CECOS, 14 rue Gaffarel, F-21000 Dijon, France. [3]USMR, Dijon Bourgogne University Hospital, F-21000 Dijon, France. [4]Institut Curie, PSL University, CNRS, INSERM, 26 rue d'Ulm, F-75248 Paris, France. [5]Laboratoire de Biologie de la Reproduction, CHU Dijon, BP 77908, 14, rue Gaffarel, 21079 Dijon Cedex, France.

Received: 7 July 2022 Accepted: 21 November 2022
Published online: 05 December 2022

References

1. Alpha Consensus. The Alpha consensus meeting on cryopreservation key performance indicators and benchmarks: proceedings of an expert meeting. Reprod BioMed Online. 2012;25:146–67.

2. Amoushahi M, Salehnia M, Mowla SJ. Vitrification of Mouse MII Oocyte Decreases the Mitochondrial DNA Copy Number, TFAM gene expression and mitochondrial enzyme activity. J Reprod Infertil. 2017;18:343–51.
3. Andrews S. FastQC: a quality control tool for high throughput sequence data. 2010;Available from: https://www.bioinformatics.babraham.ac.uk/projects/fastqc/.
4. Aoki S, Ito J, Hara S, Shirasuna K, Iwata H. Effect of maternal aging and vitrification on mitochondrial DNA copy number in embryos and spent culture medium. Reprod Biol. 2021;21:100506.
5. Barberet J, Barry F, Choux C, Guilleman M, Karoui S, Simonot R, et al. What impact does oocyte vitrification have on epigenetics and gene expression? Clin Epigenetics. BioMed Central Ltd; 2020.
6. Barberet J, Bruno C, Valot E, Antunes-Nunes C, Jonval L, Chammas J, et al. Can novel early non-invasive biomarkers of embryo quality be identified with time-lapse imaging to predict live birth? Hum Reprod. 2019;34:1439–49.
7. Barragán M, Pons J, Ferrer-Vaquer A, Cornet-Bartolomé D, Schweitzer A, Hubbard J, et al. The transcriptome of human oocytes is related to age and ovarian reserve. Mol Hum Reprod. 2017;23:535–48.
8. Bourc'his D, Bestor TH. Meiotic catastrophe and retrotransposon reactivation in male germ cells lacking Dnmt3L. Nature. 2004;431:96–9.
9. Chamayou S, Bonaventura G, Alecci C, Tibullo D, Di Raimondo F, Guglielmino A, et al. Consequences of metaphase II oocyte cryopreservation on mRNA content. Cryobiology. 2011;62:130–4.
10. Chen C. Pregnancy after human oocyte cryopreservation. Lancet. 1986;1:884–6.
11. Cobo A, García-Velasco JA, Remohí J, Pellicer A. Oocyte vitrification for fertility preservation for both medical and nonmedical reasons. Fertil Steril. 2021;115:1091–101.
12. Cobo A, Meseguer M, Remohí J, Pellicer A. Use of cryo-banked oocytes in an ovum donation programme: a prospective, randomized, controlled, clinical trial. Hum Reprod. 2010;25:2239–46.
13. Cornet-Bartolomé D, Rodriguez A, García D, Barragán M, Vassena R. Efficiency and efficacy of vitrification in 35 654 sibling oocytes from donation cycles. Hum Reprod. 2020;35:2262–71.
14. Crawford S, Boulet SL, Kawwass JF, Jamieson DJ, Kissin DM. Cryopreserved oocyte versus fresh oocyte assisted reproductive technology cycles, United States, 2013. Fertil Steril. 2017;107:110–8.
15. D'Aurora M, Budani MC, Franchi S, Sarra A, Stuppia L, Tiboni GM, et al. Dynactin pathway-related gene expression is altered by aging, but not by vitrification. Reprod Toxicol. 2019;88:48–55.
16. Di Pietro C, Vento M, Guglielmino MR, Borzì P, Santonocito M, Ragusa M, et al. Molecular profiling of human oocytes after vitrification strongly suggests that they are biologically comparable with freshly isolated gametes. Fertil Steril. 2010;94:2804–7.
17. Dobin A, Davis CA, Schlesinger F, Drenkow J, Zaleski C, Jha S, et al. STAR: ultrafast universal RNA-seq aligner. Bioinformatics. 2013;29:15–21.
18. Ferrero H, Corachán A, Aguilar A, Quiñonero A, Carbajo-García MC, Alamá P, et al. Single-cell RNA sequencing of oocytes from ovarian endometriosis patients reveals a differential transcriptomic profile associated with lower quality. Hum Reprod. 2019;34:1302–12.
19. Frankish A, Diekhans M, Jungreis I, Lagarde J, Loveland JE, Mudge JM, et al. GENCODE 2021. Nucleic Acids Res. 2021;49:D916–23.
20. Gatimel N, Moreau J, Bettiol C, Parinaud J, Léandri RD. Semi-automated versus manual embryo vitrification: inter-operator variability, time-saving, and clinical outcomes. J Assist Reprod Genet. 2021;38:3213–22.
21. Gianaroli L, Ferraretti AP, Perruzza D, Terzuoli G, Azzena S, Crippa A, et al. Oocyte donation: not all oocyte cryobanks are the same. Reprod BioMed Online. 2022;44:271–9.
22. Hajek J, Baron R, Sandi-Monroy N, Schansker S, Schoepper B, Depenbusch M, et al. A randomised, multi-center, open trial comparing a semi-automated closed vitrification system with a manual open system in women undergoing IVF. Hum Reprod. 2021;36:2101–10.
23. Huo Y, Yuan P, Qin Q, Yan Z, Yan L, Liu P, et al. Effects of vitrification and cryostorage duration on single-cell RNA-Seq profiling of vitrified-thawed human metaphase II oocytes. Front Med. 2021;15:144–54.
24. Krueger F. Trim Galore!: a wrapper tool around Cutadapt and FastQC to consistently apply quality and adapter trimming to FastQ files, with some extra functionality for MspI-digested RRBS-type libraries. 2012;Available from: https://www.bioinformatics.babraham.ac.uk/projects/trim_galore/.
25. Kushnir VA, Darmon SK, Barad DH, Gleicher N. New national outcome data on fresh versus cryopreserved donor oocytes. J Ovarian Res. 2018;11:2.
26. Liao Y, Smyth GK, Shi W. featureCounts: an efficient general purpose program for assigning sequence reads to genomic features. Bioinformatics. 2014;30:923–30.
27. Love MI, Huber W, Anders S. Moderated estimation of fold change and dispersion for RNA-seq data with DESeq2. Genome Biol. 2014;15:550.
28. Malki S, van der Heijden GW, O'Donnell KA, Martin SL, Bortvin A. A Role for Retrotransposon LINE-1 in Fetal Oocyte Attrition in Mice. Dev Cell. 2014;29:521–33.
29. Miwa A, Noguchi Y, Hosoya K, Mori Y, Sato T, Kasahara Y, et al. Equivalent clinical outcome after vitrified-thawed blastocyst transfer using semi-automated embryo vitrification system compared with manual vitrification method. Reprod Med Biol. 2020;19:164–70.
30. Monzo C, Haouzi D, Roman K, Assou S, Dechaud H, Hamamah S. Slow freezing and vitrification differentially modify the gene expression profile of human metaphase II oocytes. Hum Reprod. 2012;27:2160–8.
31. Parmegiani L, Cognigni GE, Bernardi S, Cuomo S, Ciampaglia W, Infante FE, et al. Efficiency of aseptic open vitrification and hermetical cryostorage of human oocytes. Reprod BioMed Online. 2011;23:505–12.
32. Peaston AE, Evsikov AV, Graber JH, de Vries WN, Holbrook AE, Solter D, et al. Retrotransposons Regulate Host Genes in Mouse Oocytes and Preimplantation Embryos. Dev Cell. 2004;7:597–606.
33. Pérez-Palacios R, Fauque P, Teissandier A, Bourc'his D. Deciphering the early mouse embryo transcriptome by low-input RNA-seq. Methods Mol Biol. 2021;2214:189–205.
34. Reynier P, May-Panloup P, Chrétien M-F, Morgan CJ, Jean M, Savagner F, et al. Mitochondrial DNA content affects the fertilizability of human oocytes. Mol Hum Reprod. 2001;7:425–9.
35. Rienzi L, Gracia C, Maggiulli R, LaBarbera AR, Kaser DJ, Ubaldi FM, et al. Oocyte, embryo and blastocyst cryopreservation in ART: systematic review and meta-analysis comparing slow-freezing versus vitrification to produce evidence for the development of global guidance. Hum Reprod Update. 2017;23:139–55.
36. Rienzi L, Romano S, Albricci L, Maggiulli R, Capalbo A, Baroni E, et al. Embryo development of fresh 'versus' vitrified metaphase II oocytes after ICSI: a prospective randomized sibling-oocyte study. Hum Reprod. 2010;25:66–73.
37. Roy TK, Brandi S, Peura TT. Chapter 20 Gavi-Automated Vitrification Instrument. In: Nagy ZP, Varghese AC, Agarwal A, editors. Cryopreservation of mammalian gametes and embryos: methods and protocols: Springer; 2017. p. 261–77.
38. Shalgi R, Pilpel Y, Oren M. Repression of transposable-elements – a microRNA anti-cancer defense mechanism? Trends Genet. 2010;26:253–9.
39. Shoubridge EA, Wai T. Mitochondrial DNA and the mammalian oocyte. Curr Top Dev Biol. 2007;77:87–111.
40. Stephens M. False discovery rates: a new deal. Biostatistics. 2017;18:275–94.
41. Stigliani S, Moretti S, Anserini P, Casciano I, Venturini PL, Scaruffi P. Storage time does not modify the gene expression profile of cryopreserved human metaphase II oocytes. Hum Reprod. 2015;30:2519–26.
42. Szklarczyk D, Gable AL, Nastou KC, Lyon D, Kirsch R, Pyysalo S, et al. The STRING database in 2021: customizable protein–protein networks, and functional characterization of user-uploaded gene/measurement sets. Nucleic Acids Res. 2021;49:D605–12.
43. Teissandier A, Servant N, Barillot E, Bourc'his D. Tools and best practices for retrotransposon analysis using high-throughput sequencing data. Mobile. DNA. 2019;10:52.
44. Walter M, Teissandier A, Pérez-Palacios R, Bourc'his D. An epigenetic switch ensures transposon repression upon dynamic loss of DNA methylation in embryonic stem cells. In: Ferguson-Smith AC, editor. , vol. 5: eLife; 2016. p. e11418.
45. Wang L, Nie J, Sicotte H, Li Y, Eckel-Passow JE, Dasari S, et al. Measure transcript integrity using RNA-seq data. BMC Bioinformatics. 2016;17:58.

46. Yan L, Yang M, Guo H, Yang L, Wu J, Li R, et al. Single-cell RNA-Seq profiling of human preimplantation embryos and embryonic stem cells. Nat Struct Mol Biol. 2013;20:1131–9.
47. Yan R, Gu C, You D, Huang Z, Qian J, Yang Q, et al. Decoding dynamic epigenetic landscapes in human oocytes using single-cell multi-omics sequencing. Cell Stem Cell. 2021;28:1641–56.
48. Ye M, Yang ZY, Zhang Y, Xing YX, Xie QG, Zhou JH, et al. Single-cell multiomic analysis of in vivo and in vitro matured human oocytes. Human Reproduction. Oxford University Press; 2020;35:886–900.
49. Yu G, Wang L-G, Han Y, He Q-Y. clusterProfiler: an R Package for Comparing Biological Themes Among Gene Clusters. OMICS: A Journal of. Integr Biol. 2012;16:284–7.
50. Zhao H, Li T, Zhao Y, Tan T, Liu C, Liu Y, et al. Single-cell transcriptomics of human oocytes: Environment-driven metabolic competition and compensatory mechanisms during oocyte maturation. Antioxid Redox Signal. Mary Ann Liebert Inc.; 2019;30:542–59.
51. Zhao Z-H, Meng T-G, Li A, Schatten H, Wang Z-B, Sun Q-Y. RNA-Seq transcriptome reveals different molecular responses during human and mouse oocyte maturation and fertilization. BMC Genomics. 2020;21:475.

Publisher's Note

Additional file 1. Oocyte surfaces before and after vitrification process.

Oocyte surfaces (µm²)	Manual	GAVI	β (95%CI)	*p*-value[a]
Before vitrification	10053.91 (± 757.87)	9987.90 (± 612.05)	66.01 (-102.14 ; 234.16)	0.443
T0 post thawing	10236.12 (± 781.85)	10251.20 (± 713.44)	-8.56 (-210.11 ; 192.99)	0.934
T1 hour	10157.81 (± 701.70)	10085.63 (± 688.46)	77.01 (-106.77 ; 260.79)	0.414
T2 hours	10134.40 (± 681.80)	10065.49 (± 687.80)	72.16 (-106.44 ; 250.76)	0.431
T3 hours	10055.58 (± 656.25)	10015.83 (± 642.80)	42.34 (-130.15 ; 214.83)	0.632

For continuous variables, mean (± SD) are presented. 95%CI: 95% Confidence Interval.

[a] Linear mixed models with random effect on donor were estimated

Additional file 2. A. Comparison of mean medTIN between FH and FZ oocytes. Significance was assessed using a linear mixed model with random effects. B. Gene body scRNA-seq read coverage across all samples. C. Comparison of the proportion of mitochondrial DNA (%mtDNA) between FH and FZ oocytes. Significance was assessed using a linear mixed model with random effects.

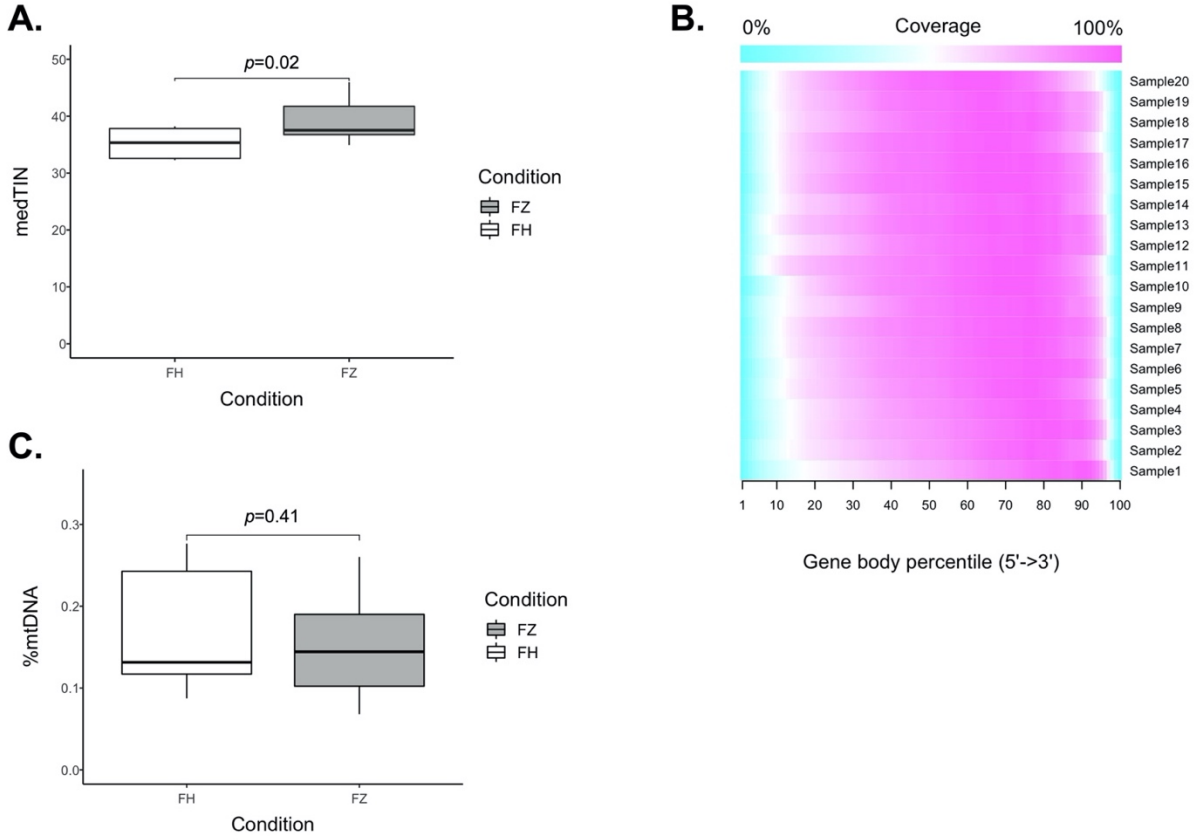

Additional file 3. Semi-automated vs. manual vitrification differential expression analysis results for all genes.

Available at https://static-content.springer.com/esm/art%3A10.1186%2Fs13048-022-01064-3/MediaObjects/13048_2022_1064_MOESM3_ESM.xlsx

Additional file 4. Semi-automated vs. manual vitrification differential expression analysis results for all genes only for in vivo mature oocytes.

Available at https://static-content.springer.com/esm/art%3A10.1186%2Fs13048-022-01064-3/MediaObjects/13048_2022_1064_MOESM4_ESM.xlsx

Additional file 5. FH vs. FZ oocytes differential expression analysis results for all genes.

Available at https://static-content.springer.com/esm/art%3A10.1186%2Fs13048-022-01064-3/MediaObjects/13048_2022_1064_MOESM5_ESM.zip

Additional file 6. Expression of DNA methylation-related genes across fresh, manual and semi-automated vitrification groups. None of these genes were significantly differentially expressed in the comparisons between semi-automated vs manual and FH vs FZ.

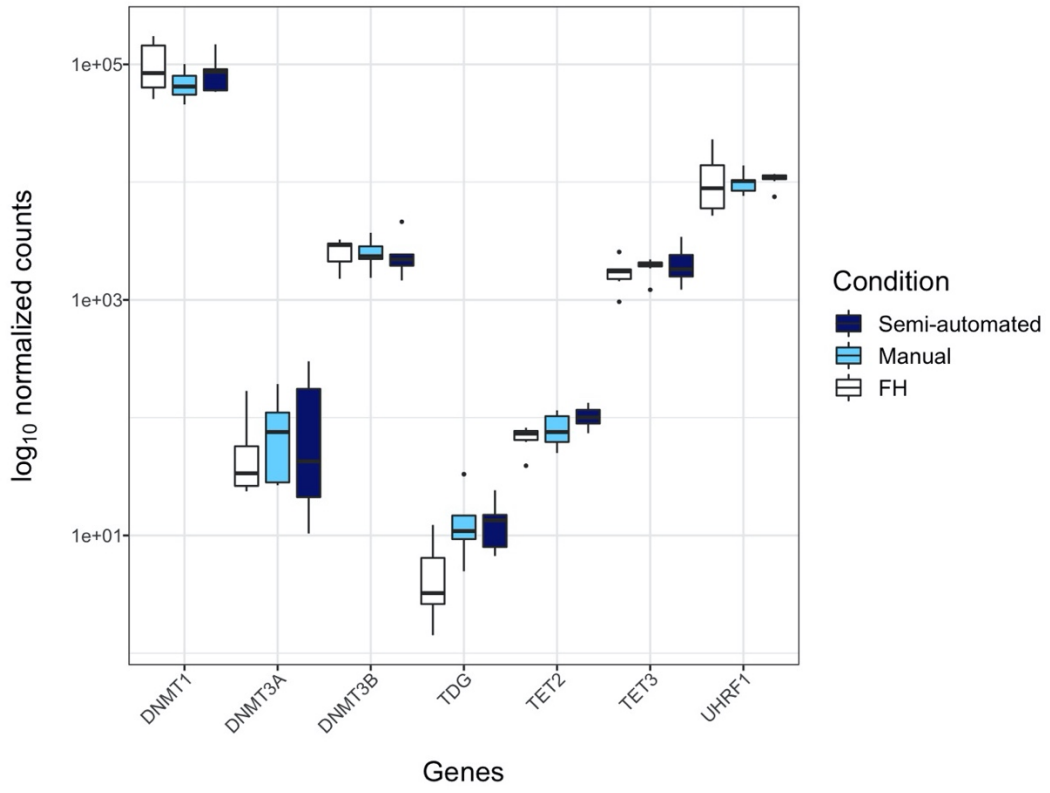

2) Évaluation de l'influence de milieux de culture embryonnaire distincts sur le transcriptome préimplantatoire humain

2.1) Objectifs

Plusieurs interventions artificielles qui se déroulent lors d'un protocole d'AMP sont suspectées d'engendrer des perturbations du transcriptome et ainsi diminuer la qualité des embryons et les chances de grossesse. Parmi elles, l'utilisation de différents milieux de culture a été ciblée (Mantikou *et al.*, 2016). Historiquement, des données avaient suggéré que la présence d'acides aminés était toxique pour l'embryon pré-implantatoire. Ces résultats ont conduit à la mise sur le marché de milieux de culture totalement dépourvus en ces composés organiques (Ménézo *et al.*, 2013). Aujourd'hui, cette vision a été rectifiée et la tendance à l'utilisation de milieux riches en acides aminés semble un meilleur choix, dans des concentrations optimisées, même si ce n'est pas la norme dans toutes les cliniques (Menezo *et al.*, 2019). Ici, nous nous proposons d'étudier l'effet de plusieurs milieux de culture au stade embryonnaire en pré-implantatoire (Ferticult, dépourvu en acides aminés ; Global, riche en acides aminés ; et SSM, plus utilisé en raison de sa sous-performance en termes de taux de préimplantation et de grossesse). Nous avons ainsi étudié le transcriptome d'embryons cultivés jusqu'au jour 2 (J2) et 5 après fécondation (J5, stade blastocyste) dans ces différents milieux de culture. L'effet d'une supplémentation en méthionine, un acide aminé essentiel au bon fonctionnement de la machinerie épigénétique, mais qui en excès peut affecter négativement la méthylation et la régulation épigénétique des gènes soumis à empreinte (Hoeijmakers *et al.*, 2016) a aussi été testé.

2.2) Matériels et méthodes

Des embryons cryoconservés au laboratoire de biologie de la reproduction du CHU de Dijon ont été donnés pour la recherche. Nous avons analysé par RNA-seq uniquement les embryons cultivés dans trois milieux de culture différents (Global medium, LifeGlobal ; FertiCult IVF medium, FertiPro ; SSM, Irvine Scientific) mais avec des critères morphologiques identiques, c'est-à-dire au stade 4-cellules avec moins de 15% de fragments anucléés et un clivage régulier.

Dans une autre expérience, nous avons sélectionné des embryons cryoconservés au jour 2 avec des critères morphologiques identiques à ceux décrits ci-dessus à partir de cohortes d'embryons cultivés jusqu'au jour 2 soit dans FertiCult soit dans Global, qui ont ensuite été cultivés jusqu'au jour 5 dans Global. Tous les embryons ont été traités suivant la méthode de Pérez-Palacios *et al.* (2021) pour mettre en place des analyses single-embryo RNA-sequencing et établir leur profil transcriptomique (Pérez-Palacios *et al.*, 2021).

Enfin, pour la supplémentation en méthionine, nous avons inclus des embryons cryoconservés au jour 2 provenant de cohortes des mêmes patients (embryons frères) avec au moins quatre embryons présentant des critères morphologiques identiques (stade 4-cellules). Ces embryons frères ont été cultivés au hasard dans le milieu Global sans ou avec supplémentation en méthionine (200µM ; concentration près de trois fois supérieure à celle du milieu Global) et nous avons analysé les ARNm totaux par single-embryo RNA-seq. La concentration en méthionine après supplémentation entre dans une gamme observée parmi les milieux de culture commercialisés aujourd'hui.

Le traitement bioinformatique des données de séquençage a inclus le contrôle qualité des données avec *FastQC*, le « trimming » avec *TrimGalore!*, l'alignement sur le génome de référence hg38 avec *STAR*, la quantification de l'expression brute des gènes avec *featureCounts*. La normalisation des données d'expression a été effectuée avec la méthode

TMM de *edgeR* et l'analyse différentielle avec *limma-voom* qui est particulièrement performante avec les données issues de single-cell RNA-seq (Soneson & Robinson, 2018).

Par ailleurs, nous avons comparé nos données avec trois études de single-cell RNA-seq sur des embryons précoces (Xue *et al.*, 2013; Yan *et al.*, 2013; Petropoulos *et al.*, 2016). Pour identifier les gènes dont l'expression change dynamiquement au cours du développement embryonnaire précoce, de manière continue, indépendamment du stade de l'embryon, nous avons appliqué la réduction de la dimensionnalité PHATE, une méthode récemment développée qui a déjà été appliquée aux cellules souches embryonnaires humaines (Moon *et al.*, 2019). Nous avons ensuite inféré les lignées existantes et le « pseudotime » à l'aide de *slingshot*, une méthode adaptée aux structures de lignées ramifiées dans les données de faible dimension.

2.3) Résultats

Nous avons pu mettre en évidence des différences d'expression pour 266 gènes à J2 entre les milieux Ferticult et Global, alors que le SSM a révélé très peu de différences avec les deux autres milieux. Par l'intermédiaire d'analyse de Gene Ontology et de Gene Set Enrichment Analysis, ces différences transcriptomiques se sont avérées en lien avec le développement embryonnaire et la division cellulaire. A J5, les différences étaient atténuées avec seulement 18 gènes différentiellement exprimés, différents de ceux observés à J2, suggérant une plasticité de l'embryon face aux différentes conditions de culture. Les embryons cultivés dans le Ferticult jusqu'au jour 2 présentaient des anomalies de surexpression de quelques gènes à effets maternels au jour 5 (qui codent des facteurs d'origine ovocytaire et impliqués dans le développement embryonnaire) comme *PADI6* et *TUBB8*, et d'autres identifiés comme jouant un rôle dans les premières divisions cellulaires. Spécifiquement, ces transcrits affichaient un retard de dégradation chez les embryons cultivés dans le Ferticult jusqu'au jour 2 en comparaison de données modélisant la cinétique attendue du transcriptome embryonnaire précoce. Il reste inconnu si le retard de dégradation spécifique à ces transcrits

impacte réellement le phénotype du fœtus et du nouveau-né. Dans leur globalité, nos résultats montrent la capacité de l'embryon à s'adapter à un environnement suboptimal pré-compaction (dépourvu en acides aminés) par une modulation de son activité transcriptomique et suggèrent que les milieux riches en acides aminés placent l'embryon dans une cinétique transcriptomique optimisée et donc favorable pour son développement.

2.4) Article 5 - Assessing the influence of distinct IVF culture media on human pre-implantation development using single-embryo transcriptomics

frontiers | Frontiers in Cell and Developmental Biology

TYPE Original Research
PUBLISHED 26 June 2023
DOI 10.3389/fcell.2023.1155634

OPEN ACCESS

EDITED BY
Mellissa Mann,
University of Pittsburgh, United States

REVIEWED BY
Paolo Rinaudo,
University of California, San Francisco, United States
Nicolas Rivron,
Austrian Academy of Sciences (OeAW), Austria

*CORRESPONDENCE
Patricia Fauque,
patricia.fauque@chu-dijon.fr

RECEIVED 31 January 2023
ACCEPTED 13 June 2023
PUBLISHED 26 June 2023

CITATION
Ducreux B, Barberet J, Guilleman M, Pérez-Palacios R, Teissandier A, Bourc'his D and Fauque P (2023), Assessing the influence of distinct culture media on human pre-implantation development using single-embryo transcriptomics.
Front. Cell Dev. Biol. 11:1155634.
doi: 10.3389/fcell.2023.1155634

Assessing the influence of distinct culture media on human pre-implantation development using single-embryo transcriptomics

Bastien Ducreux[1], Julie Barberet[1,2], Magali Guilleman[1,2], Raquel Pérez-Palacios[3], Aurélie Teissandier[4], Déborah Bourc'his[4] and Patricia Fauque[1,2]*

[1]Université Bourgogne Franche-Comté—Equipe Génétique des Anomalies du Développement (GAD), INSERM UMR1231, Dijon, France, [2]CHU Dijon Bourgogne, Laboratoire de Biologie de la Reproduction—CECOS, Dijon, France, [3]Departamento de Anatomía, Embriología y Genética Animal, Facultad de Veterinaria, Universidad de Zaragoza, Zaragoza, Spain, [4]Institut Curie, CNRS, INSERM, PSL University, Paris, France

The use of assisted reproductive technologies is consistently rising across the world. However, making an informed choice on which embryo culture medium should be preferred to ensure satisfactory pregnancy rates and the health of future children critically lacks scientific background. In particular, embryos within their first days of development are highly sensitive to their micro-environment, and it is unknown how their transcriptome adapts to different embryo culture compositions. Here, we determined the impact of culture media composition on gene expression in human pre-implantation embryos. By employing single-embryo RNA-sequencing after 2 or 5 days of the post-fertilization culture in different commercially available media (Ferticult, Global, and SSM), we revealed medium-specific differences in gene expression changes. Embryos cultured pre-compaction until day 2 in Ferticult or Global media notably displayed 266 differentially expressed genes, which were related to essential developmental pathways. Herein, 19 of them could have a key role in early development, based on their previously described dynamic expression changes across development. When embryos were cultured after day 2 in the same media considered more suitable because of its amino acid enrichment, 18 differentially expressed genes thought to be involved in the transition from early to later embryonic stages were identified. Overall, the differences were reduced at the blastocyst stage, highlighting the ability of embryos conceived in a suboptimal *in vitro* culture medium to mitigate the transcriptomic profile acquired under different pre-compaction environments.

KEYWORDS

assisted reproductive technologies, culture media, embryo, RNA-seq, transcriptome

1 Introduction

Assisted reproductive technologies (ARTs) have allowed the birth of millions of children worldwide. In Europe, for instance, over two million children were born following ARTs (Wyns et al., 2021), and numbers continuously rise, proving that tackling infertility is a huge challenge for decades to come (de Geyter et al., 2020). However, significant variability in

ART practice and effectiveness exists between countries and even at the regional scale (Munné et al., 2017; Chambers et al., 2021). In particular, embryo culture is at the core of ARTs, but making an informed decision on which culture medium to use is still a subtle task (Lane and Gardner, 2007). Embryo culture media are not expected to perfectly mirror *in vivo* environment conditions (Vajta et al., 2010), but they should, nonetheless, provide the required biological content to sustain satisfactory embryo development compared to natural conceptions. A myriad of embryo culture media is nowadays commercially available. However, owing to trade confidentiality, their exact composition is unknown, which obscures the scientific decisions for choosing one culture medium over another for embryologists (Biggers and Summers, 2008). Although the competitive commercial race to optimize embryo culture media greatly contributed to increased pregnancy rates in ARTs, the scientific basis behind their formulation is unclear, which is a matter of concern for ART-related biovigilance (Sunde et al., 2016). Very few studies have followed up the health of children born in relation to different embryo culture media used in ART cycles, but they tend to indicate that certain media may be suboptimal, with a potential long-term health impact (Kleijkers et al., 2014; Zandstra et al., 2015; Bouillon et al., 2016).

The early embryo closely interacts with its environment, particularly during the cleavage stage (Zander et al., 2006; Bolnick et al., 2017). After fertilization, the embryo transits through the oviduct until reaching the uterus, where it may be implanted. This journey throughout the maternal track exposes the embryo to multiple molecules, including growth factors, hormones, and metabolites, which promote complex reactions (Paria and Dey, 1990; Kölle et al., 2020; Saint-Dizier et al., 2020). This period also coincides with critical epigenetic reprogramming, which influences gene expression (Morgan et al., 2005; Messerschmidt et al., 2014). Substantial evidence has linked adverse environmental maternal exposures and transcriptome changes in human embryonic stem cells and newborns' cord blood (Winckelmans et al., 2017; Guo et al., 2019). This likely reflects the adaptation of the embryo to external stressors, displaying remarkable plasticity at the molecular and cellular levels (Bateson et al., 2004; Ramos-Ibeas et al., 2019).

Compared to natural conception, *in vitro* conditions inherent to ARTs can be a source of additional stress (Roseboom, 2018). Indeed, the *in vitro* environment could adversely affect the postnatal phenotype of the offspring born via *in vitro* fertilization (IVF: with or without sperm microinjection) (Fernández-Gonzalez et al., 2004; Watkins and Fleming, 2009; Gardner and Kelley, 2017). The many processes involved in ARTs and, in particular, the osmotic stress, substrate imbalance, volatile organics, and contaminant pollution linked to *in vitro* culture can trigger embryonic stress response mechanisms, but this has been barely assessed to date (Leese, 2002; Puscheck et al., 2015; Cagnone and Sirard, 2016). As Thompson et al. (2007) highlighted, "there is no adaptation by an embryo to its environment that has no consequence." In particular, differences in embryo culture medium composition may lead to differences in adaptive responses to stress.

The embryo is mostly transcriptionally silent until day 3 (four- to eight-cell stage), when embryonic genome activation (EGA) mainly occurs and relies on maternally provided mRNAs for early embryo development (Braude et al., 1988; Vassena et al., 2011; Leng et al., 2019), although transcription initiation has been reported in human embryos at the one-cell stage, acting as a proxy for early epigenetic programming (Asami et al., 2022). During this period, the capacity of the embryo to maintain metabolism and cellular homeostasis may, thus, be limited (Edwards et al., 1998; Lane and Gardner, 2001). Accordingly, short exposure to ammonium before compaction was shown to compromise the ability to further develop compared with the same exposure after compaction in mice (Zander et al., 2006). After EGA, dynamic changes in gene expression accompany embryonic lineage specification, and anomalies in these sequential expression changes can lead to developmental arrest (Sha et al., 2020). These examples highlight that the early embryo is sensitive to its micro-environment and that many parameters in IVF centers should be tightly controlled, especially embryo culture.

Evidence from animal models showed that *in vitro* culture can affect embryonic gene expression and epigenetic marks compared with *in vivo* conditions (Mann et al., 2004; Rinaudo and Schultz, 2004; Fauque et al., 2007; Wright et al., 2011). Most importantly, these molecular effects can be worsened depending on the culture medium (Rinaudo and Schultz, 2004; Schwarzer et al., 2012; Feuer et al., 2017), with a reported sensitivity of imprinted gene expression (Market-Velker et al., 2010; Ramos-Ibeas et al., 2019). Comparatively, studies in humans have mainly focused on the clinical efficiency of various culture media (live birth rate, implantation rate, clinical pregnancy rate, birthweight, placental weight, and pre-term birth rate) (Dumoulin et al., 2010; Eskild et al., 2013; Youssef et al., 2015; Kleijkers et al., 2016). Only two studies compared the transcriptomic profile of blastocysts cultured in two different media: using microarrays, they reported misregulation of genes involved in cell cycle, apoptosis, protein degradation, and metabolism, which have the capacity to impair embryo development (Kleijkers et al., 2015; Mantikou et al., 2016). This justifies pursuing efforts to identify the biological origin of embryo culture effects.

In this study, we investigated, for the first time, the impact of different culture media used in IVF centers (Ferticult, Global, and SSM) on the transcriptome of a unique collection of day-2 and -5 human embryos using single-embryo RNA sequencing. Analyzing day-2 embryos (four-cell stage) will provide insight into effects of culture media on maternal-provided transcripts and early embryonic gene activation (epigenetic programming). The importance of analyzing day-5 embryos (blastocyst stage) is that it will increase our understanding of effects on molecular processes after compaction. Embryo culture media rich in amino acids, such as Global, are nowadays preferentially used among IVF centers over media depleted in amino acids, such as Ferticult. The SSM medium evaluated in this study is no longer used due to under-performance in terms of pre-implantation and pregnancy rates (Bouillon et al., 2016). In addition, we tested whether supplementation with methionine, an essential amino acid for embryo development, could modulate the embryonic transcriptome.

We found evidence for medium-specific transcriptomic differences at day 2 (embryos at the four-cell stage), affecting major genes involved in embryonic development. In a second experiment, embryos cultured in two different media until day 2 were cultured until the blastocyst stage (day 5) in the same media considered more suitable because of its amino acid

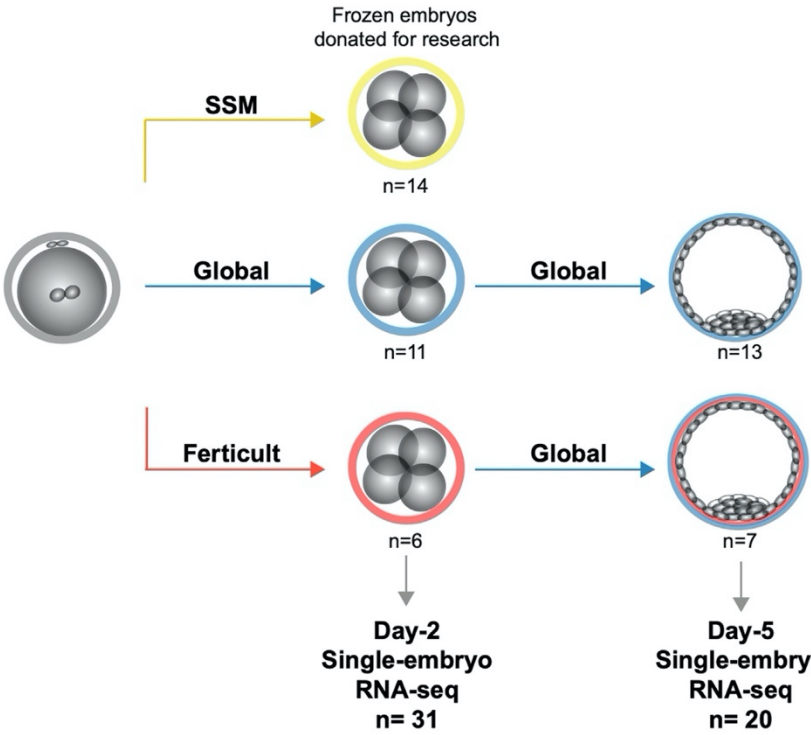

FIGURE 1
Study design for the transcriptomic analysis of human embryos cultured until days 2 and 5.

enrichment, and differences tended to reduce, reflecting the possible adaptation of the embryonic transcriptome to the culture medium. Using an expression pseudotime approach based on previously described datasets, altered expression of some genes thought to be involved in the transition from early to later embryonic stages was still identified in these blastocysts depending on their culture media pre-compaction. In addition, supplementing the embryo culture medium with methionine nearly four times the concentration found in culture media did not modify gene expression.

2 Materials and methods

2.1 Ethics statement

This research was authorized by the National Biomedicine Agency (legal decision published in the Journal Officiel under the reference JORF N°0233- 6 October 2016 and extended under the reference JORF n°0303- 31 December 2019).

2.2 Embryo selection- experimental design

We used embryos donated for research by couples and cryopreserved at the Reproductive Lab of Dijon Hospital during a relatively short period (maximum 2 years long). Embryos were included if they originated from couples ≤42 years of age, in conventional IVF or intracytoplasmic sperm injection (ICSI) attempt. Embryos from attempts with surgical spermatozoa (testicular or epididymal sperm) or performed in a viral context (HIV or viral hepatitis) were excluded. Clinical information and the number of embryos per couple are available in Supplementary Table S1. Freezing and thawing were performed with strict procedures as previously described (Bechoua et al., 2009) and detailed in Supplementary Methods. In brief, all embryos used in this study were cryopreserved individually 2 days post-fertilization by a slow-cooling protocol. Then, embryos were *in vitro* cultured in different culture media (Global medium, LifeGlobal; Ferticult IVF medium, FertiPro; SSM, and Irvine Scientific). However, to limit environmental variability, experiments were performed in parallel from different groups, using the same consumables and equipment. We analyzed only embryos cultured in these three different culture media but with identical morphological criteria, i.e., at the four-cell stage with less than 15% of anucleate fragments and regular cleavage (Figure 1). In another experiment, we selected day-2 cryopreserved embryos with identical morphological criteria as described previously from embryo cohorts cultured up to day 2 either in Ferticult or Global, which were then cultured up to day 5 in Global. Finally, for methionine supplementation, we included day-2 cryopreserved embryos from cohorts from the same patients (sibling embryos) with at least four embryos with identical embryo morphological criteria (four-cell stage). Precisely, after

thawing, these sibling embryos were randomly cultured in the Global medium without or with methionine supplementation (200 μM; concentration nearly thrice that in the Global medium), and we analyzed by single-embryo RNA-seq sibling embryos that reached the blastocyst stage in both groups (without or with methionine supplementation).

Embryos were thawed according to the strict protocol routinely used in human IVF-clinic to maintain their integrity as much as possible (Bechoua et al., 2009). Immediately after thawing, embryos were transferred into pre-equilibrated embryoslides (Unisense Fertilitech, Vitrolife) with 25 μL of the culture medium and covered with 1.2 mL of oil (Nidoil, Nidacon). They were cultured up to the blastocyst stage at 37°C and tri-gas atmosphere (6%CO2, 5%O2, and 89% N2). According to the classification of Gardner and Schoolcraft (1999), only blastocysts with at least a B2 blastocoel cavity without lysis were analyzed. At the time of sequencing, embryos were between the B2 and B4 blastocyst stages (Supplementary Table S1). We also paid attention to using the same batches of culture media in all experiments.

2.3 Single-embryo RNA sequencing

A previously described scRNA-seq method was applied to single embryos (Pérez-Palacios et al., 2021). In brief, zona pellucida-free embryos (after using acidic Tyrode's solution) were individually placed in a lysis buffer containing 1.35 mM MgCl2 (4379878, Applied Biosystems), 4.5 mM DTT, 0.45% Nonidet P-40 (11332473001, Roche), 0.18 U/mL SUPERase-In (AM2694, Ambion), and 0.36 U/mL RNase-inhibitor (AM2682, Ambion). Then, we performed a reverse transcription reaction (SuperScript III reverse transcriptase—18,080–044, Invitrogen, final concentration: 13.2 U/mL) and poly(A) tailing to the 3' end of the first-strand cDNA (by using terminal deoxynucleotidyl transferase—10,533–073, Invitrogen, final concentration: 0.75 U/mL). After the second-strand cDNA synthesis, 20 and 18 cycles (at day 2 and day 5, respectively) of PCR were performed to amplify the embryo cDNA using the TaKaRa ExTaq HS (TAKRR006B, Takara, final concentration: 0.05 U/mL) and IS PCR primer (IDT, final concentration: 1 mM). Following purification using a Zymoclean Gel DNA Recovery Kit (ZD4008, Takara), product size distribution and quantity were assessed on a Bioanalyzer using an Agilent 2,100 high-sensitivity DNA assay kit (5,067–4,626, Agilent Technologies).

The library preparation (KAPA Hyper Plus Library prep kit) and sequencing were performed by the ICGex – NGS platform (Institut Curie) on HiSeq 2,500 for day-2 embryos and on NovaSeq 6,000 Illumina sequencer for day-5 embryos for 100 bp paired-end sequencing.

2.4 Data pre-processing and quality control

We computed sequencing quality checks with FastQC v0.11.9 and trimming of adapters and low-quality sequences using TrimGalore! V0.6.6. Paired-end read alignment was performed onto human reference genome (hg38) with STAR v2.7.9a (Dobin et al., 2013) reporting randomly one position, allowing 6% of mismatches. Following previous recommendations (Teissandier et al., 2019), repeat annotation was downloaded from RepeatMasker and joined with basic gene annotation from Gencode v19. The merged file was used as an input for quantification with featureCounts v2.0.1. Genes with a minimum of count per million (cpm) > 1 in at least four samples were retained for further analysis. Principal component analyses were implemented with PCAtools v2.8.0 on log2(cpm+1) for all genes for single datasets and common genes for multiple datasets, excepting the 10% genes with the lowest variance.

2.5 Differential expression analysis

Differential expression analysis was performed using *edgeR*'s normalization (v3.38.1) combined with *voom* transformation from the *limma* package v3.52.1. *p*-values were computed using *limma* and adjusted with the Benjamini–Hochberg correction for multiple testing. Genes were declared as differentially expressed if FDR<0.1.

2.6 Gene Ontology and gene set enrichment analysis

We used Metascape v3.5 to calculate and visualize over-representation of gene ontologies in our list of differentially expressed genes (DEGs) (Zhou et al., 2019). Metascape applies hypergeometric tests and FDR corrections to identify ontology terms that comprise significantly more genes in a given gene list than what would be expected with a random gene list. For each gene list tested, we provided an appropriate background gene list corresponding to all expressed genes in all samples for a given experiment. We selected "Express Analysis" to capture relevant gene annotations from multiple sources (GO, KEGG, Reactome, canonical pathways, and CORUM). The *p*-value cutoff was kept at 0.01.

Gene set enrichment analysis (GSEA) was implemented with the *clusterProfiler* R package (v4.4.1) setting the adjusted *p*-value significance threshold at 0.05. Beforehand, imputed gene lists were pre-ranked by logFC.

2.7 Processing of public single-cell RNA-seq datasets in human embryos

We compared our data with three early embryos single-cell RNA-seq studies (Xue et al., 2013; Yan et al., 2013; Petropoulos et al., 2016). Reads alignment and quantification were executed as described previously onto raw reads downloaded from the European Nucleotide Archive (study accessions PRJNA153427, PRJNA189204, and PRJEB11202).

2.8 Trajectory inference and pseudotime computing

After pre-processing, read counts data from all 1,529 cells from the work of Petropoulos et al. were pre-clustered and normalized

with *scran* and *scater* packages (v1.24.0) after removing lowly expressed genes. Next, *Seurat* (v4.1.1) was used to scale the data and regress variables on total RNA. To identify genes whose expression dynamically changes across early embryonic development, in a continuous manner, independently of the embryo stage, we applied PHATE dimensionality reduction, a recently developed method that has been previously applied to human embryonic stem cells (Moon et al., 2019). We chose PHATE because of its ability to capture heterogeneity and reduce noise better than other dimensionality reduction methods (Moon et al., 2019). As the information geometry relies on diffusion dynamics, PHATE is especially suitable for early development (Moon et al., 2019). PHATE dimension reduction was applied with *phateR* v1.0.7 embedding three dimensions. We then inferred existing lineages and pseudotime using *slingshot* v2.4.0, a method adapted for branching lineage structures in low-dimensional data.

2.9 Differential expression along pseudotime

We used *tradeSeq* v1.10.0 (van den Berge et al., 2020) to fit a negative binomial generalized additive model (NB-GAM) for each gene. After examining diagnostic plots of the optimal number of knots (k) according to the Akaike Information Criterion (AIC), k was set to 6 as an optional parameter in the NB-GAM model. We selected DEGs along pseudotime with *associationTest*() function if p-value<0.05 and meanLogFC>2. This function relies on Wald tests to assess the null hypothesis that the expression of a gene is constant along pseudotime. DEGs with the culture medium were cross-checked with the list of DEGs along pseudotime according to Petropoulos et al.'s (2016) dataset. For further investigation, a dataset from Yan et al. (2013) was used to visualize these changes in a larger window, from the oocyte to late blastocyst stage.

3 Results

3.1 Study design and quality control analysis by comparison with previous studies

To analyze the impact of embryo culture media on the embryonic transcriptome, we performed single-embryo RNA-seq (Pérez-Palacios et al., 2021) on 51 frozen/thawed donated embryos after day 2 or day 5 of culture (Figure 1). Clinical characteristics of donors, embryo origin, and morphology are available in Supplementary Table S1, and information regarding survival after thawing can be retrieved from Supplementary Table S2. We compared three different media: Global (LifeGlobal, United States), SSM (Irvine Scientific, United States), and Ferticult (FertiPro, Belgium). Global and SSM have very similar components, except different forms of glutamine and the presence of taurine in SSM (Bouillon et al., 2016), and are intended to be used as one-step media up to day 5/6 of human embryo development (Supplementary Table S3). Ferticult differs from both in that it does not contain amino acids and is fitted to be used up to day 2/3. We processed 31 day-2 embryos (SSM: n = 14, Global: n = 11, and Ferticult: n = 6) and 20 day-5 embryos (Global: n = 13 without (n = 9) or with (n = 4) methionine supplementation and Ferticult: n = 7). At day 5, the number of samples was independent of the rate of embryos that survived the thawing process and reached at least the B2 stage (42.3% and 50.0% in Global and Ferticult groups, respectively). An average of 3.3 million reads per embryo at day 2 and 13.1 million reads at day 5 were generated, with an average mapping rate of 90.1% across all samples (Supplementary Table S4). We were able to detect the expression of 30% and 26% of all RefSeq genes and transposable elements at day 2 and day 5, respectively.

To assess the quality of our generated single-embryo RNA-seq datasets, we relied on previous high-quality studies that performed single-cell RNA-seq (scRNA-seq) in human early embryos. According to the criteria that an expressed gene should have a count per million (cpm) value greater than 1 in at least half of the samples in each embryo stage, we found consistent numbers of 12,056, 10,022, and 11,213 genes being expressed in four-cell stage embryos in the work of Yan et al. (2013), the work of Xue et al. (2013), and our own dataset, respectively (Supplementary Figure S1). In blastocysts, we identified 12,790 expressed genes in our data, compared with 8,204 genes in Yan et al.'s (2013) dataset in which blastocysts were collected a day later, at day 6.

Principal component analysis (PCA) and hierarchical clustering of global gene expression further confirmed the high similarity of our data with those two previous studies: our day-2 embryo samples clustered near four-cell samples, and our day-5 embryos samples clustered beyond morula and before late blastocyst stages (Supplementary Figures S2A,B).

3.2 Transcriptomic comparison of day-2 embryos cultured in different media

We first focused on transcriptome differences in short-term culture, at the four-cell stage (day-2), between embryos conceived in different media. The highest number of DEGs was found comparing Ferticult and Global media groups, with 266 DEGs (1.5% of all transcripts analyzed) showing adjusted p-value<0.1 (Figure 2A; Supplementary Table S5). In contrast, only one and five DEGs were found comparing SSM with either Ferticult or Global groups, respectively (Supplementary Table S5). However, the global transcriptomic analysis showed that SSM was transcriptionally closer to Global than to Ferticult (r = 0.95 versus r = 0.9, Spearman's correlation), which is consistent with their similar composition (Supplementary Figure S3A). Histograms of p-value distribution for all genes corroborate the observation of a strong effect of the culture medium on transcriptomic differences between Ferticult and Global and to a lesser extent between Ferticult and SSM, whereas p-values tended to be uniformly distributed between SSM and Global and far from statistical significance (Supplementary Figure S3B; Supplementary Table S5).

Among the 266 DEGs in the Ferticult-to-Global comparison, 145 were upregulated and 121 downregulated. Most of them (88.3%) displayed absolute log2(fold change, FC) > 2.5, which revealed substantial differences in the transcriptome of day-2 embryos depending on the culture medium (Supplementary Table S5; Supplementary Figures S4, S5A). Only eight DEGs are likely to be maternal transcripts because their expression is strictly declining in embryonic stages succeeding oocyte as assessed with Yan et al.'s

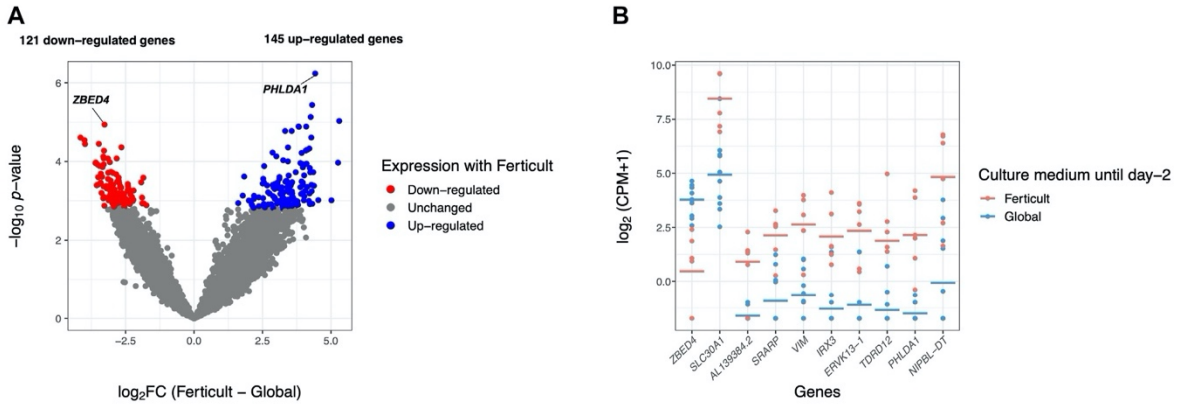

FIGURE 2
Differential gene expression analysis in day-2 embryos between Ferticult and Global media. **(A)** Volcano plot of gene expression between Ferticult and Global media at day 2. **(B)** Dot plot of the expression of top 10 Ferticult-to-Global DEGs, ordered by ascending log2FC (from left to right). Group mean is represented by the line. Dots represent individual embryos.

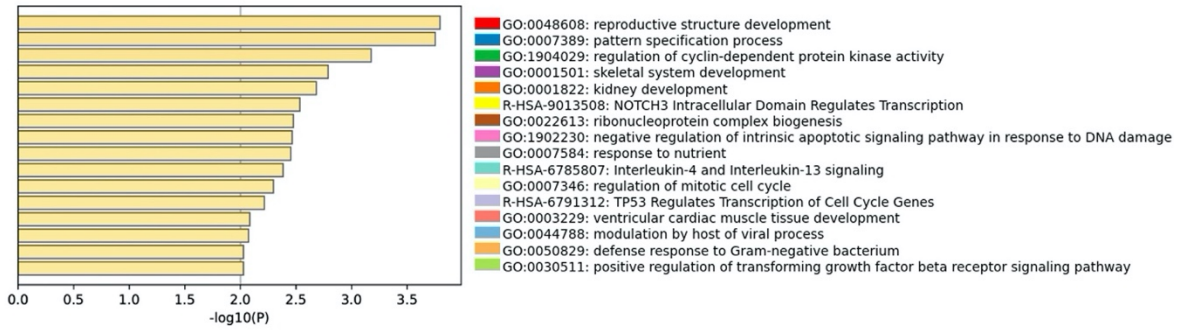

FIGURE 3
Gene Ontology analyses of Ferticult-to-Global DEGs at day 2. Bar plot of the most significant GO terms from clusters of significant pathways over-represented in day-2 DEGs, ordered by significance. Each term was selected by Metascape using a heuristic algorithm that selected the most informative term from clusters of proximal significant GO terms.

(2013) reference dataset (Supplementary Figure S5B). Top 10 most dysregulated genes including *ZBED4*, *SLC30A1*, AL139384.2, *SRARP*, *VIM*, *IRX3*, *ERVK13-1*, *TDRD12*, *PHLDA1*, and *NIPBL-DT* are shown in Figure 2B for each individual embryo according to the culture medium group. Six of them can be considered as mixed maternal/embryonic transcripts, while the four others appear to be transcribed from the embryonic genome. Gene Ontology (GO) analysis with Metascape revealed an over-representation of DEGs related to development (pattern specification process, reproductive structure development, skeletal system development, and kidney development), regulation (regulation of the mitotic cell cycle, regulation of cyclin-dependent protein kinase activity, negative regulation of the intrinsic apoptotic signaling pathway in response to DNA damage, and positive regulation of the transforming growth factor), ribonucleoprotein biogenesis complex, and response to nutrients (Figure 3; Supplementary Figure S6). Adjustments for maternal age or fertilization method were performed in all differential expression analyses, but the top DEGs remained the same (Supplementary Table S5). In parallel, we decided to perform a GSEA which provides a broader view of the overall biological processes that may be up- or downregulated with the use of either Ferticult or Global, which may not be detected by focusing on DEG interpretation. Top 10 significant ontologies indicate that genes involved in embryonic development and cell division are, respectively, likely to be differentially up- and downregulated with Ferticult (Supplementary Figure S7; Supplementary Table S6).

Focusing on major genes involved in chromatin-based processes such as DNA methylation, heterochromatin modulators, histone modifiers, and remodeling complexes, we found two histone modifiers to be significantly downregulated among the Ferticult-to-Global DEGs: the Aurora kinase A gene *AURKA* (FDR<0.1, log2FC = −1.84), which regulates many aspects of mitosis, and *SETDB1* (FDR<0.1, log2FC = −2.92), which catalyzes trimethylation

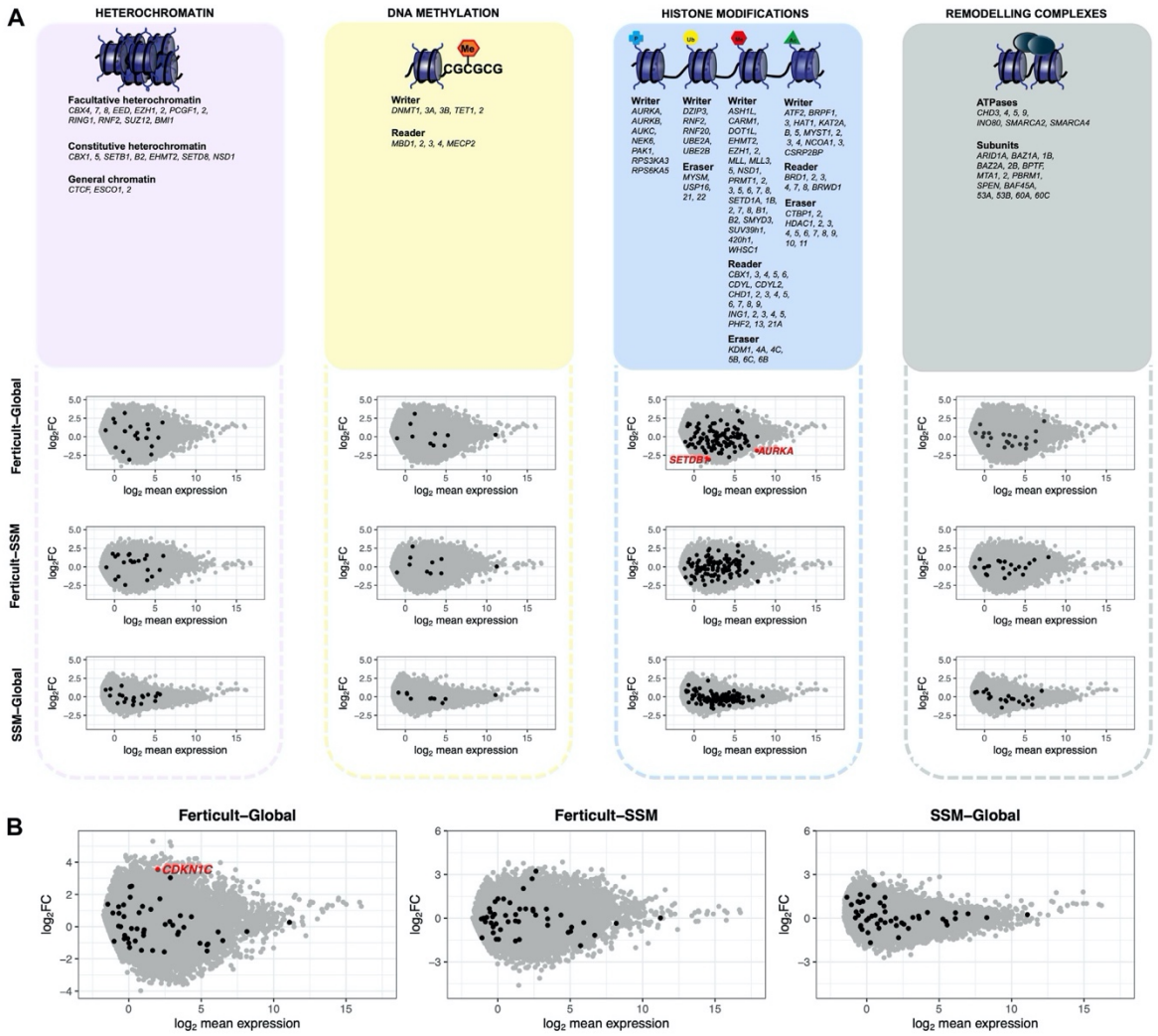

FIGURE 4
Expression differences of genes involved in chromatin-based mechanisms, imprinted genes, and transposable elements between Ferticult, SSM, and Global samples (day-2 embryos). **(A)** List of major genes identified as involved in chromatin-based processes with their scatter plot of differential expression analysis. Log2 mean expression was calculated by taking the average log2(cpm+1) expression in compared culture media groups. Each point represents a gene: misregulated genes from the aforementioned list (red dots), unchanged genes from the aforementioned list (black dots), and other expressed genes (gray dots). **(B)** Scatter plot of differential expression analysis focused on imprinted genes. Log2 mean expression was calculated by taking the average log2(cpm+1) expression in compared culture media groups. Each point represents a gene: misregulated imprinted genes (red dots), unchanged imprinted genes (black dots), and other expressed genes (gray dots).

of lysine 9 of histone H3 (H3K9me3) (Figure 4A). Additionally, focusing on imprinted genes, we only found the cyclin-dependent kinase inhibitor 1 (*CDKN1C*) gene among the 266 Ferticult-to-Global DEGs (Figure 4B). Finally, we also analyzed transposable elements and found three families to be differentially expressed between Ferticult and Global media (*CR1-12_1Mi*, *LTR6A*, and *LTR7C*). Although the top 20 expressed transposable element families were not differentially expressed in any comparison, their expression was higher in Ferticult, which resulted in fold change intensities higher in Ferticult comparisons (Supplementary Figures S8A,B).

3.3 Monitoring 2-day culture medium-induced differences at the blastocyst stage

Given the transcriptomic differences of day-2 embryos resulting from the amino-acid-free Ferticult medium over Global medium, we wanted to further analyze whether amino acid deprivation during the first 2 days of development may have extended effects on the transcriptome of blastocyst embryos. For that purpose, a second batch of embryos cultured until day 2 in Global (n = 13) or Ferticult (n = 7) media was selected for their strict identical embryo morphology and subsequently cultured until the blastocyst stage,

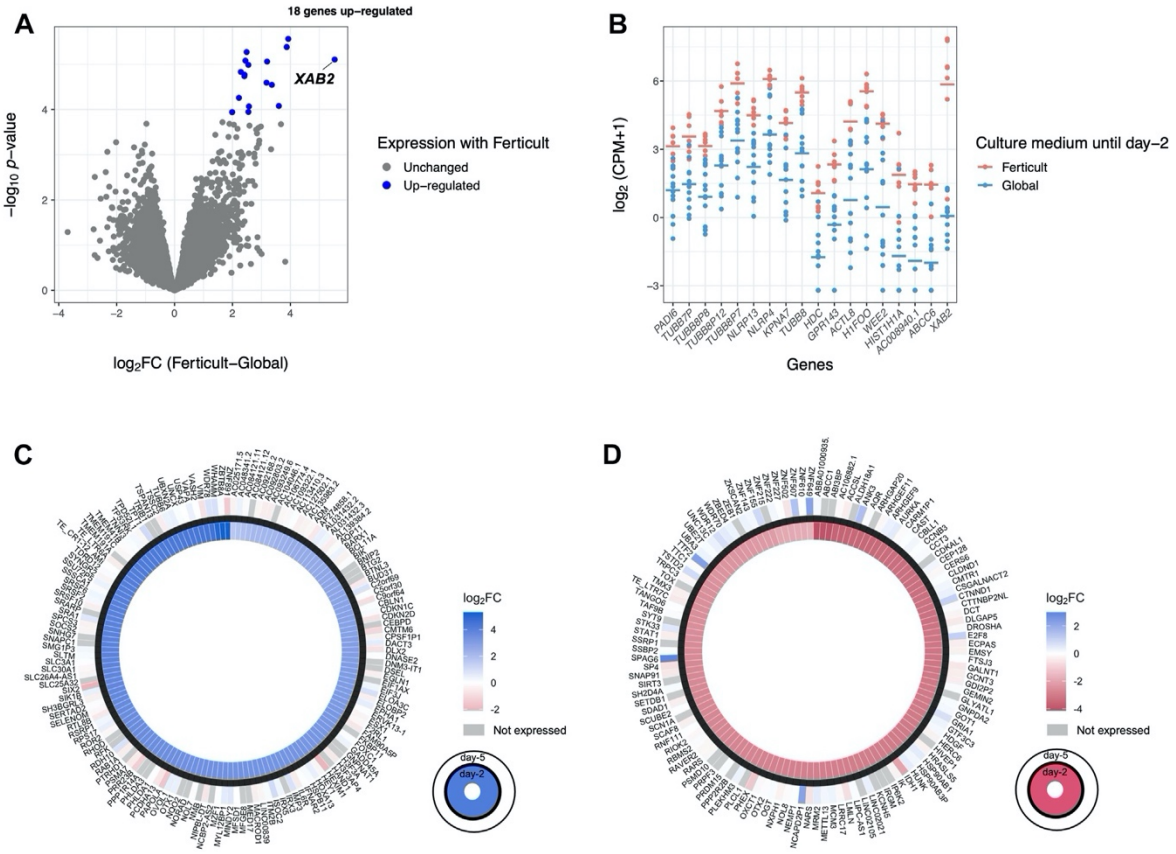

FIGURE 5
Differential expression analysis at day 5 of culture. **(A)** Volcano plot of differential gene expression between Ferticult and Global media. **(B)** Dot plot of the expression of all 18 Ferticult-to-Global DEGs, ordered by ascending log2FC (from left to right). Group mean is represented by the line. Dots represent individual embryos. **(C)** Circle plot of the expression of upregulated Ferticult-to-Global DEGs at day 2 and their expression at day 5. Plot displays the log2 fold change of the 147 DEGs upregulated with Ferticult at day 2 (interior layer) and the log2 fold change with Ferticult for the same genes at day 5 (exterior layer). Cells colored in gray correspond to genes that were not expressed at day 5. **(D)** Circle plot of the expression of downregulated Ferticult-to-Global DEGs at day 2 Global and their expression at day 5. Plot displays the log2 fold change of the 122 DEGs downregulated with Ferticult at day 2 (interior layer) and the log2 fold change with Ferticult for the same genes at day 5 (exterior layer). Cells colored in gray correspond to genes that were not expressed at day 5.

all in the Global medium (Figure 1A). Performing differential expression analysis after single-embryo RNA-seq, we found 18 DEGs in blastocysts that were previously cultured in the Ferticult medium until day 2 versus blastocysts cultured all along in Global: *ABCC6*, AC008940.1, *ACTL8*, *GPR143*, *H1FOO*, *HDC*, *HIST1H1A*, *KPNA7*, *NLRP4*, *NLRP13*, *PADI6*, *TUBB7P*, *TUBB8*, *TUBB8P7*, *TUBB8P8*, *TUBB8P12*, *WEE2*, and *XAB2* (Figures 5A,B; Supplementary Table S7). These genes were all upregulated with the Ferticult medium condition until day 2, with half showing a log2FC > 2.5 and the *XAB2* gene showing the highest overexpression score (>5.5) (Figure 5A). The GO analysis indicated a functional link with the meiotic cycle (DEGs associated with this pathway: *H1FOO*, *TUBB8*, and *WEE2*). Importantly, none of the previous expression differences observed at day 2 remained significant at day 5. Circular plots showed that fold changes of gene differences observed at day 2 were largely minimized by day 5 (Figures 5C,D). Conclusions were unchanged when adjusting for maternal age (Supplementary Table S7).

3.4 Effects of methionine supplementation

Methionine is an essential amino acid present in embryo culture media that serves as a precursor for protein synthesis and DNA methylation and, therefore, could modulate the transcriptome. We tested whether the addition of methionine at day 2 would impact the transcriptome of day-5 blastocysts cultured in Global by comparing nine samples cultured in Global and four samples cultured in Global supplemented with methionine after day 2, from sibling embryos (i.e., a pair of embryos of each condition were coming from the same couples) (Supplementary Figure S9). The differential expression analysis revealed no significant DEG.

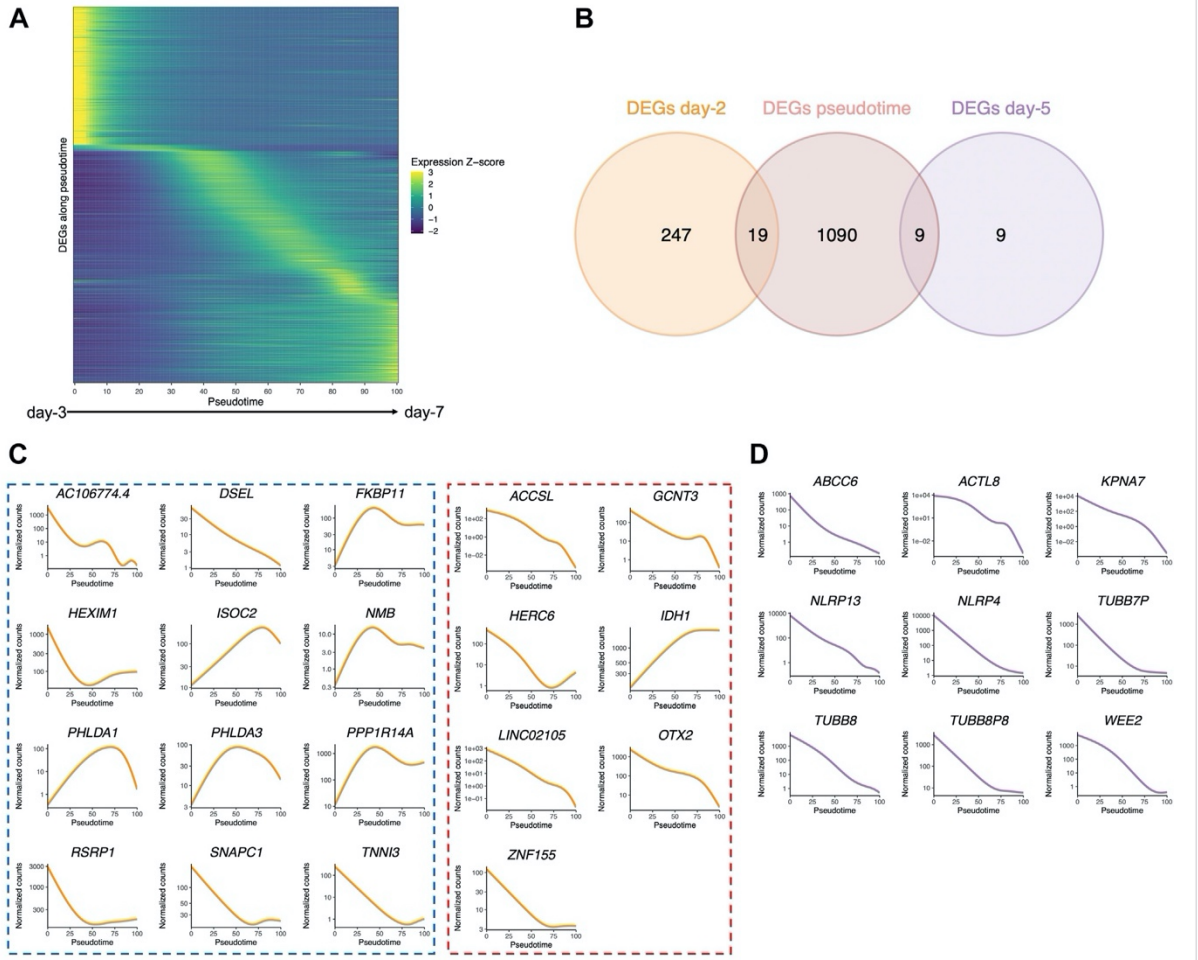

FIGURE 6
Pseudotime differential expression during human preimplantation development. Pseudotime is a metric that could be interpreted as a timing distance between one cell and its precursor cell and helps identify the ordering of cells along a lineage based on their gene expression profile. **(A)** Heatmap of the expression of the 1,110 genes that were found to be differentially expressed along pseudotime (from public datasets established from the eight-cell stage (Petropoulos et al., 2016), ordered by the timing of peak expression (arbitrary unit). Expression Z-score: Z-score of TMM-adjusted cpm. **(B)** Venn diagram of the number of DEGs along pseudotime that are differentially expressed between Ferticult and Global at days 2 and 5 of the embryonic culture. **(C)** Dynamics of the expression of the 19 day-2 Ferticult-to-Global DEGs that are differentially expressed along pseudotime according to Petropoulos et al.'s (2016) dataset. The curve corresponds to the NB-GAM fitted normalized counts (TMM-adjusted cpm). Left panel surrounded by a blue line corresponds to genes upregulated with Ferticult. Right panel surrounded by a red line corresponds to genes downregulated with Ferticult. **(D)** Expression dynamics of the nine day-5 Ferticult-to-Global DEGs that are differentially expressed along pseudotime according to Petropoulos et al.'s (2016) dataset. The curve corresponds to the NB-GAM fitted normalized counts (TMM-adjusted cpm).

3.5 Effects of the culture medium on the transcriptional trajectory of early embryos

Early embryos undergo profound transcriptional changes during the first stages of development. In an attempt to address whether the embryo culture medium may affect these sequential modifications of gene expression, we used a public dataset of 1,529 single-cell RNA-seq of human embryos from days 3 to 7 (cultured in either CCM (Vitrolife) or G-1 Plus (Vitrolife) media) (Petropoulos et al., 2016), which previously allowed delineating the transcription signature of each embryonic lineage and their dynamics during embryonic lineage segregation (Meistermann et al., 2021). Our objective was to identify genes whose expression dynamically changes across early embryonic development, in a continuous manner, independent of the embryo stage. For that purpose, we applied the PHATE dimensionality reduction method (Moon et al., 2019) and inferred existing lineages and pseudotime (van den Berge et al., 2020)—a metric that could be interpreted as a timing distance between 1 cell and its precursor cell. On the public scRNA-seq dataset (Petropoulos et al., 2016), we were able to identify eight clusters by using k-means clustering to group cells with high transcriptomic similarities. We also identified three distinct lineages (Supplementary Figure S10A) that shared the same

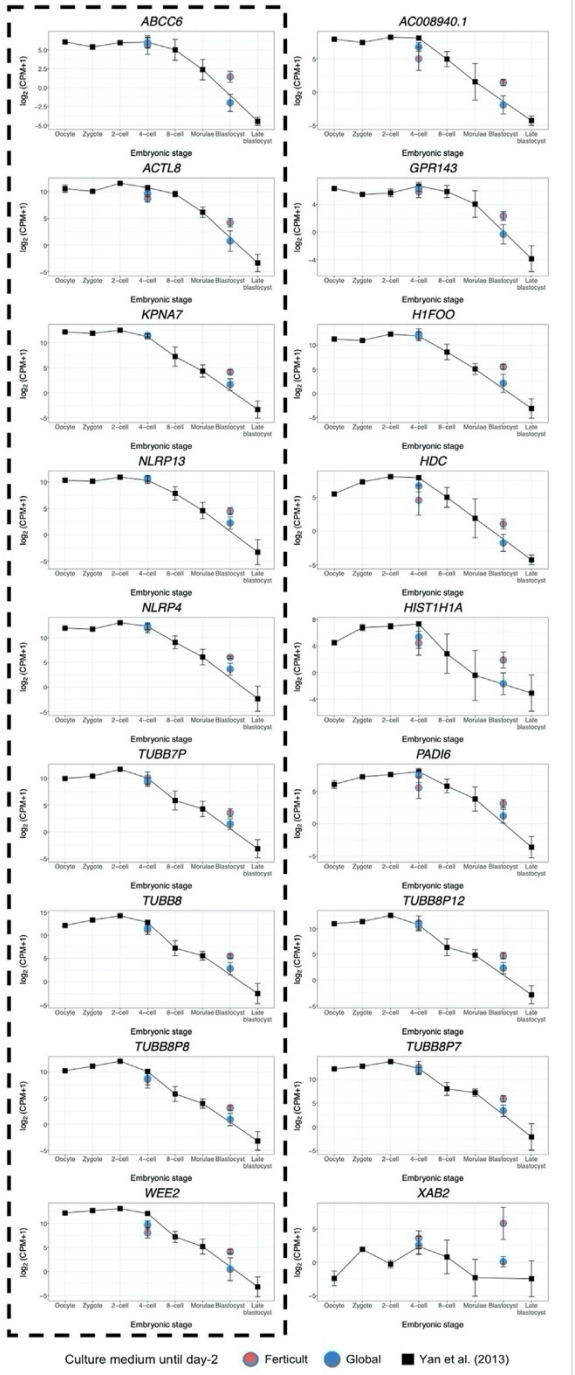

FIGURE 7
Expression dynamics of day-5 Ferticult-to-Global DEGs from the oocyte to the blastocyst stage as compared to the literature. We plotted the public scRNA-seq dataset from the work of Yan et al. (2013) obtained from the oocyte to the late blastocyst stage as the reference level of the expression of early embryonic genes. Each colored point represents the mean log2(cpm+1) value of all samples for each culture medium group. Black squares represent the mean log2(cpm+1) for all samples from the work of Yan et al. (2013) for each embryonic stage. Error bars represent the standard deviation between (*Continued*)

FIGURE 7 (Continued)
samples from the same group. Day-2 embryos were represented at the four-cell stage. Day-5 embryos were represented at the blastocyst stage. DEGs surrounded by a dashed black line were also found to be differentially expressed along pseudotime according to Petropoulos et al.'s (2016) dataset.

structure when considering cells from clusters 1 to 5 but separated into clusters 6, 7, and 8. Using the cell classification adopted in previous studies (Petropoulos et al., 2016; Meistermann et al., 2021), the three lineages corroborated with the demarcation into epiblast (EPI), primitive endoderm (PrE), and trophectoderm (TE) cells (Supplementary Figures S10B,C). Each cell was then assigned a pseudotime to reflect its "transcriptomic age" along each of the three lineages (Supplementary Figure S10D). Along with this inferred pseudotime, we identified 1,110 genes with a dynamic expression pattern (Figure 6A).

Considering the question of the impact of the culture medium, we crossed these 1,110 dynamic genes with our list of DEGs identified at days 2 and 5 in the Ferticult-to-Global comparison. Remarkably, 19 out of 266 DEGs at day 2 and 9 out of 18 DEGs at day 5 showed dynamic expression changes across pre-implantation pseudotime, meaning that the choice of the culture medium has an impact on the expression of genes that are dynamically regulated during early development (Figure 6B). Temporal expression of those genes is shown in Figures 6C,D. While the 19 DEGs at day 2 that were also differentially expressed pseudotime showed a diverse profile of expression (Figure 6C), the 9 DEGs at day 5 that are also differentially expressed along pseudotime displayed a declining expression over embryo development in the reference pseudotime (Figure 6D). To confirm these results, we used an independent public scRNA-seq dataset from the work of Yan et al. (2013) obtained with a broader window, from the oocyte to late blastocyst (Figure 7). When considering our own datasets, embryos continuously cultured in Global up to day 5 also showed this declining trend of expression from days 2 to 5, with levels that were congruent with the reference dataset from the work of Yan et al. (2013) (Figure 7). However, day-5 embryos previously cultured in Ferticult until the four-cell stage showed over-expression for all DEGs, suggesting that these embryos retained abnormally high levels for their embryonic stage. On average, these blastocyst embryos showed expression levels that were closer to the morula stages.

4 Discussion

We provide here in-depth characterization of the transcriptomic effects exerted by different culture media on human embryos after 2 and 5 days of culture. In this study, media determined as a worse-case scenario, Ferticult and SSM, were compared to Global, as a better-case scenario, providing insight into the impact of culture media on the transcriptome of early ART-produced human embryos. It should be noted that for the best-case scenario, *in vivo*-derived embryos cannot ethically be obtained. It yields several insights into how culture medium composition can induce transcriptomic responses as an adaptation of the embryo

to its micro-environment, pre- and post-compaction. In line with the importance of our research questions, two of the media we tested are no longer used for human embryo culture (one was removed from the market).

First, we focused on embryos cultured until day 2, as this pre-compaction period is likely to be sensitive to environmental stressors. The most pronounced transcriptional divergence was between Ferticult and Global, with 266 DEGs. Among these DEGs, the majority were transcribed from the embryonic genome or consisted of mixed maternal/embryonic transcripts. It is in agreement with studies using animal models, where it has been shown that the culture environment influences the maternal-to-embryonic transition, which itself influences the maternal transcript clearance (Tesfaye et al., 2004; Zhang et al., 2022). A total of 19 of these DEGs could have a key role in early development, based not only on their dynamic expression changes across development but also on their association with GO terms related to essential developmental pathways, and were mostly upregulated in Ferticult. GSEA also depicted global differential regulation of important developmental pathways regarding the use of different culture media, notably cell division and pattern specification processes. Our results are congruent with two previous microarray studies that measured transcriptomic differences between embryos cultured in two culture media (G5 and HTF) related to cell cycle and metabolism-associated genes (Kleijkers et al., 2015; Mantikou et al., 2016). Despite SSM and Global having proximal components, the Ferticult–SSM comparison yielded only one DEG, but the overview of global patterns of expression still assumes the existence of transcriptomic differences between Ferticult and SSM media. The few composition disparities between SSM and Global would explain why the embryonic response to the SSM culture is not completely equal to that of Global.

Imprinted genes are candidates for high susceptibility to environmental conditions, and disruption of imprinted expression has been linked to developmental pathologies in humans (Maher and Reik, 2000). Accordingly, animal studies indicated that some embryo culture media were associated with hypomethylation of maternally expressed genes (such as *H19* and *SNRPN*), resulting in aberrant biallelic expression (Mann et al., 2004; Market-Velker et al., 2012). In our study, only one imprinted gene, *CDKN1C*, was upregulated after 2 days in culture in Ferticult compared to Global. *CDKN1C* is a key regulator of cell growth and proliferation, and aberrant expression is observed in syndromes with overgrowth, tumor predisposition, and congenital malformations, such as Beckwith–Wiedemann syndrome, notably in mouse embryos and fetuses (Andrews et al., 2007; Tunster et al., 2011). We also found that the expression of *SETDB1*, which is involved in histone methylation, was downregulated in Ferticult samples. These elements may reflect direct and indirect influences of the culture medium on the embryonic epigenome.

The link between culture medium composition and transcriptomic effects is still unclear, but transcriptional changes may reflect an adaptation to a sub-optimal environment. For those reasons, we further tested whether the differences observed at day 2 in Ferticult over Global were maintained later on, at the blastocyst stage, after being cultured in Global, which is considered more suitable because of its amino acid enrichment (Rinaudo and Schultz, 2004). Only 18 DEGs were retrieved, and importantly, none of the early differences observed at day 2 were conserved at this later stage. Notably, the differences in expression levels of *AURKA*, *SETDB1*, and the imprinted *CDKN1C* gene observed at day 2 no longer existed at day 5. The original transcriptional changes may not have persisted because, in post-compaction, the embryo acquires an increasing ability to mitigate the transcriptomic profile acquired under different pre-compaction environments and to correct transcriptional errors (Wale and Gardner, 2016). A second hypothesis is that the Global medium composition itself may have allowed the embryo to recover a favorable transcriptomic landscape. Finally, we cannot rule out that only viable embryos were able to develop until the blastocyst stage, and only embryos with functional abilities were, therefore, selected in our analysis.

Our analysis of genes that are differentially expressed along pseudotime brought evidence that the use of distinct culture media prior to compaction can alter the sequential gene expression changes linked to later embryo development. Genes activated or downregulated at the wrong time may impact development and cause lasting effects (Calle et al., 2012; Bertoldo et al., 2015). Notably, Ferticult was associated with the over-expression of some genes at day 5. It is, therefore, possible that 2-day culture in Ferticult induces a delay in clearance of some maternal RNAs. Accordingly, two of the 18 DEGs at day 5 were maternal effect genes (*PADI6* and *TUBB8*) (Mitchell, 2022), which may indeed reflect longer retention of maternal transcripts. *PADI6* is a member of the subcortical oocyte complex (Yu et al., 2014; Bebbere et al., 2016), while *TUBB8* is the major constituent of the oocyte meiotic spindle assembly in primates (Feng et al., 2016).

Nevertheless, our pseudotime analysis of genes differentially expressed over the course of development also identified genes that are thought to be involved in the transition from early to later embryonic stages, such as *ABCC6*, *ACTL8*, *KPNA7*, *NLRP4*, *NLRP13*, *TUBB7P*, *TUBB8P8*, and *WEE2*. *TUBB7P* and *TUBB8P8* encode beta-tubulins of major importance in cell division and morphology. Karyopherin subunit alpha 7 (*KPNA7*) is involved in nuclear protein transport (Tejomurtula et al., 2009), and *Kpna7*-deficient mice fail to develop to the blastocyst stage or show developmental delays (Hu et al., 2010). Whether *ABCC6*, *ACTL8*, *NLRP4*, *NLRP13*, and *WEE2* are involved in early embryogenesis remains unknown. Additionally, XPA-binding protein 2 (*XAB2*), whose expression does not appear to be stage specific, was particularly high in Ferticult (log2FC>5.5). *XAB2* plays a role in DNA repair (Hou et al., 2016) and is required for embryo viability (Yonemasu et al., 2005; Yanez et al., 2016). The activation of DNA repair mechanisms may be reflective of stress conditions experienced by pre-implantation embryos. Because embryos were cultured in the same medium after day 2 in our study and because the embryo is transcriptionally silent until EGA, we can hypothesize that the blastocyst transcriptome was influenced by alterations that occurred pre-compaction.

Finally, we investigated whether adding methionine to the culture medium, an essential amino acid whose concentration varies greatly between commercial media (Tarahomi et al., 2019), could affect embryo gene expression. Methionine is a precursor of S-adenosylmethionine, a key component in the one-carbon metabolism and methylation processes (Steegers-Theunissen et al., 2013). Methionine is necessary for proper embryo development, but in excessive concentration, it could negatively affect embryo abilities, as demonstrated in several animal models (Dunlevy et al., 2006; Rees et al., 2006; Kwong et al., 2010). Reassuringly, we did not identify any DEGs in sibling embryos cultured in Global until day 5, with or without methionine

supplementation (concentration nearly thrice that in the Global medium), suggesting that excessive methionine concentration from day 2 did not have a major influence on the blastocyst's transcriptome. It is possible that the original methionine concentration in the Global medium (50 μM as evaluated in Morbeck et al. (2014)) and the supplementation concentration (200 μM) assessed in this study are both within the physiological range. Consequently, the absence of significant differences after supplementation would be normal. Analyzing the early effects of methionine addition before EGA could be important.

Evidence that the embryo culture medium can impact gene expression has long been described in animals (Rinaudo and Schultz, 2004; Schwarzer et al., 2012; Feuer et al., 2017). Interestingly, in pig, adding reproductive fluids during *in vitro* culture allows producing blastocysts with closer chromatin and transcriptomic profiles compared to natural conditions (Canovas et al., 2017). It will be important to develop culture media closer to natural fluid even if we showed that the embryo is highly adaptable to different conditions. Additionally, if this study is reassuring, we might not forget that many other processes in the IVF laboratory environment constitute environmental stressors (temperature, pH, co-culture, light, oxygen tension, and manipulation). In our design, culture conditions other than culture media were identical for all samples, but a gamete or an embryo exposed to a stressful condition might be even more vulnerable to other stressors. In addition, identical freezing protocol was used, the slow freezing protocol, now optimized by vitrification. This freezing protocol might be a factor of the cumulative stress effect.

We cannot rule out that some differential expression observed at the blastocyst stage did stem from differences in embryo morphology between the groups, even if the blastocysts included were mostly B2. However, it is likely that if there are morphological differences, they may be substantially related to the use of the different culture media. In this study, we cannot exclude specific effects of couple characteristics (stimulation protocol, age, and infertility causes) on the embryonic transcriptome, but we showed that maternal age did not change the overall results.

For the first time in humans, we employed single-embryo RNA-seq on a unique collection of day-2 and -5 embryos to assess to what extent different culture conditions might affect the developing embryo transcriptome. Even though marked transcriptomic differences were observed between culture media at day 2, when embryos totally deprived in amino acids during their first days of development were returned to favorable culture conditions, these differences were reduced at the blastocyst stage. The few differences observed at day 5 may be attributed to a delay in molecular processes specific to the use of one medium. Altogether, our study emphasizes the abilities of the embryo to recover an expected transcriptomic landscape post-compaction. Consecutively, to rule out potential long-lasting epigenetic effects, it would be important to investigate whether the methylome also adapts to different media formulations. In addition, whether different embryo culture media used post-compaction could modulate the embryonic transcriptome, and notably, the expression of genes characteristic of lineage specification remains to be elucidated.

Data availability statement

The datasets presented in this study can be found in online repositories. The names of the repository/repositories and accession number(s) can be found below: GEO accession number: GSE212811.

Ethics statement

The studies involving human participants were reviewed and approved by the National Biomedicine Agency. The patients/participants provided their written informed consent to participate in this study.

Author contributions

PF, JB, and BD took primary responsibility for conceptualization and investigation. PF and RP-P were responsible for the methodology. MG, JB, and PF were involved in resources, experiments, and visualization. BD and AT conducted the data curation and formal analysis. BD and PF were involved in original draft preparation. DB participated in review and editing. All authors contributed to the article and approved the submitted version.

Funding

This work was supported by funding from the "Agence Nationale pour la Recherche ("CARE"-ANR JCJC 2017)."

Acknowledgments

We thank Fuchou Tang for hosting PF in his lab to learn the scRNA-seq method, Nicolas Lieury for his assistance in preparing and obtaining the samples and Maud Carpentier of the "Direction de la Recherche Clinique et de l'Innovation" of Dijon University Hospital for the adminitrative management of the study. We acknowledge the ICGex NGS platform of Institut Curie (supported by grants ANR-10-EQPX-03, Equipex and ANR-10-INBS-09-08, France Génomique).

Conflict of interest

The authors declare that the research was conducted in the absence of any commercial or financial relationships that could be construed as a potential conflict of interest.

Publisher's note

All claims expressed in this article are solely those of the authors and do not necessarily represent those of their

affiliated organizations, or those of the publisher, the editors, and the reviewers. Any product that may be evaluated in this article, or claim that may be made by its manufacturer, is not guaranteed or endorsed by the publisher.

Supplementary material

The Supplementary Material for this article can be found online at: https://www.frontiersin.org/articles/10.3389/fcell.2023.1155634/full#supplementary-material

References

Andrews, S. C., Wood, M. D., Tunster, S. J., Barton, S. C., Surani, M. A., and John, R. M. (2007). Cdkn1c (p57Kip2) is the major regulator of embryonic growth within its imprinted domain on mouse distal chromosome 7. *BMC Dev. Biol.* 7, 53. doi:10.1186/1471-213X-7-53

Asami, M., Lam, B. Y. H., Ma, M. K., Rainbow, K., Braun, S., VerMilyea, M. D., et al. (2022). Human embryonic genome activation initiates at the one-cell stage. *Cell Stem Cell* 29, 209–216.e4. doi:10.1016/j.stem.2021.11.012

Bateson, P., Barker, D., Clutton-Brock, T., Deb, D., D'Udine, B., Foley, R. A., et al. (2004). Developmental plasticity and human health. *Nature* 430, 419–421. doi:10.1038/nature02725

Bebbere, D., Masala, L., Albertini, D. F., and Ledda, S. (2016). The subcortical maternal complex: Multiple functions for one biological structure? *J. Assist. Reprod. Genet.* 33, 1431–1438. doi:10.1007/s10815-016-0788-z

Bechoua, S., Astruc, K., Thouvenot, S., Girod, S., Chiron, A., Jimenez, C., et al. (2009). How to demonstrate that eSET does not compromise the likelihood of having a baby? *Hum. Reprod.* 24, 3073–3081. doi:10.1093/humrep/dep321

Bertoldo, M. J., Locatelli, Y., O'Neill, C., and Mermillod, P. (2015). Impacts of and interactions between environmental stress and epigenetic programming during early embryo development. *Reprod. Fertil. Dev.* 27, 1125–1136. doi:10.1071/RD14049

Biggers, J. D., and Summers, M. C. (2008). Choosing a culture medium: Making informed choices. *Fertil. Steril.* 90, 473–483. doi:10.1016/j.fertnstert.2008.08.010

Bolnick, A., Abdulhasan, M., Kilburn, B., Xie, Y., Howard, M., Andresen, P., et al. (2017). Two-cell embryos are more sensitive than blastocysts to AMPK-dependent suppression of anabolism and stemness by commonly used fertility drugs, a diet supplement, and stress. *J. Assist. Reprod. Genet.* 34, 1609–1617. doi:10.1007/s10815-017-1028-x

Bouillon, C., Léandri, R., Desch, L., Ernst, A., Bruno, C., Cerf, C., et al. (2016). Does embryo culture medium influence the health and development of children born after *in vitro* fertilization? *PLoS One* 11. doi:10.1371/journal.pone.0150857

Braude, P., Bolton, V., and Moore, S. (1988). Human gene expression first occurs between the four-and eight-cell stages of preimplantation development. *Nature* 332, 459–461. doi:10.1038/332459a0

Cagnone, G., and Sirard, M. A. (2016). The embryonic stress response to *in vitro* culture: Insight from genomic analysis. *Reproduction* 152, R247–R261. doi:10.1530/REP-16-0391

Calle, A., Fernandez-Gonzalez, R., Ramos-Ibeas, P., Laguna-Barraza, R., Perez-Cerezales, S., Bermejo-Alvarez, P., et al. (2012). Long-term and transgenerational effects of *in vitro* culture on mouse embryos. *Theriogenology* 77, 785–793. doi:10.1016/j.theriogenology.2011.07.016

Canovas, S., Ivanova, E., Romar, R., García-Martínez, S., Soriano-Úbeda, C., García-Vázquez, F. A., et al. (2017). DNA methylation and gene expression changes derived from assisted reproductive technologies can be decreased by reproductive fluids. *Elife* 6, e23670. doi:10.7554/eLife.23670

Chambers, G. M., Dyer, S., Zegers-Hochschild, F., de Mouzon, J., Ishihara, O., Banker, M., et al. (2021). International committee for monitoring assisted reproductive technologies world report: Assisted reproductive technology, 2014. *Hum. Reprod.* 36, 2921–2934. doi:10.1093/humrep/deab198

de Geyter, C., Wyns, C., Calhaz-Jorge, C., de Mouzon, J., Ferraretti, A. P., Kupka, M., et al. (2020). 20 years of the European IVF-monitoring consortium registry: What have we learned? A comparison with registries from two other regions. *Hum. Reprod.* 35, 2832–2849. doi:10.1093/humrep/deaa250

Dobin, A., Davis, C. A., Schlesinger, F., Drenkow, J., Zaleski, C., Jha, S., et al. (2013). Star: Ultrafast universal RNA-seq aligner. *Bioinformatics* 29, 15–21. doi:10.1093/bioinformatics/bts635

Dumoulin, J. C., Land, J. A., van Montfoort, A. P., Nelissen, E. C., Coonen, E., Derhaag, J. G., et al. (2010). Effect of *in vitro* culture of human embryos on birthweight of newborns. *Hum. Reprod.* 25, 605–612. doi:10.1093/humrep/dep456

Dunlevy, L. P. E., Burren, K. A., Chitty, L. S., Copp, A. J., and Greene, N. D. E. (2006). Excess methionine suppresses the methylation cycle and inhibits neural tube closure in mouse embryos. *FEBS Lett.* 580, 2803–2807. doi:10.1016/j.febslet.2006.04.020

Edwards, L. J., Williams, D. A., and Gardner, D. K. (1998). Intracellular pH of the preimplantation mouse embryo: Effects of extracellular pH and weak acids. *Mol. Reprod. Dev.* 50, 434–442. doi:10.1002/(SICI)1098-2795

Eskild, A., Monkerud, L., and Tanbo, T. (2013). Birthweight and placental weight; do changes in culture media used for IVF matter? Comparisons with spontaneous pregnancies in the corresponding time periods. *Hum. Reprod.* 28, 3207–3214. doi:10.1093/humrep/det376

Fauque, P., Jouannet, P., Lesaffre, C., Ripoche, M. A., Dandolo, L., Vaiman, D., et al. (2007). Assisted reproductive technology affects developmental kinetics, H19 imprinting control region methylation and H19 gene expression in individual mouse embryos. *BMC Dev. Biol.* 7, 116. doi:10.1186/1471-213X-7-116

Feng, R., Sang, Q., Kuang, Y., Sun, X., Yan, Z., Zhang, S., et al. (2016). Mutations in TUBB8 and human oocyte meiotic arrest. *N. Engl. J. Med.* 374, 223–232. doi:10.1056/nejmoa1510791

Fernández-Gonzalez, R., Moreira, P., Bilbao, A., Jiménez, A., Pérez-Crespo, M., Ramírez, M. A., et al. (2004). Long-term effect of *in vitro* culture of mouse embryos with serum on mRNA expression of imprinting genes, development, and behavior. *Proc. Natl. Acad. Sci. U. S. A.* 101, 5880–5885. doi:10.1073/pnas.0308560101

Feuer, S., Liu, X., Donjacour, A., Simbulan, R., Maltepe, E., and Rinaudo, P. (2017). Transcriptional signatures throughout development: The effects of mouse embryo manipulation *in vitro*. *Reproduction* 153, 107–122. doi:10.1530/rep-16-0473

Gardner, D. K., and Kelley, R. L. (2017). Impact of the IVF laboratory environment on human preimplantation embryo phenotype. *J. Dev. Orig. Health Dis.* 8, 418–435. doi:10.1017/S2040174417000368

Gardner, D. K., and Schoolcraft, W. B. (1999). Culture and transfer of human blastocysts. *Curr. Opin. Obstet. Gynecol.* 11, 307–311. doi:10.1097/00001703-199906000-00013

Guo, H., Tian, L., Zhang, J. Z., Kitani, T., Paik, D. T., Lee, W. H., et al. (2019). Single-cell RNA sequencing of human embryonic stem cell differentiation delineates adverse effects of nicotine on embryonic development. *Stem Cell Rep.* 12, 772–786. doi:10.1016/j.stemcr.2019.01.022

Hou, S., Li, N., Zhang, Q., Li, H., Wei, X., Hao, T., et al. (2016). XAB2 functions in mitotic cell cycle progression via transcriptional regulation of CENPE. *Cell Death Dis.* 7, e2409. doi:10.1038/cddis.2016.313

Hu, J., Wang, F., Yuan, Y., Zhu, X., Wang, Y., Zhang, Y., et al. (2010). Novel importin-alpha family member Kpna7 is required for normal fertility and fecundity in the mouse. *J. Biol. Chem.* 285, 33113–33122. doi:10.1074/jbc.M110.117044

Kleijkers, S. H. M., Eijssen, L. M. T., Coonen, E., Derhaag, J. G., Mantikou, E., Jonker, M. J., et al. (2015). Differences in gene expression profiles between human preimplantation embryos cultured in two different IVF culture media. *Hum. Reprod.* 30, 2303–2311. doi:10.1093/humrep/dev179

Kleijkers, S. H. M., Mantikou, E., Slappendel, E., Consten, D., van Echten-Arends, J., Wetzels, A. M., et al. (2016). Influence of embryo culture medium (G5 and HTF) on pregnancy and perinatal outcome after IVF: A multicenter rct. *Hum. Reprod.* 31, 2219–2230. doi:10.1093/humrep/dew156

Kleijkers, S. H. M., van Montfoort, A. P. A., Smits, L. J. M., Viechtbauer, W., Roseboom, T. J., Nelissen, E. C. M., et al. (2014). IVF culture medium affects post-natal weight in humans during the first 2 years of life. *Hum. Reprod.* 29, 661–669. doi:10.1093/humrep/deu025

Kölle, S., Hughes, B., and Steele, H. (2020). Early embryo-maternal communication in the oviduct: A review. *Mol. Reprod. Dev.* 87, 650–662. doi:10.1002/mrd.23352

Kwong, W. Y., Adamiak, S. J., Gwynn, A., Singh, R., and Sinclair, K. D. (2010). Endogenous folates and single-carbon metabolism in the ovarian follicle, oocyte and pre-implantation embryo. *Reproduction* 139, 705–715. doi:10.1530/REP-09-0517

Lane, M., and Gardner, D. K. (2001). Blastomere homeostasis. *ART Hum. Blastocyst*, 69–90. doi:10.1007/978-1-4613-0149-3_7

Lane, M., and Gardner, D. K. (2007). Embryo culture medium: Which is the best? *Best. Pract. Res. Clin. Obstet. Gynaecol.* 21, 83–100. doi:10.1016/j.bpobgyn.2006.09.009

Leese, H. J. (2002). Quiet please, do not disturb: A hypothesis of embryo metabolism and viability. *BioEssays* 24, 845–849. doi:10.1002/bies.10137

Leng, L., Sun, J., Huang, J., Gong, F., Yang, L., Zhang, S., et al. (2019). Single-cell transcriptome analysis of uniparental embryos reveals parent-of-origin effects on human preimplantation development. *Cell Stem Cell* 25, 697–712. doi:10.1016/j.stem.2019.09.004

Maher, E. R., and Reik, W. (2000). Beckwith-Wiedemann syndrome: Imprinting in clusters revisited. *J. Clin. Investigation* 105, 247–252. doi:10.1172/jci9340

Mann, M. R. W., Lee, S. S., Doherty, A. S., Verona, R. I., Nolen, L. D., Schultz, R. M., et al. (2004). Selective loss of imprinting in the placenta following preimplantation development in culture. *Development* 131, 3727–3735. doi:10.1242/dev.01241

Mantikou, E., Jonker, M. J., Wong, K. M., van Montfoort, A. P. A., de Jong, M., Breit, T. M., et al. (2016). Factors affecting the gene expression of *in vitro* cultured human preimplantation embryos. *Hum. Reprod.* 31, 298–311. doi:10.1093/humrep/dev306

Market-Velker, B. A., Denomme, M. M., and Mann, M. R. W. (2012). Loss of genomic imprinting in mouse embryos with fast rates of preimplantation development in culture. *Biol. Reprod.* 86, 1–16. doi:10.1095/biolreprod.111.096602

Market-Velker, B. A., Fernandes, A. D., and Mann, M. R. W. (2010). Side-by-side comparison of five commercial media systems in a mouse model: Suboptimal *in vitro* culture interferes with imprint maintenance. *Biol. Reprod.* 83, 938–950. doi:10.1095/biolreprod.110.085480

Meistermann, D., Bruneau, A., Loubersac, S., Reignier, A., Firmin, J., François-Campion, V., et al. (2021). Integrated pseudotime analysis of human pre-implantation embryo single-cell transcriptomes reveals the dynamics of lineage specification. *Cell Stem Cell* 28, 1625–1640.e6. doi:10.1016/j.stem.2021.04.027

Messerschmidt, D. M., Knowles, B. B., and Solter, D. (2014). DNA methylation dynamics during epigenetic reprogramming in the germline and preimplantation embryos. *Genes Dev.* 28, 812–828. doi:10.1101/gad.234294.113

Mitchell, L. E. (2022). Maternal effect genes: Update and review of evidence for a link with birth defects. *Hum. Genet. Genomics Adv.* 3, 100067. doi:10.1016/j.xhgg.2021.100067

Moon, K. R., van Dijk, D., Wang, Z., Gigante, S., Burkhardt, D. B., Chen, W. S., et al. (2019). Visualizing structure and transitions in high-dimensional biological data. *Nat. Biotechnol.* 37, 1482–1492. doi:10.1038/s41587-019-0336-3

Morbeck, D. E., Krisher, R. L., Herrick, J. R., Baumann, N. A., Matern, D., and Moyer, T. (2014). Composition of commercial media used for human embryo culture. *Fertil. Steril.* 102, 759–766. doi:10.1016/j.fertnstert.2014.05.043

Morgan, H. D., Santos, F., Green, K., Dean, W., and Reik, W. (2005). Epigenetic reprogramming in mammals. *Hum. Mol. Genet.* 14, 47–58. doi:10.1093/hmg/ddi114

Munné, S., Alikani, M., Ribustello, L., Colls, P., Martínez-Ortiz, P. A., Mcculloh, D. H., et al. (2017). Euploidy rates in donor egg cycles significantly differ between fertility centers. *Hum. Reprod.* 32, 743–749. doi:10.1093/humrep/dex031

Paria, B. C., and Dey, S. K. (1990). Preimplantation embryo development *in vitro*: Cooperative interactions among embryos and role of growth factors. *Proc. Natl. Acad. Sci. U. S. A.* 87, 4756–4760. doi:10.1073/pnas.87.12.4756

Pérez-Palacios, R., Fauque, P., Teissandier, A., and Bourc'his, D. (2021). "Deciphering the early mouse embryo transcriptome by low-input RNA-Seq," in *Methods in molecular Biology* (New Jersey: Humana Press Inc.), 189–205.

Petropoulos, S., Edsgärd, D., Reinius, B., Deng, Q., Panula, S. P., Codeluppi, S., et al. (2016). Single-cell RNA-seq reveals lineage and X chromosome dynamics in human preimplantation embryos. *Cell* 165, 1012–1026. doi:10.1016/j.cell.2016.03.023

Puscheck, E. E., Awonuga, A. O., Yang, Y., Jiang, Z., and Rappolee, D. A. (2015). Molecular biology of the stress response in the early embryo and its stem cells. *Adv. Exp. Med. Biol.* 843, 77–128. doi:10.1007/978-1-4939-2480-6_4

Ramos-Ibeas, P., Heras, S., Gómez-Redondo, I., Planells, B., Fernández-González, R., Pericuesta, E., et al. (2019). Embryo responses to stress induced by assisted reproductive technologies. *Mol. Reprod. Dev.* 86, 1292–1306. doi:10.1002/mrd.23119

Rees, W. D., Wilson, F. A., and Maloney, C. A. (2006). Sulfur amino acid metabolism in pregnancy: The impact of methionine in the maternal diet. *J. Nutr.* 136, 1701S–1705S. doi:10.1093/jn/136.6.1701s

Reimand, J., Isserlin, R., Voisin, V., Kucera, M., Tannus-Lopes, C., Rostamianfar, A., et al. (2019). Pathway enrichment analysis and visualization of omics data using g:Profiler, GSEA, Cytoscape and EnrichmentMap. *Nat. Protoc.* 14, 482–517. doi:10.1038/s41596-018-0103-9

Rinaudo, P., and Schultz, R. M. (2004). Effects of embryo culture on global pattern of gene expression in preimplantation mouse embryos. *Reproduction* 128, 301–311. doi:10.1530/rep.1.00297

Roseboom, T. J. (2018). Developmental plasticity and its relevance to assisted human reproduction. *Hum. Reprod.* 33, 546–552. doi:10.1093/humrep/dey034

Saint-Dizier, M., Schoen, J., Chen, S., Banliat, C., and Mermillod, P. (2020). Composing the early embryonic microenvironment: Physiology and regulation of oviductal secretions. *Int. J. Mol. Sci.* 21, 223. doi:10.3390/ijms21010223

Schwarzer, C., Esteves, T. C., Araúzo-Bravo, M. J., le Gac, S., Nordhoff, V., Schlatt, S., et al. (2012). ART culture conditions change the probability of mouse embryo gestation through defined cellular and molecular responses. *Hum. Reprod.* 27, 2627–2640. doi:10.1093/humrep/des223

Sha, Q. Q., Zheng, W., Wu, Y. W., Li, S., Guo, L., Zhang, S., et al. (2020). Dynamics and clinical relevance of maternal mRNA clearance during the oocyte-to-embryo transition in humans. *Nat. Commun.* 11, 4917. doi:10.1038/s41467-020-18680-6

Steegers-Theunissen, R. P. M., Twigt, J., Pestinger, V., and Sinclair, K. D. (2013). The periconceptional period, reproduction and long-term health of offspring: The importance of one-carbon metabolism. *Hum. Reprod. Update* 19, 640–655. doi:10.1093/humupd/dmt041

Sunde, A., Brison, D., Dumoulin, J., Harper, J., Lundin, K., Magli, M. C., et al. (2016). Time to take human embryo culture seriously. *Hum. Reprod.* 31, 2174–2182. doi:10.1093/humrep/dew157

Tarahomi, M., Vaz, F. M., van Straalen, J. P., Schrauwen, F. A. P., van Wely, M., Hamer, G., et al. (2019). The composition of human preimplantation embryo culture media and their stability during storage and culture. *Hum. Reprod.* 34, 1450–1461. doi:10.1093/humrep/dez102

Teissandier, A., Servant, N., Barillot, E., and Bourc'His, D. (2019). Tools and best practices for retrotransposon analysis using high-throughput sequencing data. *Mob. DNA* 10, 52–12. doi:10.1186/s13100-019-0192-1

Tejomurtula, J., Lee, K. B., Tripurani, S. K., Smith, G. W., and Yao, J. (2009). Role of importin alpha8, a new member of the importin alpha family of nuclear transport proteins, in early embryonic development in cattle. *Biol. Reprod.* 81, 333–342. doi:10.1095/biolreprod.109.077396

Tesfaye, D., Ponsuksili, S., Wimmers, K., Gilles, M., and Schellander, K. (2004). A comparative expression analysis of gene transcripts in post-fertilization developmental stages of bovine embryos produced *in vitro* or *in vivo*. *Reprod. Dom. Anim.* 39, 396–404. doi:10.1111/j.1439-0531.2004.00531.x

Thompson, J. G., Mitchell, M., and Kind, K. L. (2007). Embryo culture and long-term consequences. *Reprod. Fertil. Dev.* 19, 43–52. doi:10.1071/RD06129

Tripodi, F., Castoldi, A., Nicastro, R., Reghellin, V., Lombardi, L., Airoldi, C., et al. (2018). Methionine supplementation stimulates mitochondrial respiration. *Biochim. Biophys. Acta Mol. Cell Res.* 1865, 1901–1913. doi:10.1016/j.bbamcr.2018.09.007

Tunster, S. J., van de Pette, M., and John, R. M. (2011). Fetal overgrowth in the Cdkn1c mouse model of Beckwith-Wiedemann syndrome. *DMM Dis. Models Mech.* 4, 814–821. doi:10.1242/dmm.007328

Vajta, G., Rienzi, L., Cobo, A., and Yovich, J. (2010). Embryo culture: Can we perform better than nature? *Reprod. Biomed. Online* 20, 453–469. doi:10.1016/j.rbmo.2009.12.018

van den Berge, K., Roux de Bézieux, H., Street, K., Saelens, W., Cannoodt, R., Saeys, Y., et al. (2020). Trajectory-based differential expression analysis for single-cell sequencing data. *Nat. Commun.* 11, 1201–1213. doi:10.1038/s41467-020-14766-3

Vassena, R., Boué, S., González-Roca, E., Aran, B., Auer, H., Veiga, A., et al. (2011). Waves of early transcriptional activation and pluripotency program initiation during human preimplantation development. *Development* 138, 3699–3709. doi:10.1242/dev.064741

Wale, P. L., and Gardner, D. K. (2016). The effects of chemical and physical factors on mammalian embryo culture and their importance for the practice of assisted human reproduction. *Hum. Reprod. Update* 22, 2–22. doi:10.1093/humupd/dmv034

Watkins, A. J., and Fleming, T. P. (2009). Blastocyst environment and its influence on offspring cardiovascular health: The heart of the matter. *J. Anat.* 215, 52–59. doi:10.1111/j.1469-7580.2008.01033.x

Winckelmans, E., Vrijens, K., Tsamou, M., Janssen, B. G., Saenen, N. D., Roels, H. A., et al. (2017). Newborn sex-specific transcriptome signatures and gestational exposure to fine particles: Findings from the ENVIRONAGE birth cohort. *Environ. Health* 16, 52–17. doi:10.1186/s12940-017-0264-y

Wright, K., Brown, L., Brown, G., Casson, P., and Brown, S. (2011). Microarray assessment of methylation in individual mouse blastocyst stage embryos shows that *in vitro* culture may have widespread genomic effects. *Hum. Reprod.* 26, 2576–2585. doi:10.1093/humrep/der201

Wyns, C., de Geyter, C., Calhaz-Jorge, C., Kupka, M. S., Motrenko, T., Smeenk, J., et al. (2021). ART in europe, 2017: Results generated from European registries by ESHRE. *Hum. Reprod. Open* 2021, hoab026–17. doi:10.1093/hropen/hoab026

Xue, Z., Huang, K., Cai, C., Cai, L., Jiang, C. Y., Feng, Y., et al. (2013). Genetic programs in human and mouse early embryos revealed by single-cell RNA sequencing. *Nature* 500, 593–597. doi:10.1038/nature12364

Yan, L., Yang, M., Guo, H., Yang, L., Wu, J., Li, R., et al. (2013). Single-cell RNA-Seq profiling of human preimplantation embryos and embryonic stem cells. *Nat. Struct. Mol. Biol.* 20, 1131–1139. doi:10.1038/nsmb.2660

Yanez, L. Z., Han, J., Behr, B. B., Pera, R. A. R., and Camarillo, D. B. (2016). Human oocyte developmental potential is predicted by mechanical properties within hours after fertilization. *Nat. Commun.* 7, 10809. doi:10.1038/ncomms10809

Yonemasu, R., Minami, M., Nakatsu, Y., Takeuchi, M., Kuraoka, I., Matsuda, Y., et al. (2005). Disruption of mouse XAB2 gene involved in pre-mRNA splicing, transcription and transcription-coupled DNA repair results in preimplantation lethality. *DNA Repair (Amst)* 4, 479–491. doi:10.1016/j.dnarep.2004.12.004

Youssef, M., Mantikou, E., van Wely, M., van der Veen, F., Al-Inany, H., Repping, S., et al. (2015). Culture media for human pre-implantation embryos in assistedreproductive technology cycles. *Cochrane database Syst. Rev. (Online)* 1, CD007876. doi:10.1002/14651858.CD007876

Yu, X. J., Yi, Z., Gao, Z., Qin, D., Zhai, Y., Chen, X., et al. (2014). The subcortical maternal complex controls symmetric division of mouse zygotes by regulating F-actin dynamics. *Nat. Commun.* 5, 4887. doi:10.1038/ncomms5887

Zander, D. L., Thompson, J. G., and Lane, M. (2006). Perturbations in mouse embryo development and viability caused by ammonium are more severe after exposure at the cleavage stages. *Biol. Reprod.* 74, 288–294. doi:10.1095/biolreprod.105.046235

Zandstra, H., van Montfoort, A. P. A., and Dumoulin, J. C. M. (2015). Does the type of culture medium used influence birthweight of children born after IVF? *Hum. Reprod.* 30, 530–542. doi:10.1093/humrep/deu346

Zhang, T., Zheng, Y., Kuang, T., Yang, L., Jiang, H., Wang, H., et al. (2022). Arginine regulates zygotic genome activation in porcine embryos under nutrition restriction. *Front. Vet. Sci.* 9, 921406. doi:10.3389/fvets.2022.921406

Zhou, Y., Zhou, B., Pache, L., Chang, M., Khodabakhshi, A. H., Tanaseichuk, O., et al. (2019). Metascape provides a biologist-oriented resource for the analysis of systems-level datasets. *Nat. Commun.* 10, 1523. doi:10.1038/s41467-019-09234-6

Supplementary Methods

Freezing/thawing procedure

The freezing procedure was performed following a slow freeze protocol (2°C/min from 20°C to −7°C, manual seeding, 0.3°C/min to −30°C, and 35°C/min from −30 to −150°C). An adaptation of a freezing thawing procedure (FREEZE-KIT 1™ and THAW KIT 1™, Vitrolife, Göteborg, Sweden) was performed. Briefly, the straws were loaded successively with sucrose 0.2 M, air (1 cm), the embryo in 1.5 M propanediol + 0.1 M sucrose, air (1 cm) and 1.5 M propanediol + 0.1 M sucrose. At the time of thawing, the straws were kept at RT for 2 min, at 37°C for 3 min and at RT for 1 min and the straw contents were then mixed gently for 10 s. The embryo, in a solution of propanediol and sucrose, was then transferred to IVF medium and then immediately used for the single embryo RNA-seq.

Supplementary Figure S1. Overlap of expressed genes in our study with Yan *et al.* and Xue *et al.* data. (A) Table and Venn diagram indicating the number of expressed genes that overlap between studies at day-2. (B) Venn diagram indicating the number of expressed genes that overlap between studies at day-5.

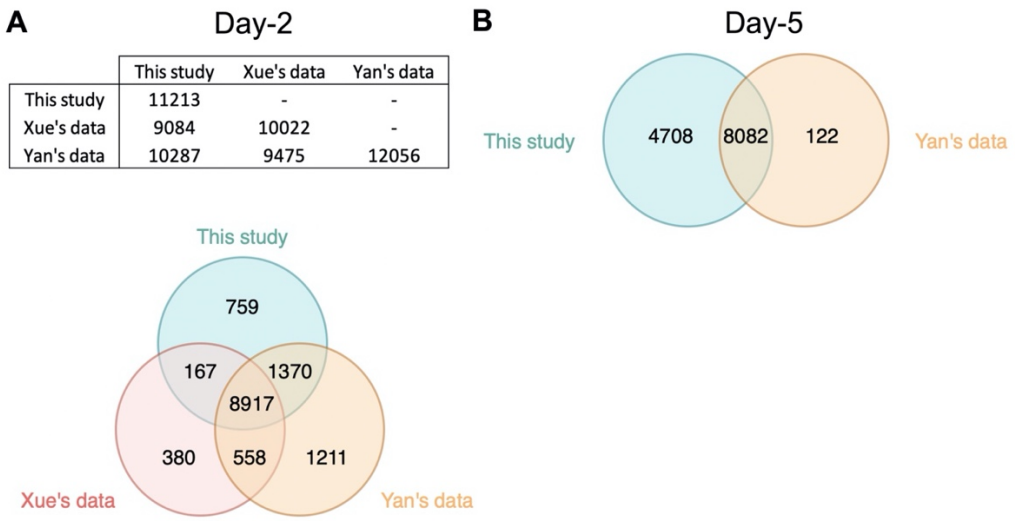

	This study	Xue's data	Yan's data
This study	11213	-	-
Xue's data	9084	10022	-
Yan's data	10287	9475	12056

Supplementary Figure S2. Comparison of global gene expression profiles between Yan *et al.*, Xue *et al.* and this study's datasets. (**A**) Principal component analysis of Yan *et al.*, Xue *et al.* and this study's datasets according to the normalized expression (log2(cpm+1)) of all expressed genes. Right panel displays PCA results for the embryos analyzed in this study only. (**B**) Hierarchical clustering of Yan *et al.*, Xue *et al.* and this study's datasets according to the normalized expression (log2(cpm+1)) of all expressed genes.

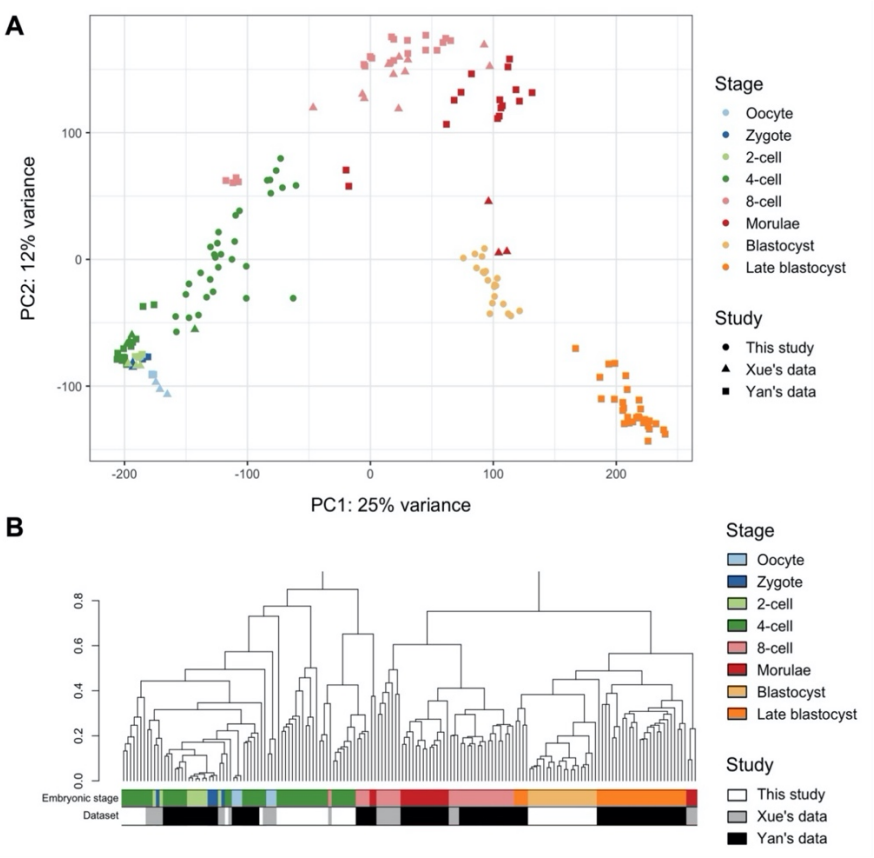

Supplementary Figure S3. Statistics of the differential expression analysis for all three group comparisons. (**A**) Pairwise comparison of the levels of expression of all genes expressed between Ferticult, Global and SSM groups. R: Spearman's correlation coefficient. Each point represents a gene. (**B**) Histogram of raw p-values in the three group comparisons.

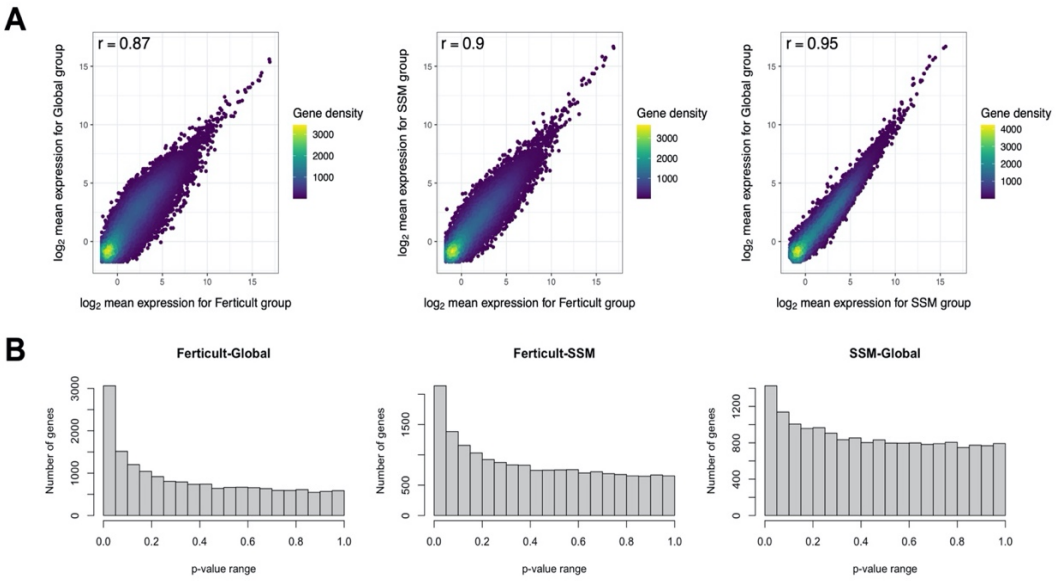

Supplementary Figure S4. PCA of Ferticult and Global samples at day-2 on the 266 DEGs.

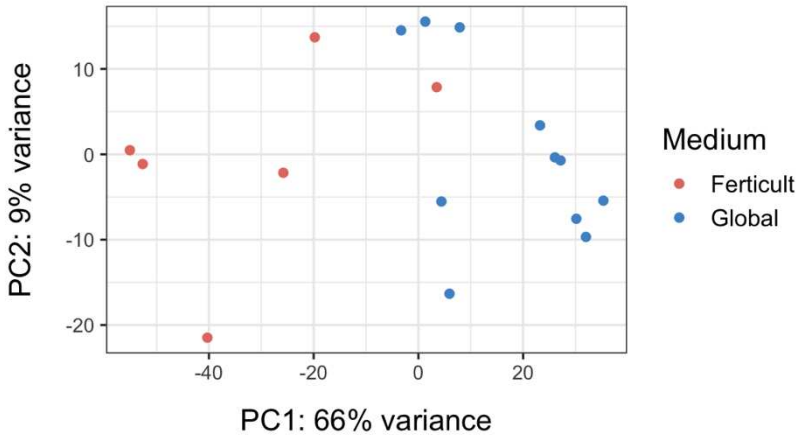

Supplementary Figure S5. Visualization of the 266 DEGs at day-2 in the Ferticult-to-Global comparison. (**A**) Heatmap according to their log2(cpm+1) expression. Samples are represented in rows and genes in columns. (**B**) Repartition of DEGs into strictly maternal, maternal and embryonic, and embryonic transcripts (from left to right) according to their pattern of expression along the first embryonic states assessed with Yan *et al.* (2013) data. Dendrograms represent the hierarchical clustering of genes per category, colored by culture medium groups.

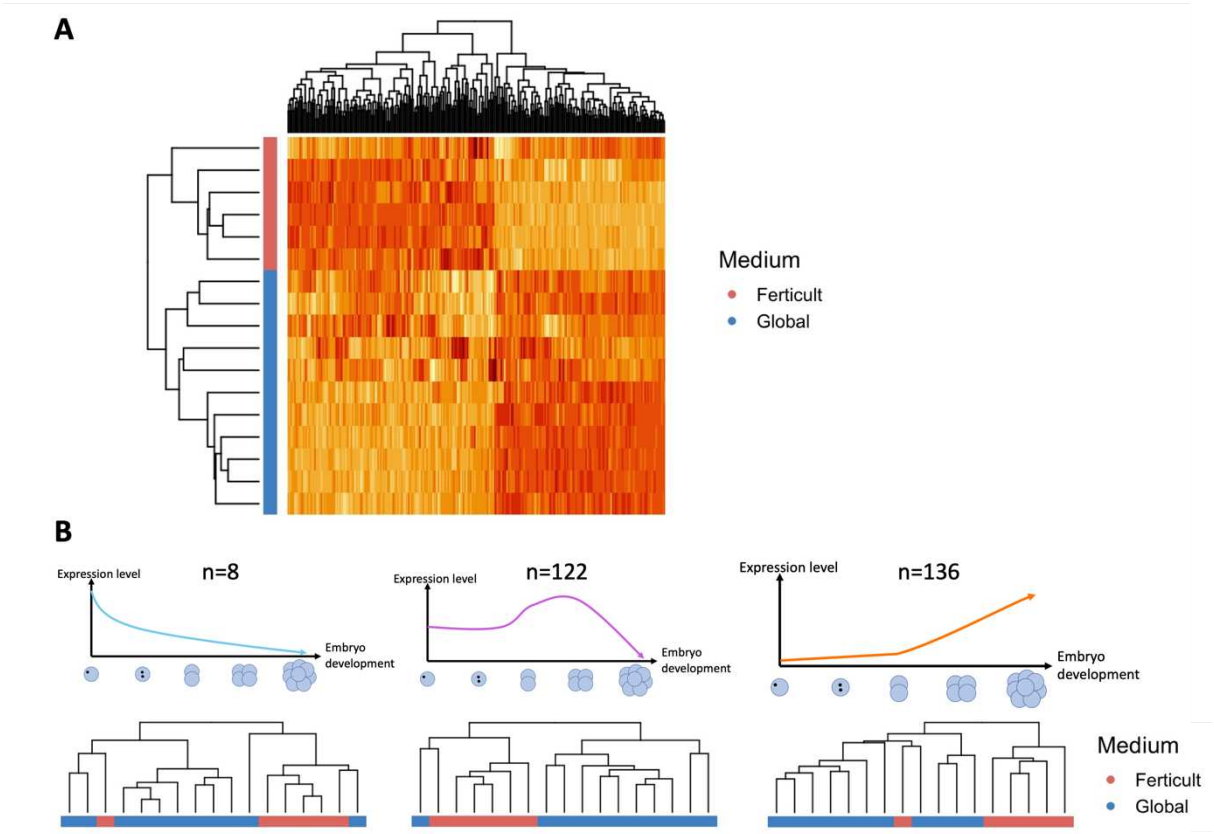

Supplementary Figure S6. Detailed analysis of significant GO terms significantly over-represented in DEGs between Ferticult and Global at day-2. (**A**) Overview of most significant GO terms from clusters of significant pathways over-represented in day-2 differentially expressed genes (DEGs). (**B**) Network of all GO significantly enriched terms, colored by their representative GO terms. Three clusters of GO terms interaction were identified. Each node is an individual GO term and its size indicates the number of genes included in the GO term. Thick links connect GO terms of high similarity. (**C**) Detailed expression of DEGs between Ferticult and Global at day-2 involved in clusters of enriched pathways. Barplot represents the expression level (log2(cpm+1)) for each gene in the cluster.

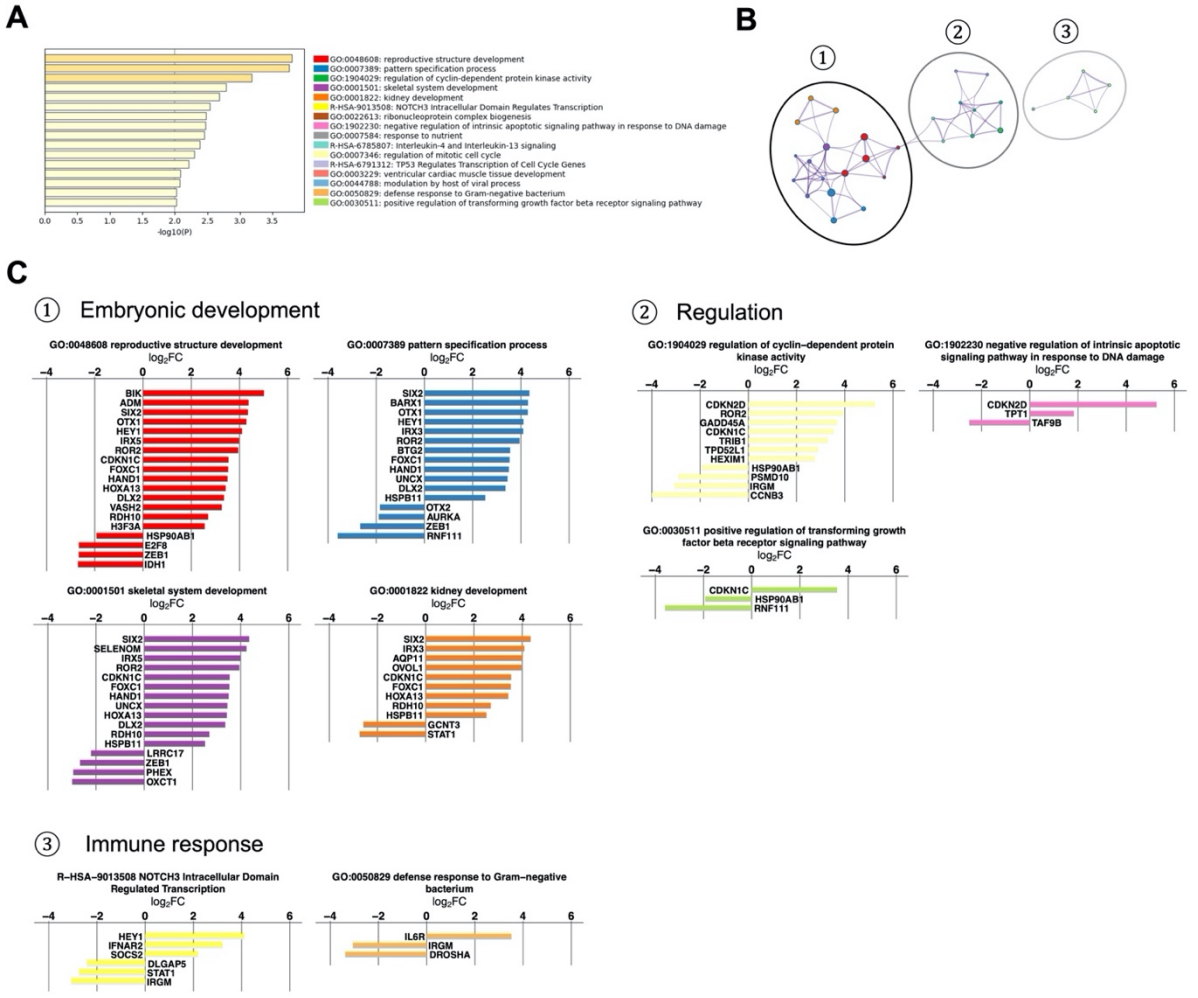

Supplementary Figure S7. Gene Set Enrichment Analysis (GSEA) of global gene expression changes in Ferticult-to-Global comparison. Only the top-10 biological processes are shown. The enrichment score, represented by the curves, reflects the degree to which genes belonging to a specific GO (each gene is represented by a point in the curve) are over-represented in the first or last position of the overall gene ranking (genes ranked from the highest positive logFC to the highest negative logFC). Walking down the ranked list of genes, GSEA increases the enrichment score when a gene is encountered in the GO considered (bars at the bottom of the plot) and decreases the score if not (absence of bars at the bottom of the plot). A positive peak enrichment score indicates that genes belonging to the GO considered are over-expressed with Ferticult. The vertical line separates genes with positive logFC (left side) from those with negative logFC (right side) with Ferticult compared to Global. For example, concerning the genes involved in the anterior/posterior pattern specification pathway, we observe high density of genes with the largest positive logFC (pink curve), symbolized by a positive peak enrichment score. This pathway appears up-regulated with Ferticult.

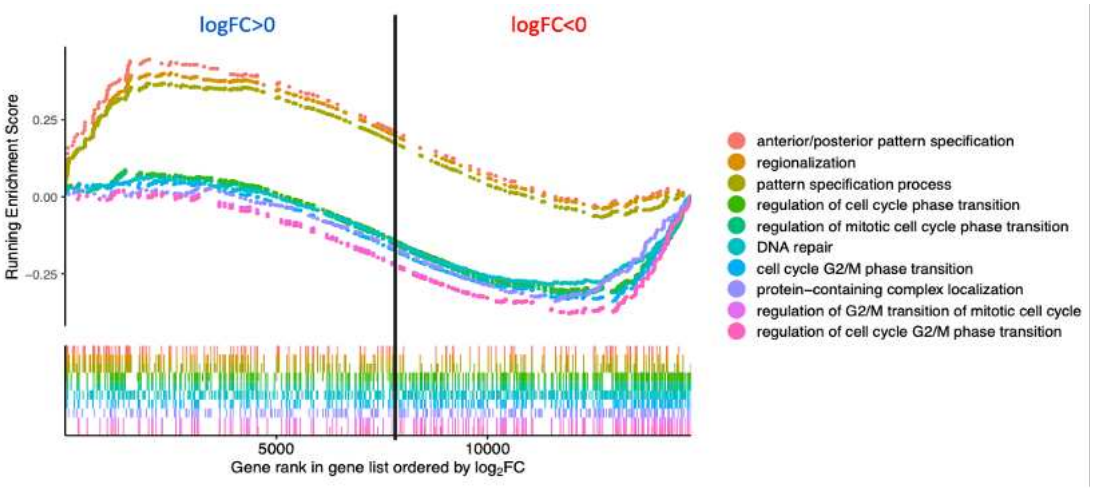

Supplementary Figure S8. Differential expression analysis at day-2 focused on top-20 expressed transposable elements for all groups. (**A**) Heatmap of log2 fold change of transposable elements in all comparisons between culture media. (**B**) Heatmap of mean expression of transposable elements in all culture media groups. Log2 mean expression was calculated by taking the average log2(cpm+1) expression.

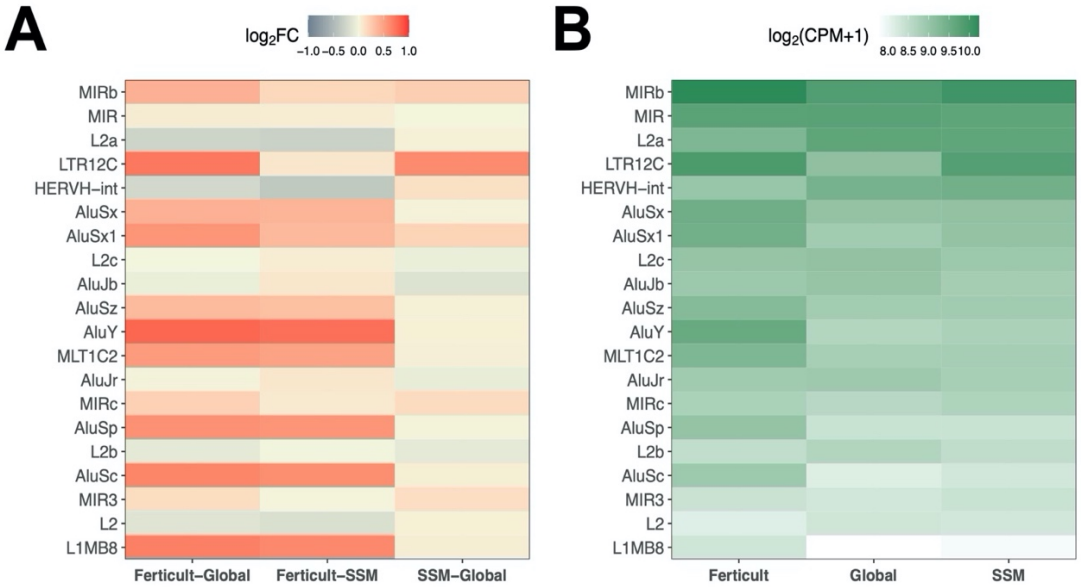

Supplementary Figure S9. Study design of the experiment regarding methionine supplementation in the culture medium at day-2.

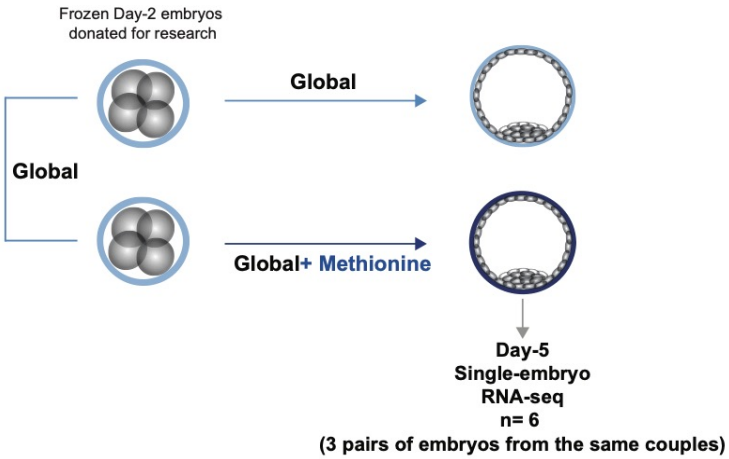

Supplementary Figure S10. PHATE reduction of Petropoulos' (2016) embryo scRNA-seq data. Each point represents one of the 1529 cells in the dataset. Curves indicate the trajectory of the three inferred lineages by slingshot. (**A**) Colored by k-means clusters identified in this study. Cells were grouped into 8 clusters according to their global expression of expressed genes. This clustering was used as input in slingshot to depict the global structure of underlying embryonic lineages. (**B**) Colored by Meistermann *et al.* lineage inference. Authors applied UMAP dimensionality reduction on module eigengenes identified with WGCNA (Langfelder and Horvath, 2008) to cluster cells according to their association with gene expression signatures specific to developmental stages and lineages. (**C**) Colored by Petropoulos *et al.* original lineage inference. Authors used PCA dimensionality reduction to infer embryonic lineages of cells after day-5. (**D**) Colored by pseudotime inferred with slingshot in this study (arbitrary unit). Pseudotime of the second lineage has been chosen for the purpose of visualization. Earliest embryonic stages in the dataset are gray colored, while dark red colored points are indicative of the latest cells timepoints.

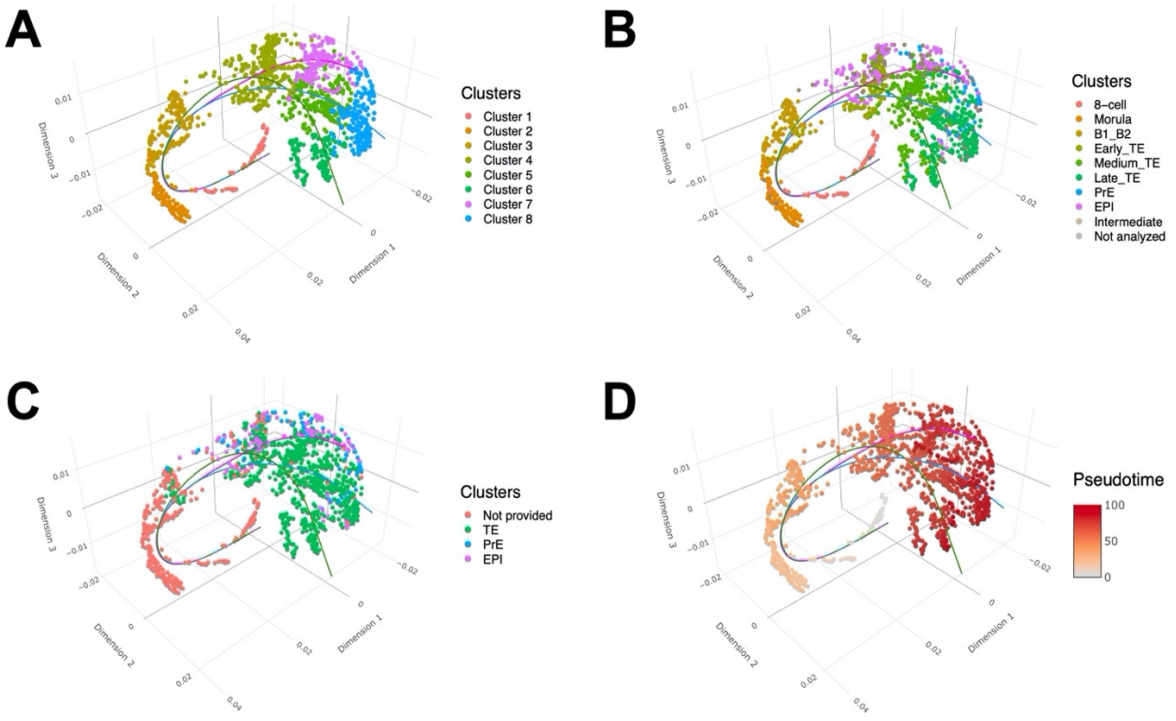

Supplementary Table S1. Clinical characteristics of patients, embryo origin and morphology.

Fertilization method *	Couple	Woman age (WA) **	Paternal age (PA) ***	Diagnosis	Type of COH	Hormonal treatment	Medium used until Day-2	Medium used until day-5	Morphology at day-2 ***	Morphology at blastocyst stage **
cIVF	Couple 1	35	36	Polycystic ovary syndrome	Long GnRH-agonist protocol	Recombinant Follicle Stimulating Hormone (FSH; Gonal-f®)	SSM		4-cell (<15%, T)	
cIVF	Couple 1	35	36	Polycystic ovary syndrome	Long GnRH-agonist protocol	Recombinant Follicle Stimulating Hormone (FSH; Gonal-f®)	SSM		4-cell (<15%, T)	
ICSI	Couple 2	36	35	Intra-uterine insemination failures	Long GnRH-agonist protocol	Recombinant follicle-stimulating hormone (FSH; Puregon®)	Global		4-cell (<15%, T)	
ICSI	Couple 2	36	35	Intra-uterine insemination failures	Long GnRH-agonist protocol	Recombinant follicle-stimulating hormone (FSH; Puregon®)	Global		4-cell (<15%, T)	
ICSI	Couple 2	36	35	Intra-uterine insemination failures	Long GnRH-agonist protocol	Recombinant follicle-stimulating hormone (FSH; Puregon®)	Global		4-cell (<15%, T)	
ICSI	Couple 2	36	35	Intra-uterine insemination failures	Long GnRH-agonist protocol	Recombinant follicle-stimulating hormone (FSH; Puregon®)	Global		4-cell (<15%, T)	
ICSI	Couple 3	32	32	Endometriosis	Long GnRH-agonist protocol	Recombinant Follicle Stimulating Hormone (FSH; Gonal-f®)	Global		4-cell (<15%, T)	
ICSI	Couple 3	32	32	Endometriosis	Long GnRH-agonist protocol	Recombinant Follicle Stimulating Hormone (FSH; Gonal-f®)	Global		4-cell (<15%, T)	
ICSI	Couple 3	32	32	Endometriosis	Long GnRH-agonist protocol	Recombinant Follicle Stimulating Hormone (FSH; Gonal-f®)	Global		4-cell (<15%, T)	
cIVF	Couple 4	33	35	Sperm cryopreservation before gonadotoxic treatment	Long GnRH-agonist protocol	Recombinant Follicle Stimulating Hormone (FSH; Gonal-f®)	Global		4-cell (<15%, T)	
cIVF	Couple 4	33	35	Sperm cryopreservation before gonadotoxic treatment	Long GnRH-agonist protocol	Recombinant Follicle Stimulating Hormone (FSH; Gonal-f®)	Global		4-cell (<15%, T)	
ICSI	Couple 5	27	39	Oligozoospermia	Long GnRH-agonist protocol	Recombinant follicle-stimulating hormone (FSH; Puregon®)	Ferticult		4-cell (<15%, T)	
ICSI	Couple 5	27	39	Oligozoospermia	Long GnRH-agonist protocol	Recombinant follicle-stimulating hormone (FSH; Puregon®)	Ferticult		4-cell (<15%, T)	
ICSI	Couple 6	31	33	Oligozoospermia	Long GnRH-agonist protocol	Recombinant Follicle Stimulating Hormone (FSH; Gonal-f®)	SSM		4-cell (<15%, T)	
ICSI	Couple 6	31	33	Oligozoospermia	Long GnRH-agonist protocol	Recombinant Follicle Stimulating Hormone (FSH; Gonal-f®)	SSM		4-cell (<15%, T)	
ICSI	Couple 6	31	33	Oligozoospermia	Long GnRH-agonist protocol	Recombinant Follicle Stimulating Hormone (FSH; Gonal-f®)	SSM		4-cell (<15%, T)	
cIVF	Couple 7	29	27	Intra-uterine insemination failures	Long GnRH-agonist protocol	Recombinant follicle-stimulating hormone (FSH; Puregon®)	SSM		4-cell (<15%, T)	
ICSI	Couple 8	36	34	Oocyte donation	Long GnRH-agonist protocol	Recombinant follicle-stimulating hormone (FSH; Puregon®)	SSM		4-cell (<15%, T)	
ICSI	Couple 8	36	34	Oocyte donation	Long GnRH-agonist protocol	Recombinant follicle-stimulating hormone (FSH; Puregon®)	SSM		4-cell (<15%, T)	
ICSI	Couple 8	36	34	Oocyte donation	Long GnRH-agonist protocol	Recombinant follicle-stimulating hormone (FSH; Puregon®)	SSM		4-cell (<15%, T)	
ICSI	Couple 8	36	34	Oocyte donation	Long GnRH-agonist protocol	Recombinant follicle-stimulating hormone (FSH; Puregon®)	SSM		4-cell (<15%, T)	
ICSI	Couple 9	25	30	Dysovulation and fertilization failure in IVF	Long GnRH-agonist protocol	Recombinant Follicle Stimulating Hormone (FSH; Gonal-f®)	SSM		4-cell (<15%, T)	
ICSI	Couple 9	25	30	Dysovulation and fertilization failure in IVF	Long GnRH-agonist protocol	Recombinant Follicle Stimulating Hormone (FSH; Gonal-f®)	SSM		4-cell (<15%, T)	
ICSI	Couple 9	25	30	Dysovulation and fertilization failure in IVF	Long GnRH-agonist protocol	Recombinant Follicle Stimulating Hormone (FSH; Gonal-f®)	SSM		4-cell (<15%, T)	
ICSI	Couple 9	25	30	Dysovulation and fertilization failure in IVF	Long GnRH-agonist protocol	Recombinant Follicle Stimulating Hormone (FSH; Gonal-f®)	SSM		4-cell (<15%, T)	
cIVF	Couple 10	34	39	Polycystic ovary syndrome	Long GnRH-agonist protocol	Recombinant Follicle Stimulating Hormone (FSH; Gonal-f®)	Ferticult		4-cell (<15%, T)	
cIVF	Couple 10	34	39	Polycystic ovary syndrome	Long GnRH-agonist protocol	Recombinant Follicle Stimulating Hormone (FSH; Gonal-f®)	Ferticult		4-cell (<15%, T)	
ICSI	Couple 11	35	37	Oligozoospermia	Long GnRH-agonist protocol	Recombinant follicle-stimulating hormone (FSH; Puregon®)	Ferticult		4-cell (<15%, T)	
ICSI	Couple 11	35	37	Oligozoospermia	Long GnRH-agonist protocol	Recombinant follicle-stimulating hormone (FSH; Puregon®)	Ferticult		4-cell (<15%, T)	

ICSI	Couple 12	35	32	Oligozoospermia	Long GnRH-agonist protocol	Recombinant follicle-stimulating hormone (FSH; Puregon®)	Global		4-cell (<15%, T)	
ICSI	Couple 12	35	32	Oligozoospermia	Long GnRH-agonist protocol	Recombinant follicle-stimulating hormone (FSH; Puregon®)	Global		4-cell (<15%, T)	
cIVF	Couple 13	37	35	Idiopathic	Long GnRH-agonist protocol	Highly Purified Human Menopausal Gonadotropin (FSH + LH; Menopur®)	Ferticult	Global	4-cell (<15%, T)	B2
cIVF	Couple 14	38	38	Dysovulation	Long GnRH-agonist protocol	Recombinant Follicle Stimulating Hormone (FSH; Gonal-f®)	Ferticult	Global	4-cell (<15%, T)	B2
cIVF	Couple 14	38	38	Dysovulation	Long GnRH-agonist protocol	Recombinant Follicle Stimulating Hormone (FSH; Gonal-f®)	Ferticult	Global	4-cell (<15%, T)	B2
cIVF	Couple 15	34	37	Intra-uterine insemination failures and unique ovary	Long GnRH-agonist protocol	Recombinant follicle-stimulating hormone (FSH; Puregon®)	Ferticult	Global	4-cell (<15%, T)	B3 BB
cIVF	Couple 15	34	37	Intra-uterine insemination failures and unique ovary	Long GnRH-agonist protocol	Recombinant follicle-stimulating hormone (FSH; Puregon®)	Ferticult	Global	4-cell (<15%, T)	B3 BA
cIVF	Couple 15	34	37	Intra-uterine insemination failures and unique ovary	Long GnRH-agonist protocol	Recombinant follicle-stimulating hormone (FSH; Puregon®)	Ferticult	Global	4-cell (<15%, T)	B2
cIVF	Couple 16	27	29	Poor ovarian reserve	Long GnRH-agonist protocol	Recombinant follicle-stimulating hormone (FSH; Puregon®)	Global	Global	4-cell (<15%, T)	B2
ICSI	Couple 17	29	34	Oligozoospermia	Long GnRH-agonist protocol	Recombinant Follicle Stimulating Hormone (FSH; Gonal-f®)	Ferticult	Global	4-cell (<15%, T)	B3 BB
cIVF	Couple 18	34	37	Idiopathic	Long GnRH-agonist protocol	Recombinant Follicle Stimulating Hormone (FSH; Gonal-f®)	Global	Global	4-cell (<15%, T)	B2
cIVF	Couple 19	38	40	Tubal factor infertility	Long GnRH-agonist protocol	Recombinant follicle-stimulating hormone (FSH; Puregon®)	Global	Global	4-cell (<15%, T)	B3 BB
cIVF	Couple 20	37	34	Endometriosis	Long GnRH-agonist protocol	Recombinant Follicle Stimulating Hormone (FSH; Gonal-f®)	Global	Global	4-cell (<15%, T)	B2
cIVF	Couple 21	29	29	Polycystic ovary syndrome	Long GnRH-agonist protocol	Recombinant follicle-stimulating hormone (FSH; Puregon®)	Global	Global	4-cell (<15%, T)	B4 AB
cIVF	Couple 21	29	29	Polycystic ovary syndrome	Long GnRH-agonist protocol	Recombinant follicle-stimulating hormone (FSH; Puregon®)	Global	Global	4-cell (<15%, T)	B3 BB
cIVF	Couple 21	29	29	Polycystic ovary syndrome	Long GnRH-agonist protocol	Recombinant follicle-stimulating hormone (FSH; Puregon®)	Global	Global + methionine supplementation	4-cell (<15%, T)	B2
ICSI	Couple 22	33	32	Poor ovarian reserve + Oligozoospermia	Short GnRH agonist protocol	Recombinant follicle-stimulating hormone and luteinizing hormone (FSH+ LH; Pergoveris®)	Global	Global	4-cell (<15%, T)	B3 BB
ICSI	Couple 22	33	32	Poor ovarian reserve + Oligozoospermia	Short GnRH agonist protocol	Recombinant follicle-stimulating hormone and luteinizing hormone (FSH+ LH; Pergoveris®)	Global	Global + methionine supplementation	4-cell (<15%, T)	B2
ICSI	Couple 23	41	37	Azoospermia (donnor sperm)	Short GnRH agonist protocol	Highly Purified Human Menopausal Gonadotropin (Menopur®)	Global	Global + methionine supplementation	4-cell (<15%, T)	B3 BB
ICSI	Couple 23	41	37	Azoospermia (donnor sperm)	Short GnRH agonist protocol	Highly Purified Human Menopausal Gonadotropin (Menopur®)	Global	Global	4-cell (<15%, T)	B2
ICSI	Couple 24	29	35	Oligozoospermia	Long GnRH-agonist protocol	Recombinant Follicle Stimulating Hormone (FSH; Gonal-f®)	Global	Global + methionine supplementation	4-cell (<15%, T)	B2
ICSI	Couple 24	29	35	Oligozoospermia	Long GnRH-agonist protocol	Recombinant Follicle Stimulating Hormone (FSH; Gonal-f®)	Global	Global	4-cell (<15%, T)	B2

* cIVF: conventional IVF; ICSI: Intra Cytoplasmic Sperm Injection

** at the 4-cell stage with less than 15% of anucleate fragments and regular cleavage (T : typical)

*** The evaluation of blastocysts was based on Gardner and Schoolcraft's blastocyst grading scale (Gardner and Schoolcraft, 1999). Briefly, this evaluation enumerates the degree of expansion and hatching represented by a numerical value (1–6) followed by the appearance of the key features of the inner cell mass then the trophectoderm in letters (A–C).

Supplementary Table S2. Statistics on survival after thawing.

	Experiments - day-2
Number of thawed embryos	50
Number of embryos* used to single-embryo RNAseq	31
	Experiments - day-5
Number of thawed embryos	68
Number of embryos* cultured up to day-5	44
Number of blastocysts used to single-embryo RNAseq**	21

*: fully survived embryos at the thawing process
**: blastocysts with at least B2 blastocoel cavity without lysis

Supplementary Table S3. Composition of the different culture media (from Morbeck *et al.* (2014), Bouillon *et al.* (2016) and Material Safety Data Sheet from manufacturers)

		Global	SSM	Ferticult
Salts and ions	Sodium Chloride	+	+	+
	Potassium Chloride	+	+	+
	Magnesium Sulfate	+	+	+
	Calcium Chloride	+	+	+
	Potassium Phosphate	+	+	Not documented
Buffer	Sodium Bicarbonate	+	+	+
Energy Substrates	Glucose	+	+	+
	Sodium Pyruvate	+	+	+
	Sodium Lactate	+	+	+
Essential Amino Acids	Arginine	+	+	-
	Cysteine	+	+	-
	Histidine	+	+	-
	Isoleucine	+	+	-
	Leucine	+	+	-
	Lysine	+	+	-
	Methionine	+	+	-
	Phenylalanine	+	+	-
	Threonine	+	+	-
	Tryptophan	+	+	-
	Tyrosine	+	+	-
	Valine	+	+	-
Non-essential Amino Acids	Alanine	+	+	-
	Asparagine	+	+	-
	Aspartic acid	+	+	-
	Glutamic acid	+	+	-
	Glycine	+	+	-
	Proline	+	+	-
	Serine	+	+	-
	Taurine	-	+	-
Di-peptide		Glycyl-L-Glutamine	Alanyl-L-Glutamine	-
Chelator		EDTA	EDTA	Albumin
Indicator	Phenol Red	+	+	+
Antibiotic	Gentamicin	+	+	+

Supplementary Table S4. Single-embryo RNA-sequencing statistics for all samples.

Sample	Day	Culture media until day-2	Culture media until day-5	# of sequenced reads after trimming	Total Mapped reads	% of mapping	# of reads mapped to multiple loci	# of uniquely mapped reads	% of uniquely mapped reads
A1132R66	day-2	Ferticult	NA	4228442	4149099	98,12	267746	3881353	93,55
A1132R67	day-2	SSM	NA	3608168	3539521	98,10	235008	3304513	93,36
A1132R68	day-2	Global	NA	3265891	3196541	97,88	254568	2941973	92,04
A1132R69	day-2	Ferticult	NA	3107262	3014947	97,03	357881	2657066	88,13
A1132R70	day-2	Global	NA	3524971	3186553	90,40	337477	2849076	89,41
A1132R71	day-2	SSM	NA	3323018	3229629	97,19	362436	2867193	88,78
A1132R72	day-2	Global	NA	3706461	3614973	97,53	256132	3358841	92,91
A1132R73	day-2	Global	NA	3385125	3261796	96,36	287680	2974116	91,18
A1132R74	day-2	Global	NA	4962136	4390664	88,48	635891	3754773	85,52
A1132R75	day-2	Global	NA	3123505	3058254	97,91	312623	2745631	89,78
A1132R76	day-2	Global	NA	2852308	1751586	61,41	245797	1505789	85,97
A1132R77	day-2	Global	NA	2821238	2750670	97,50	246123	2504547	91,05
A1132R78	day-2	Global	NA	3001231	2933449	97,74	243835	2689614	91,69
A1132R79	day-2	Global	NA	2603393	2553430	98,08	161678	2391752	93,67
A1132R80	day-2	Global	NA	4089624	4000901	97,83	289957	3710944	92,75
A1132R81	day-2	Ferticult	NA	3847971	3774294	98,09	294331	3479963	92,20
A1132R82	day-2	Ferticult	NA	3919320	3838863	97,95	395106	3443757	89,71
A1132R83	day-2	Ferticult	NA	3274348	3204632	97,87	342781	2861851	89,30
A1132R84	day-2	Ferticult	NA	3357239	3300235	98,30	425381	2874854	87,11
A1132R85	day-2	SSM	NA	2863766	2816884	98,36	217208	2599676	92,29
A1132R86	day-2	SSM	NA	3691155	3605156	97,67	294088	3311068	91,84
A1132R87	day-2	SSM	NA	3269342	3216229	98,38	182292	3033937	94,33
A1132R88	day-2	SSM	NA	2928750	2824506	96,44	328757	2495749	88,36
A1132R89	day-2	SSM	NA	2950992	2907345	98,52	186666	2720679	93,58
A1132R90	day-2	SSM	NA	3093971	3034720	98,08	309939	2724781	89,79
A1132R91	day-2	SSM	NA	2508149	2374993	94,69	203921	2171072	91,41
A1132R92	day-2	SSM	NA	2249211	2210477	98,28	119636	2090841	94,59
A1132R93	day-2	SSM	NA	2382129	2343917	98,40	148960	2194957	93,64
A1132R94	day-2	SSM	NA	3715397	3657254	98,44	263968	3393286	92,78
A1132R95	day-2	SSM	NA	4180994	4093468	97,91	284960	3808508	93,04
A1132R96	day-2	SSM	NA	3046106	2993990	98,29	253314	2740676	91,54
D655T01	day-5	Ferticult	Global	12229565	9227136	75,45	572592	8654544	93,79
D655T02	day-5	Ferticult	Global	12152896	9336972	76,83	594149	8742823	93,64
D655T03	day-5	Ferticult	Global	11975256	9655686	80,63	613940	9041746	93,64
D655T04	day-5	Ferticult	Global	11159992	9283995	83,19	719279	8564716	92,25
D655T05	day-5	Ferticult	Global	12012407	9639737	80,25	669172	8970565	93,06
D655T06	day-5	Global	Global	11535788	9516615	82,50	880594	8636021	90,75
D655T07	day-5	Ferticult	Global	14099641	11170632	79,23	725757	10444875	93,50
D655T08	day-5	Global	Global	12376085	10249418	82,82	704957	9544461	93,12

D655T09	day-5	Global	Global	13719853	10759111	78,42	794709	9964402	92,61
D655T10	day-5	Global	Global	13059421	11188226	85,67	799733	10388493	92,85
D655T11	day-5	Global	Global	12147437	10477733	86,25	680288	9797445	93,51
D655T12	day-5	Global	Global	13465108	11934905	88,64	923273	11011632	92,26
D655T13	day-5	Global	Global	13247804	10761122	81,23	793260	9967862	92,63
D655T14	day-5	Global	Global_methionine	13733614	11487304	83,64	811042	10676262	92,94
D655T15	day-5	Global	Global_methionine	13093376	11036260	84,29	869255	10167005	92,12
D655T16	day-5	Global	Global	16554515	13020861	78,65	909612	12111249	93,01
D655T17	day-5	Global	Global	13832686	10597776	76,61	787896	9809880	92,57
D655T18	day-5	Global	Global_methionine	14297614	10457102	73,14	838104	9618998	91,99
D655T19	day-5	Global	Global_methionine	12441046	9610792	77,25	739163	8871629	92,31
D655T40	day-5	Ferticult	Global	12070642	10095825	83,64	837546	9258279	91,70

Supplementary Table S5. Single-embryo RNA-sequencing results for all genes (Ferticult-Global comparison)

Supplementary Table S6. Gene Set Expression Analysis results for the Ferticult-Global comparison at day-2.

Supplementary Table S7. Differential expression analysis of all genes at day-5 (Ferticult-Global comparison)

Available at https://www.frontiersin.org/articles/10.3389/fcell.2023.1155634/full#supplementary-material

II) Profil de méthylation chez des enfants conçus par AMP

1) Objectifs

Des expositions périconceptionnelles précoces en lien avec les procédures d'AMP sont suspectées de modifier les profils de méthylation de l'ADN des gamètes et embryons et prédisposer les enfants ainsi conçus à des maladies sur le long terme. A l'échelle du génome entier, notre revue systématique et méta-analyse a pu montrer des différences à la naissance à l'échelle du génome entier, mais il restait à déterminer si ces modifications persistaient au cours de l'enfance.

Notre étude a eu pour objectif d'étudier les effets des techniques d'AMP sur le méthylome d'enfants âgés entre 7 et 8 ans suivant leur mode de conception (FIV ou ICSI) et le milieu de culture embryonnaire au sein duquel ils ont été conçus, à l'aide de puces à méthylation EPIC (Illumina).

2) Matériels et méthodes

Cette étude de cohorte monocentrique s'appuie sur une étude randomisée menée en 2008 au CHU de Dijon, dont l'objectif principal était de comparer les résultats obtenus après l'utilisation de deux milieux de culture embryonnaire : le milieu Global (LifeGlobal) et le milieu Single Step Medium (SSM, Irvine Scientific). Les données de méthylation de l'ADN à l'échelle de l'épigénome ont été obtenues à l'aide de puces EPIC (Illumina) pour 36 enfants (23 et 13 dans les groupes Global et SSM, respectivement). Parmi eux, 15 enfants ont été conçus par transferts d'embryons frais à J2 ou J3 après une FIV conventionnelle (10 et 5 dans les groupes Global et SSM, respectivement) et 21 après une ICSI (13 et 8 dans les groupes Global et SSM, respectivement).

Les fichiers .idat bruts obtenus à partir des données de puces ont été prétraités à l'aide des packages R *missMethyl* et *minfi* (Aryee *et al.*, 2014; Phipson *et al.*, 2016). La qualité des échantillons a d'abord été vérifiée avant que les données globales ne soient normalisées à l'aide de la méthode SWAN, afin d'éliminer la variance technique entre les sondes de type I et II (Maksimovic *et al.*, 2012) (Figure 27).

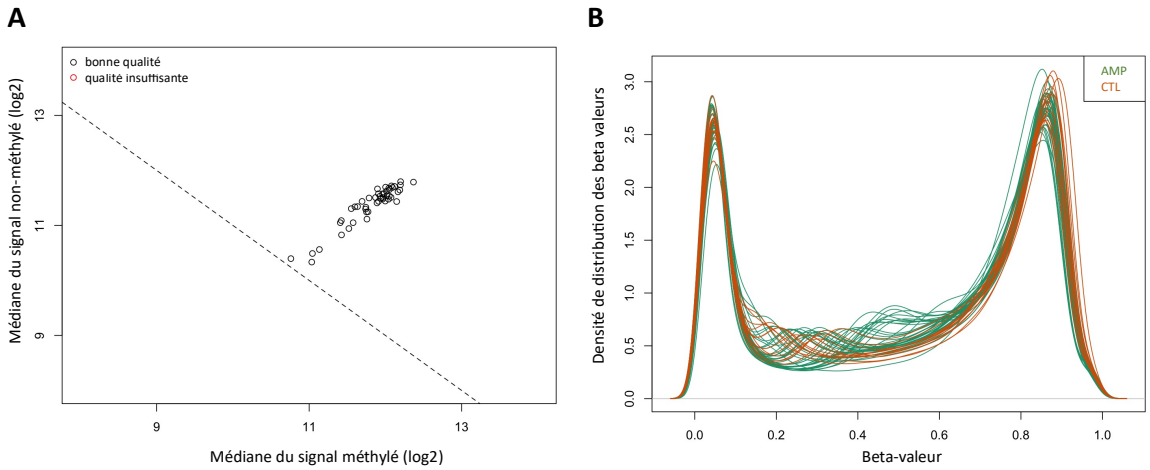

Figure 27. Contrôle qualité des données.
A. Les médianes des intensités des signaux méthylés et non-méthylés franchissent les seuils de qualité suffisante pour tous les échantillons. B. La distribution des densités des beta-valeurs apparait conforme.

Similairement aux échantillons sanguins, les frottis buccaux collectent l'ADN d'un grand nombre de types cellulaires. Cette composition des types cellulaires est souvent un facteur de confusion majeur dans les EWAS, qu'il faut prendre en compte. Ainsi les proportions en types cellulaires ont été prédites à l'aide de l'algorithme de déconvolution *HEpiDISH* (Zheng *et al.*, 2018). Au final, un total de 740 869 CpGs seront analysés et comparés entre groupes contrôle et AMP, Global et SSM, FIV et ICSI, par analyse différentielle en utilisant la régression linéaire (package *limma* (Smyth, 2005)).

3) Résultats

Nous avons identifié 127 positions différentiellement méthylées (DMP) et 16 régions différentiellement méthylées (DMR) (FDR < 0.05) avec de faibles différences de deltabeta

(>10%) entre les groupes d'enfants nés par AMP et conçus naturellement. Les DMPs étaient préférentiellement situées dans des régions promotrices et des îlots CpG et étaient principalement hyperméthylées avec AMP. Nous avons mis en évidence que l'utilisation d'un milieu de culture embryonnaire différent (Global et SSM) n'était pas associée à des différences de méthylation de l'ADN durant l'enfance. Dans l'ensemble, nous apportons des preuves supplémentaires que les enfants conçus par procréation médicalement assistée présentent une variation limitée de la méthylation de l'ADN à l'échelle du génome par rapport à ceux conçus naturellement.

4) Article 6 - Genome-wide analysis of DNA methylation in buccal cells of children conceived through IVF and ICSI

genes

MDPI

Article

Genome-Wide Analysis of DNA Methylation in Buccal Cells of Children Conceived through IVF and ICSI

Bastien Ducreux [1], Jean Frappier [1,2], Céline Bruno [1,2], Abiba Doukani [3], Magali Guilleman [1,2], Emmanuel Simon [1,4], Aurélie Martinaud [1,2], Déborah Bourc'his [5], Julie Barberet [1,2] and Patricia Fauque [1,2,*]

1 Equipe Génétique des Anomalies du Développement (GAD), Université Bourgogne Franche-Comté, INSERM UMR1231, 2 Rue Angélique Ducoudray, F-21000 Dijon, France; bastien.ducreux@outlook.fr (B.D.); jean.frappier@chu-dijon.fr (J.F.); celine.bruno@chu-dijon.fr (C.B.); magali.guilleman@chu-dijon.fr (M.G.); emmanuel.simon@chu-dijon.fr (E.S.); aurelie.martinaud@chu-dijon.fr (A.M.); julie.barberet@chu-dijon.fr (J.B.)
2 Laboratoire de Biologie de la Reproduction—CECOS, CHU Dijon Bourgogne, 14 Rue Gaffarel, F-21000 Dijon, France
3 Faculté de Médecine, Sorbonne Université, UMS 37 PASS Plateforme P3S, 91, Bd de l'hôpital, F-75634 Paris, France; habiba.doukani@sorbonne-universite.fr
4 Service de Gynécologie-Obstétrique, CHU Dijon Bourgogne, 14 Rue Gaffarel, F-21000 Dijon, France
5 Institut Curie, PSL University, CNRS, INSERM, 26 Rue d'Ulm, F-75248 Paris, France; deborah.bourchis@inserm.fr
* Correspondence: patricia.fauque@chu-dijon.fr; Fax: +333-80-29-51-16

Abstract: Early life periconceptional exposures during assisted reproductive technology (ART) procedures could alter the DNA methylation profiles of ART children, notably in imprinted genes and repetitive elements. At the genome scale, DNA methylation differences have been reported in ART conceptions at birth, but it is still unclear if those differences remain at childhood. Here, we performed an epigenome-wide DNA methylation association study using Illumina InfiniumEPIC BeadChip to assess the effects of the mode of conception on the methylome of buccal cells from 7- to 8-year-old children (48 children conceived after ART or naturally (control, CTL)) and according to the embryo culture medium in which they were conceived. We identified 127 differentially methylated positions (DMPs) and 16 differentially methylated regions (DMRs) (FDR < 0.05) with low delta beta differences between the two groups (ART vs. CTL). DMPs were preferentially located inside promoter proximal regions and CpG islands and were mostly hypermethylated with ART. We highlighted that the use of distinct embryo culture medium was not associated with DNA methylation differences in childhood. Overall, we bring additional evidence that children conceived via ART display limited genome-wide DNA methylation variation compared with those conceived naturally.

Keywords: assisted reproduction; children; DNA methylation; methylation array; culture medium

check for updates

Citation: Ducreux, B.; Frappier, J.; Bruno, C.; Doukani, A.; Guilleman, M.; Simon, E.; Martinaud, A.; Bourc'his, D.; Barberet, J.; Fauque, P. Genome-Wide Analysis of DNA Methylation in Buccal Cells of Children Conceived through IVF and ICSI. *Genes* **2021**, *12*, 1912. https://doi.org/10.3390/genes12121912

Academic Editor: Martine De Rycke

Received: 4 November 2021
Accepted: 26 November 2021
Published: 28 November 2021

1. Introduction

Assisted reproductive technologies (ARTs) have been in use for more than 40 years. They are clinically effective thanks to the improvement of diverse procedures, such as conventional in vitro fertilization (IVF) or intracytoplasmic sperm injection (ICSI). Now that ARTs are commonly used, it is estimated that children born by ART worldwide represent approximately 4% of all births [1].

However, rising concerns about the absolute safety of these techniques appeared in the early 2000s. Major adverse perinatal outcomes were first reported following ART including increased risk of preterm birth, and low and very low birthweight [2,3]. Epidemiological studies with more extensive follow-up have now been performed, and they support that the majority of ART-conceived children are healthy, even though higher cardiometabolic risk profiles exist in ART offspring [4–6]. Potential long-term health risks, including malignances, associated with ART are still unknown in humans and might not be negligible [6,7].

Furthermore, there is an increasing awareness about the potential consequences of IVF/ICSI on a number of complications potentially linked to epigenetic deregulation, such as Beckwith–Wiedemann and Silver–Russell syndromes [8,9]. It has been suggested that prenatal and early life exposure to a stressful environment could affect developmental trajectories via epigenetic mechanisms [10–12]. Indeed, epigenetic processes control numerous major cellular functions that occur during development, including changes in gene expression directed by epigenetic marks (notably DNA methylation). Reprogramming of the epigenome is also essential for genomic imprinting and for the control of repeated sequences, which are major factors regulating development and growth of the conceptus. Specifically, a partial erasure of parental DNA methylation occurs during early embryogenesis, sparing imprinted controlled regions, followed by a remodeling of the methylome landscape [13] that persists into adulthood [14,15]. In ART, additional periconceptional exposure occurs during epigenetic reprogramming (controlled ovarian hyperstimulation, embryo culture medium), with the potential to alter DNA methylation set up [16].

There have been continuous efforts to improve the culture media used for preimplantation embryos, with the primary goal of increasing live birth rates [17]. Despite these enhancements, numerous studies using mouse models, including ours, provide reliable and relevant findings concerning the impact of the culture medium composition on epigenetic regulation [18–22]. Furthermore, the type of culture medium used in human reproduction may influence the phenotypic characteristics (such as birthweight) of children born after IVF [23–26]. However, recent studies in placenta [27] and buccal cells [28] found no differences in the DNA methylation profiles of imprinted genes of ART-conceived children for whom different culture media were used. In spite of this, there is still an assumption that the culture media used has an overall influence on the human embryo epigenome [29].

It is clear that the resulting epigenetic profile arising from ART could affect development later in life and predispose to adult-onset diseases. Moreover, these epigenetic modifications may be transmitted to further generations [30], especially on sequences that do not undergo epigenetic reprogramming during gametogenesis [31]. As considerable evidence in animals indicates that the ART themselves can negatively affect epigenetics [7], the safety of ART at the epigenetic level is still not accepted [32].

In humans, DNA methylation at imprinted genes has been intensively studied, which has highlighted that ART are likely to increase imprinting methylation errors [33]. For instance, on several occasions, our team found DNA methylation changes associated with imprinted genes in ART children as compared with naturally conceived children [28,34]. We also investigated DNA methylation levels in repetitive elements in ART children in comparison with naturally conceived newborns [34] and found differences in LINE-1 elements. Nevertheless, all regions are susceptible to DNA methylation changes, and only a very small number of epigenome-wide association studies (EWASs) of ART offspring were performed to date in humans, resulting in contradictory findings. Some studies found large [35] or low differential methylation [36,37] between ART and naturally conceived neonates in cord blood. On the other hand, Choufani et al. [38] and Gentilini et al. [39] did not find significant DNA methylation differences between ART-conceived and naturally conceived children in placenta tissue and cord blood, respectively. Finally, the largest EWAS to date found that, in blood, the differential methylation observed in ART neonates was minimized in childhood [40] and adulthood [41]. Given the rising number of ART-born children, it is essential to assess the safety of such techniques on the whole epigenome and at different ages.

To address the gaps in knowledge, we performed an epigenome-wide association study assessing more than 740,000 CpGs and CpHs using EPIC BeadChip on ART and non-ART children (aged 7.7 $\pm$ 0.7 years old), and we evaluated the impact of the culture medium composition. ART children were conceived following the use of two distinct culture media, one of which turned out to be significantly underperforming in the matter of preimplantation embryo development [42] and is no longer used. This investigation offers

new insights into how ART and the culture medium remodel the epigenome in childhood, and the functional consequences.

2. Materials and Methods

2.1. Study Population

This single-center cohort study was based on an earlier randomized study conducted in 2008 at the University Hospital of Dijon with the primary aim of comparing outcomes following the use of two media: Global medium (LifeGlobal, Guelph, ON, Canada) and Single Step Medium (SSM, Irvine Scientific, Santa Ana, CA, USA). Singletons conceived in the randomized study were included in a previous study in order to collect medical data for the gestational, neonatal, and childhood period [42]. This former study was prematurely stopped 6 months after the start because the SSM medium significantly underperformed in preimplantation embryo development and pregnancy rates. The parents of all singletons from the Bouillon population (n = 73) were approached after the seventh birthday of their child to participate in an additional epigenetic study. In total, after parental consent, buccal smears of 37 singleton births were obtained for epigenetic analyses. For controls, naturally conceived singleton children born in the same period (between September 2008 and September 2009) and geographic region (Burgundy) as the ART children were included. Children were excluded from the naturally conceived group if there was any parental history of infertility or fertility treatment. One sample from the ART group was finally excluded for technical reasons (insufficient quantity of DNA). Epigenome-wide methylation data was analyzed using the EPIC array for 36 children (23 and 13 in the Global and SSM groups, respectively). Among these, 15 children were conceived using fresh embryo transfers after standard IVF (10 and 5 in the Global and SSM groups, respectively) and 21 after ICSI (13 and 8 in the Global and SSM groups, respectively). DNA methylation status was generated by EPIC array for 12 CTL children matched for gender and age. Participating children's characteristics can be found in Supplementary Materials File S1.

2.2. Sample Preparation and DNA Methylation Extraction

As previously described, buccal smear samples were collected with the Oragene DNA Collection kit (OG-250, Genotek, Ottawa, ON, Canada) [28]. We extracted DNA with the Gentra Puregene Blood Kit (Qiagen, Valencia, CA, USA) according to the manufacturer's protocol. For each sample, DNA quantity and quality was evaluated on a Nanodrop Spectrophotometer (ThermoFisher Scientific, Illkirch, France). We then performed bisulfite conversion using the EZ DNA Methylation Kit (Zymo Research, Orange, CA, USA) following the manufacturer's instructions and methylome was assessed with the state-of-the-art Infinium HumanMethylationEPIC BeadChip (Illumina, San Diego, CA, USA). Finally, chip processing was performed using an Illumina HiScan SQ fluorescent scanner at the UMS 37 PASS platform (Sorbonne University, Paris, France). Arrays were visualized and analyzed using GenomeStudio v.2011.1 (Illumina, San Diego, CA, USA).

2.3. Statistical Analyses

Raw IDAT files obtained from methylome array data were pre-processed using the *MissMethyl* [43] and *minfi* [44] R packages. Sample quality was first checked before overall data was normalized using the Subset-quantile Within Array Normalization method [45] to remove technical variance between probe designs. Probes with a poor detection p-value ($p < 0.01$) were removed from the analysis, as were those associated with SNPs and cross-reactive probes. Because cell-type composition is often a major confounder in EWAS, cell-type proportions were predicted at this step with the recent deconvolution algorithm *HEpiDISH* [46]. Briefly, *HepiDISH* uses robust partial correlation to estimate cellular proportions in epithelial tissues according to the methylation levels of highly specific CpGs of epithelial cells and seven leukocyte subtypes. As repetitive elements and imprinted genes were already analyzed by our group for the same samples in a previous study for [28], we decided to remove them for this analysis. As a result, we used

REMP package [47] to identify probes located within repetitive elements and removed them. We also removed probes located within a list of 76 imprinted genes established by Pervjakova et al. [48]. This left a total of 740,869 probes for downstream analysis. For each probe, a ß-value was calculated applying the following formula: ß = intensity of the methylated allele/(intensity of the methylated allele+intensity of the unmethylated allele + 100). ß-values are an estimator of methylation proportion at a given loci, with 0 meaning completely unmethylated and 1 fully methylated.

Singular value decomposition was next used to identify the following biological and technical confounders: Gender, Array position, Cell fractions of epithelial cells/B-lymphocytes/monocytes/neutrophils/natural killers (p-value < 0.05, Supplementary Materials File S2). We performed a differential methylation analysis using linear regression with the *limma* package (Smith, 2005) after converting ß-values to M-values, which possess more valid statistical properties to carry out differential analysis [49]. We incorporated the previously identified covariates in the final model and tested it with and without cell-type proportions. Differentially methylated positions (DMPs) associated with variables of interest were probes showing an adjusted p-value < 0.05 (Benjamini–Hochberg). A $\Delta\beta$ was calculated for each probe as the β-value difference between the two groups compared. The *DMRcate* method [50] was then used with default parameters to identify differentially methylated regions (DMRs). DMRs were those that contained at least 2 DMPs (FDR < 0.05). Probe annotations were retrieved from *ChAMP* package EPIC array annotation file [51]. A gene ontology enrichment test of DMRs was performed using the GOregion function from *MissMethyl* package. Association between genes containing DMR and diseases were tested in the DisGeNET database [52], a useful platform that computes gene–disease association scores taking into account, inter alia, the number of studies that reported the association in the literature. In addition, for each DMP found, in order to determine their potential involvement in conditions, we checked for any overlaps in the EWAS catalog and the EWAS atlas [53,54].

2.4. Comparison with Previous Studies

The location of DMPs and DMRs was compared with the results of 15 other studies on genome-wide DNA methylation and ART [35–41,55–62]. Genomic coordinates of DMPs and DMRs found in each individual study were extracted and annotated to the nearest gene. Finally, we recorded genes that contained DMP or DMR in both our study and at least one of the 15 studies included in the comparison.

3. Results

We investigated whether ART procedures could affect the buccal cell methylome in non-imprinted and non-repetitive element regions, seeing as imprinted genes and repetitive elements were already explored in this dataset [28]. We performed differential methylation analysis at a single CpG resolution in order to make comparisons between 36 ART-conceived children and 12 naturally conceived children.

Before assessing the impact of mode of conception (ART vs. CTL), type of culture medium, and method of fertilization, we analyzed the role of the cell composition in our samples.

3.1. Raw Analysis of the Buccal Cell DNA Methylation Profile of ART Children Reveals Major Variations in Cell Type Proportions

Similar to the previous study, we conducted the first EWAS without adjusting for cell fractions in our model, assuming buccal smear samples were homogenous in our cohort. From all the probes tested, 17.1% showed differential methylation between ART and the control group (CTL) (FDR < 0.05) and 9.8% were differentially methylated with a $\Delta\beta > 5\%$. In total, 20,486 differentially methylated regions (DMRs) were found, 8527 of which contained at least one probe with $\Delta\beta > 5$. Gene Ontology revealed that hypomethylated DMR genes were prevalent in immune biological pathways and hypermethylated DMR genes were prevalent in the epidermis processes. We performed a hierarchical clustering

of DMRs (Figure 1A), which failed to properly separate CTL (in grey) from ART samples (in orange). It is likely that inappropriate data preprocessing was performed and that additional confounders, such as cell composition or the presence of outliers that we did not account for, had biased the differential methylation analysis (Figure 1A).

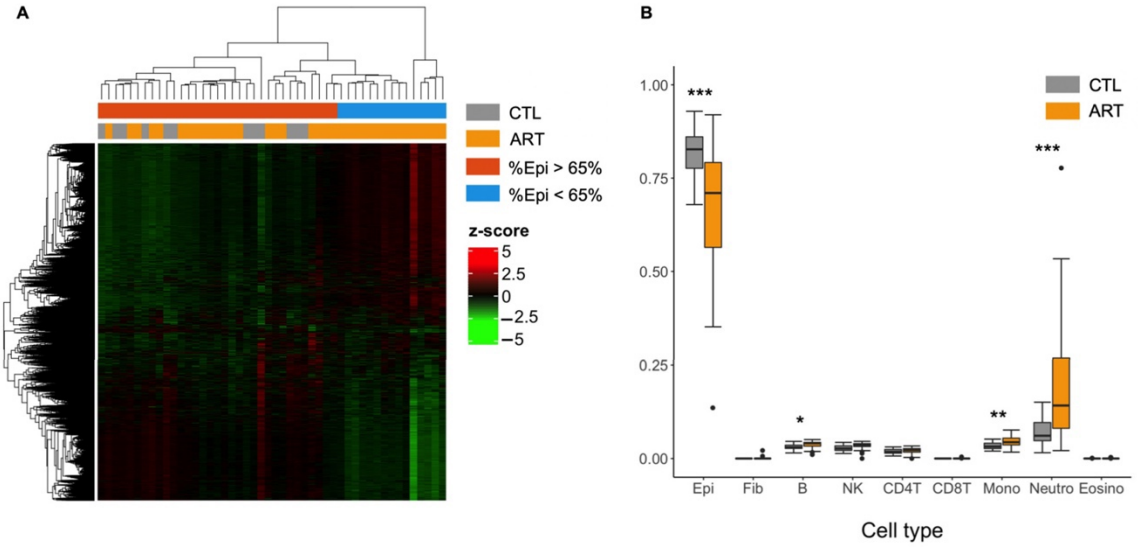

Figure 1. DMR analysis and the need to adjust for cell-type fractions. (**A**) Heatmap of differentially methylated regions (FDR < 0.05) between control and ART children in buccal cells without adjusting for cellular composition with hierarchical clustering of beta-levels (center scaled beta-values = z-scores). Epi = Epithelial buccal cells. Each row represents one of the 20,486 DMRs associated with ART. Each column corresponds to one sample. Dendrograms show how the samples and DMRs are independently clustered. The grey and orange header refers to the conception group to which children belong (grey = CTL, orange = ART). The blue and red header refers to the proportion of epithelial cells in each sample (blue = less than 65% epithelial cells, red = more than 65% epithelial cells). (**B**) Cellular proportions of buccal swab samples estimated by HEpiDISH between control and ART groups. Epi = Epithelial buccal cells, Fib = Fibroblasts, B = B cells, NK = Natural killer cells, CD4T = CD4T+ T cells, CD8T = CD8T+ T cells, Mono = Monocytes, Neutro = Neutrophils, Eosino = Eosinophils. * $p < 0.05$ ** $p < 0.01$ *** $p < 0.001$ (Student's *t*-test).

Using these observations, we estimated the cell proportions of buccal swab samples with a recent and accurate reference-based cell-type deconvolution method [46]. Surprisingly, from the DNA methylation profile estimations, predicted epithelial cell proportions ranged from 68.0% to 93.0% (mean = 81.6 ± 7.3%) for the control group whereas the ART group ranged from 13.6% to 92.0% (mean = 66.8 ± 17.0%) (Figure 1B). The ART group presented a significantly lower proportion of estimated epithelial cells ($p = 0.00014$) and a higher proportion of estimated neutrophils ($p = 0.00016$, mean control = 7.2 ± 4.1% vs. mean ART = 19.3 ± 16.1%). There was a strong negative correlation between epithelial cell and neutrophil proportions (r = −0.98) (Supplementary Materials File S3). To a lesser extent, there was also a difference in the estimated cellular fraction of monocytes ($p = 0.0061$) and B cells ($p = 0.024$) in our samples, and it was higher in the ART group. Similar to a previous study [63], estimates of CD8T cells, eosinophils, and fibroblasts were nearly null for all samples (Supplementary Materials File S4).

We finally noted that differentially methylated regions were biased by extreme ART samples that display abnormally low proportions of epithelial cells (Figure 1A). The observed differences are not related to the season of sample collection.

3.2. Impact of Mode of Conception, Type of Culture Medium, and Method of Fertilization at the CpG Level

In agreement with these previous observations, we performed a second analysis taking into account cellular fractions in our linear model. First, the average methylation level of the 740,869 probes tested was similar between ART-conceived children and controls (0.529 vs. 0.526, $p = 0.221$). Nonetheless, 127 differentially methylated positions (DMPs) were identified at FDR < 0.05 and 13 showing $\Delta\beta > 5\%$ with ART (0.02% of all the probes tested); none of the probes exceeded a 10% methylation difference between the ART and naturally conceived groups (largest effect size: 0.091) (Figure 2; Supplementary Materials File S5). The majority of DMPs were hypermethylated (75.6%) in ART children compared with non-ART children (Figure 2) and they were scattered throughout the entire genome with no apparent preferential genomic position (Figure 3). DMPs were preferentially found in the 1st Exon and TSS200 and largely in CpG islands (Figure 4). The 20 top-ranked DMPs are shown in Table 1 and Supplementary Materials File S6.

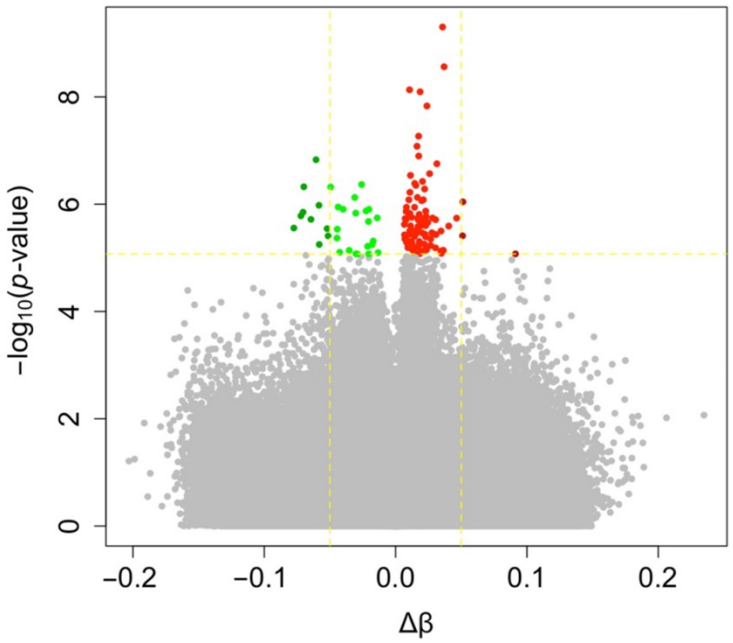

Figure 2. Volcano plot of DNA methylation changes with ART. Each point represents one of the 740,869 probes tested with mean differences in DNA methylation between ART and naturally conceived groups on the x-axis and −log10 of the unadjusted *p*-value from the moderated *t*-test computed with limma on the y-axis. Probes highlighted in green and red are respectively hypo- ($\Delta\beta < 0$) and hyper-methylated ($\Delta\beta > 0$) with ART (FDR < 0.05). Probes in dark green and dark red are those displaying $\Delta\beta > 5\%$ (FDR < 0.05).

We did not observe any DMPs in the ART group between children born via IVF or ICSI. Similarly, in vitro culture medium analysis did not reveal any DMPs between the Global and SSM groups.

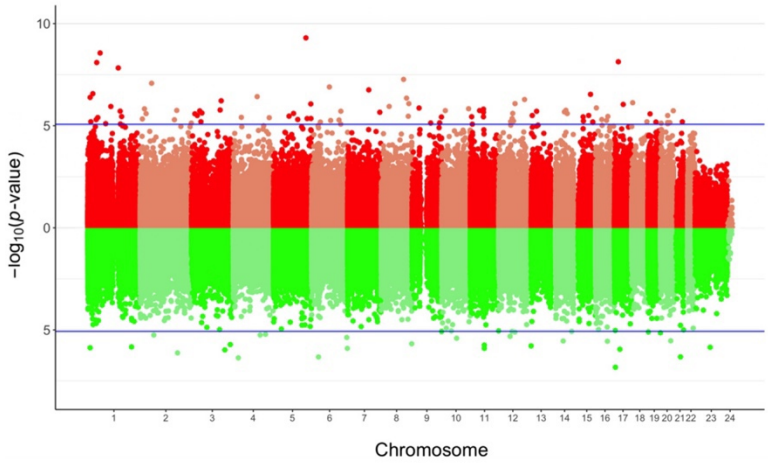

Figure 3. Bidirectional Manhattan plot of the genome-wide DNA methylation analysis of ART-conceived children compared to controls. Each point represents one of the 740,869 probes tested with their chromosomal location on the x-axis and −log10 of the unadjusted p-value from the moderated *t*-test computed with limma on the y-axis. Lines in blue separate probes that surpassed the FDR cut-off. The upper graph corresponds to hyper-methylated sites (in red) whereas the lower represents hypo-methylated sites (in green).

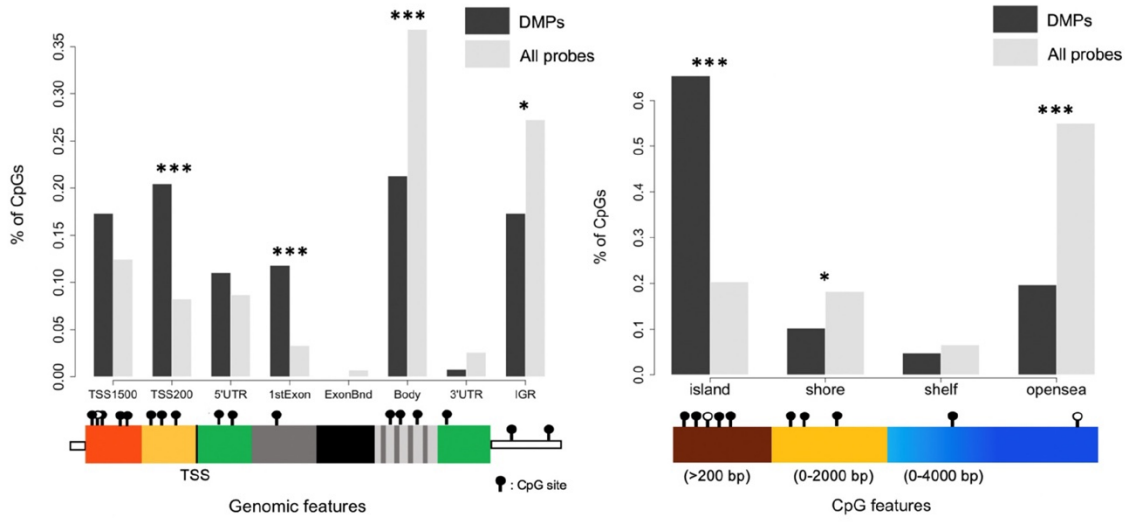

Figure 4. Distribution of DMPs across genomic and CpG regions. Significance was assessed with Chi-squared tests. * $p < 0.05$ *** $p < 0.001$. TSS = Transcription Start Site, IGR = Intergenic region.

3.3. Impact of the Mode of Conception, Type of Culture Medium, and Method of Fertilization at the Region Level

We decided to focus our downstream analysis on DMRs because they may contain more biological information and limit redundancy among the DMPs as neighboring CpGs are often highly correlated [64]. In this study, DMRs are regions that contain at least two DMPs (FDR < 0.05). We identified 16 DMRs (Table 2; Supplementary Materials File S7 and S8), none of which were contained inside gene promoters. The majority of DMRs were hypermethylated, and only one was hypomethylated. All of them had a mean

difference in methylation of <10% and only 2 had a mean difference >5%. Hierarchical clustering was managed properly to separate ART and non-ART groups (Figure 5).

Table 1. Top 20 differentially methylated positions associated with ART.

Probe ID	*p*-Value	Δβ	Genomic Feature	CpG Feature	Gene
cg25587535	0.0004	0.036	TSS200	island	*HAND1*
cg26311208	0.0010	0.037	TSS200	island	*DAB1*
cg18958584	0.0015	0.011	1stExon	island	*SHMT1*
cg24877558	0.0015	0.019	TSS1500	island	*FOXJ3*
cg18788524	0.0022	0.024	1stExon	island	*SEC22B*
cg17154315	0.0067	0.018	5′UTR	island	*ZFPM2*
cg02079951	0.0088	0.016	Body	island	*ASB3*
cg00270497	0.0117	0.018	TSS200	island	*RIPPLY2*
cg13593809	0.0122	−0.061	Body	shore	*LOC101559451*
cg19767562	0.0130	0.031	Body	island	*TFR2*
cg04856657	0.0179	0.026	TSS200	island	*PNRC2*
cg23727043	0.0179	0.011	TSS1500	island	*ADAMTS7*
cg05700616	0.0197	−0.026	IGR	opensea	*PPARGC1A*
cg11857246	0.0197	0.015	5′UTR	island	*MAD2L2*
cg14427382	0.0197	−0.070	Body	shore	*LOC100294145*
cg16866373	0.0197	0.015	5′UTR	island	*CCN3*
cg19306866	0.0197	−0.049	IGR	opensea	*KRTAP6-2*
ch.4.113910337F	0.0197	0.020	IGR	opensea	*ANK2*
cg00243897	0.0203	0.022	TSS200	island	*HPD*
cg12110529	0.0223	0.011	IGR	island	*ZBTB38*

Table 2. Differentially methylated regions associated with ART procedures identified by DMRcate. FDR corresponds to the minimum Benjamini–Hochberg FDR-corrected p-value in the region after Gaussian kernel smoothing.

Location (hg19)	Number of Probes	FDR	Maximum Difference	Mean Difference	Gene	Genomic Feature
chr19:51486901-51487968	14	4.49×10^{-22}	0.084	0.038	*KLK7*	covers exons
chr20:34204902-34205488	7	2.81×10^{-20}	0.062	0.030	*SPAG4*	covers exons
chr20:5485144-5486007	7	2.86×10^{-20}	0.127	0.094	*LINC00654*	overlaps exon upstream
chr5:153857468-153858102	7	1.10×10^{-16}	0.038	0.011	*HAND1*	overlaps exon upstream
chr20:44746392-44747351	9	2.19×10^{-12}	0.103	0.064	*CD40*	covers exons
chr1:92949813-92950575	20	1.34×10^{-11}	0.028	0.007	*GFI1*	inside intron
chr2:173292579-173292636	2	8.09×10^{-11}	0.017	0.013	*ITGA6*	inside exon
chr4:144621270-144621385	3	1.34×10^{-10}	0.017	0.013	*FREM3*	inside exon
chr1:59012392-59012820	11	1.84×10^{-10}	0.035	0.001	*DAB1*	overlaps exon upstream
chr1:47799827-47800167	3	3.11×10^{-10}	0.015	0.011	*CMPK1*	inside intron
chr20:2820742-2821472	14	8.23×10^{-10}	0.019	0.008	*PCED1A*	covers exons
chr8:106331160-106331166	2	9.47×10^{-10}	0.018	0.008	*ZFPM2*	inside exon
chr2:210444075-210444270	6	1.17×10^{-09}	−0.067	−0.043	*MAP2*	inside intron
chr17:18266764-18266775	2	1.51×10^{-09}	0.011	0.007	*SHMT1*	inside exon
chr6:32164503-32164801	7	1.88×10^{-09}	0.053	0.034	*NOTCH4*	overlaps exon downstream
chr6:32939777-32940054	10	1.88×10^{-09}	0.020	0.004	*BRD2*	inside exon

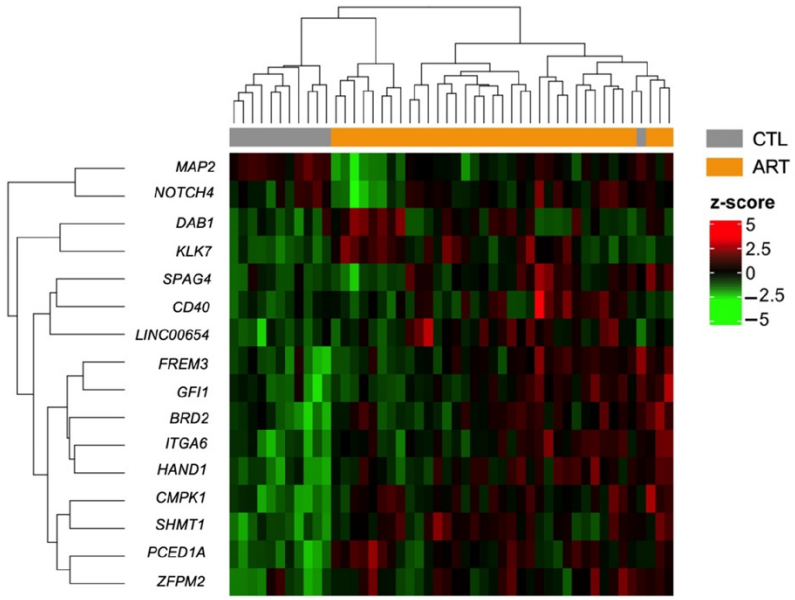

Figure 5. Heatmap of differentially methylated regions (FDR < 0.05) between control and ART children in buccal cells after adjusting for cellular composition with hierarchical clustering of beta-levels (center scaled beta-values = z-scores). Each row represents one of the 16 DMRs associated with ART. Each column corresponds to one sample. Dendrograms show how the samples and DMRs are independently clustered. The grey and orange header refers to the conception group to which children belong (grey = CTL, orange = ART).

We performed the Gene Ontology enrichment test on DMPs, but we did not find any significant ontology. Moreover, we tested our list of DMR genes in the DisGeNET database [52] in order to find if differentially methylated genes were known to be related to diseases. *ZFPM2* displayed a very high association score with tetralogy of Fallot (TOF), which is the most common form of congenital heart disease (Supplementary Materials File S9).

We did not observe any DMRs between the ART and CTL groups, ICSI and IVF groups, and Global and SSM groups.

A few studies have attempted to assess epigenome-wide effects in ART-born children. There were no DMPs or DMRs common between our study and two others performed in childhood and adolescence to date [40,61]. When we compared our results with the results of published work, regardless of the tested tissue and the age of the participants, we found six genes containing at least one DMR in common with a recent study on cord blood neonates [35] but not at the same genomic coordinates (*SHMT1*, *DAB1*, *ITGA6*, *ZFPM2*, *FREM3*, *KLK7*). We also found two genes containing one DMP in common with a study on neonates by Novakovic et al. [41]: *KAZN* and *ACTR3B*.

4. Discussion

To date, this is the only study that has performed an epigenome-wide analysis of ART outcomes in childhood assessing the impact of the culture medium in which ART children were conceived. The effects of different culture media have already been assessed in humans but only in imprinted regions and in placenta tissues [27]. This is also the second attempt to map epigenome-wide variation induced by ART in childhood [40].

For the first step, we carried out a genome-wide DNA methylation analysis to test for differences in the methylation profile of ART- and naturally conceived children. Indeed,

concerns about the epigenetic safety of ART in the beginning of the century have not yet been totally set aside [65]. Even if long-term health follow-up of ART children is reassuring [6], epigenome-wide association studies of ART status have found inconsistent and conflicting results. This led us to pursue new insights about potential modifications in the methylome of ART children. We found here a small number of DMPs in the genome of ART children. In addition, our findings suggest the Δβ of DMPs and DMRs we found between ART and control groups at childhood mostly remain low (<5%). We are not able to fully appreciate to what extent a small variation in DNA methylation can affect gene expression, though it has been shown that small-sized effects observed in environmental studies can have big outcomes [66].

Intriguingly, we found DMR in *ZFPM2* which is a gene highly related to Tetralogy of Fallot (TOF) in the DisGeNET database and *ZFPM2* promoter hypermethylation has been found in TOF patients [67]. Moreover, *HAND1* and *NOTCH4*, in which we found DMR, display abnormal methylation patterns of their promoter regions in TOF patients [68,69]. Interestingly, TOF has been shown to be more prevalent in the ART-conceived population (adjusted OR 2.4, 95% CI 1.5–3.7) [70] even if an up-to-date meta-analysis did not find any increased risk of this congenital heart defect [71]. The etiology of TOF remains poorly understood, but recent studies suggest that an aberrant epigenetic status may play an important part in the development of this heart defect [72]. None of the DMRs we found in this study were located inside promoter regions though and should have a limited phenotypic impact. As a result, we can say that the methylome in ART children is not globally altered, so it may not affect global health until adulthood [73]. One-off changes in DNA methylation in imprinted regions cannot be excluded in ART children [28,74], but their functional relevance at a later age is still unknown.

Another key point of our research is that we were able to test whether the mode of in vitro fertilization (IVF or ICSI) or the use of differing embryo culture media are associated with differential DNA methylation outcomes. In our study, no DMPs or DMRs were found between the IVF and ICSI groups, which remains consistent with other epigenome-wide studies that did not find an effect relative to the conception method [60,75]. It is regrettable that this has been very little tested in EWAS. In fact, differences according to the use of IVF or ICSI were previously highlighted in LINE-1 in placental tissues [34,76] and imprinted genes *SNRPN* in children's buccal cells [74], *PEG1/MEST* in cord blood [77], *H19* CTCF6 in children's buccal cells [78], and *PLAGL1* in cord blood [79]. Penova-Veselinovic et al. [61] also noted four CpGs were differentially methylated between IVF and ICSI after multiple correction, but this association did not persist when correcting for additional confounders, such as the type of embryo transfer. Different assisted reproductive techniques thus may not induce considerable discrepancies between ART-conceived neonates, but we advise future studies to test for differences between IVF and ICSI in order to further explore this field.

Similarly, the use of distinct culture media (Global and SSM) was associated with discrepant developmental profiles in children [42]. However, both here and previously [28], we did not find any DMP or DMR between the Global and SSM culture medium groups in the same cohort. It is important and reassuring to notice that whereas SSM culture medium was significantly underperforming in early embryo development and pregnancy rates as compared with the Global medium, no epigenetic differences were found in large-scale analyses in children thus conceived. ART procedures' specificities (i.e., IVF or ICSI, culture medium) tested in our cohort did not affect the methylome, and ART differences may thus come from the intrinsic biological features of gametes, ovarian hyperstimulation, or the use of the technique itself rather than its conditions [80,81]. Indeed, ART interferes at a time of intense physiological epigenetic reprogramming, i.e., during gametogenesis and early embryogenesis, when cells are highly sensitive to their environment. Efforts must be maintained to identify and assess the origins of epigenetic abnormalities detected in ART-conceived individuals in order to further improve ART procedures and reduce the potential health risks.

We compared our study with previous EWAS conducted in ART individuals, and again we found few gene correspondences. To date, no other EWAS was conducted on buccal cells and two were performed at childhood or adolescence. Penova-Veselinovic et al. [61] found no differences in adolescent blood methylome while Yeung et al. [40] found one DMR in children blood samples, but it was located in imprinted gene GNAS. We decided to perform a pan-tissue cross-over comparison of DNA methylation and ART studies whatever the age, which was motivated by the fact that ART could influence identical genes across different tissues and these modifications might be persistent during lifespan. The only similarities we found were with Novakovic et al. [41] (two genes containing at least one DMP in common) and Chen et al. [35] (six genes containing at least one DMR in common). We focused on buccal cells, which have less cell variability than blood and may be a more informative tissue for non-blood-based diseases in EWAS [82]. We attempted to link the DMPs we found to phenotypes thanks to the EWAS catalog [54] and the EWAS atlas [53]. Unfortunately, far too few EWAS were carried out on buccal cells, and they mostly focused on smoking, breastfeeding, and alcohol consumption, which restricts disease association.

The unique nature of our study arises from the fact that we assessed methylome in childhood (7.7 ± 0.7 years old), which has rarely been done on a genome-wide scale before, and almost all existing studies have focused on newborns. In addition, the age range of our cohort of children is very narrow, ensuring robust epigenetic assessments and comparisons. Indeed, Horvath established that DNA methylation was age dependent [83]. However, as DNA methylation is a dynamic process throughout life, it would be interesting to follow this cohort to reassess the methylome later, in the teenage years or adulthood, to fully understand how and if epigenetic variations induced by ART could be detrimental.

Finally, we found that the buccal swab samples of ART children presented a distinct composition profile. Based on estimations, immune cells were more prevalent, which is a possible biological characteristic of inflammation. More particularly, a very high proportion of neutrophils was found in ART samples compared to the control group. In line with this finding, perturbations in immune processes have already been described in the ART conceptus. Zhang et al. [84] first related differentially expressed genes implicated in the immune response in ART-treated placentas. Recently, Chen et al. [35] suggested that epigenetic modifications induced by ART could affect the immune system. This phenomenon has also been underlined in mouse experiments. Indeed, in vitro fertilization techniques dysregulated genes encoding proteins that play a role in immune regulation in placental tissues [85]. A study in ART-conceived mice also revealed disturbances in the TH1/TH2/TH17 balance [86], while another highlighted an altered helper T cell-mediated immune response [87]. It would be worth assessing whether the immune imbalance we observed in the cells of ART children shifts with age. If these observations are further confirmed by new studies, it would be interesting to explore the relation between the proportion of immune cells in the oral cavity, the epigenetic modifications potentially induced by ART, and a prospective predisposition to immune disorders.

To date, there are still gaps in our knowledge about the link between ART procedures and epigenetic variations observed in ART-conceived individuals on the epigenome-wide scale in humans. The one study that attempted to map global epigenetic changes following ART in early pregnancy by studying chorionic villus sampling did not find differences between ART and natural conception methods [58]. It has been suggested that abnormal epigenetic regulation during early embryogenesis could be a cause for abnormal placentation and may thus be the source of developmental abnormalities [88,89]. In addition, we still have a missing link between the epigenetic variation observed with ART and the disease phenotype. In our cohort, all children were born healthy and have not reported medical issues to date. Forming cohorts of individuals with identified medical conditions potentially linked to ART could be of great interest to investigate whether ART-induced epigenetic modifications could be responsible for these underlying disorders.

There are some limitations to our findings. Regarding the sample size, the statistical power of our epigenome-wide results can be debated. According to the a priori power

calculations guidance in Mansell et al. [90], we would only detect 50% of all EPIC array sites with a mean difference of 5% with >50% power with 36 cases samples. Additionally, we decided to separate the ART group to analyze the fertilization method (IVF or ICSI vs. CTL) or the culture medium effect, which reduces the reliability of these sub-group analysis conclusions. It is, however, necessary to consider the remarkable homogeneity in our tested individuals (born in the same IVF center, ensuring the same lab conditions, at the same period, and very close in age). We can also ensure gestational age at birth between the two groups was not different between the ART and CTL groups. However, early life socioeconomic status could also be associated with specific DNA methylation patterns [91]. Unfortunately, this information was non-exhaustively recorded in our study to be assessed. To date, epigenome-wide association studies of ART effects suffer from great heterogeneity in sample size and ART procedures, which has resulted in discrepancies. Further studies of this kind would be welcome to address the growing problem of the origin of ART-induced epigenetic modifications.

5. Conclusions

Overall, our findings suggest that there are modest DNA methylation differences between naturally conceived and ART-conceived children and their functional relevance in adult tissue is unknown. Additionally, we highlighted that the use of different culture media and different techniques (ICSI or IVF) is not associated with DNA methylation variations across our cohort. Even if DNA methylation modifications in imprinted regions have been reported in relation to ART, the conclusions supported by our study tend to demonstrate additional modifications are not widespread across the entire genome. In accordance with epidemiological studies, our data are reassuring about the potential epigenetic side effects of ART in childhood. However, until now, too few studies have assessed the safety of ART on an epigenetic level. In future, it will be important to continue conducting epigenome-wide association studies in ART-conceived individuals, especially at various ages.

Supplementary Materials: The following are available online at https://www.mdpi.com/article/10.3390/genes12121912/s1, Supplementary File S1: Characteristics of participating children, Supplementary File S2: Estimated Singular Value Decomposition of methylation sample analysis summary, Supplementary File S3: Correlation between estimated epithelial buccal cells fraction and other immune cells fraction (Cor: Pearson correlation coefficient), Supplementary File S4: Estimated cell proportions for each sample, Supplementary File S5: All DMPs with ART, Supplementary File S6: Dotplot of DNA methylation for control and ART samples for the top 20 top-ranked DMPs, Supplementary File S7: Dotplot of mean DNA methylation for control and ART samples for the 16 DMRs, Supplementary File S8: All DMRs with ART, Supplementary File S9: Gene-Disease heatmap from the DisGeNet database for gene containing DMRs.

Author Contributions: Conceptualization, P.F., B.D. and J.B.; methodology, P.F., B.D. and J.B.; software, B.D.; formal analysis, B.D.; investigation, M.G., J.B., C.B., J.F., E.S. and P.F.; resources, A.D., M.G., J.B., C.B., J.F., E.S., A.M. and P.F.; data curation, B.D.; writing—original draft preparation, P.F. and B.D.; writing—review and editing, P.F. and B.D.; visualization, P.F.; supervision, D.B. and P.F.; project administration, P.F.; funding acquisition, P.F. All authors have read and agreed to the published version of the manuscript.

Funding: This work was supported by funding from the Agence Nationale pour la Recherche ("CARE"-ANR JCJC 2017).

Institutional Review Board Statement: All the work described here was approved by the Ethics Evaluation Committee of INSERM (IORG0003254, FWA00005831) and the Institutional Review Board (IRB00003888).

Informed Consent Statement: Informed consent was provided by the parents of all participants.

Data Availability Statement: The datasets generated during the current study are available in NCBI's Gene Expression Omnibus under accession number GSE150901.

Acknowledgments: The authors thank the clinical and technical teams of the IVF Center of Dijon for their collaboration. We thank Maud Carpentier of the "Direction de la Recherche Clinique et de l'Innovation" of Dijon University Hospital for the financial management of the study and Suzanne Rankin for her help in proofreading the manuscript.

Conflicts of Interest: The authors declare no conflict of interest.

References

1. Adamson, G.D.; de Mouzon, J.; Chambers, G.M.; Zegers-Hochschild, F.; Mansour, R.; Ishihara, O.; Banker, M.; Dyer, S. International Committee for Monitoring Assisted Reproductive Technology: World report on assisted reproductive technology, 2011. *Fertil. Steril.* **2018**, *110*, 1067–1080. [CrossRef]
2. Hansen, M.; Kurinczuk, J.J.; Bower, C.; Webb, S. Injection and in vitro Fertilization. *N. Engl. J. Med.* **2002**, *346*, 725–730. [CrossRef]
3. Helmerhorst, F.M.; Perquin, D.A.M.; Donker, D.; Keirse, M.J.N.C. Perinatal outcome of singletons and twins after assisted conception: A systematic review of controlled studies. *Br. Med. J.* **2004**, *328*, 261–264. [CrossRef] [PubMed]
4. Chen, M.; Heilbronn, L.K. The health outcomes of human offspring conceived by assisted reproductive technologies (ART). *J. Dev. Orig. Health Dis.* **2017**, *8*, 388–402. [CrossRef]
5. Guo, X.-Y.; Liu, X.M.; Jin, L.; Wang, T.T.; Ullah, K.; Sheng, J.Z.; Huang, H.F. Cardiovascular and metabolic profiles of offspring conceived by assisted reproductive technologies: A systematic review and meta-analysis. *Fertil. Steril.* **2017**, *107*, 622–631.e5. [CrossRef]
6. Berntsen, S.; Söderström-Anttila, V.; Wennerholm, U.B.; Laivuori, H.; Loft, A.; Oldereid, N.B.; Romundstad, L.B.; Bergh, C.; Pinborg, A. The health of children conceived by ART: 'The chicken or the egg?'. *Hum. Reprod. Update* **2019**, *25*, 137–158. [CrossRef] [PubMed]
7. Duranthon, V.; Chavatte-Palmer, P. Long term effects of ART: What do animals tell us? *Mol. Reprod. Dev.* **2018**, *85*, 348–368. [CrossRef] [PubMed]
8. Fauque, P.; De Mouzon, J.; Devaux, A.; Epelboin, S.; Gervoise-Boyer, M.J.; Levy, R.; Valentin, M.; Viot, G.; Bergère, A.; De Vienne, C.; et al. Reproductive technologies, female infertility, and the risk of imprinting-related disorders. *Clin. Epigenetics* **2020**, *12*, 191. [CrossRef]
9. Argyraki, M.; Damdimopoulou, P.; Chatzimeletiou, K.; Grimbizis, G.F.; Tarlatzis, B.C.; Syrrou, M.; Lambropoulos, A. In-utero stress and mode of conception: Impact on regulation of imprinted genes, fetal development and future health. *Hum. Reprod. Update* **2019**, *25*, 777–801. [CrossRef] [PubMed]
10. Bale, T.L.; Baram, T.Z.; Brown, A.S.; Goldstein, J.M.; Insel, T.R.; McCarthy, M.M.; Nemeroff, C.B.; Reyes, T.M.; Simerly, R.B.; Susser, E.S. Nestler EJ Early Life Programming and Neurodevelopmental Disorders Tracy. *Biol. Psychiatry* **2010**, *68*, 314–319. [CrossRef]
11. Vaiserman, A.M. Epigenetic programming by early-life stress: Evidence from human populations. *Dev. Dyn.* **2015**, *244*, 254–265. [CrossRef]
12. Kundakovic, M.; Jaric, I. The epigenetic link between prenatal adverse environments and neurodevelopmental disorders. *Genes* **2017**, *8*, 104. [CrossRef]
13. Reik, W.; Dean, W.; Walter, J. Epigenetic reprogramming in mammalian development. *Science* **2001**, *293*, 1089–1093. [CrossRef]
14. Reik, W.; Romer, I.; Barton, S.C.; Surani, M.A.; Howlett, S.K.; Klose, J. Adult phenotype in the mouse can be affected by epigenetic in the early embryo. *Development* **1993**, *119*, 933–942. [CrossRef] [PubMed]
15. Murgatroyd, C.; Patchev, A.V.; Wu, Y.; Micale, V.; Bockmühl, Y.; Fischer, D.; Holsboer, F.; Wotjak, C.T.; Almeida, O.F.; Spengler, D. Dynamic DNA methylation programs persistent adverse effects of early-life stress. *Nat. Neurosci.* **2009**, *12*, 1559–1566. [CrossRef] [PubMed]
16. Ramos-Ibeas, P.; Heras, S.; Gómez-Redondo, I.; Planells, B.; Fernández-González, R.; Pericuesta, E.; Laguna-Barraza, R.; Pérez-Cerezales, S.; Gutiérrez-Adán, A. Embryo responses to stress induced by assisted reproductive technologies. *Mol. Reprod. Dev.* **2019**, *86*, 1292–1306. [CrossRef]
17. Mantikou, E.; Youssef, M.A.; van Wely, M.; van der Veen, F.; Al-Inany, H.G.; Repping, S.; Mastenbroek, S. Embryo culture media and IVF/ICSI success rates: A systematic review. *Hum. Reprod. Update* **2013**, *19*, 210–220. [CrossRef]
18. Doherty, A.S.; Mann, M.R.W.; Tremblay, K.D.; Bartolomei, M.S.; Schultz, R.M. Differential effects of culture on imprinted H19 expression in the preimplantation mouse embryo. *Biol. Reprod.* **2000**, *62*, 1526–1535. [CrossRef] [PubMed]
19. Khosla, S.; Dean, W.; Brown, D.; Reik, W.; Feil, R. Culture of preimplantation mouse embryos affects fetal development and the expression of imprinted genes. *Biol. Reprod.* **2001**, *64*, 918–926. [CrossRef] [PubMed]
20. Mann, M.R.W.; Lee, S.S.; Doherty, A.S.; Verona, R.I.; Nolen, L.D.; Schultz, R.M.; Bartolomei, M.S. Selective loss of imprinting in the placenta following preimplantation development in culture. *Development* **2004**, *131*, 3727–3735. [CrossRef]
21. Market-Velker, B.A.; Fernandes, A.D.; Mann, M.R.W. Side-by-side comparison of five commercial media systems in a mouse model: Suboptimal in vitro culture interferes with imprint maintenance. *Biol. Reprod.* **2010**, *83*, 938–950. [CrossRef] [PubMed]
22. Carmignac, V.; Barberet, J.; Iranzo, J.; Quéré, R.; Guilleman, M.; Bourc'his, D.; Fauque, P. Effects of assisted reproductive technologies on transposon regulation in the mouse pre-implanted embryo. *Hum. Reprod.* **2019**, *34*, 612–622. [CrossRef] [PubMed]
23. Dumoulin, J.C.; Land, J.A.; Van Montfoort, A.P.; Nelissen, E.C.; Coonen, E.; Derhaag, J.G.; Schreurs, I.L.; Dunselman, G.A.; Kester, A.D.; Geraedts, J.P.; et al. Effect of in vitro culture of human embryos on birthweight of newborns. *Hum. Reprod.* **2010**, *25*, 605–612. [CrossRef] [PubMed]

24. Nelissen, E.C.; Van Montfoort, A.P.; Coonen, E.; Derhaag, J.G.; Geraedts, J.P.; Smits, L.J.; Land, J.A.; Evers, J.L.; Dumoulin, J.C. Further evidence that culture media affect perinatal outcome: Findings after transfer of fresh and cryopreserved embryos. *Hum. Reprod.* **2012**, *27*, 1966–1976. [CrossRef]
25. Hassani, F.; Eftekhari-Yazdi, P.; Karimian, L.; Valojerdi, M.R.; Movaghar, B.; Fazel, M.; Fouladi, H.R.; Shabani, F.; Johansson, L. The effects of ISM1 medium on embryo quality and outcomes of IVF/ICSI cycles. *Int. J. Fertil. Steril.* **2013**, *7*, 108–115.
26. Zandstra, H.; van Montfoort, A.P.A.; Dumoulin, J.C.M. Does the type of culture medium used influence birthweight of children born after IVF? *Hum. Reprod.* **2015**, *30*, 530–542. [CrossRef] [PubMed]
27. Mulder, C.L.; Wattimury, T.M.; Jongejan, A.; de Winter-Korver, C.M.; van Daalen, S.K.; Struijk, R.B.; Borgman, S.C.; Wurth, Y.; Consten, D.; van Echten-Arends, J.; et al. Comparison of DNA methylation patterns of parentally imprinted genes in placenta derived from IVF conceptions in two different culture media. *Hum. Reprod.* **2020**, *35*, 516–528. [CrossRef] [PubMed]
28. Barberet, J.; Binquet, C.; Guilleman, M.; Doukani, A.; Choux, C.; Bruno, C.; Bourredjem, A.; Chapusot, C.; Bourc'his, D.; Duffourd, Y.; et al. Do assisted reproductive technologies and in vitro embryo culture influence the epigenetic control of imprinted genes and transposable elements in children? *Hum. Reprod.* **2021**, *36*, 479–492. [CrossRef]
29. Mani, S.; Mainigi, M. Embryo Culture Conditions and the Epigenome. *Semin. Reprod. Med.* **2018**, *36*, 211–220. [CrossRef]
30. Van Montfoort, A.P.A.; Hanssen, L.L.P.; de Sutter, P.; Viville, S.; Geraedts, J.P.M.; de Boer, P. Assisted reproduction treatment and epigenetic inheritance. *Hum. Reprod. Update* **2012**, *18*, 171–197. [CrossRef] [PubMed]
31. Bruno, C.; Carmignac, V.; Netchine, I.; Choux, C.; Duffourd, Y.; Faivre, L.; Thauvin-Robinet, C.; Le Bouc, Y.; Sagot, P.; Bourc'his, D.; et al. Germline correction of an epimutation related to Silver-Russell syndrome. *Hum. Mol. Genet.* **2015**, *24*, 3314–3321. [CrossRef] [PubMed]
32. Jiang, Z.; Wang, Y.; Lin, J.; Xu, J.; Ding, G.; Huang, H. Genetic and epigenetic risks of assisted reproduction. *Best Pract. Res. Clin. Obstet. Gynaecol.* **2017**, *44*, 90–104. [CrossRef]
33. Lazaraviciute, G.; Kauser, M.; Bhattacharya, S.; Haggarty, P.; Bhattacharya, S. A systematic review and meta-analysis of DNA methylation levels and imprinting disorders in children conceived by IVF/ICSI compared with children conceived spontaneously. *Hum. Reprod. Update* **2014**, *20*, 840–852. [CrossRef] [PubMed]
34. Choux, C.; Binquet, C.; Carmignac, V.; Bruno, C.; Chapusot, C.; Barberet, J.; Lamotte, M.; Sagot, P.; Bourc'his, D.; Fauque, P. The epigenetic control of transposable elements and imprinted genes in newborns is affected by the mode of conception: ART versus spontaneous conception without underlying infertility. *Hum. Reprod.* **2018**, *33*, 331–340. [CrossRef]
35. Chen, W.; Peng, Y.; Ma, X.; Kong, S.; Tan, S.; Wei, Y.; Zhao, Y.; Zhang, W.; Wang, Y.; Yan, L.; et al. Integrated multi-omics reveal epigenomic disturbance of assisted reproductive technologies in human offspring. *EBioMedicine* **2020**, *61*, 103076. [CrossRef] [PubMed]
36. Melamed, N.; Choufani, S.; Wilkins-Haug, L.E.; Koren, G.; Weksberg, R. Comparison of genome-wide and gene-specific DNA methylation between ART and naturally conceived pregnancies. *Epigenetics* **2015**, *10*, 474–483. [CrossRef] [PubMed]
37. El Hajj, N.; Haertle, L.; Dittrich, M.; Denk, S.; Lehnen, H.; Hahn, T.; Schorsch, M.; Haaf, T. DNA methylation signatures in cord blood of ICSI children. *Hum. Reprod.* **2017**, *32*, 1761–1769. [CrossRef]
38. Choufani, S.; Turinsky, A.L.; Melamed, N.; Greenblatt, E.; Brudno, M.; Bérard, A.; Fraser, W.D.; Weksberg, R.; Trasler, J.; Monnier, P. Impact of assisted reproduction, infertility, sex and paternal factors on the placental DNA methylome. *Hum. Mol. Genet.* **2019**, *28*, 372–385. [CrossRef] [PubMed]
39. Gentilini, D.; Somigliana, E.; Pagliardini, L.; Rabellotti, E.; Garagnani, P.; Bernardinelli, L.; Papaleo, E.; Candiani, M.; Di Blasio, A.M.; Viganò, P. Multifactorial analysis of the stochastic epigenetic variability in cord blood confirmed an impact of common behavioral and environmental factors but not of in vitro conception. *Clin. Epigenetics* **2018**, *10*, 77. [CrossRef] [PubMed]
40. Yeung, E.H.; Mendola, P.; Sundaram, R.; Zeng, X.; Guan, W.; Tsai, M.Y.; Robinson, S.L.; Stern, J.E.; Ghassabian, A.; Lawrence, D.; et al. Conception by fertility treatment and offspring deoxyribonucleic acid methylation. *Fertil. Steril.* **2021**, *116*, 493–504. [CrossRef] [PubMed]
41. Novakovic, B.; Lewis, S.; Halliday, J.; Kennedy, J.; Burgner, D.P.; Czajko, A.; Kim, B.; Sexton-Oates, A.; Juonala, M.; Hammarberg, K.; et al. Assisted reproductive technologies are associated with limited epigenetic variation at birth that largely resolves by adulthood. *Nat. Commun.* **2019**, *10*, 3922. [CrossRef] [PubMed]
42. Bouillon, C.; Léandri, R.; Desch, L.; Ernst, A.; Bruno, C.; Cerf, C.; Chiron, A.; Souchay, C.; Burguet, A.; Jimenez, C.; et al. Does embryo culture medium influence the health and development of children born after in vitro fertilization? *PLoS ONE* **2016**, *11*, e0150857. [CrossRef] [PubMed]
43. Phipson, B.; Maksimovic, J.; Oshlack, A. MissMethyl: An R package for analyzing data from Illumina's HumanMethylation450 platform. *Bioinformatics* **2016**, *32*, 286–288. [CrossRef] [PubMed]
44. Aryee, M.J.; Jaffe, A.E.; Corrada-Bravo, H.; Ladd-Acosta, C.; Feinberg, A.P.; Hansen, K.D.; Irizarry, R.A. Minfi: A flexible and comprehensive Bioconductor package for the analysis of Infinium DNA methylation microarrays. *Bioinformatics* **2014**, *30*, 1363–1369. [CrossRef]
45. Maksimovic, J.; Gordon, L.; Oshlack, A. SWAN: Subset-quantile within array normalization for illumina infinium HumanMethylation450 BeadChips. *Genome Biol.* **2012**, *13*, r44. [CrossRef]
46. Zheng, S.C.; Webster, A.P.; Dong, D.; Feber, A.; Graham, D.G.; Sullivan, R.; Jevons, S.; Lovat, L.B.; Beck, S.; Widschwendter, M.; et al. A novel cell-type deconvolution algorithm reveals substantial contamination by immune cells in saliva, buccal and cervix. *Epigenomics* **2018**, *10*, 925–940. [CrossRef]

47. Zheng, Y.; Joyce, B.T.; Liu, L.; Zhang, Z.; Kibbe, W.A.; Zhang, W.; Hou, L. Prediction of genome-wide DNA methylation in repetitive elements. *Nucleic Acids Res.* **2017**, *45*, 8697–8711. [CrossRef] [PubMed]
48. Pervjakova, N.; Kasela, S.; Morris, A.P.; Kals, M.; Metspalu, A.; Lindgren, C.M.; Salumets, A.; Mägi, R. Imprinted genes and imprinting control regions show predominant intermediate methylation in adult somatic tissues. *Epigenomics* **2016**, *8*, 789–799. [CrossRef] [PubMed]
49. Du, P.; Zhang, X.; Huang, C.C.; Jafari, N.; Kibbe, W.A.; Hou, L.; Lin, S.M. Comparison of β-value and M-value methods for quantifying methylation levels by microarray analysis. *BMC Bioinform.* **2010**, *11*, 587. [CrossRef]
50. Peters, T.J.; Buckley, M.J.; Statham, A.L.; Pidsley, R.; Samaras, K.; Lord, R.V.; Clark, S.J.; Molloy, P.L. De novo identification of differentially methylated regions in the human genome. *Epigenetics Chromatin* **2015**, *8*, 6. [CrossRef] [PubMed]
51. Tian, Y.; Morris, T.J.; Webster, A.P.; Yang, Z.; Beck, S.; Feber, A.; Teschendorff, A.E. ChAMP: Updated methylation analysis pipeline for Illumina BeadChips. *Bioinformatics* **2017**, *33*, 3982–3984. [CrossRef] [PubMed]
52. Piñero, J.; Bravo, À.; Queralt-Rosinach, N.; Gutiérrez-Sacristán, A.; Deu-Pons, J.; Centeno, E.; García-García, J.; Sanz, F.; Furlong, L.I. DisGeNET: A comprehensive platform integrating information on human disease-associated genes and variants. *Nucleic Acids Res.* **2017**, *45*, D833–D839. [CrossRef] [PubMed]
53. Li, M.; Zou, D.; Li, Z.; Gao, R.; Sang, J.; Zhang, Y.; Li, R.; Xia, L.; Zhang, T.; Niu, G.; et al. EWAS Atlas: A curated knowledgebase of epigenome-wide association studies. *Nucleic Acids Res.* **2019**, *47*, D983–D988. [CrossRef] [PubMed]
54. Battram, T.; Yousefi, P.; Crawford, G.; Prince, C.; Babei, M.S.; Sharp, G.; Hatcher, C.; Vega-Salas, M.J.; Khodabakhsh, S.; Whitehurst, O.; et al. The EWAS Catalog: A database of epigenome-wide association studies. *OSF Prepr* **2021**, 2–5. [CrossRef]
55. Katari, S.; Turan, N.; Bibikova, M.; Erinle, O.; Chalian, R.; Foster, M.; Gaughan, J.P.; Coutifaris, C.; Sapienza, C. DNA methylation and gene expression differences in children conceived in vitro or in vivo. *Hum. Mol. Genet.* **2009**, *18*, 3769–3778. [CrossRef]
56. Camprubí, C.; Iglesias-Platas, I.; Martin-Trujillo, A.; Salvador-Alarcon, C.; Rodriguez, M.A.; Barredo, D.R.; Court, F.; Monk, D. Stability of genomic imprinting and gestational-age dynamic methylation in complicated pregnancies conceived following assisted reproductive technologies. *Biol. Reprod.* **2013**, *89*, 50. [CrossRef]
57. Estill, M.S.; Bolnick, J.M.; Waterland, R.A.; Bolnick, A.D.; Diamond, M.P.; Krawetz, S.A. Assisted reproductive technology alters deoxyribonucleic acid methylation profiles in bloodspots of newborn infants. *Fertil. Steril.* **2016**, *106*, 629–639.e10. [CrossRef]
58. Xu, N.; Barlow, G.M.; Cui, J.; Wang, E.T.; Lee, B.; Akhlaghpour, M.; Kroener, L.; Williams, J.; Rotter, J.I.; Yii-der, I.C.; et al. Comparison of Genome-Wide and Gene-Specific DNA Methylation Profiling in First-Trimester Chorionic Villi from Pregnancies Conceived with Infertility Treatments. *Reprod. Sci.* **2017**, *24*, 996–1004. [CrossRef] [PubMed]
59. Castillo-Fernandez, J.E.; Loke, Y.J.; Bass-Stringer, S.; Gao, F.; Xia, Y.; Wu, H.; Lu, H.; Liu, Y.; Wang, J.; Spector, T.D.; et al. DNA methylation changes at infertility genes in newborn twins conceived by in vitro fertilisation. *Genome Med.* **2017**, *9*, 28. [CrossRef] [PubMed]
60. Tobi, E.W.; Almqvist, C.; Hedman, A.; Andolf, E.; Holte, J.; Olofsson, J.I.; Wramsby, H.; Wramsby, M.; Pershagen, G.; Heijmans, B.T.; et al. DNA methylation differences at birth after conception through ART. *Hum. Reprod.* **2021**, *36*, 248–259. [CrossRef] [PubMed]
61. Penova-Veselinovic, B.; Melton, P.E.; Huang, R.C.; Yovich, J.L.; Burton, P.; Wijs, L.A.; Hart, R.J. DNA methylation patterns within whole blood of adolescents born from assisted reproductive technology are not different from adolescents born from natural conception. *Hum. Reprod.* **2021**, *36*, 2035–2049. [CrossRef]
62. Caramaschi, D.; Jungius, J.; Page, C.M.; Novakovic, B.; Saffery, R.; Halliday, J.; Lewis, S.; Magnus, M.C.; London, S.J.; Håberg, S.E.; et al. Association of medically assisted reproduction with offspring cord blood DNA methylation across cohorts. *Human Reprod.* **2021**, *36*, 2403–2413. [CrossRef] [PubMed]
63. Van Dongen, J.; Ehli, E.A.; Jansen, R.; Van Beijsterveldt, C.E.; Willemsen, G.; Hottenga, J.J.; Kallsen, N.A.; Peyton, S.A.; Breeze, C.E.; Kluft, C.; et al. Genome-wide analysis of DNA methylation in buccal cells: A study of monozygotic twins and mQTLs. *Epigenetics Chromatin* **2018**, *11*, 54. [CrossRef]
64. Guo, S.; Diep, D.; Plongthongkum, N.; Fung, H.L.; Zhang, K.; Zhang, K. Identification of methylation haplotype blocks AIDS in deconvolution of heterogeneous tissue samples and tumor tissue-of-origin mapping from plasma DNA. *Nat. Genet.* **2017**, *49*, 635–642. [CrossRef]
65. Niemitz, E.L.; Feinberg, A.P. Epigenetics and assisted reproductive technology: A Call for Investigation. *Epigenetic Epidemiol.* **2014**, *74*, 599–609. [CrossRef] [PubMed]
66. Breton, C.V.; Marsit, C.J.; Faustman, E.; Nadeau, K.; Goodrich, J.M.; Dolinoy, D.C.; Herbstman, J.; Holland, N.; LaSalle, J.M.; Schmidt, R.; et al. Small-magnitude effect sizes in epigenetic end points are important in children's environmental health studies: The children's environmental health and disease prevention research center's epigenetics working group. *Environ. Health Perspect.* **2017**, *125*, 511–526. [CrossRef]
67. Sheng, W.; Chen, L.; Wang, H.; Ma, X.; Ma, D.; Huang, G. CpG island shore methylation of ZFPM2 is identified in tetralogy of fallot samples. *Pediatric Res.* **2016**, *80*, 151–158. [CrossRef]
68. Sheng, W.; Qian, Y.; Wang, H.; Ma, X.; Zhang, P.; Diao, L.; An, Q.; Chen, L.; Ma, D.; Huang, G. DNA methylation status of NKX2-5, GATA4 and HAND1 in patients with tetralogy of fallot. *BMC Med. Genom.* **2013**, *6*, 46. [CrossRef]
69. Zhu, Y.; Ye, M.; Xu, H.; Gu, R.; Ma, X.; Chen, M.; Li, X.; Sheng, W.; Huang, G. Methylation status of CpG sites in the NOTCH4 promoter region regulates NOTCH4 expression in patients with tetralogy of Fallot. *Mol. Med. Rep.* **2020**, *22*, 4412–4422. [CrossRef] [PubMed]

70. Tararbit, K.; Lelong, N.; Thieulin, A.C.; Houyel, L.; Bonnet, D.; Goffinet, F.; Khoshnood, B.; EPICARD Study Group. The risk for four specific congenital heart defects associated with assisted reproductive techniques: A population-based evaluation. *Hum. Reprod.* **2013**, *28*, 367–374. [CrossRef] [PubMed]
71. Giorgione, V.; Parazzini, F.; Fesslova, V.L.; Cipriani, S.O.; Candiani, M.; Inversetti, A.N.; Sigismondi, C.; Tiberio, F.; Cavoretto, P. Congenital heart defects in IVF/ICSI pregnancy: Systematic review and meta-analysis. *Ultrasound Obstet. Gynecol.* **2018**, *51*, 33–42. [CrossRef]
72. Radhakrishna, U.; Vishweswaraiah, S.; Veerappa, A.M.; Zafra, R.; Albayrak, S.; Sitharam, P.H.; Saiyed, N.M.; Mishra, N.K.; Guda, C.; Bahado-Singh, R. Newborn blood DNA epigenetic variations and signaling pathway genes associated with Tetralogy of Fallot (TOF). *PLoS ONE* **2018**, *13*, e0203893. [CrossRef]
73. Halliday, J.; Lewis, S.; Kennedy, J.; Burgner, D.P.; Juonala, M.; Hammarberg, K.; Amor, D.J.; Doyle, L.W.; Saffery, R.; Ranganathan, S.; et al. Health of adults aged 22 to 35 years conceived by assisted reproductive technology. *Fertil. Steril.* **2019**, *112*, 130–139. [CrossRef] [PubMed]
74. Whitelaw, N.; Bhattacharya, S.; Hoad, G.; Horgan, G.W.; Hamilton, M.; Haggarty, P. Epigenetic status in the offspring of spontaneous and assisted conception. *Hum. Reprod.* **2014**, *29*, 1452–1458. [CrossRef]
75. Santos, F.; Hyslop, L.; Stojkovic, P.; Leary, C.; Murdoch, A.; Reik, W.; Stojkovic, M.; Herbert, M.; Dean, W. Evaluation of epigenetic marks in human embryos derived from IVF and ICSI. *Hum. Reprod.* **2010**, *25*, 2387–2395. [CrossRef]
76. Ghosh, J.; Coutifaris, C.; Sapienza, C.; Mainigi, M. Global DNA methylation levels are altered by modifiable clinical manipulations in assisted reproductive technologies. *Clin. Epigenetics* **2017**, *9*, 14. [CrossRef] [PubMed]
77. Tierling, S.; Souren, N.Y.; Gries, J.; LoPorto, C.; Groth, M.; Lutsik, P.; Neitzel, H.; Utz-Billing, I.; Gillessen-Kaesbach, G.; Kentenich, H.; et al. Assisted reproductive technologies do not enhance the variability of DNA methylation imprints in human. *J. Med. Genet.* **2010**, *47*, 371–376. [CrossRef] [PubMed]
78. Loke, Y.J.; Galati, J.C.; Saffery, R.; Craig, J.M. Association of in vitro fertilisation (IVF) with global and IGF2/H19 methylation variation in newborn twins. *J. Paediatr. Child Health* **2015**, *51*, 21. [CrossRef]
79. Vincent, R.N.; Gooding, L.D.; Louie, K.; Wong, E.C.; Ma, S. Altered DNA methylation and expression of PLAGL1 in cord blood from assisted reproductive technology pregnancies compared with natural conceptions. *Fertil. Steril.* **2016**, *106*, 739–748.e3. [CrossRef]
80. Fauque, P. Ovulation induction and epigenetic anomalies. *Fertil. Steril.* **2013**, *99*, 616–623. [CrossRef] [PubMed]
81. Marshall, K.L.; Rivera, R.M. The effects of superovulation and reproductive aging on the epigenome of the oocyte and embryo. *Mol. Reprod. Dev.* **2018**, *85*, 90–105. [CrossRef]
82. Lowe, R.; Gemma, C.; Beyan, H.; Hawa, M.I.; Bazeos, A.; Leslie, R.D.; Montpetit, A.; Rakyan, V.K.; Ramagopalan, S.V. Buccals are likely to be a more informative surrogate tissue than blood for epigenome-wide association studies. *Epigenetics* **2013**, *8*, 445–454. [CrossRef]
83. Horvath, S. DNA methylation age of human tissues and cell types. *Genome Biol.* **2013**, *14*, 3156. [CrossRef] [PubMed]
84. Zhang, Y.; Cui, Y.; Zhou, Z.; Sha, J.; Li, Y.; Liu, J. Altered global gene expressions of human placentae subjected to assisted reproductive technology treatments. *Placenta* **2010**, *31*, 251–258. [CrossRef] [PubMed]
85. Fauque, P.; Ripoche, M.A.; Tost, J.; Journot, L.; Gabory, A.; Busato, F.; Le Digarcher, A.; Mondon, F.; Gut, I.; Jouannet, P.; et al. Modulation of imprinted gene network in placenta results in normal development of in vitro manipulated mouse embryos. *Hum. Mol. Genet.* **2010**, *19*, 1779–1790. [CrossRef] [PubMed]
86. Ahmadi, H.; Fathi, F.; Karimi, H.; Amidi, F.; Mehdinejadiani, S.; Moeini, A.; Hoseini, S.; Sobhani, A. Altered TH1, TH2, TH17 balance in assisted reproductive technology conceived mice. *J. Reprod. Immunol.* **2020**, *139*, 103117. [CrossRef] [PubMed]
87. Karimi, H.; Mahdavi, P.; Fakhari, S.; Faryabi, M.R.; Esmaeili, P.; Banafshi, O.; Mohammadi, E.; Fathi, F.; Mokarizadeh, A. Altered helper T cell-mediated immune responses in male mice conceived through in vitro fertilization. *Reprod. Toxicol.* **2017**, *69*, 196–203. [CrossRef] [PubMed]
88. Nelissen, E.C.M.; van Montfoort, A.P.A.; Dumoulin, J.C.M.; Evers, J.L.H. Epigenetics and the placenta. *Hum. Reprod. Update* **2011**, *17*, 397–417. [CrossRef] [PubMed]
89. Choux, C.; Carmignac, V.; Bruno, C.; Sagot, P.; Vaiman, D.; Fauque, P. The placenta: Phenotypic and epigenetic modifications induced by Assisted Reproductive Technologies throughout pregnancy. *Clin. Epigenetics* **2015**, *7*, 87. [CrossRef]
90. Mansell, G.; Gorrie-Stone, T.J.; Bao, Y.; Kumari, M.; Schalkwyk, L.S.; Mill, J.; Hannon, E. Guidance for DNA methylation studies: Statistical insights from the Illumina EPIC array. *BMC Genom.* **2019**, *20*, 366. [CrossRef] [PubMed]
91. Bush, N.R.; Edgar, R.D.; Park, M.; MacIsaac, J.L.; McEwen, L.M.; Adler, N.E.; Essex, M.J.; Kobor, M.S.; Boyce, W.T. The biological embedding of early-life socioeconomic status and family adversity in children's genome-wide DNA methylation. *Epigenomics* **2018**, *10*, 1445–1461. [CrossRef] [PubMed]

Supplementary File S1: Characteristics of participating children

	ART Group (n=36)	CTL group (n=12)	p*
Boys (*n*)	18 (50%)	5 (41.6%)	
Gestational age at birth (weeks)	38.8 (1.8)	39.6 (1.3)	0.15
Birthweight (grams)	3144.6 (504)	3282.5 (273)	0.30
Low birthweight (<2500 g)	3 (8.3%)	0	
Major malformations (according to EUROCAT)	2/35 (5.7%)		
Hospitalizations (day)	8/35 (22.8%)	3/19 (15.8%)	
Chronic diseases			
Cardiac	0/35 (0%)	0/19 (0%)	
Pulmonary (asthma)	2/35 (5.7%)	1/19 (5.3%)	
Neurological	1/35 (2.9%)	0/19 (0%)	
ENT with secondary deafness	1/35 (2.9%)	0/19 (0%)	
Digestive	1/35 (2.9%)	0/19 (0%)	
Haematological	1/35 (2.9%)	0/19 (0%)	
Other diseases	1/35 (2.9%)	0/19 (0%)	
Surgery	9/35 (25.7%)	4/19 (21.1%)	

Data are presented as numbers (%) or mean (SD)

EUROCAT: European Surveillance of Congenital Anomalies

SD: standard deviation

n: number of children

Student test (quantitative variables) or Fisher test (qualitative variables)

Supplementary File S2: Estimated Singular Value Decomposition of methylation sample analysis summary

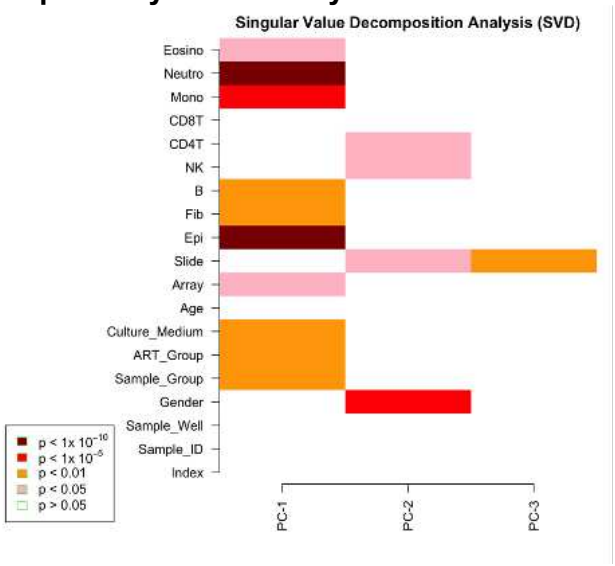

Supplementary File S3: Correlation between estimated epithelial buccal cells fraction and other immune cells fraction (Cor: Pearson correlation coefficient)

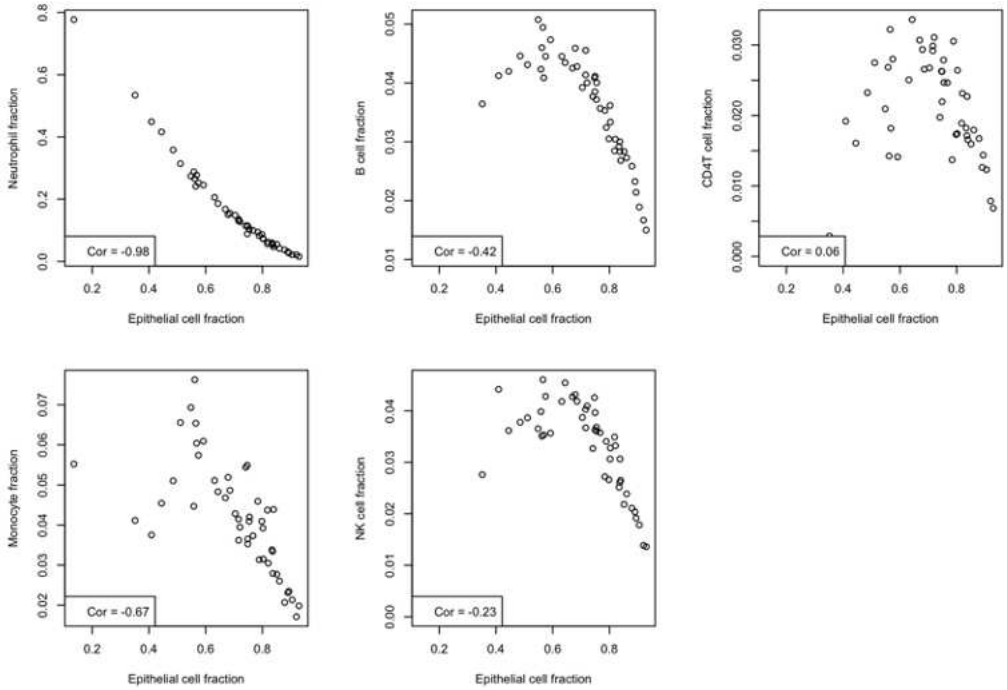

Supplementary File S4: Estimated cell proportions for each sample

Available at https://www.mdpi.com/article/10.3390/genes12121912/s1

Supplementary File S5: All DMPs with ART

Available at https://www.mdpi.com/article/10.3390/genes12121912/s1

Supplementary File S6: Dotplot of DNA methylation for control and ART samples for the top 20 top-ranked DMPs

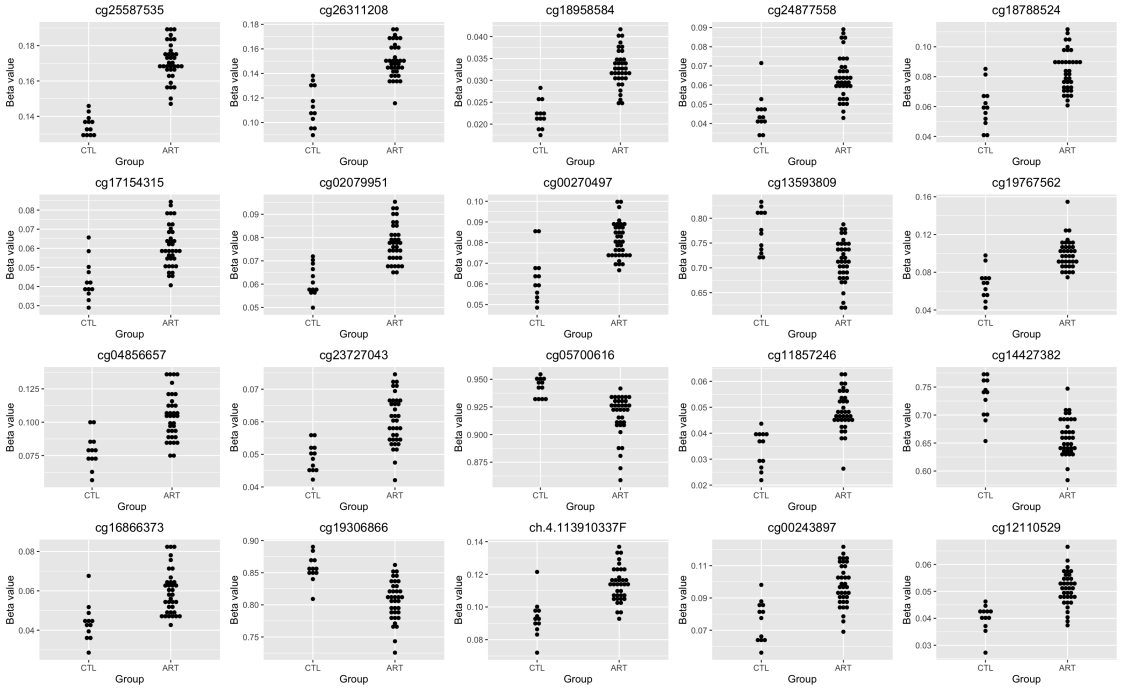

Supplementary File S7: Dotplot of mean DNA methylation for control and ART samples for the 16 DMRs

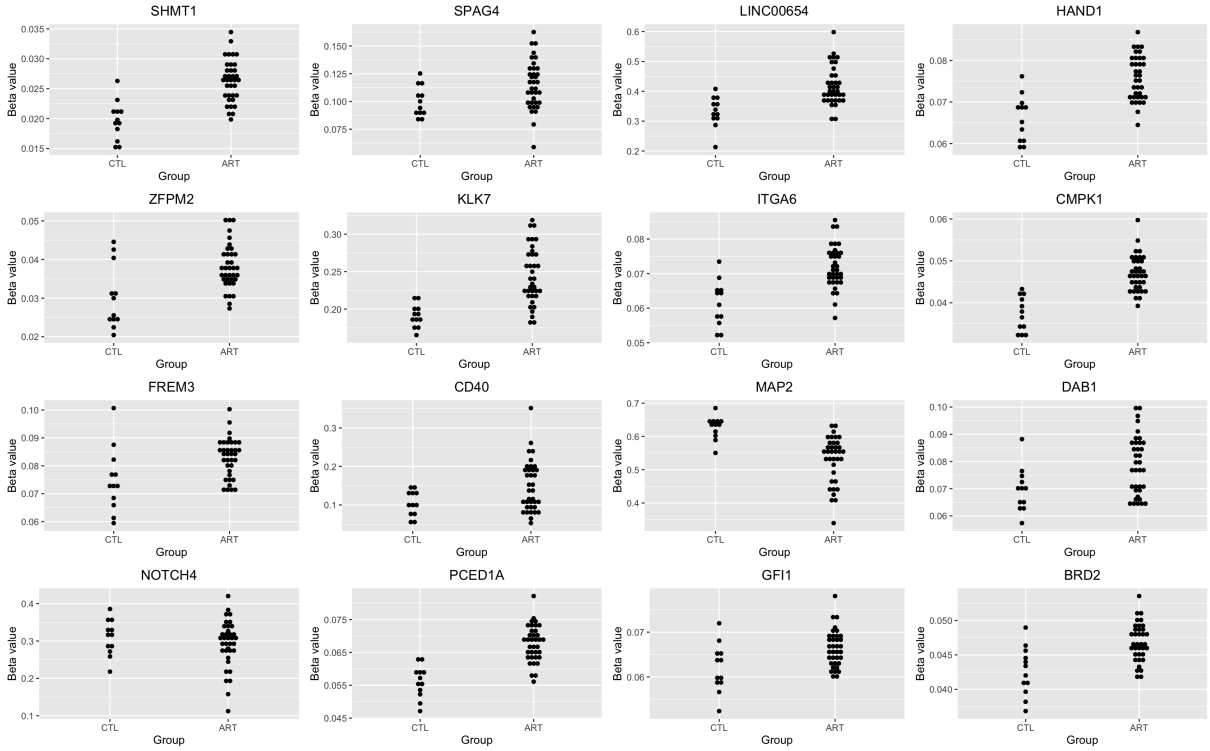

Supplementary File S8: All DMRs with ART

Available at https://www.mdpi.com/article/10.3390/genes12121912/s1

Supplementary File S9: Gene-Disease heatmap from the DisGeNet database for gene containing DMRs

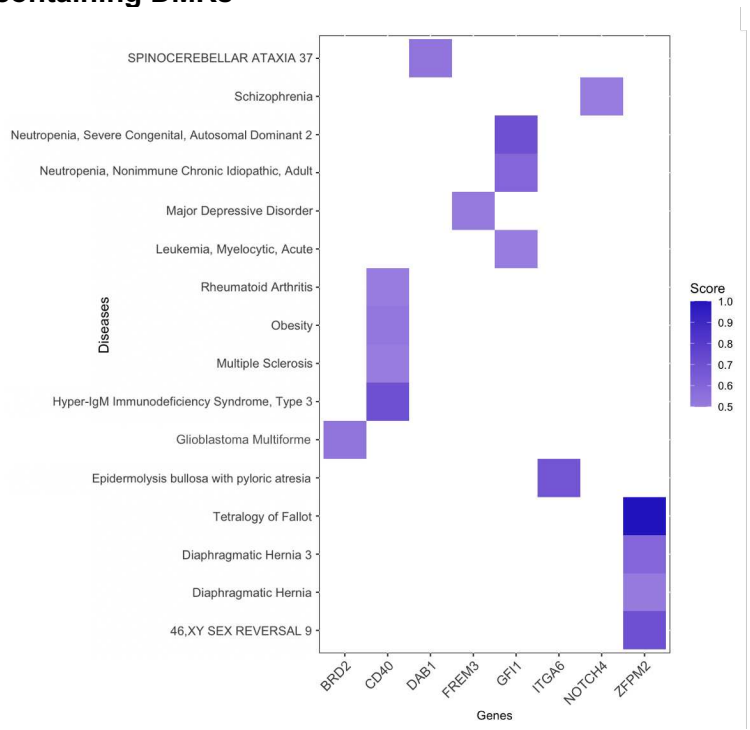

Chapitre 3 : Discussion générale

Les techniques utilisées en AMP aujourd'hui apparaissent donc comme pratiquement sans danger mais il faut encore identifier l'origine du faible surrisque de certaines pathologies et syndromes par rapport aux conceptions naturelles. Cela doit motiver la recherche à l'évolution des pratiques car il est évident que l'environnement influe directement sur la régulation de l'expression des gènes via des modifications épigénétiques. Il y a de plus une attente sociétale grandissante vis-à-vis de l'AMP, car de plus en plus de personnes vont avoir recours à l'AMP dans les décennies qui viennent. Nous nous devons de maximiser les chances de grossesse en se questionnant sur chaque pratique et leurs faiblesses. C'est dans cette optique que l'étude du transcriptome lors des premiers stades du développement peut nous aider, en comprenant comment différentes pratiques et leurs modalités d'exécution influencent les mécanismes essentiels du développement.

En ce sens, une des conclusions de cette thèse est qu'il faut attacher plus d'importance à la qualité des ovocytes utilisés en AMP. L'ovocyte est une cellule riche en ARN messager puisqu'approximativement 20% de ses ARNs totaux sont des ARNm, près de 10 fois plus que n'importe quelle autre cellule somatique (Tora & Vincent, 2021). Ce stockage en matériel transcriptomique est initié durant la folliculogenèse puis stoppé après la rupture de la vésicule germinale ; on parle de quiescence transcriptionnelle (Oh *et al.*, 2000; Zhang *et al.*, 2018). Pour être fécondable, l'ovocyte subit une maturation nucléaire et surtout cytoplasmique, lorsque les ARNs maternels stockés sont sélectivement dégradés ou transcrits pour supporter les premières étapes du développement post-fécondation jusqu'à la mise en route du génome embryonnaire (Sha *et al.*, 2020; Yu *et al.*, 2020; Llonch *et al.*, 2021). Il est impératif que ce contenu ne soit pas altéré au cours de la folliculogenèse et de la maturation ovocytaire, notamment le fonctionnement de processus biologiques majeurs comme le cycle cellulaire et la division cellulaire afin d'éviter générer du stress cellulaire et de conserver une compétence développementale optimale ainsi que celle sous-jacente de l'embryon.

Les principales observations de notre revue sur la qualité transcriptomique des ovocytes utilisés en AMP nous a permis de cibler les techniques les plus à-mêmes d'altérer des fonctions essentielles du développement ou de promouvoir l'activité de gènes pouvant compromettre la cinétique embryonnaire et/ou l'implantation. Nous décrivons que différents protocoles de stimulation ovarienne modulent le transcriptome des cellules entourant l'ovocyte, notamment au niveau du métabolisme lipidique et des interactions cellule-cellule, mais avec des différences qui restent très limitées entre eux. Le manque de données directement sur l'ovocyte même est une barrière à notre compréhension des effets de la stimulation ovarienne pour l'ovocyte. Il semble que cette procédure n'induise pas de dommages importants pour le contenu en ARN messager ovocytaire, mais elle pourrait forcer l'ovocyte à être relâché prématurément. La maturation du protéome ovocytaire ne serait alors pas totalement achevée d'après une étude sur le modèle murin, et cela nécessite d'investiguer cette question chez l'humain (Taher *et al.*, 2021). Notre synthèse met toutefois en lumière le bénéfice à utiliser la combinaison hCG+GnRH-a pour l'induction de l'ovulation, d'une part pour permettre l'achèvement de la maturation ovocytaire et par ailleurs réduire le risque de syndrome d'hyperstimulation ovarienne. Le choix d'un protocole de stimulation doit être motivé par les caractéristiques cliniques de chaque patiente.

D'autres interventions en AMP semblent plus néfastes pour la transcription des ARNm maternels requis pour la compétence ovocytaire. La maturation *in vitro* pourrait altérer les voies de signalisation énergétiques de l'ovocyte (respiration mitochondriale, métabolisme, phosphorylation oxydative) alors que les premières divisions cellulaires demandent une forte consommation d'énergie. L'amélioration de la disponibilité énergétique pourrait être un levier de développement pour optimiser cette technique parfois nécessaire chez certaines patientes. Toutes les manipulations *in vitro*, incluant les conditions de culture de la MIV (tension en oxygène, manipulation), sont génératrices de stress oxydant qui doit être évité au maximum pour limiter la survenue de modifications épigénétiques et d'autres dommages fonctionnels et structuraux. L'utilisation d'antioxydants apparaît alors judicieuse pour limiter ce risque. Des

sources de pollution existent également dans les laboratoires d'AMP mais elles sont encore trop sous-estimées, comme dans l'air ambiant ou dans les contenants et les pipettes utilisés (bisphénols) (Khoudja *et al.*, 2013; Gatimel *et al.*, 2016). Dans les ovocytes de souris, le bisphénol A a démontré une capacité à altérer l'expression de gènes du cycle cellulaire, de la signalisation hormonale et de la régulation traductionnelle, ce qui nécessite grande prudence (Ferris *et al.*, 2016).

Enfin nous avons évalué de façon critique les études sur la vitrification des ovocytes, qui tend à s'adresser à davantage de patientes. Quelques études étaient alarmistes sur l'impact de cette technique avec des modifications majeures de l'expression de gènes du cycle cellulaire et de la croissance ovocytaire en comparaison d'ovocytes frais (Monzo *et al.*, 2012; Huo *et al.*, 2021). Ces études comprenant de nombreuses failles (taille d'échantillon faible, composition du groupe contrôle inadéquate, nombre de gènes évalués), nous avons tenu à proposer la plus grande étude évaluant l'effet de la vitrification sur le transcriptome ovocytaire à ce jour. Nous avons appliqué un plan d'étude très rigoureux, incluant des patientes ayant donné à la recherche trois ovocytes par patiente répartis entre trois groupes : frais, vitrification semi-automatique et vitrification manuelle. Nos résultats affichent des différences largement limitées entre les ovocytes frais et vitrifiés ce qui est rassurant quant à la sécurité de cette technique pour l'intégrité du transcriptome ovocytaire. Il est possible que certains gènes soient sous-exprimés en lien avec la vitrification comme l'indiquent plusieurs études dont la nôtre mais la mesure du nombre d'intégrité des transcrits (TIN) nous indique que la vitrification ne dégrade pas le contenu transcriptomique ovocytaire dans sa globalité. De plus les deux modes de vitrification testés affichaient des différences très minimes (5 gènes différentiellement exprimés).

Enfin, pour conclure sur les effets de l'AMP dans sa globalité, nous avons utilisé une approche de recoupage de données et avons observé qu'une récurrence commune à différentes interventions en AMP était la dysrégulation de gènes impliqués dans des processus de modifications épigénétiques. La sensibilité de ces transcrits mérite davantage d'attention pour

éviter que ces processus majeurs pour le développement de l'embryon ne soient altérés, notamment la reprogrammation épigénétique. La qualité ovocytaire passe entre autres en première ligne par l'expression adéquate de ces transcrits.

Les interventions artificielles susceptibles de modifier la qualité des ovocytes utilisés en AMP se superposent dans la majorité des cas à un contexte d'infertilité sous-jacent. Ce paramètre est inhérent à chaque patiente, et a souvent déjà généré du stress pour l'ovocyte, incluant des dysrégulations transcriptomiques inéluctables. Parmi ces facteurs on retrouve l'âge des patientes, les pathologies du système reproductif (endométriose, SOPK), des facteurs de risque liés au mode de vie (tabac, obésité) et les expositions environnementales nuisibles (phtalates, particules fines) durant toute la vie (Steuerwald *et al.*, 2007; Mai *et al.*, 2014; Liu *et al.*, 2016; Kalo & Roth, 2017; Ferrero *et al.*, 2019; Zhang *et al.*, 2020; Guo *et al.*, 2021; Yuan *et al.*, 2021). Tous ces facteurs sont générateurs de stress oxydant et semblent altérer la bioénergie de l'ovocyte issue des mitochondries (Roth, 2018). Les ovocytes des femmes ayant recours à l'AMP sont donc déjà fragilisés avant toute intervention d'AMP et il est nécessaire de limiter les effets cumulatifs.

En ce sens, notre étude sur la vitrification des ovocytes apporte la preuve que cette technique est une avancée notable pour de nombreuses femmes car elle permet de conserver ses ovocytes à des moments opportuns, où les chances qu'ils soient fécondables sont les plus hautes. De plus, la méthylation de l'ADN est un processus réversible et pour certains facteurs, notamment ceux liés au mode de vie, il est possible d'agir favorablement sur le méthylome ovocytaire. Cette thèse ouvre ainsi quelques pistes à explorer pour les chercheurs mais aussi des réflexions des cliniciens sur leurs pratiques actuelles. Dans les grandes lignes, les futurs axes de recherche pourraient se concentrer sur l'étude de populations spécifiques (SOPK, endométriose, âge maternel avancé, expositions environnementales), des manipulations encore inexplorées (composition du milieu de manipulation des ovocytes, pipetage, délai de fécondation après collecte de l'ovocyte, antioxydants, hormones de croissance, co-culture

avec cellules cumulus) ou des paramètres physico-chimiques du laboratoire (tension en oxygène basse, sources de pollutions dans le laboratoire, exposition lumineuse).

En dernière analyse, nous avons montré que la composition du milieu de culture embryonnaire peut induire des réponses transcriptomiques en tant qu'adaptation de l'embryon à son micro-environnement, avant et après compaction. L'utilisation de milieux riches en acides aminés semble un meilleur choix, dans des concentrations optimisées, même si ce n'est pas la norme dans toutes les cliniques (Menezo *et al.*, 2019). Nos résultats ont montré une divergence dans l'expression de 266 transcrits entre les milieux Ferticult (dépourvu en acides aminés) et Global (riche en acides aminés) au stade 4-cellules, dont certains pourraient jouer un rôle clé dans le développement précoce d'après l'analyse par Gene Ontology. Ce résultat ne permet pas de soutenir l'utilisation d'un milieu plus qu'un autre, il nous indique seulement que le milieu de culture module l'expression du transcriptome.

En effectuant une culture prolongée dans le milieu Global jusqu'au stade blastocyste d'embryons cultivés jusqu'au jour 2 soit dans le milieu Global soit Ferticult, notre analyse différentielle n'a révélé plus que 18 gènes différentiellement exprimés, dont aucun n'était différentiellement exprimé dans l'analyse précédente. La non-persistance des modifications observées au stade 4-cellules peut se présumer à 2 hypothèses : après-compaction et donc l'activation du génome embryonnaire, les différences d'expression acquises dans différents environnements pré-compaction ont été atténuées par récupération de l'activité transcriptionnelle, ou alors le milieu Global, supposé plus favorable étant donné sa composition, a modulé l'expression de ces gènes vers leur zone d'optimalité. Toutefois, les embryons cultivés dans le Ferticult jusqu'au jour 2 présentaient des anomalies de surexpression de quelques gènes à effets maternels au jour 5 (qui codent des facteurs d'origine ovocytaire et impliqués dans le développement embryonnaire) comme *PADI6* et *TUBB8*, et d'autres identifiés comme jouant un rôle dans les premières divisions cellulaires (détail dans l'article 5). Spécifiquement, ces transcrits affichaient un retard de dégradation chez les embryons cultivés dans le Ferticult jusqu'au jour 2 en comparaison de données

modélisant la cinétique attendue du transcriptome embryonnaire précoce. Il reste inconnu si le retard de dégradation spécifique à ces transcrits impacte réellement le phénotype du fœtus et du nouveau-né. Dans leur globalité, nos résultats montrent la capacité de l'embryon post-compaction à s'adapter à un environnement suboptimal pré-compaction par une modulation de son activité transcriptomique et suggèrent que les milieux riches en acides aminés placent l'embryon dans une cinétique de développement optimisée.

Cette thèse a également passé en revue de façon critique les évènements d'erreur de méthylation de l'ADN et d'expression des gènes à différentes étapes du développement en lien avec les techniques d'assistance médicale à la procréation. Nous avons montré que le recours à l'AMP était souvent associé à des altérations du méthylome, même si les études restent très conflictuelles, de faible qualité de l'évidence (taille d'échantillon inadéquate pour détecter des variations de méthylation avec une grande puissance statistique) et les résultats très peu répliqués d'une étude à l'autre. Cette complexité est accentuée par l'observation que différents tissus néonataux ne semblent pas atteints de façon similaire. Une standardisation des méthodologies utilisées, l'inclusion d'un très grand nombre de patients et l'utilisation de technologies couvrant l'ensemble du génome devraient nous permettre à l'avenir d'avoir plus de clarté sur l'état de l'épigénome après AMP.

Toutefois, notre méta-analyse des études ciblées indique que seule la région *PEG1*/*MEST* est modifiée de façon consistante chez différentes cohortes dans le placenta et le sang de cordon, mais seulement d'après deux études pour chaque tissu (Tierling *et al.*, 2010; Rancourt *et al.*, 2012; Nelissen *et al.*, 2013). Pour les études à l'échelle du génome, nous avons mis en évidence très peu de gènes communément différentiellement méthylés, avec une forte variabilité d'un tissu étudié à un autre et d'une période de la vie à une autre. Ces observations nous amènent à la conclusion que l'AMP n'induit pas de modifications ciblées chez tous les individus mais elle pourrait augmenter la prévalence d'erreurs de méthylation de façon stochastique, c'est-à-dire induire des modifications aléatoirement distribuées dans tout le génome (Gentilini *et al.*, 2015). Malgré tout, la forte incidence d'évènements de perte

d'empreinte semble indiquer que les régions soumises à empreinte sont en première ligne face aux interventions artificielles de l'AMP et plus susceptibles de voir le contrôle de leur empreinte altéré qu'en conception naturelle. Cela se traduit au niveau de la santé des enfants conçus par AMP, qui sont plus à risques d'être atteints de ces syndromes liés à l'empreinte parentale (Odom & Segars, 2010; Vermeiden & Bernardus, 2013; Hattori *et al*., 2019; Fauque *et al*., 2020).

Des études pionnières avaient préalablement montré une méthylation différentielle de certains GSE entre conception par FIV et naturelle chez la souris suivant l'origine embryonnaire ou extra-embryonnaire du tissu étudié. A J10.5, *H19* DMR était notamment hypométhylée dans le placenta mais pas chez le fœtus, et dans une autre étude *H19* DMR et *SNRPN* affichaient également une hypométhylation dans le placenta mais pas dans les tissus fœtaux à J9.5 (Mann *et al.*, 2004; Fauque *et al.*, 2010). La variabilité retrouvée dans différents tissus pourrait s'expliquer précocement lors de la ségrégation des cellules depuis le stade 8-cellules en différentes lignées cellulaires embryonnaires : le trophectoderme et la masse cellulaire interne (MCI). La spécification de ces cellules implique la programmation de profils de méthylation différents qui définissent leur propre identité cellulaire, à savoir les différents tissus embryonnaires et le placenta (Fulka *et al.*, 2004; Zhou *et al.*, 2019; Olcha *et al.*, 2021). Le trophectoderme représente la couche externe de la morula puis du blastocyste, qui après nidation donne les syncytiotrophoblastes, cellules qui sont elles-mêmes à l'origine du placenta. La MCI, qui est constituée à partir des cellules internes de la morula, sont des cellules pluripotentes à l'origine des trois feuillets embryonnaires : de façon simplifiée, l'ectoderme qui donne les organes externes comme les muqueuses et le système nerveux, l'endoderme qui donne les organes des systèmes digestifs et respiratoires, et le mésoderme qui forme les autres organes internes (système circulatoire, reproducteur, muscles, reins, …). Une combinaison de facteurs de position et des caractéristiques des profils de méthylation préétablis pourrait expliquer la variabilité tissu-spécifique notamment retrouvée entre les profils de méthylation de nouveau-nés conçus par FIV ou spontanément pour le placenta et le sang

périphérique. Une hypothèse pourrait être que du fait de leur contact direct avec l'environnement extérieur, les cellules du trophoblaste soient plus vulnérables aux interventions telles que la culture embryonnaire et que des différences de méthylation soient plus prononcées dans le placenta et le sang de cordon que pour des tissus propres au fœtus. Le placenta est le régulateur exclusif de l'environnement fœtal et un témoin direct du stress épigénétique que peut subir le fœtus (Maccani & Marsit, 2009). Puisque l'AMP est susceptible d'engendrer des altérations précoces du méthylome dès les premières spécifications du trophoblaste, le placenta représente un marqueur des potentielles modifications épigénétiques subies par l'embryon précoce. En lien avec le concept de la DOHaD qui établit que des expositions à des environnements suboptimaux durant le développement prédispose à des altérations irréversibles et une mauvaise santé à long terme, il faudra à l'avenir accorder plus d'attention aux différences spécifiques à chaque tissu issu de lignées embryonnaires distinctes.

Par ailleurs, nous ne savons pas distinguer si les altérations retrouvées dans notre méta-analyse sont les conséquences de certaines techniques en particulier ou résultent de l'effet global d'une conception *in vitro* (accumulation d'interventions). Pouvoir isoler l'effet unique de chaque technique chez l'humain est difficile à mettre en place en raison de législations restrictives. Il a été soupçonné qu'en lieu et place de l'AMP, c'est l'infertilité sous-jacente des couples qui expliquerait les différences de méthylation retrouvées. Si leur influence est non-négligeable, cette théorie n'est pas confirmée par une récente étude en trio (enfant et parents) de la méthylation qui a retrouvé des altérations de méthylation chez les nouveau-nés par FIV qui n'étaient pas présentes chez les parents (Håberg *et al.*, 2022). De plus, des effets sur la méthylation sont rapportées chez de nombreux modèles animaux et en absence de toute infertilité (Doherty *et al.*, 2000; Fauque *et al.*, 2007a; Rivera *et al.*, 2008; Reis e Silva *et al.*, 2012; de Waal *et al.*, 2014; Urrego *et al.*, 2014). Toutefois cela ne garantit pas que le contexte d'infertilité ne joue pas un rôle sur ces modifications, car des pathologies du système reproductif comme l'endométriose sont génératrices de stress oxydant pour l'ovocyte, qui joue

un rôle direct sur les niveaux de méthylation (Menezo *et al.*, 2016; Scutiero *et al.*, 2017; Wyck *et al.*, 2018). Il convient donc de prendre en compte le facteur infertilité parentale dans le plan d'analyse d'études sur la méthylation et l'AMP mais également d'élargir la recherche sur des sujets trop peu approfondis comme l'endométriose et le syndrome des ovaires polykystiques.

Une des conclusions frappantes de notre synthèse est le manque de suivi à moyen et long terme de ces profils de méthylation. Nous avons tenté d'adresser cette insuffisance par la réalisation d'une étude comparative entre enfants issus de FIV/ICSI et de conception naturelle à l'âge de 7 ans. Si quelques différences de méthylation ont été retrouvées (une centaine de DMPs), leur magnitude et leur localisation n'évoquent pas d'inquiétude concernant la santé. Cela est d'autant plus confirmé par des études sur puces à méthylation et de grandes cohortes plus tardives dans le sang périphérique, à l'adolescence et à l'âge adulte, qui ont retrouvé très peu de modifications entre groupes contrôle et FIV/ICSI (Novakovic *et al.*, 2019; Penova-Veselinovic *et al.*, 2021; Yeung *et al.*, 2021). L'étude de Novakovic *et al.* est davantage rassurante au sens où les auteurs ont évalué le profil de méthylation dans le sang périphérique chez le nouveau-né puis à l'âge adulte car alors qu'ils avaient retrouvé 18 DMRs chez le nouveau-né, seulement 4 DMRs étaient présentes à l'âge adulte. Parmi elles, 3 étaient communes et avec des différences de méthylation assez similaires, localisées dans les gènes *CHRNE*, *PRSS16* et *TMEM18*. Il est donc possible que l'AMP induise des modifications de méthylation persistantes, d'où une nécessité de davantage d'études longitudinales. Toutefois en majorité, les modifications souvent observées à la naissance semblent se résorber avec le temps, ce qui est rassurant et va de pair avec l'observation que la santé à long terme chez les individus issus de FIV/ICSI est bonne, malgré quelques incertitudes résiduelles (Hart & Wijs, 2022). Il faut notamment rester prudent quant à ces conclusions pour les régions soumises à empreinte, qui sont très mal couvertes par les technologies actuelles de puces à méthylation. Au sein de notre cohorte d'enfants âgés de 7 ans, une étude menée par Julie Barberet ciblant uniquement les CpGs localisés dans ces gènes a identifié des altérations de la méthylation en lien avec l'AMP dans les régions *H19*/*IGF2* et *PEG3* à l'aide du pyroséquençage et plus

globalement dans de nombreux autres gènes d'après les données de puces, dont certains particulièrement impliqués dans le développement (*MEG3*, *BLCAP*, *DLX5*) (Barberet *et al.*, 2021a). Parallèlement, nos deux études montrent conjointement l'absence d'effet du milieu de culture (SSM ou Global) sur le profil de méthylation alors même que des différences significatives de développement pré-implantatoire et de taux de grossesse existent entre les deux.

Une inconnue qui demeure dans les études sur la méthylation et l'effet de l'environnement est dans quelle mesure des petites variations de méthylation peuvent affecter l'expression des gènes. Comme nous l'avons évoqué en AMP, >90% des études réalisées à ce jour n'ont pas une puissance statistique permettant d'affirmer que des faibles variations observées ne sont pas dues au hasard (par exemple pour détecter une différence <2% sur la puce EPIC, il faudrait plus de 500 échantillons par groupe comparé (Mansell *et al.*, 2019)). Pour celles avec un design remplissant ces conditions, ces petites différences suggèrent qu'il y a peu de variabilité dans les valeurs mesurées dans chaque groupe réfléchissant une vraie disparité entre les groupes, qu'il est nécessaire d'investiguer davantage. Il est donc crucial de s'interroger sur les conséquences fonctionnelles de ces faibles variations qui sont très souvent retrouvées dans les études liant l'épigénétique et l'environnement (Breton *et al.*, 2017). Dans l'idéal, les études sur la méthylation devraient être associées à des données d'expression, afin de déterminer la corrélation entre ces deux mesures, même si cela ne garantit pas les liens de cause à effet.

Enfin, il est également important de passer en revue de façon critique l'ensemble des méthodologies appliquées pour obtenir les résultats issus de cette thèse. Dans l'article 1, nous utilisons une méta-analyse pour synthétiser quantitativement les résultats d'études indépendantes, ce qui permet de mettre en évidence les différences d'expression entre les stades GV et MII qui sont concordantes entre les 6 jeux de données réanalysés, tout en éliminant les potentiels faux positifs inhérents à chacun d'entre eux. Cette approche permet d'augmenter la taille d'échantillon et par conséquent de maximiser la puissance statistique

permettant de détecter des différences d'expression subtiles, et d'identifier de nouvelles voies biologiques impliquées dans la transition entre ces deux stades de maturation ovocytaire. Toutefois nous ne pouvons pas exclure certains biais résiduels apportés par cette méthode puisque le kit d'extraction propre à chaque étude, et notamment l'utilisation d'oligo(dT), exerce une influence directe sur les caractéristiques des ARNm capturés, à savoir la longueur de leur queue poly(A).

Dans l'article 2, nous utilisons également les principes de la méta-analyse pour regrouper les preuves issues d'études en lien avec l'AMP et la méthylation de l'ADN, exclusivement pour les études dites « ciblées » dont les données quantitatives étaient accessibles. Cette méthode, si elle permet une synthèse robuste de l'évidence d'absence ou de présence de différences de méthylation entre les groupes AMP et contrôle, reste biaisée du fait qu'elle ne s'intéresse qu'aux régions couvertes dans de nombreuses études souvent parce que la littérature scientifique s'intéresse davantage aux régions ayant montré des différences significatives par le passé (biais de publication). C'est en ce sens que notre application d'un recoupement qualitatif des gènes contenant des DMPs/DMRs dans chaque étude globale individuelle apporte des résultats disruptifs. En effet, cette approche permet de considérer de façon uniforme l'ensemble des gènes chez l'Homme, sans biais dans le choix des régions analysées. Ainsi, retrouver une proportion élevée de GSE dans cette analyse témoigne de leur forte exposition aux techniques d'AMP. Dans l'idéal, nous aurions aimé réaliser une méta-analyse quantitative permettant par exemple d'évaluer la présence de différence de méthylation à chaque CpG couvert par les études. Cela n'a pas pu être réalisé en raison de l'absence d'accès aux données brutes ou de résultats d'analyse différentielle pour chaque publication, mais cette approche pourrait apporter davantage de précision quant aux régions génomiques vulnérables aux techniques d'AMP, au CpG près. Le même principe a été appliqué dans l'article 3 pour des données d'expression en raison de restrictions d'accès.

Les articles 4 et 5 appliquent une méthode de séquençage RNA-seq adaptée à l'étude d'échantillons obtenus lors du développement précoce, ici l'ovocyte unique ou l'embryon

unique. Dans l'étude 5, le choix a été fait de séquencer l'embryon dans son ensemble en raison de la préciosité des échantillons et d'avoir accès à l'information transcriptionnelle globale de chaque embryon. Toutefois, avoir accès à une information de l'architecture transcriptomique de chaque blastomère aurait potentiellement pu permettre de distinguer des différences d'expression inter-cellules, notamment au stade blastocyste où le trophectoderme et la MCI commencent à se différencier. La méthode détaillée ici utilise des primers oligo(dT) pour rétro-transcrire les ARN en ADNc, capturant essentiellement les ARN polyadénylés, c'est-à-dire les ARNm stables, non ciblés par la dégradation et qui sont ceux destinés à être traduits en protéine. Les ARNm avec une queue polyA courte sont susceptibles d'être perdus durant cette sélection, ce qui peut conduire à une inflation biaisée de l'expression de certains gènes. Cette approche rend également l'amplification biaisée en 3' (biais de position), ce qui limite la couverture des sites d'initiation de la transcription (TSS). Toutefois, c'est une méthode robuste et qui s'applique à toutes les cellules du développement embryonnaire précoce avec une couverture satisfaisante des gènes moyennement à fortement exprimés (Pérez-Palacios *et al.*, 2021). Dans l'article 5 nous observons notamment que les valeurs d'expression des échantillons d'embryons humains affichent des valeurs d'expression similaires à celles obtenues par l'équipe à l'origine du développement de la technique de scRNA-seq (Yan *et al.*, 2013). De plus, le traitement bioinformatique de ces données de séquençage a été réalisé en appliquant les méthodes parmi les plus reconnues pour l'analyse de données RNA-seq (Soneson & Robinson, 2018), ce qui combiné au design robuste des expériences menées dans les articles 4 et 5 apporte une réelle confiance dans les résultats obtenus.

Pour l'article 6, nous avons utilisé la technologie EPIC de chez Illumina pour mesurer la méthylation de plus de 740,000 CpGs (après contrôle qualité et exclusion des sondes dans les GSE). Même si cette puce couvre presque l'ensemble des gènes chez l'Humain, cette couverture est non uniforme puisque certains gènes sont plus représentés en CpGs couverts ce qui pourrait favoriser l'apparition de certains gènes plus que d'autres lors d'une analyse différentielle. Nous avons également choisi d'être permissif sur le seuil de différence de

méthylation considéré significatif en n'appliquant pas de règles d'exclusion. D'après les calculs de puissance de Mansell *et al.* pour les puces EPIC, nous ne détecterions que 50% de tous les CpGs avec une différence moyenne de 5% avec une puissance statistique supérieure à 50% pour les 36 échantillons AMP inclus (Mansell *et al.*, 2019). Comme l'AMP pourrait induire de faibles différences de méthylation, l'inclusion de grandes tailles d'échantillons apparaît donc plus que nécessaire pour identifier de potentielles modifications à l'échelle d'un grand nombre de CpGs.

Conclusion

En conclusion, de façon générale, la majorité des interventions en AMP sont susceptibles de modifier la reprogrammation épigénétique des gamètes et embryons. Des perturbations du cycle des folates et de la méthionine et du stress oxydant induits par différentes techniques seraient à l'origine de modifications de méthylation observées chez le fœtus, le nouveau-né, l'enfant et à plus long terme. Il semble improbable qu'une seule technique en elle-même soit responsable des anomalies de méthylation de l'ADN, mais plutôt une accumulation de petites perturbations à chaque étape qui déstabiliserait les profils globaux, via des modifications ponctuelles stochastiques de CpGs. Le surrisque de pathologies liées à l'empreinte parentale en conception par AMP ne semble toutefois pas dû au hasard, étant donné que les régions soumises à empreinte sont en première ligne de susceptibilité aux interventions artificielles lors de la reprogrammation épigénétique. Notre synthèse est toutefois rassurante sur la magnitude de ces modifications et leur implication fonctionnelle sur la santé.

Les faibles taux de réussite en AMP et surtout la variabilité inter-clinique des techniques utilisées pourraient être un témoin qu'aujourd'hui, les modifications épigénétiques (dans les lignées germinales ou chez l'embryon) et leurs conséquences sur l'échec d'une tentative d'AMP ne sont pas assez prises en compte dans les pratiques actuelles. La manipulation des gamètes et embryons devrait être minimisée davantage, mais ce sujet souffre d'un manque cruel de recherche scientifique permettant de conclure statistiquement à l'amélioration de la sécurité de certaines techniques d'AMP, qui sont suboptimales à ce jour. L'analyse du transcriptome ovocytaire peut en ce sens nous aider à comprendre les interventions qui pourraient diminuer la compétence développementale des ovocytes et des embryons pré-implantatoires. Cette thèse montre le faible impact de différents modes de vitrification pour le contenu transcriptomique ovocytaire. Elle suggère aussi que la présence d'acides aminés dans le milieu de culture constitue un environnement plus optimal pour l'embryon précoce.

Les techniques d'AMP ne doivent pas forcer l'ovocyte et l'embryon à s'adapter à un environnement modifié mais doivent les placer dans les meilleures conditions possibles pour ne pas avoir d'impact sur le développement embryonnaire et la santé à long terme. Face à une infertilité croissante pour diverses raisons à travers le monde, le recours à l'AMP est grandissant. En revanche, il est difficilement possible d'agir sur certains paramètres tels que l'âge maternel et il est nécessaire d'éviter tout stress cumulatif lors de la manipulation des gamètes et des embryons. Dans le prolongement de cette thèse, des protocoles d'AMP plus sûrs sont nécessaires et la recherche doit aller en ce sens.

Bibliographie

Adalsteinsson BT, Ferguson-Smith AC. Epigenetic control of the genome — Lessons from genomic imprinting. *Genes (Basel)* 2014;**5**:635–655. MDPI AG.

Adriaenssens T, Wathlet S, Segers I, Verheyen G, Vos A De, Elst J Van Der, Coucke W, Devroey P, Smitz J. Cumulus cell gene expression is associated with oocyte developmental quality and influenced by patient and treatment characteristics. *Human Reproduction* 2010;**25**:1259–1270. Oxford University Press.

Affinito O, Palumbo D, Fierro A, Cuomo M, Riso G De, Monticelli A, Miele G, Chiariotti L, Cocozza S. Nucleotide distance influences co-methylation between nearby CpG sites. *Genomics* 2020;**112**:144–150. Academic Press Inc.

Agarwal A, Rosas IM, Anagnostopoulou C, Cannarella R, Boitrelle F, Munoz LV, Finelli R, Durairajanayagam D, Henkel R, Saleh R. Oxidative Stress and Assisted Reproduction: A Comprehensive Review of Its Pathophysiological Role and Strategies for Optimizing Embryo Culture Environment. *Antioxidants* 2022;**11**:. MDPI.

Agence de la biomédecine. Rapport médical et scientifique 2022. 2023;

Alles J, Fehlmann T, Fischer U, Backes C, Galata V, Minet M, Hart M, Abu-Halima M, Grässer FA, Lenhof HP, *et al.* An estimate of the total number of true human miRNAs. *Nucleic Acids Res* 2019;**47**:3353–3364. Oxford University Press.

Amor DJ, Halliday J. A review of known imprinting syndromes and their association with assisted reproduction technologies. *Human Reproduction* 2008;**23**:2826–2834. Oxford University Press.

Anckaert E, Romero S, Adriaenssens T, Smitz J. Effects of low methyl donor levels in culture medium during mouse follicle culture on oocyte imprinting establishment. *Biol Reprod* 2010;**83**:377–386.

Argyle CE, Harper JC, Davies MC. Oocyte cryopreservation: Where are we now? *Hum Reprod Update* 2016;**22**:440–449. Oxford University Press.

Argyraki M, Damdimopoulou P, Chatzimeletiou K, Grimbizis GF, Tarlatzis BC, Syrrou M, Lambropoulos A. In-utero stress and mode of conception: impact on regulation of imprinted genes, fetal development and future health. *Hum Reprod Update* 2019;**25**:777–801. England.

Aryee MJ, Jaffe AE, Corrada-Bravo H, Ladd-Acosta C, Feinberg AP, Hansen KD, Irizarry RA. Minfi: A flexible and comprehensive Bioconductor package for the analysis of Infinium DNA methylation microarrays. *Bioinformatics* 2014;**30**:1363–1369.

Asami M, Lam BYH, Ma MK, Rainbow K, Braun S, VerMilyea MD, Yeo GSH, Perry ACF. Human embryonic genome activation initiates at the one-cell stage. *Cell Stem Cell* 2022;**29**:209-216.e4. Cell Press.

Assou S, Haouzi D, Dechaud H, Gala A, Ferrières A, Hamamah S. Comparative gene expression profiling in human cumulus cells according to ovarian gonadotropin treatments. *Biomed Res Int* 2013;**2013**:.

Baak NA, Cantineau AE, Farquhar C, Brison DR. Temperature of embryo culture for assisted reproduction. *Cochrane Database of Systematic Reviews* 2019; Wiley.

Baker TG. A quantitative and cytological study of germ cells in human ovaries. *Proc R Soc Lond* [Internet] 1963;**158**:417–433.

Barberet J, Barry F, Choux C, Guilleman M, Karoui S, Simonot R, Bruno C, Fauque P. What impact does oocyte vitrification have on epigenetics and gene expression? *Clin Epigenetics* 2020;**12**:. BioMed Central Ltd.

Barberet J, Binquet C, Guilleman M, Doukani A, Choux C, Bruno C, Bourredjem A, Chapusot C, Bourc'his D, Duffourd Y, *et al.* Do assisted reproductive technologies and in vitro embryo culture influence the epigenetic control of imprinted genes and transposable elements in children? *Hum Reprod* 2021a;**36**:479–492. England.

Barberet J, Boucret L, Fauque P, May-Panloup P. Assistance médicale à la procréation : techniques actuelles et nouveaux horizons. *Revue Francophone des Laboratoires* 2018;**2018**:43–51. Elsevier BV.
Barberet J, Ducreux B, Bruno C, Guilleman M, Simonot R, Lieury N, Guilloteau A, Bourc'his D, Fauque P. Comparison of oocyte vitrification using a semi-automated or a manual closed system in human siblings: survival and transcriptomic analyses. *ResearchSquare* 2022a;.
Barberet J, Ducreux B, Guilleman M, Simon E, Bruno C, Fauque P. DNA methylation profiles after ART during human lifespan: a systematic review and meta-analysis. *Hum Reprod Update* 2022b;**28**:.
Barberet J, Romain G, Binquet C, Guilleman M, Bruno C, Ginod P, Chapusot C, Choux C, Fauque P. Do frozen embryo transfers modify the epigenetic control of imprinted genes and transposable elements in newborns compared with fresh embryo transfers and natural conceptions? *Fertil Steril* 2021b;**116**:1468–1480. Elsevier Inc.
Barberi M, Ermini B, Morelli MB, Ermini M, Cecconi S, Canipari R. Follicular fluid hormonal profile and cumulus cell gene expression in controlled ovarian hyperstimulation with recombinant FSH: Effects of recombinant LH administration. *J Assist Reprod Genet* 2012;**29**:1381–1391.
Barrero MJ, Boué S, Izpisúa Belmonte JC. Epigenetic Mechanisms that Regulate Cell Identity. *Cell Stem Cell* 2010;**7**:565–570.
Barrès R, Zierath JR. The role of diet and exercise in the transgenerational epigenetic landscape of T2DM. *Nat Rev Endocrinol* 2016;**12**:441–451. Nature Publishing Group.
Barroso M, Handy DE, Castro R. The link between hyperhomocysteinemia and hypomethylation: Implications for cardiovascular disease. *J Inborn Errors Metab Screen* 2017;**5**:. SAGE Publications Inc.
Beck D, Maamar M Ben, Skinner MK. Genome-wide CpG density and DNA methylation analysis method (MeDIP, RRBS, and WGBS) comparisons. *Epigenetics* 2022;**17**:518–530. Taylor and Francis Ltd.
Berntsen S, Söderström-Anttila V, Wennerholm UB, Laivuori H, Loft A, Oldereid NB, Romundstad LB, Bergh C, Pinborg A. The health of children conceived by ART: "The chicken or the egg?" *Hum Reprod Update* 2019;**25**:137–158.
Bertoldo MJ, Locatelli Y, O'Neill C, Mermillod P. Impacts of and interactions between environmental stress and epigenetic programming during early embryo development. *Reprod Fertil Dev* 2015;**27**:1125–1136.
Biggers JD, Summers MC. Choosing a culture medium: making informed choices. *Fertil Steril* 2008;**90**:473–483.
Bird AP. CpG-rich islands and the function of DNA methylation. *Nature* 1986;**325**:209–213.
Boks MP, Derks EM, Weisenberger DJ, Strengman E, Janson E, Sommer IE, Kahn RS, Ophoff RA. The relationship of DNA methylation with age, gender and genotype in twins and healthy controls. *PLoS One* 2009;**4**:.
Borgbo T, Povlsen BB, Andersen CY, Borup R, Humaidan P, Grøndahl ML. Comparison of gene expression profiles in granulosa and cumulus cells after ovulation induction with either human chorionic gonadotropin or a gonadotropin-releasing hormone agonist trigger. *Fertil Steril* 2013;**100**:. Elsevier Inc.
Borghol N, Lornage J, Blachère T, Sophie Garret A, Lefèvre A. Epigenetic status of the H19 locus in human oocytes following in vitro maturation. *Genomics* 2006;**87**:417–426.
Bourc'his D, Xu G-L, Lin C-S, Bollman B, Bestor TH. Dnmt3L and the Establishment of Maternal Genomic Imprints. *Science (1979)* [Internet] 2001;**294**:2536–2539.
Boxmeer JC, Steegers-Theunissen RPM, Lindemans J, Wildhagen MF, Martini E, Steegers EAP, Macklon NS. Homocysteine metabolism in the pre-ovulatory follicle during ovarian stimulation. *Human Reproduction* 2008;**23**:2570–2576. Oxford University Press.
Brannian J, Eyster K, Mueller BA, Bietz MG, Hansen K. Differential gene expression in human granulosacells from recombinant FSH versus humanmenopausal gonadotropin ovarian stimulationprotocols. *Reproductive Biology and Endocrinology* 2010;**8**:.

Braude P, Bolton V, Moore S. Human gene expression first occurs between the four-and eight-cell stages of preimplantation development. *Nature* 1988;**332**:459–461.
Breton C V., Marsit CJ, Faustman E, Nadeau K, Goodrich JM, Dolinoy DC, Herbstman J, Holland N, LaSalle JM, Schmidt R, *et al.* Small-magnitude effect sizes in epigenetic end points are important in children's environmental health studies: The children's environmental health and disease prevention research center's epigenetics working group. *Environ Health Perspect* 2017;**125**:511–526.
Camprubí C, Iglesias-Platas I, Martin-Trujillo A, Salvador-Alarcon C, MA R, DR B, Court F, Monk D. Stability of genomic imprinting and gestational-age dynamic methylation in complicated pregnancies conceived following assisted reproductive technologies. *Biol Reprod* [Internet] 2013;**89**:50. United States.
Caramaschi D, Jungius J, Page CM, Novakovic B, Saffery R, Halliday J, Lewis S, Magnus MC, London SJ, Håberg SE, *et al.* Association of medically assisted reproduction with offspring cord blood DNA methylation across cohorts. *Hum Reprod* 2021; England.
Castillo-Fernandez JE, Loke YJ, Bass-Stringer S, Gao F, Xia Y, Wu H, Lu H, Liu Y, Wang J, Spector TD, *et al.* DNA methylation changes at infertility genes in newborn twins conceived by in vitro fertilisation. *Genome Med* 2017;**9**:28.
Chambers GM, Dyer S, Zegers-Hochschild F, Mouzon J de, Ishihara O, Banker M, Mansour R, Kupka MS, Adamson GD. International Committee for Monitoring Assisted Reproductive Technologies world report: assisted reproductive technology, 2014†. *Human Reproduction* 2021;**36**:2921–2934. Oxford University Press.
Chan Wong E, Hatakeyama C, Robinson WP, Ma S, Wong EC, Hatakeyama C, Robinson WP, Ma S. DNA methylation at H19/IGF2 ICR1 in the placenta of pregnancies conceived by in vitro fertilization and intracytoplasmic sperm injection. *Fertil Steril* [Internet] 2011;**95**:2524-2526.e3. S. Ma, D6-4500 Oak Street, Vancouver, BC, V6H-3N1, Canada, United States.
Chen M, Heilbronn LK. The health outcomes of human offspring conceived by assisted reproductive technologies (ART). *J Dev Orig Health Dis* 2017;**8**:388–402.
Chen SL, Shi XY, Zheng HY, Wu FR, Luo C. Aberrant DNA methylation of imprinted H19 gene in human preimplantation embryos. *Fertil Steril* 2010;**94**:. Elsevier Inc.
Chen T, Ueda Y, Dodge JE, Wang Z, Li E. Establishment and Maintenance of Genomic Methylation Patterns in Mouse Embryonic Stem Cells by Dnmt3a and Dnmt3b. *Mol Cell Biol* 2003;**23**:5594–5605. Informa UK Limited.
Chen W, Peng Y, Ma X, Kong S, Tan S, Wei Y, Zhao Y, Zhang W, Wang Y, Yan L, *et al.* Integrated multi-omics reveal epigenomic disturbance of assisted reproductive technologies in human offspring. *EBioMedicine* [Internet] 2020;**61**:. Elsevier B.V.: Y. Wang, Center for Reproductive Medicine of Peking University Third Hospital, NO 49 North Garden Rd., Haidian District, Beijing, China.
Chen X-J, Chen F, Lv P-P, Zhang D, Ding G-L, Hu X-L, Feng C, Sheng J-Z, Huang H-F. Maternal high estradiol exposure alters CDKN1C and IGF2 expression in human placenta. *Placenta* 2018;**61**:72–79. Netherlands.
Chen YA, Lemire M, Choufani S, Butcher DT, Grafodatskaya D, Zanke BW, Gallinger S, Hudson TJ, Weksberg R. Discovery of cross-reactive probes and polymorphic CpGs in the Illumina Infinium HumanMethylation450 microarray. *Epigenetics* 2013;**8**:203–209. Taylor and Francis Inc.
Chen ZX, Riggs AD. DNA methylation and demethylation in mammal. *Journal of Biological Chemistry* 2011;**286**:18347–18353.
Choufani S, Turinsky AL, Melamed N, Greenblatt E, Brudno M, Bérard A, Fraser WD, Weksberg R, Trasler J, Monnier P. Impact of assisted reproduction, infertility, sex and paternal factors on the placental DNA methylome. *Hum Mol Genet* 2019;**28**:372–385.
Choux C, Binquet C, Carmignac V, Bruno C, Chapusot C, Barberet J, Lamotte M, Sagot P, Bourc'his D, Fauque P. The epigenetic control of transposable elements and imprinted genes in newborns is affected by the mode of conception: ART versus spontaneous conception without underlying infertility. *Human Reproduction* [Internet] 2018;**33**:331–

340. P. Fauque, Laboratoire de Biologie de la Reproduction, CHU Dijon, BP 77908, 14, rue Gaffarel, Dijon, Cedex, France.
Choux C, Petazzi P, Sanchez-Delgado M, Hernandez Mora JR, Monteagudo A, Sagot P, Monk D, Fauque P. The hypomethylation of imprinted genes in IVF/ICSI placenta samples is associated with concomitant changes in histone modifications. *Epigenetics* [Internet] 2020;**15**:1386–1395. C. Choux, Service de Gynécologie Et Biologie de la Reproduction, Dijon Cedex, France.
Christensen BC, Houseman EA, Marsit CJ, Zheng S, Wrensch MR, Wiemels JL, Nelson HH, Karagas MR, Padbury JF, Bueno R, *et al.* Aging and environmental exposures alter tissue-specific DNA methylation dependent upon CPG island context. *PLoS Genet* 2009;**5**:.
Chronopoulou E, Harper JC. IVF culture media: Past, present and future. *Hum Reprod Update* 2015;**21**:39–55. Oxford University Press.
Cimadomo D, Fabozzi G, Vaiarelli A, Ubaldi N, Ubaldi FM, Rienzi L. Impact of maternal age on oocyte and embryo competence. *Front Endocrinol (Lausanne)* 2018;**9**:. Frontiers Media S.A.
Cobo A, Diaz C. Clinical application of oocyte vitrification: A systematic review and meta-analysis of randomized controlled trials. *Fertil Steril* 2011;**96**:277–285.
Cobo A, Remohí J, Chang CC, Nagy ZP. Oocyte cryopreservation for donor egg banking. *Reprod Biomed Online* 2011;**23**:, p. 341–346.
Cochran WG. The Combination of Estimates from Different Experiments. *Biometrics* 1954;**10**:101–129.
Combelles CMH, Gupta S, Agarwal A. Could oxidative stress influence the in-vitro maturation of oocytes? *Reprod Biomed Online* 2009;**18**:864–880. Reproductive Healthcare Ltd.
Consensus Group C. 'There is only one thing that is truly important in an IVF laboratory: everything' Cairo Consensus Guidelines on IVF Culture Conditions. *Reprod Biomed Online* [Internet] 2020;**40**:33–60.
Conti M, Franciosi F. Acquisition of oocyte competence to develop as an embryo: Integrated nuclear and cytoplasmic events. *Hum Reprod Update* 2018;**24**:245–266. Oxford University Press.
Cordaux R, Batzer MA. The impact of retrotransposons on human genome evolution. *Nat Rev Genet* 2009;**10**:691–703.
Cornet-Bartolomé D, Barragán M, Zambelli F, Ferrer-Vaquer A, Tiscornia G, Balcells S, Rodriguez A, Grinberg D, Vassena R. Human oocyte meiotic maturation is associated with a specific profile of alternatively spliced transcript isoforms. *Mol Reprod Dev* 2021;**88**:605–617. John Wiley and Sons Inc.
Crawford NM, Steiner AZ. Age-related infertility. *Obstet Gynecol Clin North Am* 2015;**42**:15–25. W.B. Saunders.
Cruz M, Requena A, Agudo D, García-Velasco JA. Type of gonadotropin used during controlled ovarian stimulation induces differential gene expression in human cumulus cells: A randomized study. *European Journal of Obstetrics and Gynecology and Reproductive Biology* 2017;**215**:124–133. Elsevier Ireland Ltd.
Daca-Roszak P, Pfeifer A, Zebracka-Gala J, Rusinek D, Szybińska A, Jarzab B, Witt M, Zietkiewicz E. Impact of SNPs on methylation readouts by Illumina Infinium HumanMethylation450 BeadChip Array: Implications for comparative population studies. *BMC Genomics* 2015;**16**:. BioMed Central Ltd.
Dedeurwaerder S, Defrance M, Calonne E, Denis H, Sotiriou C, Fuks F. Evaluation of the Infinium Methylation 450K technology. *Epigenomics* 2011;**3**:771–784.
Delaval K, Feil R. Epigenetic regulation of mammalian genomic imprinting. *Curr Opin Genet Dev* 2004;**14**:188–195.
Delcuve GP, Rastegar M, Davie JR. Epigenetic control. *J Cell Physiol* 2009;**219**:243–250.
Denomme MM, Zhang L, Mann MRW. Embryonic imprinting perturbations do not originate from superovulation-induced defects in DNA methylation acquisition. *Fertil Steril* 2011;**96**:. Elsevier Inc.

Derakhshan-Horeh M, Abolhassani F, Jafarpour F, Moini A, Karbalaie K, Hosseini SM, Nasr-Esfahani MH. Vitrification at Day3 stage appears not to affect the methylation status of H19/IGF2 differentially methylated region of in vitro produced human blastocysts. *Cryobiology* 2016;**73**:168–174. Academic Press Inc.

Devjak R, Fon Tacer K, Juvan P, Virant Klun I, Rozman D, Vrtačnik Bokal E. Cumulus Cells Gene Expression Profiling in Terms of Oocyte Maturity in Controlled Ovarian Hyperstimulation Using GnRH Agonist or GnRH Antagonist. *PLoS One* 2012;**7**:1–9.

Dieamant F, Petersen CG, Mauri AL, Comar V, Mattila M, Vagnini LD, Renzi A, Petersen B, Ricci J, Oliveira JBA, *et al.* Single versus sequential culture medium: Which is better at improving ongoing pregnancy rates? a systematic review and meta-analysis. *J Bras Reprod Assist* 2017;**21**:240–246. SBRA - Associação Brasileira de Reprodução Assistida (Brazilian Society of Assisted Reproduction).

Dillies MA, Rau A, Aubert J, Hennequet-Antier C, Jeanmougin M, Servant N, Keime C, Marot NS, Castel D, Estelle J, *et al.* A comprehensive evaluation of normalization methods for Illumina high-throughput RNA sequencing data analysis. *Brief Bioinform* 2013;**14**:671–683.

Doherty AS, Mann MRW, Tremblay KD, Bartolomei MS, Schultz RM. *Differential Effects of Culture on Imprinted H19 Expression in the Preimplantation Mouse Embryo 1* [Internet]. *Biol Reprod* [Internet] 2000;**62**:.

Dong J, Wen L, Guo X, Xiao X, Jiang F, Li B, Jin N, Wang J, Wang X, Chen S, *et al.* The increased expression of glucose transporters in human full-term placentas from assisted reproductive technology without changes of mTOR signaling. *Placenta* 2019;**86**:4–10. Netherlands.

Du P, Zhang X, Huang CC, Jafari N, Kibbe WA, Hou L, Lin SM. Comparison of Beta-value and M-value methods for quantifying methylation levels by microarray analysis. *BMC Bioinformatics* 2010;**11**:.

Ducreux B, Barberet J, Guilleman M, Pérez-Palacios R, Teissandier A, Bourc'his D, Fauque P. Assessing the influence of distinct culture media on human pre-implantation development using single-embryo transcriptomics. *Front Cell Dev Biol* 2023;**11**:. Frontiers Media SA.

Ducreux B, Frappier J, Bruno C, Doukani A, Guilleman M, Simon E, Barberet J, Fauque P. Genome-Wide Analysis of DNA Methylation in Buccal Cells ofChildren Conceived through IVF and ICSI. *Genes (Basel)* 2021;**12**:.

Duranthon V, Chavatte-Palmer P. Long term effects of ART: What do animals tell us? *Mol Reprod Dev* 2018;**85**:348–368.

Edgar DH, Gook DA. A critical appraisal of cryopreservation (slow cooling versus vitrification) of human oocytes and embryos. *Hum Reprod Update* 2012;**18**:536–554.

Edwards LJ, Williams DA, Gardner DK. Intracellular pH of the preimplantation mouse embryo: Effects of extracellular pH and weak acids. *Mol Reprod Dev* 1998;**50**:434–442.

Eppig JJ. *Coordination of Nuclear and Cytoplasmic Oocyte Maturation in Eutherian Mammals*. *Reprod Fertil Dev* 1996;**8**:.

Estill MS, Bolnick JM, Waterland RA, Bolnick AD, Diamond MP, Krawetz SA. Assisted reproductive technology alters deoxyribonucleic acid methylation profiles in bloodspots of newborn infants. *Fertil Steril* [Internet] 2016;**106**:629-639.e10. S.A. Krawetz, Wayne State University School of Medicine, 253 C. S. Mott Center, 275 E. Hancock Ave., Detroit, Michigan, United States.

Falkenberg KJ, Johnstone RW. Histone deacetylases and their inhibitors in cancer, neurological diseases and immune disorders. *Nat Rev Drug Discov* 2014;**13**:673–691.

Fauque P. Ovulation induction and epigenetic anomalies. *Fertil Steril* 2013;**99**:616–623.

Fauque P, Jouannet P, Lesaffre C, Ripoche MA, Dandolo L, Vaiman D, Jammes H. Assisted reproductive technology affects developmental kinetics, H19 imprinting control region methylation and H19 gene expression in individual mouse embryos. *BMC Dev Biol* 2007a;**7**:1–19.

Fauque P, Léandri R, Merlet F, Juillard JC, Epelboin S, Guibert J, Jouannet P, Patrat C. Pregnancy outcome and live birth after IVF and ICSI according to embryo quality. *J Assist Reprod Genet* 2007b;**24**:159–165.
Fauque P, Mouzon J De, Devaux A, Epelboin S, Gervoise-Boyer MJ, Levy R, Valentin M, Viot G, Bergère A, Vienne C De, *et al.* Reproductive technologies, female infertility, and the risk of imprinting-related disorders. *Clin Epigenetics* [Internet] 2020;**12**:1–9. BioMed Central.
Fauque P, Ripoche M-A, Tost J, Journot L, Gabory A, Busato F, Digarcher A Le, Mondon F, Gut I, Jouannet P, *et al.* Modulation of imprinted gene network in placenta results in normal development of in vitro manipulated mouse embryos. *Hum Mol Genet* 2010;**19**:1779–1790. England.
Fernández-Gonzalez R, Moreira P, Bilbao A, Jiménez A, Pérez-Crespo M, Angel Ramírez M, Rodríguez De Fonseca F, Pintado B, Gutiérrez-Adá A. *Long-term effect of in vitro culture of mouse embryos with serum on mRNA expression of imprinting genes, development, and behavior* [Internet]. 2004;Available from: www.pnas.orgcgidoi10.1073pnas.0308560101.
Ferrero H, Corachan A, Aguilar A, Quiñonero A, Carbajo-Garcia MC, Alama P, Tejera A, Taboas E, Munoz E, Pellicer A, *et al.* Single-cell RNA sequencing of oocytes from ovarian endometriosis patients reveals a differential transcriptomic profile associated with lower quality. *Human Reproduction* 2019;**34**:1302–1312. Oxford University Press.
Ferrick L, Lee YSL, Gardner DK, Sakkas D. Reducing time to pregnancy and facilitating the birth of healthy children through functional analysis of embryo physiology. *Biol Reprod* 2019;**101**:1124–1139. Oxford University Press.
Ferris J, Mahboubi K, MacLusky N, King WA, Favetta LA. BPA exposure during in vitro oocyte maturation results in dose-dependent alterations to embryo development rates, apoptosis rate, sex ratio and gene expression. *Reproductive Toxicology* 2016;**59**:128–138. Elsevier Inc.
Fiedler K, Ezcurra D. Predicting and preventing ovarian hyperstimulation syndrome (OHSS): The need for individualized not standardized treatment. *Reproductive Biology and Endocrinology* 2012;**10**:.
Frommer M, Mcdonald LE, Millar DS, Collist CM, Wattt F, Griggt GW, Molloyt PL, Paul CL. *A genomic sequencing protocol that yields a positive display of 5-methylcytosine residues in individual DNA strands (genomic sequencing/DNA methylation/bisulfite modiflication/PCR/kininogen gene)* [Internet]. 1992;**89**:.
Fuchs Weizman N, Wyse BA, Gat I, Balakier H, Sangaralingam M, Caballero J, Kenigsberg S, Librach CL. Triggering method in assisted reproduction alters the cumulus cell transcriptome. *Reprod Biomed Online* 2019;**39**:211–224. Elsevier Ltd.
Fujimoto T, Miyayama Y, Fuyuta M. The origin, migration and fine morphology of human primordial germ cells. *Anat Rec* 1977;**188**:315–329.
Fulka H, Mrazek M, Tepla O, Fulka J. DNA methylation pattern in human zygotes and developing embryos. *Reproduction* 2004;**128**:703–708.
Gardner DK. Changes in requirements and utilization of nutrients during mammalian preimplantation embryo development and their significance in embryo culture. *Thenogenology* 1998;**49**:83–102.
Gatimel N, Lacroix MZ, Chanthavisouk S, Picard-Hagen N, Gayrard V, Parinaud J, Léandri RD. Bisphenol A in culture media and plastic consumables used for ART. *Human Reproduction* 2016;**31**:1436–1444. Oxford University Press.
Gatta V, Tatone C, Ciriminna R, Vento M, Franchi S, D'Aurora M, Sperduti S, Cela V, Borzì P, Palermo R, *et al.* Gene expression profiles of cumulus cells obtained from women treated with recombinant human luteinizing hormone + recombinant human follicle-stimulating hormone or highly purified human menopausal gonadotropin versus recombinant human follicle-stimulating hormone alone. *Fertil Steril* 2013;**99**:. Elsevier Inc.
Gentilini D, Rabellotti E, Pagliardini L, Somigliana E, Zanirato M, Vanni VS, Papaleo E, Blasio AM Di, Viganò P. Genome-wide epigenetic evaluation of cord blood from in vitro-

conceived babies. *Human Reproduction* [Internet] 2015;**30**:i86–i87. D. Gentilini, Istituto Auxologico Italiano, Molecular Biology Laboratory, Milan, Italy.
Geyter C De, Calhaz-Jorge C, Kupka MS, Wyns C, Mocanu E, Motrenko T, Scaravelli G, Smeenk J, Vidakovic S, Goossens V, *et al.* ART in Europe, 2014: Results generated from European registries by ESHRE. *Human Reproduction* 2018;**33**:1586–1601.
Geyter C de, Wyns C, Calhaz-Jorge C, Mouzon J de, Ferraretti AP, Kupka M, Nyboe Andersen A, Nygren KG, Goossens V. 20 years of the European IVF-monitoring Consortium registry: What have we learned? A comparison with registries from two other regions. *Human Reproduction* 2020;**35**:2832–2849. Oxford University Press.
Ghosh J, Coutifaris C, Sapienza C, Mainigi M. Global DNA methylation levels are altered by modifiable clinical manipulations in assisted reproductive technologies. *Clin Epigenetics* 2017;**9**:14.
Gomes M V, Huber J, Ferriani RA, Amaral Neto AM, Ramos ES. Abnormal methylation at the KvDMR1 imprinting control region in clinically normal children conceived by assisted reproductive technologies. *Mol Hum Reprod* 2009;**15**:471–477. England.
Gonzalez TL, Schaub AM, Lee B, Cui J, Taylor KD, Dorfman AE, Goodarzi MO, Wang ET, Chen YDI, Rotter JI, *et al.* Infertility and treatments used have minimal effects on first-trimester placental DNA methylation and gene expression. *Fertil Steril* 2023;**119**:301–312. Elsevier Inc.
Greenberg MVC, Bourc'his D. The diverse roles of DNA methylation in mammalian development and disease. *Nat Rev Mol Cell Biol* [Internet] 2019;**20**:590–607. Springer US.
Gremeau AS, Andreadis N, Fatum M, Craig J, Turner K, McVeigh E, Child T. In vitro maturation or in vitro fertilization for women with polycystic ovaries? A case-control study of 194 treatment cycles. *Fertil Steril* 2012;**98**:355–360.
Grøndahl ML, Borup R, Lee YB, Myrhøj V, Meinertz H, Sørensen S. Differences in gene expression of granulosa cells from women undergoing controlled ovarian hyperstimulation with either recombinant follicle-stimulating hormone or highly purified human menopausal gonadotropin. *Fertil Steril* 2009;**91**:1820–1830.
Grynberg M, Sermondade N, Sellami I, Benoit A, Mayeur A, Sonigo C. In vitro maturation of oocytes for fertility preservation: a comprehensive review. *F and S Reviews* 2022;**3**:211–226. Elsevier Inc.
Gu C, Liu S, Wu Q, Zhang L, Guo F. Integrative single-cell analysis of transcriptome, DNA methylome and chromatin accessibility in mouse oocytes. *Cell Res* 2019;**29**:110–123. Nature Publishing Group.
Gu TP, Guo F, Yang H, Wu HP, Xu GF, Liu W, Xie ZG, Shi L, He X, Jin SG, *et al.* The role of Tet3 DNA dioxygenase in epigenetic reprogramming by oocytes. *Nature* 2011;**477**:606–612.
Guibert S, Forné T, Weber M. Global profiling of DNA methylation erasure in mouse primordial germ cells. *Genome Res* 2012;**22**:633–641.
Guo F, Yan L, Guo H, Li L, Hu B, Zhao Y, Yong J, Hu Y, Wang X, Wei Y, *et al.* The transcriptome and DNA methylome landscapes of human primordial germ cells. *Cell* 2015;**161**:1437–1452. Cell Press.
Guo H, Zhu P, Yan L, Li R, Hu B, Lian Y, Yan J, Ren X, Lin S, Li J, *et al.* The DNA methylation landscape of human early embryos. *Nature* 2014;**511**:606–610. Nature Publishing Group.
Guo S, Diep D, Plongthongkum N, Fung HL, Zhang K, Zhang K. Identification of methylation haplotype blocks AIDS in deconvolution of heterogeneous tissue samples and tumor tissue-of-origin mapping from plasma DNA. *Nat Genet* 2017a;**49**:635–642. Nature Publishing Group.
Guo X-Y, Liu X-M, Jin L, Wang T-T, Ullah K, Sheng J-Z, Huang H-F. Cardiovascular and metabolic pro fi les of offspring conceived by assisted reproductive technologies : a systematic review and. *Fertil Steril* [Internet] 2017b;**107**:622-631.e5. Elsevier Inc.
Guo Y, Cao Z, Jiao X, Bai D, Zhang Y, Hua J, Liu W, Teng X. Pre-pregnancy exposure to fine particulate matter (PM2.5) increases reactive oxygen species production in oocytes

and decrease litter size and weight in mice. *Environmental Pollution* 2021;**268**:. Elsevier Ltd.
Gurgan T, Montjean D, Demirol A, Menezo YJR. Sequential (hFSH + recFSH) vs homogenous (hFSH or recFSH alone) stimulation: Clinical and biochemical (cumulus cell gene expression) aspects. *J Assist Reprod Genet* 2014;**31**:657–665. Springer New York LLC.
Haas J, Ophir L, Barzilay E, Machtinger R, Yung Y, Orvieto R, Hourvitz A. Standard human chorionic gonadotropin versus double trigger for final oocyte maturation results in different granulosa cells gene expressions: a pilot study. *Fertil Steril* 2016;**106**:653-659.e1. Elsevier Inc.
Haas J, Ophir L, Barzilay E, Yerushalmi GM, Yung Y, Kedem A, Maman E, Hourvitz A. GnRH agonist vs. hCG for triggering of ovulation - Differential effects on gene expression in human granulosa cells. *PLoS One* 2014;**9**:. Public Library of Science.
Håberg SE, Page CM, Lee Y, Nustad HE, Magnus MC, Haftorn KL, Carlsen E, Denault WRP, Bohlin J, Jugessur A, *et al.* DNA methylation in newborns conceived by assisted reproductive technology. *Nat Commun* 2022;**13**:. Nature Research.
Hackett JA, Sengupta R, Zylicz JJ, Murakami K, Lee C, Down TA, Surani MA. Germline DNA demethylation dynamics and imprint erasure through 5-hydroxymethylcytosine. *Science (1979)* 2013;**339**:448–452. American Association for the Advancement of Science.
Haggarty P, Hoad G, Campbell DM, Horgan GW, Piyathilake C, McNeill G. Folate in pregnancy and imprinted gene and repeat element methylation in the offspring. *American Journal of Clinical Nutrition* 2013;**97**:94–99.
Hajj N El, Haaf T. Epigenetic disturbances in in vitro cultured gametes and embryos: Implications for human assisted reproduction. *Fertil Steril* 2013;**99**:632–641.
Hajkova P, Jeffries SJ, Lee C, Miller N, Jackson SP, Surani A. Genome-Wide Reprogramming in the Mouse Germ Line Entails the Base Excision Repair Pathway. *Science (1979)* 2010;**329**:78–82.
Hanna CW, Demond H, Kelsey G. Epigenetic regulation in development: Is the mouse a good model for the human? *Hum Reprod Update* 2018;**24**:556–576. Oxford University Press.
Hansen M, Kurinczuk JJ, Bower C, Webb S. The Risk of Major Birth Defects after Intracytoplasmic Sperm Injection and in Vitro Fertilization. *N Engl J Med* 2002;**346**:725–730.
Hargan-Calvopina J, Taylor S, Cook H, Hu Z, Lee SA, Yen MR, Chiang YS, Chen PY, Clark AT. Stage-Specific Demethylation in Primordial Germ Cells Safeguards against Precocious Differentiation. *Dev Cell* 2016;**39**:75–86. Cell Press.
Hart RJ, Wijs LA. The longer-term effects of IVF on offspring from childhood to adolescence. *Frontiers in Reproductive Health* 2022;**4**:. Frontiers Media SA.
Hatırnaz Ş, Ata B, Hatırnaz ES, Dahan MH, Tannus S, Tan J, Tan SL. Oocyte in vitro maturation: A sytematic review. *Turk J Obstet Gynecol* 2018;**15**:112–125.
Hattori H, Hiura H, Kitamura A, Miyauchi N, Kobayashi N, Takahashi S, Okae H, Kyono K, Kagami M, Ogata T, *et al.* Association of four imprinting disorders and ART. *Clin Epigenetics* 2019;**11**:. BioMed Central Ltd.
Haute Autorité de Santé. *Évaluation des actes de vitrification et réchauffement ovocytaire-vitrification et réchauffement embryonnaire* [Internet]. 2017;Available from: www.has-sante.fr.
Hellman A, Chess A. Gene body-specific methylation on the active X chromosome. *Science (1979)* 2007;**315**:1141–1143.
Herbemont C, Labrosse J, Bennani-Smires B, Cedrin-Durnerin I, Peigne M, Sermondade N, Sarandi S, Vivot A, Vicaut E, Talib Z, *et al.* Impact of oxygen tension according to embryo stage of development: a prospective randomized study. *Sci Rep* 2021;**11**:. Nature Research.
Hicks SC, Irizarry RA. quantro: A data-driven approach to guide the choice of an appropriate normalization method. *Genome Biol* 2015;**16**:. BioMed Central Ltd.

Hirasawa R, Chiba H, Kaneda M, Tajima S, Li E, Jaenisch R, Sasaki H. Maternal and zygotic Dnmt1 are necessary and sufficient for the maintenance of DNA methylation imprints during preimplantation development. *Genes Dev* 2008;**22**:1607–1616.
Hiura H, Hattori H, Kobayashi N, Okae H, Chiba H, Miyauchi N, Kitamura A, Kikuchi H, Yoshida H, Arima T. Genome-wide microRNA expression profiling in placentae from frozen-thawed blastocyst transfer. *Clin Epigenetics* 2017;**9**:79.
Hoeijmakers L, Kempe H, Verschure PJ. Epigenetic imprinting during assisted reproductive technologies: The effect of temporal and cumulative fluctuations in methionine cycling on the DNA methylation state. *Mol Reprod Dev* [Internet] 2016;**83**:94–107. P.J. Verschure, Swammerdam Institute for Life Sciences, University of Amsterdam, Science Park 904, Amsterdam, Netherlands.
Horvath S. DNA methylation age of human tissues and cell types. *Genome Biol* 2013;**14**:.
Horvath S, Raj K. DNA methylation-based biomarkers and the epigenetic clock theory of ageing. *Nat Rev Genet* 2018;**19**:371–384. Nature Publishing Group.
Houseman EA, Accomando WP, Koestler DC, Christensen BC, Marsit CJ, Nelson HH, Wiencke JK, Kelsey KT. *DNA methylation arrays as surrogate measures of cell mixture distribution* [Internet]. 2012;Available from: http://www.biomedcentral.com/1471-2105/13/86.
Houseman EA, Kelsey KT, Wiencke JK, Marsit CJ. Cell-composition effects in the analysis of DNA methylation array data: A mathematical perspective. *BMC Bioinformatics* 2015;**16**:. BioMed Central Ltd.
Howell CY, Bestor TH, Ding F, Latham KE, Mertineit C, Trasler JM, Chaillet JR. Genomic Imprinting Disrupted by a Maternal Effect Mutation in the Dnmt1 Gene. *Cell* 2001;**104**:829–838.
Huo Y, Yuan P, Qin Q, Yan Z, Yan L, Liu P, Li R, Yan J, Qiao J. Effects of vitrification and cryostorage duration on single-cell RNA-Seq profiling of vitrified-thawed human metaphase II oocytes. *Front Med* 2021;**15**:144–154. Higher Education Press Limited Company.
Ibala-Romdhane S, Al-Khtib M, Khoueiry R, Blachère T, Guérin JF, Lefèvre A. Analysis of H19 methylation in control and abnormal human embryos, sperm and oocytes. *European Journal of Human Genetics* 2011;**19**:1138–1143.
Ikeda S, Sugimoto M, Kume S. *Importance of Methionine Metabolism in Morula-to-blastocyst Transition in Bovine Preimplantation Embryos*. *Original Article-Published online in J-STAGE* 2011;**58**:.
Inoue A, Zhang Y. Replication-Dependent Loss of 5-Hydroxymethylcytosine in Mouse Preimplantation Embryos. *Science (1979)* 2011;**334**:194.
Iqbal K, Jin SG, Pfeifer GP, Szabó PE. Reprogramming of the paternal genome upon fertilization involves genome-wide oxidation of 5-methylcytosine. *Proc Natl Acad Sci U S A* 2011;**108**:3642–3647.
Jenuwein T, David Allis C. Translating the Histone Code. *Science (1979)* [Internet] 2001;**293**:1074–1080.
Jiang Y, Adhikari D, Li C, Zhou X. Spatiotemporal regulation of maternal mRNAs during vertebrate oocyte meiotic maturation. *Biological Reviews* 2023;**98**:900–930. John Wiley and Sons Inc.
Jouannet P, Claris O, Bouc Y Le. *Santé à moyen et à long terme des enfants conçus par fécondation in vitro (FIV)*. *Académie Natio* 2023;
Kalo D, Roth Z. Low level of mono(2-ethylhexyl) phthalate reduces oocyte developmental competence in association with impaired gene expression. *Toxicology* 2017;**377**:38–48. Elsevier Ireland Ltd.
Kanber D, Buiting K, Zeschnigk M, Ludwig M, Horsthemke B. Low frequency of imprinting defects in ICSI children born small for gestational age. *Eur J Hum Genet* 2009;**17**:22–29.
Kaneda M, Okano M, Hata K, Sado T, Tsujimoto N, Li E, Sasaki H. *Essential role for de novo DNA methyltransferase Dnmt3a in paternal and maternal imprinting* [Internet]. 2004;Available from: www.nature.com/nature.

Karimi M, Johansson S, Stach D, Corcoran M, Grandér D, Schalling M, Bakalkin G, Lyko F, Larsson C, Ekström TJ. LUMA (LUminometric Methylation Assay)-A high throughput method to the analysis of genomic DNA methylation. *Exp Cell Res* 2006;**312**:1989–1995. Academic Press Inc.

Katari S, Turan N, Bibikova M, Erinle O, Chalian R, Foster M, Gaughan JP, Coutifaris C, Sapienza C. DNA methylation and gene expression differences in children conceived in vitro or in vivo. *Hum Mol Genet* [Internet] 2009;**18**:3769–3778. C. Sapienza, Fels Institute for Cancer Research and Molecular Biology, Temple University School of Medicine, Philadelphia, PA 19140, United States.

Kawasaki Y, Lee J, Matsuzawa A, Kohda T, Kaneko-Ishino T, Ishino F. Active DNA demethylation is required for complete imprint erasure in primordial germ cells. *Sci Rep* 2014;**4**:.

Kerjean A, Couvert P, Heams T, Chalas C, Poirier K, Chelly J, Jouannet P, Paldi A, Poirot C. In vitro follicular growth affects oocyte imprinting establishment in mice. *European Journal of Human Genetics* 2003;**11**:493–496.

Khodavirdilou R, Pournaghi M, Oghbaei H, Rastgar Rezaei Y, Javid F, Khodavirdilou L, Shakibfar F, Latifi Z, Hakimi P, Nouri M, *et al.* Toxic effect of light on oocyte and pre-implantation embryo: a systematic review. *Arch Toxicol* 2021;**95**:3161–3169. Springer Science and Business Media Deutschland GmbH.

Khosla S, Dean W, Brown D, Reik W, Feil R. *Culture of Preimplantation Mouse Embryos Affects Fetal Development and the Expression of Imprinted Genes 1* [Internet]. *Biol Reprod* [Internet] 2001;**64**:.

Khoudja RY, Xu Y, Li T, Zhou C. Better IVF outcomes following improvements in laboratory air quality. *J Assist Reprod Genet* 2013;**30**:69–76.

Khoureiry R, Ibala-Rhomdane S, Méry L, Blachère T, Guérin JF, Lornage J, Lefèvre A. Dynamic CpG methylation of the KCNQ1OT1 gene during maturation of human oocytes. *J Med Genet* 2008;**45**:583–588. BMJ Publishing Group.

Kleijkers SHM, Eijssen LMT, Coonen E, Derhaag JG, Mantikou E, Jonker MJ, Mastenbroek S, Repping S, Evers JLH, Dumoulin JCM, *et al.* Differences in gene expression profiles between human preimplantation embryos cultured in two different IVF culture media. *Human Reproduction* 2015;**30**:2303–2311. Oxford University Press.

Kobayashi H, Hiura H, John RM, Sato A, Otsu E, Kobayashi N, Suzuki R, Suzuki F, Hayashi C, Utsunomiya T, *et al.* DNA methylation errors at imprinted loci after assisted conception originate in the parental sperm. *Eur J Hum Genet* 2009;**17**:1582–1591.

Koeck RM, Busato F, Tost J, Consten D, Echten-Arends J van, Mastenbroek S, Wurth Y, Remy S, Langie S, Nawrot TS, *et al.* Methylome-wide analysis of IVF neonates that underwent embryo culture in different media revealed no significant differences. *NPJ Genom Med* 2022a;**7**:. Nature Research.

Koeck RM, Busato F, Tost J, Zandstra H, Remy S, Langie S, Gielen M, Golde R van, Dumoulin JCM, Brunner H, *et al.* At age 9, the methylome of assisted reproductive technology children that underwent embryo culture in different media is not significantly different on a genome-wide scale. *Hum Reprod* 2022b;**37**:2709–2721. NLM (Medline).

Krisher RL. The effect of oocyte quality on development. *J Anim Sci* 2004;**82**:E14–E23.

Krisher RL. In vivo and in vitro environmental effects on mammalian oocyte quality. *Annu Rev Anim Biosci* 2013;**1**:393–417. Annual Reviews Inc.

Kumar N, Singh A. Trends of male factor infertility, an important cause of infertility: A review of literature. *J Hum Reprod Sci* 2015;**8**:191–196. Medknow Publications.

Kuo KC, McCune RA, Gehrke CW, Midgett R, Ehrlich M. Quantitative reversed-phase high performance liquid chromatographic determination of major and modified deoxvribonudeosides in DNA*. *Nucleic Acids Res* [Internet] 1980;**8**:4763–4776.

Kurdyukov S, Bullock M. DNA methylation analysis: Choosing the right method. *Biology (Basel)* 2016;**5**:1–21.

Kurimoto K, Yabuta Y, Ohinata Y, Shigeta M, Yamanaka K, Saitou M. Complex genome-wide transcription dynamics orchestrated by Blimp1 for the specification of the germ cell lineage in mice. *Genes Dev* 2008;**22**:1617–1635.

Kushnir VA, Barad DH, Albertini DF, Darmon SK, Gleicher N. Systematic review of worldwide trends in assisted reproductive technology 2004-2013. *Reproductive Biology and Endocrinology* 2017;**15**:. BioMed Central Ltd.

Lan X, Adams C, Landers M, Dudas M, Krissinger D, Marnellos G, Bonneville R, Xu M, Wang J, Huang THM, *et al.* High resolution detection and analysis of CpG dinucleotides methylation using MBD-seq technology. *PLoS One* 2011;**6**:.

Lane M, Gardner DK. Blastomere Homeostasis. *ART and the Human Blastocyst* 2001;69–90.

Lazaraviciute G, Kauser M, Bhattacharya S, Haggarty P, Bhattacharya S. A systematic review and meta-analysis of DNA methylation levels and imprinting disorders in children conceived by IVF/ICSI compared with children conceived spontaneously. *Hum Reprod Update* [Internet] 2014;**20**:840–852. S. Bhattacharya, Division of Applied Health Sciences, University of Aberdeen, Head, Foresterhill, Aberdeen, United Kingdom.

Lee AWT, Ng JKW, Liao J, Luk AC, Suen AHC, Chan TTH, Cheung MY, Chu HT, Tang NLS, Zhao MP, *et al.* Single-cell RNA sequencing identifies molecular targets associated with poor in vitro maturation performance of oocytes collected from ovarian stimulation. *Human Reproduction* 2021;**36**:1907–1921. Oxford University Press.

Leese HJ, McKeegan P, Sturmey RG. Amino acids and the early mammalian embryo: Origin, fate, function and life-long legacy. *Int J Environ Res Public Health* 2021;**18**:. MDPI.

Li L, Wang L, Le F, Liu X, Yu P, Sheng J, Huang H, Jin F. Evaluation of DNA methylation status at differentially methylated regions in IVF-conceived newborn twins. *Fertil Steril* 2011a;**95**:1975–1979. United States.

Li L, Wang L, Xu X, Lou H, Le F, Li L, Sheng J, Huang H, Jin F. Genome-wide DNA methylation patterns in IVF-conceived mice and their progeny: A putative model for ART-conceived humans. *Reproductive Toxicology* 2011b;**32**:98–105.

Li S, Tollefsbol TO. DNA methylation methods: Global DNA methylation and methylomic analyses. *Methods* 2021;**187**:28–43. Academic Press Inc.

Li Y, Zhang Z, Chen J, Liu W, Lai W, Liu B, Li X, Liu L, Xu S, Dong Q, *et al.* Stella safeguards the oocyte methylome by preventing de novo methylation mediated by DNMT1. *Nature* 2018;**564**:136–140. Nature Publishing Group.

Lim M, Thompson JG, Dunning KR. Hypoxia and ovarian function: follicle development, ovulation, oocyte maturation. 2021;

Lira-Albarrán S, Liu X, Lee SH, Rinaudo P. DNA methylation profile of liver of mice conceived by in vitro fertilization. *J Dev Orig Health Dis* 2022;**13**:358–366. Cambridge University Press.

Litzky JF, Deyssenroth MA, Everson TM, Armstrong DA, Lambertini L, Chen J, Marsit CJ. Placental imprinting variation associated with assisted reproductive technologies and subfertility. *Epigenetics* 2017;**12**:653–661.

Liu J, Siegmund KD. An evaluation of processing methods for HumanMethylation450 BeadChip data. *BMC Genomics* 2016;**17**:. BioMed Central Ltd.

Liu Q, Li Y, Feng Y, Liu C, Ma J, Li Y, Xiang H, Ji Y, Cao Y, Tong X, *et al.* Single-cell analysis of differences in transcriptomic profiles of oocytes and cumulus cells at GV, MI, MII stages from PCOS patients. *Sci Rep* 2016;**6**:. Nature Publishing Group.

Liu X, Mai H, Chen P, Zhang Z, Wu T, Chen J, Sun P, Zhou C, Liang X, Huang R. Comparative analyses in transcriptome of human granulosa cells and follicular fluid micro-environment between poor ovarian responders with conventional controlled ovarian or mild ovarian stimulations. *Reproductive Biology and Endocrinology* 2022;**20**:. BioMed Central Ltd.

Liu Y, Li X, Chen S, Wang L, Tan Y, Li X, Tang L, Zhang J, Wu D, Wu Y, *et al.* Comparison of Genome-Wide DNA Methylation Profiles of Human Fetal Tissues Conceived by in vitro Fertilization and Natural Conception. *Front Cell Dev Biol* 2021;**9**:. Frontiers Media S.A.

Liu Y, Tang Y, Ye D, Ma W, Feng S, Li X, Zhou X, Chen X, Chen S. Impact of Abnormal DNA Methylation of Imprinted Loci on Human Spontaneous Abortion. *Reprod Sci* 2018;**25**:131–139. United States.

Llonch S, Barragán M, Nieto P, Mallol A, Elosua-Bayes M, Lorden P, Ruiz S, Zambelli F, Heyn H, Vassena R, *et al.* Single human oocyte transcriptome analysis reveals distinct maturation stage-dependent pathways impacted by age. *Aging Cell* 2021;**20**:. John Wiley and Sons Inc.

Loke YJ, Galati JC, Saffery R, Craig JM. Association of in vitro fertilisation (IVF) with global and IGF2/H19 methylation variation in newborn twins. *J Paediatr Child Health* [Internet] 2015;**51**:21. Y.J. Loke, Murdoch Childrens Research Institute, Parkville, VIC, Australia.

Lopes S, Lewis A, Hajkova P, Dean W, Oswald J, Forné T, Murrell A, Constância M, Bartolomei M, Walter J, *et al.* Epigenetic modifications in an imprinting cluster are controlled by a hierarchy of DMRs suggesting long-range chromatin interactions. *Hum Mol Genet* 2003;**12**:295–305.

Los Santos MJ De, Garca-Lez V, Beltrn-Torregrosa D, Horcajadas JA, Martnez-Conejero JA, Esteban FJ, Pellicer A, Labarta E. Hormonal and molecular characterization of follicular fluid, cumulus cells and oocytes from pre-ovulatory follicles in stimulated and unstimulated cycles. *Human Reproduction* 2012;**27**:1596–1605. Oxford University Press.

Lou H, Le F, Hu M, Yang X, Li L, Wang L, Wang N, Gao H, Jin F. Aberrant DNA Methylation of IGF2-H19 Locus in Human Fetus and in Spermatozoa From Assisted Reproductive Technologies. *Reproductive Sciences* 2019;**26**:997–1004. SAGE Publications Inc.

Lou H, Le F, Zheng Y, Li L, Wang L, Wang N, Zhu Y, Huang H, Jin F. Assisted reproductive technologies impair the expression and methylation of insulin-induced gene 1 and sterol regulatory element-binding factor 1 in the fetus and placenta. *Fertil Steril* 2014;**101**:. Elsevier Inc.

Lowe R, Shirley N, Bleackley M, Dolan S, Shafee T. Transcriptomics technologies. *PLoS Comput Biol* 2017;**13**:. Public Library of Science.

Lu CL, Yan ZQ, Song XL, Xu YY, Zheng XY, Li R, Liu P, Feng HL, Qiao J. Effect of exogenous gonadotropin on the transcriptome of human granulosa cells and follicular fluid hormone profiles. *Reproductive Biology and Endocrinology* 2019;**17**:. BioMed Central Ltd.

Luciano AM, Lodde V, Franciosi F, Tessaro I, Corbani D, Modina SC. Large-scale chromatin morpho-functional changes during mammalian oocyte growth and differentiation. *European Journal of Histochemistry* 2012;**56**:231–235. Luigi Ponzio e figlio Editori.

Maccani MA, Marsit CJ. Epigenetics in the placenta. *American Journal of Reproductive Immunology* 2009;**62**:78–89.

Mai Z, Lei M, Yu B, Du H, Liu J. The effects of cigarette smoke extract on ovulation, oocyte morphology and ovarian gene expression in mice. *PLoS One* 2014;**9**:. Public Library of Science.

Maksimovic J, Gordon L, Oshlack A. SWAN: Subset-quantile within array normalization for illumina infinium HumanMethylation450 BeadChips. *Genome Biol* 2012;**13**:.

Maksimovic J, Oshlack A, Phipson B. Gene set enrichment analysis for genome-wide DNA methylation data. *Genome Biol* 2021;**22**:. BioMed Central Ltd.

Mandelbaum RS, Awadalla MS, Smith MB, Violette CJ, Klooster BL, Danis RB, Mcginnis LK, Ho JR, Bendikson KA, Paulson RJ, *et al.* Developmental potential of immature human oocytes aspirated after controlled ovarian stimulation. *J Assist Reprod Genet* [Internet] 2021;**38**:2291–2299.

Mani S, Ghosh J, Rhon-Calderon EA, Lan Y, Ord T, Kalliora C, Chan J, Schultz B, Vaughan-Williams E, Coutifaris C, *et al.* Embryo cryopreservation leads to sex-specific DNA methylation perturbations in both human and mouse placentas. *Hum Mol Genet* 2022;**31**:3855–3872. NLM (Medline).

Manipalviratn S, DeCherney A, Segars J. Imprinting disorders and assisted reproductive technology. *Fertil Steril* 2009;**91**:305–315.

Mann MRW, Lee SS, Doherty AS, Verona RI, Nolen LD, Schultz RM, Bartolomei MS. Selective loss of imprinting in the placenta following preimplantation development in culture. *Development* 2004;**131**:3727–3735.

Mansell G, Gorrie-Stone TJ, Bao Y, Kumari M, Schalkwyk LS, Mill J, Hannon E. Guidance for DNA methylation studies: Statistical insights from the Illumina EPIC array. *BMC Genomics* 2019;**20**:. BioMed Central Ltd.
Mantikou E, Jonker MJ, Wong KM, Montfoort APA Van, Jong M De, Breit TM, Repping S, Mastenbroek S. Factors affecting the gene expression of in vitro cultured human preimplantation embryos. *Human Reproduction* 2016;**31**:298–311.
Mantikou E, Youssef MAFM, wely M van, veen F van der, Al-inany HG, Repping S, Mastenbroek S. Embryo culture media and IVF/ICSI success rates: A systematic review. *Hum Reprod Update* 2013;**19**:210–220.
Marjonen H, Auvinen P, Kahila H, Tšuiko O, Kõks S, Tiirats A, Viltrop T, Tuuri T, Söderström-Anttila V, Suikkari A-M, *et al.* rs10732516 polymorphism at the IGF2/H19 locus associates with genotype-specific effects on placental DNA methylation and birth weight of newborns conceived by assisted reproductive technology. *Clin Epigenetics* 2018;**10**:80.
Market-Velker BA, Zhang L, Magri LS, Bonvissuto AC, Mann MRW. Dual effects of superovulation: Loss of maternal and paternal imprinted methylation in a dose-dependent manner. *Hum Mol Genet* 2009;**19**:36–51.
Maunakea AK, Nagarajan RP, Bilenky M, Ballinger TJ, Dsouza C, Fouse SD, Johnson BE, Hong C, Nielsen C, Zhao Y, *et al.* Conserved role of intragenic DNA methylation in regulating alternative promoters. *Nature* 2010;**466**:253–257.
McRae AF, Marioni RE, Shah S, Yang J, Powell JE, Harris SE, Gibson J, Henders AK, Bowdler L, Painter JN, *et al.* Identification of 55,000 Replicated DNA Methylation QTL. *Sci Rep* 2018;**8**:. Nature Publishing Group.
Meissner A, Gnirke A, Bell GW, Ramsahoye B, Lander ES, Jaenisch R. Reduced representation bisulfite sequencing for comparative high-resolution DNA methylation analysis. *Nucleic Acids Res* 2005;**33**:5868–5877.
Melamed N, Choufani S, Wilkins-Haug LE, Koren G, Weksberg R. Comparison of genome-wide and gene-specific DNA methylation between ART and naturally conceived pregnancies. *Epigenetics* [Internet] 2015;**10**:474–483. R. Weksberg, Genetics and Genome Biology Program, The Hospital for Sick Children, Toronto, ON, Canada.
Menezo Y, Clément P, Dale B. DNA Methylation Patterns in the Early Human Embryo and the Epigenetic/Imprinting Problems: A Plea for a More Careful Approach to Human Assisted Reproductive Technology (ART). *Int J Mol Sci* 2019;**20**:.
Menezo Y, Clement P, Dale B, Elder K. Modulating oxidative stress and epigenetic homeostasis in preimplantation IVF embryos. *Zygote* 2022a;**30**:149–158.
Menezo Y, Elder K, Clement P, Clement A, Patrizio P. Biochemical Hazards during Three Phases of Assisted Reproductive Technology: Repercussions Associated with Epigenesis and Imprinting. *Int J Mol Sci* 2022b;**23**:. MDPI.
Ménézo Y, Lichtblau I, Elder K. New insights into human pre-implantation metabolism in vivo and in vitro. *J Assist Reprod Genet* 2013;**30**:293–303.
Ménézo YJR, Hérubel F. Mouse and bovine models for human IVF. *Reprod Biomed Online* 2002;**4**:170–175.
Menezo YJR, Silvestris E, Dale B, Elder K. Oxidative stress and alterations in DNA methylation: two sides of the same coin in reproduction. *Reprod Biomed Online* [Internet] 2016;**33**:668–683. Y.J.R. Menezo, London Fertility Associates, Harley St, London, United Kingdom.
Mermillod P, Dalbiès-Tran R, Uzbekova S, Thélie A, Traverso JM, Perreau C, Papillier P, Monget P. Factors Affecting Oocyte Quality: Who is Driving the Follicle? *Reproduction in Domestic Animals* 2008;**43**:393–400.
Messerschmidt DM, Knowles BB, Solter D. DNA methylation dynamics during epigenetic reprogramming in the germline and preimplantation embryos. *Genes Dev* 2014;**28**:812–828. Cold Spring Harbor Laboratory Press.
Millán-Zambrano G, Burton A, Bannister AJ, Schneider R. Histone post-translational modifications — cause and consequence of genome function. *Nat Rev Genet* 2022;**23**:563–580. Nature Research.

Molyneaux K, Wylie C. *Primordial germ cell migration* [Internet]. *Int J Dev Biol* [Internet] 2004;**48**:.
Monk D, Morales J, Dunnen JT den, Russo S, Court F, Prawitt D, Eggermann T, Beygo J, Buiting K, Tümer Z. Recommendations for a nomenclature system for reporting methylation aberrations in imprinted domains. *Epigenetics* 2018;**13**:117–121. Taylor and Francis Inc.
Montfoort APA Van, Arts EGJM, Wijnandts L, Sluijmer A, Pelinck M-J, Land JA, Echten-Arends J Van. Reduced oxygen concentration during human IVF culture improves embryo utilization and cumulative pregnancy rates per cycle. *Hum Reprod Open* 2020;**2020**:. Oxford University Press (OUP).
Montfoort APA Van, Hanssen LLP, Sutter P De, Viville S, Geraedts JPM, Boer P De. Assisted reproduction treatment and epigenetic inheritance. *Hum Reprod Update* 2012;**18**:171–197.
Monzo C, Haouzi D, Roman K, Assou S, Dechaud H, Hamamah S. Slow freezing and vitrification differentially modify the gene expression profile of human metaphase II oocytes. *Human Reproduction* 2012;**27**:2160–2168. Oxford University Press.
Moon KR, Dijk D van, Wang Z, Gigante S, Burkhardt DB, Chen WS, Yim K, Elzen A van den, Hirn MJ, Coifman RR, *et al.* Visualizing structure and transitions in high-dimensional biological data. *Nat Biotechnol* [Internet] 2019;**37**:1482–1492. Springer US.
Moore GE, Ishida M, Demetriou C, Al-Olabi L, Leon LJ, Thomas AC, Abu-Amero S, Frost JM, Stafford JL, Chaoqun Y, *et al.* The role and interaction of imprinted genes in human fetal growth. *Philosophical Transactions of the Royal Society B: Biological Sciences* 2015;**370**:. Royal Society of London.
Morbeck DE, Krisher RL, Herrick JR, Baumann NA, Matern D, Moyer T. Composition of commercial media used for human embryo culture. *Fertil Steril* 2014;**102**:. Elsevier Inc.
Mulder CL, Wattimury TM, Jongejan A, Winter-Korver CM De, Daalen SKM Van, Struijk RB, Borgman SCM, Wurth Y, Consten D, Echten-Arends J Van, *et al.* Comparison of DNA methylation patterns of parentally imprinted genes in placenta derived from IVF conceptions in two different culture media. *Human Reproduction* 2020;**35**:516–528.
Munck N De, Verheyen G, Landuyt L Van, Stoop D, Velde H Van De. Survival and post-warming in vitro competence of human oocytes after high security closed system vitrification. *J Assist Reprod Genet* 2013;**30**:361–369.
Munné S, Alikani M, Ribustello L, Colls P, Martínez-Ortiz PA, Mcculloh DH. Euploidy rates in donor egg cycles significantly differ between fertility centers. *Human Reproduction* 2017;**32**:743–749. Oxford University Press.
Naillat F, Saadeh H, Nowacka-Woszuk J, Gahurova L, Santos F, Tomizawa S ichi, Kelsey G. Oxygen concentration affects de novo DNA methylation and transcription in in vitro cultured oocytes. *Clin Epigenetics* 2021;**13**:. BioMed Central Ltd.
National Human Genome Research Institute. Transcriptome Fact Sheet. 2020;
Nelissen ECM, Dumoulin JCM, Daunay A, Evers JLH, Tost J, Montfoort APA van. Placentas from pregnancies conceived by IVF/ICSI have a reduced DNA methylation level at the H19 and MEST differentially methylated regions. *Hum Reprod* 2013;**28**:1117–1126. England.
Novakovic B, Lewis S, Halliday J, Kennedy J, Burgner DP, Czajko A, Kim B, Sexton-Oates A, Juonala M, Hammarberg K, *et al.* Assisted reproductive technologies are associated with limited epigenetic variation at birth that largely resolves by adulthood. *Nat Commun* [Internet] 2019;**10**:. R. Saffery, Murdoch Children's Research Institute, Parkville, VIC, Australia.
Nurk S, Koren S, Rhie A, Rautiainen M, Bzikadze A V, Mikheenko A, Vollger MR, Altemose N, Uralsky L, Gershman A, *et al.* The complete sequence of a human genome. *Science (1979)* [Internet] 2022;**376**:43–55.
Odom LN, Segars J. Imprinting disorders and assisted reproductive technology. *Curr Opin Endocrinol Diabetes Obes* 2010;**17**:517–522.
Oh B, Hwang S-Y, McLaughlin J, Solter D, Knowles BB. Timely translation during the mouse oocyte-to-embryo transition. *Development* 2000;**127**:3795–3803.

Ohno R, Nakayama M, Naruse C, Okashita N, Takano O, Tachibana M, Asano M, Saitou M, Seki Y. A replication-dependent passive mechanism modulates DNA demethylation in mouse primordial germ cells. *Development (Cambridge)* 2013;**140**:2892–2903.
Okae H, Chiba H, Hiura H, Hamada H, Sato A, Utsunomiya T, Kikuchi H, Yoshida H, Tanaka A, Suyama M, *et al.* Genome-Wide Analysis of DNA Methylation Dynamics during Early Human Development. *PLoS Genet* 2014;**10**:. Public Library of Science.
Okano M, Bell DW, Haber DA, Li E. *DNA Methyltransferases Dnmt3a and Dnmt3b Are Essential for De Novo Methylation and Mammalian Development*. *Cell* 1999;**99**:.
Olcha M, Dong X, Feil H, Hao X, Lee M, Jindal S, Buyuk E, Vijg J. A workflow for simultaneous DNA copy number and methylome analysis of inner cell mass and trophectoderm cells from human blastocysts. *Fertil Steril* 2021;**115**:, p. 1533–1540. Elsevier Inc.
Oliver VF, Miles HL, Cutfield WS, Hofman PL, Ludgate JL, Morison IM. Defects in imprinting and genome-wide DNA methylation are not common in the in vitro fertilization population. *Fertil Steril* 2012;**97**:147-53.e7. United States.
Ondičová M, Irwin RE, Thursby SJ, Hilman L, Caffrey A, Cassidy T, McLaughlin M, Lees-Murdock DJ, Ward M, Murphy M, *et al.* Folic acid intervention during pregnancy alters DNA methylation, affecting neural target genes through two distinct mechanisms. *Clin Epigenetics* 2022;**14**:. BioMed Central Ltd.
O'Neill C, Li Y, Jin XL. Survival signaling in the preimplantation embryo. *Theriogenology* 2012;**77**:773–784.
Papler TB, Bokal EV, Tacer KF, Juvan P, Klun IV, Devjak R. Differences in cumulus cells gene expression between modified natural and stimulated in vitro fertilization cycles. *J Assist Reprod Genet* 2014;**31**:79–88. Springer New York LLC.
Penova-Veselinovic B, Melton PE, Huang RC, Yovich JL, Burton P, Wijs LA, Hart RJ. DNA methylation patterns within whole blood of adolescents born from assisted reproductive technology are not different from adolescents born from natural conception. *Hum Reprod* 2021;**36**:2035–2049. England.
Pérez-Palacios R, Fauque P, Teissandier A, Bourc'his D. Deciphering the early mouse embryo transcriptome by low-input RNA-Seq. *Methods in Molecular Biology* 2021;**2214**:, p. 189–205. Humana Press Inc.
Perry ACF, Asami M, Lam BYH, Yeo GSH. The initiation of mammalian embryonic transcription: to begin at the beginning. *Trends Cell Biol* 2022; Elsevier BV.
Peters TJ, Buckley MJ, Statham AL, Pidsley R, Samaras K, Lord R V, Clark SJ, Molloy PL. De novo identification of differentially methylated regions in the human genome. *Epigenetics Chromatin* 2015;**8**:.
Petropoulos S, Edsgärd D, Reinius B, Deng Q, Panula SP, Codeluppi S, Plaza Reyes A, Linnarsson S, Sandberg R, Lanner F. Single-Cell RNA-Seq Reveals Lineage and X Chromosome Dynamics in Human Preimplantation Embryos. *Cell* 2016;**165**:1012–1026.
Pham N V, Nguyen MT, Hu J-F, Vu TH, Hoffman AR. *Dissociation of IGF2 and H19 imprinting in human brain*. *Brain Res* 1998;**810**:.
Phipson B, Maksimovic J, Oshlack A. MissMethyl: An R package for analyzing data from Illumina's HumanMethylation450 platform. *Bioinformatics* 2016;**32**:286–288.
Pidsley R, Zotenko E, Peters TJ, Lawrence MG, Risbridger GP, Molloy P, Djik S Van, Muhlhausler B, Stirzaker C, Clark SJ. Critical evaluation of the Illumina MethylationEPIC BeadChip microarray for whole-genome DNA methylation profiling. *Genome Biol* 2016;**17**:. BioMed Central Ltd.
Pliushch G, Schneider E, Schneider T, Hajj N El, Rösner S, Strowitzki T, Haaf T. In vitro maturation of oocytes is not associated with altered deoxyribonucleic acid methylation patterns in children from in vitro fertilization or intracytoplasmic sperm injection. *Fertil Steril* 2015;**103**:720-727.e1. Elsevier Inc.
Popp C, Dean W, Feng S, Cokus SJ, Andrews S, Pellegrini M, Jacobsen SE, Reik W. Genome-wide erasure of DNA methylation in mouse primordial germ cells is affected by AID deficiency. *Nature* 2010;**463**:1101–1105.

Puscheck EE, Awonuga AO, Yang Y, Jiang Z, Rappolee DA. Molecular biology of the stress response in the early embryo and its stem cells. *Adv Exp Med Biol* 2015;**843**:77–128.
Puumala SE, Nelson HH, Ross JA, Nguyen RHN, Damario MA, Spector LG. Similar DNA methylation levels in specific imprinting control regions in children conceived with and without assisted reproductive technology: a cross-sectional study. *BMC Pediatr* 2012;**12**:33.
Quenneville S, Verde G, Corsinotti A, Kapopoulou A, Jakobsson J, Offner S, Baglivo I, Pedone P V., Grimaldi G, Riccio A, *et al.* In embryonic stem cells, ZFP57/KAP1 recognize a methylated hexanucleotide to affect chromatin and DNA methylation of imprinting control regions. *Mol Cell* 2011;**44**:361–372.
Rakyan VK, Down TA, Maslau S, Andrew T, Yang TP, Beyan H, Whittaker P, McCann OT, Finer S, Valdes AM, *et al.* Human aging-associated DNA hypermethylation occurs preferentially at bivalent chromatin domains. *Genome Res* 2010;**20**:434–439.
Ramos-Ibeas P, Heras S, Gómez-Redondo I, Planells B, Fernández-González R, Pericuesta E, Laguna-Barraza R, Pérez-Cerezales S, Gutiérrez-Adán A. Embryo responses to stress induced by assisted reproductive technologies. *Mol Reprod Dev* 2019;**86**:1292–1306.
Rancourt RC, Harris HR, Michels KB. Methylation levels at imprinting control regions are not altered with ovulation induction or in vitro fertilization in a birth cohort. *Hum Reprod* 2012;**27**:2208–2216.
Redding GP, Bronlund JE, Hart AL. Theoretical investigation into the dissolved oxygen levels in follicular fluid of the developing human follicle using mathematical modelling. *Reprod Fertil Dev* 2008;**20**:408–417.
Reik W, Walter J. Genomic imprinting: parental influence on the genome. *Nature Reviews* 2001;**2**:21–32.
Reis e Silva AR, Bruno C, Fleurot R, Daniel N, Archilla C, Peynot N, Lucci CM, Beaujean N, Duranthon V. Alteration of DNA demethylation dynamics by in vitro culture conditions in rabbit pre-implantation embryos. *Epigenetics* 2012;**7**:440–446. Taylor and Francis Inc.
Reynier P, May-Panloup P, Chrétien M-F, Morgan CJ, Jean M, Savagner F, Barrière P, Malthièry Y. *Mitochondrial DNA content affects the fertilizability of human oocytes*. *Mol Hum Reprod* 2001;**7**:.
Rezazadeh Valojerdi M, Eftekhari-Yazdi P, Karimian L, Hassani F, Movaghar B. Vitrification versus slow freezing gives excellent survival, post warming embryo morphology and pregnancy outcomes for human cleaved embryos. *J Assist Reprod Genet* 2009;**26**:347–354.
Richardson BE, Lehmann R. Mechanisms guiding primordial germ cell migration: Strategies from different organisms. *Nat Rev Mol Cell Biol* 2010;**11**:37–49.
Richmond RC, Sharp GC, Herbert G, Atkinson C, Taylor C, Bhattacharya S, Campbell D, Hall M, Kazmi N, Gaunt T, *et al.* The long-term impact of folic acid in pregnancy on offspring DNA methylation: Follow-up of the Aberdeen folic acid supplementation trial (AFAST). *Int J Epidemiol* 2018;**47**:928–937. Oxford University Press.
Rivera CM, Ren B. Mapping human epigenomes. *Cell* 2013;**155**:. Elsevier B.V.
Rivera RM, Stein P, Weaver JR, Mager J, Schultz RM, Bartolomei MS. Manipulations of mouse embryos prior to implantation result in aberrant expression of imprinted genes on day 9.5 of development. *Hum Mol Genet* 2008;**17**:1–14.
Roadmap Epigenomics Consortium, Kundaje A, Meuleman W, Ernst J, Bilenky M, Yen A, Heravi-Moussavi A, Kheradpour P, Zhang Z, Wang J, *et al.* Integrative analysis of 111 reference human epigenomes. *Nature* 2015;**518**:317–329. Nature Research.
Romanowska J, Nustad HE, Page CM, Denault WRP, Lee Y, Magnus MC, Haftorn KL, Gjerdevik M, Novakovic B, Saffery R, *et al.* The X-factor in ART: does the use of assisted reproductive technologies influence DNA methylation on the X chromosome? *Hum Genomics* [Internet] 2023;**17**:35.
Roth Z. Reduction in oocyte developmental competence by stress is associated with alterations in mitochondrial function. *J Dairy Sci* 2018;**101**:3642–3654. Elsevier Inc.

Rougier N, Bourc'his D, Molina Gomes D, Niveleau A, Plachot M, Pàldi A, Viegas-Péquignot E. Chromosome methylation patterns during mammalian preimplantation development. *Genes Dev* [Internet] 1998;**12**:2108–2113.
Russell DL, Gilchrist RB, Brown HM, Thompson JG. Bidirectional communication between cumulus cells and the oocyte: Old hands and new players? *Theriogenology* 2016;**86**:62–68. Elsevier Inc.
Saare M, Modhukur V, Suhorutshenko M, Rajashekar B, Rekker K, Sõritsa D, Karro H, Soplepmann P, Sõritsa A, Lindgren CM, *et al.* The influence of menstrual cycle and endometriosis on endometrial methylome. *Clin Epigenetics* 2016;**8**:1–10. Springer Verlag.
Saenz-De-Juano MD, Ivanova E, Billooye K, Herta AC, Smitz J, Kelsey G, Anckaert E. Genome-wide assessment of DNA methylation in mouse oocytes reveals effects associated with in vitro growth, superovulation, and sexual maturity. *Clin Epigenetics* 2019;**11**:. BioMed Central Ltd.
Saini A, Rawat Y, Jain K, Mani I. State-of-the-art techniques to study epigenetics. *Prog Mol Biol Transl Sci* 2023;**197**:, p. 23–50. Elsevier B.V.
Sakian S, Louie K, Wong EC, Havelock J, Kashyap S, Rowe T, Taylor B, Ma S. Altered gene expression of H19 and IGF2 in placentas from ART pregnancies. *Placenta* 2015;**36**:1100–1105. Netherlands.
Sala C, Lena P Di, Durso DF, Prodi A, Castellani G, Nardini C. Evaluation of pre-processing on the meta-analysis of DNA methylation data from the Illumina HumanMethylation450 BeadChip platform. *PLoS One* 2020;**15**:. Public Library of Science.
Santos F, Hyslop L, Stojkovic P, Leary C, Murdoch A, Reik W, Stojkovic M, Herbert M, Dean W. Evaluation of epigenetic marks in human embryos derived from IVF and ICSI. *Human Reproduction* 2010;**25**:2387–2395. Oxford University Press.
Santos TA, Shourbagy S El, John JC St. Mitochondrial content reflects oocyte variability and fertilization outcome. *Fertil Steril* 2006;**85**:584–591.
Sato A, Otsu E, Negishi H, Utsunomiya T, Arima T. Aberrant DNA methylation of imprinted loci in superovulated oocytes. *Human Reproduction* 2007;**22**:26–35. Oxford University Press.
Sato S, Yoshida W, Soejima H, Nakabayashi K, Hata K. Methylation dynamics of IG-DMR and Gtl2-DMR during murine embryonic and placental development. *Genomics* 2011;**98**:120–127.
Schier AF. The maternal-zygotic transition: Death and birth of RNAs. *Science (1979)* 2007;**316**:406–407.
Schieve LA, Rasmussen SA, Buck GM, Schendel DE, Reynolds MA, Wright VC. Are children born after assisted reproductive technology at increased risk for adverse health outcomes? *Obstetrics and Gynecology* 2004;**103**:1154–1163.
Schoenherr CJ, Levorse JM, Tilghman SM. CTCF maintains differential methylation at the Igf2/H19 locus. *Nat Genet* 2003;**33**:66–69.
Schultz MD, He Y, Whitaker JW, Hariharan M, Mukamel EA, Leung D, Rajagopal N, Nery JR, Urich MA, Chen H, *et al.* Human body epigenome maps reveal noncanonical DNA methylation variation. *Nature* 2015;**523**:212–216.
Schultz RM. The molecular foundations of the maternal to zygotic transition in the preimplantation embryo. *Hum Reprod Update* 2002;**8**:323–331.
Schulz KN, Harrison MM. Mechanisms regulating zygotic genome activation. *Nat Rev Genet* 2019;**20**:221–234. Nature Publishing Group.
Scutiero G, Iannone P, Bernardi G, Bonaccorsi G, Spadaro S, Volta CA, Greco P, Nappi L. Oxidative Stress and Endometriosis: A Systematic Review of the Literature. *Oxid Med Cell Longev* 2017;**2017**:. Hindawi Limited.
Seale K, Horvath S, Teschendorff A, Eynon N, Voisin S. Making sense of the ageing methylome. *Nat Rev Genet* 2022;**23**:585–605. Nature Research.
Seisenberger S, Andrews S, Krueger F, Arand J, Walter J, Santos F, Popp C, Thienpont B, Dean W, Reik W. The Dynamics of Genome-wide DNA Methylation Reprogramming in Mouse Primordial Germ Cells. *Mol Cell* 2012;**48**:849–862.

Sepúlveda S, Garcia J, Arriaga E, Diaz J, Noriega-Portella L, Noriega-Hoces L. In vitro development and pregnancy outcomes for human embryos cultured in either a single medium or in a sequential media system. *Fertil Steril* 2009;**91**:1765–1770.
Sha QQ, Zheng W, Wu YW, Li S, Guo L, Zhang S, Lin G, Ou XH, Fan HY. Dynamics and clinical relevance of maternal mRNA clearance during the oocyte-to-embryo transition in humans. *Nat Commun* [Internet] 2020;**11**:4917. Springer US.
Shen L, Song CX, He C, Zhang Y. Mechanism and function of oxidative reversal of DNA and RNA methylation. *Annu Rev Biochem* 2014;**83**:585–614. Annual Reviews Inc.
Shi X, Chen S, Zheng H, Wang L, Wu Y. Abnormal DNA methylation of imprinted loci in human preimplantation embryos. *Reproductive Sciences* 2014;**21**:978–983. SAGE Publications Inc.
Shi X, Ni Y, Zheng H, Chen S, Zhong M, Wu F, Xia R, Luo Y. Abnormal methylation patterns at the IGF2/H19 imprinting control region in phenotypically normal babies conceived by assisted reproductive technologies. *Eur J Obstet Gynecol Reprod Biol* 2011;**158**:52–55. Ireland.
Shirane K, Toh H, Kobayashi H, Miura F, Chiba H, Ito T, Kono T, Sasaki H. Mouse Oocyte Methylomes at Base Resolution Reveal Genome-Wide Accumulation of Non-CpG Methylation and Role of DNA Methyltransferases. *PLoS Genet* 2013;**9**:.
Smith ZD, Chan MM, Mikkelsen TS, Gu H, Gnirke A, Regev A, Meissner A. A unique regulatory phase of DNA methylation in the early mammalian embryo. *Nature* 2012;**484**:339–344.
Smyth GK. limma: Linear Models for Microarray Data. *Bioinformatics and Computational Biology Solutions Using R and Bioconductor* 2005;397–420.
Söderström-Anttila V, Salokorpi T, Pihlaja M, Serenius-Sirve S, Suikkari AM. Obstetric and perinatal outcome and preliminary results of development of children born after in vitro maturation of oocytes. *Human Reproduction* 2006;**21**:1508–1513. Oxford University Press.
Soneson C, Robinson MD. Bias, robustness and scalability in single-cell differential expression analysis. *Nat Methods* 2018;**15**:255–261. Nature Publishing Group.
Song S, Ghosh J, Mainigi M, Turan N, Weinerman R, Truongcao M, Coutifaris C, Sapienza C. DNA methylation differences between in vitro- and in vivo-conceived children are associated with ART procedures rather than infertility. *Clin Epigenetics* 2015;**7**:41.
Steegers-Theunissen RP, Obermann-Borst SA, Kremer D, Lindemans J, Siebel C, Steegers EA, Slagboom PE, Heijman BT. Periconceptional maternal folic acid use of 400 µg per day is related to increased methylation of the IGF2 gene in the very young child. *PLoS One* 2009;**4**:.
Steuerwald NM, Bermúdez MG, Wells D, Munné S, Cohen J. Maternal age-related differential global expression profiles observed in human oocytes. *Reprod Biomed Online* 2007;**14**:700–708. Reproductive Healthcare Ltd.
Suetake I, Shinozaki F, Miyagawa J, Takeshima H, Tajima S. DNMT3L stimulates the DNA methylation activity of Dnmt3a and Dnmt3b through a direct interaction. *Journal of Biological Chemistry* 2004;**279**:27816–27823.
Sun H, Gong T-T, Jiang Y-T, Zhao Y-H, Wu Q-J. Global, regional, and national prevalence and disability-adjusted life-years for infertility in 195 countries and territories, 1990–2017: results from a global burden of disease study, 2017. *Aging* 2019;**11**:10952–10991.
Sunde A, Brison D, Dumoulin J, Harper J, Lundin K, Magli MC, Abbeel E Van Den, Veiga A. Time to take human embryo culture seriously. *Human Reproduction* 2016;**31**:2174–2182. Oxford University Press.
Surani A. Reprogramming of genome function through epigenetic inheritance. *Nature* [Internet] 2001;**414**:122–128.
Suzuki MM, Bird A. DNA methylation landscapes: Provocative insights from epigenomics. *Nat Rev Genet* 2008;**9**:465–476.
Tadros W, Lipshitz HD. The maternal-to-zygotic transition: A play in two acts. *Development* 2009;**136**:3033–3042.

Taher L, Israel S, Drexler HCA, Makalowski W, Suzuki Y, Fuellen G, Boiani M. The proteome, not the transcriptome, predicts that oocyte superovulation affects embryonic phenotypes in mice. *Sci Rep* 2021;**11**:. Nature Research.
Takashima T, Fujimaru T, Obata Y. Effect of in vitro growth on mouse oocyte competency, mitochondria and transcriptome. *Reproduction* 2021;**162**:307–318. BioScientifica Ltd.
Tang F, Barbacioru C, Wang Y, Nordman E, Lee C, Xu N, Wang X, Bodeau J, Tuch BB, Siddiqui A, *et al.* mRNA-Seq whole-transcriptome analysis of a single cell. *Nat Methods* 2009;**6**:377–382.
Tang L, Liu Z, Zhang R, Su C, Yang W, Yao Y, Zhao S. Imprinting alterations in sperm may not significantly influence ART outcomes and imprinting patterns in the cord blood of offspring. *PLoS One* 2017;**12**:e0187869.
Tarahomi M, Vaz FM, Straalen JP Van, Schrauwen FAP, Wely M Van, Hamer G, Repping S, Mastenbroek S. The composition of human preimplantation embryo culture media and their stability during storage and culture. *Human Reproduction* 2019;**34**:1450–1461. Oxford University Press.
Teschendorff AE, Breeze CE, Zheng SC, Beck S. A comparison of reference-based algorithms for correcting cell-type heterogeneity in Epigenome-Wide Association Studies. *BMC Bioinformatics* 2017;**18**:. BioMed Central Ltd.
Teschendorff AE, Marabita F, Lechner M, Bartlett T, Tegner J, Gomez-Cabrero D, Beck S. A beta-mixture quantile normalization method for correcting probe design bias in Illumina Infinium 450 k DNA methylation data. *Bioinformatics* 2013;**29**:189–196.
Thompson JG, Brown HM, Kind KL, Russell DL. The ovarian antral follicle: Living on the edge of hypoxia or not? *Biol Reprod* 2015;**92**:. Society for the Study of Reproduction.
Tierling S, Souren NY, Gries J, Loporto C, Groth M, Lutsik P, Neitzel H, Utz-Billing I, Gillessen-Kaesbach G, Kentenich H, *et al.* Assisted reproductive technologies do not enhance the variability of DNA methylation imprints in human. *J Med Genet* 2010;**47**:371–376. England.
Tobi EW, Almqvist C, Hedman A, Andolf E, Holte J, Olofsson JI, Wramsby H, Wramsby M, Pershagen G, Heijmans BT, *et al.* DNA methylation differences at birth after conception through ART. *Hum Reprod* 2021;**36**:248–259.
Tora L, Vincent SD. What defines the maternal transcriptome? *Biochem Soc Trans* 2021;**49**:2051–2062. Portland Press Ltd.
Tsai PC, Glastonbury CA, Eliot MN, Bollepalli S, Yet I, Castillo-Fernandez JE, Carnero-Montoro E, Hardiman T, Martin TC, Vickers A, *et al.* Smoking induces coordinated DNA methylation and gene expression changes in adipose tissue with consequences for metabolic health 06 Biological Sciences 0604 Genetics. *Clin Epigenetics* 2018;**10**:. BioMed Central Ltd.
Tsukada YI, Akiyama T, Nakayama KI. Maternal TET3 is dispensable for embryonic development but is required for neonatal growth. *Sci Rep* 2015;**5**:. Nature Publishing Group.
Turan N, Katari S, Gerson LF, Chalian R, Foster MW, Gaughan JP, Coutifaris C, Sapienza C. Inter- and intra-individual variation in allele-specific DNA methylation and gene expression in children conceived using assisted reproductive technology. *PLoS Genet* 2010;**6**:e1001033.
Turner BM. Histone acetylation and an epigenetic code. *BioEssays* 2000;**22**:836–845.
Tusnády GE, Simon I, Váradi A, Arányi T. BiSearch: primer-design and search tool for PCR on bisulfite-treated genomes. *Nucleic Acids Res* 2005;**33**:.
Tyler JK, Canovas S, Ivanova E, Romar R, García-Martínez S, Soriano-U ´ Beda C, García-Vá Zquez FA, Saadeh H, Andrews S, Kelsey G, *et al.* DNA methylation and gene expression changes derived from assisted reproductive technologies can be decreased by reproductive fluids. 2017;
Urrego R, Rodriguez-Osorio N, Niemann H. Epigenetic disorders and altered gene expression after use of assisted reproductive technologies in domestic cattle. *Epigenetics* 2014;**9**:803–815. Taylor and Francis Inc.

Varrault A, Dubois E, Digarcher A Le, Bouschet T. Quantifying genomic imprinting at tissue and cell resolution in the brain. Epigenomes 2020;**4**:. MDPI.
Vassena R, Boué S, González-Roca E, Aran B, Auer H, Veiga A, Belmonte JCI. Waves of early transcriptional activation and pluripotency program initiation during human preimplantation development. *Development* 2011;**138**:3699–3709.
Vermeiden JPW, Bernardus RE. Are imprinting disorders more prevalent after human in vitro fertilization or intracytoplasmic sperm injection? *Fertil Steril* [Internet] 2013;**99**:642–651. Elsevier Inc.
Vincent RN, Gooding LD, Louie K, Chan Wong E, Ma S. Altered DNA methylation and expression of PLAGL1 in cord blood from assisted reproductive technology pregnancies compared with natural conceptions. *Fertil Steril* 2016;**106**:739-748.e3. United States.
Volders PJ, Anckaert J, Verheggen K, Nuytens J, Martens L, Mestdagh P, Vandesompele J. Lncipedia 5: Towards a reference set of human long non-coding rnas. *Nucleic Acids Res* 2019;**47**:D135–D139. Oxford University Press.
Vos M De, Grynberg M, Ho TM, Yuan Y, Albertini DF, Gilchrist RB. Perspectives on the development and future of oocyte IVM in clinical practice. *J Assist Reprod Genet* [Internet] 2021;**38**:1265–1280.
Vuong TNL, Ho MT, Ha TQ, Jensen MB, Andersen CY, Humaidan P. Effect of GnRHa ovulation trigger dose on follicular fluid characteristics and granulosa cell gene expression profiles. *J Assist Reprod Genet* 2017;**34**:471–478. Springer New York LLC.
Waal E de, Mak W, Calhoun S, Stein P, Ord T, Krapp C, Coutifaris C, Schultz RM, Bartolomei MS. In vitro culture increases the frequency of stochastic epigenetic errors at imprinted genes in placental tissues from mouse concepti produced through assisted reproductive technologies. *Biol Reprod* 2014;**90**:22.
waal E De, Yamazaki Y, Ingale P, Bartolomei MS, Yanagimachi R, McCarrey JR. Gonadotropin stimulation contributes to an increased incidence of epimutations in ICSI-derived mice. *Hum Mol Genet* 2012;**21**:4460–4472.
Wallace SE, Bean LJ. *Resources for Genetics Professionals-Genetic Disorders Caused by Imprinting Errors and Uniparental Disomy Not Detectable by Sequence Analysis*. 2017;
Wang K, Li M, Hakonarson H. ANNOVAR: Functional annotation of genetic variants from high-throughput sequencing data. *Nucleic Acids Res* 2010;**38**:.
Wang L, Zhang J, Duan J, Gao X, Zhu W, Lu X, Yang L, Zhang J, Li G, Ci W, *et al.* Programming and inheritance of parental DNA methylomes in mammals. *Cell* 2014;**157**:979–991. Elsevier B.V.
Wang Y-X, Yue L-F, Zhang J-W, Xiong Y-W, Hu J-J, Wang L-L, Li Z, Liu Y, Yang L, Sun L-J. Expression and DNA Methylation Status of the Imprinted Genes PEG10 and L3MBTL1 in the Umbilical Cord Blood and Placenta of the Offspring of Assisted Reproductive Technology. *Reprod Sci* 2021;**28**:1133–1141. United States.
Watson AJ. Oocyte cytoplasmic maturation: a key mediator of oocyte and embryo developmental competence. *J Anim Sci* 2007;**85**:.
Weber M, Davies JJ, Wittig D, Oakeley EJ, Haase M, Lam WL, Schübeler D. Chromosome-wide and promoter-specific analyses identify sites of differential DNA methylation in normal and transformed human cells. *Nat Genet* 2005;**37**:853–862.
Wei JW, Huang K, Yang C, Kang CS. Non-coding RNAs as regulators in epigenetics (Review). *Oncol Rep* 2017;**37**:3–9. Spandidos Publications.
Whitelaw N, Bhattacharya S, Hoad G, Horgan GW, Hamilton M, Haggarty P. Epigenetic status in the offspring of spontaneous and assisted conception. *Human Reproduction* [Internet] 2014;**29**:1452–1458. P. Haggarty, Division of Lifelong Health, Rowett Institute of Nutrition and Health, University of Aberdeen, Greenburn Road, Bucksburn, Aberdeen AB21 9SB, United Kingdom.
Willer CJ, Li Y, Abecasis GR. METAL: Fast and efficient meta-analysis of genomewide association scans. *Bioinformatics* 2010;**26**:2190–2191.

Winship AL, Stringer JM, Liew SH, Hutt KJ. The importance of DNA repair for maintaining oocyte quality in response to anti-cancer treatments, environmental toxins and maternal ageing. *Hum Reprod Update* 2018;**24**:119–134. Oxford University Press.
Wolkers WF, Oldenhof H. *Cryopreservation and Freeze-Drying Protocols* [Internet]. 2015;Available from: http://www.springer.com/series/7651.
Wu D, Dean J. EXOSC10 sculpts the transcriptome during the growth-to-maturation transition in mouse oocytes. *Nucleic Acids Res* 2020;**48**:5349–5365. Oxford University Press.
Wu H, Zhang Y. Reversing DNA methylation: Mechanisms, genomics, and biological functions. *Cell* 2014;**156**:45–68. Elsevier B.V.
Wu X, Zhang Y. TET-mediated active DNA demethylation: Mechanism, function and beyond. *Nat Rev Genet* 2017;**18**:517–534. Nature Publishing Group.
Wyck S, Herrera C, Requena CE, Bittner L, Hajkova P, Bollwein H, Santoro R. Oxidative stress in sperm affects the epigenetic reprogramming in early embryonic development. *Epigenetics Chromatin* 2018;**11**:. BioMed Central Ltd.
Wyns C, Geyter C De, Calhaz-Jorge C, Kupka MS, Motrenko T, Smeenk J, Bergh C, Tandler-Schneider A, Rugescu IA, Goossens V. ART in Europe, 2018: results generated from European registries by ESHRE. *Hum Reprod Open* [Internet] 2022;**2022**:.
Xu J, Sinclair KD. One-carbon metabolism and epigenetic regulation of embryo development. *Reprod Fertil Dev* 2015;**27**:667–676. CSIRO.
Xu N, Barlow GM, Cui J, Wang ET, Lee B, Akhlaghpour M, Kroener L, Williams J 3rd, Rotter JI, Chen YI, *et al.* Comparison of Genome-Wide and Gene-Specific DNA Methylation Profiling in First-Trimester Chorionic Villi From Pregnancies Conceived With Infertility Treatments. *Reprod Sci* 2017;**24**:996–1004.
Xue Z, Huang K, Cai C, Cai L, Jiang CY, Feng Y, Liu Z, Zeng Q, Cheng L, Sun YE, *et al.* Genetic programs in human and mouse early embryos revealed by single-cell RNA sequencing. *Nature* [Internet] 2013;**500**:593–597. Nature Publishing Group.
Yabuta Y, Kurimoto K, Ohinata Y, Seki Y, Saitou M. Gene expression dynamics during germline specification in mice identified by quantitative single-cell gene expression profiling. *Biol Reprod* 2006;**75**:705–716.
Yamaguchi S, Shen L, Liu Y, Sendler D, Zhang Y. Role of Tet1 in erasure of genomic imprinting. *Nature* 2013;**504**:460–464.
Yan L, Yang M, Guo H, Yang L, Wu J, Li R, Liu P, Lian Y, Zheng X, Yan J, *et al.* Single-cell RNA-Seq profiling of human preimplantation embryos and embryonic stem cells. *Nat Struct Mol Biol* 2013;**20**:1131–1139. Nature Publishing Group.
Yang AS, Estécio MRH, Doshi K, Kondo Y, Tajara EH, Issa JPJ. A simple method for estimating global DNA methylation using bisulfite PCR of repetitive DNA elements. *Nucleic Acids Res* 2004;**32**:.
Yang ZY, Ye M, Xing YX, Xie QG, Zhou JH, Qi XR, Kee K, Chian RC. Changes in the Mitochondria-Related Nuclear Gene Expression Profile during Human Oocyte Maturation by the IVM Technique. *Cells* 2022;**11**:. MDPI.
Yao J-F, Huang Y-F, Huang R-F, Lin S-X, Guo C-Q, Hua C-Z, Wu P-Y, Hu J-F, Li Y-Z. Effects of vitrification on the imprinted gene Snrpn in neonatal placental tissue. *Reproductive and Developmental Medicine* [Internet] 2020;**4**:25–31. J.-F. Hu, Department of Obstetrics and Gynecology, First Affiliated Hospital, Fujian Medical University, Fuzhou, China.
Yao Q, Chen Y, Zhou X. The roles of microRNAs in epigenetic regulation. *Curr Opin Chem Biol* 2019;**51**:11–17. Elsevier Ltd.
Ye M, Yang ZY, Zhang Y, Xing YX, Xie QG, Zhou JH, Wang L, Xie W, Kee KK, Chian RC. Single-cell multiomic analysis of in vivo and in vitro matured human oocytes. *Human Reproduction* 2020;**35**:886–900. Oxford University Press.
Yeung EH, Mendola P, Sundaram R, Zeng X, Guan W, Tsai MY, Robinson SL, Stern JE, Ghassabian A, Lawrence D, *et al.* Conception by fertility treatment and offspring deoxyribonucleic acid methylation. *Fertil Steril* [Internet] 2021; E.H. Yeung,

Epidemiology Branch, Eunice Kennedy Shriver National Institute of Child Health and Human Development, 6710B Rockledge Drive, Room 3122, MSC 7004, Bethesda, MD, United StatesAvailable from: https://www.embase.com/search/results?subaction=viewrecord&id=L2011596204&from=export.

Young LE, Fernandes K, McEvoy TG, Butterwith SC, Gutierrez CG, Carolan C, Broadbent PJ, Robinson JJ, Wilmut I, Sinclair KD. Epigenetic change in IGF2R is associated with fetal overgrowth after sheep embryo culture. *Nat Genet* 2001;**27**:153–154.

Yu B, Jayavelu ND, Battle SL, Mar JC, Schimmel T, Cohen J, Hawkins RD. Single-cell analysis of transcriptome and DNA methylome in human oocyte maturation. *PLoS One* 2020;**15**:. Public Library of Science.

Yuan L, Yin P, Yan H, Zhong X, Ren C, Li K, Chin Heng B, Zhang W, Tong G. Single-cell transcriptome analysis of human oocyte ageing. *J Cell Mol Med* 2021;**25**:6289–6303. John Wiley and Sons Inc.

Zander DL, Thompson JG, Lane M. Perturbations in mouse embryo development and viability caused by ammonium are more severe after exposure at the cleavage stages. *Biol Reprod* 2006;**74**:288–294.

Zandstra H, Montfoort APA Van, Dumoulin JCM. Does the type of culture medium used influence birthweight of children born after IVF? *Human Reproduction* 2015;**30**:530–542.

Zechner U, Pliushch G, Schneider E, Hajj N El, Tresch A, Shufaro Y, Seidmann L, Coerdt W, Müller AM, Haaf T. Quantitative methylation analysis of developmentally important genes in human pregnancy losses after ART and spontaneous conception. *Mol Hum Reprod* 2010;**16**:704–713. England.

Zhang J-J, Liu X, Chen L, Zhang S, Zhang X, Hao C, Miao Y-L. Advanced maternal age alters expression of maternal effect genes that are essential for human oocyte quality. *Aging* 2020;**12**:3950–3961.

Zhang Y, Yan Z, Qin Q, Nisenblat V, Chang HM, Yu Y, Wang T, Lu C, Yang M, Yang S, *et al.* Transcriptome Landscape of Human Folliculogenesis Reveals Oocyte and Granulosa Cell Interactions. *Mol Cell* 2018;**72**:1021-1034.e4. Cell Press.

Zhao H, Li T, Zhao Y, Tan T, Liu C, Liu Y, Chang L, Huang N, Li C, Fan Y, *et al.* Single-cell transcriptomics of human oocytes: Environment-driven metabolic competition and compensatory mechanisms during oocyte maturation. *Antioxid Redox Signal* 2019a;**30**:542–559. Mary Ann Liebert Inc.

Zhao P, Zhou X, Shen K, Liu Z, Cheng T, Liu D, Cheng Y, Peng X, Sun M xiang. Two-Step Maternal-to-Zygotic Transition with Two-Phase Parental Genome Contributions. *Dev Cell* 2019b;**49**:882-893.e5. Cell Press.

Zheng H-Y, Shi X-Y, Wang L-L, Wu Y-Q, Chen S-L, Zhang L. Study of DNA methylation patterns of imprinted genes in children born after assisted reproductive technologies reveals no imprinting errors: A pilot study. *Exp Ther Med* 2011;**2**:751–755.

Zheng H-Y, Tang Y, Niu J, Li P, Ye D-S, Chen X, Shi X-Y, Li L, Chen S-L. Aberrant DNA methylation of imprinted loci in human spontaneous abortions after assisted reproduction techniques and natural conception. *Hum Reprod* 2013;**28**:265–273. England.

Zheng SC, Webster AP, Dong D, Feber A, Graham DG, Sullivan R, Jevons S, Lovat LB, Beck S, Widschwendter M, *et al.* A novel cell-type deconvolution algorithm reveals substantial contamination by immune cells in saliva, buccal and cervix. *Epigenomics* 2018;**10**:925–940.

Zheng Y, Joyce BT, Liu L, Zhang Z, Kibbe WA, Zhang W, Hou L. Prediction of genome-wide DNA methylation in repetitive elements. *Nucleic Acids Res* 2017;**45**:8697–8711. Oxford University Press.

Zhou F, Wang R, Yuan P, Ren Y, Mao Y, Li R, Lian Y, Li J, Wen L, Yan L, *et al.* Reconstituting the transcriptome and DNA methylome landscapes of human implantation. *Nature* 2019;**572**:660–664. England.

Zhu H, Wang G, Qian J. Transcription factors as readers and effectors of DNA methylation. *Nat Rev Genet* 2016;**17**:551–565. Nature Publishing Group.

Zhu L, Zeng X, Liu W, Han W, Huang G, Li J. Comparison of DNA methylation profiles of human embryos cultured in either uninterrupted or interrupted incubators. *J Assist Reprod Genet* 2023;**40**:113–123. Springer.
Zhu P, Guo H, Ren Y, Hou Y, Dong J, Li R, Lian Y, Fan X, Hu B, Gao Y, *et al.* Single-cell DNA methylome sequencing of human preimplantation embryos. *Nat Genet* 2018;**50**:12–19. Nature Publishing Group.
Zwart R, Sleutels F, Wutz A, Schinkel AH, Barlow DP. Bidirectional action of the Igf2r imprint control element on upstream and downstream imprinted genes. *Genes Dev* 2001;**15**:2361–2366.